

ANNUAL REPORTS ON NMR SPECTROSCOPY

Edited by

G. A. WEBB

Department of Chemical Physics, University of Surrey, Guildford, Surrey, England

VOLUME 8

1978



ACADEMIC PRESS

London · New York · San Francisco

A Subsidiary of Harcourt Brace Jovanovich, Publishers

ACADEMIC PRESS INC. (LONDON) LTD.
24-28 Oval Road,
London, NW1 7DX

U.S. Edition Published by

ACADEMIC PRESS INC.
111 Fifth Avenue
New York, New York 10003

Copyright ©1978 by ACADEMIC PRESS INC. (LONDON) LTD.

All Rights Reserved

No part of this book may be reproduced in any form by photostat, microfilm, or
any other means, without written permission from the publishers

Library of Congress Catalog Card Number: 68-17678
ISBN: 0-12-505308-8

Printed in Great Britain by Spottiswoode Ballantyne Ltd.
Colchester and London

LIST OF CONTRIBUTORS

- T. A. CRABB, *Department of Chemistry, Portsmouth Polytechnic, Hampshire, England*
- A. GRYFF-KELLER, *Institute of Organic Chemistry and Technology, Polytechnical University, Warsaw, Poland*
- P. J. SMITH, *International Tin Research Institute, Greenford, Middlesex, UB6 7AQ, England*
- W. B. SMITH, *Department of Chemistry, Texas Christian University, Fort Worth, Texas, USA*
- S. SZYMAŃSKI, *Institute of Organic Chemistry, Polish Academy of Sciences, Warsaw, Poland*
- A. P. TÚPČIAUSKAS, *Institute of Biochemistry, Academy of Sciences of the Lithuanian SSR, Lenino av. 3, 232600 Vilnius MTP-1, USSR*
- M. WITANOWSKI, *Institute of Organic Chemistry, Polish Academy of Sciences, Warsaw, Poland*

PREFACE

The present volume consists of state-of-the-art accounts on four distinct areas of NMR spectroscopy. The relevant literature has been covered up to the first half of 1977.

Dr. Crabb has updated his review on alkaloids which appeared in Volume 6A of this series. This valuable report includes a timely account of the published work on indole alkaloids. A previous review on the ^{13}C NMR spectroscopy of steroids has been brought up to date by Professor W. B. Smith. The more theoretical aspects of dynamic NMR are covered by Dr. Witanowski and his co-workers. Finally, it is a pleasure to include a review on ^{119}Sn NMR spectroscopy for the first time in this series.

It is with gratitude that I acknowledge the encouraging remarks made by various reviewers and readers following the appearance of Volume 7 of this series. Such comments reflect on the considerable efforts made by the authors of the reviews presented. I am very grateful both to them and the authors of the present volume for the cooperation and enthusiasm they have shown in preparing their contributions and submitting them promptly.

*University of Surrey,
Guildford, Surrey,
England*

G. A. WEBB

Nuclear Magnetic Resonance of Alkaloids

TREVOR A. CRABB

*Department of Chemistry, Portsmouth Polytechnic,
Hampshire, England*

I. Introduction	2
A. General remarks	2
B. ^{13}C NMR spectra of alkaloids	3
II. Isoquinoline alkaloids	5
A. Simple isoquinoline alkaloids	5
B. Benzyloisoquinoline alkaloids	7
C. Aporphine, oxa-aporphine, and proaporphine alkaloids (including dioxo- aporphine, aristolactams, and phenanthrene alkaloids)	8
1. Aporphines	8
2. Oxa-aporphines	13
3. Proaporphines	14
4. Dioxoaporphines, aristolactams, and phenanthrene alkaloids	15
D. Bisbenzyloisoquinolines and benzyloisoquinoline-aporphine dimers	17
1. Bisbenzyloisoquinolines	17
2. Benzyloisoquinoline-aporphine dimers	24
E. Cularines	29
F. Protoberberines and protopines	31
G. Spirobenzyloisoquinolines	40
H. Benzophenanthridines	43
I. Phthalideisoquinolines	45
J. Other isoquinoline alkaloids: phenethylisoquinolines, emetine, pavines, tetra- hydrodibenzopyrrococlines, and azafluoranthenes	49
III. Amaryllidaceae alkaloids	52
IV. Erythrina, dibenz[d,f]azonine, and cephalotaxine alkaloids	55
V. Morphine alkaloids	57
A. Alkaloids containing the 4,5-oxide bridge	57
1. Morphine type alkaloids	57
2. Compounds related to canconine	61
B. Alkaloids possessing the morphine skeleton but lacking the 4,5-oxide bridge	62
C. Alkaloids possessing the hasubane skeleton	65
VI. Pyrrolizidine and pyrrole alkaloids	66
VII. Indolizidine alkaloids	70

VIII. Quinolizidine alkaloids	71
A. Lupanine and related alkaloids	71
B. Nuphar alkaloids	76
C. Lythraceae alkaloids	82
IX. Piperidine and pyridine alkaloids	85
A. Tropane alkaloids	85
B. Other alkaloids containing the piperidine moiety	90
C. Pyridine alkaloids	94
X. Quinoline, acridone, and quinazoline alkaloids	98
XI. Imidazole alkaloids	103
XII. Indole alkaloids	106
A. Simple indoles, carbazoles, carbolines, and physostygmine type alkaloids	106
B. Mould metabolites	109
C. Ergot alkaloids	112
D. Yohimbine, corynantheine, ajmalicine, and related alkaloids	117
1. ^{13}C NMR spectra	117
2. ^1H NMR spectra	124
E. Oxindole alkaloids	127
F. Strychnine and related alkaloids	130
1. ^1H NMR spectra	130
2. ^{13}C NMR spectra	133
G. Sarpagine type alkaloids (including gardneria bases)	135
H. Vincamine and related alkaloids	136
I. Aspidospermine, quebrachamine, and ibogamine alkaloids	139
1. ^{13}C NMR spectra of aspidospermine and quebrachamine alkaloids	139
2. ^1H NMR spectra of aspidospermine type alkaloids	146
3. NMR spectra of iboga type alkaloids	149
J. Other indole alkaloids (including andranguinine, adina bases, and cinchona bases)	152
K. Bisindole alkaloids	158
1. Roxburghines	158
2. Vincaleucoblastine and related alkaloids	160
3. Other bisindole alkaloids	163
XIII. Diterpene alkaloids	177
XIV. Lycopodium alkaloids	186
References	189

I. INTRODUCTION

A. General remarks

This review updates the one written for Volume 6A of the series (1) and describes characteristic features of the ^1H and ^{13}C NMR spectra of alkaloids with selected examples taken from papers published during the period from June 1972 to the early part of 1977. Steroidal alkaloids and

peptide alkaloids are not included since these are best covered in reviews on steroids and on peptides, but the NMR spectra of some intermediates in the synthesis of a particular alkaloid and of selected alkaloid degradation products are described.

In some of the papers taken from the period under consideration the NMR spectra of previously described alkaloids are recorded when, for example, comparison between synthetic and natural material is being made. In such cases, and where these alkaloids were not included in the last review, only reference to the most recent paper is given. In addition, reference to work carried out prior to mid-1972 is normally made to Volume 6A of this series rather than to the original literature.

In Sections II–XIV chemical shifts and coupling constants of many of the alkaloids and related systems are given with the structural formulae in order to provide a reference collection of alkaloid NMR data. Many of the recorded proton–proton coupling constants are in fact splittings and are therefore only an approximation to the true coupling constants. ^1H and ^{13}C chemical shifts are in ppm to high frequency from internal TMS unless otherwise stated; coupling constants (or splittings) are in Hz. In the displays and tables of ^{13}C NMR data asterisks signify possible reversal of shift assignments.

B. ^{13}C NMR spectra of alkaloids

Since the period covered by the last review there has been a great increase in the number of papers describing the ^{13}C NMR spectra of alkaloids, and an excellent introduction to this area of research is available. (2) The books by Stothers (3) and by Levy and Nelson (4) on ^{13}C NMR spectroscopy are invaluable and are quoted in the majority of papers concerned with the ^{13}C NMR spectra of alkaloids.

Certain ^{13}C NMR substituent effects (3, 4) are utilized so frequently in the assignment of alkaloid structure that these are summarized in Tables I–III in order to facilitate reference. The γ -effect [illustrated by a

TABLE I

^{13}C NMR substituent effects in substituted benzenes (4)

--	--	--

Negative sign denotes shift to lower frequency; positive sign denotes shift to higher frequency.

TABLE II

Effects of α -, β -, and γ -methyl substituents on ^{13}C shifts in alkanes (5)

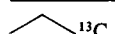
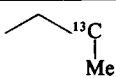
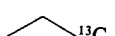
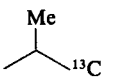
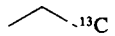
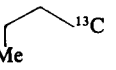
	\longrightarrow		α -effect	shift of <i>ca.</i> 9 ppm to higher frequency
	\longrightarrow		β -effect	shift of <i>ca.</i> 9 ppm to higher frequency
	\longrightarrow		γ -effect	shift of <i>ca.</i> 2 ppm to lower frequency

TABLE III

Effects of α -, β -, and γ -methyl substituents on ^{13}C shifts in cyclohexanes (6)

Equatorial methyl	α -effect	+5.6 ppm	Axial methyl	α -effect	+1.1 ppm
	β -effect	+9.8 ppm		β -effect	+5.2 ppm
	γ -effect	0.0 ppm		γ -effect	-5.4 ppm

substituent methyl in Tables II (5) and III (6)] is of particular importance. Detailed discussions of these effects are available. (3, 4)

In the work described in the following sections, ^{13}C assignments are made utilizing a variety of ^1H decoupling methods which are conveniently summarized here.

In wide-band proton decoupled spectra complete proton decoupling is achieved and all carbon resonances appear as singlets. Enhancement of the ^{13}C signals is observed as a result of the NOE and collapse of the C-H spin multiplets.

In the noise off-resonance decoupling experiment inefficient decoupling conditions are maintained and, since residual coupling is related to coupling constants, the band widths of the signals arising from the methine, methylene, and methyl carbon nuclei, characterized by large $^1J(\text{C-H})$ values, are affected most strongly. Quaternary carbon nuclei, characterized by very small long-range couplings, are decoupled under the off-resonance conditions and absorb as singlets. (7)

In single-frequency off-resonance decoupled (SFORD) spectra the magnitude of the coupling interaction between ^{13}C and ^1H is reduced so that normally only one bond C-H coupling patterns are observed and an A_nX situation is assumed. In such a decoupling the residual coupling J_R is less than $^1J(\text{C-H})$ and depends upon the decoupling power (γB_2) and the decoupler offset ($\Delta\nu$). For most applications to structural work

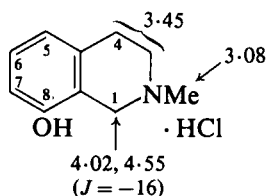
the equation $J_R = J(C-H)\Delta\nu(\gamma B_2)^{-1}$ is permissible. Differences in residual coupling, to their directly bound protons, provide a method of distinction between carbon nuclei (see discussion, for example, on vindoline in Section XII.I). Some problems associated with geminal non-equivalence and second-order coupling in SFORD spectra with reference to some examples taken from the alkaloid field have been discussed by Hagaman. (8) In particular it has been emphasized that the A_nX treatment in SFORD spectra is only legitimate when, for example, in a $^{13}C^1H_A^1H_B$ system $J(C-H_A) = J(C-H_B)$ and $\delta(H_A) = \delta(H_B)$. When $\delta(H_A) - \delta(H_B) > 3 \times J_{gem}$ a doublet of doublets is observed in the SFORD spectrum. Since differences between the chemical shifts of methylene group protons exceeding 0.5 ppm are quite frequently observed in the 1H NMR spectra of natural products, care must be exercised in the interpretation of the SFORD spectra of such systems.

II. ISOQUINOLINE ALKALOIDS

The spectral features of all classes of the isoquinoline alkaloids have been described, (9) and NMR data on thirty-six thalictrum alkaloids described before 1970 have been tabulated. (10)

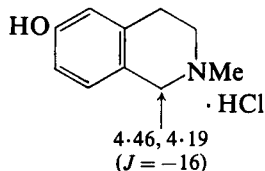
A. Simple isoquinoline alkaloids

The presence of the 8-hydroxyl in longimammidine hydrochloride [1]



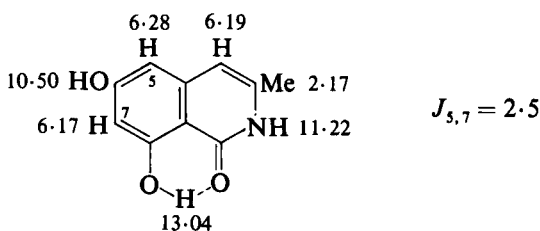
[1] Longimammidine hydrochloride (in D_2O)

produces a chemical shift difference of 0.53 ppm between the C(1) methylene group protons. In longimammosine hydrochloride [2] the corresponding chemical shift difference is 0.27 ppm. (11)

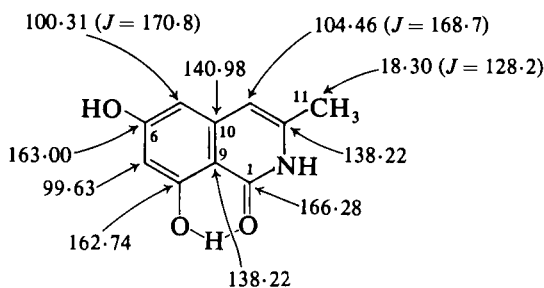


[2] Longimammosine hydrochloride (in D_2O)

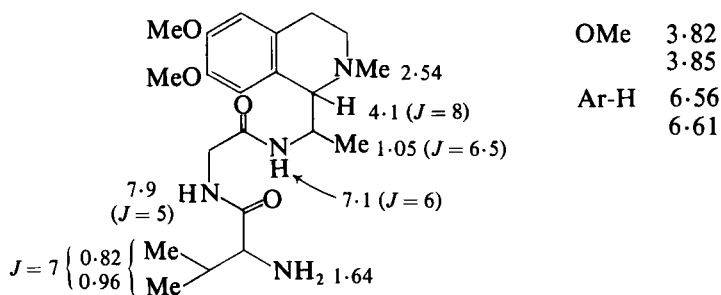
The ^1H and ^{13}C NMR spectra of siamin are summarized in [3] and [4], (12) and of amphibin in [5]. (13) The ^{13}C shifts of 163.00 and



[3] Siamin

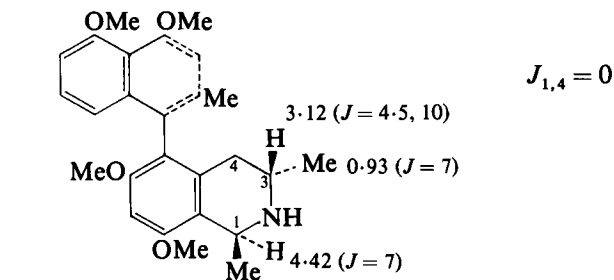
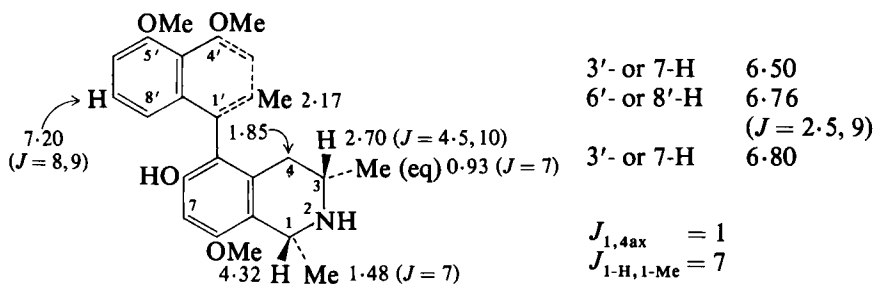


[4]

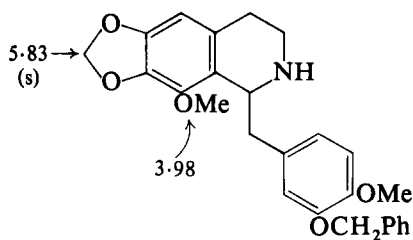
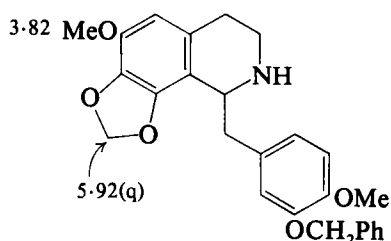


[5] Amphibin (in CDCl_3)

162.74 are typical of the resorcinol moiety. In both *O*-methylancistrocladine [6] and isoancistrocladine [7] the 3-methyl group is shown to be equatorial by vicinal couplings between the 3ax-proton and the 4-methylene protons of 4.5 and 10 Hz. The stereochemical assignments of the 1-methyl groups in [6] and [7] are based on the observation of homoallylic coupling of 1 Hz between the 1ax-proton and the 4ax-proton in the spectrum of [7] which is not observed in that of [6]. (14)

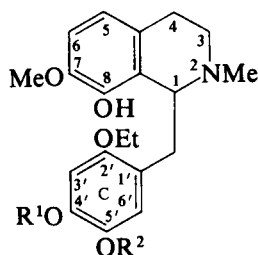
[6] *O*-Methylancistrocladine (in CDCl_3)[7] Isoancistrocladine (in CDCl_3)**B. Benzylisoquinoline alkaloids**

In line with previous correlations (15) the 8-methoxyl protons in the spectrum of [8] absorb at higher frequency than, for example, the 6-methoxyl protons in that of [9]. In the spectrum of [9] the

[8] (in CDCl_3)[9] (in CDCl_3)

methylenedioxy protons absorb as an AB quartet as a result of the neighbouring bulky group. (16)

The 7-methoxyl proton resonances in [10] and [11] are shifted to lower frequency on changing solvent from CDCl_3 to $\text{CDCl}_3\text{-C}_6\text{H}_6$ [$\delta(\text{CDCl}_3) - \delta(\text{C}_6\text{H}_6)$ 0.50 ppm]. The ring-c methoxyl proton



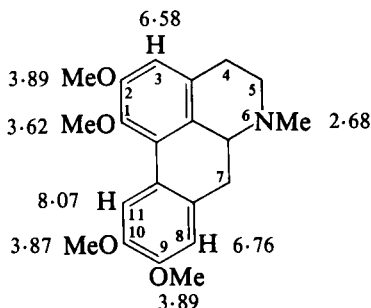
[10]	R¹ = Me	R² = Et	7-OMe	3.86 (CDCl₃)
				3.36 (CDCl₃ + C₆H₆)
			4'-OMe	3.86 (CDCl₃)
				3.72 (C₆H₆)
[11]	R¹ = Et	R² = Me	7-OMe	3.86 (CDCl₃)
				3.36 (CDCl₃ + C₆H₆)
			5'-OMe	3.77 (CDCl₃)
				3.62 (CDCl₃ + C₆H₆)

resonances are shifted to a smaller extent [$\delta(\text{CDCl}_3) - \delta(\text{C}_6\text{H}_6)$ *ca.* 0.14 ppm]. (17)

C. Aporphine, oxa-aporphine, and proaporphine alkaloids (including dioxoaporphine, aristolactams, and phenanthrene alkaloids)

1. Aporphines

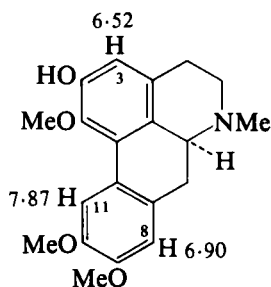
The ^1H NMR spectrum of glaucine [12] (18) shows features typical of aporphine alkaloid spectra, with low frequency absorption of the



[12] (\pm)-Glaucine (in CDCl₃)

C(1)-methoxyl protons and the 3-proton, and high frequency absorption of the 11-proton. (9)

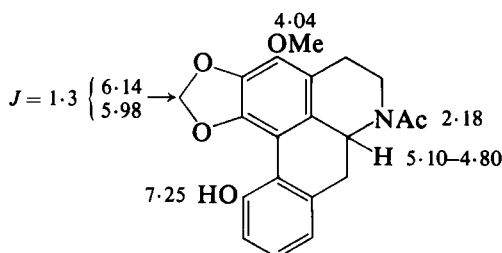
Addition of the chiral lanthanide reagent tris-(3-trifluoromethyl-hydroxymethylene-*d*-camphorato)europium(III) to a solution of (\pm)-

[13] 2-*O*-Demethylglaucine (in DMSO- d_6)

glaucine in $CDCl_3$ shifts the signals from the C(1)-methoxyl protons and from the 11-proton in the *S*-enantiomer to lower frequencies. Shifts of these types permit an estimation of the enantiomeric purity of a variety of isoquinoline alkaloids. (19)

The position of demethylation in 2-*O*-demethylglaucine, a metabolite of glaucine, is located by the observation of 1H chemical shift changes on the addition of NaOD to a DMSO- d_6 solution of the metabolite. The 8-proton signal is not shifted and the 11-proton signal moves to higher frequency (0.08 ppm). In contrast the signal arising from the 3-proton, *ortho* to the phenolic function, moves to lower frequency (0.14 ppm). (20)

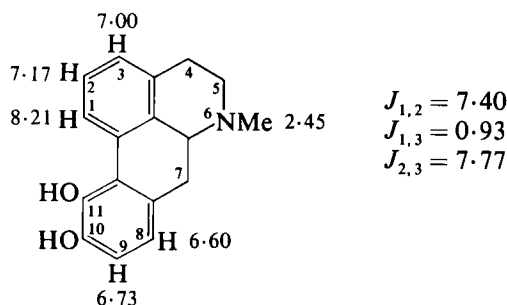
The methoxyl and hydroxyl substituents in *N*-acetylmerrillicine [14]

[14] *N*-Acetylmerrillicine (in $CDCl_3$)

were located (21) at C(3) and C(11) after a consideration of the normally encountered chemical shifts of the 11- and 3-protons and C(1)- and C(11)-methoxyl protons. (9)

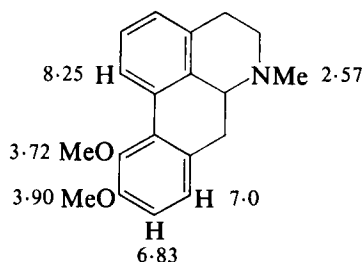
1,2-Methylenedioxyaporphines are characterized by a low frequency shift of the 11-proton signals (δ 7.47 to 7.86) [cf. δ 7.80 to 8.21 for the 11-protons in C(1) hydroxylated or methoxylated aporphines]. (22)

In the spectrum of apomorphine [15] the 1-proton absorbs at high frequency as a consequence of deshielding by the 11-hydroxyl and the D ring. Assignment of the 8- and 9-proton signals is possible since the low

[15] Apomorphine (in DMSO- d_6)

frequency signals of the AB pattern due to these protons show long range coupling. (23) The dihedral angle between C(8)-H and C(7)-H_{ax} is *ca.* 90° so the magnitude of 4J for this system is maximal. (24)

With increasing amounts of Eu(fod)₃ a large deshielding of the signal from the 10-methoxyl protons in 10,11-dimethoxyaporphine [16] is

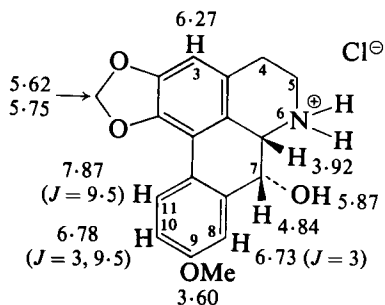


[16] 10,11-Dimethoxyaporphine

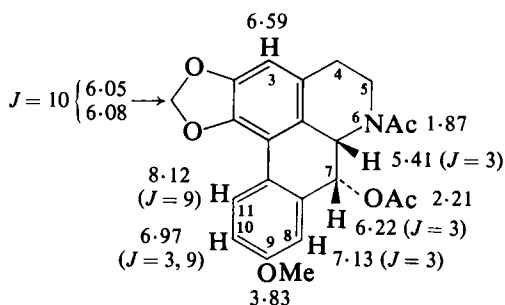
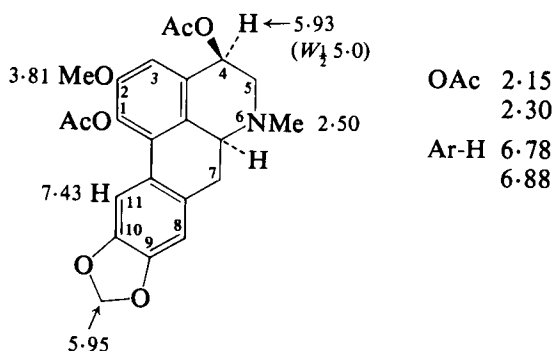
observed. (25) This suggests that the high frequency doublet of the signals arising from the 8- and 9-protons should be assigned to the 9-protons. On this basis, and plotting shifts against the ratio of concentration of Eu(fod)₃ to the concentration of [16], evidence for the low frequency absorption of the 9-proton in the absence of Eu(fod)₃ is obtained. The observation of a NOE between the 10-methoxyl protons and the 9-protons at δ 6.83 supports this conclusion.

The *cis*-relationship between the 6a- and 7-protons in michelanugine hydrochloride [17] is shown by the small vicinal coupling constant (3 Hz) in the spectrum of *O,N*-diacetylmichelanugine [18]. (26)

If the 6a-proton in the 1,4-diacetoxyaporphines [19] and [20] is assumed to be α -orientated, the stereochemistry may be assigned largely on the basis of an analysis of the 4-proton signals in their spectra. (27) Similar 1H NMR studies on 4,*O*-diacetylthaliporphines (methylenedioxy



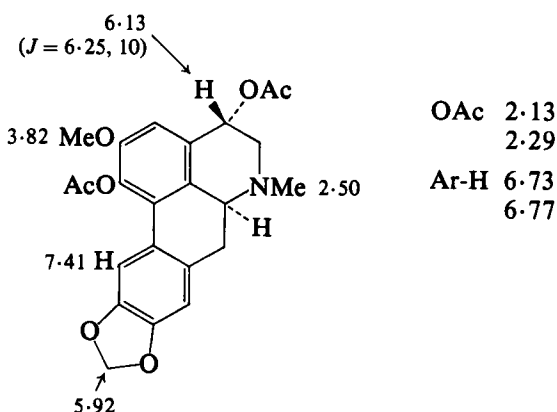
[17] Michelanugine hydrochloride (in TFA)

[18] *O,N*-Diacetylmichelanugine (in CDCl_3)[19] (\pm)-1,4 β -Diacetoxyporphine (in CDCl_3)

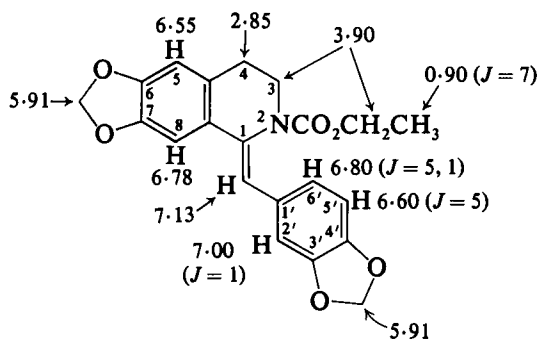
group replacing 9- and 10-methoxyl in [19] and [20]) have been described. (28)

The lower frequency absorption of the $\text{COOCH}_2\text{CH}_3$ protons in the spectrum of the *Z*-isomer [21] compared with the corresponding

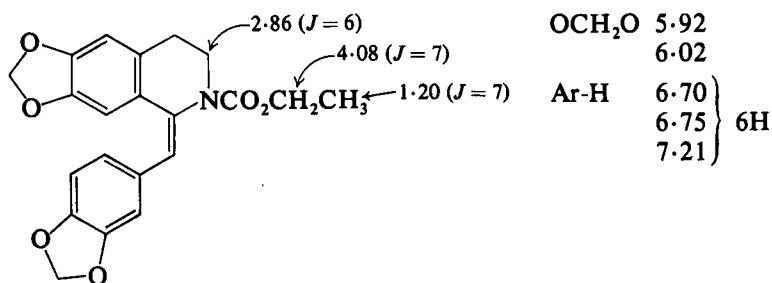
absorption in the *E*-isomer [22] as a result of the differing orientations of the benzyldiene ring has been noted. (29)



[20] (±)-1,4 α -Diacetoxyporphine (in CDCl_3)



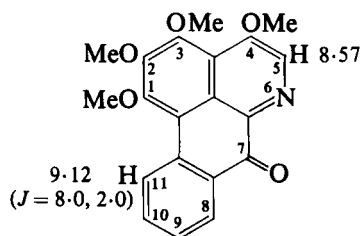
[21] (in CDCl_3)



[22] (in CDCl_3)

2. Oxa-aporphines

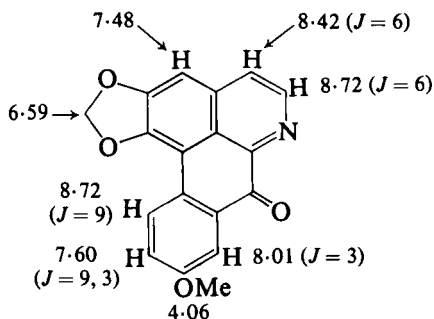
In the ^1H NMR spectra of the oxa-aporphines, a high frequency absorption for the 11-proton is observed [see imenine [23] (30) and



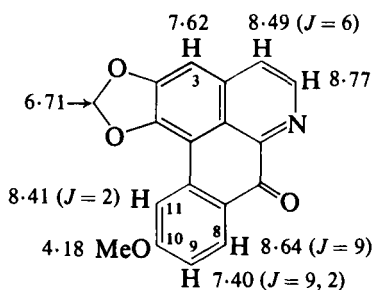
OMe	4.02
	4.07
	4.12
	4.22
Ar-H	8.56, 7.80–7.35 (3H)

[23] Imenine (in CDCl_3)

lanuginosine [24] (26)] and lower frequency absorption for the 3-proton (see [24]). In the spectrum of oxolaureline [25] the 8-proton actually

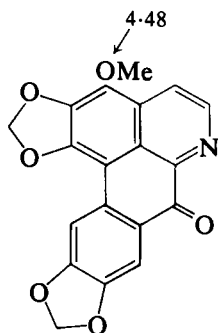


[24] Lanuginosine (in TFA)



[25] Oxolaureline (in TFA-d)

absorbs to high frequency of the 11-proton. (31) ^1H NMR parameters for cassamedine are shown in [26]. (32)

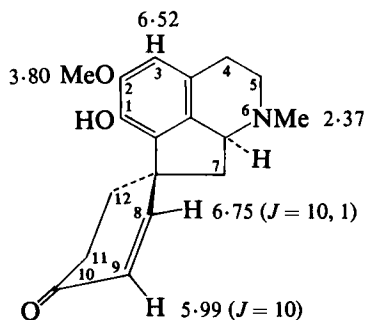


[26] Cassamedine (in TFA-d)

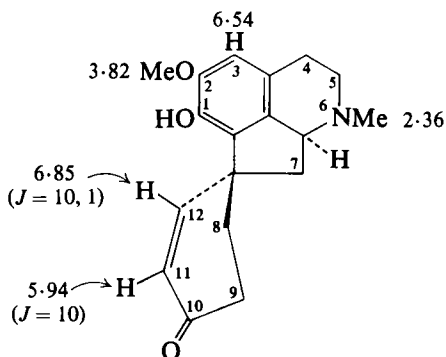
OCH_2O	6.21
	6.61
Ar-H	7.83
	8.18
	8.83 (2H)

3. Proaporphines

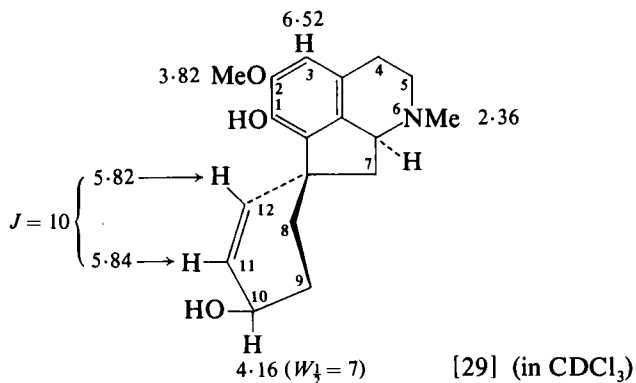
^1H NMR parameters for pairs of 8,9-dihydro- and 11,12-dihydro-proaporphines are shown in [27] and [28] (33) and in [29] and [30]. (34) A value of 3.5 Hz for $J_{10,11}$ in [29] is obtained on a solution in deuterio-pyridine.



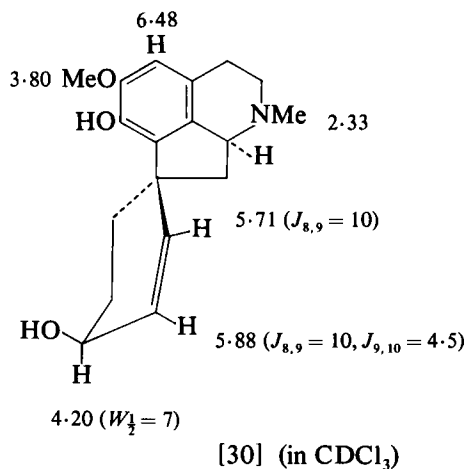
[27] (±)-11,12-Dihydroglaziovine (in CDCl_3)



[28] (±)-8,9-Dihydroglaziovine (in CDCl_3)

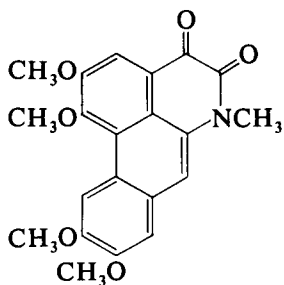


[29] (in CDCl_3)

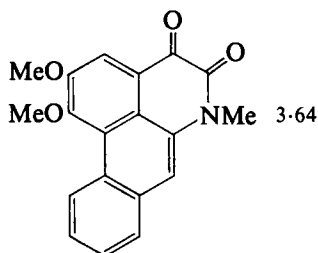


4. Dioxoaporphines, aristolactams, and phenanthrene alkaloids

The structure of pontevedrine [31] has been revised since the ^{13}C NMR spectrum (CDCl_3) shows the presence of the C(4) and C(5) carbonyl groups (δ 48 and 55). (35) The ^1H NMR spectrum of cepharadione B is shown in [32]. The highest frequency aromatic proton



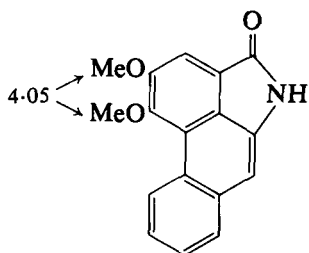
[31] Pontevedrine



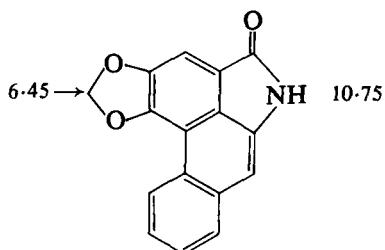
OMe	4.00
	4.03
Ar-H	7.22
	7.5–7.8 (3H)
	7.98
	9.37

[32] Cepharadione B (in CDCl_3)

(δ 9.12) in cepharanone B [33] absorbs at higher frequency than the corresponding proton (δ 8.5) in cepharanone A [34]. (36)



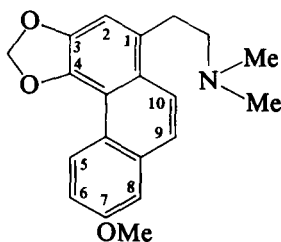
[33] Cepharanone B (in DMSO)



Ar-H 7.10
7.60
7.5-7.7 (2H)
7.9
8.5

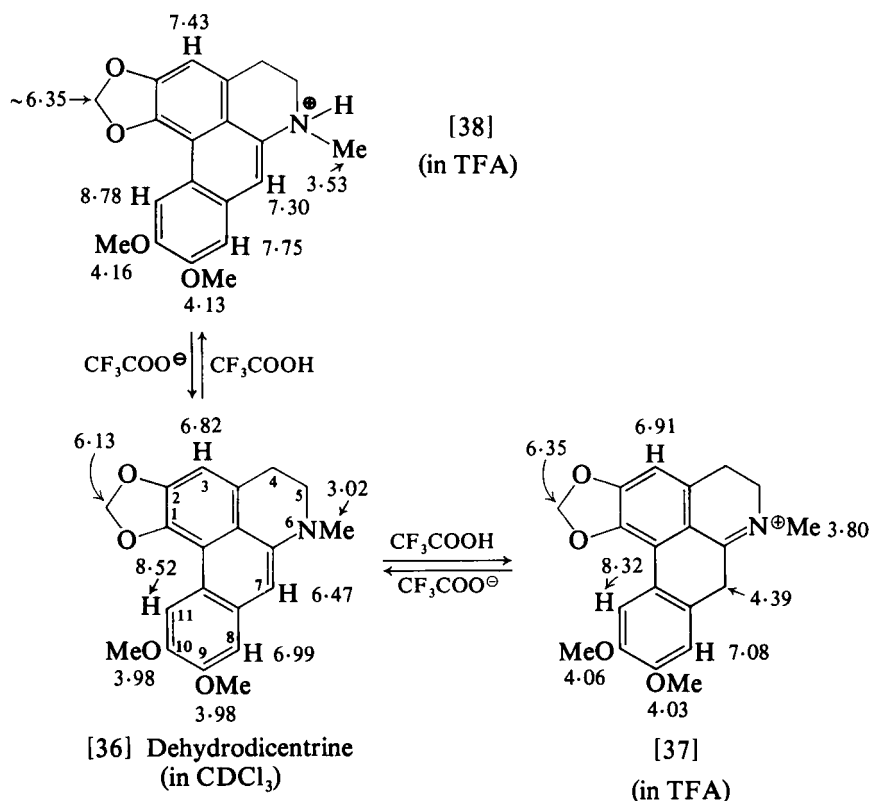
[34] Cepharanone A (in DMSO)

In the phenanthrene alkaloids the 3,4-methylenedioxy group causes an increase in shielding of the 5-proton signals (δ 9.00 in uvariopsine [35] compared with δ 9.3-9.9 in 3,4-dihydroxylated or 3,4-



[35] Uvariopsine

dimethoxylated phenanthrenes). (22) Protonation studies on dehydrodicentrine [36] are summarized in [37] and [38]. The C-protonated salt [37] is the major species. Similar results are obtained with dehydrocopolodine. (37)



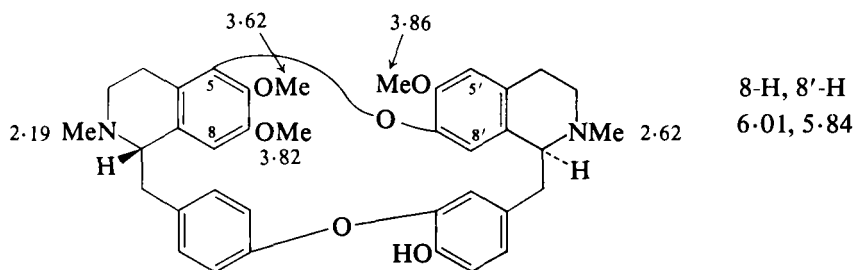
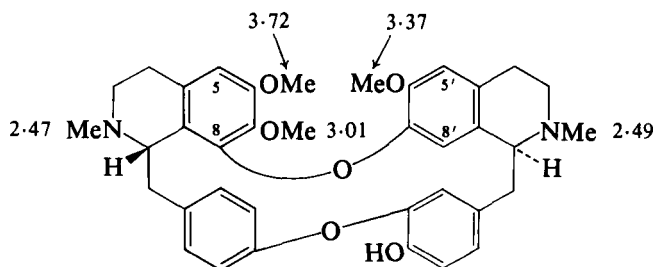
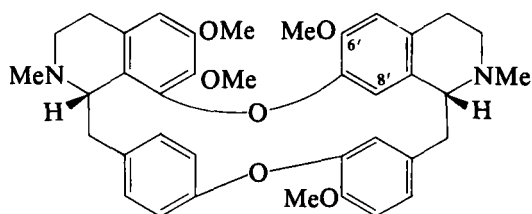
D. Bisbenzylisoquinolines and benzylisoquinoline-aporphine dimers

1. Bisbenzylisoquinolines

In the bisbenzylisoquinolines the size of the macrocyclic system affects the chemical shifts of some groupings of protons in a characteristic way. In certain conformations of the 21-membered ring in 5–7' ether linked systems the 2- and 6-substituents lie over aryl rings with a consequent shift to lower frequency. This is illustrated by the ^1H NMR spectrum of thalictine [39] (38) which shows absorption for the 8- and 8'-protons to low frequency of the other aromatic protons.

Comparison may be made with repandine [40] (8–7' ether linked system) in which the 18-membered ring forces close approach of parts of the molecule so that some of the methoxyl group protons absorb at lower frequency (see δ 3.37 6'-OMe, δ 3.01 7-OMe).

O-Methylrepandine may be distinguished from *O*-methoxyacanthine [41] by the differing shifts of the C(6)-methoxyl protons (δ 3.4 in

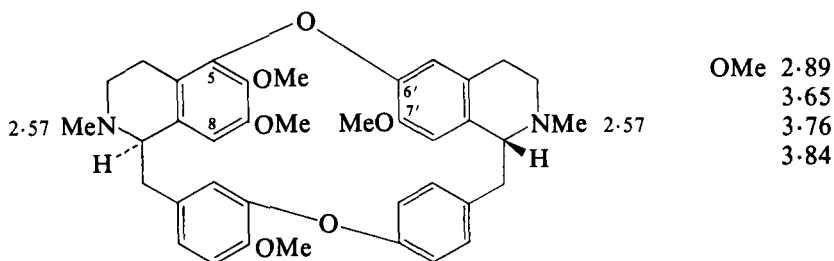
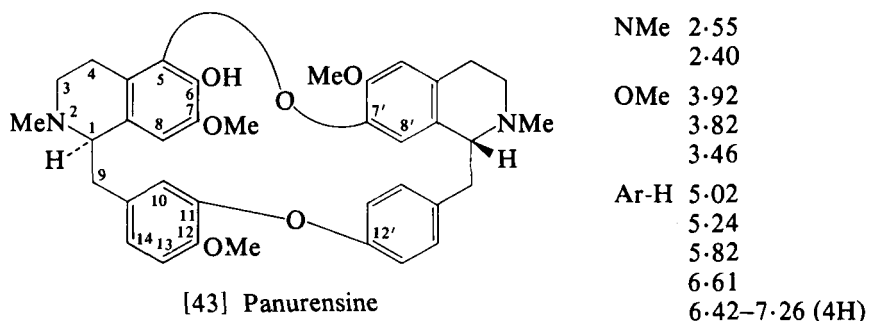
[39] Thalictine (in CDCl₃)[40] Repandine (in CDCl₃)

[41] O-Methoxyacanthine

repandine series, δ 3.6 in oxyacanthine series) and the low frequency absorption (δ 5.5) of the 8'-proton in oxyacanthine. (39) In the repandine series there is no aromatic proton signal in this region of the spectrum.

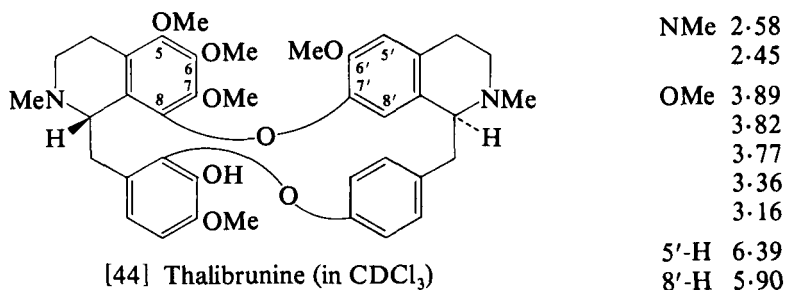
The unusual low frequency absorption (δ 2.89) of the protons of one methoxyl group in the spectrum of *O*-methylnemuarine [42] points to a previously unencountered type (5-6' ether linked) of bisbenzylisoquinoline alkaloid. (40)

In the ¹H NMR spectrum of panurensine [43] the three highly shielded aromatic protons [δ 5.02(s), 5.24(s), and 5.82(s)] are assigned to the 8-, 8'-, and 10'-protons which lie over aromatic rings. These shifts appear diagnostic of the 5-7' and 11-12' ether linked dimers. (41)

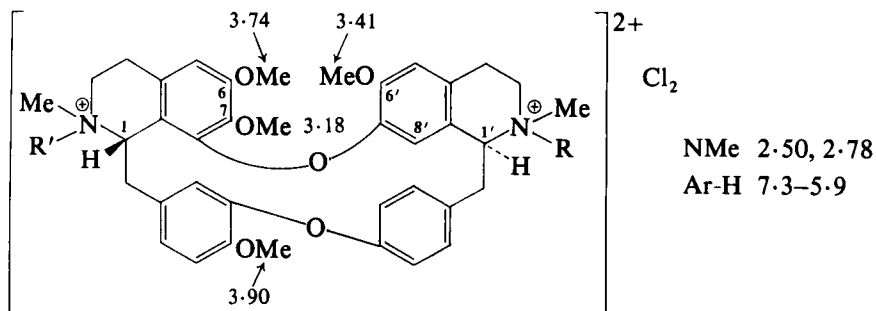
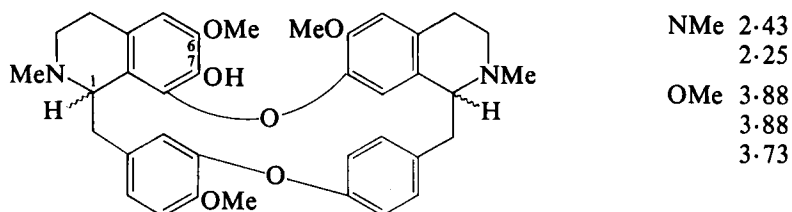
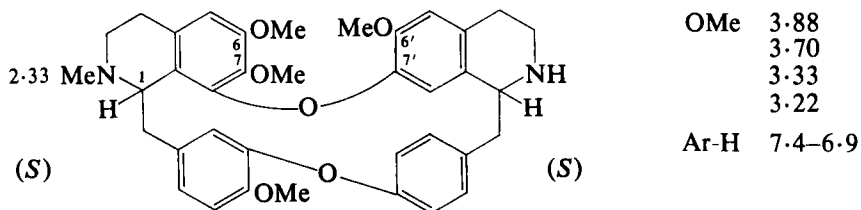
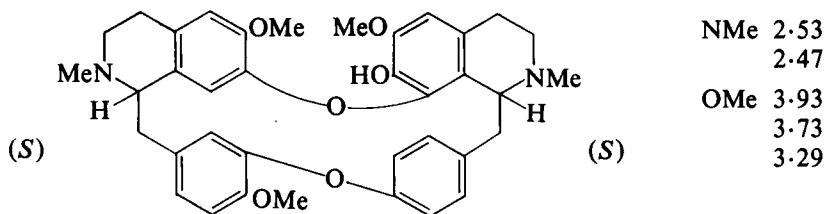
[42] *O*-Methylnemuarine

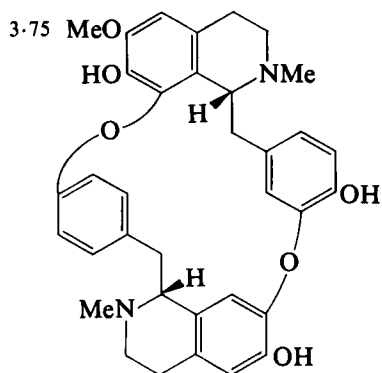
[43] Panurensine

The ^1H NMR spectra of thalibrunine (42) and of monomethyl-tetrandrinium chloride (43) are as shown in [44] and [45] respectively.

[44] Thalibrunine (in CDCl_3)

In cycleadrine (mixture of two antipodal diastereoisomers) two structures were considered (as in [46] or with the C(6) and C(7) substituents reversed). In the spectra of alkaloids of this latter type the C(7)-methoxyl protons normally absorb at low frequency (δ 3.20), and since such absorption was not observed in cycleadrine structure [46] was assigned. The ^1H NMR spectra of cycleanorine and cycleapeltine (possibly antipode of limacusine) are as shown in [47] and [48]. Absorption of the methoxyl protons assisted in the elucidation of the structure of cycleacurine [49]. In the spectrum of tri-*O*-ethyl-

[45] Monomethyltetrandrinium chloride (in CDCl_3)[46] Cycleadrine (in CDCl_3)[47] Cycleanorine (in CDCl_3)[48] Cycleapeltine (in CDCl_3)

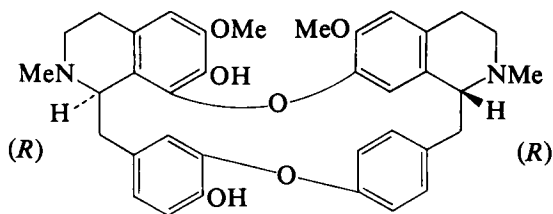


NMe 2.48, 2.18

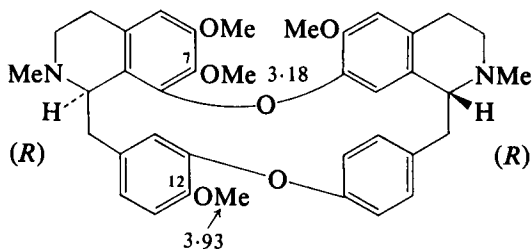
[49] Cycleacurine (in DMSO- d_6)

cycleacurine the methoxyl protons absorbed at δ 3.85, suggesting the C(6) location. (44)

The ^1H NMR spectrum of krukovine is shown in [50]. Comparison of the spectra of *O,O*-dimethylkrukovine [51] and *O,O*-bistrideuterio-



NMe 2.28
2.58
OMe 3.30
3.73
Ar-H 5.97 (1H)
7.11 ($J = 8$, 2H)
7.32 ($J = 8$, 2H)
6.28–6.75

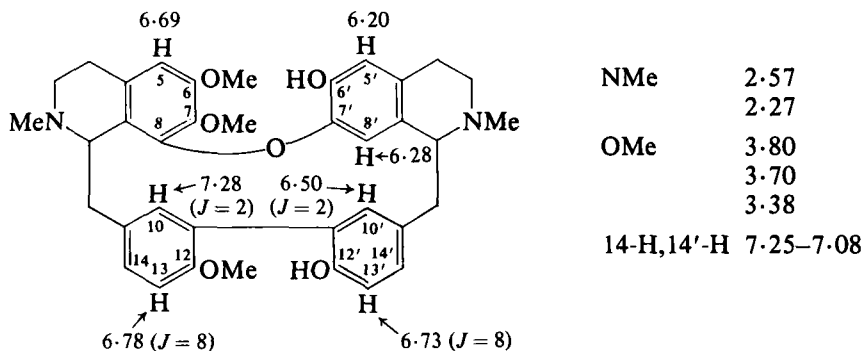
[50] Krukovine (in CDCl_3 + DMSO- d_6)

NMe 2.33
2.62
OMe 3.18
3.37
3.74
3.93
Ar-H 6.00 (1H)
6.30–7.26

[51] *O,O*-Dimethylkrukovine (in CDCl_3)

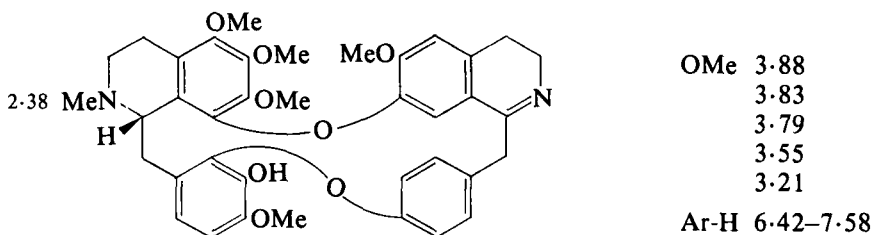
methylkrukovine enabled the chemical shifts of the introduced methyl protons in the dimethyl compound to be determined as δ 3.18 and 3.93. The low frequency absorption at 3.18 is characteristic of a 7-methoxyl group (cf. [40]) and the "normal" absorption at δ 3.93 is consonant with the 12-methoxyl group. (45)

Base catalysed deuteration of phlebicine [52] resulted in the replacement of the hydrogen atoms at C(5') and C(13') *ortho* to the phenolic groups. This was shown by loss of the signals at δ 6.20 and 6.78 ($J = 8$ Hz). (46)



[52] Phlebicine (in CDCl_3)

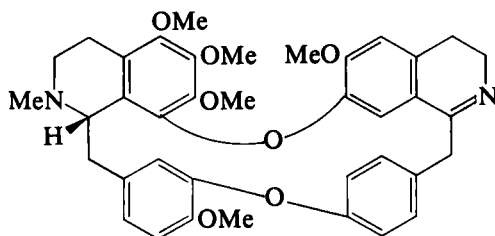
An unusually deshielded benzylic methylene signal (δ 4.40) is observed in the spectrum of thalibrunimine [53]. (47) Of importance is



[53] Thalibrunimine (in $\text{C}_5\text{D}_5\text{N}$)

the room temperature ^1H NMR spectrum of thalsimine [54] which shows ten methoxyl and two *N*-methyl signals. Since on heating to 95°C only the normal number of methyl peaks are observed, this indicates the presence of two stable conformers at room temperature. Thalsimine is the first example of a natural bisbenzylisoquinoline alkaloid exhibiting such a potentially misleading room temperature NMR spectrum due to conformers. (47)

The NMR spectrum of [55] obtained by Na-NH_3 cleavage of thalistryline [56] shows two single peaks at δ 6.43 and 6.33 in a 2:1 ratio but together integrating for one proton. These signals are assigned to the aromatic protons of the pentasubstituted ring in two conformers. (48)



[54] Thalsimine

In C_5D_5N at room temperature:

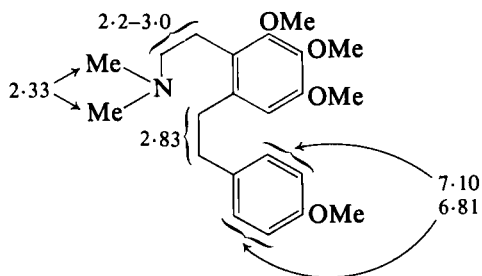
OMe 3.93, 3.91, 3.88, 3.83, 3.83, 3.78,
3.63, 3.52, 3.46, 3.39

NMe 2.33, 2.28

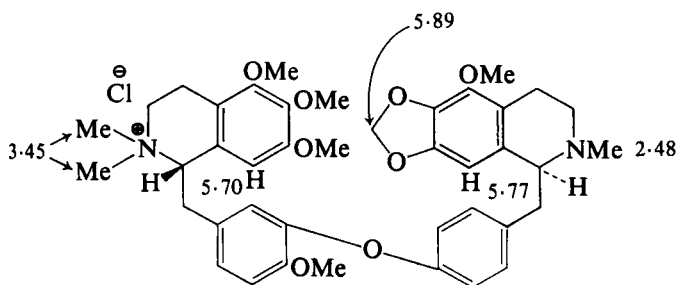
In C_5D_5N at 95° :

OMe 3.89, 3.82, 3.82, 3.54, 3.47

NMe 2.29



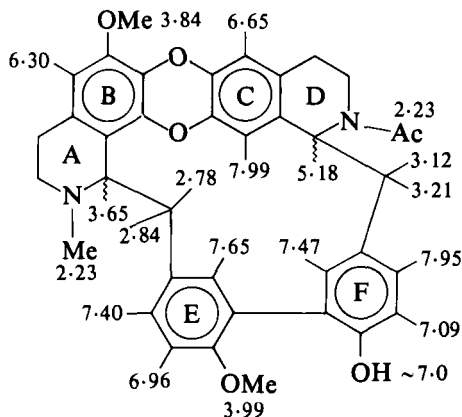
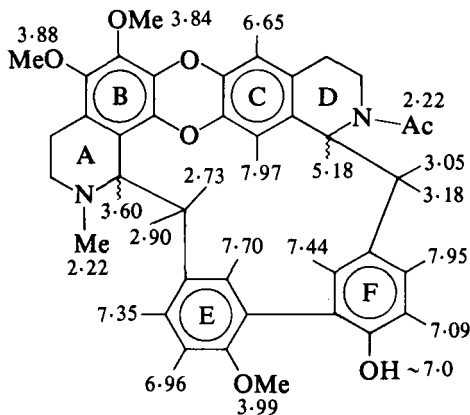
OMe 3.89
3.85
3.78
3.78

[55] (in $CDCl_3$)

OMe 3.85
3.80
3.80
3.77
3.63
Ar-H $\left. \begin{matrix} 6.98 \\ 6.63 \end{matrix} \right\} (J = 8, 4H)$

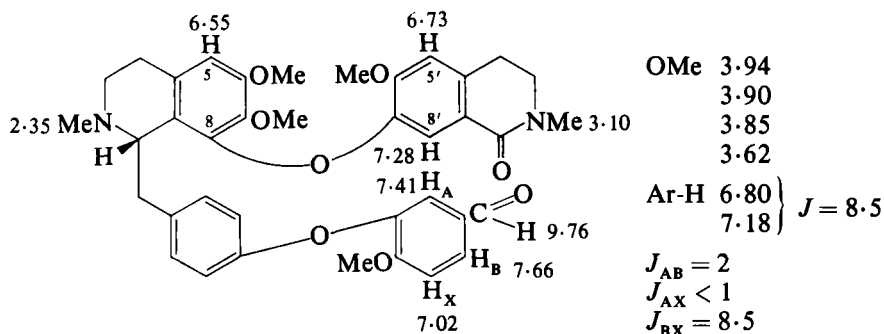
[56] Thalistyline chloride (in $CDCl_3$)

The results of a very detailed 1H NMR study (49) on *N*-acetylnortiliacorinine A and on *N*-acetyltiliamosine are displayed in [57] and [58].

[57] *N*-Acetylnortiliacorinine A[58] *N*-Acetyltiliamosine

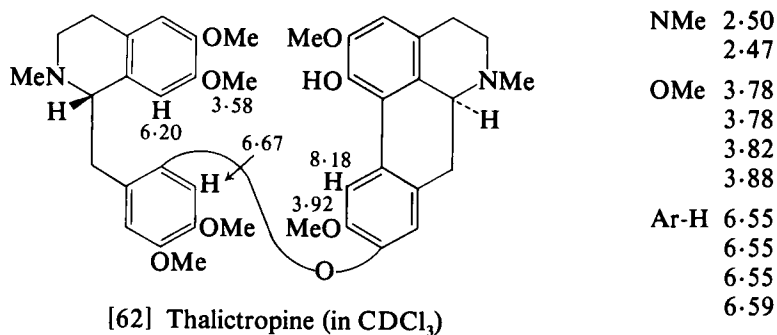
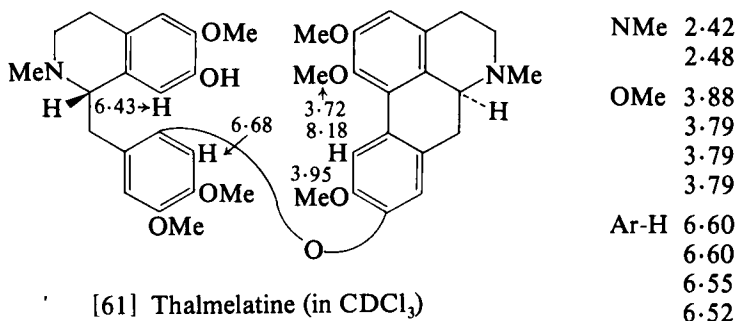
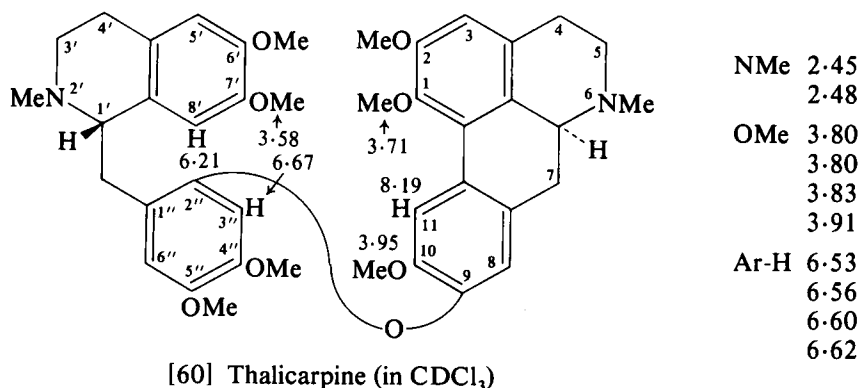
The methylene bridge protons show a J_{gem} of -12 Hz and vicinal couplings of 11 and <1 Hz ($\phi = 180^\circ$ or $\sim 0^\circ$ and $\sim 90^\circ$).

The ^1H NMR spectrum of an oxidation product of obaberine is summarized in [59]. (50) [See also the spectrum of baluchistanamine (51).]

[59] (in CDCl_3)

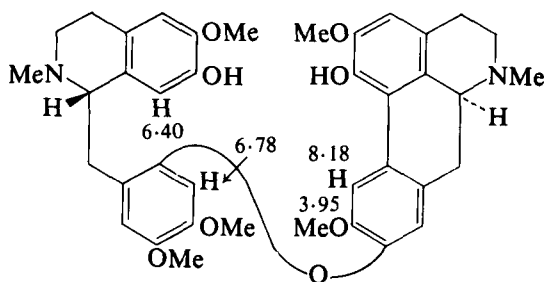
2. Benzyloquinoline-aporphine dimers

A survey of the ^1H NMR spectra of the benzyloquinoline-aporphine alkaloids [60]–[65] enables assignment of some of the methoxyl proton resonances. The lowest frequency methoxyl proton signals at *ca.* δ 3.58 are characteristic of a 7'-methoxyl function, and the 10-methoxyl protons are found to absorb to higher frequency of δ 3.90. (52) This latter shift is also shown in the spectrum of fetedine [66] the aromatic proton signals of which are completely resolved at 220 MHz. (53) In the

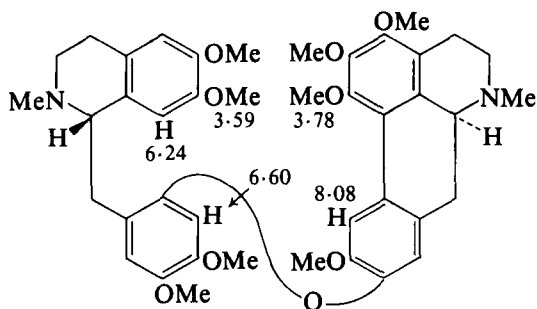


spectrum of thalictropine [62] the 8'-proton is shielded and the 11-proton is deshielded. (54) The low frequency shift of the 11-proton in the spectrum of thalictropine acetate (δ 7.60) relative to that in the spectrum of thalictropine denotes a C(1) acetoxy function. (10)

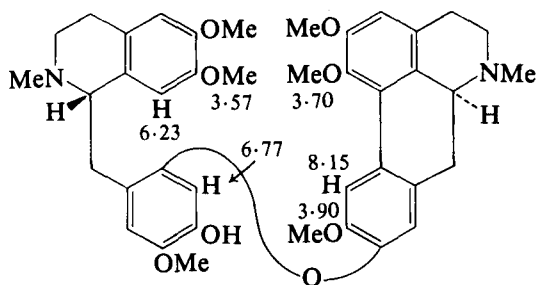
In the NMR spectrum of thalictrogamine [63] the 8'-proton signal is observed to high frequency as for thalmelatine [61] at δ 6.40, but not for

[63] Thalictrogamine (in CDCl_3)

NMe	2.49
	2.52
OMe	3.79
	3.83
	3.83
	3.92
Ar-H	6.51
	6.57
	6.57
	6.57

[64] Adiantifoline (in CDCl_3)

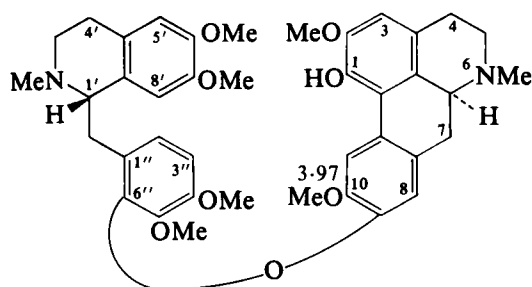
NMe	2.44
	2.47
OMe	3.78
	3.78
	3.82
	3.89
	3.94
	3.96
Ar-H	6.55
	6.55
	6.60

[65] Thalidoxine (in CDCl_3)

NMe	2.47
	2.48
OMe	3.75
	3.78
	3.88
Ar-H	6.50
	6.50
	6.50
	6.57

thalicarpine [60] or thalictropine [62] at δ 6.25 and 6.20 respectively. Thalictrogamine [63] is also characterized by the absence of the low frequency signal (δ 3.58) in its spectrum characteristic of the 7'-methoxyl group in thalicarpine, thalictropine, and other 7'-methoxylated benzyloquinoline-aporphine alkaloids.

In the spectrum of thalictrogamine diacetate (δ 8'-H 6.43; δ 11-H 7.60) the deshielding of the 8'-proton relative to thalictrogamine [63] is

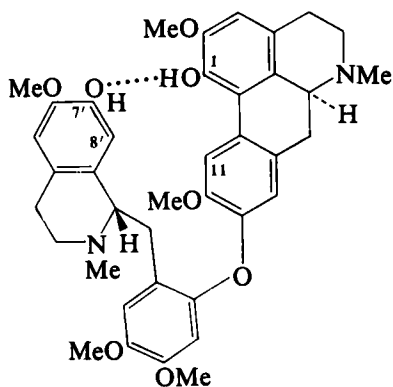


Ar-H	6.14
	6.42
	6.52
	6.52
	6.75
	6.81
	8.12

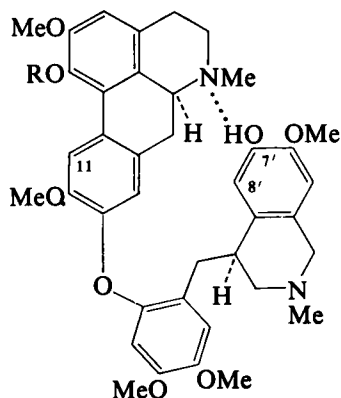
$J = 8.5$

[66] Fetidine

consistent with an aromatic proton *ortho* to an acetate function. (55) In these benzylisoquinoline-aporphine dimers of the thalicarpine [60] series it has been suggested that absorption of the 8'-proton at δ 6.4 indicates the presence of a 7'-hydroxyl function. This suggestion is based on an examination of models which shows that in these dimers the change in conformation brought about by hydrogen bonding between the 7'-hydroxyl and the 1-hydroxyl or the aporphine nitrogen as in [67] and [68] results in a deshielding of the 8'-proton to δ 6.4 from the usual



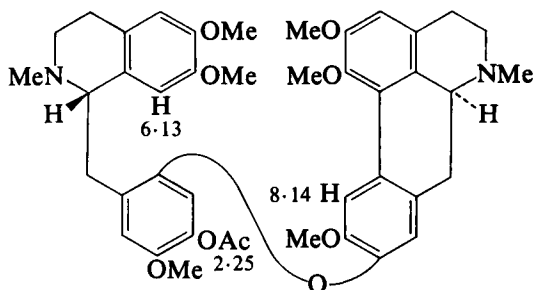
[67]



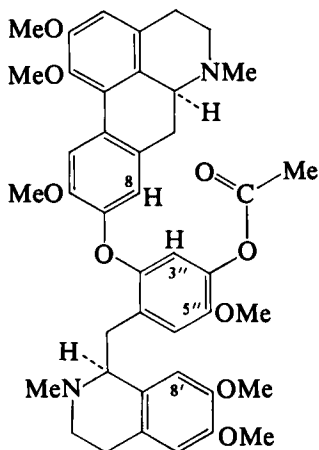
[68]

position of absorption at δ 6.2. In the acetate this hydrogen bonding cannot occur so the 8'-proton is again shielded as in thalicarpine [60] and thalictropine [62]. (54)

A comparison of the spectrum of thalidoxine [65] with that of thalidoxine acetate [69] shows that one of the aryl protons in thalidoxine absorbing at δ either 6.50 or 6.57 is shifted to lower frequency to δ 6.40 in thalidoxine acetate as a result of the presence of the acetoxyl function. This has led to the suggestion of structure [70] for thalidoxine

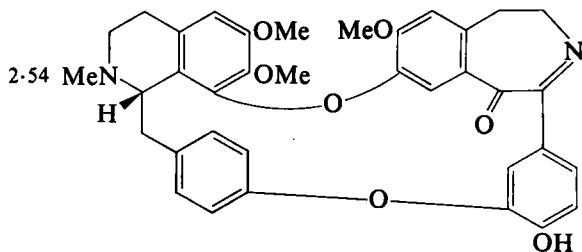
[69] Thalidoxine acetate (in CDCl_3)

NMe	2.57
	2.61
OMe	3.54
	3.67
	3.70
	3.84
	3.85
	3.90
Ar-H	6.40
	6.54
	6.54
	6.60
	6.87



[70]

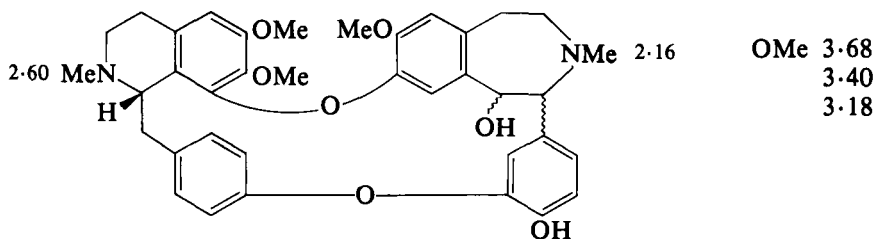
acetate with the acetoxyl group located at C(4'') in a conformation able to shield the 3''-proton. (More usually conversion of phenolic hydroxyl into acetoxyl results in a high frequency shift of the *ortho* aromatic proton.) Accordingly the highest frequency signal at δ 6.77 in the

[71] Stepinonine (in CDCl_3)

OMe	3.96
	3.85
	3.37
Ar-H	7.37-5.60

spectrum of thalidoxine [65] and related thalicarpine type alkaloids may be assigned to the 3''-proton. (52).

The ^1H NMR spectrum of stepinonine is summarized in [71]. In the spectrum of the derived *N*-methyltetrahydrostepinonine [72] the

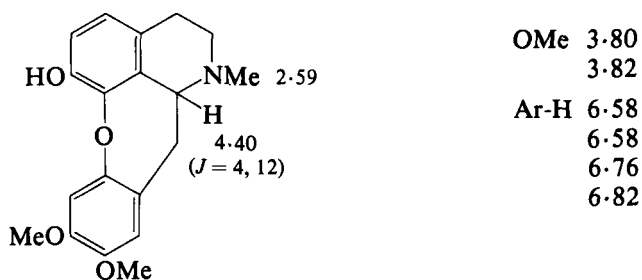


[72] *N*-Methyltetrahydrostepinonine

N-methyl protons in the seven-membered ring absorb (δ 2.16) at abnormally low frequency compared with those in normal tetrahydro-isoquinoline alkaloids. (56)

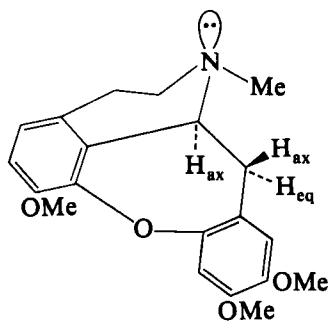
E. Cularines

The NMR spectrum of cularidine summarized in [73] (57) shows typical 12a-angular proton absorption at δ 4.40 and vicinal coupling



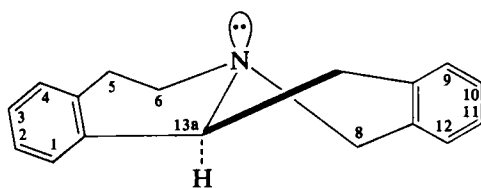
[73] (\pm)-Cularidine (in CDCl_3)

constants of 4 and 12 Hz between the 12a-proton and the adjacent methylene group. Shamma (9) has provided a detailed discussion of the ^1H NMR spectrum of cularine (*O*-methyl derivative of [73]) in terms of the conformation [74]. The high frequency absorption of the 12a-proton is attributed to its proximity to the ring oxygen atom. In addition the plane of the benzene ring approaches bisection of the H–H internuclear axis of the methylene group accounting for the decrease in magnitude of J_{gem} (–16 Hz) over that in methane (–12.4 Hz). (58)

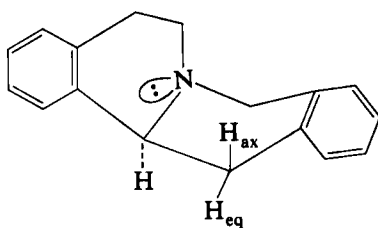


[74]

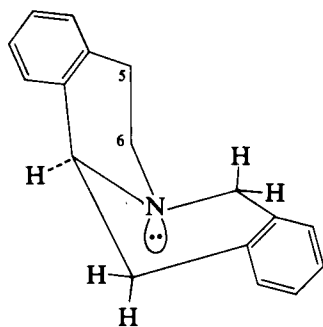
$$\begin{aligned} J_{ax,eq} &= 4 \\ J_{ax,ax} &= 12 \\ J_{gem} &= -16 \end{aligned}$$



[75]



[76]

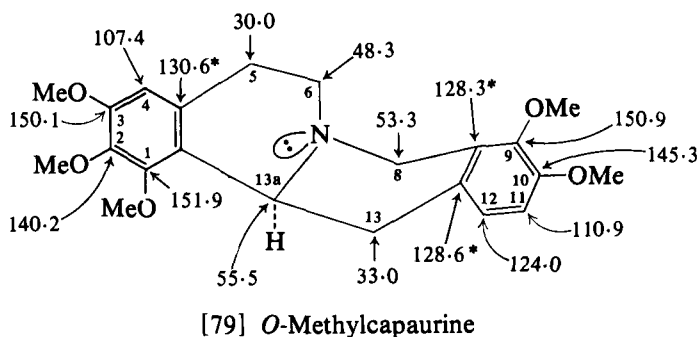
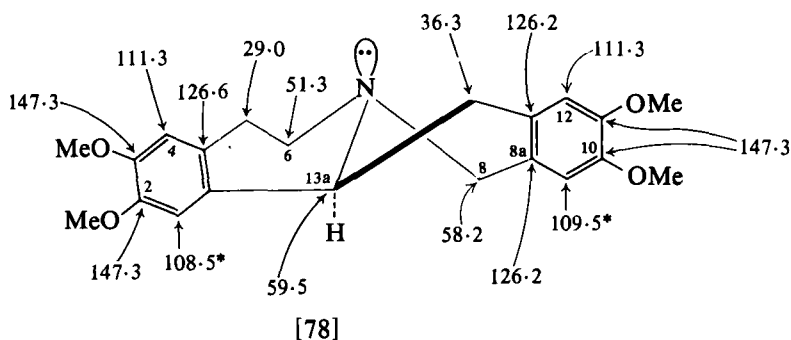


[77]

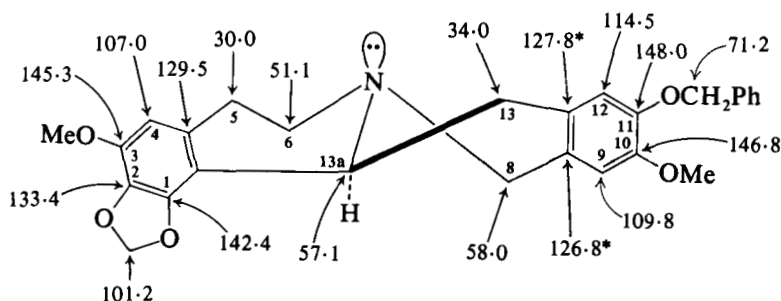
F. Protoberberines and protopines

The tetrahydroprotoberberines may exist in solution as an equilibrium mixture of the *trans*-fused conformation [75] and two *cis*-fused conformations [76] and [77] interconvertible by nitrogen inversion [75] \rightleftharpoons [76] and by ring inversion [76] \rightleftharpoons [77].

The ^{13}C NMR spectra of [78] and [79] existing in *trans*-fused and predominantly *cis*-fused conformation respectively show an increase in shielding of C(6) in the *cis*-fused conformation [79]. The shift of δ ca.



51.3 for C(6) seems diagnostic of *trans*-fused structures and shifts of δ ca. 48.3 for C(6) of *cis*-fused structures in this type of ring B and ring C unsubstituted derivatives. The *cis*-fused conformation [76] is favoured by the presence of the C(1) substituent. It is of interest therefore to note the adoption of the *trans*-fused conformation by the C(1) substituted compound [80] [shown by C(6) absorption at δ 51.1]. (59) In the spectrum of capaurimine (structure as for *O*-methylcapaurine [79] with replacement of the C(1)- and C(10)-methoxyls by phenolic groups) C(6) absorbs at δ 49.3 intermediate between the values observed for [78] and [79] indicating a shift in the equilibrium away from the predominantly

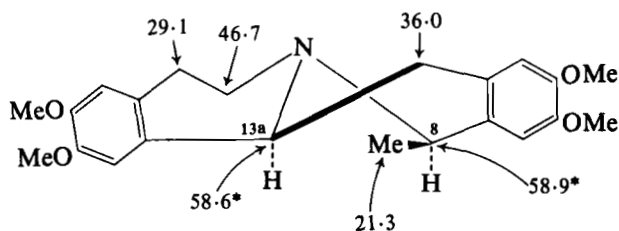
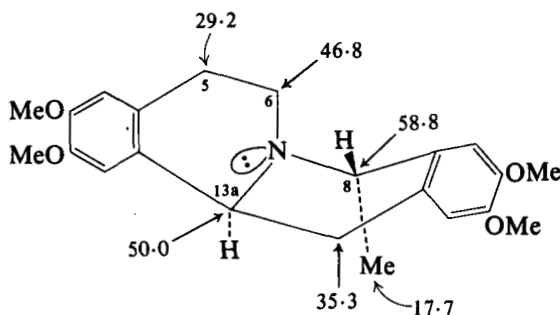


[80]

cis-fused conformation [76] observed for [79] towards the *trans*-fused conformation [75]. (60)

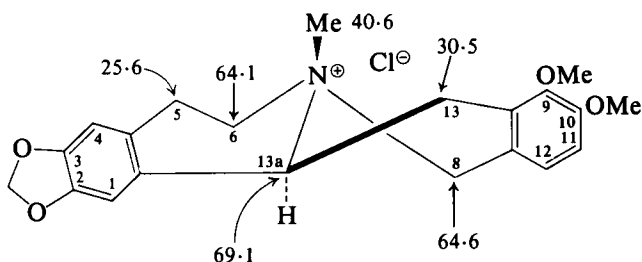
These variations in C(6) shifts are manifestations of the γ -effect (6) in which replacement of a hydrogen atom γ to a ^{13}C nucleus by a methyl group ($\text{C}-\text{C}-\text{C}-\text{H} \rightarrow \text{C}-\text{C}-\text{C}-\text{Me}$) results in a stereochemically dependent increase in shielding (Table III).

On moving to a consideration of the 8-methyl substituted derivatives the importance of the γ -effect is illustrated by the shift in coralydine [81] and *O*-methylcorytenchirine [82]. (61) Here the C(13a) shifts differ markedly in the *trans*-fused [81] from the *cis*-fused [82]. In addition the

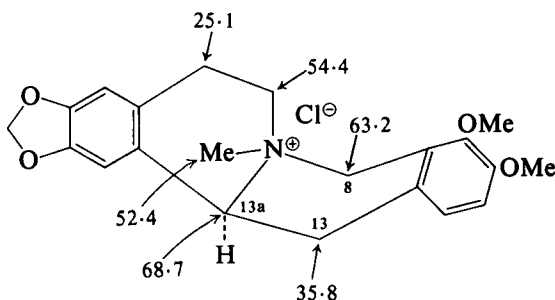
[81] Coralydine (in CDCl_3)[82] *O*-Methylcorytenchirine (in CDCl_3)

presence of the 8-methyl substituent disturbs the pattern of shifts set by the compounds [78]–[80]. Of possible application in structural work is the observation of a low frequency shift of C(8) in 9,10-dimethoxylated compared with 10,11-dimethoxylated tetrahydropprotoberberines. (59)

^{13}C NMR spectroscopy has also been used in the structural analysis of quaternary tetrahydropprotoberberine alkaloids. (62) This is illustrated by the spectra of β - and α -canadine methochlorides [83] and [84] in



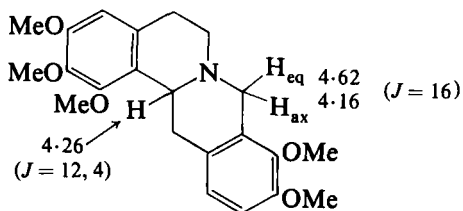
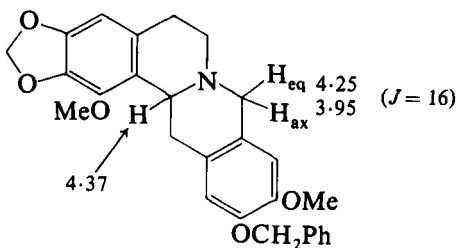
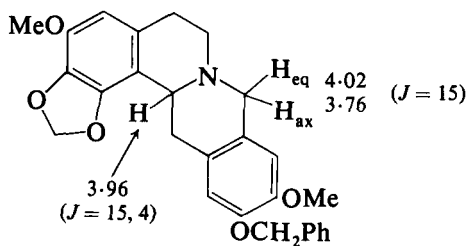
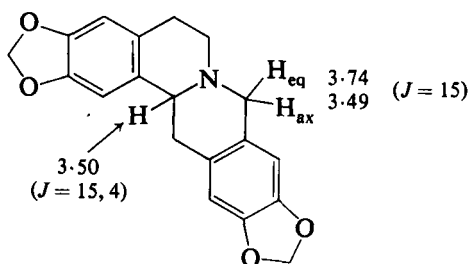
[83] β -Canadine methochloride (in TFA)



[84] α -Canadine methochloride (in TFA)

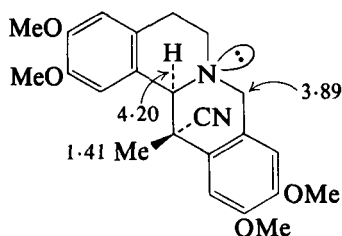
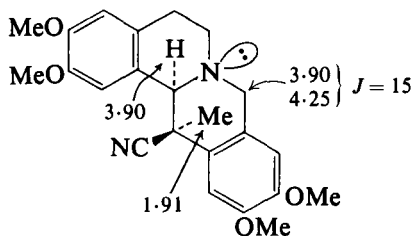
which the NMe and C(13) signals appear at higher frequency in the *cis*-fused methochloride than in the *trans*-fused methochloride. In addition, the C(6) nucleus resonates at lower frequency in the *cis*-fused than in the *trans*-fused methochloride.

Before the advent of ^{13}C NMR spectroscopy the conformational analysis of the tetrahydropprotoberberines rested in part on the chemical shift of the angular 13a-proton (to low frequency of δ 3.8 in *trans*-fused derivatives and to high frequency of δ 3.8 in *cis*-fused derivatives). (63) In spectra run in CDCl_3 solution the 13a-proton signals may be hidden by those arising from methoxyl group protons but have been found to be visible in spectra recorded in deuteriotoluene solutions. Thus [85] and [86] are shown to adopt the *cis*-fused conformation and [87] and [88]

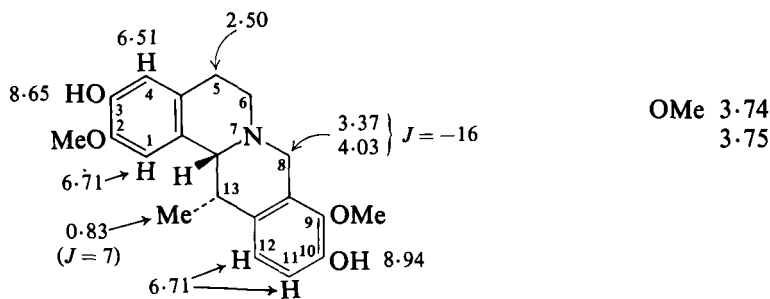
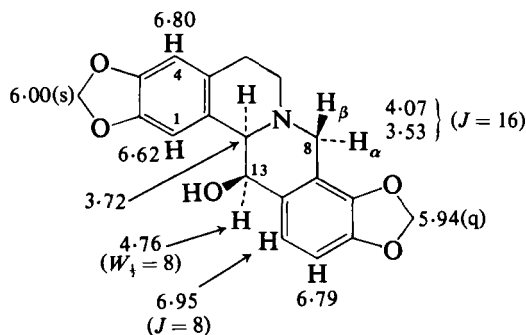
[85] *O*-Methylcapaurine (in toluene- d_8)[86] (in toluene- d_8)[87] (in toluene- d_8)[88] (in toluene- d_8)

the *trans*-fused conformation. The deshielding of the 13a-proton in [87] results from the presence of the C(1) oxygen function. (60) An apparent exception to the angular proton shift–stereochemical correlation in the

case of [89] and [90] (both *trans*-fused but with angular proton shifts of δ 4.20 and 3.90) is due to the anisotropy of the cyano group. (64)

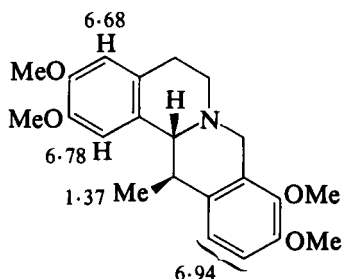
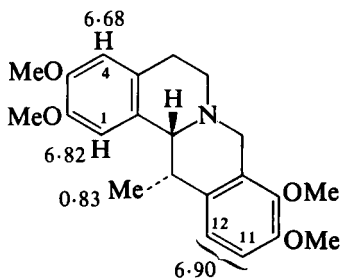
[89] (in CDCl_3)[90] (in CDCl_3)

In the spectra of the tetrahydropyroberberines the chemical shift difference between the C(8) methylene protons is greater in *trans*-fused than in *cis*-fused conformations but in both cases is enhanced by the presence of a C(9) substituent. Both effects are illustrated by the spectra of [85]–[88], (60) of corydaldizine [91], (65) and of 13β -hydroxystylophine [92]. (66) [The spectrum of the acetate of 13β -

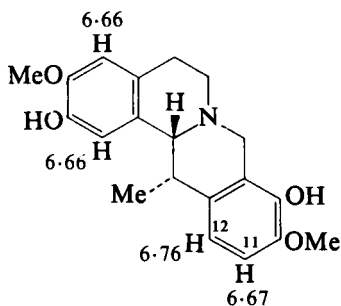
[91] Corydaldizine (in DMSO-d_6)[92] 13β -Hydroxystylophine (in CDCl_3)

hydroxystylopine shows abnormally low frequency absorption of the OCOMe protons as a result of shielding by the D ring. (66)]

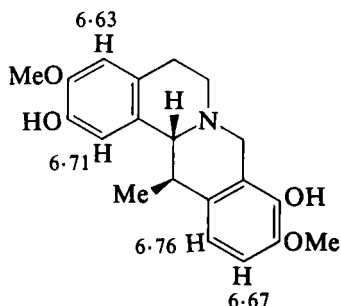
The chemical shifts of the aromatic protons in 2,3,9,10-tetra-substituted tetrahydropprotoberberines of the type [93]–[96] show



[93] (\pm)-Corydaline (in DMSO-d_6) [94] (\pm)-*meso*-Corydaline (in DMSO-d_6)



[95] (in DMSO-d_6)

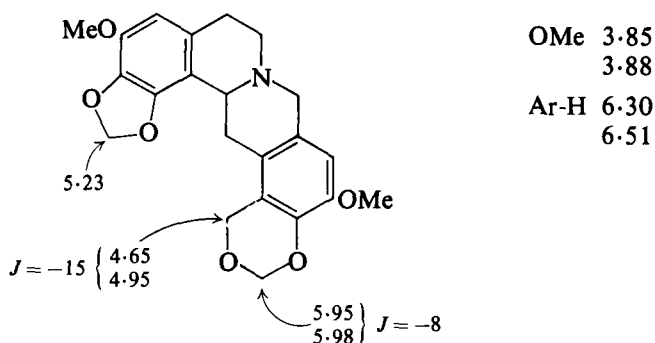


[96] (in DMSO-d_6)

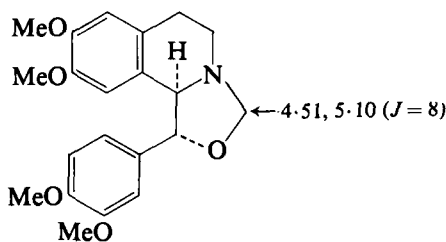
variations with change in substituent. (67) These four compounds, together with corydalidine [91], show the lower frequency absorption of the 13-methyl protons in *trans*-fused tetrahydropprotoberberines (δ ca. 0.83) than in the *cis*-fused analogues (δ ca. 1.35–1.37).

The spectrum of corydalyne [81] shows the 8-methyl protons to absorb to higher frequency (δ 1.53) than those in *O*-methylcorytencherine (δ 1.40) [82]. The corresponding 8-proton signals appear at δ ca. 3.7 for [81] and at δ 4.06 for [82]. (68)

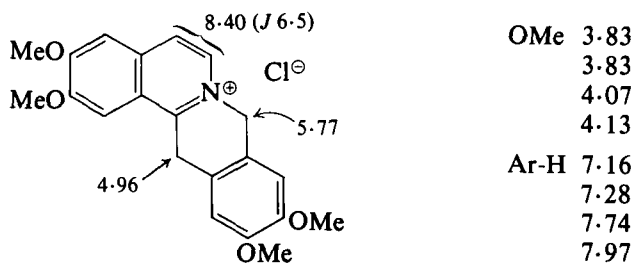
In the spectrum of the positional isomer [97] of orientolidine (69) the singlet absorption at δ 5.23 should be assigned to the OCH_2O protons in the dioxolan ring and the AB quartet at δ 5.95, 5.98 ($J = -8$ Hz) to the OCH_2O protons in the 1,3-dioxan ring in accordance with the known variation in the geminal coupling constants in dioxymethylene fragments with the incorporating ring size. (58) A related geminal

[97] (in CDCl_3)

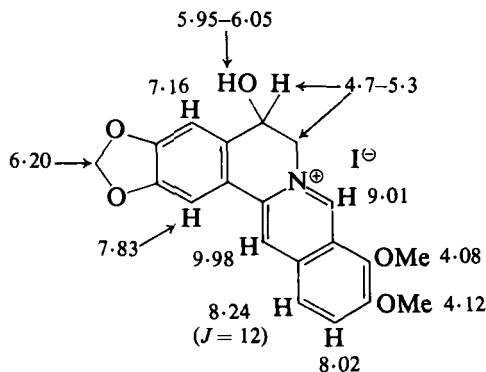
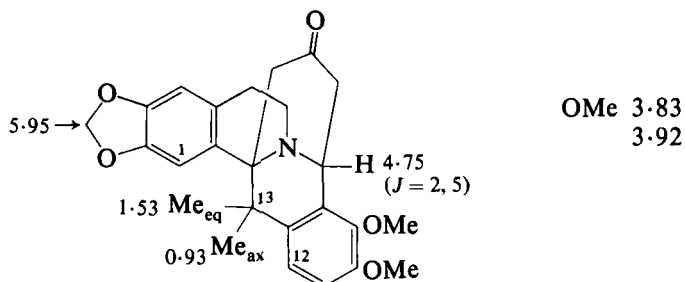
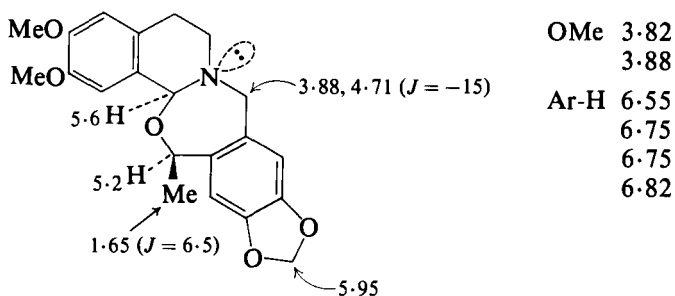
coupling constant problem is provided by [98] obtained during a berberine synthesis. Two AB quartets were observed (δ 4.51, 5.10, $J = 8$ Hz; δ 4.68, 4.81, $J = 12$ Hz) in its spectrum. The published assignments (70) should be reversed since the J_{gem} of 8 Hz is in accord with the expected value for NCH_2O protons in a *cis*-fused conformation of [98]. (71)

[98] (in CDCl_3)

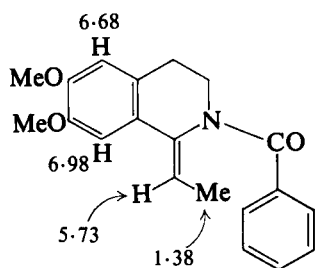
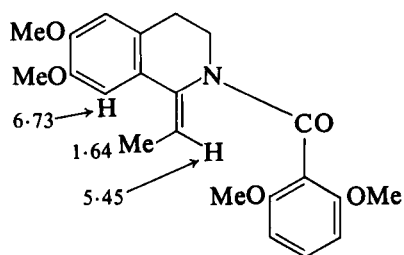
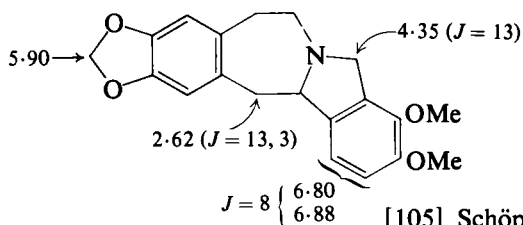
Chemical shift data on the protoberberinium salts [99] (72) and [100] (73) are as recorded in the structures. The NMR spectra of the alkaloid derivatives [101] (74) and [102] (75) have been recorded. In the

[99] (in DMSO-d_6)

T. A. CRABB

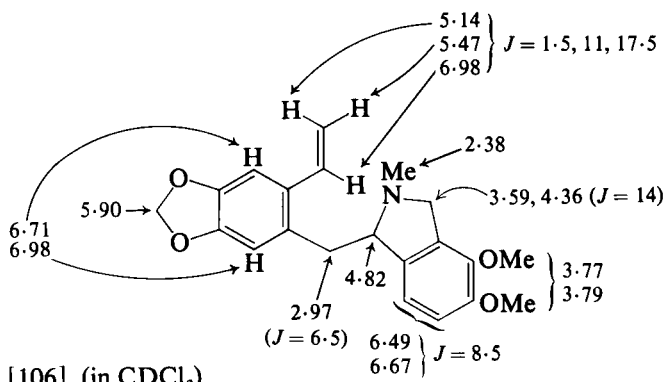
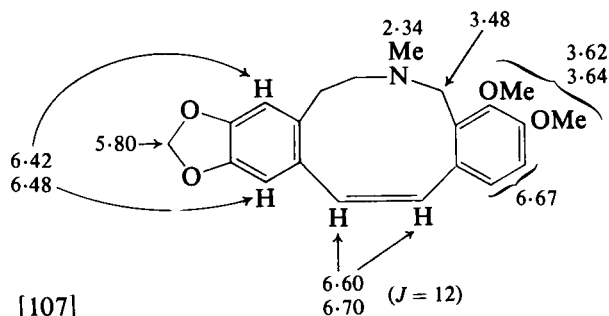
[100] Berberastine iodide (in DMSO- d_6)[101] (in CDCl₃)[102] (in CDCl₃)

spectrum of [101] the shifts of the axial and equatorial methyl group protons at C(13) have been determined by NOE measurements. In connection with a synthesis of (\pm)-cavidine the configurations of the enamides [103] and [104] (76) were determined by NOE measurements. As expected the shifts of the ethylidene groupings are diagnostic of the stereochemistry.

[103] (in CDCl_3)[104] (in CDCl_3)

OMe 3.84
3.86

Ar-H 6.65
6.74

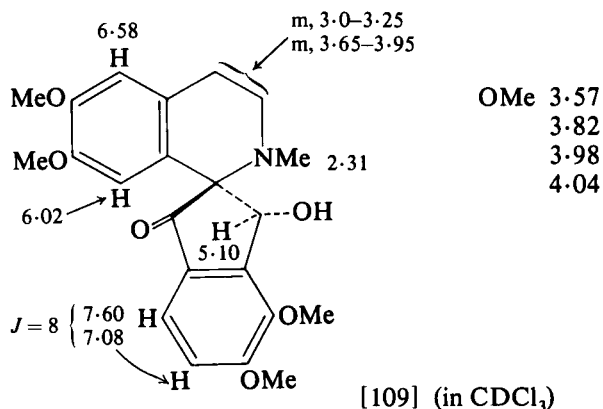
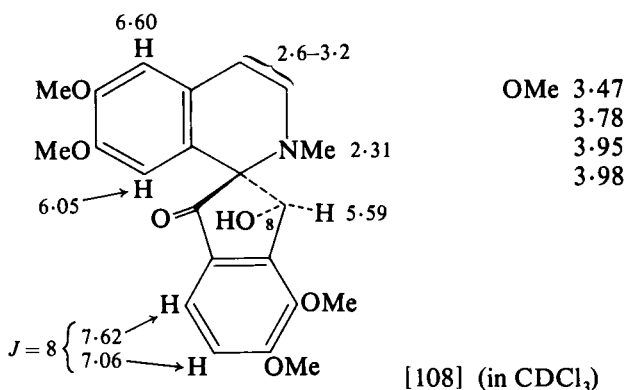
[105] Schöpf's base-VI (in CDCl_3)[106] (in CDCl_3)

[107]

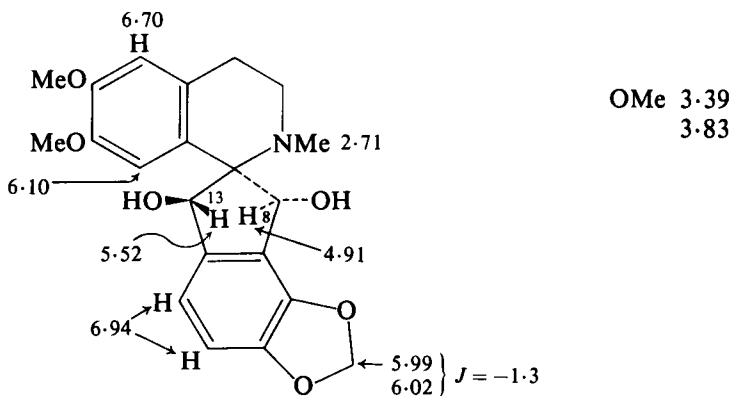
The NMR spectra of Schöpf's base-VI [105] (77) and some of its degradation products [106] and [107] (78) have been recorded.

G. Spirobenzylisoquinolines

In the ^1H NMR spectra of spirobenzylisoquinoline alkaloids substituted at C(8) the chemical shift of the 8-proton is diagnostic of its stereochemistry with respect to the nitrogen atom. This is exemplified by the spectra of the diastereoisomeric pair of compounds [108] and [109]

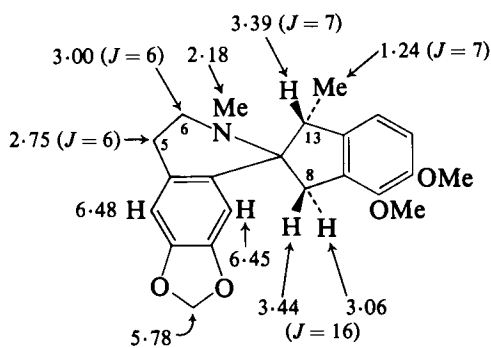


(79) and of yenusomine [110] (68) which show the high frequency absorption (δ 5.59) of the 8-proton in [108] (*syn* to the nitrogen atom) relative to that (δ 5.10) in [109] and in yenusomine [110] (*anti* to the nitrogen atom). Similar effects for other spirobenzylisoquinolines have been reported. (80) In yenusomine the protons of one of the methoxyl groups are unusually shielded (δ 3.39).

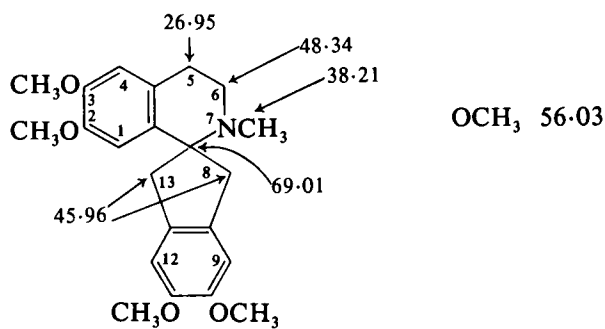


[110] Yenhusomine (in CDCl_3)

In the spectrum of 2,3-methylenedioxy-9,10-dimethoxy-13-methylchotensane [111] the 13-methyl protons absorb (*syn* to the nitrogen



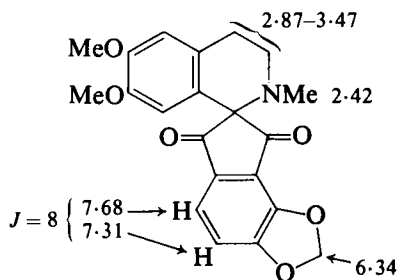
[111] (in CDCl_3)



[112] (in CDCl_3)

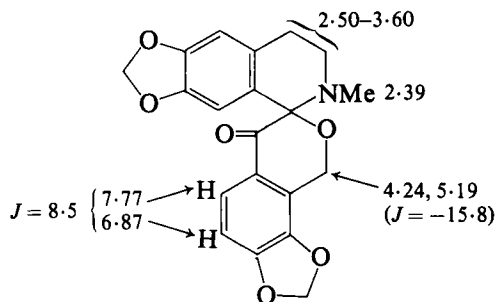
atom) at δ 1.24. In C(13) epimeric structures the 13-methyl protons absorb at *ca.* δ 0.95. (81, 82)

NMR parameters of synthetic spirobenzylisoquinolines are shown in [112] (83) and [113]. (84) NMR data on corydalispirone (85) are recorded in [114].



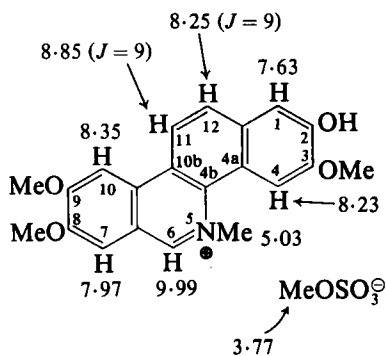
OMe 3.55
3.90
Ar-H 6.00
6.70

[113] (in CDCl_3)



OCH_2O 5.85
6.08
Ar-H 6.52
6.60

[114] Corydalispirone (in CDCl_3)



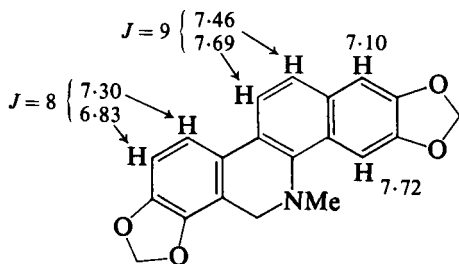
OMe 4.08
4.15
4.26

[115] Fagaronine methosulphate (in DMSO-d_6)

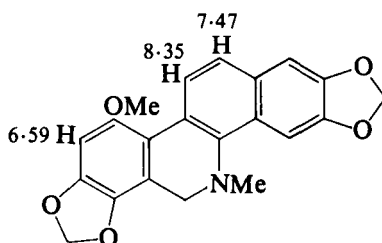
H. Benzophenanthridines

The ^1H NMR spectrum of fagaronine methosulphate is shown in [115]. (86) Partly on the basis of NMR evidence (cf. dihydrosanguinarine [116]) the structure [117] has now been suggested (87) for dihydrochelirubine (dihydroboconine). (1)

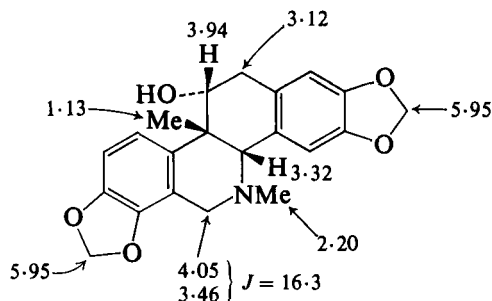
The ^1H NMR spectra of derivatives of corynoline [118] have been described. The spectrum of the synthetic analogue of [118] shown in [119] closely resembles that of [118]. (88) The chemical shift of the



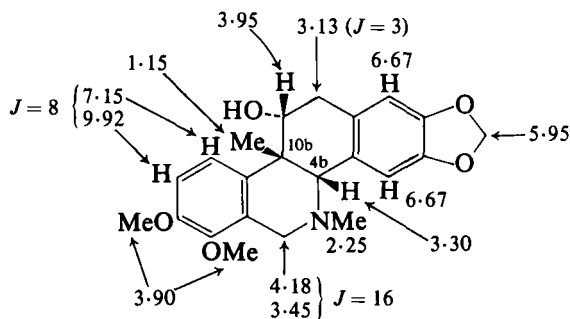
[116] Dihydrosanguinarine



[117] Dihydrochelirubine

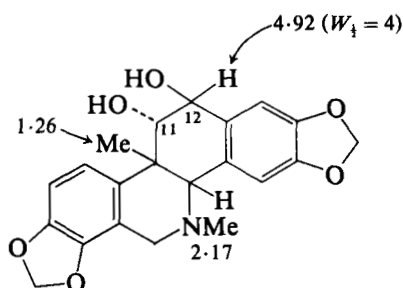


[118] Corynoline (in CDCl_3)



[119] (in CDCl_3)

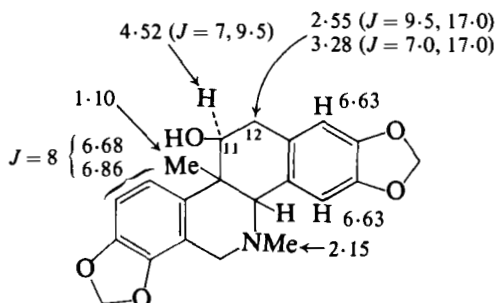
multiplet at δ 4.92 (12-H) in the spectrum of 12-hydroxycorynoline [120] is to high frequency of that (δ 3.12) in corynoline [118] indicating



OCH ₂ O	5.96
	5.98
Ar-H	6.65-7.10

[120] 12-Hydroxycorynoline

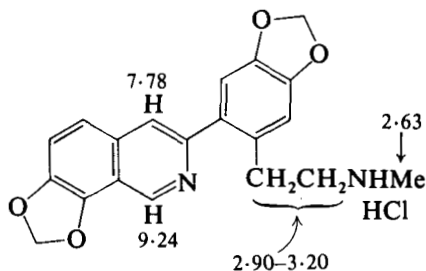
the 11,12-diol. (89) Analysis of the 11- and 12-proton signals in the spectrum of 11-epicorynoline [121] established the stereochemistry



OCH ₂ O	5.92
	5.95

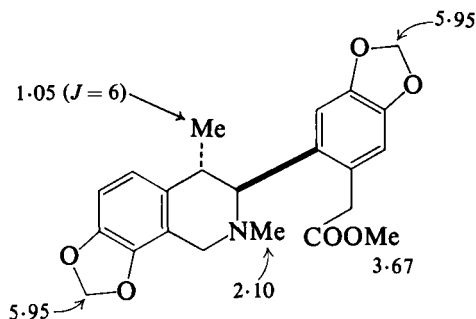
[121] 11-Epicorynoline

shown (89) and some analysis of the spectrum of 14-epicorynoline has been given. (90) Spectra of corydamine hydrochloride (91) and of corydalic acid methyl ester (92) are recorded in [122] and [123] respectively.



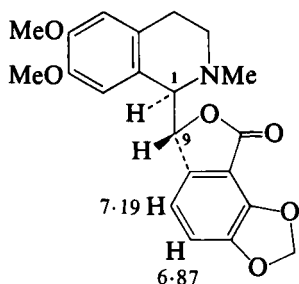
OCH ₂ O	6.10
	6.38
Ar-H	6.77
	7.00
	7.49
	7.63
	$J = 9$

[122] Corydamine hydrochloride (in D₂O)

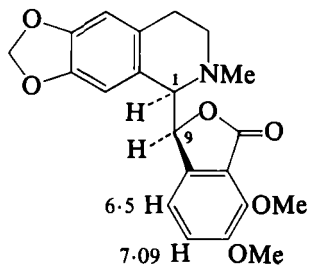
[123] Corydalic acid methyl ester (in CDCl_3)

I. Phthalideisoquinolines

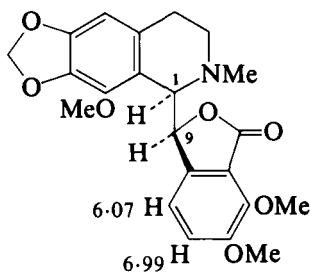
The vicinal coupling $J_{1,9}$ of 3.4–4.3 Hz in the spectra of adlumine [124], hydrastine [125], and narcotine [126] implies a *syn*-clinal relationship between C(1)–H and C(9)–H. Considering conformation consonant with this, together with the chemical shifts of the aromatic protons which are related to the mutual orientation of the two aromatic rings, it is possible to assign the *threo*-configuration to adlumine and the



[124] Adlumine

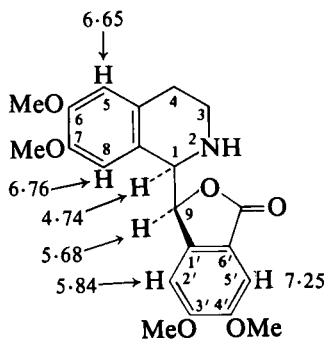


[125] Hydrastine

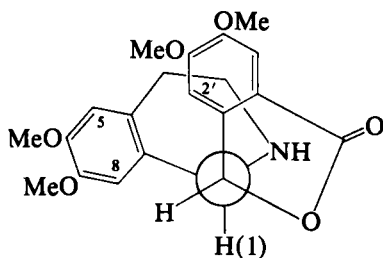


[126] Narcotine

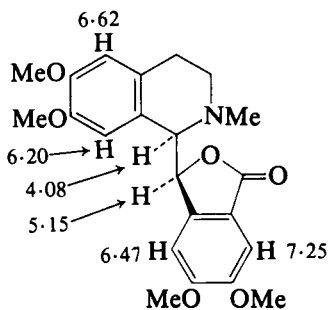
erythro-configuration to hydrastine and narcotine. (93) This has been taken up again (94) with special reference to the four compounds [127]–[130]. As for the tetrahydrobenzylisoquinolines, the two nor-compounds [127] and [129] will adopt conformations with the phthalide moiety near the N/H grouping. In the corresponding *N*-methyl compounds [128] and [130] the steric effect involving the *N*-methyl forces the phthalide



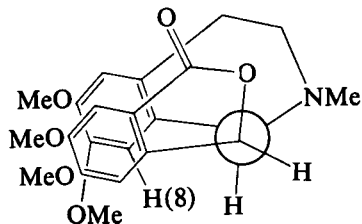
[127]



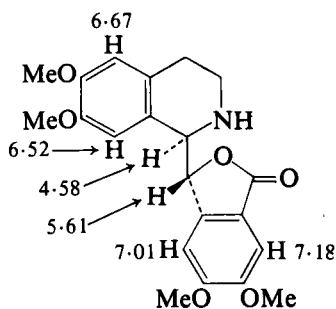
[127A]



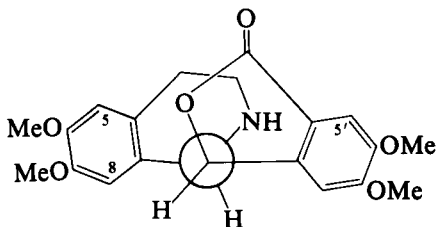
[128]



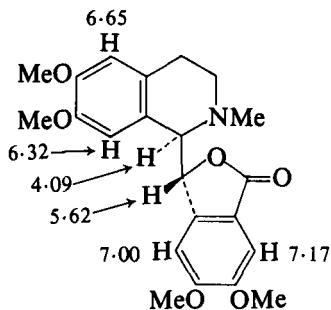
[128A]



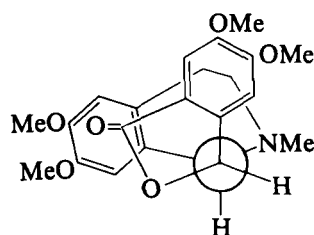
[129]



[129A]



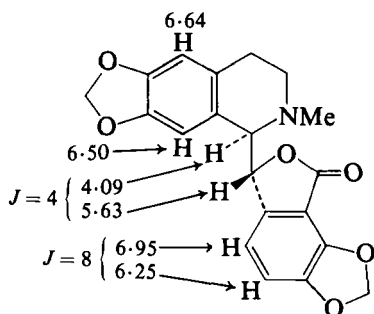
[130]



[130A]

moiety away from the nitrogen towards ring A. These conformational changes are reflected in the chemical shifts of the aromatic protons. In [127]–[130] the most deshielded proton is expected to be that *cis* to the lactone carbonyl, i.e. the 5'-proton and this absorbs at δ 7.17–7.25. In all four compounds one of the aromatic protons absorbs between δ 6.62 and 6.67, and because of the lack of variation in chemical shift with structure this is assigned to the 5-proton (remote from the centre of stereochemical changes). The other shifts are consonant with the conformational structures [127A]–[130A]. In [127] ([127A]) the 2'-proton and the 3'-methoxyl protons are to low frequency as a result of shielding by the A ring. In [128] ([128A]) the 8-proton is to low frequency as a result of shielding by the D ring. The 8-proton in [130] ([130A]) is shielded by the lactone grouping which is not operative in [129] ([129A]). Narcotine [126] adopts a conformation of type [130A] in order to minimize interactions involving the 8-methoxyl group.

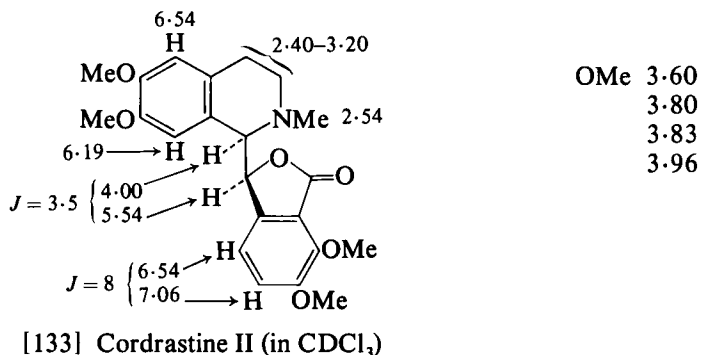
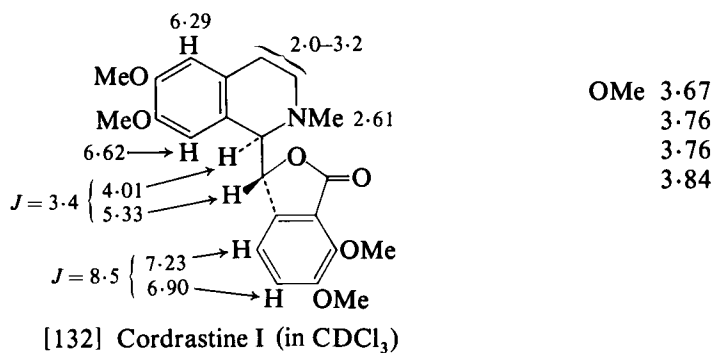
These results now enable signal assignments to be made in the spectrum of the *erythro* alkaloid bicuculline [131]. (95)



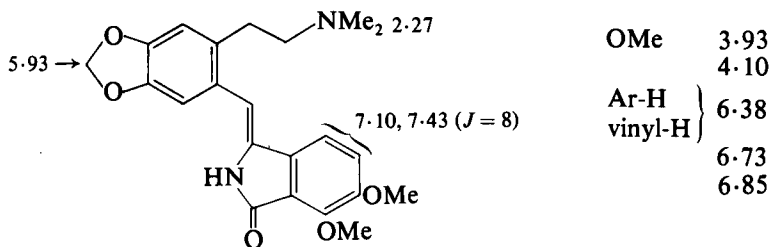
OCH₂O 5.97
6.20

[131] Bicuculline (in CDCl₃)

The ^1H NMR spectra of two other phthalideisoquinolines—cordrastine I [132] and cordrastine II [133] (95)—have been

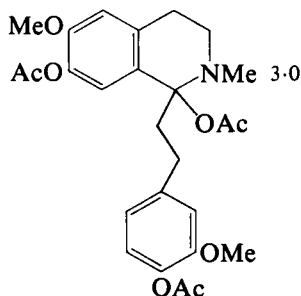


discussed in some detail. (96) Irradiation of the δ 4.01 (1-H) signal in [132] sharpens the aromatic singlet at δ 6.62, and irradiation at δ 5.33 (9-H) sharpens the high frequency half (δ 7.23) of the AB quartet. Experiments such as these permit assignment of the aromatic proton signals in [132] and [133] to be made. Couplings, e.g. between the 9- and 2'-protons of *ca.* 0.8 Hz had been noted previously. (93) The ^1H NMR spectrum of hydrastine imide is summarized in [134]. (97)



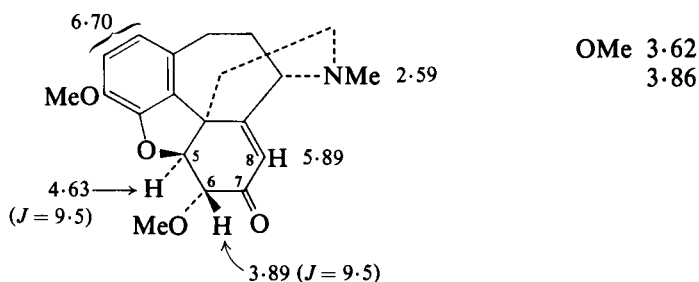
J. Other isoquinoline alkaloids: phenethylisoquinolines, emetine, pavines, tetrahydrodibenzopyrrocolines, and azafluoranthenes

Further details concerning the ^1H NMR spectra of kreysigine, floramultine, and multifloramine (1) have been published. (98) The high frequency absorption of the *N*-methyl protons (δ 3.0) in [135], isolated



[135] (in CDCl_3)

by oxidation of homo-orientaline followed by acetylation, was in part used as evidence for location of an acetoxyl function at C(1) [cf. *N*-methyl δ 2.5 in 4-acetoxy-2-methyltetrahydroisoquinoline (99)]. (100) The NMR spectrum of the kreysigine type compound [136] has been described. (101)

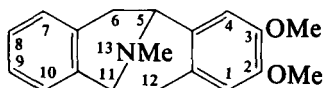
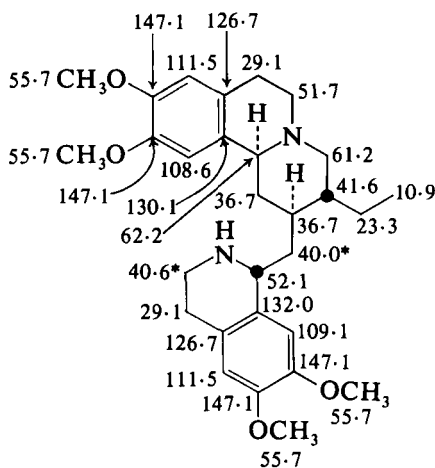
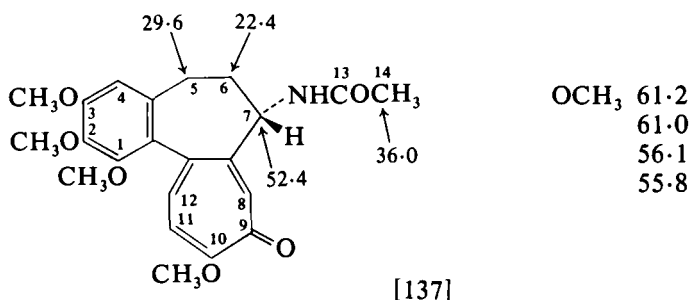


[136] (in CDCl_3)

Partial ^{13}C NMR assignments on colchicine are shown in [137]. (102)

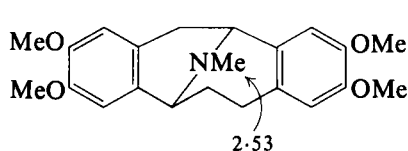
The benzylic methylene carbon nuclei in the ^{13}C NMR spectrum of emetine [138] absorb (δ 29.1) at much higher frequency than in related carbolines (see ochrolifuanine—Section XII.K). (103)

The ^1H NMR spectra of a pavinane derivative (104) and of a homopavinane, homoargemonine, (105) are summarized in [139] and [140].



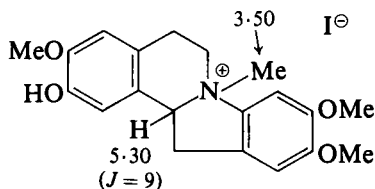
NMe	2.56
OMe	3.79
	3.87
Ar-H	7.26–7.00 (4H)
	6.67
	6.49
Ring CH + CH ₂	2.92–2.47 (m, 2H)
	3.69–3.32 (m, 2H)
	4.07 (d, 1H)
	4.13 (d, 1H)

The 12a-proton in the ¹H NMR spectrum of cryptaustoline [141] absorbs as a triplet at δ 5.30 with $J = 9$ Hz. (106) The NMR spectra of the azafluoranthene alkaloids imeluteine, rufescine, (107) and nor-



OMe	3.85
	3.85
	3.90
	3.90
Ring CH + CH ₂	4.23–2.37 (8H)
Ar-H	6.67–6.5

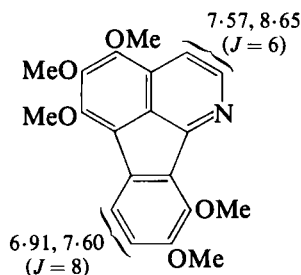
[140] (+)-Homoargemonine (in CDCl_3)



OMe	3.78
	3.84
Ar-H	6.73
	6.81
	7.07
	7.55

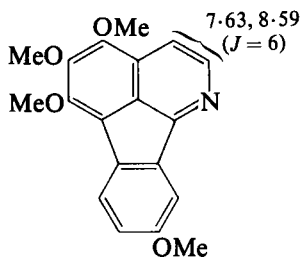
[141] Cryptaustoline (in DMSO- d_6)

rufescine (108) are summarized in [142], [143], and [144] respectively. The tropoloisoquinoline structure [145] has been assigned to imerubrine. (108)



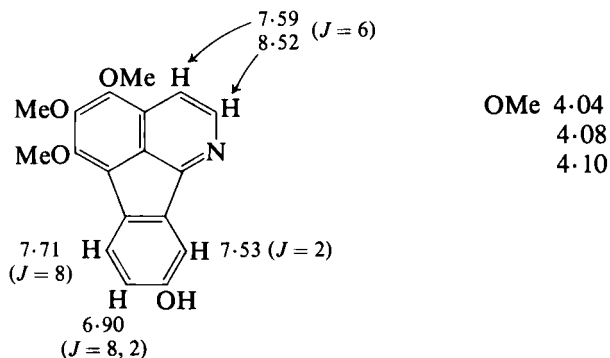
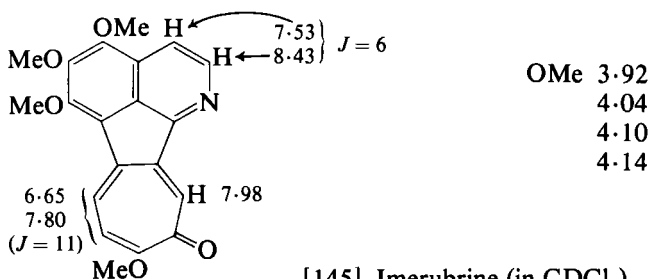
OMe 3.94
4.02
4.08
4.10
4.17

[142] Imeluteine (in CDCl_3)



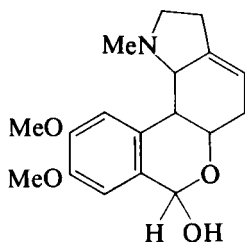
Ome 3.94
4.05
4.11
4.13
Ar-H 7.82, 7.68, 6.96
(ABC system with $J_{AC} = 8$, $J_{BC} = 2$)

[143] Rufescine (in CDCl_3)

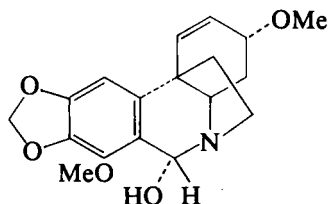
[144] Nor-rufescine (in CDCl_3 + DMSO-d_6)[145] Imerubrine (in CDCl_3)

III. AMARYLLIDACEAE ALKALOIDS

The presence of the hemiacetal moiety in lycorenine [146] and of the carbinolamine moiety in 6-hydroxybuphanidrine [147] is shown by the chemical shifts of the benzylic protons (δ 6.04 in [146], δ 5.31 in [147]). (109)

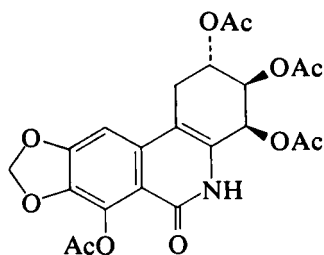


[146] Lycorenine

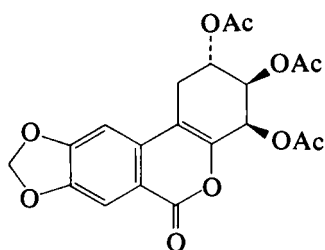


[147] 6-Hydroxybuphanidrine

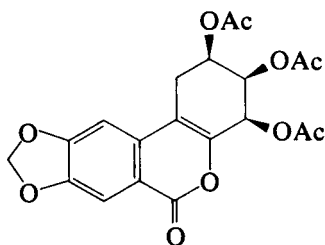
The ^1H NMR of isonarciclasine tetra-acetate [148] shows multiplets at δ 2.8 and 3.2 for the methylene group protons as does the model compound [149] of known stereochemistry. The all-*cis*-acetate [150] does not show this type of absorption. (110)



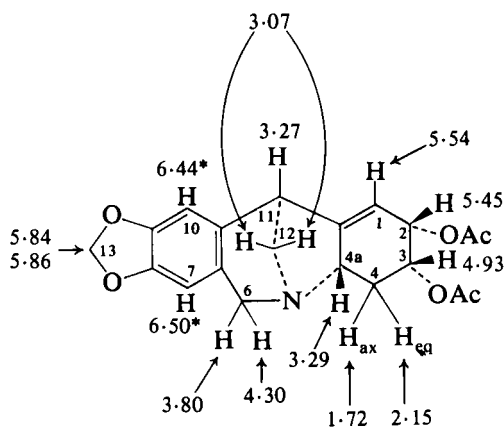
[148]



[149]



[150]



OAc 2.08
2.00

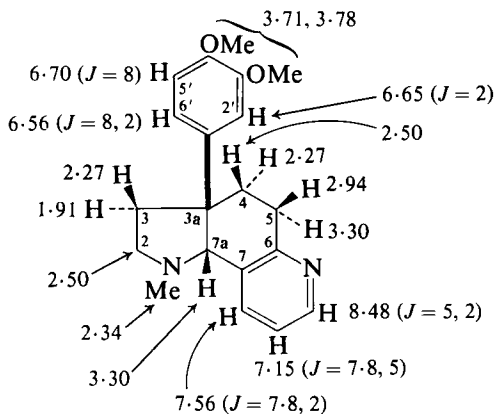
[151] *O,O'*-Diacetylbrunsvigine (in CDCl_3)

$$\begin{aligned} J_{1,2} &= 3.8 \\ J_{1,4a} &= 2.0 \\ J_{2,3} &= 4.3 \\ J_{3,4eq} &= 3.3 \\ J_{3,4ax} &= 12.2 \\ J_{4ax,4eq} &= -10.8 \end{aligned}$$

$$\begin{aligned} J_{4a,4eq} &= 5.3 \\ J_{4a,4ax} &= 11.8 \\ J_{6,6'} &= -16.6 \\ J_{11,12} &\leq 3^* \quad (\text{in } \text{C}_6\text{D}_6) \\ J_{11,12'} &\leq 2^* \quad (\text{in } \text{C}_6\text{D}_6) \\ J_{12,12'} &= -11.5 \quad (\text{in } \text{C}_6\text{D}_6) \end{aligned}$$

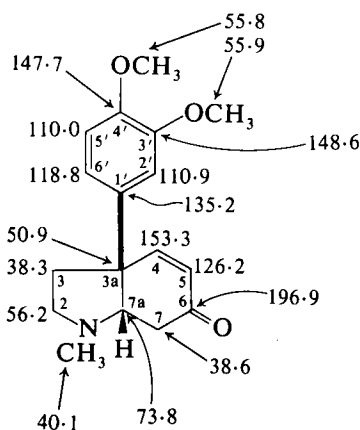
A complete analysis of the ^1H NMR spectrum of *O,O'*-diacetylbrunsvigine [151] has been made. (111)

The ^1H NMR spectrum of sceletium alkaloid A_4 , a tetracyclic system related to the octahydroindole members of the mesembrine alkaloids, is summarized in [152]. The close similarity of the ^{13}C NMR spectra of

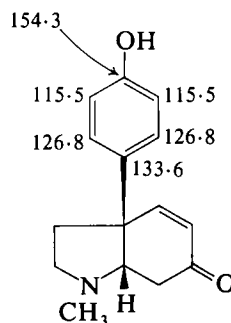


[152] Sceletium alkaloid A_4

mesembrenone [153] and of sceletenone [154] permitted the structural assignment shown. (112) The aromatic carbon shifts are in accord with calculated values based on Table I. (4)



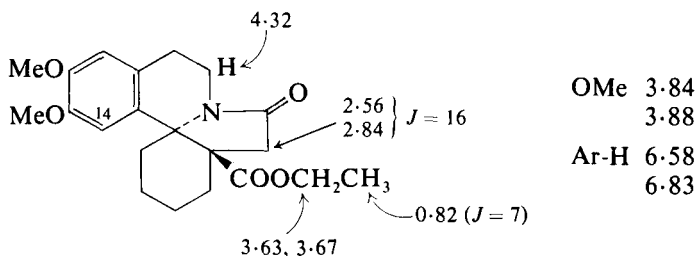
[153] Mesembrenone (in CDCl_3)



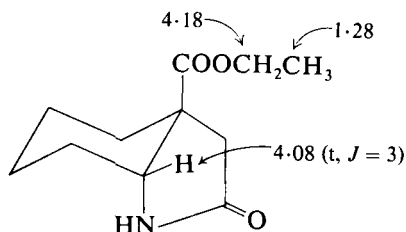
[154] Sceletenone

IV. ERYTHRINA, DIBENZ[*df*]AZONINE, AND CEPHALOTAXINE ALKALOIDS

In the NMR spectrum of the *cis*-fused erythrinanone [155] the chemical shifts of the ethyl group protons are to low frequency of those in model compounds [156] as a result of the *cis*-relationship between the

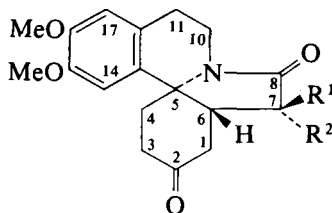


[155] (in CDCl_3)



[156]

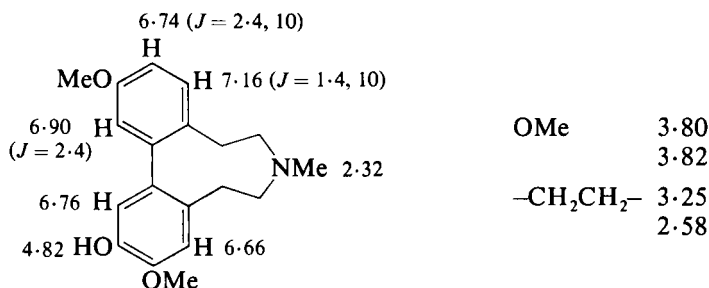
ester and the aromatic ring. (113) *cis*-Fusion between the B and C rings in [155] is also indicated by the low frequency shift of the 14-proton. (1) The 7-proton chemical shift in the spectra of erythrinan-diones is diagnostic of stereochemistry, e.g. [157] (δ 5.04) and [158] (δ 5.52) (CDCl_3). (114) ^1H NMR data on other erythrina alkaloids are available. (115, 116)



[157] $\text{R}^1 = \text{OAc}$, $\text{R}^2 = \text{H}$

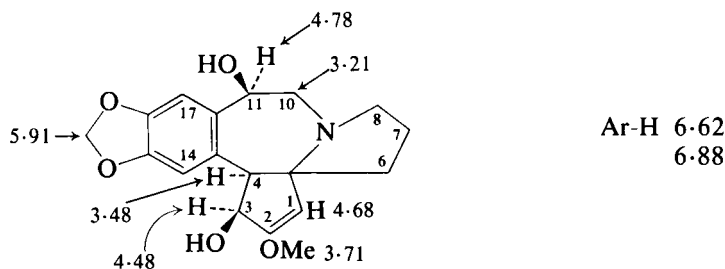
[158] $\text{R}^1 = \text{H}$, $\text{R}^2 = \text{OAc}$

In the spectrum of laurifinine [159] the broadened singlet at δ 6.66 was assigned to the 4-proton since this was sharpened by irradiation of the benzylic proton at *ca.* δ 3.25. (117)

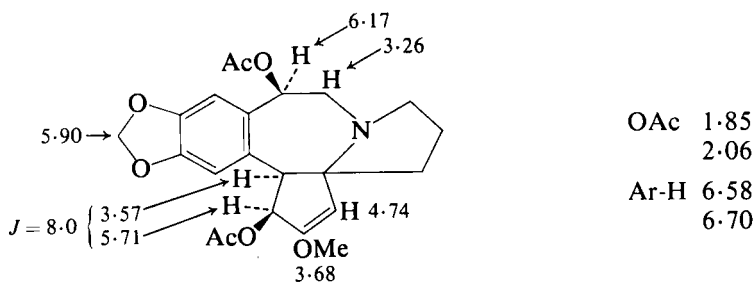


[159] Laurifinine (in CDCl_3)

The NMR spectrum of 11-hydroxycephalotaxine is summarized in [160]. (118) The vinyl proton signal (δ 4.74) in the spectrum of the derived 3,11-*O,O*-diacetylhydroxycephalotaxine [161] is to high fre-

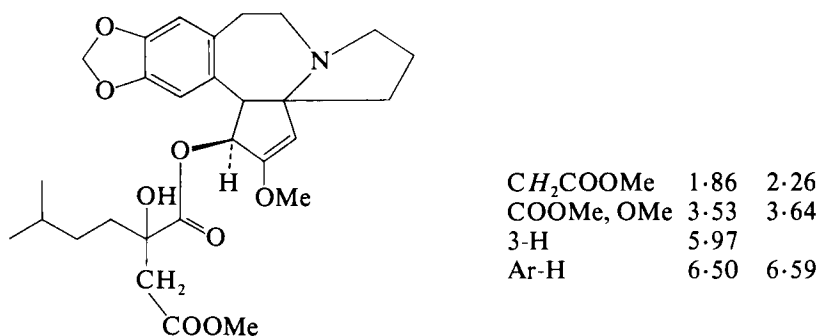
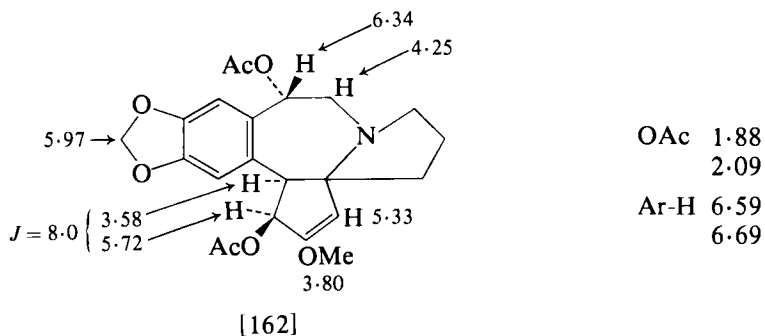


[160] 11-Hydroxycephalotaxine (in CDCl_3)



[161] 3,11-*O,O*-Diacetylhydroxycephalotaxine

quency of that in the 11-epimeric structure [162]. The spectrum of deoxyharringtonine [163; stereochemistry of side chain undefined]

[163] Deoxyharringtonine (in CDCl₃)

differs most from that of an isomer containing an epimeric side chain in the absorption for the CH₂COOMe protons (δ 2.46, 2.66 in side chain epimer of [163]). (119)

V. MORPHINE ALKALOIDS

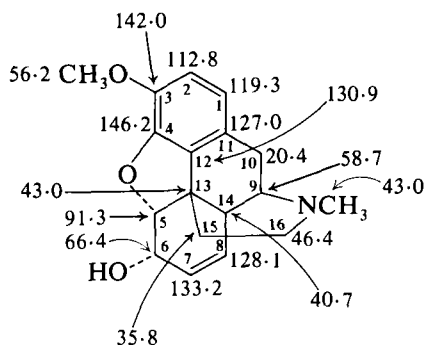
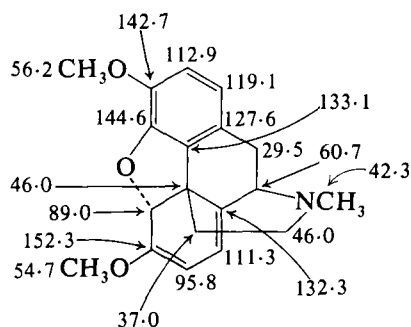
A. Alkaloids containing the 4,5-oxide bridge

1. Morphine type alkaloids

The quaternary ¹³C NMR signals in codeine [164] can be assigned from spin-lattice relaxation time (*T*₁) measurements. Values of *T*₁ for large molecules in which dipole-dipole relaxation dominates may be described by the equation

$$1/T_1 = (\mu_0/4\pi)^2 \hbar^2 \gamma_C^2 \gamma_H^2 \sum_i r_{CH_i}^{-6} \tau_C$$

which implies a proportionality between 1/*T*₁ and the inverse sixth power of the internuclear distance between the ¹³C atom and the proton

[164] Codeine (in CDCl_3)[165] Thebaine (in CDCl_3)

i. To an approximation this means that the rate of relaxation is proportional to the number of α CH protons. (120) Thus in codeine C(12) and C(4) which have no α CH protons exhibit the longest relaxation time and C(13) with four α CH protons exhibits the shortest relaxation time (Table IV). (121)

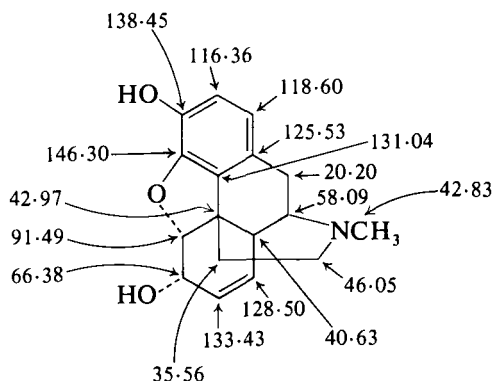
TABLE IV

^{13}C chemical shifts (CDCl_3) and spin-lattice relaxation times for codeine [164] (121)

^{13}C nucleus	$\delta(^{13}\text{C})$	T_1 (s)	No. of α CH protons
C(11)	127.04	1.82	3
C(13)	42.89	1.53	4
C(12)	130.91	5.1	0
C(4)	146.60	8.9	0
C(3)	141.73	5.2	1

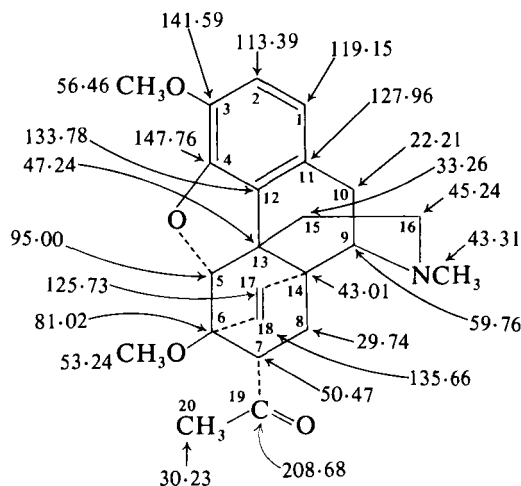
The ^{13}C shifts in codeine [164], thebaine [165], (122) and morphine [166] (123) are displayed on the structures. Quaternary carbon signals were assigned by relative signal intensity ratios following Wehrli. (121) For morphine these were found to be *ca.* 3:2:2:1 for C(11), C(12), C(3), and C(4) respectively. (122)

The change from morphine to 3,6-diacetylmorphine is accompanied by a low frequency shift of C(7) (δ 133.43 to 129.24) due to the γ -effect of the acetoxyl group. C(10) appears at unusually low frequency [γ -effects from C(8), C(16), and *N*-methyl] in a number of morphine alkaloids with the exception of thebaine (cf. δ 20.20 in morphine, δ 29.5 in thebaine) in which the *gauche* relationship between C(10) and C(8),

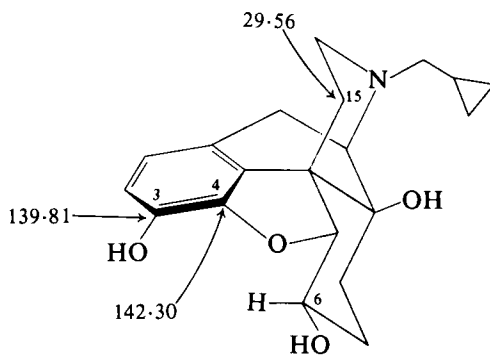
[166] Morphinine (in DMSO- d_6)

present in morphine, is lost as a result of the differences in geometry brought about by the presence of the ring c diene system. (123)

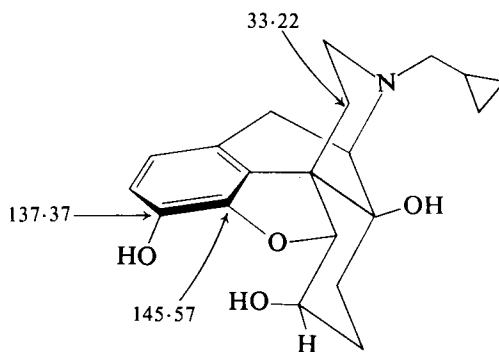
^{13}C NMR spectral characteristics of 6,14-*endo*-ethenotetrahydrothebaines are exemplified by [167]. (123) The C(15) shift in the 6 β - and

[167] (in CDCl_3)

6 α -naltrexols [168] and [169] is markedly affected by the C(6) configuration. It has been suggested that this is a steric effect arising from congestion around the C(6) substituent and the oxygen bridge in the 6 α -compound which would alter the magnitude of the γ -effects on C(15). Smaller effects on C(3) and C(4) are noted. (124) In the ^{13}C



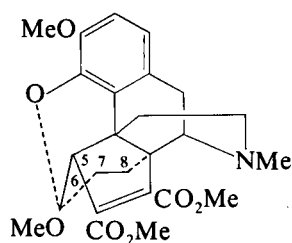
[168] 6β-Naltrexol



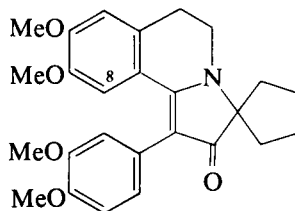
[169] 6α-Naltrexol

NMR spectrum (CDCl_3) of 6α-naltrexol-3-acetate C(7) absorbs to high frequency (0.83 ppm) and C(8) to low frequency (2.45 ppm) relative to the corresponding absorptions in 6α-naltrexol. Since these changes were not noted in DMSO-d_6 the shifts were explained in terms of hydrogen bonding between C(6)—OH and C(3)—OAc with a consequent distortion of ring c. (124) In the ^1H NMR spectra of the triacetates of [168] and [169] the 6-acetoxyl protons in the 6α-series absorb to lower frequency than in the 6β-series as a result of shielding by ring A. (124)

The expected high frequency shift of the *N*-methyl protons (δ 3.40, cf. δ 2.46 in thebaine) in the ^1H NMR spectrum of 16-hydroxythebaine is noted. In addition the 5-, 7-, and 8-protons absorb to higher frequency than in thebaine. (125) It was originally suspected that the 8β-proton gave rise to the δ 3.68 signal in the spectrum of the photoadduct [170] derived from thebaine. This signal has now been assigned to the 5-proton since the δ 3.68 signal is unaffected by *N*-oxide formation. (126)



[170]

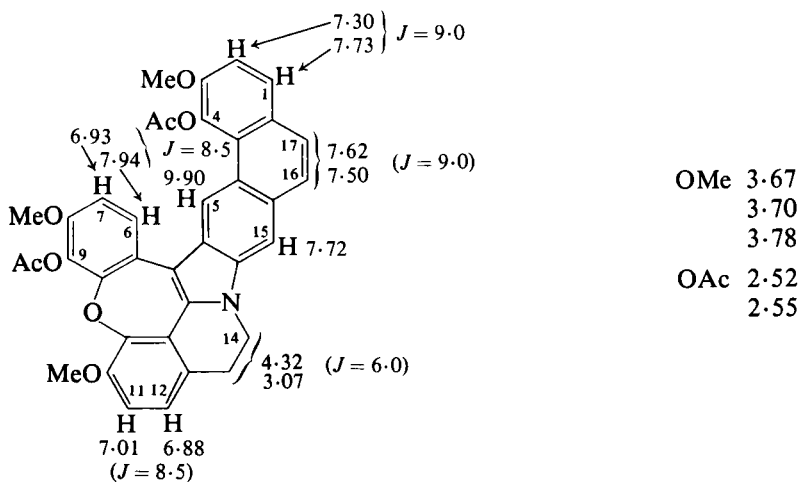


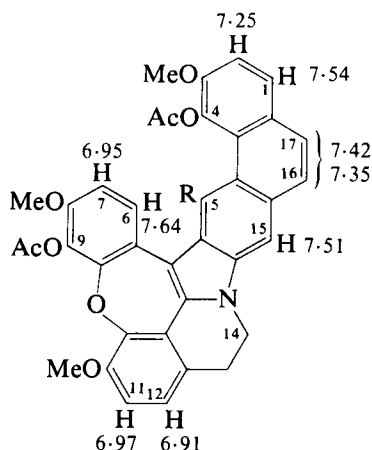
[171]

2. Compounds related to cancentrine

In the spectrum of the cancentrine model compound [171] one of the methoxyl group of protons absorbs at low frequency (δ 3.38) compared with absorption for the other methoxyl protons at δ 3.85, 3.85, and 3.90. This low frequency signal was assigned to the 7-methoxyl protons. In the hydrogenated derivative the lowest frequency methoxyl proton absorption is at δ 3.65. The low frequency aromatic proton absorption (δ 6.59) in [171] was assigned to the 8-proton. Both low frequency shifts are attributed to the shielding effects of ring c. (127)

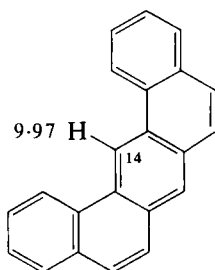
^1H NMR spectra of acetolysis products of cancentrine methiodides are shown in [172] and [173]. (128) In the spectrum of [172] the high frequency absorption of the 5-proton at δ 9.90 is typical of a "bay" proton (compare absorption for the "bay" proton in benz[*a,j*]anthracene [174] at δ 9.97 with the absorption of the 4-proton at δ 8.7 in

[172] (in CDCl_3)

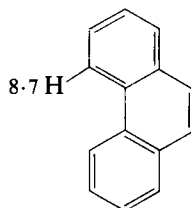


At 95°	
NMe	1.3
NAc	2.15
OMe	3.88
	3.94
	3.96
OAc	2.26
	2.44

[173] R = CH₂CH₂N(Me)Ac (in CDCl₃)



[174]

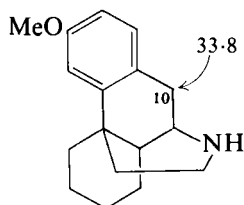
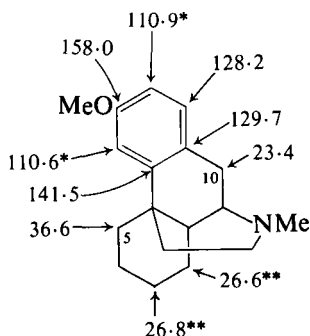
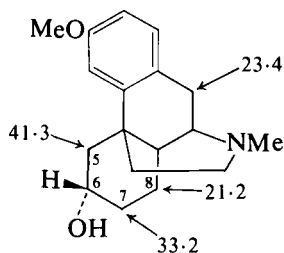
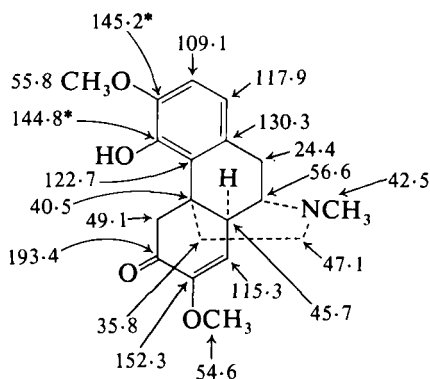


[175]

phenanthrene [175]). The ¹H NMR spectrum of [173] is complex at room temperature owing to restricted rotation in the side chain. In addition the *N*-methyl protons of the ethanamine side chain absorb at unusually low frequency (δ 1.3) suggesting shielding by the aromatic system and location of the chain at C(5).

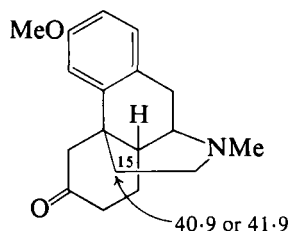
B. Alkaloids possessing the morphine skeleton but lacking the 4,5-oxide bridge

The increase in screening of C(10) on going from [176] (δ 33.8) to [177] (δ 23.4) is due to the γ -effect of the *N*-methyl group. Similarly the low frequency shift of C(8) on going from [177] (δ 26.6 or 26.8) to [178] (δ 21.2) is a γ -effect of the axial C(6)-hydroxyl group. Aromatic ring ¹³C resonances in the spectrum of sinomenine [179] were assigned from substituent additivity rules (Table I). For example, comparing

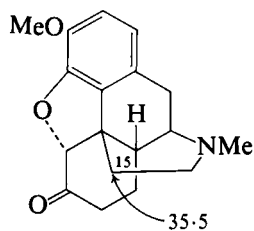
[176] (in CDCl_3)[177] (in CDCl_3)[178] (in CDCl_3)[179] Sinomenine (in CDCl_3)

sinomenine [179] and [177], the hydroxyl group shifts the C(1) absorption to lower frequency by 10.3 ppm. A marked increase in screening of C(15) (δ 40.9 or 41.9 to δ 35.5) accompanies the change from [180] to the oxide bridged structure [181]. (122)

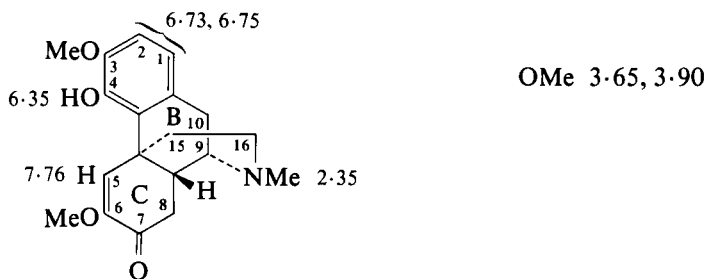
In the *trans*-B/c-8,14-dihydromorphinandienone, ocobitrine [182], (129) there is close approach of the 4-hydroxyl group and the olefinic



[180]

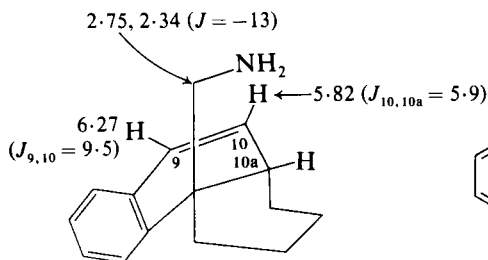


[181]

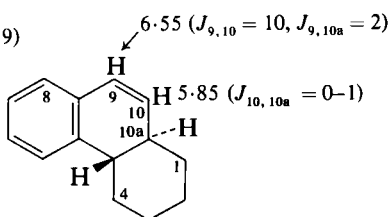
[182] Ocobitrine (in CDCl_3)

proton at C(5) resulting in a high frequency shift of the 5-proton in the ^1H NMR spectrum. In the spectrum of the *cis*-B/C analogue, isosinomenine, (1) the 5-proton absorbs at δ 6.75.

4a-Aminomethylhexahydrophenanthrenes of the type [183] have been obtained as intermediates in the synthesis of D-normorphinans. The *cis*-B/C fusion was assigned (130) to [183] from the value of $J_{10,10a}$ of 5.9 Hz corresponding to $\phi_{10,10a} \simeq 20^\circ$ (cf. $J_{10,10a}$ of 0–1 Hz ($\phi_{10,10a} \simeq 100^\circ$) in the *trans*-fused [184]). (131) Assuming the primary coor-

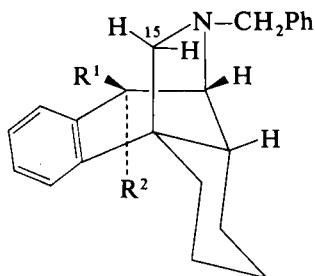


[183]



[184]

dination site with $\text{Eu}(\text{fod})_3$ to be the hydroxyl group, the smaller lanthanide induced shifts of the C(15) protons in [185; $\text{R}^1 = \text{H}$, $\text{R}^2 =$

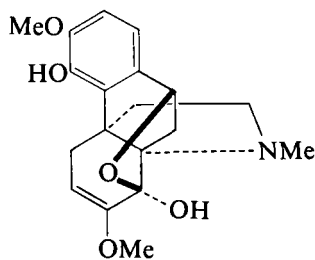
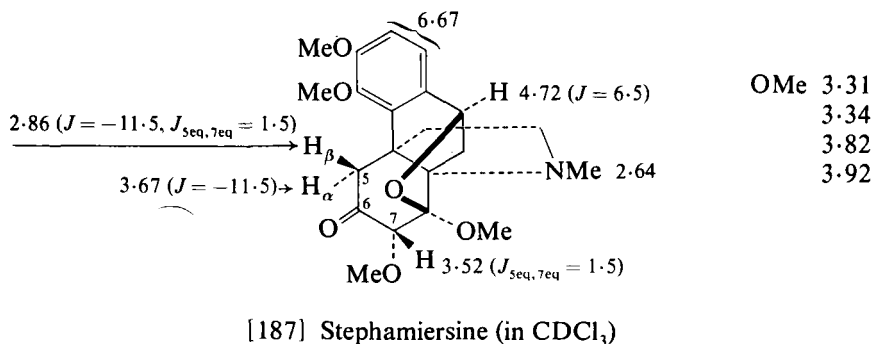
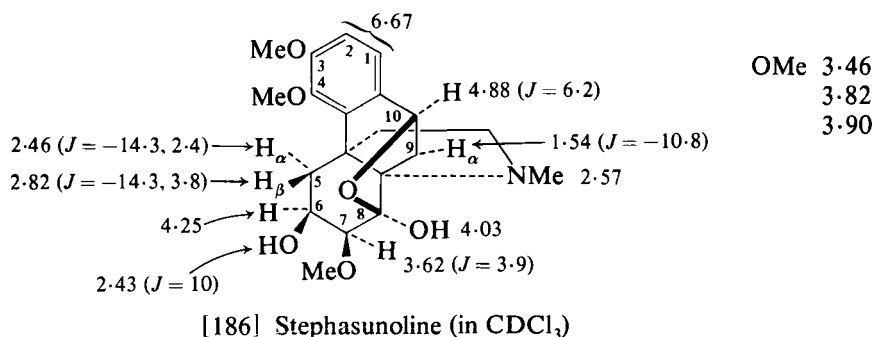


[185]

OH] than in [185; $R^1 = \text{OH}$, $R^2 = \text{H}$] are indicative of the assigned stereochemistry. (130)

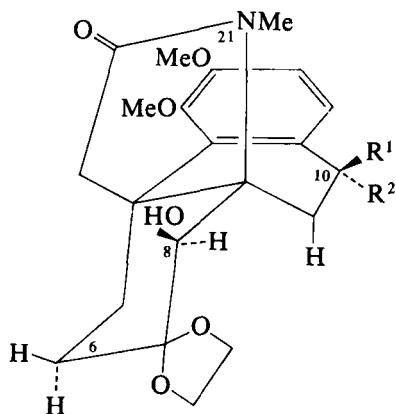
C. Alkaloids possessing the hasuban skeleton

NOE enhancement of the 7 α -proton signal on irradiation of the δ 2.46 signal permitted assignment of the latter to the *syn* axial proton at C(5) in the spectrum of stephasunoline [186]. The value (1.5 Hz) of $J_{5\text{eq},7\text{eq}}$ in the spectrum of stephamiersine [187] helped establish the axial nature of the 7-methoxyl. (132) Prostephabyssine [188] shows a



[188] Prostephabyssine

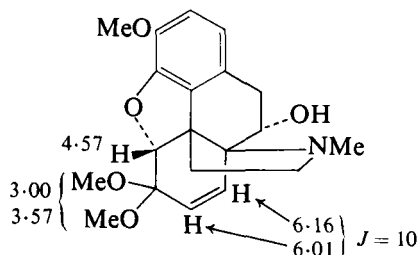
complex ^1H NMR spectrum due to the presence of the hemiketal = keto-alcohol equilibrium. (133) In [189] and [190] the 10-proton shifts permit the assignment of the pseudoaxial acetoxyl in [189] and the pseudoequatorial acetoxyl in [190]. (134)



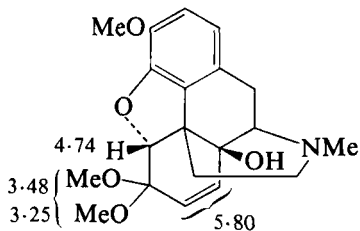
[189] $\text{R}^1 = \text{OAc}$, $\text{R}^2 = \text{H}$ $\delta \text{H-10}$ 6.03 $J = 3$

[190] $\text{R}^1 = \text{H}$, $\text{R}^2 = \text{OAc}$ $\delta \text{H-10}$ 5.75 $J = 7$

In [191] one of the methoxyl group of protons and the 5-proton absorb to low frequency of the corresponding protons in [192]. (135)



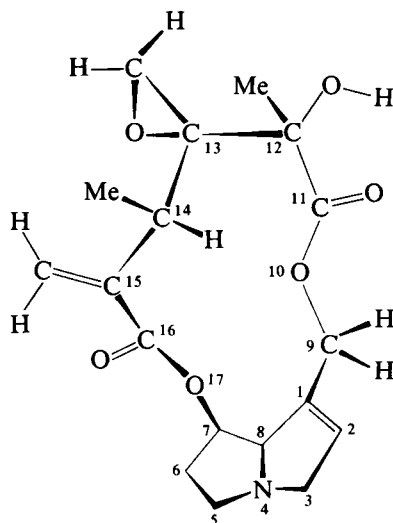
[191]



[192]

VI. PYRROLIZIDINE AND PYRROLE ALKALOIDS

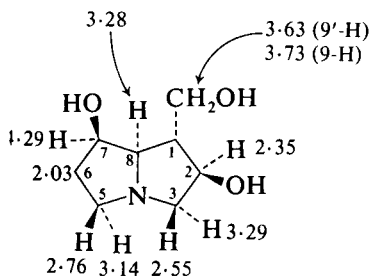
Details concerning the conformation of swazine [193] have been obtained from its ^1H NMR spectrum. The $\text{C}(14)\text{-H}$ bond is shown to lie in the plane of the exocyclic methylene by the virtual absence of allylic coupling. The large difference in chemical shift (1.39 ppm) between the $\text{C}(9)$ methylene protons (9-H δ 4.12, $9'\text{-H}$ δ 5.48) indicates one of these



[193] Swazine

protons to be lying near the intersection of the ester and olefin planes. The width (9 Hz) of the 7-proton multiplet shows normal buckling (*ca.* 40°) of the pyrrolidine ring as in retronecine, and the chemical shift (δ 5.05) for the 7-proton shows the ester carbonyl and C(7)–H to be *cis*-coplanar. (136)

In the NMR spectrum of croalbinecine [194] (in D₂O; shifts relative to the methyl signals of sodium 3-trimethylsilylpropane-1-sulphonate)

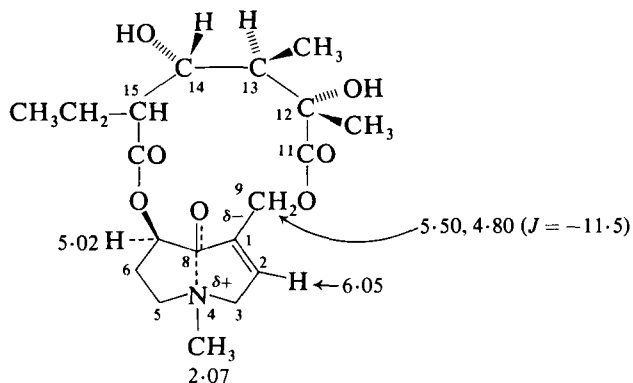


$J_{1,2} = 8.0$	$J_{3\alpha,3\beta} = -10.0$	$J_{7,8} = ca. 4.0$
$J_{1,8} = 8.0$	$J_{2,3\alpha} = 5.8$	$J_{1,8} = 8.0$
$J_{1,9'} = 6.2$	$J_{5\alpha,5\beta} = -10.0$	$J_{9',9} = -11.5$
$J_{1,9} = 5.5$	$J_{5\beta,6} = 7.0, 10.0$	$J_{1,9'} = 6.4$
$J_{2,3\beta} = 8.0$	$J_{5\alpha,6} = 4.0, 5.5$	$J_{1,9} = 5.8$
$J_{2,3\alpha} = 5.8$	$J_{6,7} = ca. 4.0$	

[194] Croalbinecine (in D₂O)

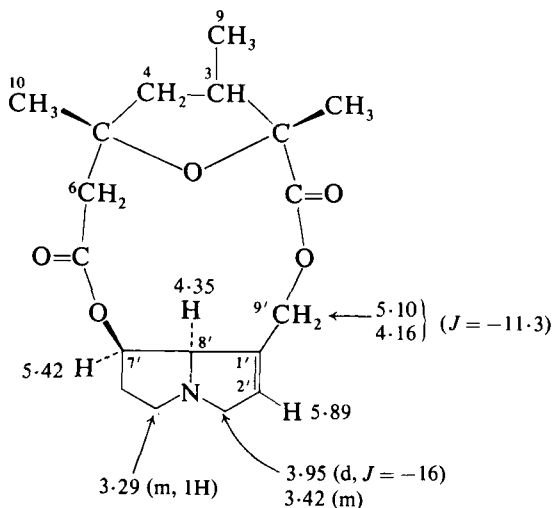
the values of $J_{1\beta,2}$ and $J_{2,3\beta}$ both of 8 Hz are best in accord with *trans*-C–H bonds (ϕ *ca.* 160°) and that of $J_{2,3\alpha}$ of 5.8 Hz with *cis*-C–H bonds (ϕ *ca.* 30–40°). These values indicate an *exo*-buckled B ring and therefore a 2 β -hydroxyl group. (137)

The rather large difference (0.70 ppm) between the chemical shifts of the C(9) methylene protons (δ 5.50 and 4.80; $J_{\text{gem}} -11.5$ Hz) in the ^1H NMR spectrum of syneilesine [195] (137) is characteristic of a 12-membered macrocyclic secopyrrolizidine alkaloid. (138) In the ^{13}C



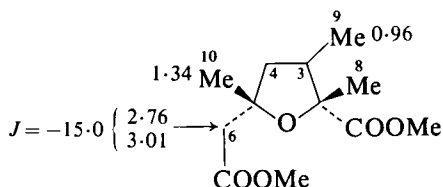
[195] Syneilesine

NMR spectrum of [195] C(16) and C(11) absorb at δ 171.4 and 176.7 while the signals at δ 134.2, 136, and 189.4 correspond to the $\alpha\beta$ -unsaturated carbonyl moiety. Transannular interaction involving the nitrogen atom is responsible for the increase in screening (δ 189.4) of C(8) [cf. δ 208.1 in cyclopent-2-enone, δ 197.1 in cyclohex-2-enone (3)].

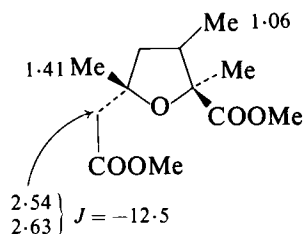


[196] Retroisosenine

The ^1H NMR spectrum of retroisosenine is summarized in [196]. The 9- and 10-methyl group protons absorb at higher frequency in [198] (as a result of their *cis*-orientation to the methoxycarbonyl group) than in [197]. Such a structural relationship has also been invoked to explain the larger chemical shift difference between the C(6) methylene protons in [197] than in [198]. (139)

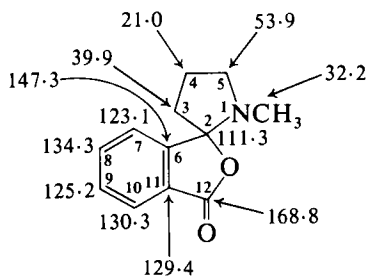


[197]

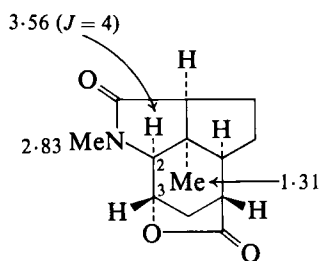


[198]

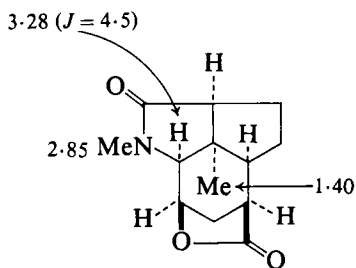
The ^{13}C NMR spectrum of shihunine is summarized in [199], (140) and the shifts in the nitrogen-containing ring may be compared with those in *N*-methylpyrrolidine [δ 41.7 NCH_3 , 55.7 C(2), 23.7 C(3) (2)].

[199] Shihunine (in CD_2Cl_2)

In the spectra of [200] and [201] (synthetic intermediates in the synthesis of *Dendrobium* alkaloids) the shifts of the 2-protons are



[200]

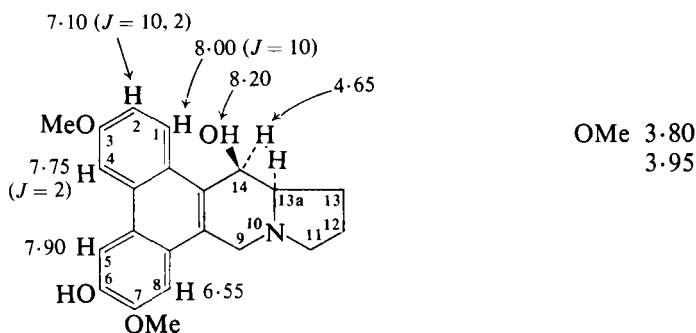


[201]

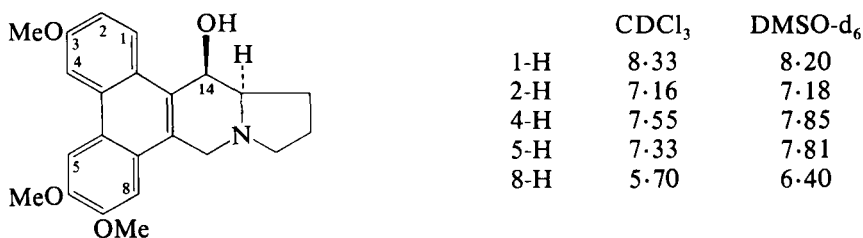
diagnostic of their stereochemistry with respect to the oxygen function at C(3). (141)

VII. INDOLIZIDINE ALKALOIDS

X-ray analysis (142) has established a structure for tylophorinidine with a *trans*-diaxial arrangement of the 14-hydroxyl and C(13a)-H. The NMR spectrum of this compound is given in [202] and of *O*-methyltylophorinidine in [203]. (143) The spectra of [203] in



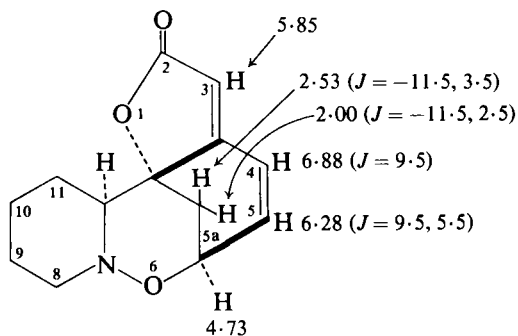
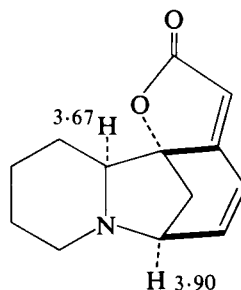
[202] Tylophorinidine (in DMSO- d_6)



[203] *O*-Methyltylophorinidine

CDCl₃ and in DMSO- d_6 show solvent shifts attributed to the occurrence of dimerization in CDCl₃ involving hydrogen bonding between the hydroxyl and the nitrogen atom which is reduced in DMSO- d_6 as solvent. Such hydrogen bonding, it is argued, would be facilitated by an axial hydroxyl group. The deshielding effect of an acetoxyl group on an *ortho* proton is shown by the chemical shift of the 5-proton in the spectrum of diacetyltylophorinidine (δ 8.18) compared with that (δ 7.88) in the spectrum of 14-acetyl-*O*-methyltylophorinidine. (143)

Phyllantidine [204] which may be obtained by oxidation of allosecurinine [205] shows a higher frequency resonance for the 5a-protons than in [205] (δ 3.90) as a result of the presence of the oxygen

[204] Phyllantidine (in CDCl_3)

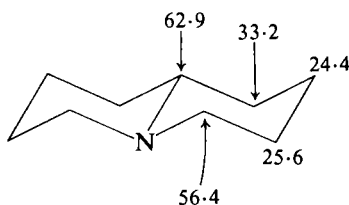
[205] Allosecurinine

atom. Since the shifts of the other protons α to nitrogen in [204] and [205] are similar, structure [204] rather than an *N*-oxide structure is assigned to phyllantidine. (144)

VIII. QUINOLIZIDINE ALKALOIDS

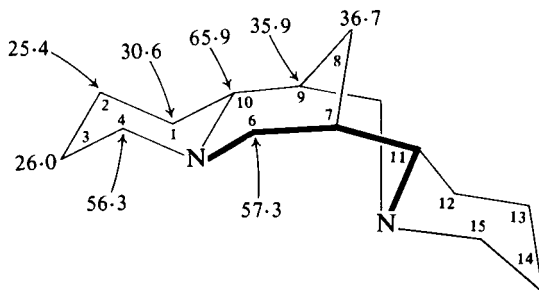
A. Lupanine and related alkaloids

The ^{13}C chemical shifts in the basic quinolizidine unit are displayed in [206]. These assignments were aided by the ^{13}C NMR spectrum of 3,3'-

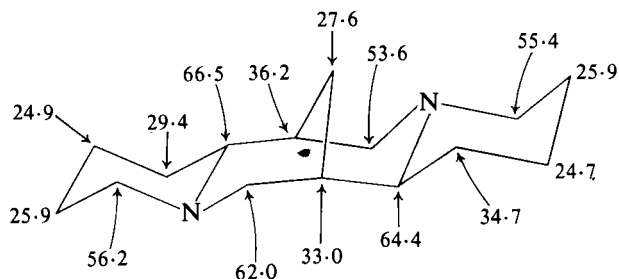


[206]

dideuterioquinolizidine. (2) The importance of ^{13}C NMR spectroscopy in the elucidation of the structures of the lupin alkaloids has been demonstrated, and an important collection of ^{13}C shift data (CDCl_3) obtained on forty-seven quinolizidines and piperidines is available. (145) While many of the shifts follow rules developed on carbocyclic systems, important differences are observed. Comparison of shifts for quinolizidine [206] and α -isosparteine [207] shows only a small β -effect on C(6) in [207] (δ 56.4 in [206], δ 57.3 in [207]) whereas C(8) in [207] absorbs 12.3 ppm to high frequency of the corresponding signal, C(2), in [206]. Comparison of the C(8) resonances in isosparteine [207] and

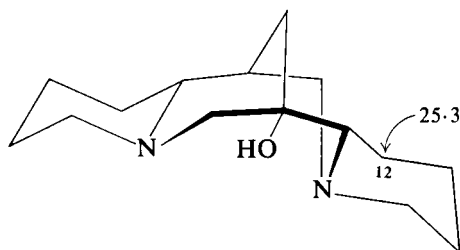
[207] α -Isosparteine

in sparteine [208] shows a marked shielding in the latter presumably as a result of the close approach of the bridge carbon, C(8), and the

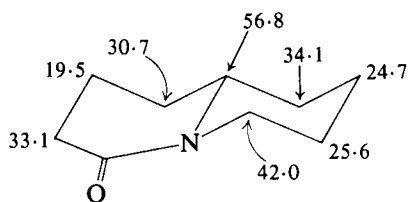


[208] Sparteine

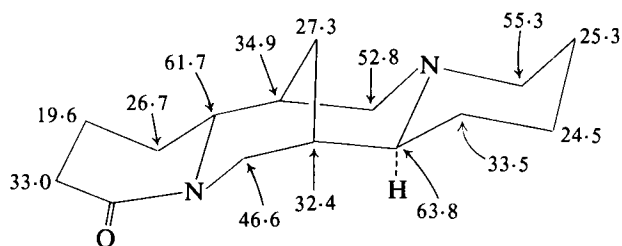
nitrogen lone pair in sparteine [208]. The low frequency absorption of C(12) in 7-hydroxy- α -isosparteine [209] is a steric effect of the 7-

[209] 7-Hydroxy- α -isosparteine

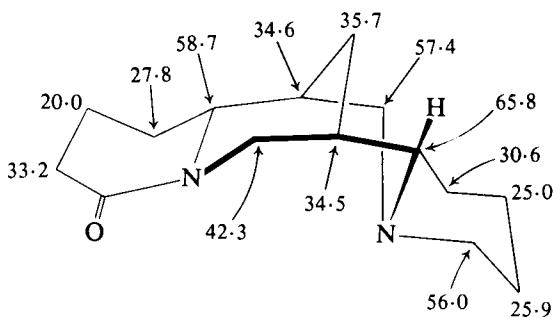
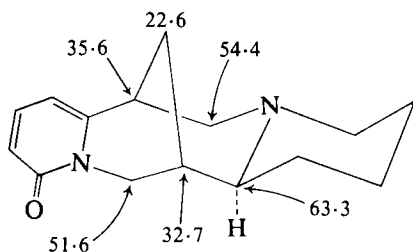
hydroxyl group. The ^{13}C NMR spectral features of some of the quinolizidinones, oxosparteines, and oxo- α -isosparteines described by Bohlmann are exemplified by those of quinolizidin-4-one [210], 4-oxo-sparteine [211], and 4-oxo- α -isosparteine [212]. In anagyrin [213] the bridge carbon, C(8), is at lower frequency than in 4-oxosparteine. In



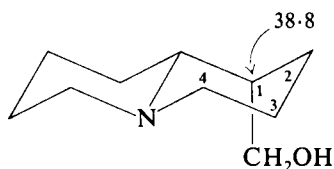
[210]



[211] 4-Oxosparteine (Lupinin)

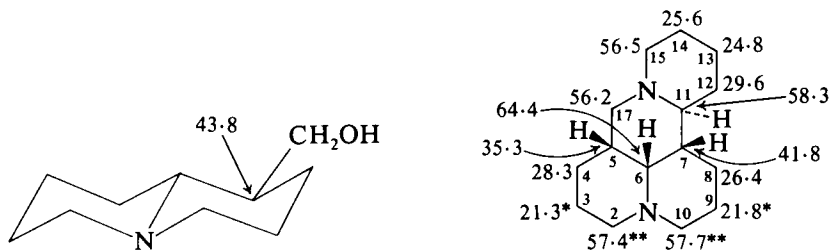
[212] 4-Oxo- α -isosparteine

[213] Anagyrin



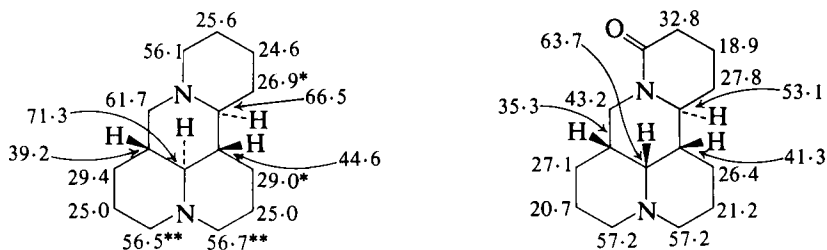
[214] Lupinin

lupinin [214] and epilupinin [215] the orientation of the CH_2OH group is indicated by the C(1) chemical shifts. Chemical shifts of matrine derivatives are shown in [216]–[219]. (145)



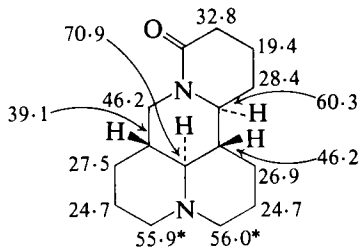
[215] Epilupinin

[216]



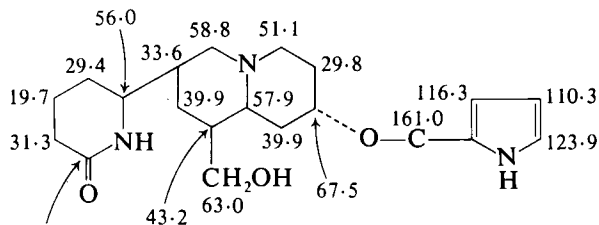
[217]

[218]

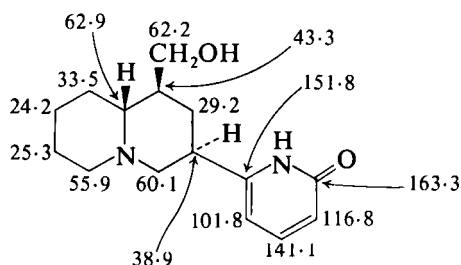


[219]

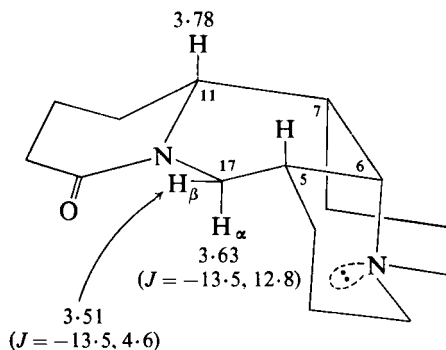
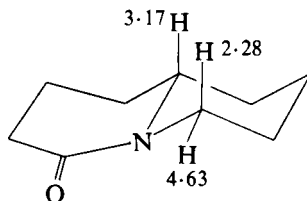
The ^{13}C shifts of the alkaloid [220] (146) from *Cadia purpurea* and of maminine [221] (147) are in accord with the structures shown. ^1H NMR data for [221] and for the tetrahydro derivative of [221] (pohakuline) are available. (147)



[220]

[221] (in DMSO- d_6)

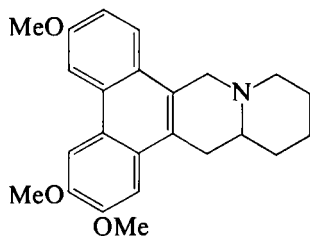
In the ^1H NMR spectrum of (+)-isomatrine [222] (148) the 17-methylene shifts differ markedly from those in octahydroquinolizin-4-one [223] (149) owing to changes in orientation of the methylene group

[222] (+)-Isomatrine (in CDCl_3)

[223]

with respect to the amido carbonyl [see also shifts in matrine and allomatrine (1)].

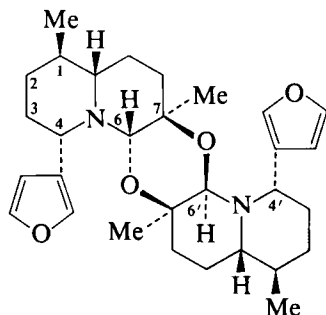
The ^1H NMR spectrum of cryptopleurine is summarized in [224]. (150)

[224] Cryptopleurine (in CDCl_3)

OMe	3.97
	4.00
	4.04
Ar-H	7.12 ($J = 10, 2$)
	7.17
	7.75 ($J = 10$)
	7.83 ($J = 2$)
	7.80

B. Nuphar alkaloids

The structure [225] has been assigned to a dimer alkaloid of 6,7 β -oxidodeoxynupharidine. (151) On changing solvent from CDCl_3 to



1-, 1'-, 7-, 7'-Me	0.87, 0.89, 0.91
4-H, 4'-H	3.75-4.10
6-H, 6'-H	3.89
β -furyl-H	6.08
α -furyl-H	7.11

[225] (in CCl_4)

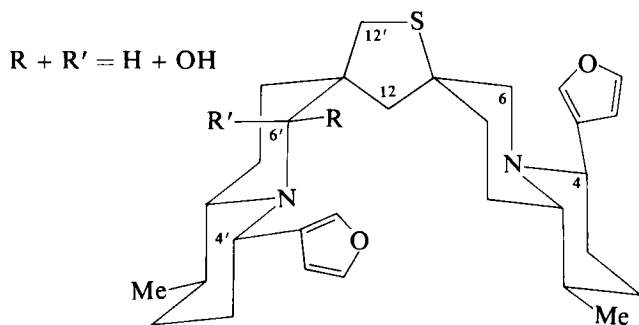
C_6D_6 the 1- and 1'-methyl signals shift to low frequency and the 7- and 7'-methyl signals shift to high frequency consistent with *trans*-fused quinolizidine systems containing axial angular methyl groups and equatorial 1- and 1'-methyl groups. (152) The observation of the non-equivalence of the 4- and 4'-protons (in CCl_4) and the 6- and 6'-protons (in C_6D_6) together with studies on Dreiding models indicate the stereochemistry shown in [225] with differing configurations at C(6) and C(6').

The hemiaminals, 6'-hydroxythiobinupharidine [226] and 6-hydroxythionupharlutine-B [227], are characterized in particular by their absorption in the δ 4 region. (153)

The results of a detailed examination of the 220 MHz ^1H NMR spectra of thionupharoline (6-hydroxythiobinupharidine) and of thiobinupharidine are summarized in [228] and [229] respectively. (154) Some of the assignments are based on the ^1H NMR spectra of deoxynupharidine [230] and 7-epideoxynupharidine [231].

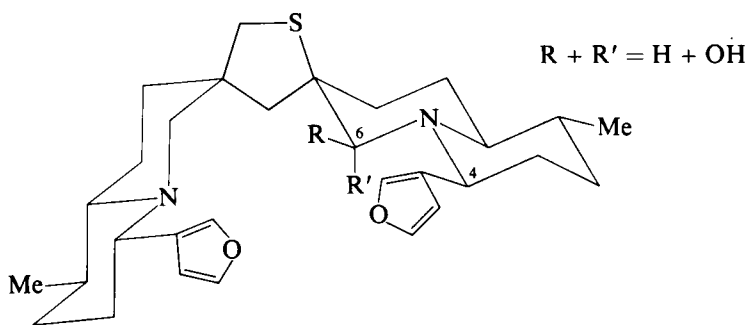
Comparison of the spectrum of thiobinupharidine [229] with that of neothiobinupharidine [232] shows the higher frequency absorption of the axial CH_2S group protons (in [232]) than of the equatorial CH_2S group protons (in [229]) (155) as noted for model quinolizidines with thiomethylene substituents. (156)

^{13}C NMR spectra of nine *Nuphar* alkaloids and of model compounds have been reported. (157) Reference to the spectra of deoxynupharidine [233], 7-epideoxynupharidine [234], and the thiomethylquinolizidines [235] and [236] illustrates the low frequency absorption of axial $^{13}\text{CH}_3$ and axial $^{13}\text{CH}_2\text{SMe}$ nuclei in *trans*-fused quinolizidine derivatives



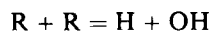
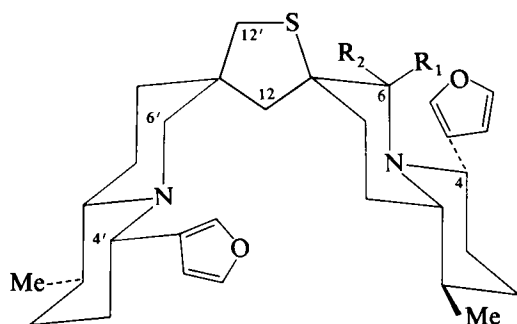
[226] 6'-Hydroxythiobinupharidine
(in $CDCl_3$)

Me	0.92 ($J = 3$)
OH	2.46 ($J = 4$)
$12'_{a,e}\text{-H}$	2.53 ($J = -11.5$)
6_e-H	2.83 ($J = -11, 1.5$)
4_a-H	2.94
$4'_a\text{-H}$	3.62
$6'\text{-H}$	4.25
Furan $\beta\text{-H}$	6.36
Furan $\alpha\text{-H}$	7.35



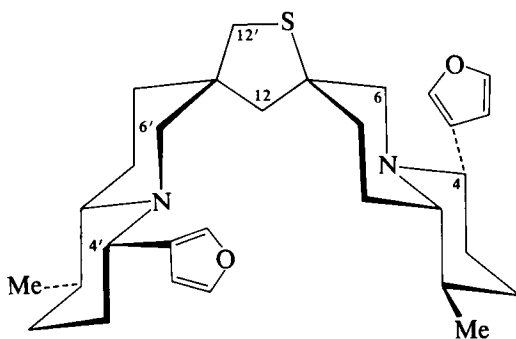
[227] 6-Hydroxythionuphlutine-B (in $CDCl_3$)

Me	0.88 ($J = 5$)
$12'_{a,e}\text{-H}$	2.32 ($J = -12.0$)
6-H	4.08 (s)
4_a-H	3.55
$4'_a\text{-H}$	2.88
$6'_e\text{-H}$	2.88
Furan $\beta\text{-H}$	6.41, 6.22
Furan $\alpha\text{-H}$	7.27



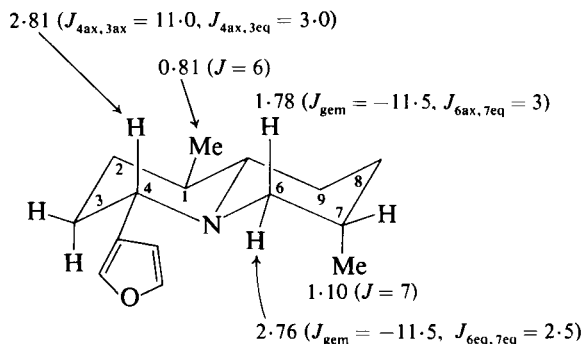
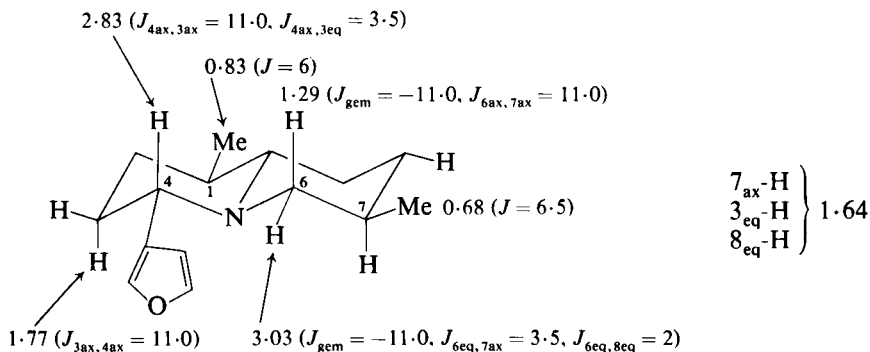
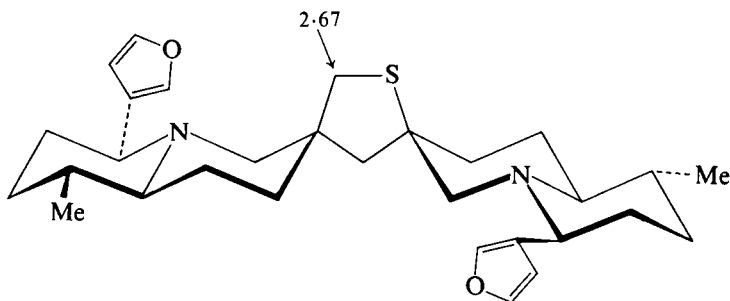
[228] Thionupharoline (6-Hydroxythiobinupharidine)

	CDCl ₃		C ₆ D ₆
Me	0.88 (<i>J</i> = 5)	Me	0.75 (<i>J</i> = 6)
OH	2.26	OH	2.42
12' _{a,e} -H	2.20 (<i>J</i> = 12)	12' _{a,e} -H	2.11 (<i>J</i> = 12)
4'-H	2.89 (<i>J</i> = 5.6, 8)	4'-H	2.79 (<i>J</i> = 3, 11)
4-H	3.70 (<i>J</i> = 7.5, 7)	4-H	3.90 (<i>J</i> = 4, 10)
6' _e -H	2.92 (<i>J</i> = -11.5, 2)	6' _e -H	3.18 (<i>J</i> = 2.5, -12)
6-H	3.97	6-H	4.25
Furan β-H	6.34 (<i>J</i> = 7)	Furan β-H	6.41
Furan α-H	7.21 (1H)		6.48
	7.30 (<i>J</i> = 4) (3H)	Furan α-H	7.16 (3H)
			7.22 (1H)



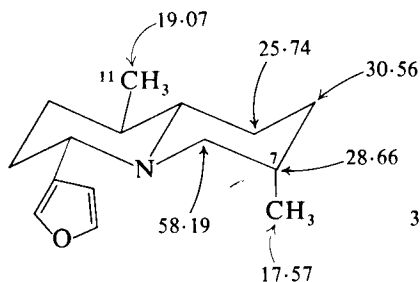
[229] Thiobinupharidine

6' _a -H	1.40 (<i>J</i> _{6'a,6'e} = -11.5)
6 _a -H	1.92 (<i>J</i> _{6a,6e} = -11.5)
6 _e -H	3.11 (<i>J</i> _{6a,6e} = -11.5, <i>J</i> _{6a,8e} = 2)
6' _e -H	3.17 (<i>J</i> _{6'a,6'e} = -11.5, <i>J</i> _{6'e,8'e} = 2.5)
4 _a -H } 4'-H }	2.80 (<i>J</i> _{4a,3a} = 10.5, <i>J</i> _{4a,3e} = 3.5)
12 _{a,e} -H	2.18 (<i>J</i> = -14.0)
12' _{a,e} -H	2.31 (<i>J</i> = -11.5)

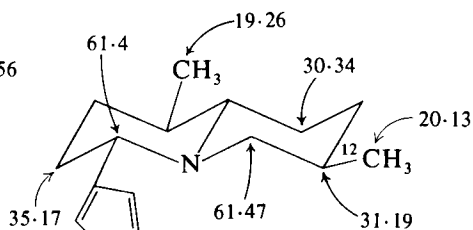
[230] Deoxynupharidine (in C_6D_6)[231] 7-Epideoxynupharidine (in C_6D_6)

[232] Neothiobinupharidine

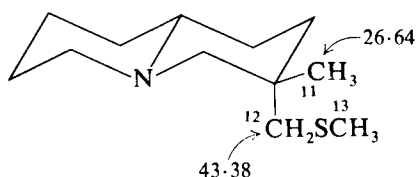
relative to the equatorial substituted isomers. Comparison of the spectra of [233] with [237] and of [234] with [238] shows the differing γ -effects of axial and equatorial hydroxyl groups in [233] and [234] on the C(9) shifts, the equatorial hydroxyl group causing deshielding and the axial



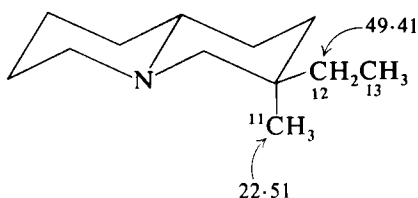
[233] Deoxynupharidine



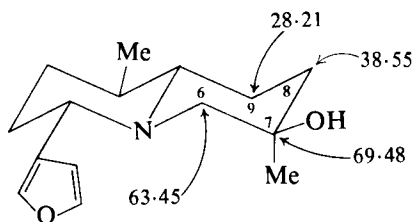
[234] 7-Epideoxynupharidine



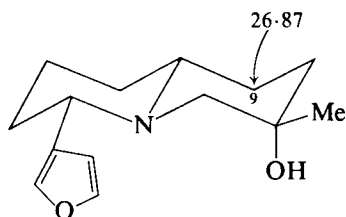
[235]



[236]

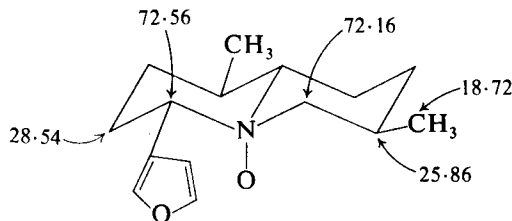


[237]

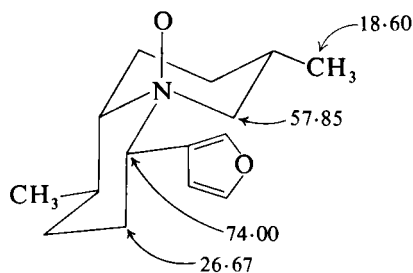


[238]

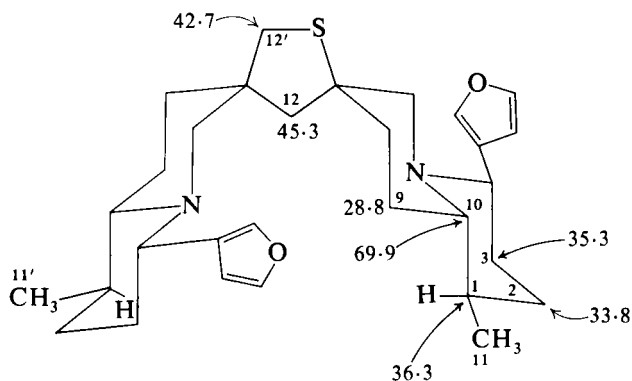
hydroxyl group causing shielding. *N*-Oxidation of 7-epideoxynupharidine [234] to give [239] results in a high frequency β -shift (*ca.* 10 ppm) of C(6) and a low frequency γ -shift (*ca.* 6 ppm) of C(7). Shifts in the *cis*-fused *N*-oxide of nupharidine are shown in [240]. (157)



[239] 7-Epinupharidine

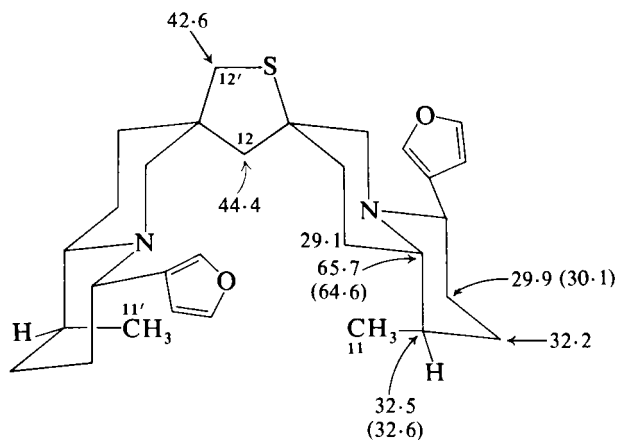


[240] Nupharidine

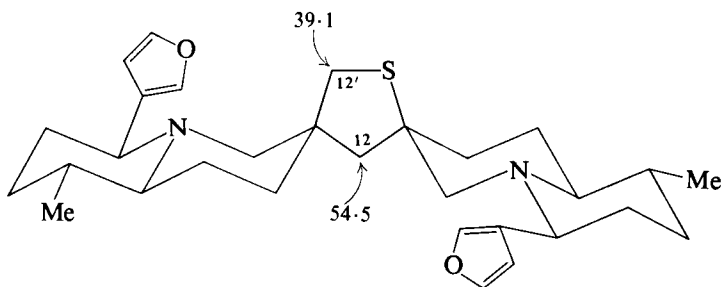


[241] Thiobinupharidine

The importance of these correlations is illustrated by the spectra of thiobinupharidine [241], 1-*epi*-1'-*epi*-thiobinupharidine [242], and neothiobinupharidine [243]. In [241] and [242] the C(12) is axial to

[242] 1-*epi*-1'-*epi*-Thiobinupharidine

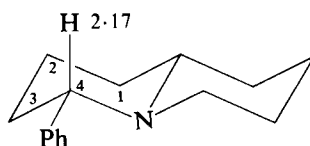
both quinolizidine systems and absorbs to low frequency of C(12) in [243]. The presence of the axial methyl groups in 1-*epi*-1'-*epi*-thio-binupharidine was shown by comparison of the α -, β -, and γ -shifts in [241] and [242] and in model quinolizidines. (158)



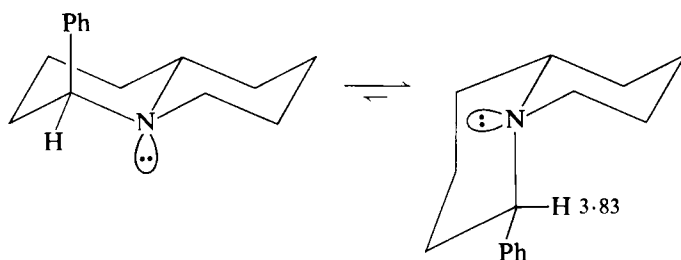
[243] Neothiobinupharidine

C. Lythraceae alkaloids

cis(4-H,9a-H)-4-Phenylquinolizidine exists in solution in the *trans*-fused ring conformation [244] whereas its epimer preferentially adopts the *cis*-fused ring conformation [245]. The ^1H NMR spectra of these

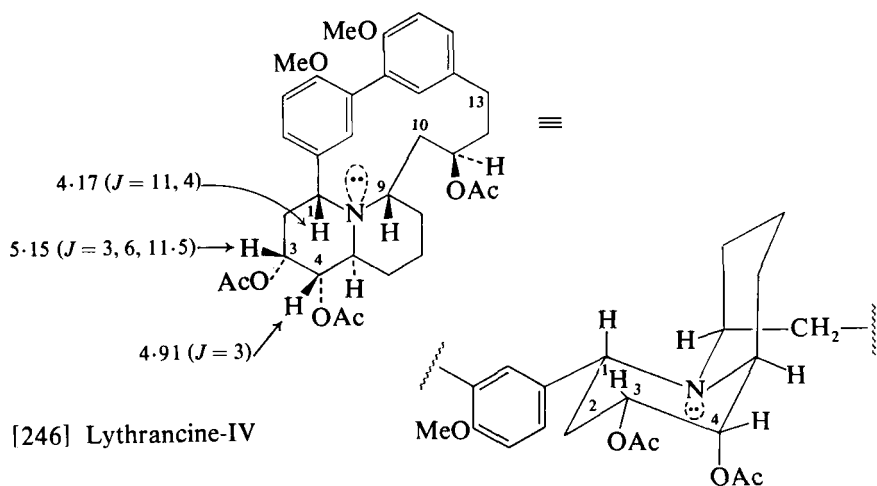


[244]

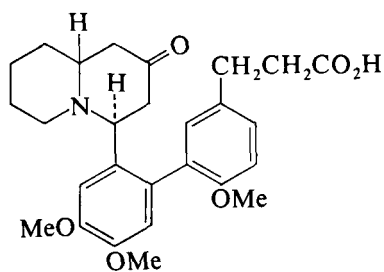


[245]

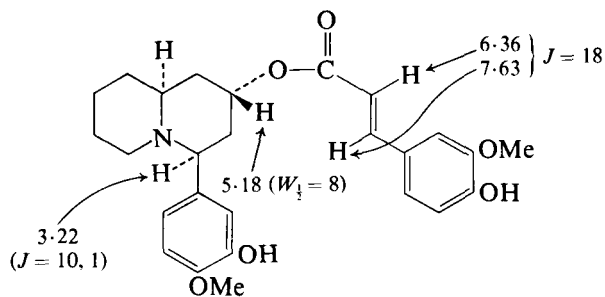
compounds show the higher frequency absorption of the 4-protons in the *cis*-fused quinolizidine. (159) This observation has been utilized in stereochemical studies on the lythraceae alkaloids [see previous discussion on methyl-lythrine and methylvertine (1)]. Thus the *cis*-fused



ring stereochemistry has been assigned to lythrancine-IV [246] on the basis of the chemical shift of the 1-proton at $\delta 4.17$ ($J = 11, 4$ Hz) (160) and to [247]. (161) The *trans*-fused ring stereochemistry has been assigned to ambresoline [248] from the lower frequency absorption of



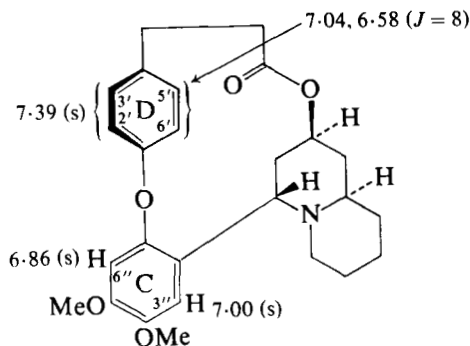
[247]



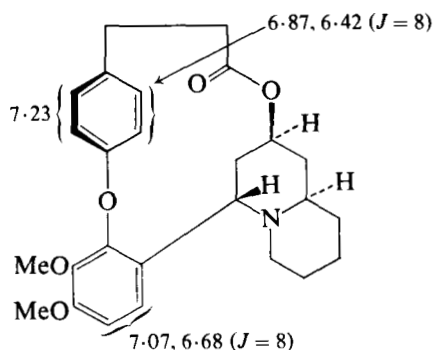
[248] Ambresoline

the 4-proton (δ 3.22, $J = 10$, 1 Hz). (162) ^1H NMR data on related lythracines are available. (163)

The structure for lagerine has been revised. (164) Comparison of the spectrum of vertaline [249] with that of methyl-lagerine indicates structure [250] for methyl-lagerine. In particular the patterns of



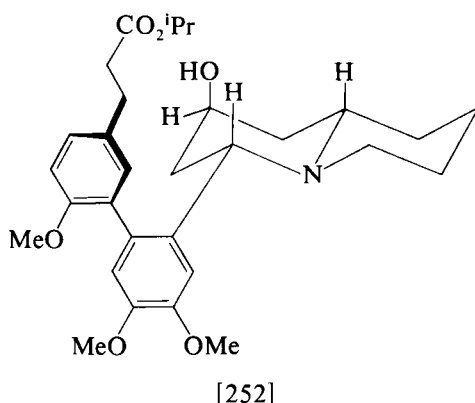
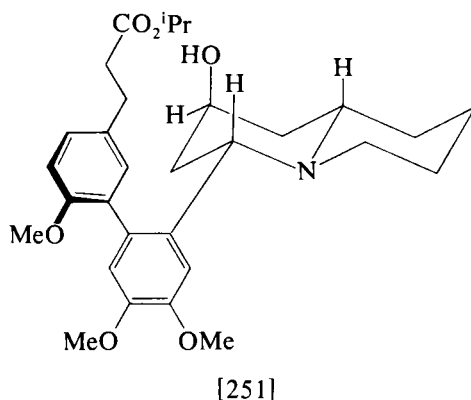
[249] Vertaline



[250] Methyl-lagerine

aromatic proton absorption are similar in both cases with the 2'- and 3'-protons absorbing as a broadened singlet with the same chemical shift and the 5'- and 6'-protons as an AB-quartet. The ring c aromatic protons absorb as singlets.

At 23°C, signals due to two atropisomers [251] and [252] of isopropyl 3-[3-{2-(2-hydroxy(a)-*Trans*-quinolizidin-4-yl(e))-4,5-dimethoxyphenyl}-4-methoxyphenyl]propionate are seen in the NMR spectrum. (165) Thus the $\text{CO}_2\text{CH}(\text{CH}_3)_2$ signals absorbing at δ 1.17 ($J = 6.5$ Hz) and δ 1.20 ($J = 6.5$ Hz), in the NMR spectrum recorded at 23°C, are



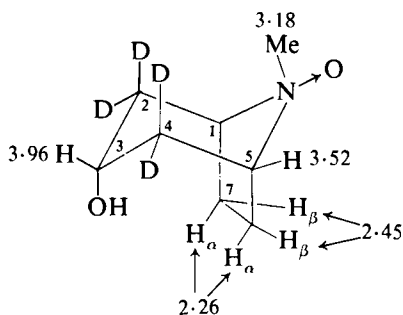
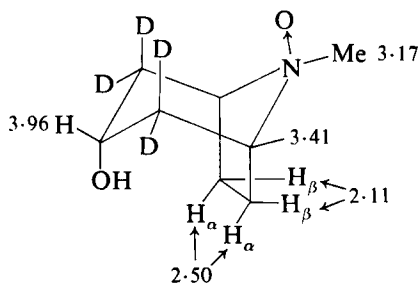
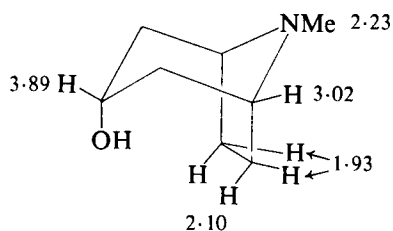
replaced by one doublet at δ 1.19 at 60°C. The 23°C spectrum also showed methoxyl proton signals at δ 3.65, 3.66, 3.77, 3.78, and 3.88, replaced at 60°C by three singlets at δ 3.68, 3.81, and 3.90.

IX. PIPERIDINE AND PYRIDINE ALKALOIDS

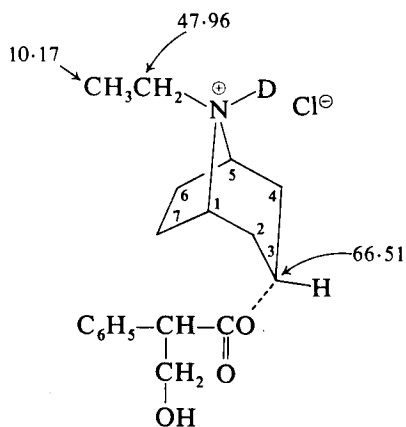
^{13}C NMR shifts of a number of alkyl substituted piperidines have been documented. (166)

A. Tropane alkaloids

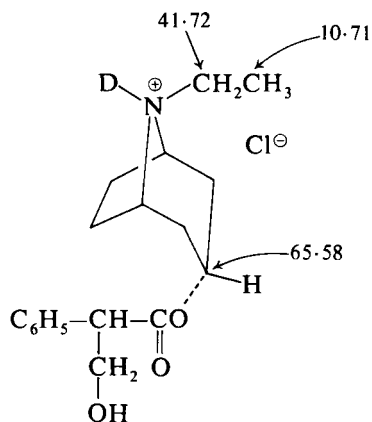
The stereochemistry of the tropane *N*-oxides is readily determined from the chemical shifts of the 6β - and 7β -protons. Thus in spectra of the isomeric 2,2,4,4- d_4 -tropine *N*-oxides [253] and [254] the 6β - and 7β -shifts in the axial *N*-oxide [254] resemble those in tropine itself [255] whereas the 6β -(7β) protons are relatively deshielded in the axial *N*-methyl isomer [253]. (167)

[253] (in CD_3OD)[254] (in CD_3OD)[255] Tropine (in CD_3OD)

The ^{13}C NMR spectra of a large number of epimeric *N*-alkylnoratropine derivatives have been studied and substituent effects suggested. The pair of compounds [256] and [257] show the expected low frequency shift of C(2) and C(4) in the axial *N*-ethyl compound [257]. (168)

[256] (in CD_3OD , DCl)

C(6), C(7) 24.39, 24.66
C(2), C(4) 35.46, 35.56
C(1), C(5) 61.11, 61.21



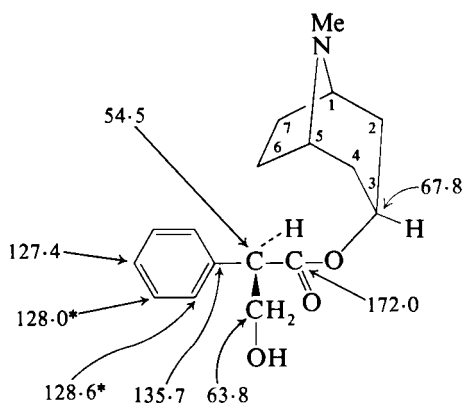
C(6), C(7) 25.88, 26.13

C(2), C(4) 29.28, 29.28

C(1), C(5) 57.62, 57.62

[257] (in CD_3OH , DCl)

The ^{13}C NMR shifts of hyoscyamine [258] and scopolamine [259] (169) are in essential agreement with those published previously. (2)



C(6), C(7) 25.2, 24.7

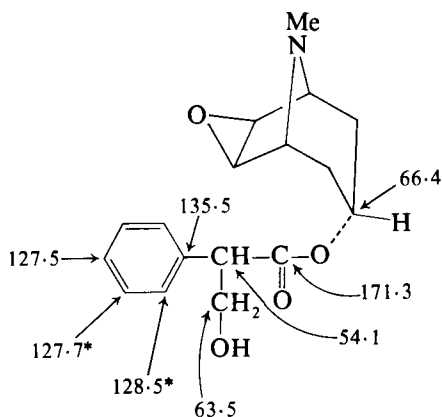
C(2), C(4) 35.9, 36.1

C(1), C(5) 59.3, 59.4

[258] Hyoscyamine (in CDCl_3)

The magnetic non-equivalence of the ^{13}C nuclei of the tropane ring in protonated scopolamine [260] and in protonated atropine [261] indicates the tropic acid group to be near C(6) and C(7) in [260] but to be in a position affecting all the carbon nuclei on one side of the tropane ring in [261]. (170) The absorption of the equatorial and axial *N*-methyl ^{13}C nuclei in [261] and [260] respectively may be compared to the corresponding absorptions in methylatropine [262].

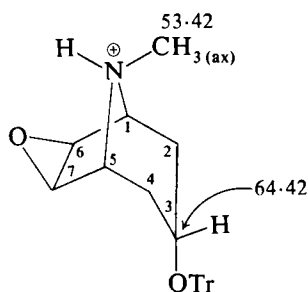
A study of second order coupling in the ^{13}C NMR spectrum of tropine [263] has confirmed the original assignment of the C(6) and



C(6), C(7) 55.6, 56.0

C(2), C(4) 30.3, 30.4

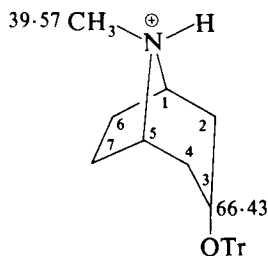
C(1), C(5) 57.3, 57.4

[259] Scopolamine (in CDCl₃)

C(1), C(5) 53.75

C(6), C(7) 58.26, 58.05

C(2), C(4) 25.20

[260] (in H₂O + 2% v/v dioxan)

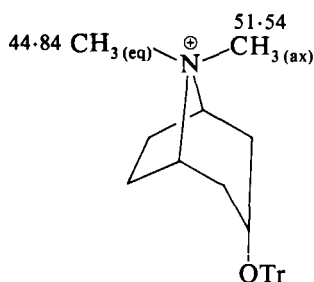
C(1), C(5) 63.03, 62.92

C(6), C(7) 35.26, 35.09

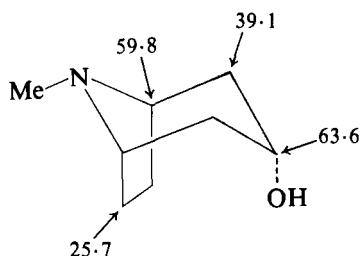
C(2), C(4) 24.03, 23.76

[261]

C(2) resonances. The identical chemical shifts of the 6 α - and 7 α -protons together with the strong ¹³C(6)–¹H(6 α) coupling and the weak ¹³C(6)–¹H(7 α) coupling lead to the expectation of the observed second order coupling of the C(6) signals. Since the chemical shifts of the C(2) methylene protons are very different from those of the protons at C(1)

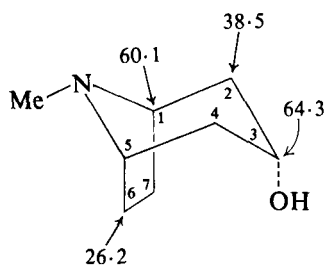
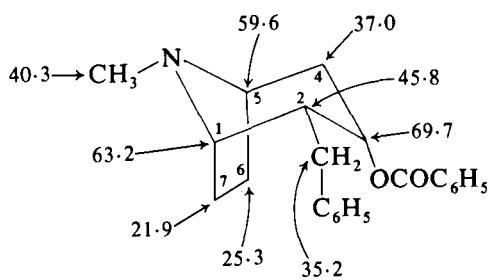


[262]

[263] (in CDCl_3)

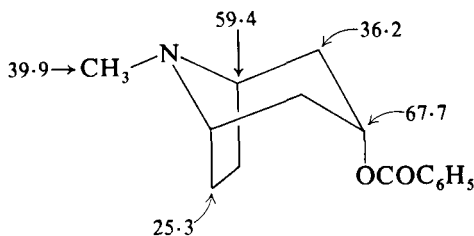
and C(3), second order coupling of the $^{13}\text{C}(2)$ nucleus is not expected. The ^{13}C NMR spectrum of tropine in aqueous solution [264] has also been re-examined. A SFORD spectrum with a decoupling signal at the low frequency end of the ^1H NMR spectrum showed lower residual coupling of the C(1) doublet than of the C(3) doublet.

Following on from this work the structures of five 2-benzyltropine type alkaloids have been assigned. One of these [265] shows a low

[264] Tropine (in D_2O)

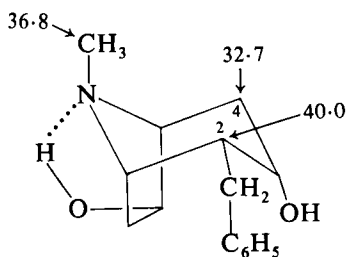
[265]

frequency shift of C(7) relative to C(7) in the tropine benzoate [266] as a result of the presence of the equatorial benzyl group at C(2). Large increases in screening are noted for the NCH_3 and the C(2) and C(4)

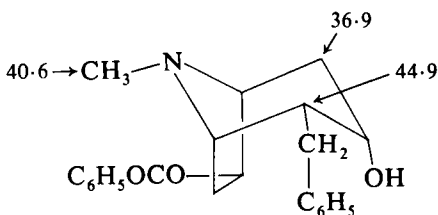


[266]

signals in [267] compared with [268] corresponding to the depicted change in stereochemistry at nitrogen. (171)



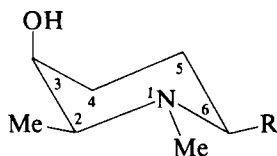
[267]



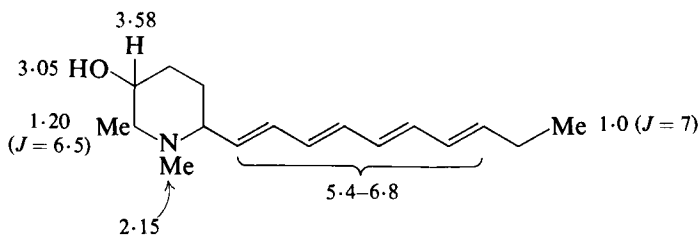
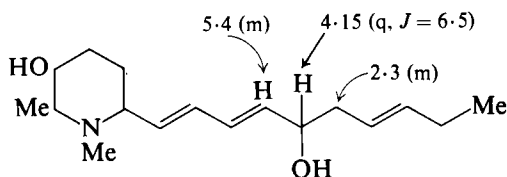
[268]

B. Other alkaloids containing the piperidine moiety

The value (2.5 Hz) of $J_{2,3}$ in octahydrocryptophorine indicates the stereochemistry shown in [269; R = C₁₀H₂₁]. This permits configurational assignment to cryptophorine [270] and cryptophorinine [271].



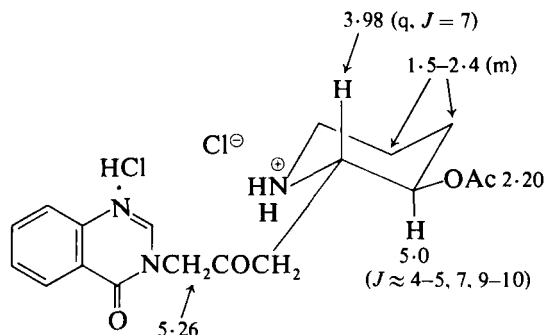
[269]

[270] Cryptophorine (in CDCl₃)

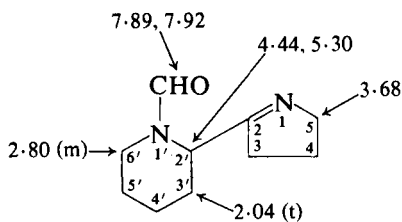
[271] Cryptophorinine

(172) Largely on the basis of the magnitude (7 Hz) of $J_{2,3}$ (obtained by irradiation at the side chain methylene) in febrifugine acetate di-hydrochloride [272] this derivative of the hydrangea alkaloid was assigned the *trans* configuration shown. (173)

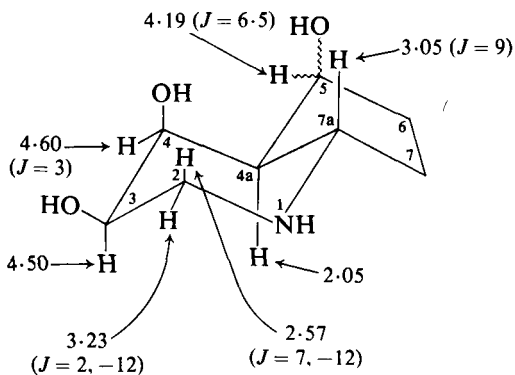
^1H NMR data on the unusual alkaloid smipine (174) and on the octahydropyridine (175) are included in [273] and [274] respectively,



[272] Febrifugine acetate di-hydrochloride (in D_2O)



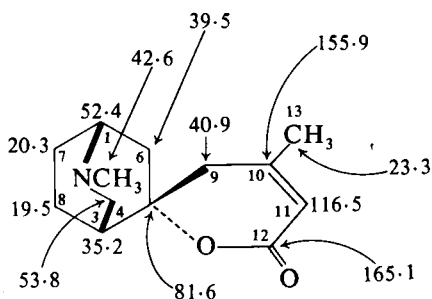
[273] Smipine (in C_6D_6)



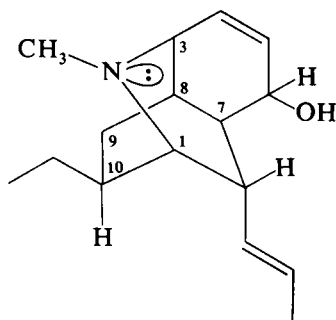
[274] (in D_2O)

$$\begin{aligned} J_{4a, 7a} &= 9 \\ J_{4, 4a} &= 3 \\ J_{2ax, 3} &= 7 \\ J_{3, 4} &= 4.5 \end{aligned}$$

and ^{13}C NMR data on dioscorine in [275]. (176) Nickel acetylacetonate induced ^{13}C shifts for cannivonine [276] have been interpreted in

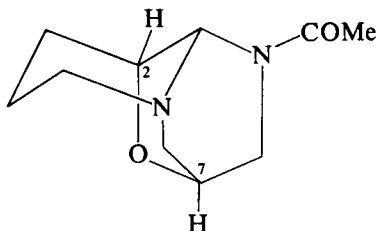


[275] Dioscorine (in CDCl_3 and in C_6D_6)



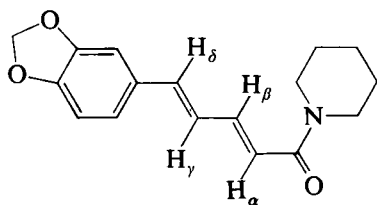
[276] Cannivonine

terms of the *N*-methyl orientation shown with the acetylacetonate lying between the nitrogen and oxygen atoms. These induced shifts for carbon nuclei β to the nitrogen are greater for the anticoplanar arrangement between the nitrogen lone pair and the β carbon, so the large induced shift for C(10) is in agreement with the suggested stereochemistry. (177)



[277] Lepistine

An X-ray study (178) on lepidine [277] has permitted the clarification of its NMR spectrum. The two-proton broadened singlet at δ 4.1

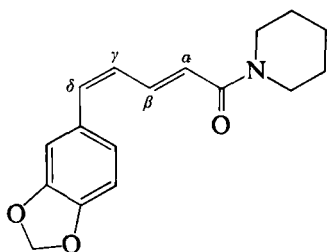


[278] Piperine (in CDCl_3)

$$\begin{aligned} J_{\alpha,\beta} &= 15.2 \\ J_{\beta,\gamma} &= 11.5 \\ J_{\gamma,\delta} &= 15.8 \end{aligned}$$

is due to the 2- and 7-protons. In the spectrum of deacetyl-lepistine these signals appear at δ 4.15 and 3.75.

Vicinal coupling constants (obtained from 300 MHz ^1H spectra) provide a means of differentiating between piperine [278], isochavicine [279], isopiperine [280], and chavicine [281]. (179) ^1H NMR shifts for the related alkaloid [282] (180) and for histrionicotoxin [283] (181) are given with the structures.

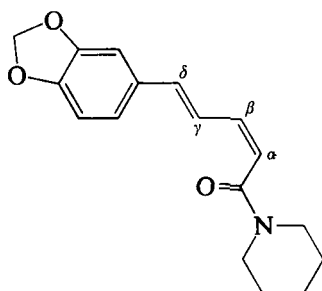


$$J_{\alpha,\beta} = 15.0$$

$$J_{\beta,\gamma} = 11.5$$

$$J_{\gamma,\delta} = 13.0$$

[279] Isochavicine

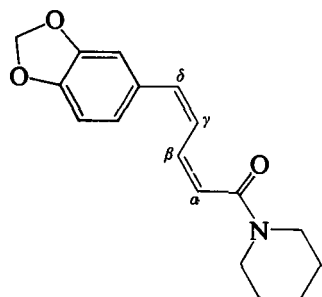


$$J_{\alpha,\beta} = 11.0$$

$$J_{\beta,\gamma} = 11.0$$

$$J_{\gamma,\delta} = 16.3$$

[280] Isopiperine (in CDCl_3)

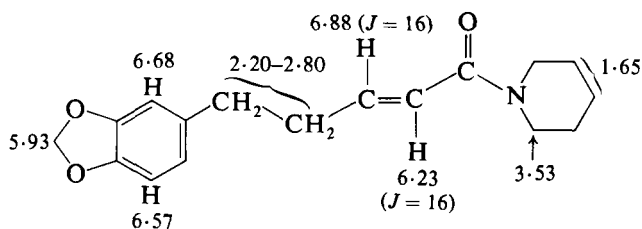


$$J_{\alpha,\beta} = 11.6$$

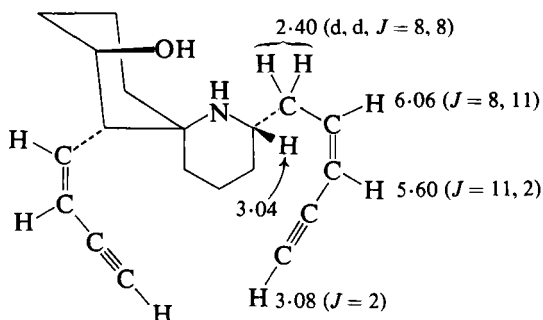
$$J_{\beta,\gamma} = 11.1$$

$$J_{\gamma,\delta} = 12.6$$

[281] Chavicine (in CDCl_3)



[282]

[283] Histronicotoxin (in CDCl_3)

C. Pyridine alkaloids

Full details of the previously discussed (1) ^1H NMR spectra of evonine and neoevonine have now been published. (182) The positions of the acetate functions in evonimine [284] have been determined by comparison (Table V) of the spectrum with that of the pentadesacetyl

TABLE V

NMR spectra (CD_3OD) of evonimine and its desacetyl derivative

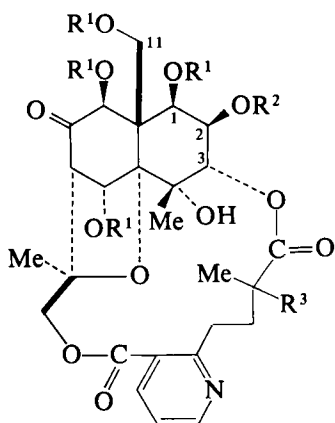
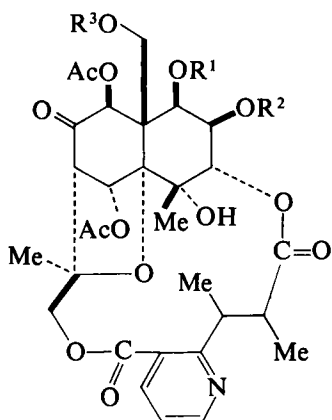
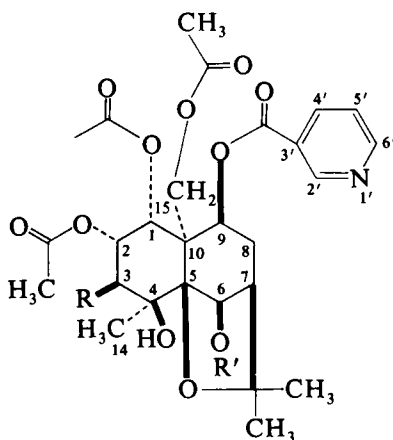
	1-H	2-H	3-H	5-H	6-H	8-H	11-H	15-H
[284]	5.73	5.10	4.97	6.71	3.05	5.55	4.50, 4.86	3.82, 5.81
[285]	4.35	3.70	5.00	5.61	3.00	4.53	4.20	3.92, 5.90

derivative [285]. (183) Comparison of the chemical shifts of the 1-, 2-, 3-, and 11-protons and of the acetyl methyl protons in the spectrum of alatamine [286] with those in the benzoates [287]–[289] derived from evonine (Table VI) permits location of the benzoyl group in alatamine at the C(2) position. (184)

TABLE VI

NMR spectra (CDCl₃) of alatamine [286] and benzoates from evonine [287]–[289]

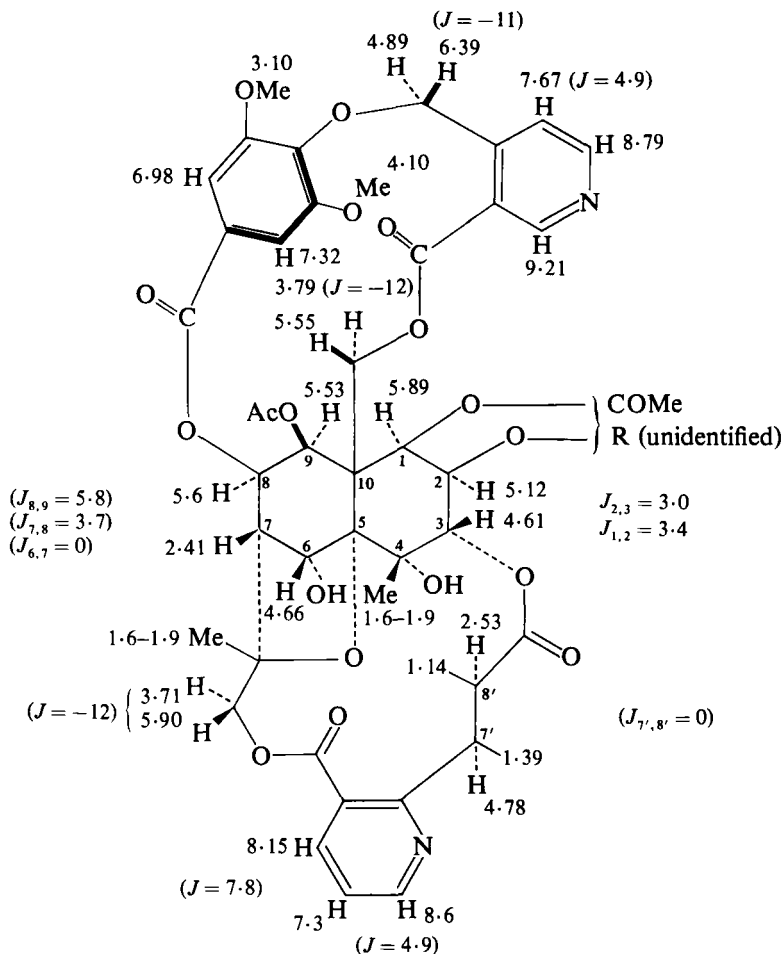
	1-H	2-H	3-H	11-H	CH ₃ CO
[286]	5.90	5.46	5.18	4.85	1.95, 2.10, 2.13, 2.24
[287]	6.07	5.42	4.90	4.70, 5.12	1.52, 2.05, 2.20, 2.26
[288]	5.85	5.57	4.95	4.70, 5.00	1.90, 2.10, 2.10, 2.25
[289]	5.78	5.35	4.75	4.99	1.92, 2.06, 2.25, 2.20

[284; R¹ = R² = Ac, R³ = H] Evonimine[285; R¹ = R² = R³ = H][286; R¹ = Ac, R² = C⁶H₅, R³ = H] Alatamine[287] R¹ = C⁶H₅, R² = R³ = OAc[288] R¹ = R³ = Ac, R² = C⁶H₅[289] R¹ = R² = Ac, R³ = C⁶H₅

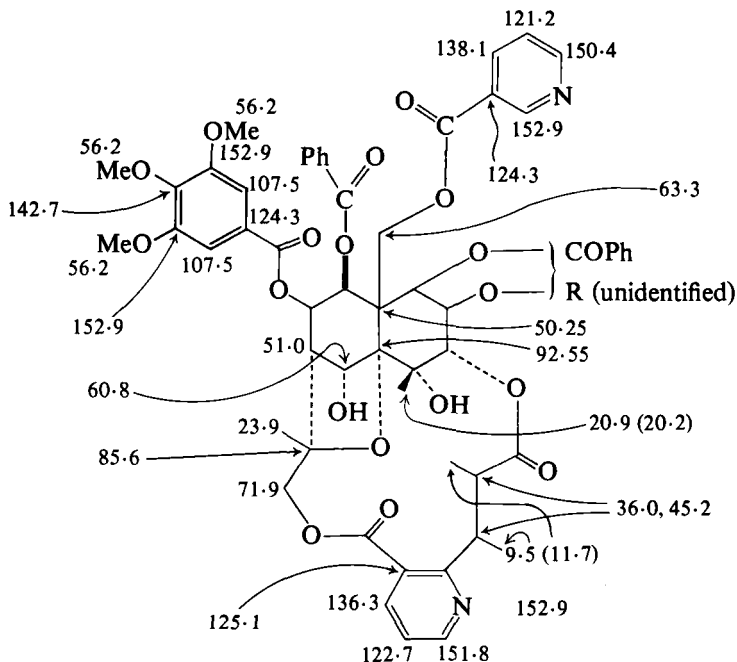
[290; R = OH, R' = Ac] Maytoline

[291; R = H, R' = Ac] Maytine

[292; R = OAc, R' = C⁶H₅] Maytolidine

[293] Cathedulin-4 (in CDCl_3)

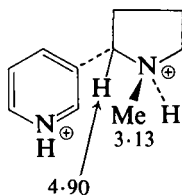
The ^1H NMR spectra (CDCl_3) of maytoline [290], maytine [291], and maytolidine [292] have been extensively analysed and the methyl shifts are noteworthy. In the spectrum (CDCl_3) of [291], for example, the *CMe* protons absorb at δ 1.56, 1.51, and 1.51 and the *COMe* protons at δ 2.26, 2.10, 2.09, and 1.60. The signal arising from the low frequency *COMe* protons at δ 1.60, distinguished from the signals from the *CMe* protons by its sharpness, is assigned to the C(1) *OCOMe* protons since these are expected to be shielded by the pyridine ring. In the spectrum of tetrahydromaytine the methyl group signals are observed at δ 2.22, 2.10, 2.10, 1.82, 1.54, 1.54, and 1.48, showing the

[294] Cathedulin-6 (in CDCl_3)

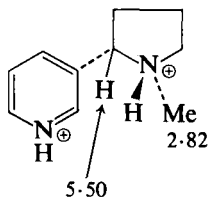
decrease in screening of the C(1) OCOMe signal at δ 1.60 in maytine to δ 1.82 in the tetrahydro-derivative. (185)

¹H NMR data for cathedulin-4 [293] and ¹³C NMR data for cathedulin-6 [294] are as displayed. (186) The $J_{7',8'}$ of ca. 0 Hz is typical of structures containing the evoninate section in a C(13)–C(3) bridge. NMR data on the related cathedulin-2 and cathedulin-8 are available. (187)

NOE studies on nicotine in trifluoroacetic acid, when the rate of deprotonation is slow on the NMR time scale, enable assignment of signals to be made to the diastereoisomeric salts [295] and [296]. The



[295]



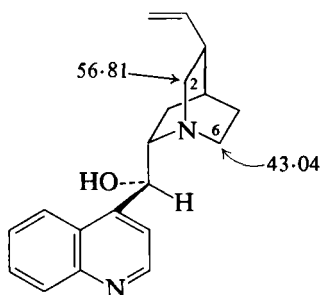
[296]

(in TFA-d)

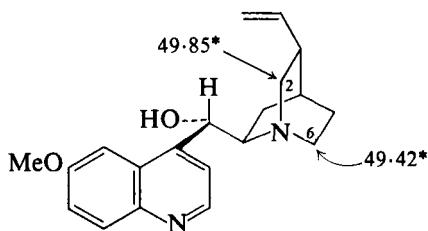
complexities of NOE studies on this type of configurationally mobile systems have been emphasized. (188)

X. QUINOLINE, ACRIDONE, AND QUINAZOLINE ALKALOIDS

The ^{13}C NMR spectra of quinine, quinidine, dihydroquinine, dihydroquinidine, and their N_b -oxides, (2) cinchonidine, 9-epiquinine, 9-epiquinidine, and dihydro-9-epiquinidine (189) have been described. Some of the assignment problems are illustrated with reference to cinchonidine [297] and quinidine [298]. Assignment of the C(2) and

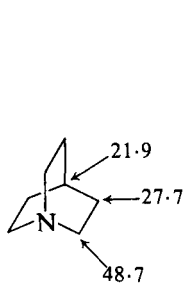


[297] Cinchonidine

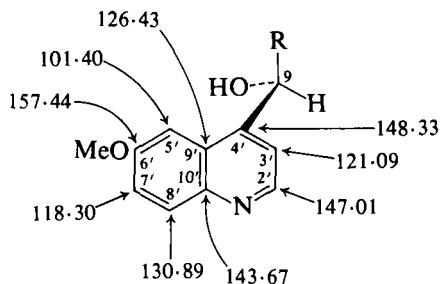


[298] Quinidine

C(6) resonances may be made by reference to the shifts in quinuclidine [299] and to substituent effects on ^{13}C shifts (Table II). In cinchonidine there is a β -effect (high frequency) on C(2) and a γ -effect (low frequency) on C(6) permitting the assignment shown. In quinidine the shifts for C(2) and C(6) are much as in quinuclidine, showing the combination of a high frequency β -effect and a low frequency γ -effect on C(2) and the absence of a γ -effect on C(6). Typical assignments for the aromatic carbon nuclei are given for quinine [300]. These assignments

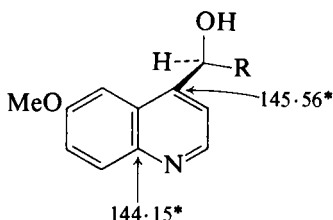


[299]



[300] Quinine

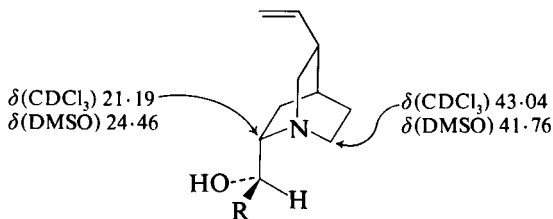
are aided by methoxyl substituent shifts (Table I). The assignment of the C(4') and C(10') signals in the spectra of, for example, quinine [300] and epiquinidine [301], is based on the expectation that the C(10') shift



[301] Epi-quinidine

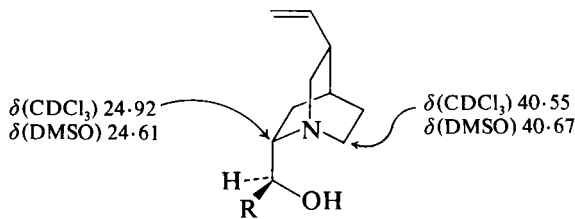
should be least affected by changes in stereochemistry at C(9). (189) In the spectrum of 3(*S*)-3-hydroxyquinidine the C(5) absorption at δ 20.69 shows the γ -effect involving the hydroxyl function. (190)

Marked solvent effects [$\delta(\text{CDCl}_3) - \delta(\text{DMSO})$] on some of the ^{13}C shifts in the spectrum of cinchonidine (*erythro*-series) [302] but not in



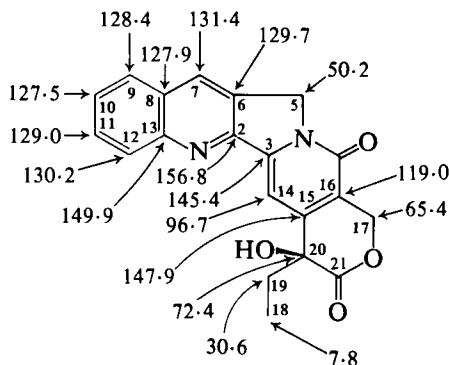
[302] Cinchonidine

that of epiquinine (*threo*-series) [303] are attributed to hydrogen bonding with the hydrogen bond still present in a DMSO solution of the *threo*-compound. (189)



[303] Epi-quinine

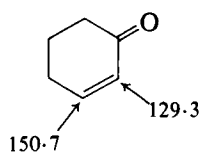
^{13}C NMR data on camptothecin are displayed in [304]. (191) The C(6) and C(2) shifts in [304] are to higher frequency than those for the corresponding nuclei in quinoline [δ C(2) 150.9, δ C(3) 121.5] as a



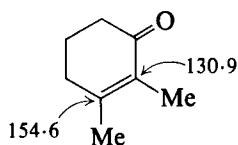
[304] Camptothecin (in DMSO)

[Shifts relative to external TMS, $\delta(\text{DMSO}) = \delta(\text{TMS}) + 39.6$ ppm]

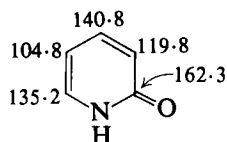
result of the attached substituents. The shift of C(16) differs little from that in 2-pyridone but that for C(15) is to higher frequency. (Compare shifts in [305], [306], and [307].) (192)



[305]

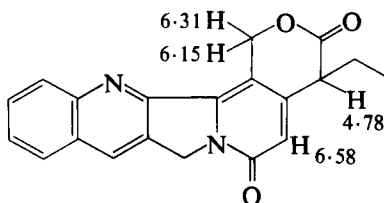


[306]



[307]

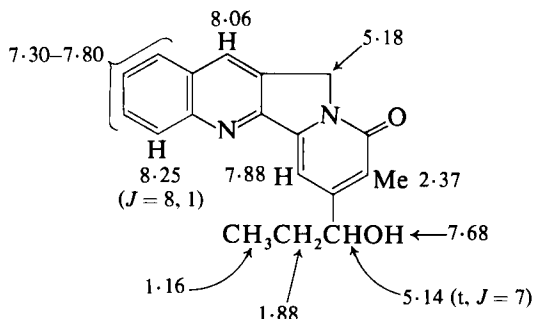
Comparison of the chemical shifts of the C(17) methylene protons (δ 5.55, 5.45) in desoxycamptothecin [304; C(20)-OH replaced by H] with those in isodesoxycamptothecin [308] reveals the higher frequency



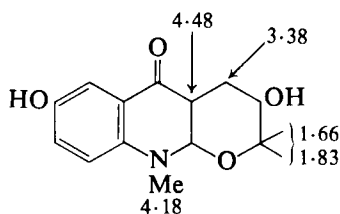
[308] Isodesoxycamptothecin (in CDCl_3)

absorption of these protons in isodesoxycamptothecin due to their proximity to the quinoline nitrogen atom. The methine proton adjacent to the lactonic carbonyl group in the iso-compound also absorbs at higher frequency. (193)

For the purposes of reference the NMR spectra of mappicine [309], (194) ribalinidine [310], (195) methylbicycloatalaphylline [311], (196) and alkaloid A from *Atalantia ceylanica* [312] (197) are given in the structures. A *trans* relationship between the C(11') hydroxyl and the

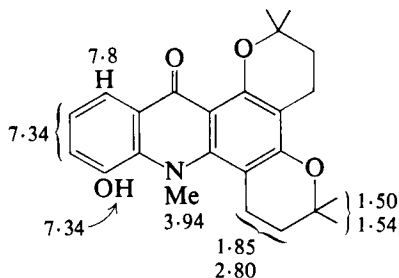


[309] Mappicine (in C₃D₃N)

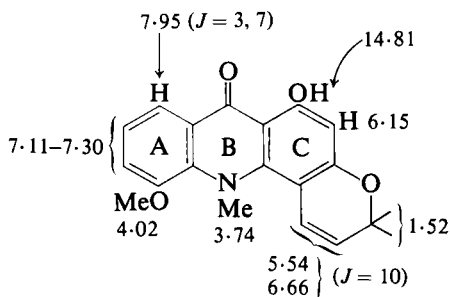


Ar-H 7.86-8.06

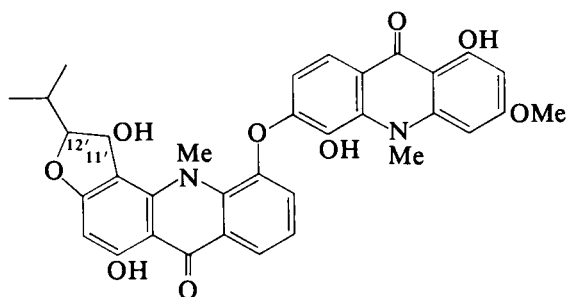
[310] Ribalinidine (in TFA)



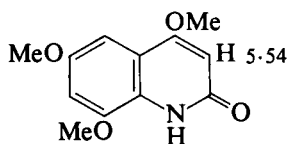
[311] Methylbicycloatalaphylline
(in CDCl₃ + few drops DMSO-d₆)

[312] (in CDCl_3)

C(12') isopropyl group in atalanine [313] was based on the value (7 Hz) of $J_{11',12'}$. (198) The ^1H NMR spectra of some 2-quinolones are given in [314] (199) and [315]. (200)

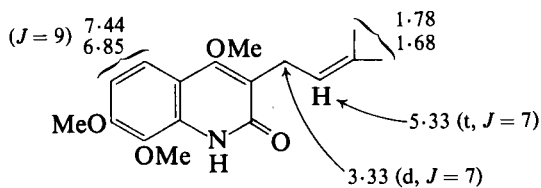
($J_{11',12'} = 7$)

[313] Atalanine



OMe 2.88
2.98
3.13
Ar-H 5.94 } $J = 2$
6.11

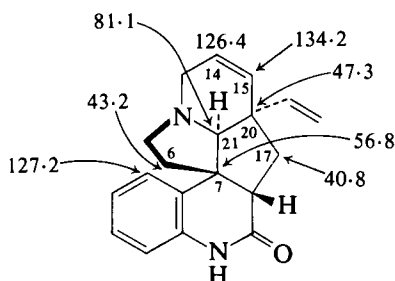
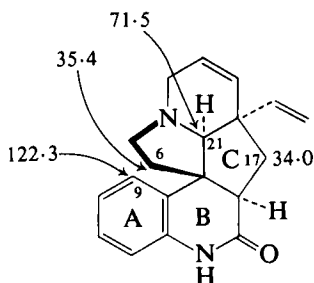
[314] Halfordamine (in TFA)



OMe 3.90
3.95
3.95

[315] (in CDCl_3)

In the SFORD ^{13}C NMR spectrum of meloscine [316], in which the decoupler frequency is at the low frequency end of the ^1H NMR spectrum, the double bond carbon nuclei are differentiated from the aromatic methines by the lower residual coupling of the former signals. The C(20) absorption shows long range coupling characteristic of carbon nuclei attached to vinyl groups, permitting a distinction to be made between C(20) and C(7). C(14) is differentiated from C(15) by C(20) substituent effects. The *b/c-trans* stereochemistry of epimeloscine [317] ensures the close approach of C(9)–H and C(21)–H resulting in a

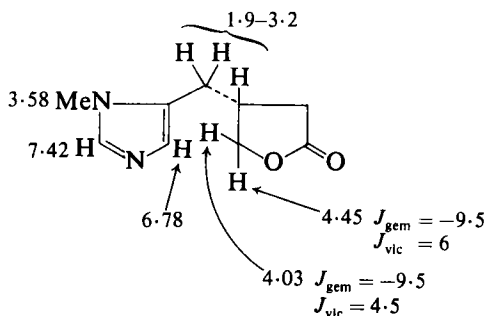
[316] Meloscine (in CDCl_3)

[317] Epimeloscine

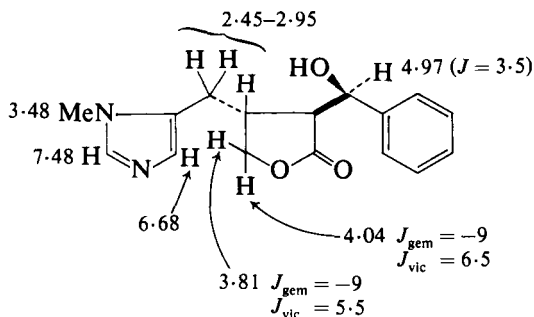
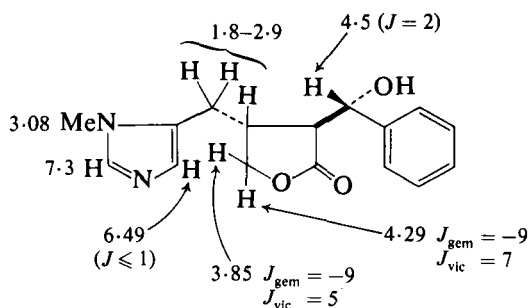
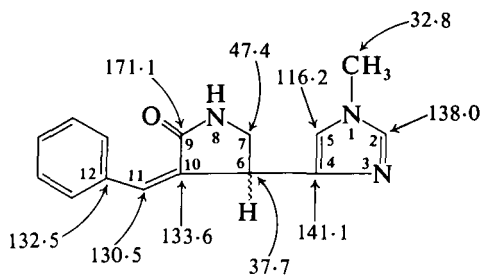
strong reciprocal γ -effect between C(9) and C(21) (cf. shifts of C(9) and C(21) in [316] and [317]). Similar reciprocal γ -effects between C(6) and C(17) are observed in epimeloscine. (201)

XI. IMIDAZOLE ALKALOIDS

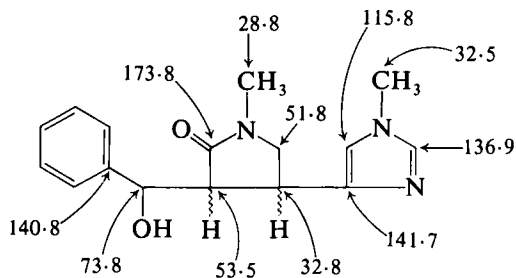
The NMR spectra of some *Pilocarpus* alkaloids, pilosinine, isopilosine, and epi-isopilosine, are summarized in structures [318], [319],

[318] Pilosinine (in CDCl_3)

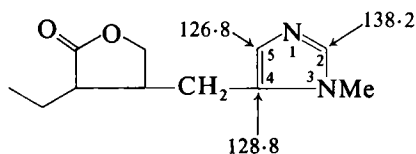
T. A. CRABB

[319] Isopilosine (in DMSO- d_6)[320] Epi-isopilosine (in DMSO- d_6)[321] Anantine (in CDCl_3)

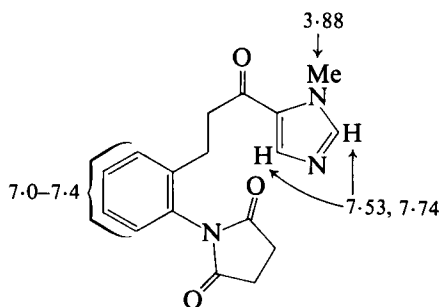
and [320]. (202) Comparison of the NMR spectra of anantine [321] and cynometrine [322] with those of pilocarpine [323] and other imidazoles establishes the position of attachment of the lactam ring to C(4) of the imidazole nucleus in [321] and [322]. (203) Spectra of dehydroisolongistrobine [324], isolongistrobine [325], (204) paragraccine [326], (205) and alchorneine [327] (206) are given for reference.



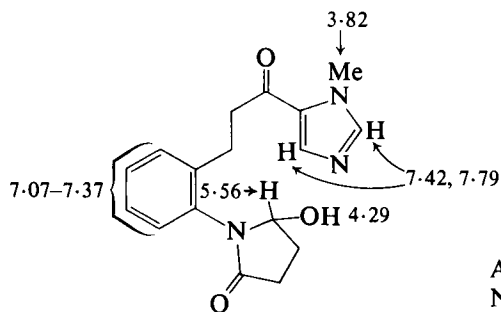
[322] Cynometrine



[323] Pilocarpine

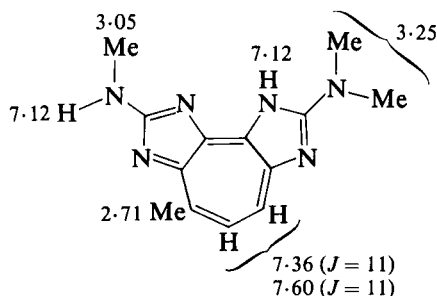
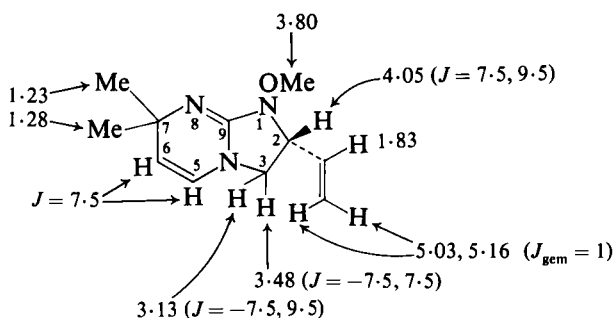


ArCH₂CH₂CO } 2.93 (4H)
Succinimide } 2.7-3.2 (4H)

[324] Dehydroisolongistrobine (in CDCl₃)

ArCH₂CH₂CO } 2.17-3.35 (8H)
NCOCH₂CH₂ } 2.17-3.35 (8H)

[325] Isolongistrobine

[326] Paragracine (in DMSO-d_6)[327] Alchorneine (in CDCl_3)

XII. INDOLE ALKALOIDS

The NMR spectra of the major groups of indole alkaloids are discussed below. Section J describes the NMR spectral characteristics of a variety of indole alkaloids which, although biogenetically related to alkaloids in Sections A–I, are discussed separately because of formal structural dissimilarities.

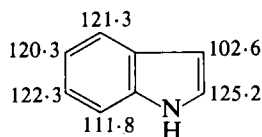
A. Simple indoles, carbazoles, carbolines, and physostygmine type alkaloids

The original assignment (207) of ^{13}C chemical shifts to C(5) and C(6) in indole and in a number of ring A unsubstituted tetrahydrocarboline alkaloids should be reversed. (208) Reassignment of ^{13}C shifts to a variety of methyl substituted indoles has been made, and the methyl substituent effects relative to indole [328] are given in Table VII. (209) These reassigned shifts are taken from the literature and converted using $\delta(\text{TMS}) = \delta(\text{CS}_2) + 192.8$ ppm. Dilution effects on ^{13}C shifts in these indoles have been noted. (209)

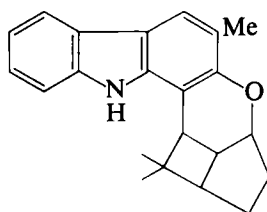
TABLE VII

Methyl substituent effects in indoles (ppm relative to indole)

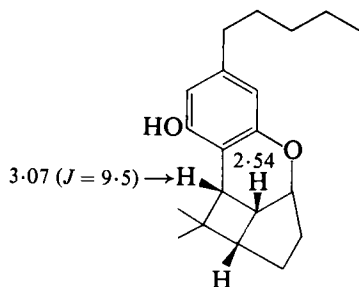
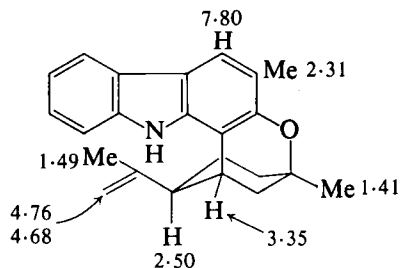
The structure of bicyclomahanimbine has been revised to [329] (210) which resembles the structure of cannabicyclol [330]. (211) The structure of curryanin [331] has also been revised. (210)



[328]

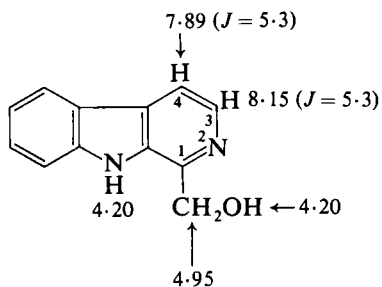


[329] Bicyclomahanimbine

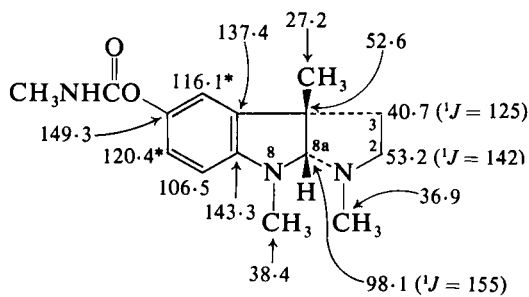
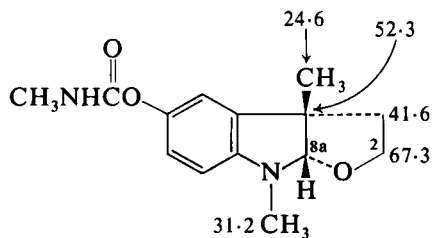
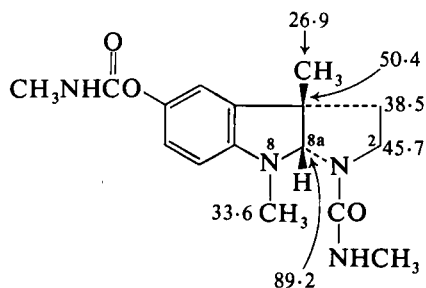
[330] Cannabicyclol (in CDCl₃)[331] Curryanin (in CDCl₃)

¹H NMR parameters for 1-hydroxymethyl- β -carboline from *Picrasma ailanthoides* PLANCHON (212) are shown in [332].

Structurally diagnostic ¹³C shifts are observed for C(2), C(8a), and 8-CH₃ in the spectra of physostigmine [333] and related alkaloids [334] and [335]. (213)



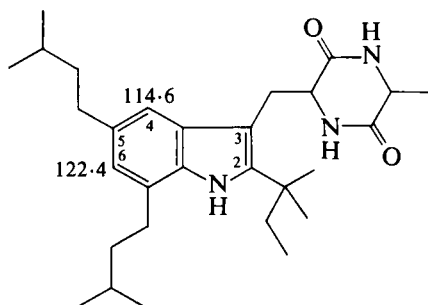
Ar-H 6.99–8.15

[332] (in DMSO- d_6)[333] Physostigmine (in CHCl_3)[334] Physovenine (in CHCl_3)

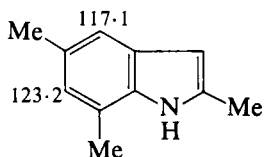
[335] Eseramine (in DMSO)

B. Mould metabolites

The ^{13}C shifts at 114.6 and 122.4 in hexahydroechinulin [336] may be assigned to C(4) and C(6) respectively on the basis of the shifts in 2,5,7-trimethylindole [337] and utilizing the value of the 3-methyl



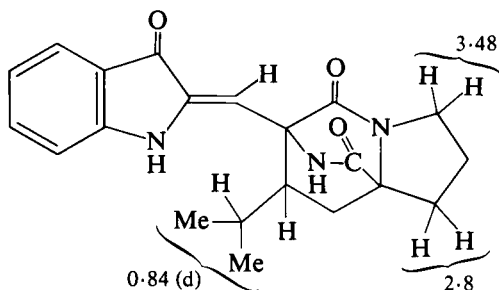
[336] Hexahydroechinulin (0.25 M in CDCl_3)



[337] 2,5,7-Trimethylindole (0.4 m in CDCl_3)

substituent effect (-1.9 ppm relative to indole) on C(4) (Table VII). In bromohexahydroechinulin the bromine substituent was located at C(4) on the basis of the ^{13}C shifts [C(6) 124.0, C(4) 116.8, and C(6) 124.6] and the expected *meta* shielding parameter of a bromo substituent ($+2.2$ ppm). (209)

The ^1H NMR spectrum of brevianamide C [338] differs from that of

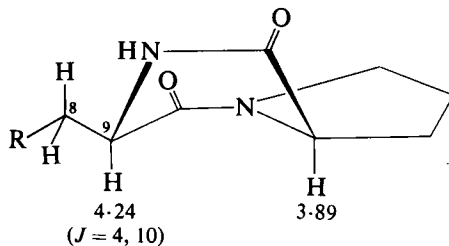


[338] Brevianamide C (in CDCl_3)

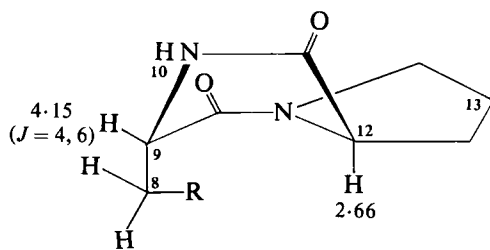
NH	7.98
	7.34
Ar-H	7.7–6.8

its geometrical isomer brevianamide D by the doublet absorption for the CHMe_2 protons in [338] replaced by the double doublet absorption in its isomer. In addition brevianamide D shows a high frequency NH absorption at δ 10.40. (214)

The conformations [339] and [340] ($\text{R} = 3\text{-indolyl}$) have been suggested for the diastereoisomeric diketopiperazines related to the



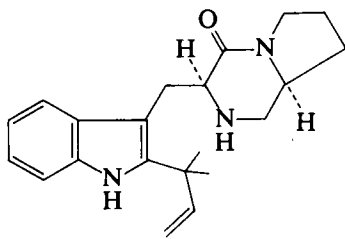
[339] (in CDCl_3)



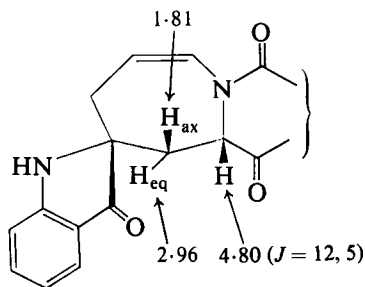
[340] (in CDCl_3)

natural product [341]. The shift of the 12-proton is diagnostic of C(9) stereochemistry and accordingly [341] is considered to adopt conformation [339] (δ 12-H 4.05).

Details of the ^1H NMR spectrum of austamide have been given previously. (1) The high frequency shift of the 9-proton in the spectrum



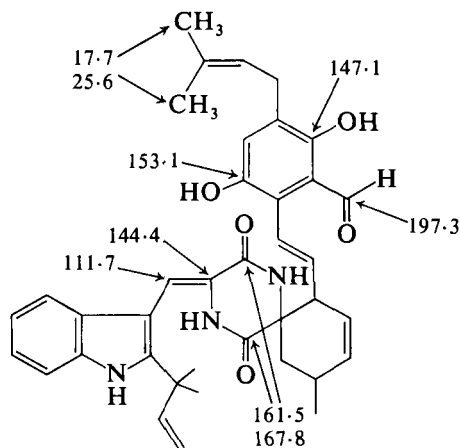
[341]



[342] Austamide (in CDCl_3)

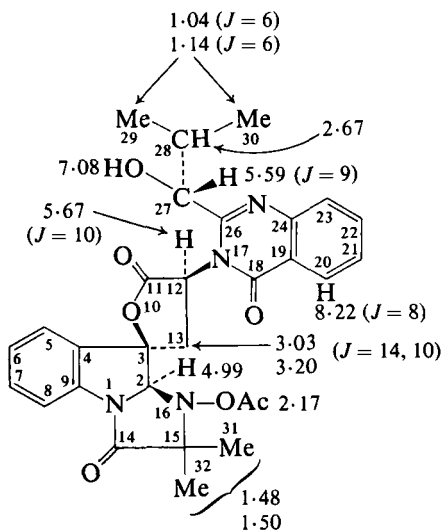
of austamide, relative to the corresponding absorption in [339] and [340], is presumably a result of the anisotropy of the ψ -indoxyl carbonyl group indicating the stereochemistry shown in [342]. (215)

^{13}C NMR data for a substance isolated from *Aspergillus amstelodami* are given in [343]. (216) ^1H NMR parameters for eight metabolites from



[343] (in DMSO-d_6)

Aspergillus fumigatus have been reported (217) and data for one of these (isotryptoquivaline) are recorded in [344].

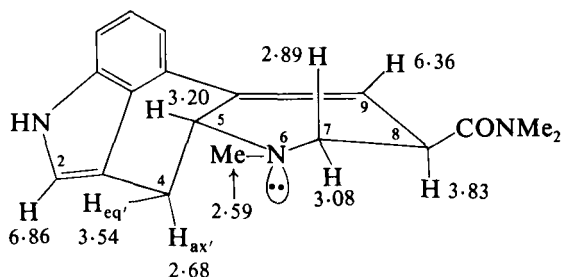


Ar-H 7.33–7.93(7H)

[344] Isotryptoquivaline (in CDCl_3)

C. Ergot alkaloids

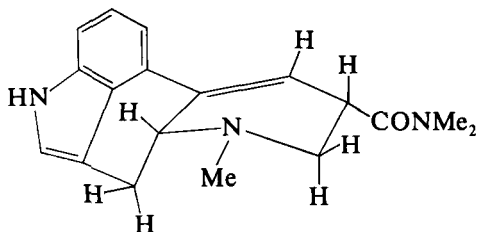
The conformation of the D-ring in the dimethylamides of lysergic acid and of isolysergic acid has been studied by ^1H NMR spectroscopy. The lysergic acid derivative exists in the conformation [345] with the half-chair D-ring and the pseudo-equatorial amide function. This conformation is supported by allylic coupling between the 5- and 9-protons of



[345] D-Lysergic acid dimethylamide (in CDCl_3)

$J_{2,4ax'} = 1.6$
$J_{2,4eq'} = 0.5$
$J_{4ax',4eq'} = -14.8$
$J_{4ax',5ax'} = 11.5$
$J_{4eq',5ax'} = 5.5$
$J_{5ax',8ax'} = 3.8$
$J_{5ax',9} = 1.0$
$J_{7ax',7eq'} = -11.2$
$J_{7ax',8ax'} = 10.4$
$J_{7eq',8ax'} = 5.3$
$J_{7eq',9} = 1.0$

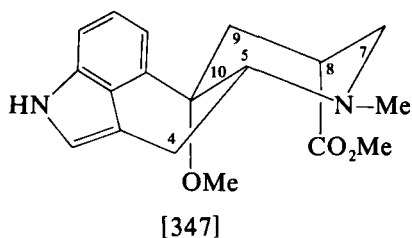
1.0 Hz and the homoallylic coupling of 3.8 Hz between the 5- and 8-protons. In addition the $7eq'$ -proton and the 9-proton are long range coupled (1.0 Hz), consistent with the presence of the planar W pathway in the half chair shown. Other data are displayed in the structure [345]. A similar detailed ^1H NMR investigation of the isolysergic acid derivative has been made which supports conformation [346] with the



[346] D-Isolysergic acid dimethylamide

other half-chair ring-D conformation and the pseudo-equatorial amide function. (218)

On going from the lysergic acid system to the dihydrolysergic acid system the problem of assigning the *cis* or *trans* nature of the C/D ring junction arises. A complete analysis of the 270 MHz ^1H NMR spectra of the four stereoisomeric 10-methoxy-dihydrolysergic acids has been made and the coupling constant data permit the assignments shown in [347]–[350]. (219)



7ax-H 2.29

7eq-H 3.59

8eq-H 2.66

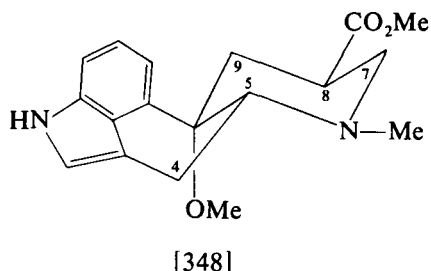
9ax-H 1.78

9eq-H 3.58

4ax-H 2.92

4eq-H 3.11

5ax-H 2.25

 $J_{4ax,4eq} = -14.4$ $J_{4ax,5ax} = 11.4$ $J_{4eq,5ax} = 4.1$ $J_{2,4ax} = 1.2$ 

7ax-H 2.31

7eq-H 3.31

8ax-H 3.13

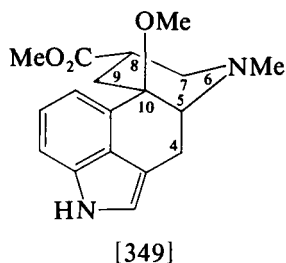
9ax-H 1.65

9eq-H 3.24

4ax-H 3.02

4eq-H 3.19

5ax-H 2.35

 $J_{4ax,4eq} = -14.4$ $J_{4ax,5ax} = 11.3$ $J_{4eq,5ax} = 4.4$ $J_{2,4ax} = 1.6$ 

7ax-H 2.81

7eq-H 2.97

8ax-H 3.37

9ax-H 1.86

9eq-H 2.17

4ax-H 3.07

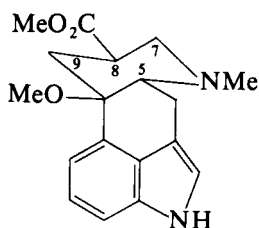
4eq-H 3.12

5eq-H 3.54

 $J_{4ax,4eq} = -15.1$ $J_{4ax,5} = 11.6$ $J_{4eq,5} = 5.2$

^1H NMR studies permitting stereochemical assignment to the structurally related festuclavine [351] and its stereoisomers costaclavine, epicostaclavine, and pyroclavine, with emphasis on the analysis of the 9- and 4-methylene proton signals, have also been reported. (220)

The stereochemistry of the 10-methoxy-dihydrolysergic acids [352]–[355] has been confirmed by ^{13}C NMR spectroscopy. (219) Com-



[350]

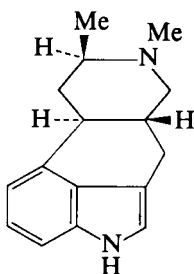
7 _{ax} -H	2.29
7 _{eq} -H	2.98
8 _{ax} -H	2.62
9 _{ax} -H	1.73
9 _{eq} -H	3.27
4 _{ax} -H	3.33
4 _{eq} -H	3.09
5 _{ax} -H	2.55

$$J_{4ax,4eq} = -16.3$$

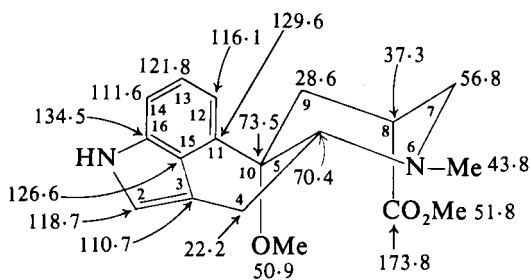
$$J_{4ax,5} = 2.5$$

$$J_{4eq,5} = 3.1$$

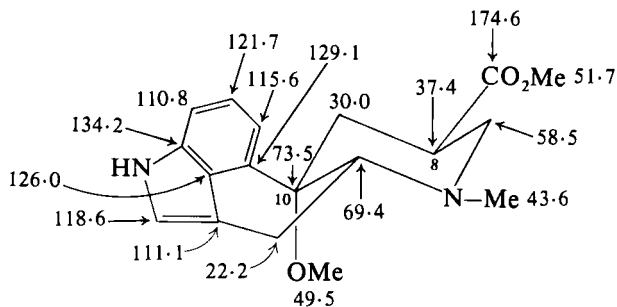
$$J_{2,4ax} = 1.8$$



[351] Festuclavine

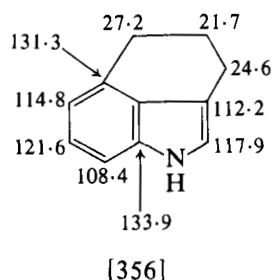
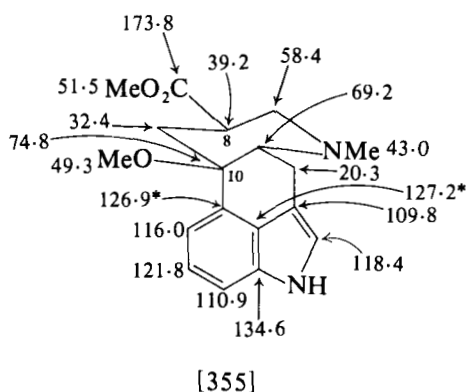
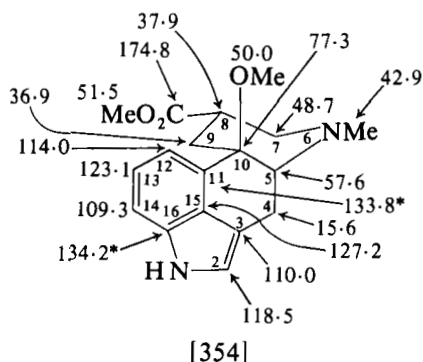


[352]

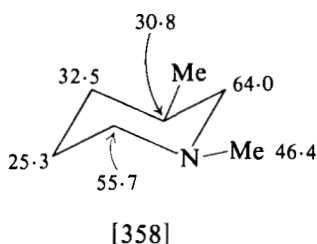
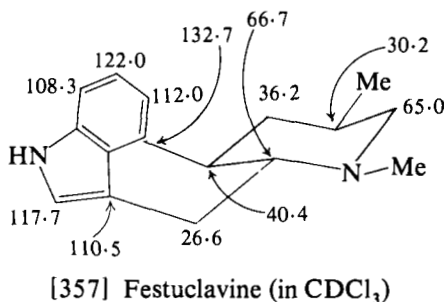


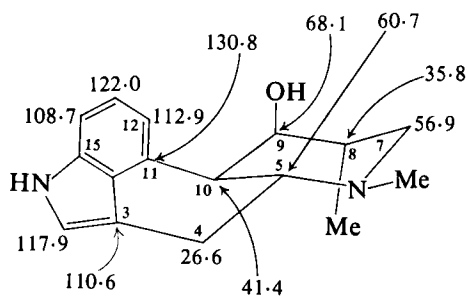
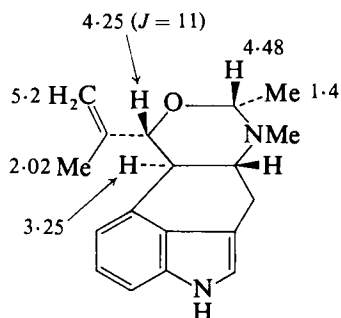
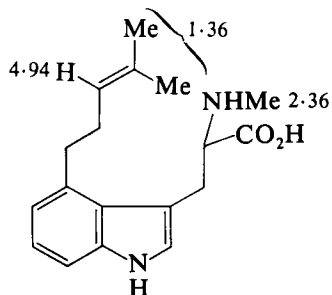
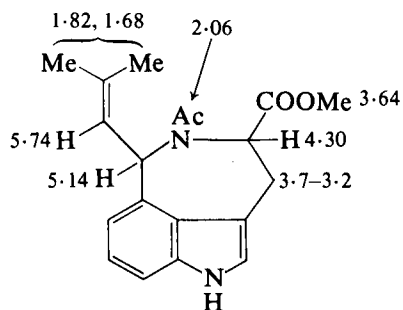
[353]

parison of the spectrum of the 8 α ,10 β -isomer [354] with that of the 8 β ,10 β -isomer [355] shows a set of diagnostically important ^{13}C shifts. C(11) in [355] absorbs 6.9 ppm to low frequency of C(11) in [354] consistent with the axial nature of C(11) in [355], and the related change in shift of C(4) is noted. Other shift differences involve C(5) and C(7) which are dependent *inter alia* upon CH_2Ar orientation.



To assist ^{13}C shift assignments in the spectra of the ergot alkaloids the spectrum of the cyclohexanoindole [356] was studied and showed low frequency shifts of C(2) and C(6) (relative to those of corresponding ^{13}C nuclei in 3- and 4-methylindole) as a result of the strain imposed by the trimethylene bridge. (221) The equatorial C-methyl group in festuclavine [357] is suggested from a comparison of the ^{13}C NMR spectrum of [357] with that of 1,3-dimethylpiperidine [358]. In fumigaclavine [359]



[359] Fumigaclavine B (in pyridine-d₅)[360] (in CDCl₃)[361] (in CD₃COOD)[362] (in CDCl₃)

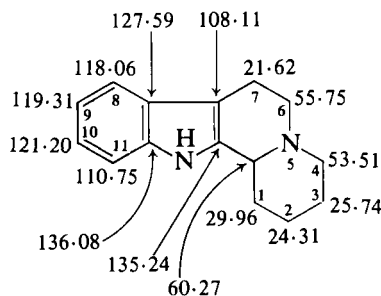
C(7) absorbs to low frequency of C(7) in festuclavine as a result of the β -effect of the axial hydroxyl group and the reduced β -effect of the axial methyl (Table III).

Some ^1H NMR data for ergot derivatives of differing types—paspaclovine [360], (222) *N*-methyl-4-dimethylallyltryptophan [361], (223) and the *N*-acetyl methyl ester of clavicipitic acid [362] (224)—are shown in the structures.

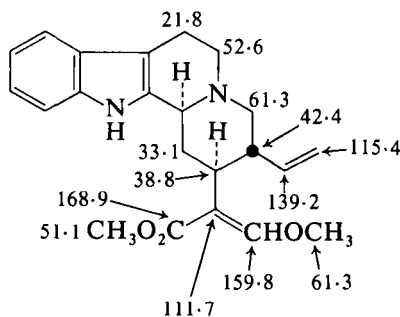
D. Yohimbine, corynantheine, ajmalicine, and related alkaloids

1. ^{13}C NMR spectra

The ^{13}C shifts of the octahydroindolo[2,3-*a*]quinolizine [363] provide an important basis for the analysis of the ^{13}C NMR spectra of the yohimbine and related group of alkaloids. The shifts shown in [363] (208) represent a revision of those originally made for C(9) and C(10) (225) since these were based on misassigned signals in the spectrum of indole itself (see Section XII.A). In addition, Wenkert (226) has suggested the interchange of the shifts for C(4) and C(6) and the correction has been made in [363].

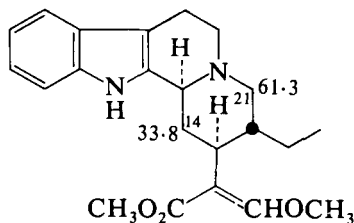


[363] (in CDCl_3)

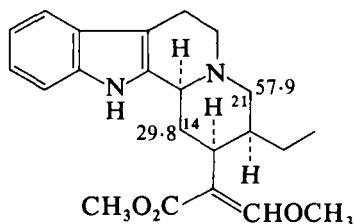


[364] Corynantheine (in CDCl_3)

The shift assignments to corynantheine [364], (2) dihydrocorynantheine [365], and corynantheidine [366] (103) are easily made

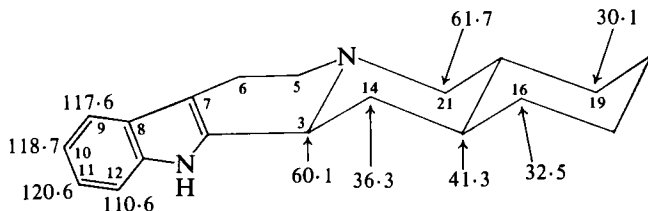


[365] Dihydrocorynantheine (in CDCl_3)



with reference to the shifts for [363]. In corynantheidine the C(21) and C(14) shifts show the β - and γ -effects respectively of the axial ethyl group. In these alkaloids the C(18) and C(19) shifts are diagnostic of the axial/equatorial orientation of the ethyl group.

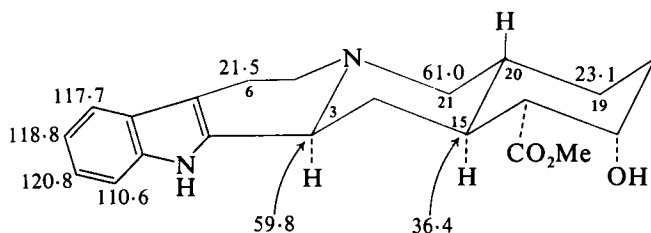
On going from [363] to the pentacyclic system exemplified by yohimbane [367] similar $\Delta\delta$ values are encountered for the C(14) and



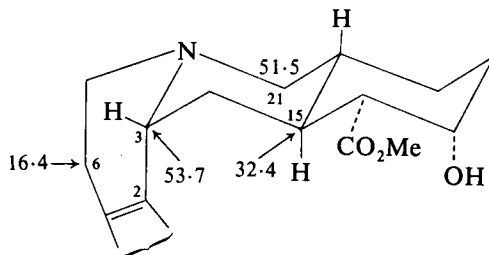
[367] Yohimbane (in CDCl_3)

C(21) nuclei. (226) In addition [367] shows the marked γ -anti-periplanar effect of the nitrogen atom on the C(19) shift [cf. C(16) shift]. (227)

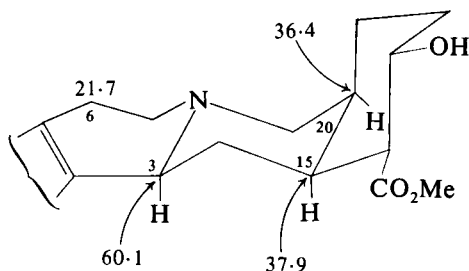
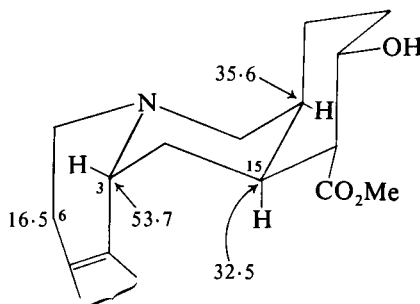
The four major stereochemical types of yohimbine alkaloids are illustrated by yohimbine (normal) [368], pseudoyohimbine (pseudo) [369], α -yohimbine (allo) [370], and 3-*epi*- α -yohimbine (epiallo) [371]. Of particular diagnostic importance are the C(3), C(6), and C(15) shifts



[368] Yohimbine (in CDCl_3)



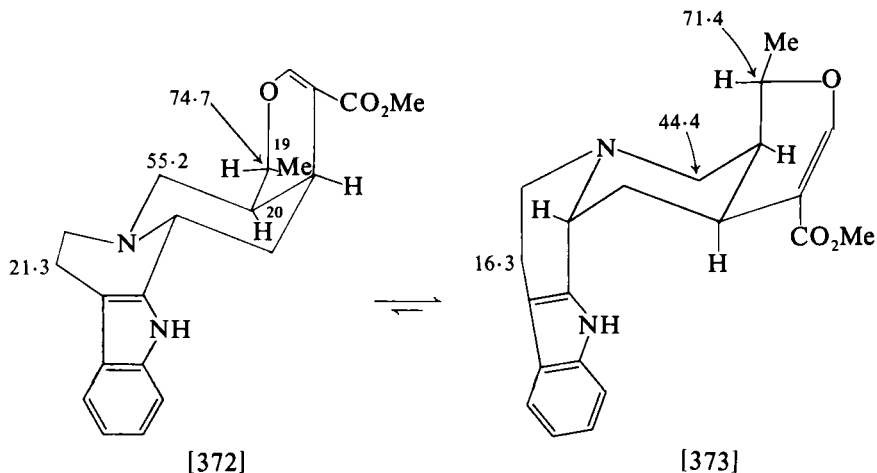
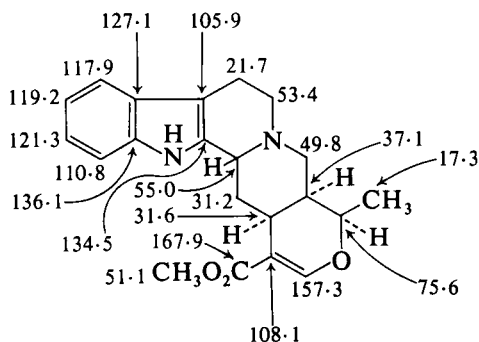
[369] Pseudoyohimbine (in CDCl_3)

[370] α -Yohimbine (in CDCl_3)[371] 3-*epi*- α -Yohimbine (in CDCl_3)

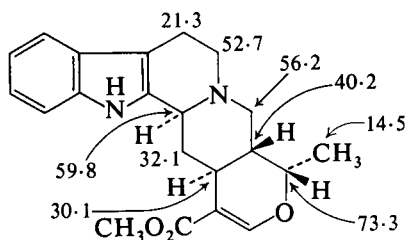
which are to lower frequency in the *cis*-C/D structures as a result of γ -effects. Among these γ -effects are those induced by π -bond-H interactions [see γ -effect on C(15) by C(2) in pseudoyohimbine].

Substituent effects in ring E may be illustrated with reference to yohimbine [368]: here the β -effect of the equatorial methoxycarbonyl appears to be *ca.* 2 ppm which suggests approximately equal γ -effects of the axial hydroxyl on C(15) and C(19).

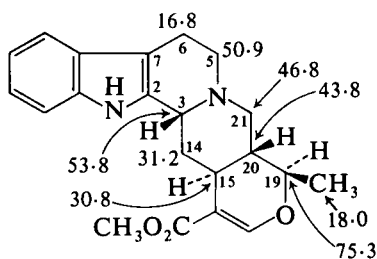
Akuammigine exists in solution at room temperature as an equilibrium mixture of *trans*-C/D and *cis*-C/D conformations [372] and [373], and at low temperatures the ^{13}C NMR spectrum shows signals for both conformations. Comparison of the shifts of C(6) and C(14) in the room temperature spectrum (δ 19.2 and 50.3) with those in the separate conformations permits an estimation of the position of equilibrium. (226) Iso-3-raunitiveine [374] (228) is shown to adopt the *trans*-C/D conformation by its similar C(3), C(5), and C(6) shifts to those in [372]. For reference purposes, particularly in connection with the analysis of the ^{13}C NMR spectra of the roxburghines (Section XII.K), ^{13}C shifts for ajmalicine (normal series) and for 3-iso-19-*epi*-ajmalicine (pseudo series) are shown in [375] and [376]. (226)

Akuammigine (in CDCl_3)

[374] Iso-3-rauniticine



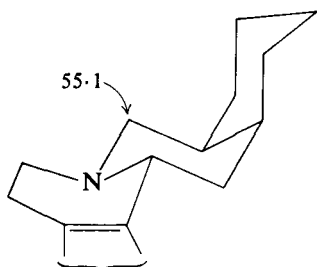
[375] Ajmalicine



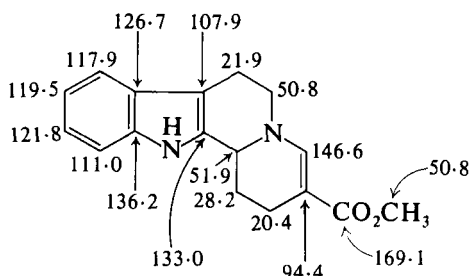
[376] 3-Iso-19-epi-ajmalicine

γ -Effects originating from heteroatom lone-pair-H interactions appear to be of comparable magnitude to the more commonly observed effects from H-H interactions (see similar C(21) shifts in epialloyohim-

bane [377] and in *c/D-trans* akuammigine [372]). (226) Other ^{13}C NMR data on Rauwolfia alkaloids are available. (229)

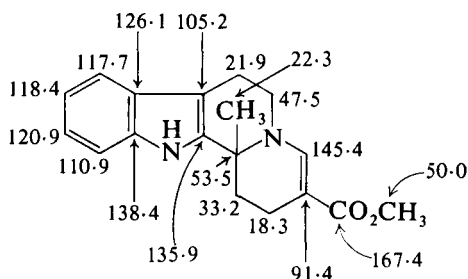


[377] Epialloyohimbane



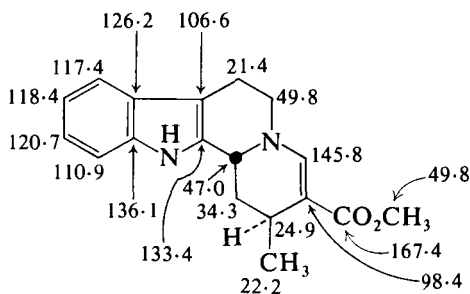
[378] (in CDCl_3)

The stereochemistry of the tetracycles [378], [379], and [380] has also been assigned by ^{13}C NMR analysis. Diminished γ -effects of the angular methyl group in [379] are observed as a result of flattening of

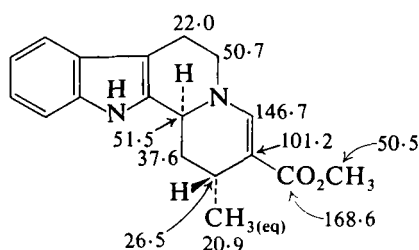


[379] (in DMSO-d_6)

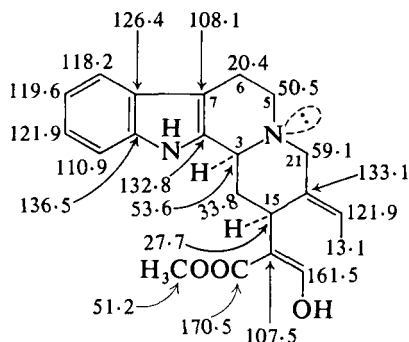
the system by the presence of the double bond. (226) Shifts for the epimer of [380] are given in [381]. (230)



[380] (in DMSO-d_6)

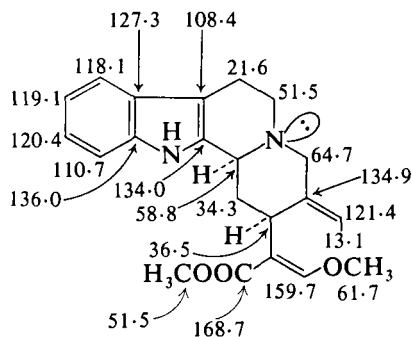


[381]



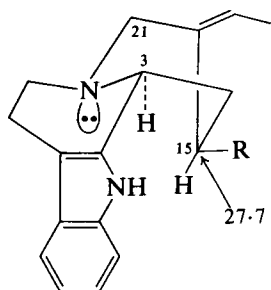
[382] Geissoschizine

The ^{13}C NMR spectrum of geissoschizine is given in [382]. (231) It has been known for some time that geissoschizine [382] possesses the $3\alpha\text{-H-cis}$ -quinolizidine structure ($3\text{-H } \delta 4.5$, $J = 11$ and 2 Hz) and *O*-methylgeissoschizine [383] the $3\alpha\text{-H-trans}$ -quinolizidine structure (absence of absorption between $\delta 3.8$ and 4.6). Confirmation of this is

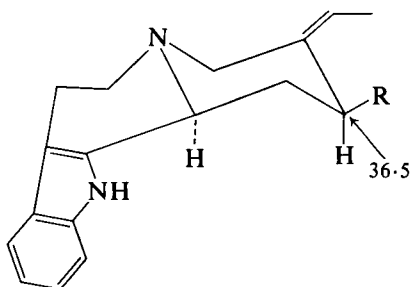
[383] *O*-Methylgeissoschizine

provided by the ^{13}C NMR spectral data summarized in [382] and [383]. The shifts in the *O*-methyl compound differ little from those of dihydrocorynantheine [365] but those of geissoschizine at C(3) and at C(6) are typical of the *cis-c/D* structure. The C(15) shift in geissoschizine is unusual and this has been explained in terms of the conformation [384]. In [384] there is close approach of C(15) to the nitrogen lone pair which will shield C(15) (compare sparteine and isosparteine). *O*-Methylgeissoschizine adopts the *trans*-fused conformation [385]. (231)

The ^{13}C NMR spectra of a range of alkaloids and derivatives bearing an oxo function at C(21) have been recorded ([386]–[391]). In the

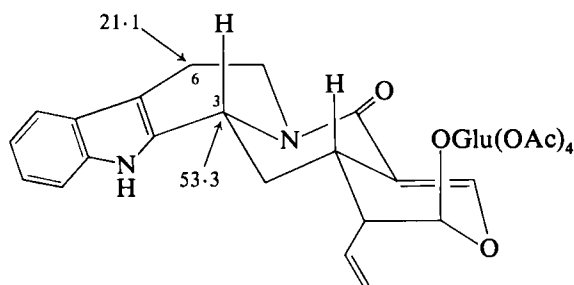


[384]

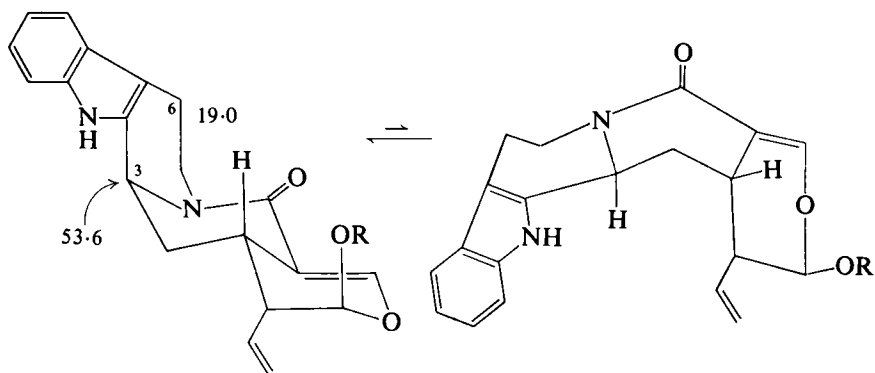


[385]

spectra of the quinolizidone derivatives [386] and [387] \Rightarrow [388] the shift of C(3) is of little diagnostic value in evaluating the *cis* or *trans* nature of the C/D ring fusion since the $-N-C(O)-C=C-$ moiety flattens part of the molecule with a consequent reduction in the magnitude of the γ -effects observed in, for example, *cis*-fused yohimbine derivatives. The C(6) shifts for [386] and [387] \Rightarrow [388] do, however, point to a *trans*-



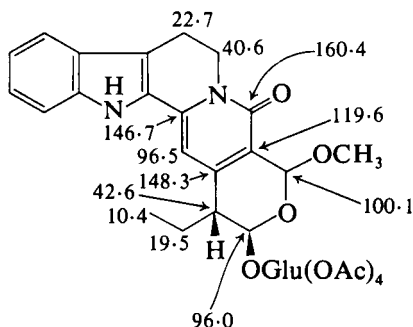
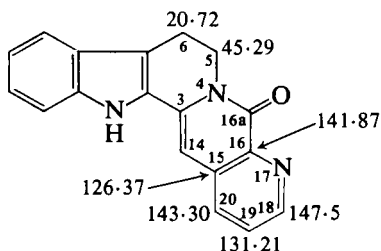
[386]



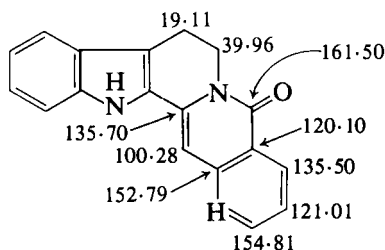
[387]

[388]

c/D fusion for [386] and an equilibrium favouring the *cis*-c/D conformation for [387] = [388]. (232) ^{13}C shifts for [389] (233) and for nauclefine [390] and isonauclefine [391] (234) are displayed in the structures.

[389] (in CDCl_3)

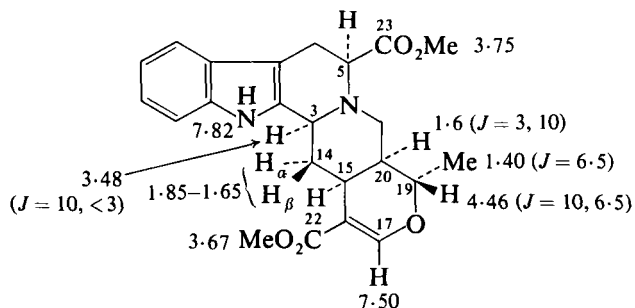
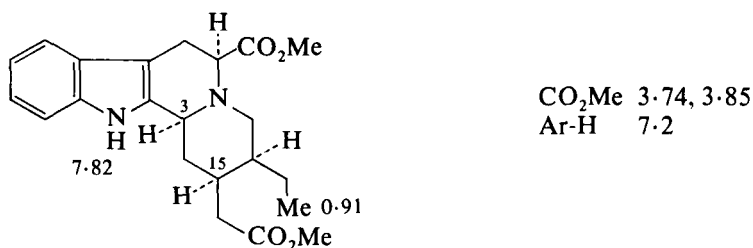
[390] Nauclefine (in TFA)

[391] Isonauclefine (in DMSO-d_6)

The use of $^1J(\text{C-H})$ values in the conformational analysis of yohimbine and reserpine has been examined. (235) For yohimbine $^1J(\text{C}(3)\text{-H})$ is 133 ± 2 Hz and for reserpine it is 140 ± 2 Hz.

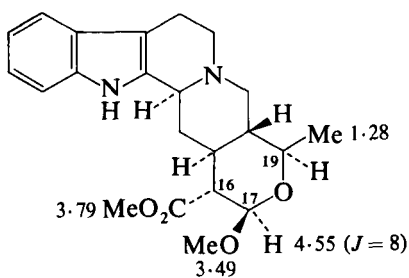
2. ^1H NMR spectra

In the ^1H NMR spectra of $19\beta\text{-H}, 20\alpha\text{-H}$ -heteroyohimbine series of alkaloids, e.g. akuammigine [372] = [373], the 19-proton absorbs at δ 4.2–4.5 whereas in the $19\alpha\text{-H}, 20\beta\text{-H}$ -series, e.g. 19-epi-ajmalicine, the corresponding proton absorbs at δ 3.4–3.5. Such a correlation aided the assignment of the stereochemistry shown in [392] to 5α -carbomethoxy-tetrahydroalstonine (δ 19-H 4.46). (236) Similarly the stereochemistry of 3-iso-19-epiajmalicine was partially assigned on the chemical shift of the 19-proton at δ 3.55 and the value of $J_{19,20}$ of 9.5 Hz. (237) The well defined 18-methyl triplet in [393] (238) is

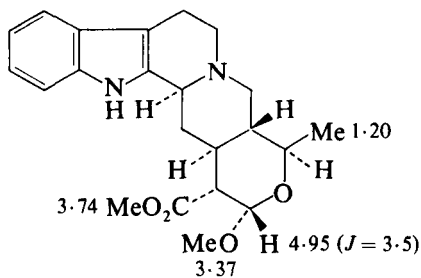
[392] 5 α -Carbomethoxytetrahydroalstonine

[393]

characteristic of an axial ethyl group in corynantheidine derivatives. (1) ^1H NMR spectral data on acetals of the type [394] and [395] are



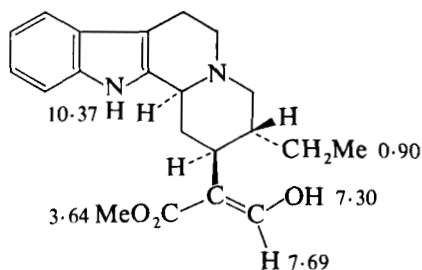
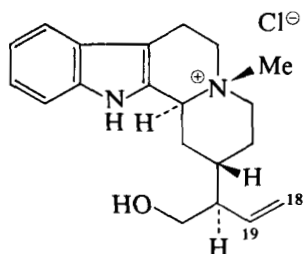
[394]



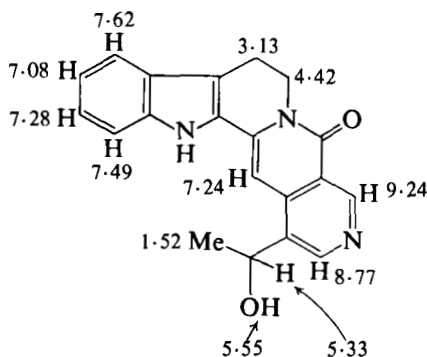
[395]

available, (239, 240) showing the higher frequency absorption of the equatorial anomeric proton. ^1H NMR shifts show that, in DMSO as solvent, 90% of the enol form [396] is present. (241) ^1H NMR spectral data on some stereoisomers of geissoschizine are also available. (242)

The ^1H NMR spectrum (TFA) of the *O*-acetate of the dihydro derivative of antirhine- β -methochloride [397] showed the ^9NMe signal

[396] (in DMSO- d_6)[397] Antirrhine- β -methochloride

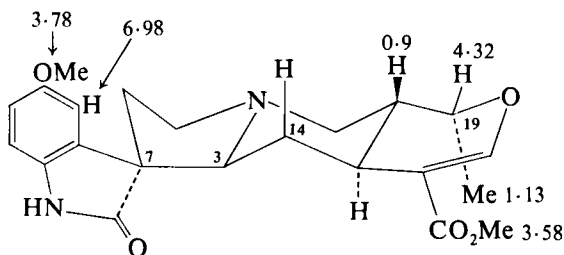
at δ 3.2 whereas an isomeric methochloride prepared by demethylation of the β -methochloride followed by methylation showed the $^{\oplus}\text{NMe}$ absorption at δ 3.5. This is consistent with a *trans*-fused c/d ring structure for the β -methochloride and a *cis*-fused structure for the isomeric methochloride. (243) The use of long range proton-proton coupling constants in structural studies is well illustrated by the spectrum of angustoline [398], (244) which shows benzylic coupling of

[398] Angustoline (in DMSO- d_6)

0.4 Hz between the MeCHOH proton and the 21-proton and a 4J (zig-zag pathway) of 0.6 Hz between the 14- and 17-protons. The signals for the 17-proton and for the 19-proton in the spectrum of nauclefine [390] in TFA solution appear as a doublet and triplet respectively as a result of protonation of the nitrogen atom. This does not occur with isonauclefine but protonation appears to take place on the oxygen atom of the amide function as suggested by a deshielding (0.72 ppm) of the 17-proton signal on changing solvent from DMSO to TFA. (234)

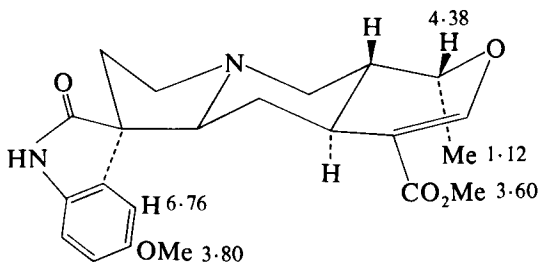
E. Oxindole alkaloids

In the elucidation of the stereochemistry about C(7) in the oxindole alkaloids the chemical shifts of the 9-proton and of the 14_{ax}-proton are of importance. Thus in the spectrum of cabucine oxindole A (7*S*) [399]



[399] Cabucine oxindole A (in CDCl₃)

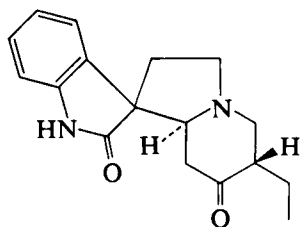
the 9-proton absorbs to high frequency of that in cabucine oxindole B (7*R*) [400] as a result of its proximity to the nitrogen atom in the



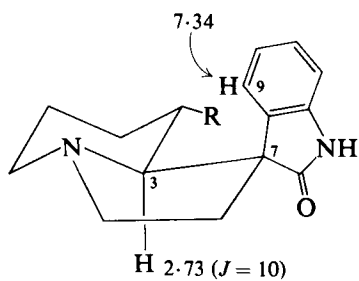
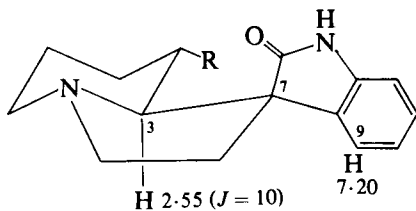
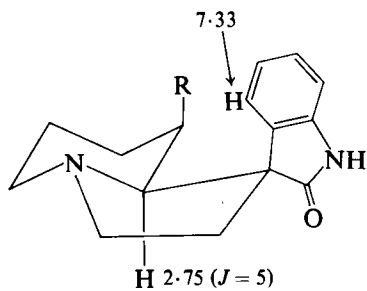
[400] Cabucine oxindole B (in CDCl₃)

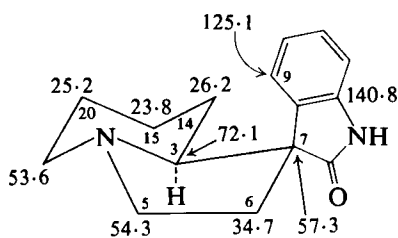
oxindole A. In cabucine oxindole A, the 14_{ax}-proton absorbs at δ 0.9 as a result of shielding by the aromatic system. (245) This latter effect is seen more clearly in the *cis*-D/E ring analogues of the cabucines. (246) Here the 7*S* series is characterized by 14_{ax}-proton absorption in the NMR spectrum at δ 0.91 in contrast to the spectrum of the 7*R* series in which the 14_{ax}-proton absorbs at δ 1.40. Similar effects have been noted in the spectra (CDCl₃) of [401] (7*S* δ 9-H 7.60; 7*R* δ 9-H 7.35) (247) and in the model oxindoles [402], [403], and [404]. (248) In this latter group of three compounds the absorption of the COOMe protons also reflects their orientation with respect to the aromatic ring.

The C(7) stereochemistry is also reflected by ¹³C(3) and ¹³C(9) shifts as illustrated by the spectra of the model oxindoles [405] and [406] and

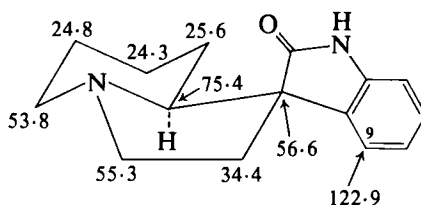


[401]

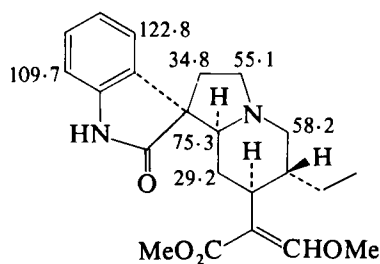
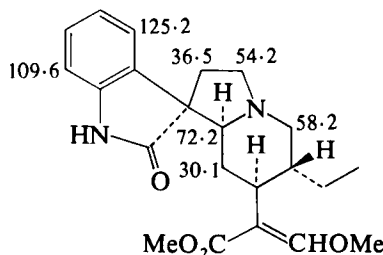
CO₂Me 3.30[402] R = CO₂Me (in CDCl₃)CO₂Me 2.98[403] R = CO₂Me (in CDCl₃)CO₂Me 2.89[404] R = CO₂Me (in CHCl₃)



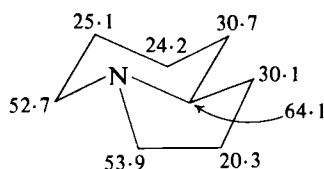
[405]



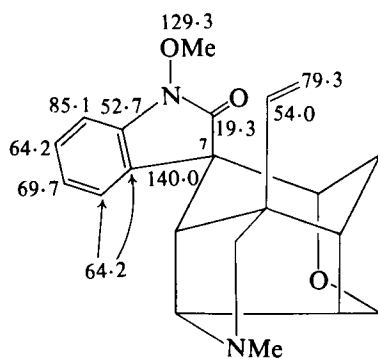
[406]

[407] Rhyncophylline (in CDCl₃)[408] Isorhyncophylline (in CDCl₃)

of rhyncophylline [407] and isorhyncophylline [408]. ¹³C assignments were assisted in this series by the shifts of indolizidine [409]. (2)

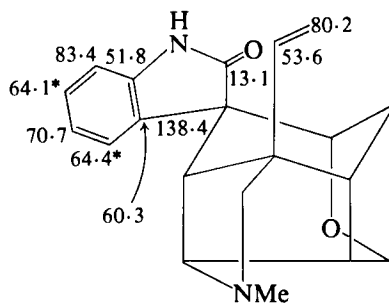


[409]



(in CHCl₃; δ ppm to lower frequency from CS₂)

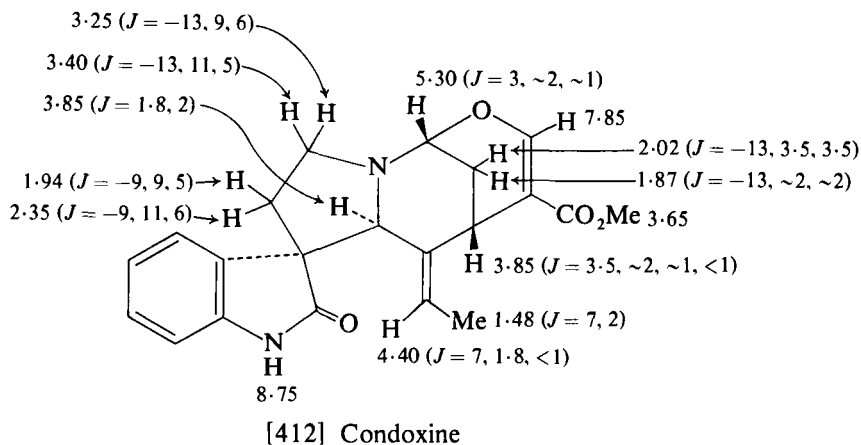
[410] Gelseverine



[411] Gelsemine

The presence of the methoxyl group in gelseverine [410] largely affects the ^{13}C shifts of the oxindole moiety and of the *cis*-orientated ethylidene side chain compared with shifts in gelsemine [411]. (249)

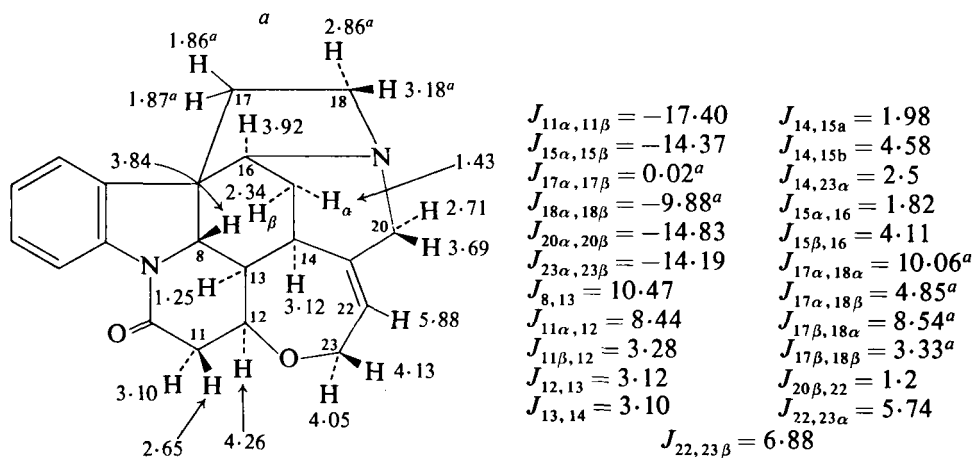
^1H NMR parameters for condoxine are displayed in structure [412]. (250)



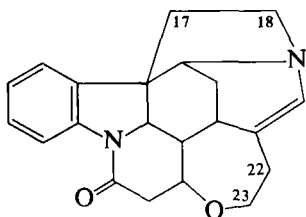
F. Strychnine and related alkaloids

1. ^1H NMR spectra

Detailed analysis of the 250 MHz ^1H NMR spectra of strychnine [413], (251) neostrychnine [414], and 18-oxostrychnine (252) has been



^a Some of these values may require correction



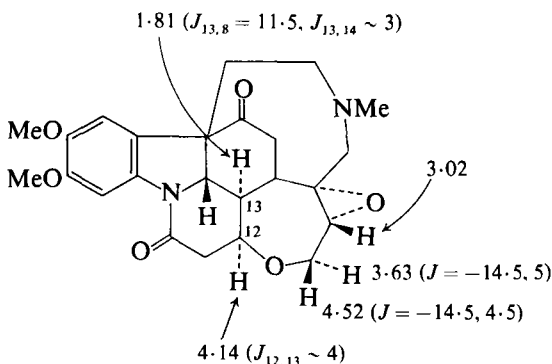
$$\begin{aligned}
 J_{17\alpha, 17\beta} &= -13.41 \\
 J_{18\alpha, 18\beta} &= -12.18 \\
 J_{17\alpha, 18\alpha} &= 10.01 \\
 J_{17\alpha, 18\beta} &= 3.62 \\
 J_{17\beta, 18\alpha} &= 7.74 \\
 J_{17\beta, 18\beta} &= 9.03
 \end{aligned}$$

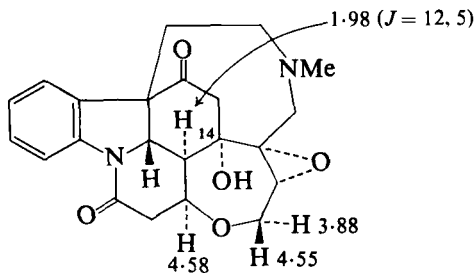
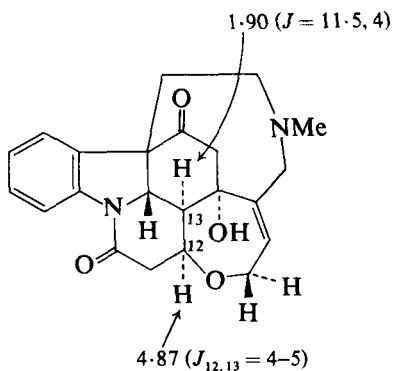
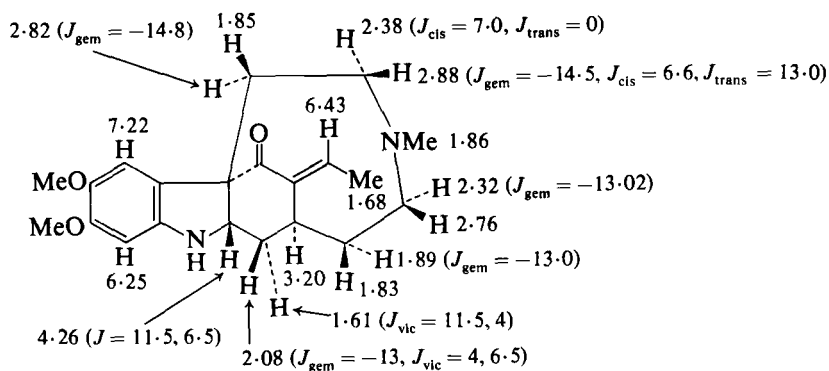
[414] Neostrychnine (in CDCl_3)

made with the aid of double resonance techniques, aromatic solvent induced shifts, and computer simulation of spectra (LAOCOON III). The results for strychnine are summarized in [413]. The values obtained for $J_{17\alpha, 17\beta}$ of 0.02 Hz cannot possibly be correct (58) and comparison of the vicinal coupling constant values between the 17- and 18-methylene group protons in the spectrum of [413] with those extracted from the neostrychnine spectrum [414] shows a marked difference for $J_{17\beta, 18\beta}$ (3.33 Hz in [413], 9.03 Hz in [414]). Thus the analysis of the $\text{C}(17)\text{H}_2\text{--C}(18)\text{H}_2$ moiety in the spectrum of strychnine appears to be incorrect.

In the *sec*-pseudostrychnine derivatives [415], [416], and [417], (253) the shifts of the 12-proton are of interest. If a chair conformation with the oxygen up is assumed for the seven-membered ether ring, then the α -oriented epoxide will shield the 12α -proton in [415] and [416]. In addition, in [416] and [417] the 12α -hydrogen and the 14α -hydroxyl are *syn*-axial resulting in a deshielding of the 12α -proton.

The low frequency absorption of the *N*-methyl protons in the spectrum of deacetylgeissovelline [418] results from the transannular

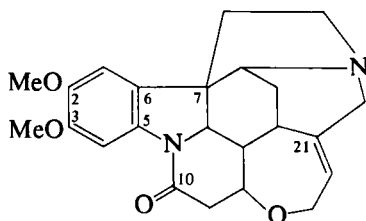
[415] (in CDCl_3)

[416] (in CDCl_3)[417] (in CDCl_3)[418] Deacetylgeissovelline (in CDCl_3)

nitrogen-carbonyl interaction. Of the four methylene protons α to the indoline unit, one at δ 2.82 is deshielded by the aromatic ring and another at δ 1.61 is shielded by the aromatic ring. (254)

2. ^{13}C NMR spectra

^{13}C spin-lattice relaxation time measurements (Table VIII) have been used in the assignment of quaternary ^{13}C signals in brucine [419] (121) (for details see discussion on codeine in Section V).



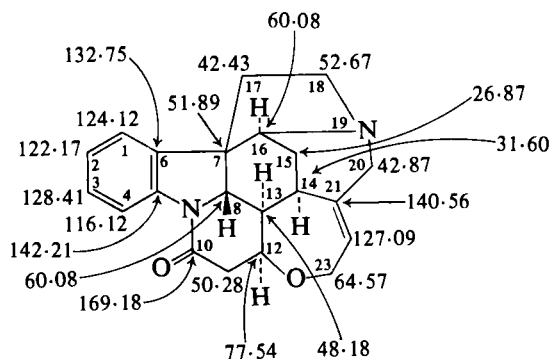
[419] Brucine

TABLE VIII

^{13}C chemical shifts and spin-lattice relaxation times for brucine [419] in CDCl_3 (121)

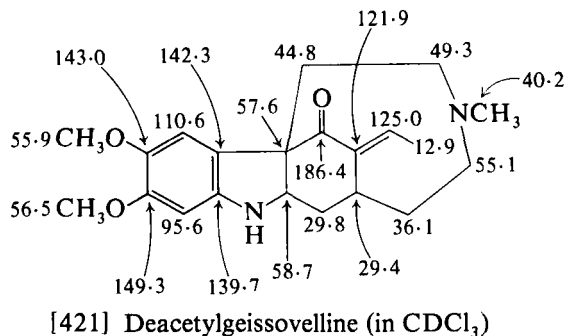
^{13}C nucleus	$\delta(^{13}\text{C})$	T_1 (s)	No. of α CH protons
C(2)	149.13*	9.35*	1
C(3)	146.14*	10.70*	1
C(5)	135.97	7.25	1
C(6)	123.46	11.75	1
C(7)	51.83	2.62	4
C(10)	168.64	4.30	2
C(21)	140.29	2.90	4

The ^{13}C NMR spectrum of strychnine is summarized in [420] and protonation shifts (TFA) have been studied. (255) In CDCl_3 solution

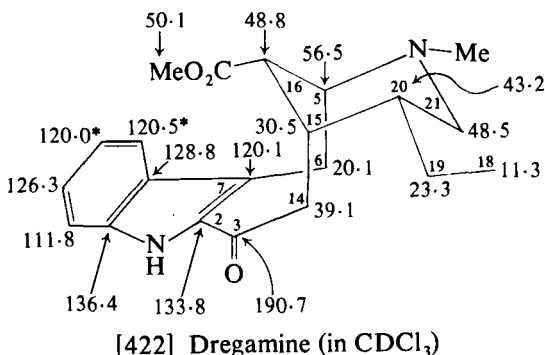
[420] Strychnine (in CDCl_3)

C(8) and C(16) absorb at δ 60.08, and on the addition of TFA C(16) moves to low frequency by 0.9 ppm and C(8) to high frequency by 2.0 ppm. The increase in screening of C(16) is as expected since α and β carbons in saturated nitrogen heterocycles are shifted to low frequency on protonation. (3) The C(8) shift suggests partial protonation of the amide.

In the ^{13}C NMR spectrum of deacetylgeissovelline [421] the $\text{C}=\text{O}$ peak present at δ 186.4 in CDCl_3 solution shifts to δ 104.5 in 0.1 N

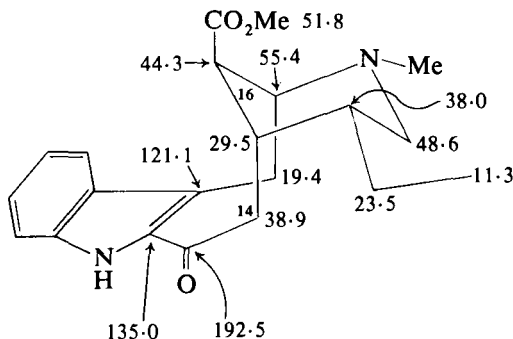


$\text{DCl-D}_2\text{O}$ as a result of formation of the HO-C-N^+ system. The assignment of the two aromatic CH and the olefinic CH signals in the spectrum of [421] provides an example of the use of residual coupling (J_R) measurements in SFORD spectra in structural studies. With the decoupling frequency set at δ 14 the separations of these proton signals from the applied decoupling frequency are 7.57 (olefin), 6.78 (*meta* to indoline nitrogen), and 7.75 ppm [*ortho* to indoline nitrogen (see proton shifts in [418])]. The J_R values then for the 125.0, 110.6, and 95.6 ppm doublets under these conditions are observed as 26.6, 24.9, and 27.5 Hz, thus permitting the carbon signals to be assigned as in [421]. (254)



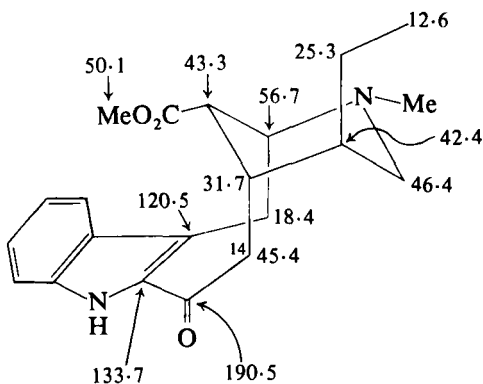
G. Sarpagine type alkaloids (including gardneria bases)

The axial nature of the C(20)–H bond in dregamine [422] and 16-epidregamine [423] is shown by the observation of a γ -effect of the axial methoxycarbonyl on C(20) in [423]. In addition, the C(2), C(3), and COOCH₃ shifts are diagnostic of the stereochemistry at C(16). (256)

[423] 16-Epidregamine (in CDCl_3)

In the ^1H NMR spectra of compounds of the dregamine type C(16) stereochemistry the COOCH_3 protons absorb 0.58 ppm to low frequency of those in the 16-*epi*-isomers (257) owing to the influence of the indole moiety. The shielding of the COOCH_3 nucleus in dregamine may be a related phenomenon.

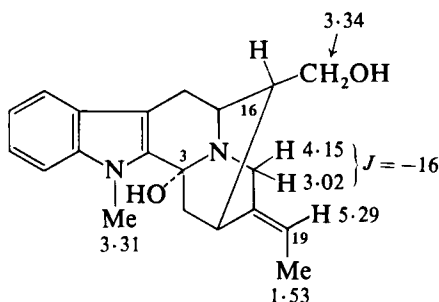
Comparison of the ^{13}C NMR spectra of dregamine [422] and tabernaemontanine [424] shows the γ -effect of the ethyl side chain on C(14) in dregamine and on C(16) in tabernaemontanine. The C(18) and



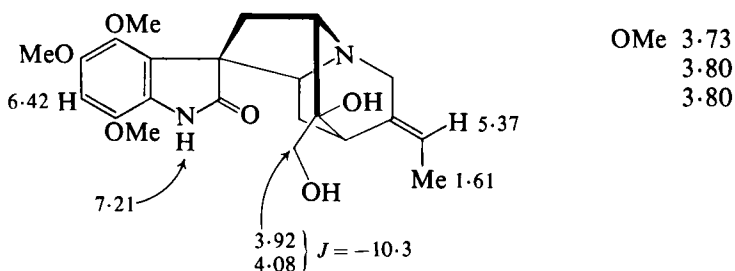
[424] Tabernaemontanine (in CDCl_3)

C(19) shifts are also diagnostic of the axial/equatorial nature of the ethyl side chain. (256)

^1H NMR data on accedine [425] (258) and on chitosenine [426] (259) are displayed in the structures.



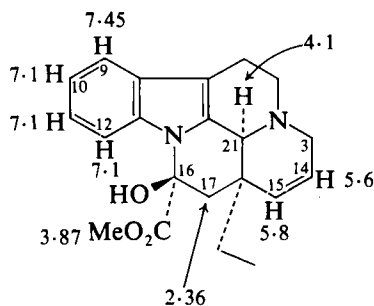
[425] Accedine (in CDCl_3)



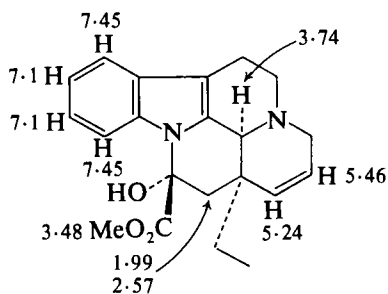
[426] Chitosenine

H. Vincamine and related alkaloids

Differences in the C(16) stereochemistry of Δ^{14} -vincamine (normal series) and Δ^{14} -16-epivincamine (epi series) ([427] and [428] respec-

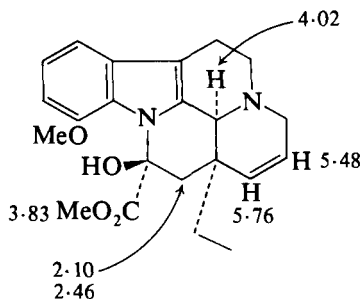


[427] Δ^{14} -Vincamine (in CDCl_3)



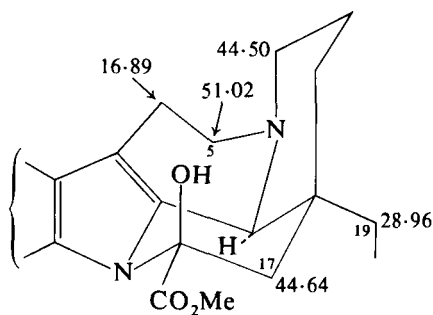
[428] Δ^{14} -16-Epivincamine (in CDCl_3)

tively) are shown by the variations in absorption for the methoxycarbonyl protons, the olefinic protons (14-H and 15-H), the C(21) proton, and the absorption for the C(17) methylene protons. On most counts 12-methoxy- Δ^{14} -vincamine [429] falls into the normal series, the



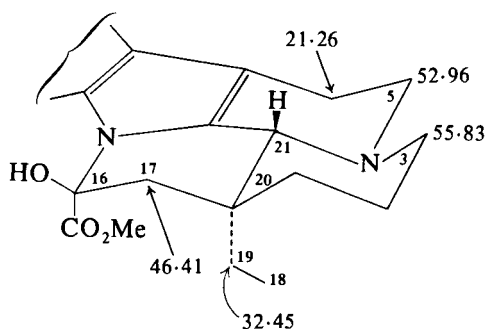
[429] 12-Methoxy- Δ^{14} -vincamine (in CDCl_3)

only exceptional feature being the AB quartet for the C(17) methylene protons. This non-equivalence must be due to interactions involving the C(12) methoxyl group. (260) The C(17) methylene absorption is also of use in the configurational assignments to vincamine and its stereoisomer. In vincamine [430] the C(17) methylene protons absorb as an



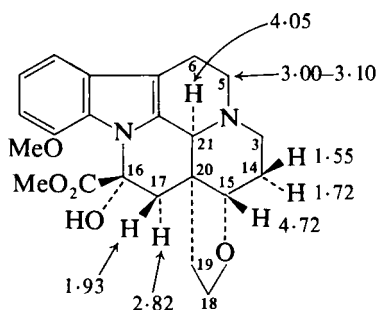
[430] Vincamine (in CDCl_3)

AB quartet (δ 2.11 and 2.24). This small $\Delta\delta$ contrasts with the large chemical shift difference between the corresponding protons in 16-epivincamine (δ 1.85 and 2.67). This large chemical shift difference is diagnostic of the axial methoxycarbonyl group since it is present (δ 1.88 and 2.63) in 21-epivincamine [431] but not in 16-epi,21-epivincamine (δ 1.98 and 2.26). The 21-epi series is characterized by a 4J coupling (W pathway) between the 17ax'-proton and one of the C(19) methylene protons. (261) ^{13}C shifts of diagnostically important carbon nuclei in the

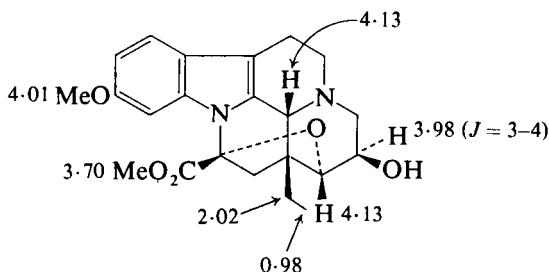
[431] 21-Epivincamine (in CDCl_3)

spectra of vincamine and 21-epivincamine are provided in [430] and [431] and show the expected shieldings in the *cis*-C/D quinolizidine system. In the spectrum of 16-epivincamine C(17) absorbs at δ 47.05 and in that of 16-epi,21-epivincamine C(17) absorbs at δ 43.90.

^1H NMR shifts for cuanzine are depicted in [432]. The 21-proton is coupled to one of the C(5) methylene protons consonant with a *cis*-C/D

[432] Cuanzine (in C_6D_6)

$$\begin{aligned} J_{19\alpha, 19\beta} &= -11.5 \\ J_{15, 14\beta} &= 7 \\ J_{14\alpha, 14\beta} &= -13 \\ J_{14\beta, 3\beta} &= 3.5 \\ J_{14\beta, 3\alpha} &= 3.5 \\ J_{15, 14\alpha} &= 10 \\ J_{14\alpha, 3\beta} &= 12 \\ J_{14\alpha, 3\alpha} &= 5 \\ J_{17\alpha, 17\beta} &= -15 \end{aligned}$$

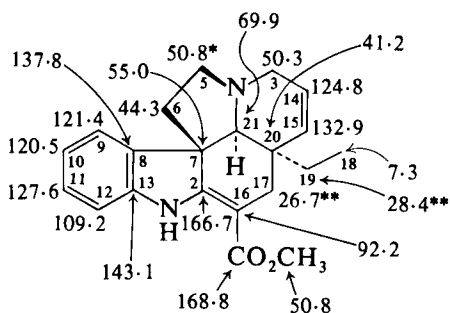
[433] Vincarodine (in pyridine-d_5)

ring fusion, and the 17β -proton is coupled to one of the C(19) methylene protons. ^{13}C shifts for cuanzine are also available, (262) as are ^1H NMR data on decarbomethoxyapocuanzine. (263) Some ^1H NMR data on vincarodine (264) are given in [433].

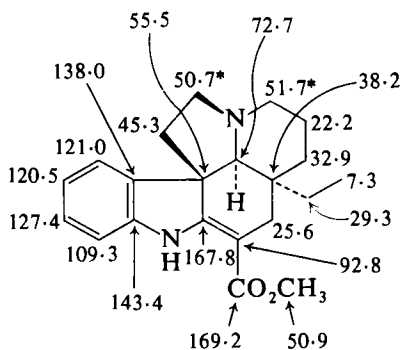
I. Aspidospermine, quebrachamine, and ibogamine alkaloids

1. ^{13}C NMR spectra of aspidospermine and quebrachamine alkaloids

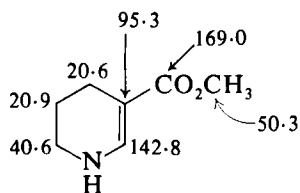
^{13}C shifts of tabersonine and of vincadifformine are shown in [434] and [435] respectively. Aromatic ring ^{13}C signals are similar to those in the oxindoles rhyncophylline, isorhyncophylline, and gelsemine (Section XII.E), and the c ring resonances are assigned on the basis of those in methyl 1,4,5,6-tetrahydronicotinate [436]. Signals arising from the



[434] Tabersonine (in CHCl_3)



[435] Vincadifformine (in CHCl_3)

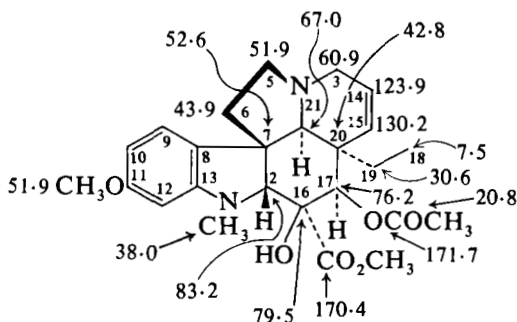


[436]

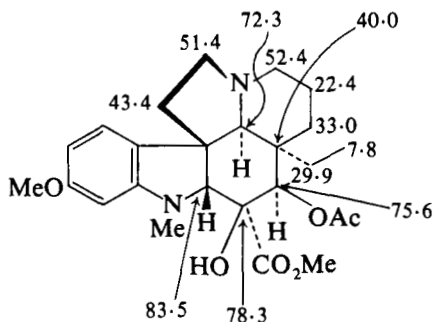
quaternary carbon nuclei C(7) and C(20) are identified by the noise off-resonance decoupling technique with the C(20) shift showing a dependence upon the piperidine or piperideine nature of the D ring. In

the spectrum of tabersonine C(21) at δ 69.9 is to low frequency of C(21) (δ 72.7) in vincadifformine. This effect of the D ring double bond appears to be general for a range of piperidine, tetrahydropyran, and cyclohexane derivatives and has been termed the "endocyclic homoallyl effect". (265)

Shifts for vindoline and dihydrovindoline are shown in [437] and [438] respectively. The assignment of the δ 76.2 and 83.2 signals in the



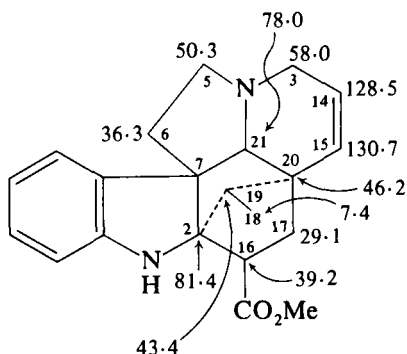
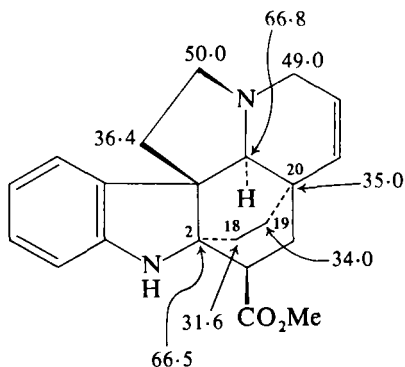
[437] Vindoline (in CDCl_3)



[438] Dihydrovindoline (in CDCl_3)

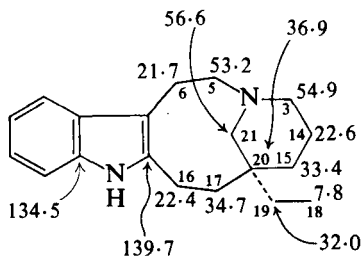
spectrum of vindoline to C(17) and C(2) respectively provides an excellent example of the use of residual coupling (J_R) measurements in SFORD spectra. Such an experiment is feasible since in the ^1H NMR spectrum of vindoline absorption of the 2β - and 17α -protons at δ 3.75 and 5.43 respectively is widely separated. J_R values for the δ 83.2 signals in SFORD with irradiation at 0–1 and 8–9 ppm are 45 and 46 Hz respectively, and under the same conditions the δ 76.2 signals display J_R values of 59 and 34 Hz respectively. This shows the δ 76.2 signal to be related to the δ 5.43 ^1H NMR signal. (265)

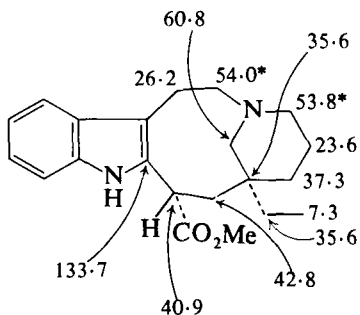
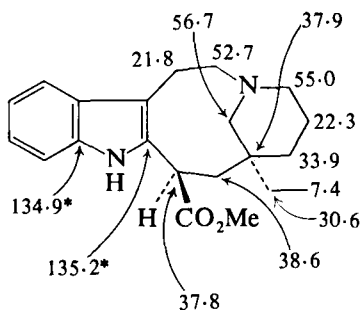
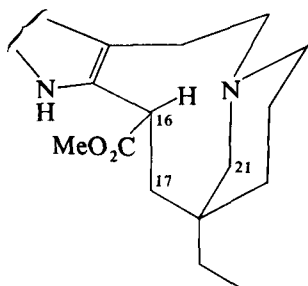
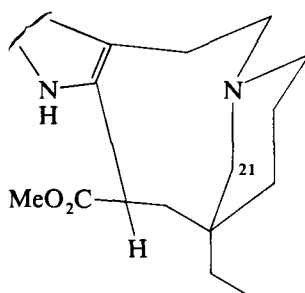
The endocyclic homoallyl effect (see C(21) in [437] and [438]) is not noted on changing structure from vindolinine [439] to 14,15-dihydrovindolinine [δ C(21) in vindoline 78.0, δ C(21) in dihydrovindolinine 78.8]. In addition the C(3) and C(21) shifts in vindolinine are abnormal and this has been attributed to the strain induced by the presence of the norbornane moiety. Comparison of the C(2) and C(20) shifts in vindolinine with those in venalstonine [440] shows the deshielding of *ca.*

[439] Vindolinine (in CDCl_3)[440] Venalstonine (in CDCl_3)

12–15 ppm in the former consistent with a change from the norbornane to the bicyclo[2,2,2]octane structure. (266)

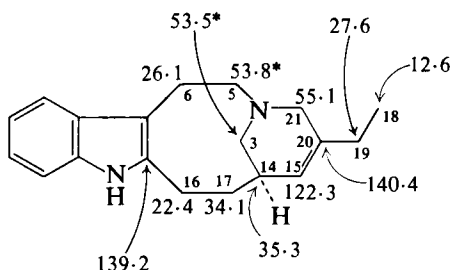
The solution conformation of the azacyclononane ring in quebrachamine [441], 16 α -carbomethoxyquebrachamine [442], 16 β -carbomethoxyquebrachamine [443], and related systems is of interest in view of its presence in the medicinally important alkaloids of the vincalkeboline type. Conformations [444] and [445] have been assigned to [442] and [443] respectively, and cleavamine [446] has been shown to adopt a conformation analogous to [442]. In the 16 β -carbomethoxy series the difference in chemical shift between the C(21) methylene

[441] Quebrachamine (in CDCl_3)

[442] 16 α -Carbomethoxyquebrachamine (in CDCl₃)[443] 16 β -Carbomethoxyquebrachamine (in CDCl₃)[444] 16 α -Carbomethoxy series[445] 16 β -Carbomethoxy series

protons must be greater than 0.5 ppm resulting in ¹³C(21) absorbing as a doublet of doublets in the SFORD spectra. In the 16 α -series a corresponding triplet is observed. Interaction between C(6) and C(16) in [445] results in mutual shielding. The additional shielding of C(21) in [445] results from an interaction with C(16). (267)

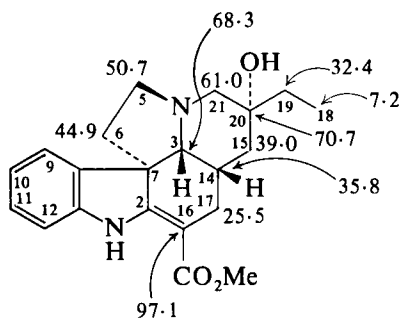
A plot of the residual couplings (J_R) of the C(16) methylene resonance of cleavamine [446] against the position of the decoupling



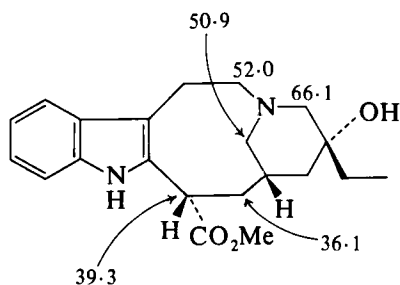
[446] Cleavamine (in CDCl_3)

field shows simplification of the doublet of doublet pattern to a doublet when the decoupler frequency coincides with the 16α - or 16β -proton resonance. In this way the chemical shifts of the 16-methylene protons were calculated as δ 3.60 and 2.65 (for the β - and α -protons respectively). (8) ^{13}C shifts of cleavamine are shown in [446]. (267)

The similarity of ^{13}C shifts in pandoline [447] and epipandoline (20 β -OH) prevented assignment of the stereochemistry about C(20). This was determined by comparison of the shifts in the derived 3,7-secopandoline A [448] with those in velbanamine [449] which shows the same relative

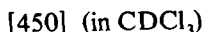
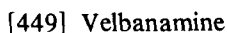


[447] Pandoline (in CDCl_3)

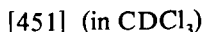


[448] 3,7-Secopandoline A

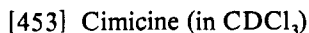
C(20), C(14) configuration. Since velbanamine, like quebrachamine, adopts the 16β -substitution type of conformation shown in [445], the conformational identity of [448] and [449] also shows the *cis* relationship between 14-H and 16-H, permitting assignment of stereochemistry to pandoline. (268) Other ^{13}C NMR data on pandoline derivatives are available. (269)



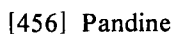
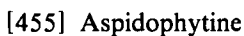
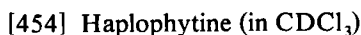
The spectrum of [450] illustrates the γ -effect of the hydroxyl group on C(3) and C(19), and that of [451] the β -effect of the hydroxyl group on C(3). (270)



The ^{13}C NMR spectrum of melobaline is summarized in [452], (271) that of cimicine in [453], (272) and that of haplophytine in [454]. (273) Peaks for the aspidophytine moiety [455] are present in the spectrum of

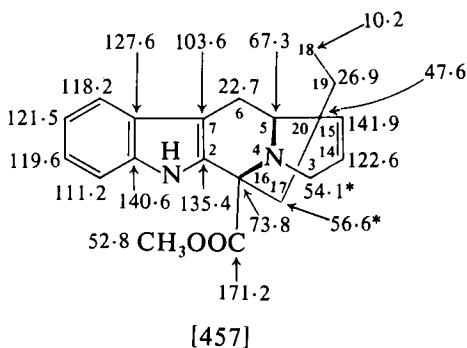


2-H	3.98
CH ₂ CH ₃	2.64, 1.32
OH	10.70



haplophytine with the exception of the C(15) absorption in the spectrum of aspidophytine at δ 102.3. The signal is replaced by a signal at δ 124.1 in the spectrum of haplophytine consonant with the linkage shown. Features of the ^1H NMR spectrum of haplophytine are discussed below.

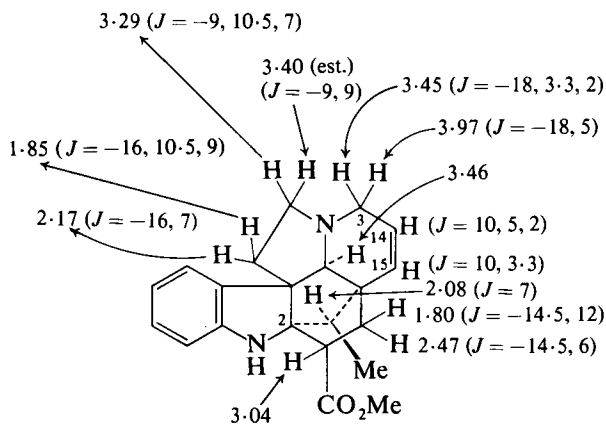
¹³C NMR data on pandine [456] (274) and on a rearranged product [457] derived from chloro-16-dehydro-1-tabersonine (275) are displayed in the structures.



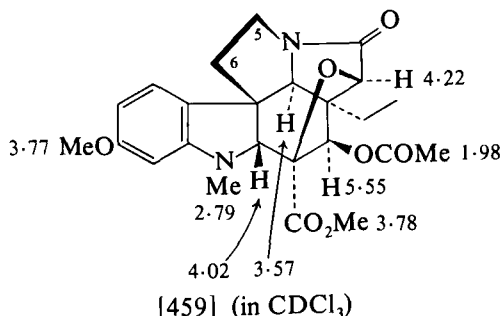
2. ¹H NMR spectra of aspidospermine type alkaloids

¹H NMR studies show the differing orientations of the 16-hydrogen to the nitrogen lone pair in [444] and [445] with deshielding of the 16-proton in [444] as a result of the proximity to the nitrogen atom. (267)

The spin-lattice relaxation times of essentially all the protons in vindoline, measured by a Fourier transform method, show values reflecting the degree of steric interaction with other protons. (276) A wealth of coupling constant data has been made available by first order analysis of the 300 MHz ¹H NMR spectrum of vindolinine [458]. (277) ¹H NMR shifts for the metabolite of vindoline [459] (278) are shown on the structure.

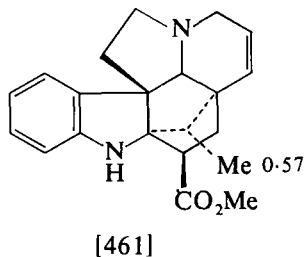
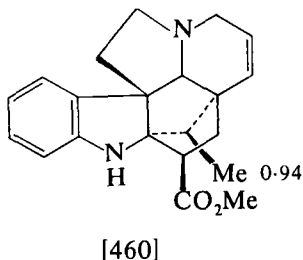


[458] Vindolinine (in CDCl_3)

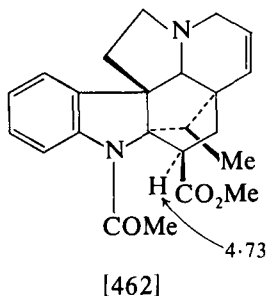


In the ^1H NMR spectrum of haplophytine [454] the C(16) methoxyl group protons absorb at unusually low frequency (δ 3.00) and the 11'-protons at δ 6.27. The 11'-proton is shielded by the aspidophytine aromatic ring and the 16-methoxyl protons by the haplophytine aromatic ring in the preferred conformation of the molecule. (273)

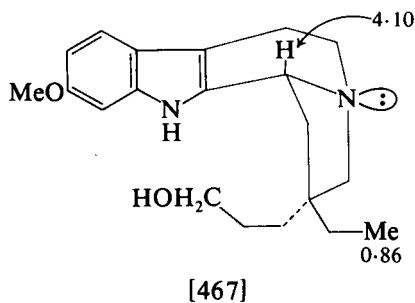
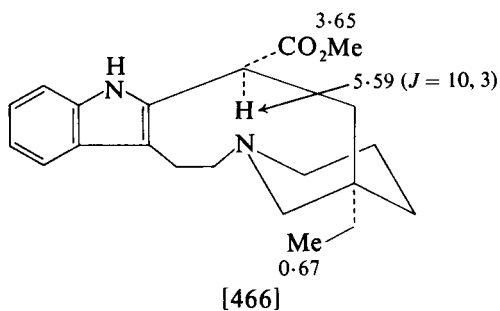
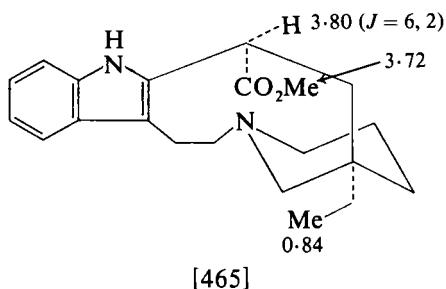
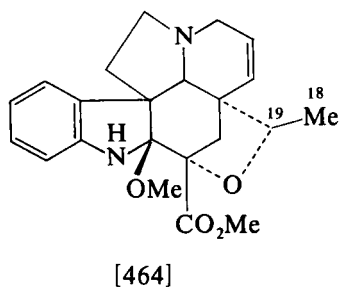
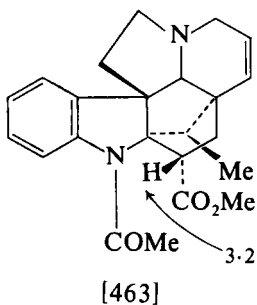
Additional examples of variations in ^1H NMR parameters with stereochemistry are provided by the spectra of the compounds [460]–[468]. In the vindolinine derivatives [460]–[463] (279) the pair of compounds [460] and [461] show the influence of the aromatic ring on



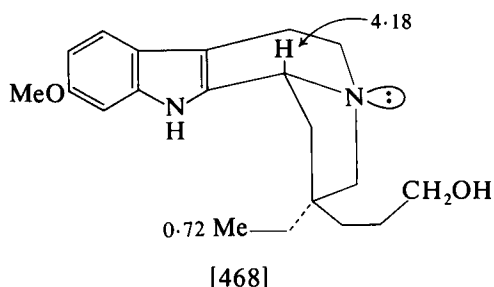
the shifts of the CHMe group protons. This influence is also shown by the 19*R* (18-Me δ 1.02, 19-H δ 3.42) and 19*S* (18-Me δ 0.55, 19-H δ 3.81) isomers of [464]. (280) The spectra of compounds [462] and



[463] show the differing influence of the *N*-acetyl function on the shifts of the 16-protons. Nitrogen lone pair effects are shown in [465]–[468]. (281) The spectra of [465] and [466] show the lone pair effect on the

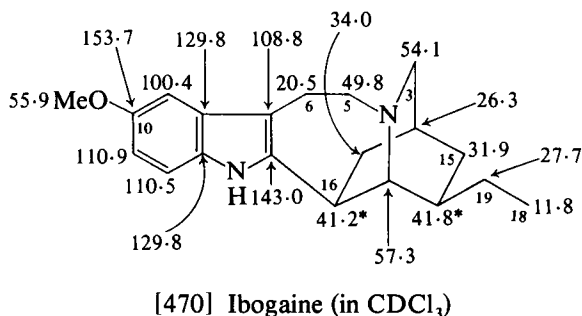
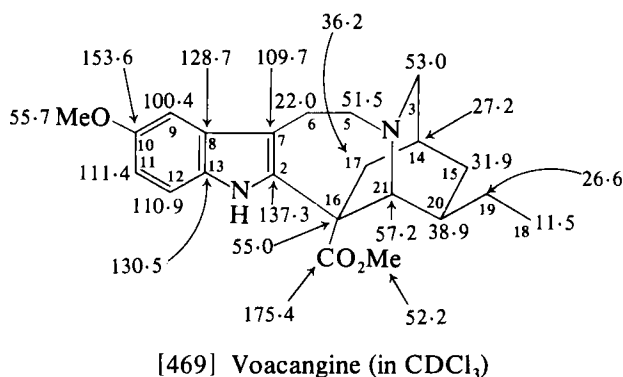


shifts of the 16-protons, and the spectra of [467] and [468] show the lone pair effects on the shifts of the CH_2CH_3 protons.



3. NMR spectra of iboga type alkaloids

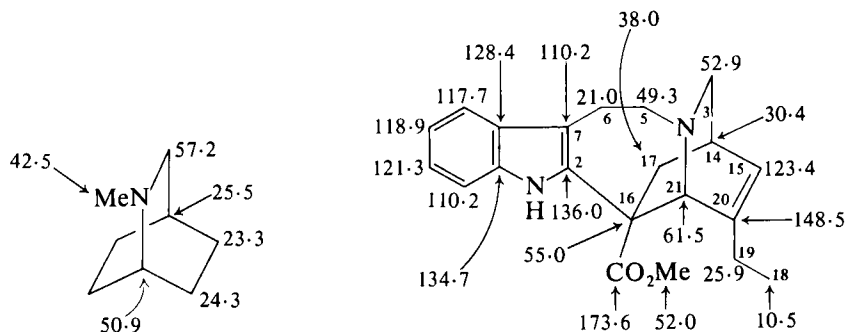
The ^{13}C NMR spectrum of voacangine [469] and ibogaine [470] show the γ -effect of the methoxycarbonyl group to be less than that in



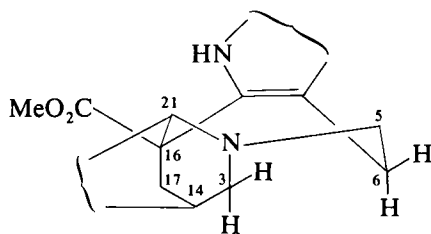
the bicyclo[2,2,2]octane analogues as a result of the hydrogen bond between the indolic NH and the oxygen atom of the carbonyl group which alters the conformation from that present in the bicyclo[2,2,2]-

octane in which a γ -hydrogen is exposed to the effect of the carbonyl group.

Comparison of the shifts in *N*-methylisoquinuclidine [471] with those in the corresponding part of catharanthine [472] shows a γ -effect on

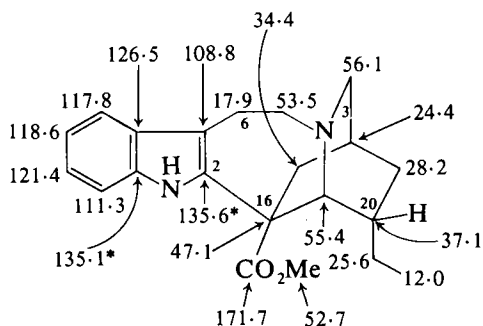
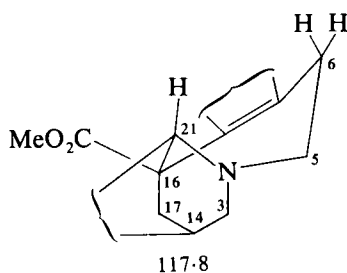
[471] *N*-Methylisoquinuclidine[472] Catharanthine (in CDCl_3)

C(3). This is consistent with the adoption of conformation [473] for catharanthine [γ -effect between C(3) and C(6)]. Marked changes in ^{13}C



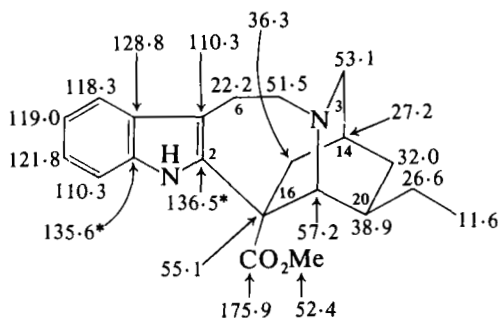
[473]

shifts are observed for dihydrocatharanthine [474], and here the isoquinuclidine twist boat conformation [475] has been suggested. The γ -

[474] Dihydrocatharanthine (in DMSO-d_6)

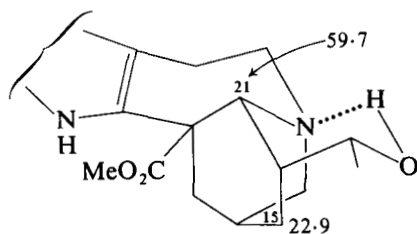
[475]

effect between C(3) and C(6) present in catharanthine is lost but is replaced by a γ -effect between C(6) and C(21). The effect of differences in C(20) stereochemistry on shifts in the isoquinuclidine moiety of iboga type alkaloids is exemplified by coronaridine [476] and dihydro-

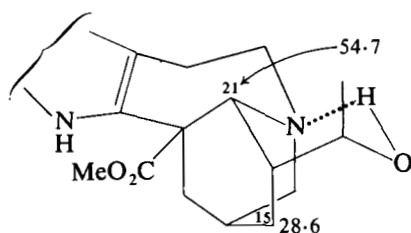


[476] Coronaridine (in CDCl_3)

catharanthine [474]. Intramolecular hydrogen bonding effects on C(15) and C(21) shifts are illustrated by heyneanine [477] and 19-isoheyneanine [478]. (282)

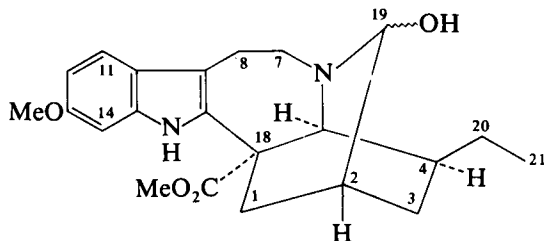


[477] Heyneanine



[478] 19-Isoheyneanine

For reference purposes the NMR spectra of 19a- and 19b-hydroxy-isoavoacangin [479], (283) voaketone [480], (284) the spiran [481] derived from conopharynginol tosylate, (285) and the rearrangement

[479] 19-Hydroxy-isovoacangin (in CDCl_3)

	19a-Hydroxy		19b-Hydroxy
NH	7.90	NH	7.83
19-H	4.46 ($J = 7$, ~1) (+ D_2O 4.43, $J = 1$)	19-H	4.16 (d, $J = 1$)
OMe	3.82	OMe	3.80
CO_2Me	3.70	CO_2Me	3.69
CH_2CH_3	0.94 ($J = 7$)	CH_2CH_3	0.92 ($J = 7$)

Chemical structure of Voaketone (in CDCl_3) showing ^{13}C NMR chemical shifts (ppm):

- 153.7 (C12)
- 127.0 (C10)
- 112.7 (C9)
- 21.1 (C8)
- 52.7 (C7)
- 42.3 (C19)
- 61.4 (C19)
- 36.4 (C19)
- 31.8 (C2)
- 31.0 (C20)
- 46.2 (C22)
- 206.0 (C18)
- 111.3 (C11)
- 111.3 (C13)
- 100.2 (C14)
- 132.3 (C15)
- 131.3 (C17)
- 67.1 (C17)
- 8.1 (C21)
- 31.8 (C2)

[480] Voaketone (in CDCl_3)

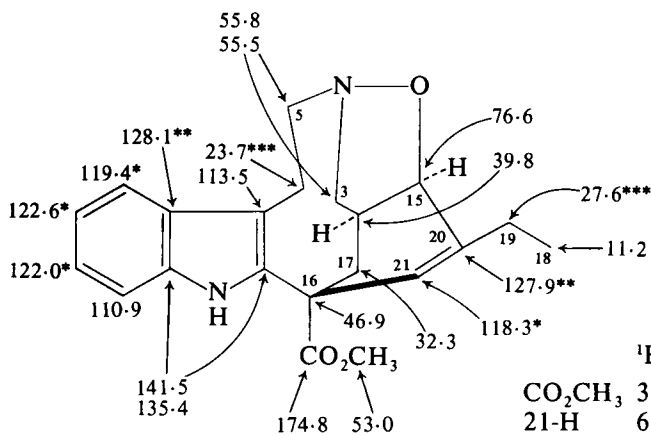
	^1H NMR
NH	7.72
OCH_3	3.82
1-H	2.2–2.4 (2H)
2-H	2.25–2.95
3-H	1.82 (2H)
5-H	3.45
7- H_β	2.84 ($J = -10$)
7- H_α	2.71 ($J = -10$)
8-H	2.35–2.56 (2H)
11-H	6.89 ($J = 2$)
13-H	6.75 ($J = 8, 2$)
14-H	7.15 ($J = 8$)
19-H	2.6–2.9 (2H)
20-H	1.60 (2H)
21- CH_3	1.08 ($J = 8$)
22- H_β	1.6–1.85
22- H_α	2.1 ($J = -16$)

[480] Voaketone (in CDCl_3)

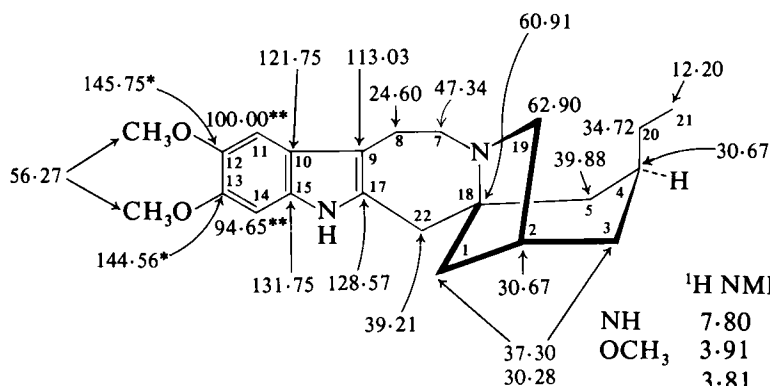
product [482] (286) from catharanthine *N*-oxide are displayed in the structures.

J. Other indole alkaloids (including andranginine, adina bases, and cinchona bases)

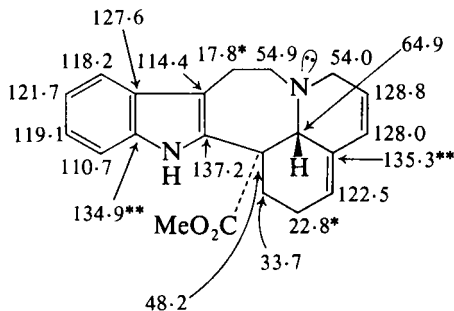
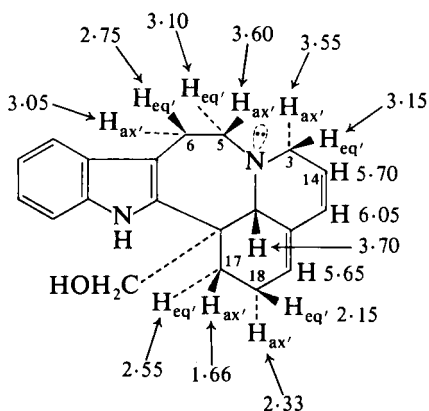
The ^{13}C NMR spectrum of andranginine [483] and the ^1H NMR spectrum of the derived andrangininol [484] are given in the formulae.

[481] (in CDCl_3) ^1H NMR

CO_2CH_3	3.77
21-H	6.14
15-H	4.50 ($J = 9.5$)
14-H	3.19
3-H'	2.60 ($J = -9.7, 4.5$)
19-H	2.41
	2.25
17-H	2.30 ($J \sim -13.6$)
17-H'	2.02 ($J = -13.6, 5.4$)
18- CH_3	1.19 ($J = 7.2$)

[482] (in CDCl_3) ^1H NMR

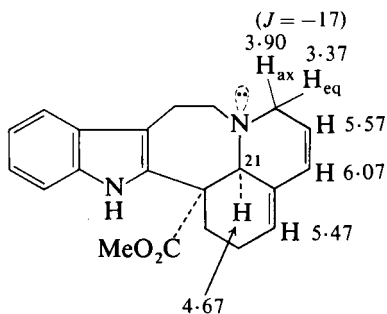
NH	7.80
OCH_3	3.91
	3.81
14-H	6.90
11-H	6.76
19- H_β	3.42 ($J = -10, 7$)
22-H	2.96 ($J = 15$)
	2.78
19- H_α	2.23 ($J = -10$)
2-H	2.20
1- H_β	1.96 ($J = -14, 7$)
21- CH_3	0.79 ($J = 7$)

[483] Andranginine (in CDCl_3)

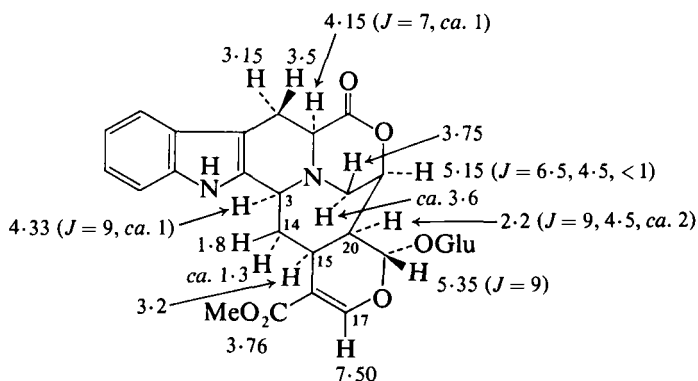
$$\begin{aligned}
 J_{3\text{ax}', 3\text{eq}'} &= -16 \\
 J_{3\text{eq}', 14} &= 5 \\
 J_{5\text{ax}', 5\text{eq}'} &= -14 \\
 J_{6\text{ax}', 6\text{eq}'} &= -16 \\
 J_{17\text{ax}', 17\text{eq}'} &= -15 \\
 J_{18\text{ax}', 18\text{eq}'} &= -18 \\
 J_{17\text{eq}', 18\text{eq}'} &= 6 \\
 J_{17\text{ax}', 18\text{ax}'} &= 15 \\
 J_{17\text{ax}', 18\text{eq}'} &= 6
 \end{aligned}$$

[484] Andranginolinol (in CDCl_3 -TFA)

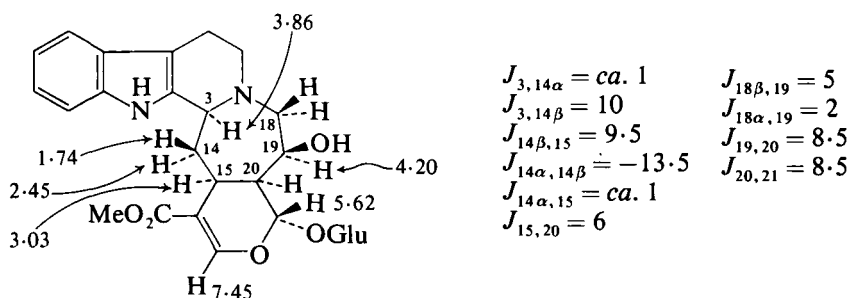
(287, 288) In the ^1H NMR spectrum of 21-epiandranginine [485] the 21-protons now *cis* to the nitrogen lone pair absorb at δ 4.67 (cf. δ 3.70 in andranginine [483]). (289)

[485] 21-Epiandranginine (in CDCl_3)

Vicinal coupling constant data have established the stereochemistry of rubenine [486] (290) and of 3α -dihydrocadambine [487]. (291, 292) The 3α -configuration for isodihydrocadambine acetate [488] is suggested by the absorption for the 3-proton at δ 3.70. (293) ^1H NMR data for palinine tetra-acetate [489] (294) and for cadamine acetate [490] (295) are included in the structures.

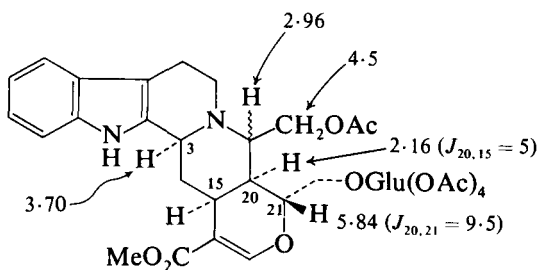


[486] Rubenine (in DMSO- d_6 -D₂O)

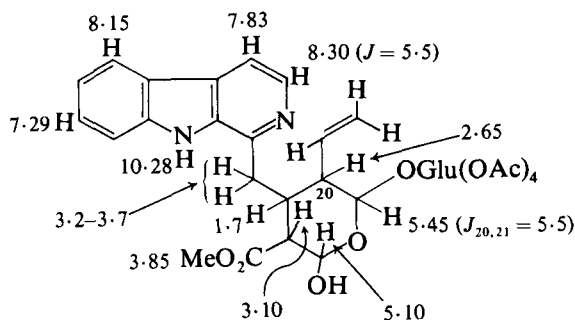
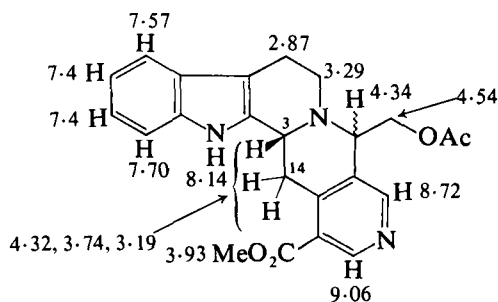


$$\begin{array}{ll}
 J_{3,14\alpha} = \text{ca. } 1 & J_{18\beta,19} = 5 \\
 J_{3,14\beta} = 10 & J_{18\alpha,19} = 2 \\
 J_{14\beta,15} = 9.5 & J_{19,20} = 8.5 \\
 J_{14\alpha,14\beta} = -13.5 & J_{20,21} = 8.5 \\
 J_{14\alpha,15} = \text{ca. } 1 & \\
 J_{15,20} = 6 &
 \end{array}$$

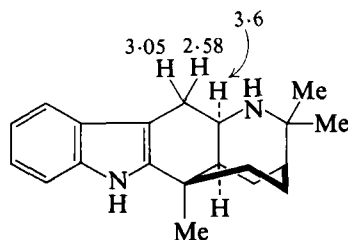
[487] 3α -Dihydrocadambine



[488] Isodihydrocadambine acetate

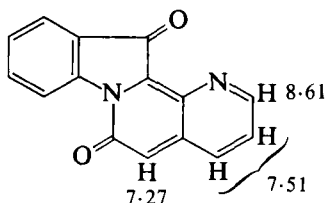
[489] Palinine tetra-acetate (in CDCl_3)

[490] Cadamine acetate

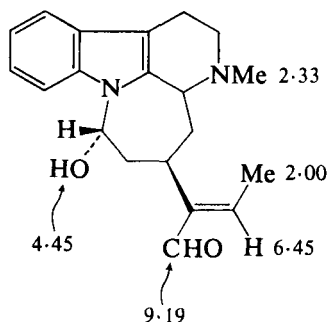
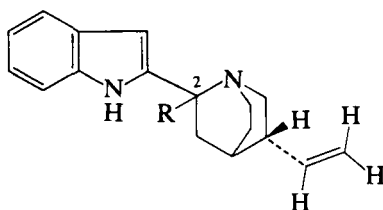


[491] Aristoteline

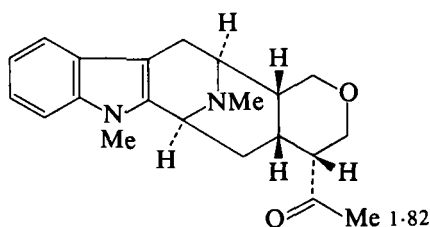
In the ^1H NMR spectrum of aristoteline [491] the two C-methyl singlets adjacent to the non-indolic nitrogen atom undergo large shifts to high frequency on the addition of TFA or europium shift reagent. (296) Some ^1H NMR spectral data on couroupitine A [492] (297) and in akagerine [493] (298) have been published.

[492] Couroupitine A (in CDCl_3)

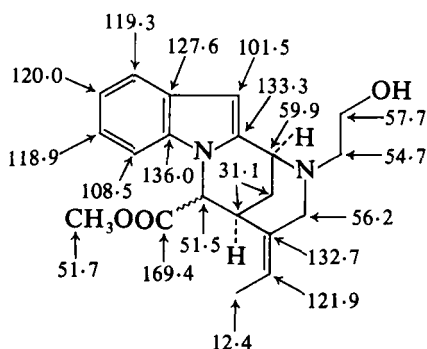
The C(2) configuration of [494] and [495] is reflected in the chemical shifts of the methylene protons of the vinyl group. Shielding of these protons by the anisotropic effect of the indole group is observed in [495] (δ 4.96) (cf. δ 5.08 in [494]). (299)

[493] Akagerine (in CDCl_3)[494] R = α -H[495] R = β -H

If chair conformations of the D and E rings in dihydroalstonerine [496] are assumed then the COMe group lies above the indole nucleus. This group has an unusually low frequency absorption (δ 1.82) for its COMe protons. (300) ^{13}C NMR parameters for vinoxine are shown in [497]. (301)



[496] Dihydroalstonerine

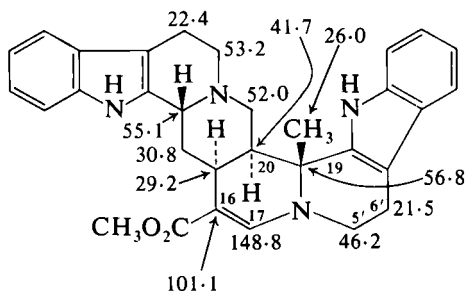


[497] Vinoxine

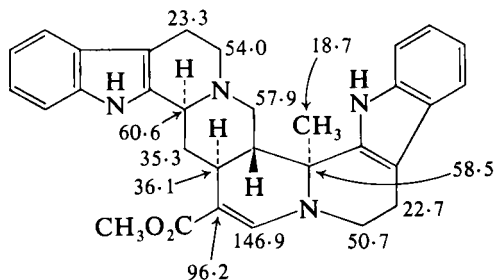
K. Bisindole alkaloids

1. *Roxburghines*

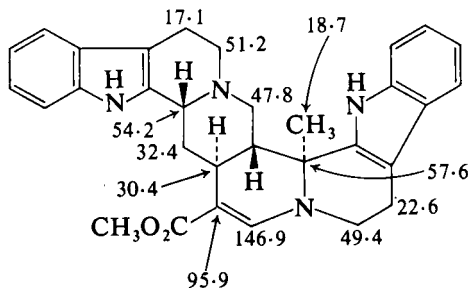
The ^{13}C NMR spectra of roxburghine B, C, D, and E are summarized in [498]–[501]. (302) The ^{13}C shift assignments are aided by data on the ajmalicinoid alkaloids (Sections XII.D). Thus roxburghine D and E are related to 3-iso-19-epi-ajmalicine (pseudo series) and roxburghine C to ajmalicine (normal series). The angular methyl group in roxburghine E is



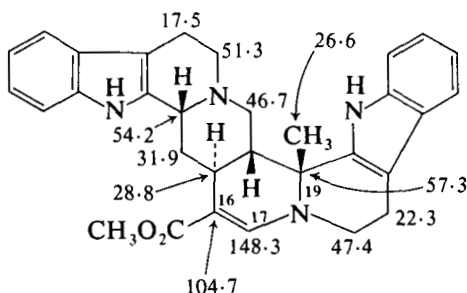
[498] Roxburghine B (in CDCl_3)



[499] Roxburghine C (in acetone)

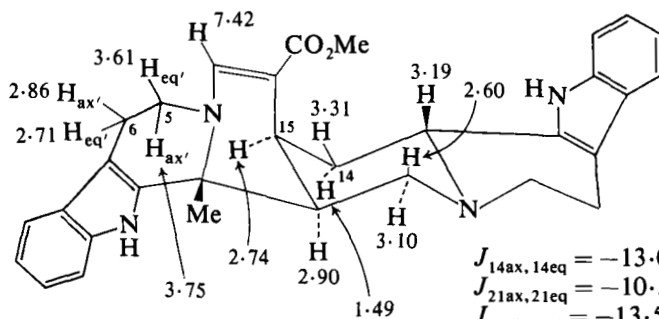


[500] Roxburghine D (in CDCl_3)

[501] Roxburghine E (in CDCl_3)

equatorial [only one γ -effect from C(21)] and that in roxburghine D axial as shown by their differing ^{13}C shifts. The C(16) shifts in roxburghine D and C are unusual and result from conjugation in the system $\text{N}-\text{CH}=\text{C}-\text{COOMe}$. This conjugation is sterically inhibited in roxburghine E. The ^{13}C NMR spectrum of roxburghine B is in best accord with the *c/d-trans* conformation of akuammigine (epi-allo series), and the ^{13}C methyl shifts in roxburghine B and E (equatorial methyl) are similar, suggesting an equatorial methyl in roxburghine B as shown in [502]. (302)

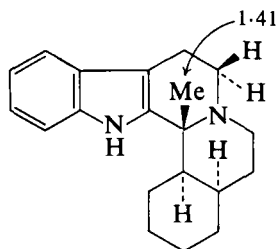
The 300 MHz ^1H NMR spectrum of roxburghine B is in accord with the conformation [502]. (303) The chemical shift (δ 3.19) of the 3-proton in roxburghine B [cf. δ 4.31 and δ 4.45 for the 3-protons in roxburghine D and E (304)] indicates the anticoplanar arrangement of C(3)-H and the nitrogen lone pair. ^1H NMR data for roxburghine E

[502] Roxburghine B (in CD_3COCD_3)

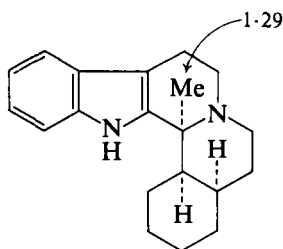
$J_{14\text{ax}, 14\text{eq}} = -13.0$	$J_{20, 21\text{eq}} = 5.0$
$J_{21\text{ax}, 21\text{eq}} = -10.5$	$J_{20, 21\text{ax}} = 11.0$
$J_{5\text{ax}', 5\text{eq}'} = -13.5$	$J_{15, 20} \leq 2$
$J_{6\text{ax}', 6\text{eq}'} = -15.0$	$J_{15, 17} = 2.0$
$J_{3, 14\text{ax}} = 11.5$	$J_{5\text{ax}', 6\text{ax}'} = 11.0$
$J_{3, 14\text{eq}} = 2.5$	$J_{5\text{ax}', 6\text{eq}'} = 5.0$
$J_{14\text{ax}, 15} = 3.8$	$J_{5\text{eq}', 6\text{ax}'} = 6.5$
$J_{14\text{eq}, 15} = 2.5$	$J_{5\text{eq}', 6\text{eq}'} \leq 1$
	$J_{5\text{eq}', 17} \leq 1$

support the *cis*-C/D,*trans*-D/E stereochemistry (305), and the equatorial nature of the angular methyl group is shown by the chemical shift (δ 1.63) of the methyl protons compared with that (δ 1.11) of the axial methyl protons in roxburghine D.

Methyl group proton chemical shifts in structurally related inside yohimbanes are shown in [503] and [504]. (306)



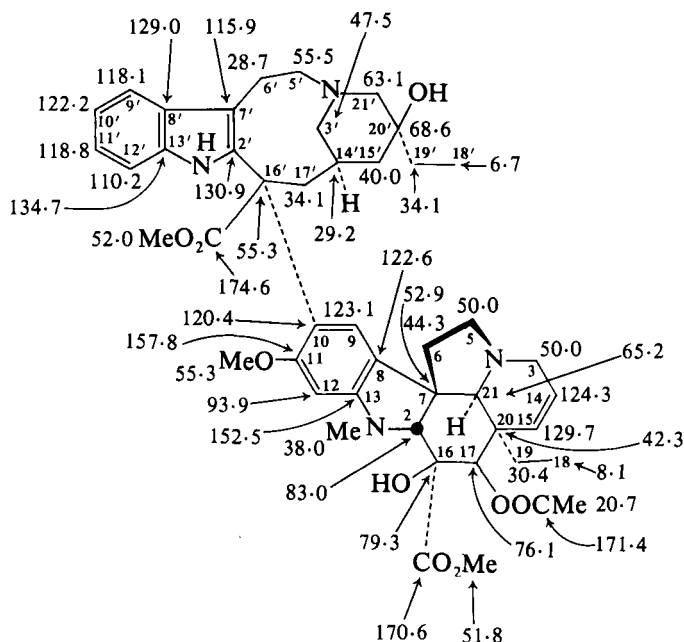
[503] (in CDCl_3)



[504] (in CDCl_3)

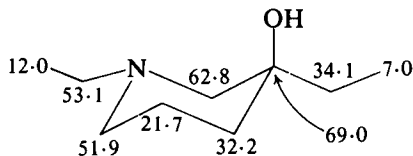
2. Vincaleucoblastine and related alkaloids

Unlike the sharp lines in the vindoline part of the ^{13}C NMR spectrum of vincaleucoblastine [505], the signals arising from the velbanamine

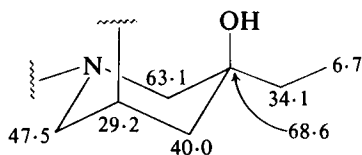


[505] Vincaleucoblastine (in CDCl_3)

portion are broadened presumably as a result of the flexibility of the nine-membered ring. Operation at lower frequency, and using a 0.10 M solution at 33–38°C, gave a spectrum suitable for complete analysis. The very similar chemical shifts of C(21'), C(20'), C(19'), and C(18') and the corresponding signals in the spectrum of 1,3-diethylpiperidinol [506] suggest a similar conformation [507] for the piperidine moiety in

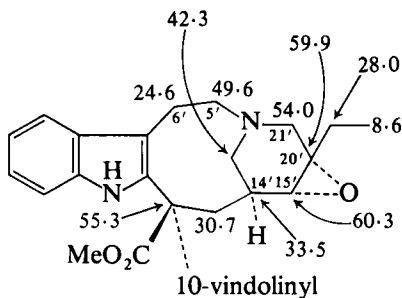


[506]

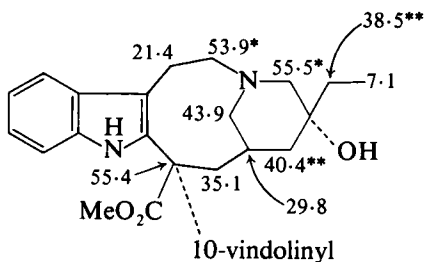
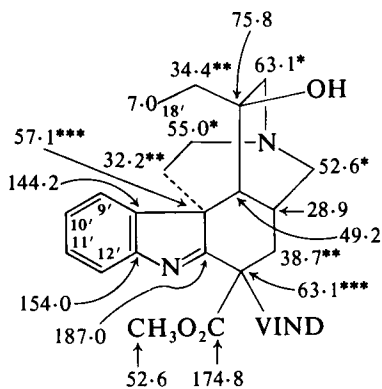


[507]

vincaleucoblastine. In the ^{13}C NMR spectrum of leurosine [508] the C(20') and C(15') shifts and the value of $^1J(\text{C}_{15'}-\text{H}_{15'})$ of 170 ± 5 Hz are typical of the oxiran function. Largely on the basis of ^{13}C shifts the structure of leurosine has been revised to [509]. (307) The

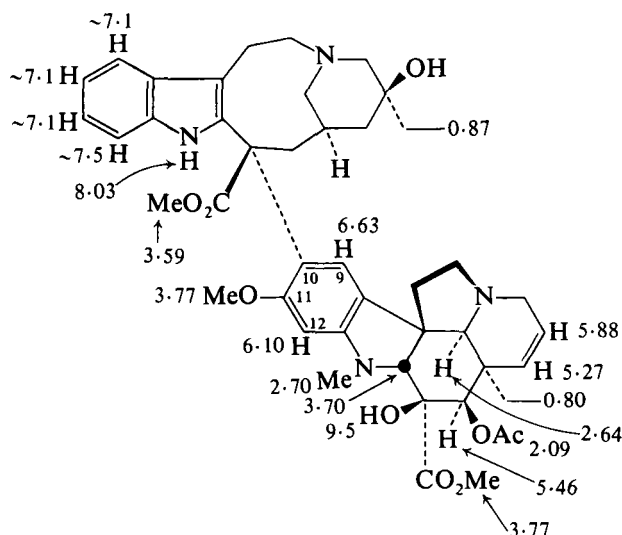
[508] Leurosine (in CDCl_3)

$$J_{\text{C}(15'), \text{H}(15')} = 170 \pm 5$$

[509] Leurosine (in CDCl_3)[510] Vincathicine (in CHCl_3)

inversion-recovery pulse sequence technique has been used as an aid to the analysis of the spectra of vincaleucoblastine type alkaloids. Spin-lattice relaxation time measurements on alkaloids have shown T_1 values of greater than 2 s for quaternary carbon atoms, of 0.1–0.25 s for methine and methylene carbons, and of 0.5–1.0 s for methyl carbons. Thus when a waiting time T_1 of ± 0.35 s is used in an inversion-recovery pulse sequence, methine and methylene resonances are upright and the quaternary carbons are inverted. This method has been applied to the analysis of the ^{13}C NMR spectrum of leurocolombine, vincadioline, (308) and vincathicine [510]. (309)

Comparison of the ^1H shifts (CDCl_3) of vincaleucoblastine [511] with those in the spectrum of vincathicine shows significant difference for the



[511] Vincaleucoblastine (in CDCl_3)

9-proton and 18-methyl resonances in the vindoline portion (vincathicine δ 9-H 6.45, δ 18-Me 0.57) and for the aromatic protons in the "indole" portion [vincathicine 9'-H and 12'-H (δ 7.60 or 7.66), 10'-H and 11'-H (δ 7.33 or 7.57)]. (309)

The 9-, 12-, and 18-proton resonances in the vindoline moiety of the vincaleucoblastine type of dimer are particularly sensitive to changes in the velbanamine type moiety. Thus in [512] these resonances appear at δ 6.03 (12-H), δ 6.52 (9-H), and δ 0.81 (18-H), values close to those in vincaleucoblastine [511], in contrast to the corresponding shifts in the 16-epimer of [512] [δ 5.92 (12-H), δ 6.85 (9-H), δ 0.60 (18-H)]. (310)



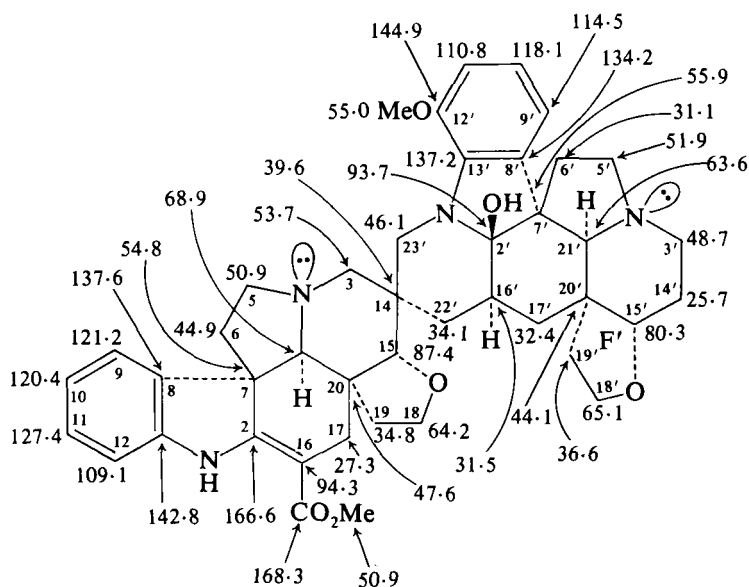
[513] Vincovaline (in CDCl_3)

[514] Vincalencoblastine ether (in CDCl_3)

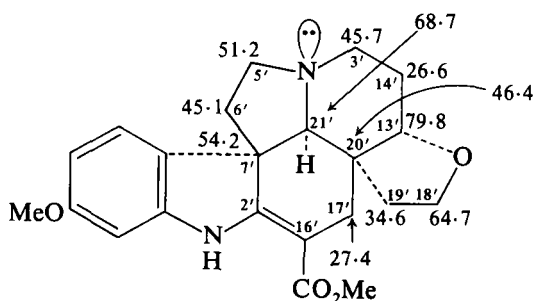
The tritium NMR spectrum of "[G-³H]" vincalencoblastine sulphate in D₂O gave ³H signals at δ 6.45 (12-³H), δ 7.25 (10'-³H, 11'-³H), δ 7.40 (9'-³H), and δ 7.72 (12'-³H). (313)

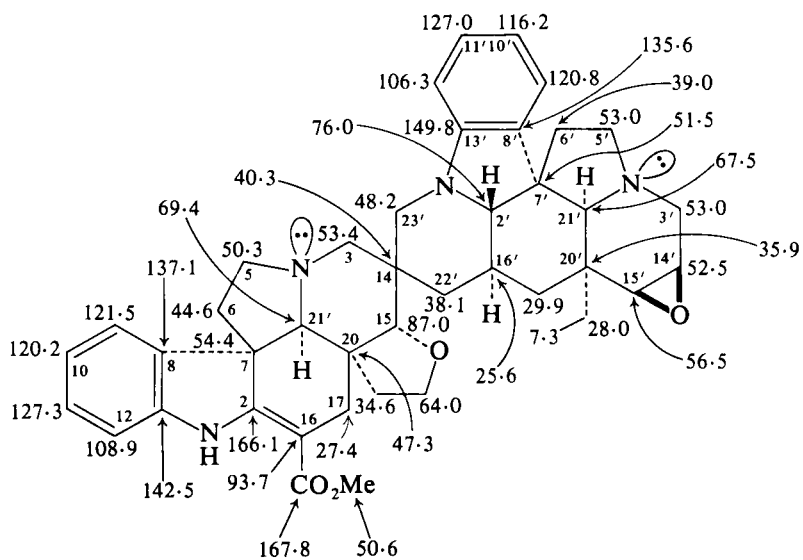
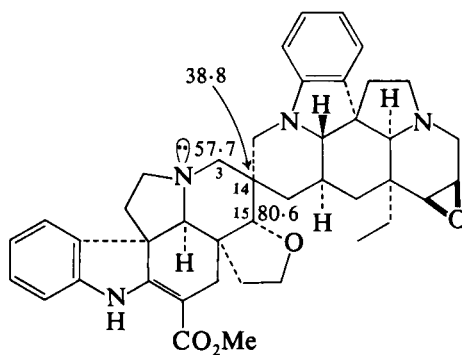
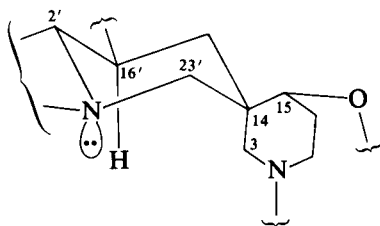
3. Other bisindole alkaloids

The ^{13}C NMR spectrum of vobtusine is summarized in [515]. Assignments are aided by comparison with the ^{13}C NMR spectra of

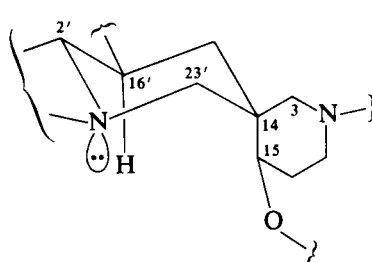
[515] Vobtusine (in CDCl_3)

vandrikinine [516] and of tabersonine [434]. C(3') in vandrikinine absorbs at δ 45.7 and in vobtusine at δ 48.7. This high frequency shift in vobtusine has been interpreted in terms of a reduced γ -effect from the ring F' oxygen atom arising from conformational changes consequent upon loss of the C(2'),C(16') double bond in vandrikinine. C(3) and

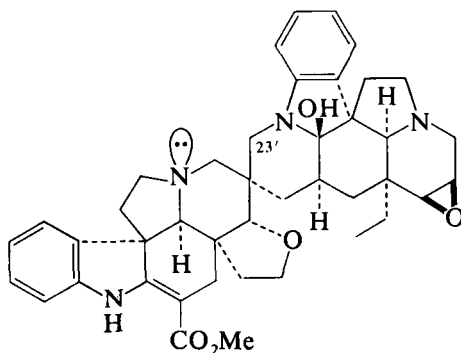


[517] Voafoline (in CDCl₃)[518] Isovoafoline (in CDCl₃)

[519]



[520]

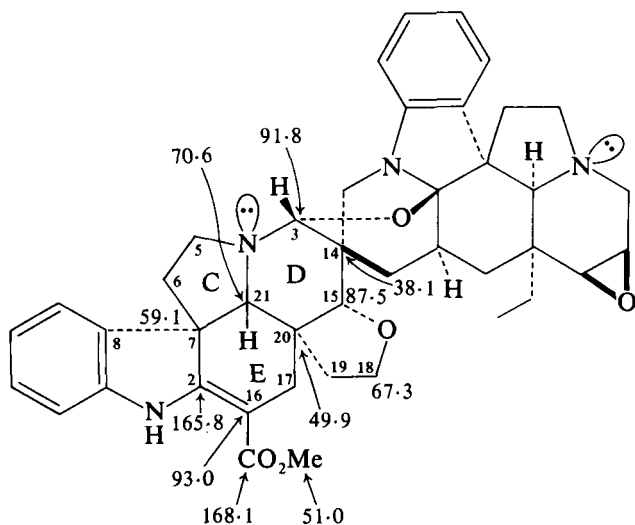


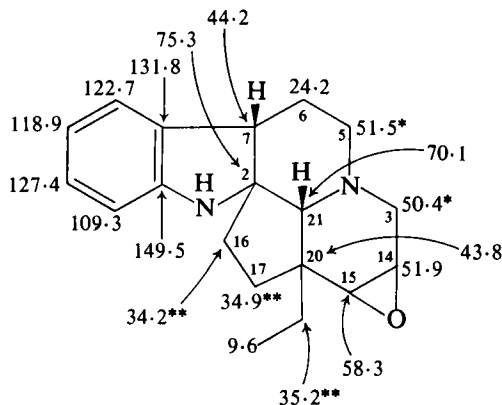
[521] Voafolidine

operative on C(15) in [520] with a resultant lower frequency absorption than in [519].

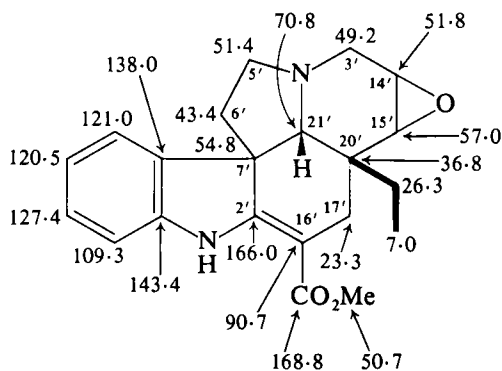
Differing γ -effects of the angular hydroxyl group on C(23') in the voafoline–voafolidine [521] series compared with those in the vobtusine series reflect changes in conformation brought about by interactions involving the 12'-methoxyl group in the vobtusine series.

The presence of the ether linkage in folicangine [522] causes such drastic changes in shifts of the ^{13}C nuclei in the C, D, E, and tetrahydropyran rings that the alkaloid is assigned the $3\beta\text{-H}$ configuration

[522] Folicangine (in CDCl_3)

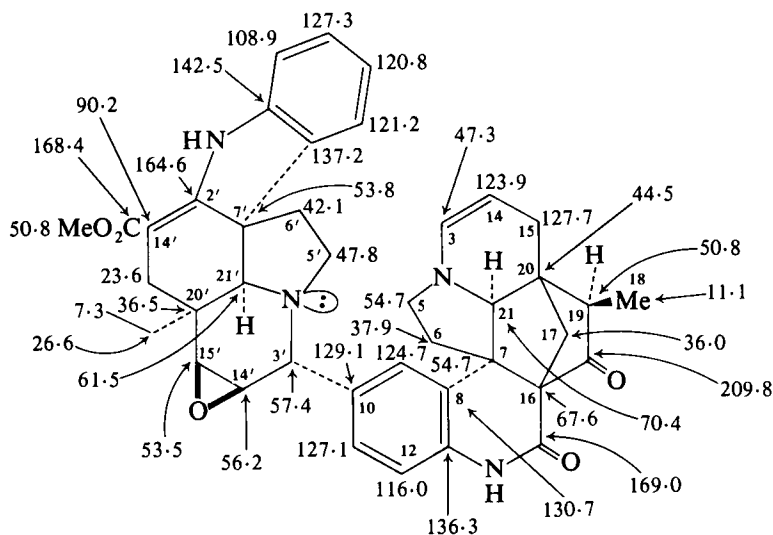


[525] Andragline

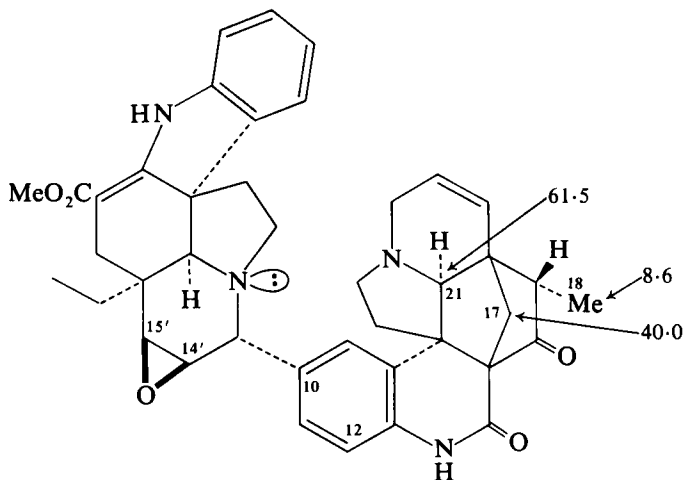
[526] 14,15 β -Epoxytabersonine

spectra were run under conditions such that the value of $^1J(\text{C}-\text{H})$ was reduced by *ca.* 50% when aromatic methine carbons show couplings only with *ipso* and *meta* protons. Under these conditions the SFORD spectrum of scandomelonine showed that, of the aromatic methines, only C(12) absorbed as a sharp doublet indicating dimer linkage at C(10). The change in C(19) stereochemistry on going from scandomelonine [527] to episcandomelonine [528] is reflected in the C(17), C(18), and C(21) shifts. The presence of the epoxide group in both compounds was confirmed by the $^1J(\text{C}-\text{H})$ value of *ca.* 180 Hz for one bond couplings involving C(15') and C(14'). (317)

The structure [529] was assigned to pleiocorine largely on the basis of a comparison of its ^{13}C NMR spectrum with the spectra of villalstonine

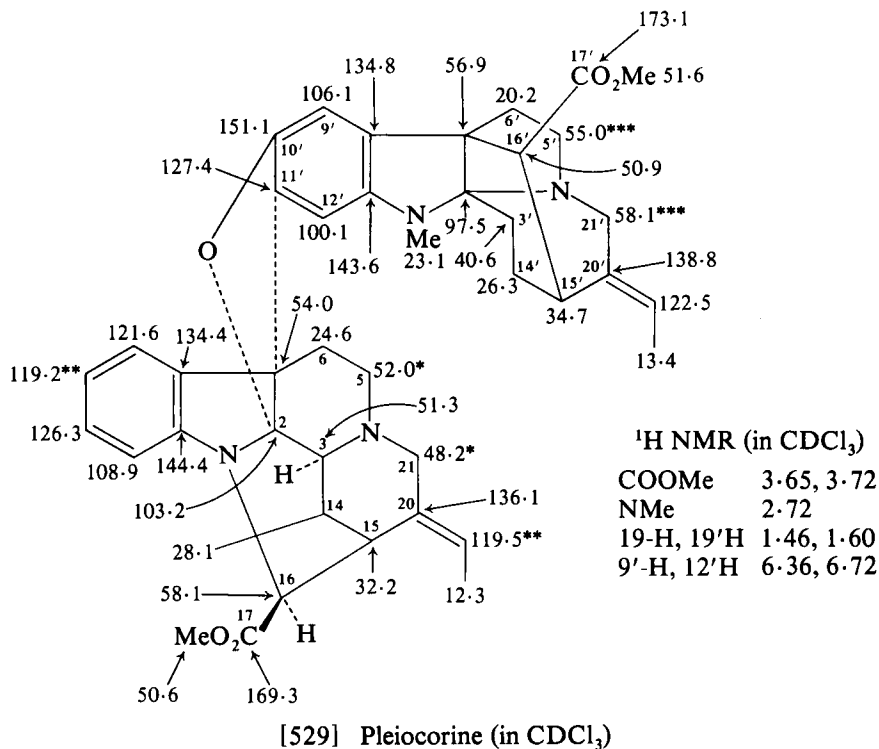


[527] Scandomelonine



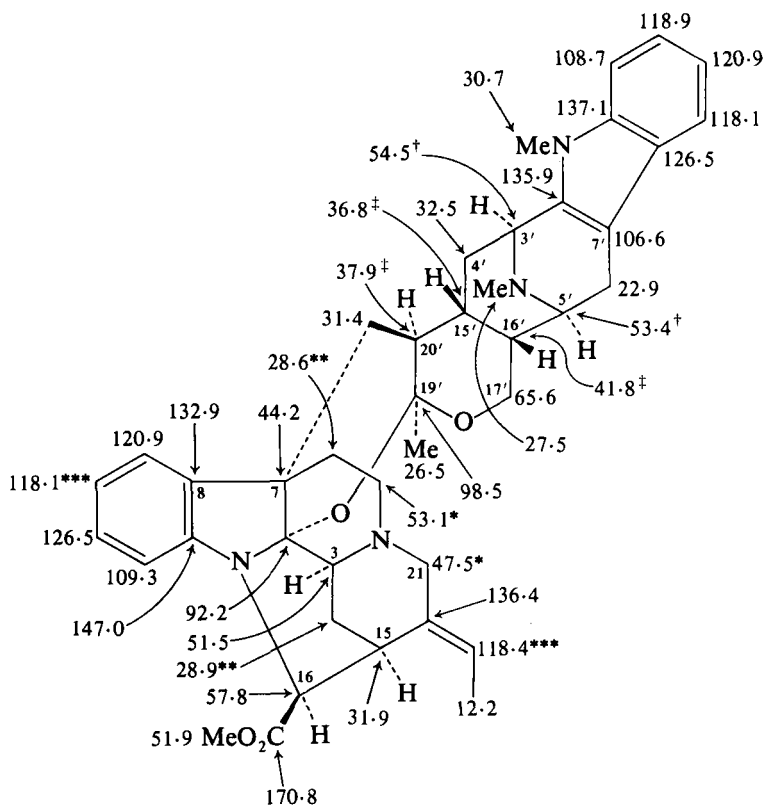
[528] Episcandomelonine

[530], macralstonidine [531], and vincorine [532]. The absorption at δ 6.36 and 6.72 in the ^1H NMR spectrum of [529] indicated the 9'- and 12'-protons and a 10',11'-disubstituted aromatic ring. Assignment of the signals at δ 151.1 and 100.1 to C(10') and C(12') respectively indicated the linkage shown in [529]. (318)



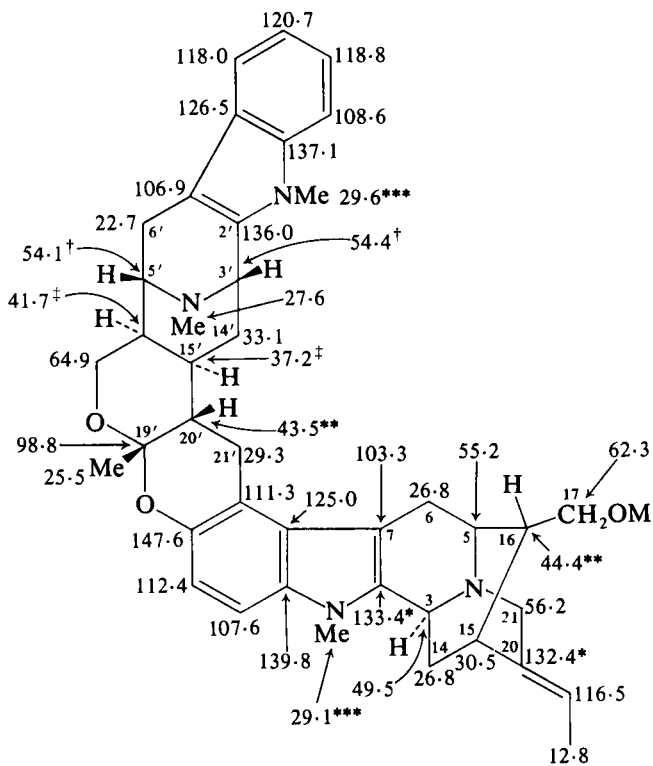
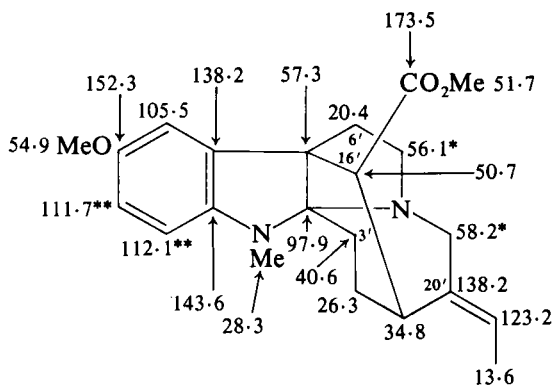
The structure of 14',15'-dihydropycnanthine has been revised to [533] from a comparison of its ¹³C NMR spectrum with that of villalstonine [530] and of vindolinine [439]. That [533] belongs to the 19'*S* series is shown by the similarity of its 18'-proton and carbon parameters to those in 19'-epivindolinine [534] (compare values in vindolinine [535]). The similarity of C(21') shifts in 19'-epivindolinine and in 14',15'-dihydropycnanthine shows the absence of the endocyclic homoallyl effect. (319)

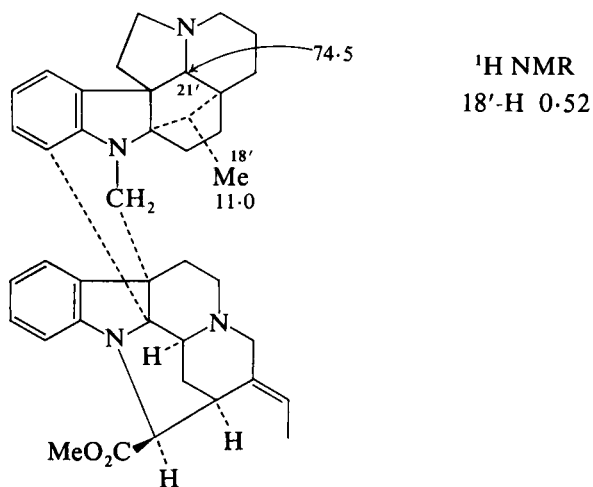
The tabernaelegantines [536]–[539] are dimers consisting of vobasine and voacangine type moieties. The ¹H NMR spectra show typical features of these systems (δ 3.9 OMe and δ 3.7 CO₂Me in voacangine moiety; δ 2.6 and δ 2.5 NMe and CO₂Me in vobasine moiety). In dregamine [422] and tabernaemontanine [424] the configuration of the ethyl substituent [analogous to C(20) in the tabernaelegantines] may be assigned from the 19- and 20-proton shifts [19-H δ 1.88 and 20-H 1.32 in dregamine (α -Et); 19-H and 20-H δ 1.50 in tabernaemontanine (β -Et)]. The complexity of the spectra of the dimers does not enable this criterion to be used, and resort has to be made to ¹³C NMR spectro-

[530] Villalstonine (in CDCl_3)

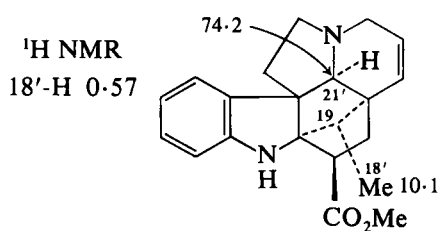
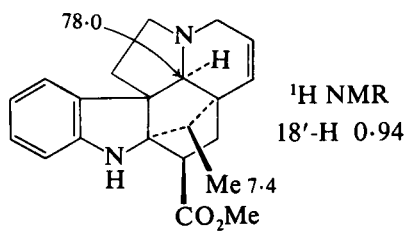
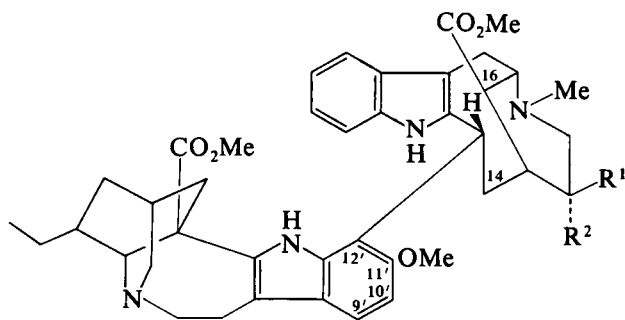
scopy. For example, in tabernaegantaine A [536] (β -Et) C(16) and C(14) absorb at δ 44.0 and 36.8 respectively in contrast to the corresponding shifts (δ 49.9 and 29.2) in tabernaegantaine C [537] (α -Et). The C(10') or C(12') linkage point in [536]–[539] is shown by the aromatic carbon shifts [tabernaegantaine A [536]: C(9') 117.1, C(10') 105.1, C(11') 152.1, C(12') 114.9; tabernaegantaine B [538]: C(9') 117.6, C(10') 127.9, C(11') 153.8, C(12') 93.0]. (320) The ^1H NMR spectrum of a related alkaloid, tabernamine, has been described. (321)

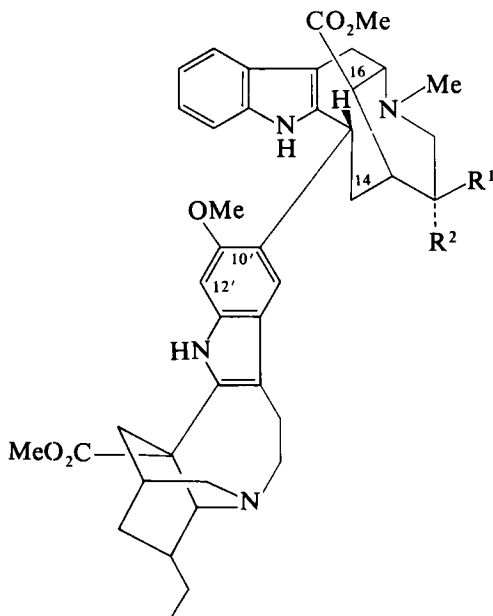
The dimer linkage in accedinisine [540] is considered to involve C(10'). The aromatic ring proton shifts are assigned as shown in [540] by comparison with vobasinol [541] and affinisine [542]. Since the 4-proton in indole absorbs at lowest frequency the low frequency singlet at δ 7.20 in [540] is assigned to the corresponding proton at C(9') which gives C(10') as the linkage carbon. (322)

[531] Macralstonidine (in CDCl_3)[532] Vincorine (in CDCl_3)



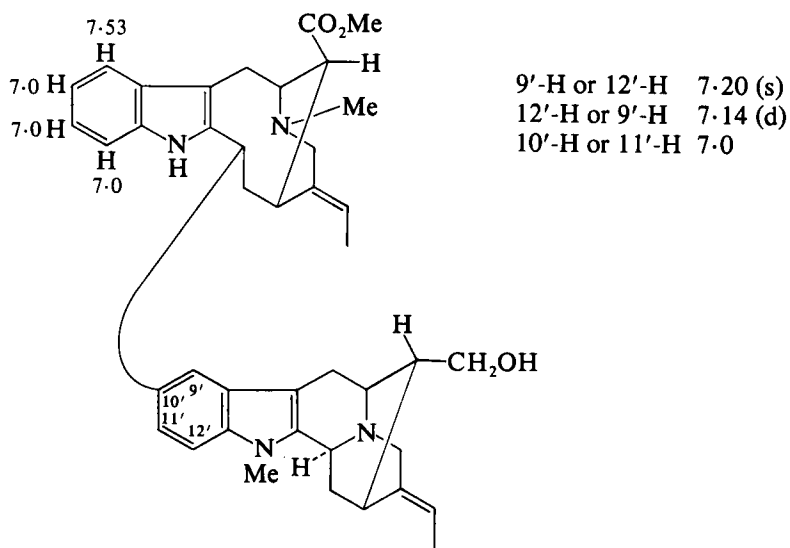
[533] 14',15'-Dihydropycnanthine

[534] 19'-Epivindoline (19*S*)[535] Vindoline (19*R*)[536; R¹ = Et, R² = H] Tabernaelegantine A[537; R¹ = H, R² = Et] Tabernaelegantine C

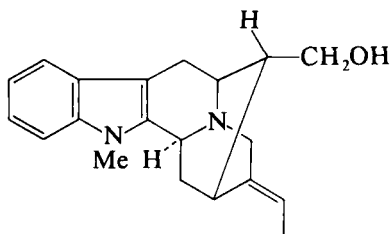
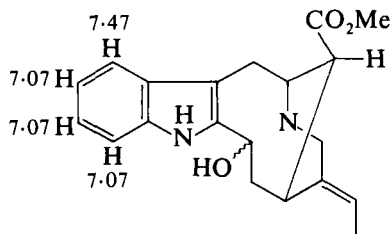


[538; $R^1 = \text{Et}$, $R^2 = \text{H}$] Tabernaegantine B

[539; $R^1 = \text{H}$, $R^2 = \text{Et}$] Tabernaegantine D



[540] Accedinisine (in CDCl_3)



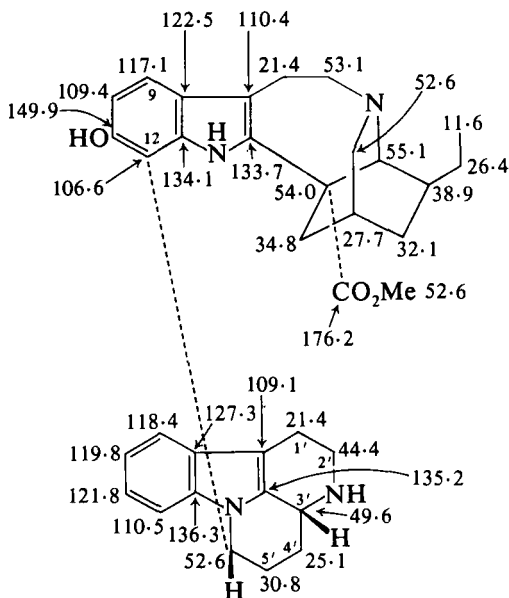
Ar-H 7.33, 7.25, 7.14, 7.02

[541] Vobasinol (in CDCl_3)

[542] Affinisine (in CDCl_3)

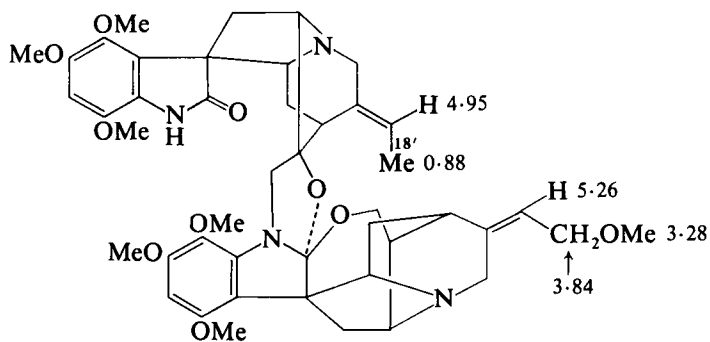
The ^{13}C NMR spectra of bonafousine is summarized in [543]. (323)

In a model of gardmultine [544] the 18'-methyl is seen to lie over the indoline moiety thus providing an explanation of its low frequency absorption (δ 0.88). Treatment of [544] with hydrochloric acid gives the conformationally more mobile oxindole [545] which now shows absorption for the 18'-methyl protons at δ 1.43. (324)

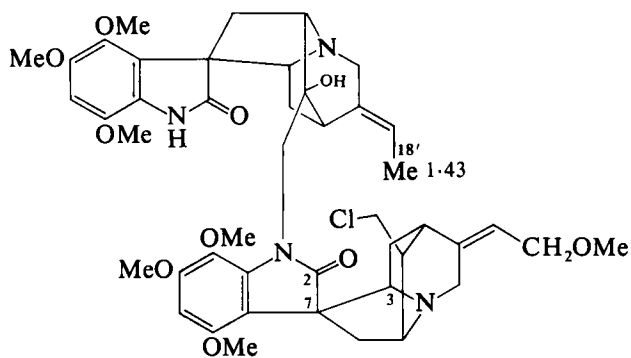


[543] Bonafousine (in CDCl_3)

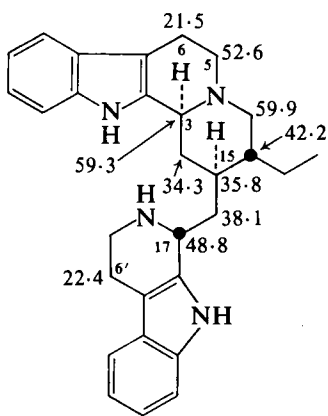
The preferred conformations of ochrolifuanine A [546] and ochrolifuanine B [547] are assigned as [548] and [549] respectively on the basis of C(14) shift differences. In the yohimbane series C(14) absorbs at δ 37.2 and the differences arising in [548] and [549] result from the



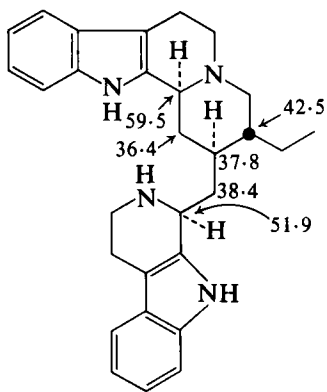
[544] Gardmultine



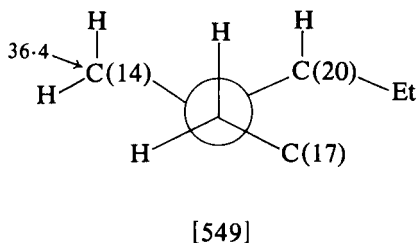
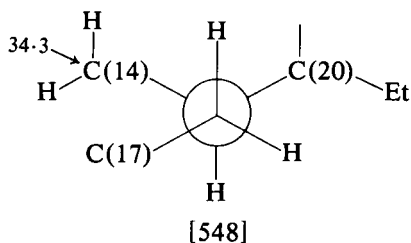
[545]



[546] Ochrolifuanine A



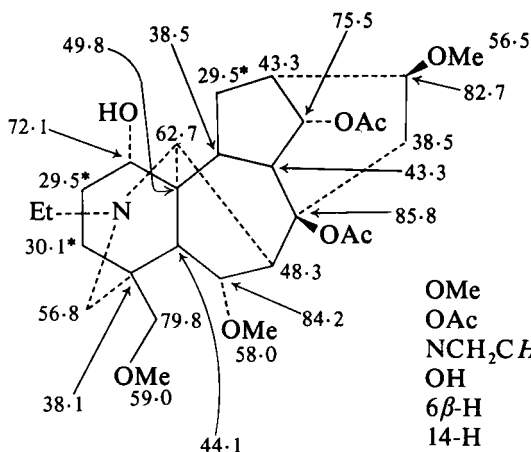
[547] Ochrolifuanine B



differing γ -effects. The C(15) and C(20) signals are differentiated on the basis of the corresponding shifts in the indoloquinoline [363] with C(15) shielded by the C(17) substituent. (103)

XIII. DITERPENE ALKALOIDS

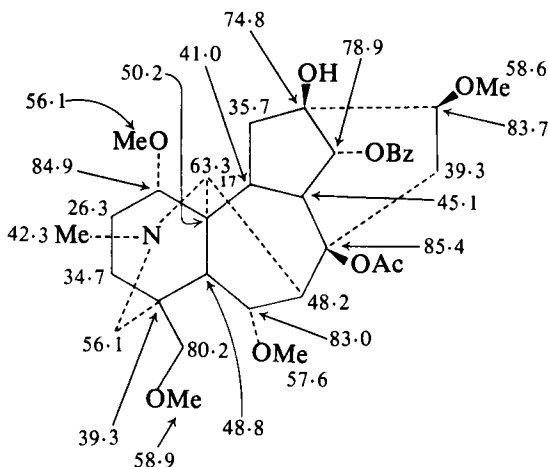
The ^1H NMR spectrum of delphisine is summarized alongside [550]. The absorption of the 1β -proton (δ 3.65) as a multiplet ($W_4 \sim 6$ Hz)



¹ H NMR in CDCl ₃	
OMe	3.25, 3.30, 3.31
OAc	1.96, 2.02
NCH ₂ CH ₃	1.12 (<i>J</i> = 7)
OH	7.10
6β-H	4.04 (<i>J</i> = 1, 7)
14-H	4.80 (<i>J</i> _{14,9β} = <i>J</i> _{14,13β} = 4.5)
1β-H	3.65 (<i>W</i> _i = 6)
CH ₃ OMe	3.09, 3.58 (<i>J</i> = -9)

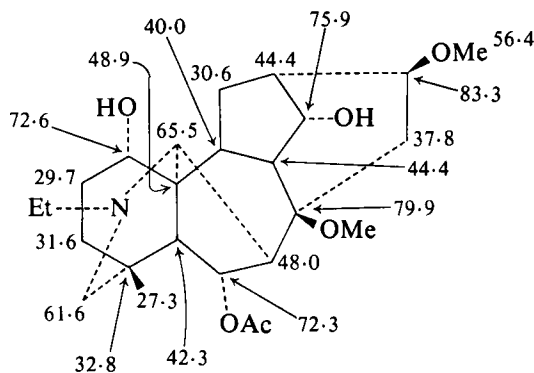
[550] Delphisine (in CDCl_3)

indicates the hydrogen bonded boat conformation of ring A [551] in which the dihedral angles between C(1)–H and the C(2) methylene bonds are both *ca.* 60°. In delphisine 1-acetate, in which the intramolecular hydrogen bond is no longer possible, the 1 β -proton (δ 4.86) shows vicinal coupling constants with the C(2) methylene protons of 9 and 5.5 Hz in agreement with a chair conformation of ring A. (325) These conformational changes are also reflected in the ¹³C NMR spectra of delphisine [550] and delphisine 1-acetate (326) with marked

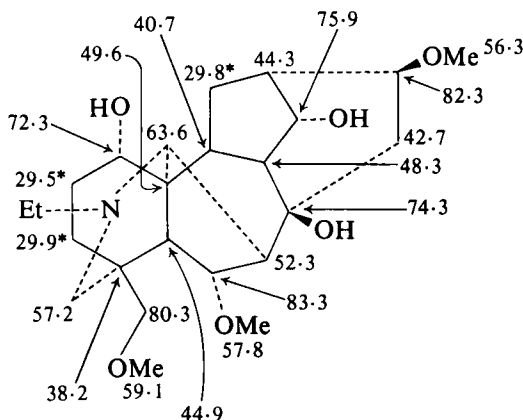
[553] Delphinine (in CDCl_3)

and delphinium species) have been described (326) and corrections made to some assignments (327) for delphonine and isotalatizidine.

Structure [554] has been assigned to alkaloid A from *Delphinium bicolor* Nutt. from a comparison of its ^{13}C NMR spectrum with the

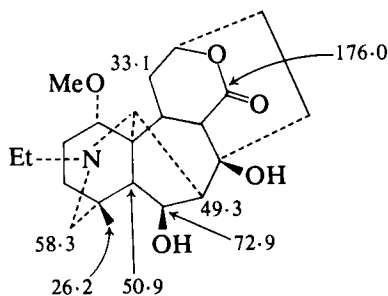
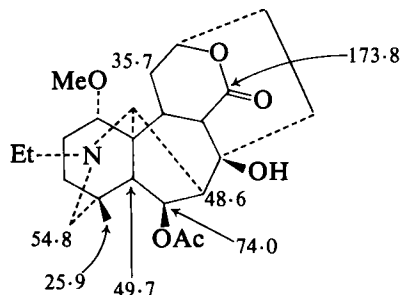
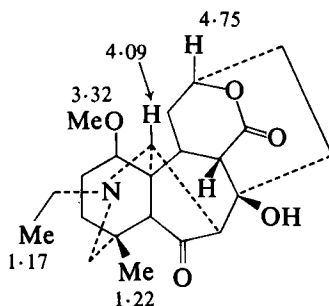
[554] (in CDCl_3)

spectra of neoline [555], 8-acetylneoline, trimethoxyneoline, and delphisine [550]. In all known diterpene alkaloids the $\text{C}(6)\text{-OCH}_3$ nucleus absorbs at δ 57.8–58.0, and the absence of such a signal in the spectrum of [554] indicates the absence of the $\text{C}(6)$ methoxyl group. The secondary acetate function in alkaloid A [554] is indicated from a comparison of its acetate shifts (δ 170.9, 21.5) with those in 8-acetyl-

[555] Neoline (in CDCl_3)

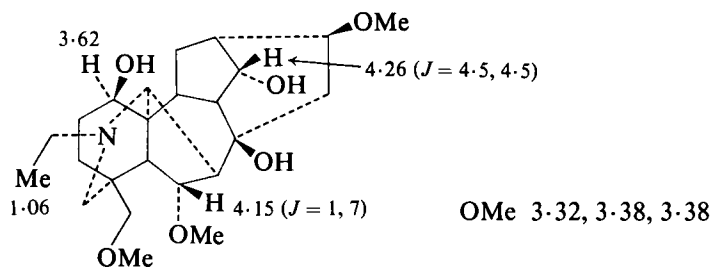
neoline (δ 169.9, 22.5), and its α configuration by comparison with heteratisine [556] and 6-acetylheteratisine [557]. (328)

In the ^1H NMR spectrum of 19-oxodehydroheteratisine [558] the 9β -proton absorbs to low frequency of the corresponding absorption (δ

[556] Heteratisine (in CDCl_3)[557] 6-Acetylheteratisine (in CDCl_3)[558] 19-Oxodehydroheteratisine (in CDCl_3)

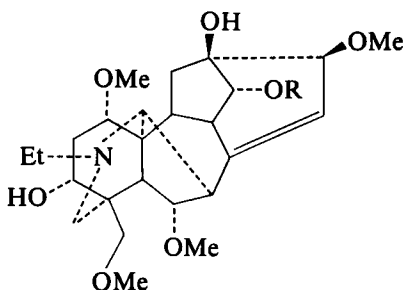
4.03) in heteratisine since this proton lies in the shielding region of the C(6) carbonyl group. In addition the C(18)-methyl protons absorb (δ 1.22) to high frequency of those in heteratisine acetate (δ 0.85). (329)

^1H NMR data for delphirine are summarized in [559]. Since the ^{13}C NMR spectrum of [559] resembles that of neoline (with the exception of



[559] Delphirine (in CDCl_3)

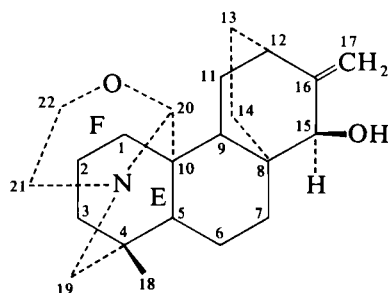
ring A and C(19) shifts which resemble those of 1-epidelphisine), delphirine is shown to be 1-epineoline. (330) The presence of the C(8)–C(15) double bond in falaconitine [560] is shown by the C(8) and C(15) absorption at δ 146.6 and 116.1 (cf. pyrodelphinine [552]). (331)



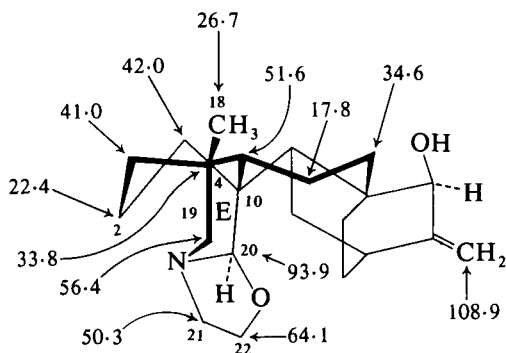
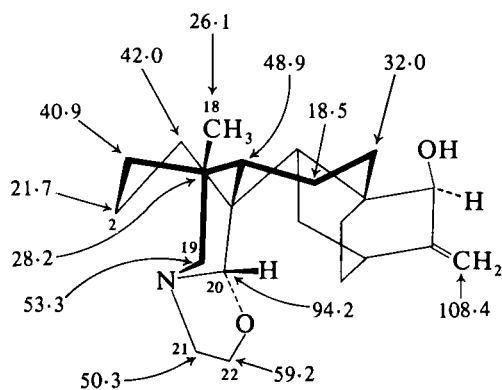
[560; $\text{R} = 3,4-(\text{MeO})_2\text{C}_6\text{H}_3\text{CO}$] Falaconitine

Agreement has now been reached on the origin of the two C(4)-methyl signals in the room temperature ^1H NMR spectrum of atisine [561] (1) arising as a result of the configurational equilibrium [562] = [563] with [562] predominating. The room temperature ^{13}C NMR spectrum of atisine in CDCl_3 shows two sets of signals corresponding to [562] and [563]. (332)

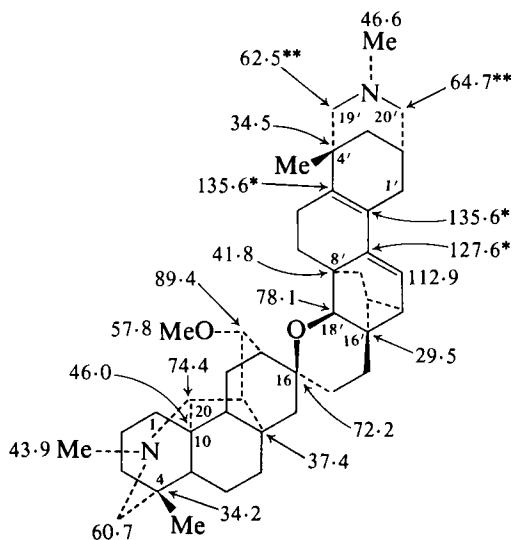
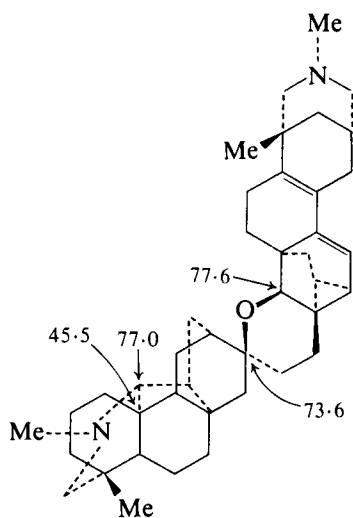
The *N*-methyl signals in the ^1H NMR spectrum (CDCl_3) of staphisine [564] may be individually assigned (*N*Me δ 2.27; *N*Me' δ 2.13) since on changing structure from staphisine to staphidine [565] the δ 2.27



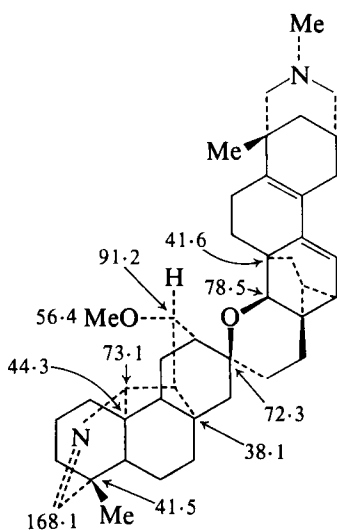
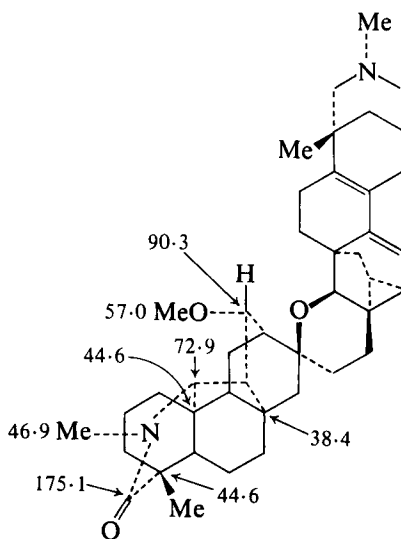
[561] Atisine

[562] (in CDCl₃)[563] (in CDCl₃)

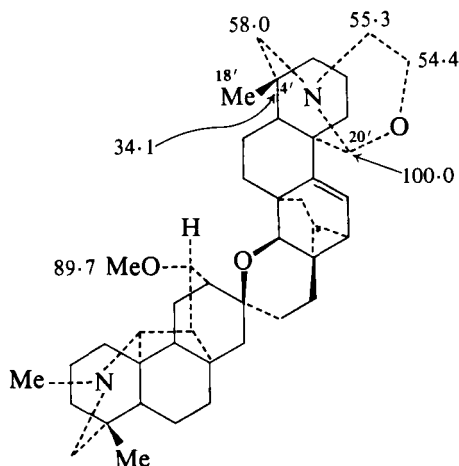
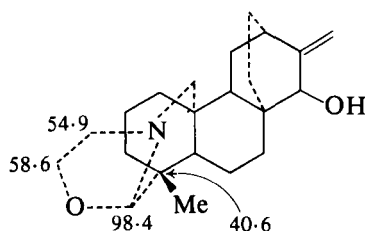
signal moves to δ 2.21. The ¹³C NMR spectrum of staphisine is summarized in [564], and where differences are noted ¹³C shifts for staphidine [565] and staphinine [566] are given. (333) In the lactam

[564] Staphisine (in CDCl_3)[565] Staphidine (in CDCl_3)

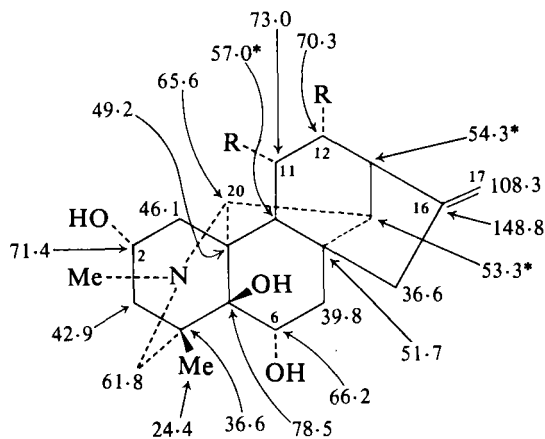
derivatives of these systems, e.g. staphigine [567], changes in the ^{13}C shifts resulting from the presence of the C(19) oxo function are shown. In addition the ^1H NMR spectrum of [567] shows the absorption for the *N*-methyl proton of the lactam group at δ 2.98 and for the 18-methyl

[566] Staphinine (in CDCl_3)[567] Staphigine (in CDCl_3)

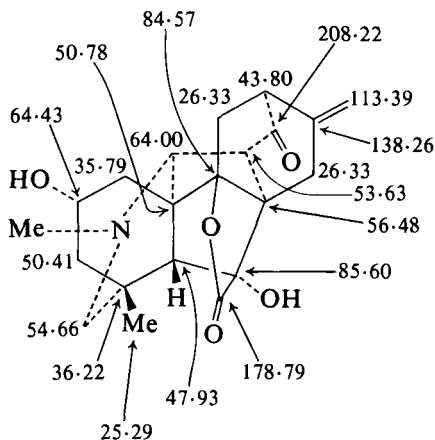
proton at δ 1.12 (cf. δ 6.91 in staphisine [564]). (334) In the ^{13}C NMR spectrum of staphisagnine [568] the oxazolidine ring, also present in atisine, is characterized by the similarity of the shifts of C(4') in these two alkaloids (δ 34.1 in staphisagnine [568], δ 33.8 in atisine [562]) and its difference from the corresponding absorption (δ 40.6) in isoatisine [569]. This is confirmed by the ^1H NMR spectrum of staphisagnine which shows absorption for the 18'-methyl protons at δ 0.82 in [568]

[568] Staphisagnine (in CDCl_3)

[569] Isoatisine

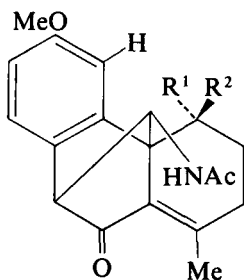
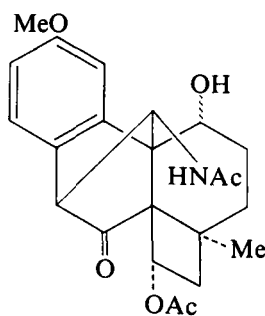
[570] Anopterine (in CDCl_3) R = O-Tigloyl ^1H NMR in CDCl_3

NMe	2.24
CMe	1.15
6-OH	10.00
2-H	4.07
6-H	3.49 ($J = 6$, after D_2O exchange)
11-H	5.48 ($J = 6, 4$)
12-H	5.11 ($J = 6, 3$)
13-H	2.90
17-H	4.82, 5.02
19-H	2.60, 3.64 ($J = -11$)
20-H	3.94

[571] Miyaconine (in CDCl_3)

(cf. δ 0.82 in atisine, δ 1.06 in isoatisine). In the spectrum of [568] the C(20') absorbs at δ 100.0 (cf. 93.9 in atisine [562]) showing the effect of the double bond. (335)

^1H and ^{13}C NMR data for anopterine [570] have been reported, (336) and the ^{13}C NMR spectrum of miyaconine [571] suggests α -orientation of the 2-hydroxyl group. (337)

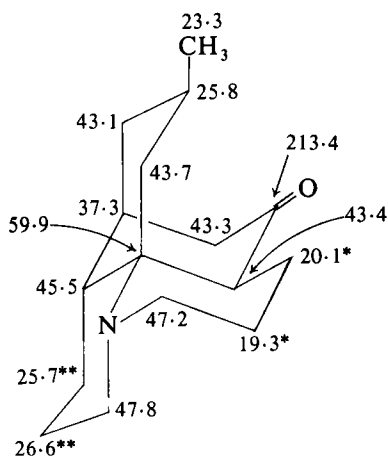
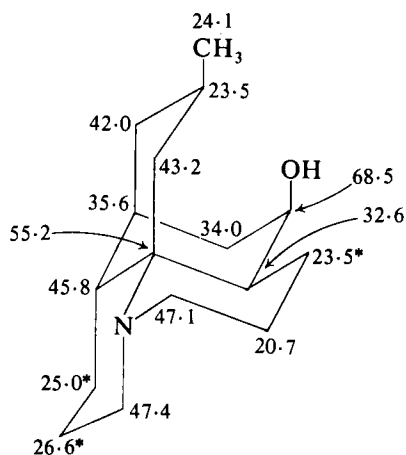
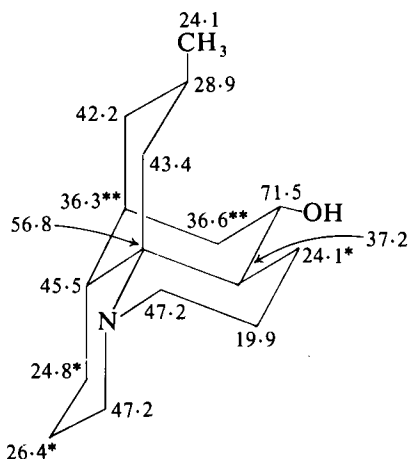
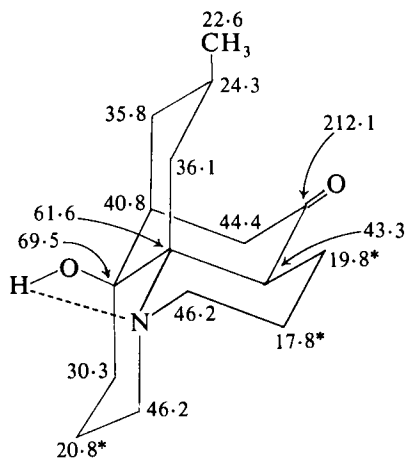
[572; $\text{R}^1 = \text{OH}$, $\text{R}^2 = \text{H}$][573; $\text{R}^1 = \text{H}$, $\text{R}^2 = \text{OH}$]

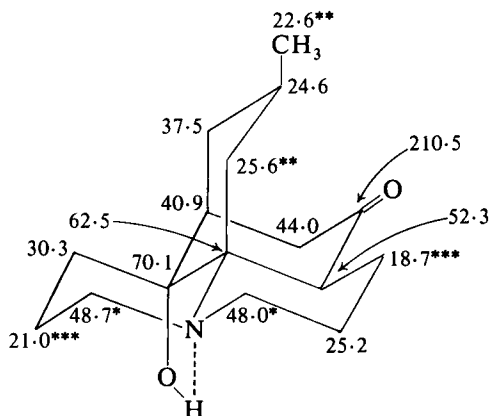
[574]

In the spectra of the synthetic intermediates [572] and [573] the chemical shifts of the depicted aryl protons are dependent upon the stereochemistry at the carbinol position (δ 7.13 in [572], δ 6.76 in [573]). In both α - and β -epimers of [574] the angular methyl group protons absorb at low frequency (δ 0.30, 0.34) as a result of shielding by the aryl ring. (338)

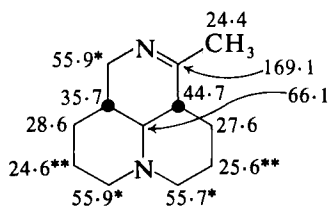
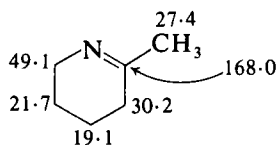
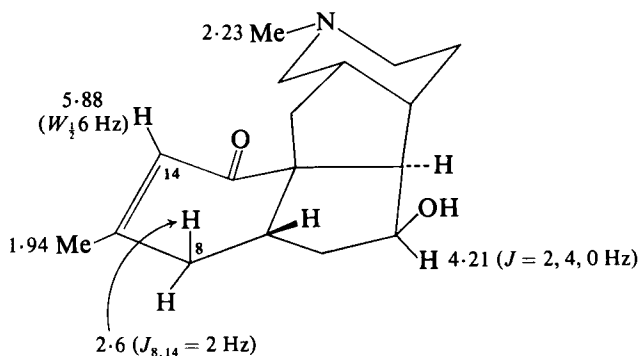
XIV. LYCOPODIUM ALKALOIDS

To illustrate some of the published work on the spectra of lycopodium alkaloids the ^{13}C NMR spectra of [575]–[579] are given. The spectra of [575]–[577] show the effect of the C(5) substituent on the C(15) shifts, and the *cis*-quinolizidine to *trans*-quinolizidine change [578] to [579] is reflected particularly in the C(4) and C(14) shifts. In all of the compounds except [579], C(4) is deshielded and C(14) shielded on *N*-protonation. (339) ^{13}C NMR data on a variety of synthetic intermedi-

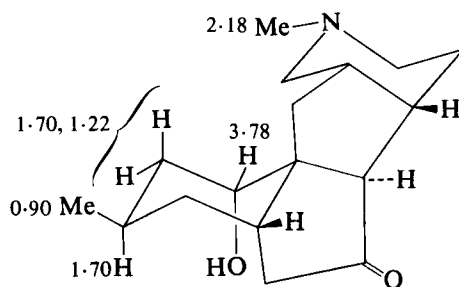
[575] Lycopodine (in CDCl_3)[576] Dihydrolycopodine (in CDCl_3)[577] Epidihydrolycopodine (in CDCl_3)[578] Lycodoline (in CDCl_3)

[579] Alkaloid-L23 (in CDCl_3)

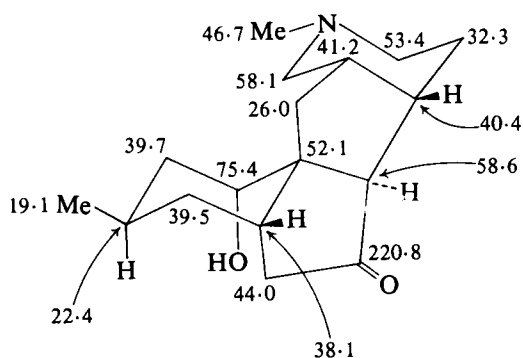
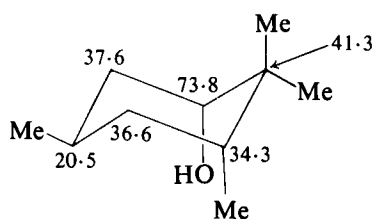
ates related to isosphoramine, e.g. [580], are available. (340) The C(3) and C(5) shifts in the spectrum of [580] show the *trans*-fusion of the quinolizidine moiety, and the C(2) and C(6) shifts show the di-equatorial attachment of the third ring. The shifts in the spectrum of the model

[580] (in CDCl_3)[581] (in CDCl_3)

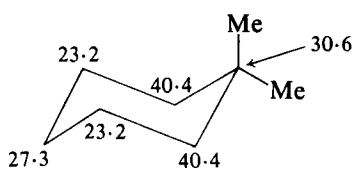
[582] Magellanine



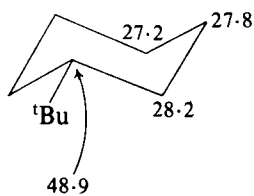
[583] Paniculatin

[584] (in CDCl_3)

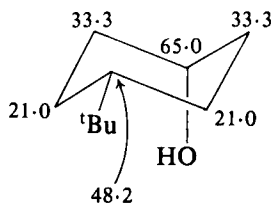
[585]



[586]



[587]



[588]

compound [581] show that the imino group, like the olefinic bond, can also exert the shielding endocyclic homoallyl effect (see Section XII.I).

The ^1H NMR spectra of magellanine and of paniculatine are summarized in [582] (341) and [583]. (342) The ^{13}C NMR spectrum of the latter alkaloid [584] provides an example of the use of model compounds in aiding signal assignment. For example, shifts were calculated for the model compound [585] from the shifts in [586], [587], and [588] (3) together with the methyl substituent effects shown in Table III.

REFERENCES

1. T. A. Crabb, in "Annual Reports on NMR Spectroscopy", Vol. 6A, E. F. Mooney (ed.), Academic Press, London, 1975, p. 249.
2. E. Wenkert, J. S. Bindra, C.-J. Chang, D. W. Cochran and F. M. Schell, *Accounts Chem. Res.*, 1974, 7, 46.
3. J. B. Stothers, "Carbon-13 NMR Spectroscopy", Academic Press, New York, 1972.
4. G. C. Levy and G. L. Nelson, "Carbon-13 Nuclear Magnetic Resonance for Organic Chemists", Wiley-Interscience, New York, 1972.
5. D. M. Grant and E. G. Paul, *J. Amer. Chem. Soc.*, 1964, **86**, 2984.
6. D. K. Dalling and D. M. Grant, *J. Amer. Chem. Soc.*, 1967, **89**, 6612.
7. E. Wenkert, A. O. Clouse, D. W. Cochran and D. Doddrell, *J. Amer. Chem. Soc.*, 1969, **91**, 6879; R. R. Ernst, *J. Chem. Phys.*, 1966, **45**, 3845.
8. E. W. Hagaman, *Org. Magn. Resonance*, 1976, **8**, 389.
9. M. Shamma, "The Isoquinoline Alkaloids", Academic Press, New York and London, 1972.
10. P. L. Schiff, Jr. and R. W. Doskotch, *Lloydia*, 1970, **33**, 403.
11. R. L. Ranieri and J. L. McLaughlin, *J. Org. Chem.*, 1976, **41**, 319.
12. B. Z. Ahn and F. Zymalkowski, *Tetrahedron Lett.*, 1976, 821.
13. R. Tschesche, C. Spilles and G. Eckhardt, *Chem. Ber.*, 1974, **107**, 1329.
14. T. R. Govindachari, K. Nagarajan, P. C. Parthasarathy, T. G. Rajagopalan, H. K. Desai, G. Kartha, S. L. Chen and K. Nakanishi, *J. Chem. Soc., Perkin I*, 1974, 1413.
15. M. Tomita, T. Singu, K. Fujitani and H. Furukawa, *Chem. Pharm. Bull. (Japan)*, 1965, **13**, 921; T. Kametani and K. Ohkubo, *Chem. Pharm. Bull. (Japan)*, 1968, **16**, 909; T. Kametani, H. Sugi, S. Shibuya and K. Fukumoto, *Tetrahedron*, 1971, **27**, 5375.
16. T. Kametani, A. Ujiie and K. Fukumoto, *J. Chem. Soc., Perkin I*, 1974, 1954.
17. A. J. Birch, A. H. Jackson, P. V. R. Shannon and G. W. Stewart, *J. Chem. Soc., Perkin I*, 1975, 2492.
18. O. Hoshino, T. Toshioka and B. Umezawa, *Chem. Pharm. Bull. (Japan)*, 1974, **22**, 1302.
19. N. A. Shaath and T. O. Soine, *J. Org. Chem.*, 1975, **40**, 1987.
20. P. J. Davis, D. Wiese and J. P. Rosazza, *J. Chem. Soc., Perkin I*, 1977, 1.
21. L. Cleaver, S. Nimgirawath, E. Ritchie and W. C. Taylor, *Austral. J. Chem.*, 1976, **29**, 2003.
22. M. Shamma and J. L. Moniot, *Experientia*, 1976, **32**, 282.
23. J. Z. Ginos, A. LoMonte, G. C. Cotzias, A. K. Bose and R. J. Brambilla, *J. Amer. Chem. Soc.*, 1973, **95**, 2991.
24. S. Sternhell, *Quart. Rev. (London)*, 1969, **23**, 236.
25. R. V. Smith and A. W. Stocklinski, *Tetrahedron Lett.*, 1973, 1819.
26. S. K. Talapatra, A. Patra and B. Talapatra, *Tetrahedron*, 1975, **31**, 1105.

27. O. Hoshino, H. Hara, N. Serizawa and B. Umezawa, *Chem. Pharm. Bull. (Japan)*, 1975, **23**, 2048.
28. O. Hoshino, H. Hara, M. Ogawa and B. Umezawa, *Chem. Pharm. Bull. (Japan)*, 1975, **23**, 2578.
29. G. Y. Moltriasio, R. M. Sotelo and D. Giacobello, *J. Chem. Soc., Perkin I*, 1973, 349.
30. M. P. Cava and I. Noguchi, *J. Org. Chem.*, 1973, **38**, 60.
31. A. Urzuà and B. K. Cassels, *Heterocycles*, 1976, **4**, 1881.
32. M. P. Cava and S. S. Libsch, *J. Org. Chem.*, 1974, **39**, 577.
33. C. Casagrande, L. Canonica and G. Severini-Ricca, *J. Chem. Soc., Perkin I*, 1975, 1652.
34. C. Casagrande, L. Canonica and G. Severini-Ricca, *J. Chem. Soc., Perkin I*, 1975, 1659.
35. L. Castedo, R. Suau and A. Mouriño, *Tetrahedron Lett.*, 1976, 501, and personal communication from Professor L. Castedo.
36. M. Akasu, H. Itokawa and M. Fujita, *Tetrahedron Lett.*, 1974, 3609.
37. A. Venkateswarlu and M. P. Cava, *Tetrahedron*, 1976, **32**, 2079.
38. T. Tomimatsu and M. Sasakawa, *Chem. Pharm. Bull. (Japan)*, 1975, **23**, 2279.
39. T. Ibuka, T. Konoshima and Y. Inubushi, *Chem. Pharm. Bull. (Japan)*, 1975, **23**, 133.
40. I. R. C. Bick, H. M. Leow and N. W. Preston, *Chem. Commun.*, 1972, 980.
41. M. P. Cava, J. M. Saá, M. V. Lakshmikantham and M. J. Mitchell, *J. Org. Chem.*, 1975, **40**, 2647.
42. M. P. Cava, J. M. Saá, M. V. Lakshmikantham and M. J. Mitchell, *Tetrahedron Lett.*, 1974, 4259.
43. B. Hoffstadt, D. Moecke, P. Pachaly and F. Zymalkowski, *Tetrahedron*, 1974, **30**, 307.
44. S. M. Kupchan, A. J. Liepa, R. L. Baxter and H. P. J. Hintz, *J. Org. Chem.*, 1973, **38**, 1846.
45. J. M. Saá, M. V. Lakshmikantham, M. J. Mitchell and M. P. Cava, *J. Org. Chem.*, 1976, **41**, 317.
46. M. P. Cava, K. Wakisaka, I. Nogushi, D. L. Edie and A. I. daRocha, *J. Org. Chem.*, 1974, **39**, 3588.
47. J. M. Saá, M. V. Lakshmikantham, M. J. Mitchell and M. P. Cava, *Tetrahedron Lett.*, 1976, 513.
48. W.-N. Wu, J. L. Beal and R. W. Doskotch, *Tetrahedron Lett.*, 1976, 3687.
49. K. P. Guha, P. C. Das, B. Mukherjee, R. Mukherjee, G. P. Juneau and N. S. Bhacca, *Tetrahedron Lett.*, 1976, 4241.
50. M. Shamma and J. E. Foy, *Tetrahedron Lett.*, 1975, 2249.
51. M. Shamma, J. E. Foy and G. A. Miana, *J. Amer. Chem. Soc.*, 1974, **96**, 7809.
52. M. Shamma, S. S. Salgar and J. L. Moniot, *Tetrahedron Lett.*, 1973, 1859.
53. M. P. Cava and K. Wakisaka, *Tetrahedron Lett.*, 1972, 2309.
54. M. Shamma and J. L. Moniot, *Tetrahedron Lett.*, 1973, 775.
55. L. J. Haynes, G. E. M. Husbands and K. L. Stuart, *J. Chem. Soc. (C)*, 1966, 1680.
56. T. Ibuka, T. Konoshima and Y. Inubushi, *Chem. Pharm. Bull. (Japan)*, 1975, **23**, 114; *Tetrahedron Lett.*, 1972, 4001.
57. H. Iida, H.-C. Hsu and T. Kikuchi, *Chem. Pharm. Bull. (Japan)*, 1973, **21**, 1001.
58. R. C. Cookson, T. A. Crabb, J. J. Frankel and J. Hudec, *Tetrahedron Supplement* 7, 1966, 355.
59. T. Kametani, A. Ujiie, M. Ihara, K. Fukumoto and H. Koizumi, *Heterocycles*, 1975, **3**, 371.
60. T. Kametani, K. Fukumoto, M. Ihara, A. Ujiie and H. Koizumi, *J. Org. Chem.*, 1975, **40**, 3280.
61. T. Kametani, A. Ujiie, M. Ihara, K. Fukumoto and S.-T. Lu, *J. Chem. Soc., Perkin I*, 1976, 1218.

62. K. Yoshikawa, I. Morishima, J. Kunitomo, M. Ju-Ichi and Y. Yoshida, *Chem. Lett.* (Japan), 1975, 961.
63. M. Uskokovic, H. Bruderer, C. von Planta, T. Williams and A. Brossi, *J. Amer. Chem. Soc.*, 1964, **86**, 3364.
64. T. Kametani, T. Takahashi, T. Honda, K. Ogasawara and K. Fukumoto, *J. Org. Chem.*, 1974, **39**, 447.
65. C. Tani, N. Nagakura and S. Hattori, *Tetrahedron Lett.*, 1973, 803; *Chem. Pharm. Bull.* (Japan), 1975, **23**, 313.
66. P. W. Jeffs and J. D. Scharver, *J. Org. Chem.*, 1975, **40**, 644.
67. S. Naruto and H. Kaneko, *Yakugaku Zasshi*, 1972, **92**, 1017.
68. S. Lu, T. Su, T. Kametani, A. Ujiie, M. Ihara and K. Fukumoto, *J. Chem. Soc., Perkin I*, 1976, 63.
69. T. Kametani, A. Ujiie, M. Ihara and K. Fukumoto, *J. Chem. Soc., Perkin I*, 1975, 1822.
70. T. Kametani, H. Matsumoto, Y. Satoh, H. Nemoto and K. Fukumoto, *J. Chem. Soc., Perkin I*, 1977, 376.
71. T. A. Crabb and R. F. Newton, *Tetrahedron*, 1968, **24**, 1997.
72. M. Shamma and L. A. Smeltz, *Tetrahedron Lett.*, 1976, 1415.
73. S. F. Dyke and E. P. Tiley, *Tetrahedron*, 1975, **31**, 561; *Tetrahedron Lett.*, 1972, 5175.
74. S. Naruto, H. Nishimura and H. Kaneko, *Chem. Pharm. Bull.* (Japan), 1975, **23**, 1271.
75. S. Natarajan, B. R. Pai, R. Rajaraman, C. S. Swaminathan, K. Nagarajan, V. Sudarsanam, D. Rogers and A. Quick, *Tetrahedron Lett.*, 1975, 3573.
76. I. Ninomiya, T. Naito and H. Takasugi, *J. Chem. Soc., Perkin I*, 1975, 1791.
77. S. Teitel, W. Klötzer, J. Borgese and A. Brossi, *Canad. J. Chem.*, 1972, **50**, 2022.
78. S. Teitel, J. Borgese and A. Brossi, *Helv. Chim. Acta*, 1973, **56**, 553.
79. H. Holland, D. B. MacLean, R. G. A. Rodrigo and R. H. F. Manske, *Tetrahedron Lett.*, 1975, 4323.
80. T. Kametani, M. Takemura, M. Ihara and K. Fukumoto, *J. Chem. Soc., Perkin I*, 1977, 390.
81. J. Imai, Y. Kondo and T. Takemoto, *Tetrahedron*, 1976, **32**, 1973.
82. T. Kametani, A. Ujiie, S.-P. Huang, M. Ihara and K. Fukumoto, *J. Chem. Soc., Perkin I*, 1977, 394.
83. S. Kano, T. Yokomatsu, E. Komiyama, S. Tokita, Y. Takahagi and S. Shibuya, *Chem. Pharm. Bull.* (Japan), 1975, **23**, 1171.
84. S. O. de Silva, K. Orito, R. H. F. Manske and R. Rodrigo, *Tetrahedron Lett.*, 1974, 3243.
85. G. Nonaka and I. Nishioka, *Chem. Pharm. Bull.* (Japan), 1975, **23**, 294.
86. J. P. Gillespie, L. G. Amoros and F. R. Stermitz, *J. Org. Chem.*, 1974, **39**, 3239.
87. H. Ishii, K. Harada, T. Ishida, E. Ueda and K. Nakajima, *Tetrahedron Lett.*, 1975, 319.
88. M. Onda, K. Yuasa and J. Okada, *Chem. Pharm. Bull.* (Japan), 1974, **22**, 2365.
89. G. Nonaka and I. Nishioka, *Chem. Pharm. Bull.* (Japan), 1975, **23**, 521.
90. N. Takao, H.-W. Bersch and S. Takao, *Chem. Pharm. Bull.* (Japan), 1973, **21**, 1096.
91. N. Takao and K. Iwasa, *Chem. Pharm. Bull.* (Japan), 1973, **21**, 1410.
92. G. Nonaka, Y. Kodera and I. Nishioka, *Chem. Pharm. Bull.* (Japan), 1973, **21**, 1020.
93. S. Safe and R. Y. Moir, *Canad. J. Chem.*, 1964, **42**, 160.
94. M. Shamma and V. St. Georgiev, *Tetrahedron Lett.*, 1974, 2339.
95. S. Teitel, J. O'Brian and A. Brossi, *J. Org. Chem.*, 1972, **37**, 1879.
96. V. Smula, N. E. Cundasawmy, H. L. Holland and D. B. MacLean, *Canad. J. Chem.*, 1973, **51**, 3287.
97. M. Shamma and J. L. Moniot, *J. Chem. Soc., Chem. Commun.*, 1975, 89.
98. A. R. Battersby, R. B. Bradbury, R. B. Herbert, M. H. G. Munro and R. Ramage, *J. Chem. Soc., Perkin I*, 1974, 1394.

99. B. Umezawa, O. Hoshino, Y. Terayama, K. Ohyama, Y. Yamanashi, T. Inoue and T. Toshioka, *Chem. Pharm. Bull.* (Japan), 1971, **19**, 2138.
100. T. Kametani, M. Mizushima, S. Takano and K. Fukumoto, *Tetrahedron*, 1973, **29**, 2031.
101. T. Kametani, T. Kohno, R. Charubala and K. Fukumoto, *Tetrahedron*, 1972, **28**, 3227.
102. A. R. Battersby, P. W. Sheldrake and J. A. Milner, *Tetrahedron Lett.*, 1974, 3315.
103. M. C. Koch, M. M. Plat, N. Préaux, H. E. Gottlieb, E. W. Hagaman, F. M. Schell and E. Wenkert, *J. Org. Chem.*, 1975, **40**, 2836.
104. D. A. Walsh and R. E. Lyle, *Tetrahedron Lett.*, 1973, 3849.
105. F. R. Stermitz and D. K. Williams, *J. Org. Chem.*, 1973, **38**, 2099.
106. T. Kametani, A. Ujiie, K. Takahashi, T. Nakano, T. Suzuki and K. Fukumoto, *Chem. Pharm. Bull.* (Japan), 1973, **21**, 766.
107. M. P. Cava, K. T. Buck and A. I. daRocha, *J. Amer. Chem. Soc.*, 1972, **94**, 5931.
108. M. P. Cava, K. T. Buck, I. Noguchi, M. Srinivasan, M. G. Rao and A. I. daRocha, *Tetrahedron*, 1975, **31**, 1667. Structure of [145] given in personal communication from Professor M. P. Cava.
109. R. D. Harken, C. P. Christensen and W. C. Wildman, *J. Org. Chem.*, 1976, **41**, 2450.
110. A. Mondon and K. Krohn, *Tetrahedron Lett.*, 1972, 2085.
111. R. C. Clark, F. L. Warren and K. G. R. Pachler, *Tetrahedron*, 1975, **31**, 1855.
112. P. W. Jeffs, T. Capps, D. B. Johnson, J. M. Karle, N. H. Martin and B. Rauckman, *J. Org. Chem.*, 1974, **39**, 2703.
113. H. J. Wilkens and F. Troxler, *Helv. Chim. Acta*, 1975, **58**, 1512.
114. M. Haruna and K. Ito, *J. Chem. Soc., Chem. Commun.*, 1976, 345.
115. K. Ito, M. Haruna and H. Furukawa, *J. Chem. Soc., Chem. Commun.*, 1975, 681.
116. A. T. McPhail and K. D. Onan, *Tetrahedron Lett.*, 1976, 485.
117. H. Uprety and D. S. Bhakuni, *Tetrahedron Lett.*, 1975, 1201; H. Pande and D. S. Bhakuni, *J. Chem. Soc., Perkin I*, 1976, 2197.
118. R. G. Powell, R. V. Madrigal, C. R. Smith, Jr., and K. L. Mikolajczak, *J. Org. Chem.*, 1974, **39**, 676.
119. K. L. Mikolajczak, C. R. Smith, Jr., D. Weisleder, T. R. Kelly, J. C. McKenna and P. A. Christenson, *Tetrahedron Lett.*, 1974, 283.
120. A. Allerhand, D. Doddrell and R. Komoroski, *J. Chem. Phys.*, 1971, **55**, 189.
121. F. W. Wehrli, *J. Chem. Soc., Chem. Commun.*, 1973, 379.
122. Y. Terui, K. Tori, S. Maeda and Y. K. Sawa, *Tetrahedron Lett.*, 1975, 2853.
123. F. I. Carroll, C. G. Moreland, G. A. Brine and J. A. Kepler, *J. Org. Chem.*, 1976, **41**, 996.
124. G. A. Brine, D. Prakash, C. K. Hart, D. J. Kotchmar, C. G. Moreland and F. I. Carroll, *J. Org. Chem.*, 1976, **41**, 3445.
125. E. Brochmann-Hanssen, A. Y. Leung and W. J. Richter, *J. Org. Chem.*, 1972, **37**, 1881.
126. R. Rubinstein, R. Giger and D. Ginsberg, *Tetrahedron*, 1973, **29**, 2383.
127. S. Ruchirawat and V. Somchitman, *Tetrahedron Lett.*, 1976, 4159.
128. R. Rodrigo, R. H. F. Manske, V. Smula, D. B. MacLean and L. Baczynskyj, *Canad. J. Chem.*, 1972, **50**, 3900.
129. V. Vechietti, C. Casagrande and G. Ferrari, *Tetrahedron Lett.*, 1976, 1631.
130. T. T. Conway, T. W. Doyle, Y. G. Perron, J. Chapuis and B. Belleau, *Canad. J. Chem.*, 1975, **53**, 245.
131. W. L. Nelson, D. D. Miller and E. Shefter, *J. Org. Chem.*, 1970, **35**, 3433.
132. M. Matsui, Y. Watanabe, T. Ibuka and K. Tanaka, *Chem. Pharm. Bull.* (Japan), 1975, **23**, 1323.
133. S. M. Kupchan, A. J. Liepa and T. Fujita, *J. Org. Chem.*, 1973, **38**, 151.
134. T. Ibuka, K. Tanaka and Y. Inubushi, *Chem. Pharm. Bull.* (Japan), 1974, **22**, 907.
135. K. Abe, M. Onda and S. Okuda, *J. Chem. Soc., Perkin I*, 1973, 316.

136. C. G. Gordon-Gray and R. B. Wells, *J. Chem. Soc., Perkin I*, 1974, 1556.
137. R. S. Sawhney, C. K. Atal, C. C. J. Culvenor and L. W. Smith, *Austral. J. Chem.*, 1974, **27**, 1805.
138. M. Hikichi and T. Furuya, *Tetrahedron Lett.*, 1974, 3657.
139. N. T. Nghia, P. Sedmera, A. Klásek, A. Boeva, L. Drjanovska, L. Dolejš and F. Šantavý, *Coll. Czech. Chem. Commun.*, 1976, **41**, 2952.
140. E. Leete and G. B. Boden, *J. Amer. Chem. Soc.*, 1976, **98**, 6321.
141. M. Suzuki, Y. Hayakawa, K. Aoki, H. Nagase, H. Nakamura, K. Yamada and Y. Hirata, *Tetrahedron Lett.*, 1973, 331.
142. V. K. Wadhawan, S. K. Sikka and N. B. Mulchandani, *Tetrahedron Lett.*, 1973, 5091.
143. T. R. Govindachari, N. Viswanathan, J. Radhakrishnan, B. R. Pai, S. Natarajan and P. S. Subramaniam, *Tetrahedron*, 1973, **29**, 891.
144. Z. Horii, T. Imanishi, M. Yamauchi, M. Hanoaka, J. Parello and S. Munavalli, *Tetrahedron Lett.*, 1972, 1877.
145. F. Bohlmann and R. Zeisberg, *Chem. Ber.*, 1975, **108**, 1043.
146. J. L. van Eijk and M. H. Radema, *Tetrahedron Lett.*, 1976, 2053.
147. M. M. Kadooka, M. Y. Chang, H. Fukami and P. J. Scheuer, *Tetrahedron*, 1976, **32**, 919.
148. A. Ueno, K. Morinaga, S. Fukushima, Y. Iitaka, Y. Koiso and S. Okuda, *Chem. Pharm. Bull. (Japan)*, 1975, **23**, 2560.
149. F. Bohlmann and D. Schumann, *Tetrahedron Lett.*, 1965, 2435.
150. E. Kotani, M. Kitazawa and S. Tobinaga, *Tetrahedron*, 1974, **30**, 3027.
151. R. T. LaLonde, C. F. Wong and K. C. Das, *J. Amer. Chem. Soc.*, 1972, **94**, 8522.
152. C. F. Wong and R. T. LaLonde, *Phytochemistry*, 1970, **9**, 659.
153. R. T. LaLonde, C. F. Wong and K. C. Das, *J. Org. Chem.*, 1974, **39**, 2892.
154. T. I. Martin, D. B. MacLean, J. T. Wróbel, A. Iwanow and W. Starzec, *Canad. J. Chem.*, 1974, **52**, 2705.
155. J. T. Wróbel, B. Bobesko, T. I. Martin, D. B. MacLean, N. Krishnamachari and C. Calvo, *Canad. J. Chem.*, 1973, **51**, 2811.
156. R. T. LaLonde, C. F. Wong and H. G. Howell, *J. Org. Chem.*, 1971, **36**, 3703.
157. R. T. LaLonde, T. N. Donvito and A. I.-M. Tsai, *Canad. J. Chem.*, 1975, **53**, 1714.
158. R. T. LaLonde and C. Wong, *Canad. J. Chem.*, 1975, **53**, 3545.
159. F. Bohlmann, D. Schumann and C. Arndt, *Tetrahedron Lett.*, 1965, 2705.
160. E. Fujita and Y. Saeki, *J. Chem. Soc., Perkin I*, 1973, 297.
161. I. Lantos, C. Razgaitis, H. Van Hoeven and B. Loev, *J. Org. Chem.*, 1977, **42**, 228.
162. R. B. Hörhammer, A. E. Schwarting and J. M. Edwards, *J. Org. Chem.*, 1975, **40**, 656.
163. E. Fujita and Y. Saeki, *J. Chem. Soc., Perkin I*, 1973, 306.
164. M. Hanoaka, H. Sassa, N. Ogawa, Y. Arata and J. P. Ferris, *Tetrahedron Lett.*, 1974, 2533.
165. M. Hanaoka, H. Sassa, C. Shimezawa and Y. Arata, *Chem. Pharm. Bull. (Japan)*, 1975, **23**, 2478.
166. D. G. Hawthorne, S. R. Johns and R. I. Willing, *Austral. J. Chem.*, 1976, **29**, 315.
167. G. Werner, M. Wiechmann, P. Scheiber, A. Gieren, T. Fischer and W. Hoppe, *Annalen*, 1976, 617.
168. K.-H. Pook, W. Schulz and R. Banholzer, *Annalen*, 1975, 1499.
169. E. Leete, N. Kowanko and R. A. Newmark, *J. Amer. Chem. Soc.*, 1975, **97**, 6826.
170. L. Simeral and G. E. Maciel, *Org. Magn. Resonance*, 1974, **6**, 226.
171. M. Lounasmaa, P. M. Wovkulich and E. Wenkert, *J. Org. Chem.*, 1975, **40**, 3694.
172. J. Bruneton and A. Cavé, *Tetrahedron Lett.*, 1975, 739; J. Bruneton, A. Cavé and R. R. Paris, *Plantes médicinales et phytothérapie*, 1975, **9**, 21.
173. D. J. Barringer, Jr., G. Berkelhammer and R. S. Wayne, *J. Org. Chem.*, 1973, **38**, 1937.

174. W. L. Fitch, P. M. Dolinger and C. Djerassi, *J. Org. Chem.*, 1974, **39**, 2974.
175. F. P. Guengerich, S. J. DiMari, H. P. Broquist, *J. Amer. Chem. Soc.*, 1973, **95**, 2055.
176. E. Leete, *J. Amer. Chem. Soc.*, 1977, **99**, 648.
177. K. Jankowski, *J. Org. Chem.*, 1976, **41**, 3321.
178. M. Laing, F. L. Warren and E. P. White, *Tetrahedron Lett.*, 1975, 269.
179. R. De Cleyne and M. Verzele, *Bull. Soc. Chim. Belges*, 1975, **84**, 435.
180. B. L. Sondengam and S. F. Kimbu, *Tetrahedron Lett.*, 1977, 69.
181. T. Tokuyama, K. Uenoyama, G. Brown, J. W. Daly and B. Witkop, *Helv. Chim. Acta*, 1974, **57**, 2597.
182. Y. Shizuri, H. Wada, K. Suguira, K. Yamada and Y. Hirata, *Tetrahedron*, 1973, **29**, 1773.
183. K. Suguira, K. Yamada and Y. Hirata, *Tetrahedron Lett.*, 1973, 113.
184. Y. Shizuri, K. Yamada and Y. Hirata, *Tetrahedron Lett.*, 1973, 741.
185. S. M. Kupchan and R. M. Smith, *J. Org. Chem.*, 1977, **42**, 115.
186. R. L. Baxter, L. Crombie, D. J. Simmonds and D. A. Whiting, *J. Chem. Soc., Chem. Commun.*, 1976, 463.
187. R. L. Baxter, L. Crombie, D. J. Simmonds and D. A. Whiting, *J. Chem. Soc., Chem. Commun.*, 1976, 465.
188. J. F. Whidby and J. I. Seeman, *J. Org. Chem.*, 1976, **41**, 1585.
189. C. G. Moreland, A. Philip and F. I. Carroll, *J. Org. Chem.*, 1974, **39**, 2413.
190. F. I. Carroll, A. Philip and M. C. Coleman, *Tetrahedron Lett.*, 1976, 1757.
191. C. R. Hutchinson, A. H. Heckendorf, P. E. Daddona, E. Hagaman and E. Wenkert, *J. Amer. Chem. Soc.*, 1974, **96**, 5609.
192. U. Vögeli and W. von Philipsborn, *Org. Magn. Resonance*, 1973, **5**, 551.
193. S. Danishefsky, R. Volkmann and S. B. Horwitz, *Tetrahedron Lett.*, 1973, 2521.
194. T. R. Vondachari, K. R. Ravindranath and N. Viswanathan, *J. Chem. Soc., Perkin I*, 1974, 1215.
195. R. A. Corral, O. O. Orazi and I. A. Benages, *Tetrahedron*, 1973, **29**, 205.
196. D. Basu and S. C. Basa, *J. Org. Chem.*, 1972, **37**, 3035.
197. A. W. Fraser and J. R. Lewis, *J. Chem. Soc., Perkin I*, 1973, 1173.
198. A. W. Fraser and J. R. Lewis, *J. Chem. Soc., Chem. Commun.*, 1973, 615.
199. R. Storer and D. W. Young, *Tetrahedron*, 1973, **29**, 1215.
200. J. F. Collins, G. H. Gray, M. F. Grundon, D. M. Harrison and C. G. Spyropoulos, *J. Chem. Soc., Perkin I*, 1973, 94.
201. M. Daudon, H. M. Mehri, E. W. Hagaman, F. M. Schell and E. Wenkert, *J. Org. Chem.*, 1975, **40**, 2838.
202. H. Link and K. Bernauer, *Helv. Chim. Acta*, 1972, **55**, 1053.
203. F. Khuong-Huu, X. Monseur, G. Ratle, G. Lukacz and R. Goutarel, *Tetrahedron Lett.*, 1973, 1757.
204. M. A. Wuonola and R. B. Woodward, *Tetrahedron*, 1976, **32**, 1085.
205. Y. Komoda, S. Kaneko, M. Yamamoto, M. Ishikawa, A. Itai and Y. Iitaka, *Chem. Pharm. Bull. (Japan)*, 1975, **23**, 2464.
206. F. Khuong-Huu, J.-P. Le Forestier and R. Goutarel, *Tetrahedron*, 1972, **28**, 5207.
207. R. G. Parker and J. D. Roberts, *J. Org. Chem.*, 1970, **33**, 996.
208. G. W. Gribble, R. B. Nelson, J. L. Johnson and G. C. Levy, *J. Org. Chem.*, 1975, **40**, 3720.
209. R. R. Fraser, S. Passannanti and F. Piozzi, *Canad. J. Chem.*, 1976, **54**, 2915.
210. W. M. Bandaranayake, M. J. Begley, B. O. Brown, D. G. Clarke, L. Crombie and D. A. Whiting, *J. Chem. Soc., Perkin I*, 1974, 998.
211. L. Crombie and R. Ponsford, *Chem. Commun.*, 1968, 894; *Tetrahedron Lett.*, 1968, 5771.
212. Y. Kondo and T. Takemoto, *Chem. Pharm. Bull. (Japan)*, 1973, **21**, 837.

213. P. A. Crooks, B. Robinson and O. Meth-Cohn, *Phytochemistry*, 1976, **15**, 1092.
214. A. J. Birch and R. A. Russell, *Tetrahedron Lett.*, 1972, **28**, 2999.
215. P. S. Steyn, *Tetrahedron*, 1973, **29**, 107.
216. G. Gatti, R. Cardillo, C. Fuganti and D. Gharinghelli, *J. Chem. Soc., Chem. Commun.*, 1976, 435.
217. M. Yamazaki, H. Fujimoto and E. Okuyama, *Tetrahedron Lett.*, 1976, 2861.
218. K. Bailey and A. A. Grey, *Canad. J. Chem.*, 1972, **50**, 3876.
219. L. Zetta and G. Gatti, *Tetrahedron*, 1975, **31**, 1403.
220. I. Ninomiya and T. Kiguchi, *J. Chem. Soc., Chem. Commun.*, 1976, 624.
221. N. J. Bach, H. E. Boaz, E. C. Kornfeld, C.-J. Chang, H. G. Floss, E. W. Hagaman and E. Wenkert, *J. Org. Chem.*, 1974, **39**, 1272.
222. H. Tschertter and H. Hauth, *Helv. Chim. Acta*, 1974, **57**, 113.
223. K. D. Barrow and F. R. Quigley, *Tetrahedron Lett.*, 1975, 4269.
224. G. S. King, P. G. Mantle, C. A. Szczyrbak and E. S. Waight, *Tetrahedron Lett.*, 1973, 215.
225. G. W. Gribble, R. B. Nelson, G. C. Levy and G. L. Nelson, *Chem. Commun.*, 1972, 703.
226. E. Wenkert, C.-J. Chang, H. P. S. Chawla, D. W. Cochran, E. W. Hagaman, J. C. King and K. Orito, *J. Amer. Chem. Soc.*, 1976, **98**, 3645.
227. E. L. Eliel, W. F. Bailey, L. D. Kopp, R. L. Willer, D. M. Grant, R. Bertrand, K. A. Christensen, D. K. Dalling, M. W. Duch, E. Wenkert, F. M. Schell and D. W. Cochran, *J. Amer. Chem. Soc.*, 1975, **97**, 322.
228. J. Melchio, A. Bouquet, M. Pais and R. Goutarel, *Tetrahedron Lett.*, 1977, 315.
229. R. H. Levin, J.-Y. Lallemand and J. D. Roberts, *J. Org. Chem.*, 1973, **38**, 1983.
230. M. Lounasmaa and C.-J. Johansson, *Tetrahedron*, 1977, **33**, 113.
231. M. Damak, A. Ahond, P. Potier and M.-M. Janot, *Tetrahedron Lett.*, 1976, 4731.
232. A. H. Heckendorf, K. C. Mattes, R. C. Hutchinson, E. W. Hagaman and E. Wenkert, *J. Org. Chem.*, 1976, **41**, 2045.
233. C. R. Hutchinson, M.-T. S. Hsia, A. H. Heckendorf and G. J. O'Loughlin, *J. Org. Chem.*, 1976, **41**, 3493.
234. M. Sainsbury and N. L. Uttley, *J. Chem. Soc., Perkin I*, 1976, 2416.
235. G. van Binst and D. Tourwe, *Heterocycles*, 1973, **1**, 257.
236. R. T. Brown and A. A. Charalambides, *Tetrahedron Lett.*, 1974, 1649.
237. R. T. Brown and C. L. Chapple, *J. Chem. Soc., Chem. Commun.*, 1974, 740.
238. E. E. van Tamelen and C. Dorschell, *J. Chem. Soc., Chem. Commun.*, 1976, 529.
239. J. Boivin, M. Pais and R. Goutarel, *Tetrahedron*, 1977, **33**, 305.
240. L. A. Djakouré, F.-X. Jarreau and R. Goutarel, *Tetrahedron*, 1975, **31**, 2695.
241. M. Barczai-Beke, G. Dörnyei, G. Tóth, J. Tamás and Cs. Szántay, *Tetrahedron*, 1976, **32**, 1153.
242. G. Rackur and E. Winterfeldt, *Chem. Ber.*, 1976, **109**, 3837.
243. R. H. Burnell, A. Chapelle and M. F. Khalil, *Canad. J. Chem.*, 1974, **52**, 2327.
244. T. Y. Au, H. T. Cheung and S. Sternhell, *J. Chem. Soc., Perkin I*, 1973, 13.
245. F. Titeux, L. Le Men-Olivier and J. Le Men, *Bull. Soc. chim. France*, 1976, 1473.
246. M. P. Yagudaev and S. Y. Yunosov, *Khim. prirod. Soedinenii*, 1976, **3**, 345.
247. Y. Ban, M. Seto and T. Oishi, *Chem. Pharm. Bull. (Japan)*, 1975, **23**, 2605.
248. E. Wenkert, J. S. Bindra, C.-J. Chang, W. D. Cochran and D. E. Rearick, *J. Org. Chem.*, 1974, **39**, 1662.
249. E. Wenkert, C.-J. Chang, D. W. Cochran and R. Pellicciari, *Experientia*, 1972, **28**, 377.
250. R. T. Brown and R. Platt, *Tetrahedron Lett.*, 1976, 2721.
251. J. C. Carter, G. W. Luther, III, and T. C. Long, *J. Magn. Resonance*, 1974, **15**, 122.
252. G. W. Luther, III, J. Valentine and J. C. Carter, *J. Magn. Resonance*, 1974, **15**, 132.

253. N. G. Bisset, B. C. Das and J. Parello, *Tetrahedron*, 1973, **29**, 4137.
254. R. E. Moore and H. Rapoport, *J. Org. Chem.*, 1973, **38**, 215.
255. P. R. Srinivasan and R. L. Lichter, *Org. Magn. Resonance*, 1976, **8**, 198.
256. A. Ahond, A.-M. Bui, P. Potier, E. W. Hagaman and E. Wenkert, *J. Org. Chem.*, 1976, **41**, 1878.
257. M. P. Cava, S. K. Talapatra, J. A. Weisbach, B. Douglas and G. O. Dudek, *Tetrahedron Lett.*, 1963, 53.
258. H. Achenbach and E. Schaller, *Chem. Ber.*, 1975, **108**, 3842.
259. S. Sakai, N. Aimi, K. Yamaguchi, H. Ohhira, K. Hori and J. Haginiwa, *Tetrahedron Lett.*, 1975, 715.
260. J. Bruneton, Ad. Cavé and A. Cavé, *Tetrahedron*, 1973, **29**, 1131.
261. E. Bombardelli, A. Bonati, B. Gabetta, E. M. Martinelli, G. Mustich and B. Danieli, *Fitoterapia*, 1975, **46**, 51.
262. E. Bombardelli, A. Bonati, B. Gabetta, E. M. Martinelli, G. Mustich and B. Danieli, *Tetrahedron*, 1974, **30**, 4141.
263. E. Bombardelli, A. Bonati, B. Danieli, B. Gabetta, E. M. Martinelli and G. Mustich, *Experientia*, 1974, 979.
264. G. A. Cordell, S. G. Weiss and N. R. Farnsworth, *J. Org. Chem.*, 1974, **39**, 431.
265. E. Wenkert, D. W. Cochran, E. W. Hagaman, F. M. Schell, N. Neuss, A. S. Katner, P. Potier, C. Kan, M. Plat, M. Koch, H. Mehri, J. Poisson, N. Kunesch and Y. Rolland, *J. Amer. Chem. Soc.*, 1973, **95**, 4990.
266. A. Ahond, M.-M. Janot, N. Langlois, G. Lukacs, P. Potier, P. Rosoanaivo, M. Sangaré, N. Neuss, M. Plat, J. Le Men, E. W. Hagaman and E. Wenkert, *J. Amer. Chem. Soc.*, 1974, **96**, 633.
267. E. Wenkert, E. W. Hagaman, N. Kunesch, N. Wang and B. Zsardon, *Helv. Chim. Acta*, 1976, **59**, 2771.
268. J. Bruneton, A. Cavé, E. W. Hagaman, N. Kunesch and E. Wenkert, *Tetrahedron Lett.*, 1976, 5567.
269. J. Le Men, G. Lukacs, L. Le Men-Olivier, J. Lévy and M. J. Hoizey, *Tetrahedron Lett.*, 1974, 483.
270. G. Lukacs, M. de Bellefon, L. Le Men-Olivier, J. Lévy and L. Le Men, *Tetrahedron Lett.*, 1974, 487.
271. M. Damak, A. Ahond and P. Potier, *Tetrahedron Lett.*, 1976, 167.
272. M. P. Cava, M. V. Lakshmikantham, S. K. Talapatra, P. Yates, I. D. Rae, M. Rosenberger, A. G. Szabo, B. Douglas and J. A. Weisbach, *Canad. J. Chem.*, 1973, **51**, 3102.
273. P. Yates, F. N. MacLachlan, I. D. Rae, M. Rosenberger, A. G. Szabo, C. R. Willis, M. P. Cava, M. Behforouz, M. V. Lakshmikantham and W. Zeiger, *J. Amer. Chem. Soc.*, 1973, **95**, 7842.
274. J. Le Men, M. J. Hoizey, G. Lukacs, L. Le Men Olivier and J. Lévy, *Tetrahedron Lett.*, 1974, 3119.
275. J. Lévy, C. Pierron, G. Lukacs, G. Massiot and J. Le Men, *Tetrahedron Lett.*, 1976, 669.
276. L. D. Hall and C. M. Preston, *Canad. J. Chem.*, 1974, **52**, 829.
277. L. J. Durham, J. N. Shoolery and C. Djerassi, *Proc. Nat. Acad. Sci. USA*, 1974, **71**, 3797.
278. N. Neuss, D. S. Fukuda, G. E. Mallett, D. R. Brannon and L. L. Huckstep, *Helv. Chim. Acta*, 1973, **56**, 2418.
279. P. Rosoanaivo, N. Langlois and P. Potier, *Tetrahedron Lett.*, 1974, 3669.
280. R. Z. Andriamialisoa, N. Langlois and P. Potier, *Tetrahedron Lett.*, 1976, 163.
281. J. P. Kutney, K. K. Chan, A. Failli, J. M. Fromson, C. Gletsos, A. Leutwiler, V. R. Nelson and J. P. de Souza, *Helv. Chim. Acta*, 1975, **58**, 1648.

282. E. Wenkert, D. W. Cochran, H. E. Gottlieb, E. W. Hagaman, R. B. Filho, F. J. de Abreu Matos and M. I. L. M. Madruga, *Helv. Chim. Acta*, 1976, **59**, 2437.
283. V. C. Agwada, Y. Morita, U. Renner, M. Hesse and H. Schmid, *Helv. Chim. Acta*, 1975, **58**, 1001.
284. Y. Morita, M. Hesse, U. Renner and H. Schmid, *Helv. Chim. Acta*, 1976, **59**, 532.
285. Y. Morita, S. Savaskan, K. A. Jaeggi, M. Hesse, U. Renner and H. Schmid, *Helv. Chim. Acta*, 1975, **58**, 211.
286. Y. Langlois, F. Guéritte, R. Z. Andriamialisoa, N. Langlois, P. Potier, A. Chiaroni and C. Riche, *Tetrahedron*, 1976, **32**, 945.
287. C. Kan-Fan, G. Massiot, A. Ahond, B. C. Das, H.-P. Husson, P. Potier, A. I. Scott and C. C. Wei, *J. Chem. Soc., Chem. Commun.*, 1974, 164.
288. G. Massiot, S. K. Kan, P. Gonord and C. Duret, *J. Amer. Chem. Soc.*, 1975, **97**, 3277.
289. R. Z. Andriamialisoa, L. Diatta, P. Rosoanaivo, N. Langlois and P. Potier, *Tetrahedron*, 1975, **31**, 2347.
290. R. T. Brown and A. A. Charalambides, *J. Chem. Soc., Chem. Commun.*, 1973, 765.
291. G. I. Dimitrienko, D. G. Murray and S. McLean, *Tetrahedron Lett.*, 1974, 1961.
292. R. T. Brown and S. B. Fraser, *Tetrahedron Lett.*, 1974, 1957.
293. R. T. Brown, S. B. Fraser and J. Banerji, *Tetrahedron Lett.*, 1974, 3335.
294. K. L. Stuart and R. B. Woo-Ming, *Tetrahedron Lett.*, 1974, 3853.
295. R. T. Brown and G. L. Chapple, *Tetrahedron Lett.*, 1976, 1629.
296. B. F. Anderson, G. B. Robertson, H. P. Avey, W. F. Donovan, I. R. C. Bick, J. B. Bremner, A. J. T. Finney, N. W. Preston, R. T. Gallagher and G. B. Russel, *J. Chem. Soc., Chem. Commun.*, 1975, 511.
297. A. K. Sen, S. B. Mahato and N. L. Dutta, *Tetrahedron Lett.*, 1974, 609.
298. L. Angenot, O. Dideberg and L. Dupont, *Tetrahedron Lett.*, 1975, 1357.
299. G. Grethe, H. L. Lee and M. R. Uskokovic, *Helv. Chim. Acta*, 1976, **59**, 2268.
300. R. L. Garnick and P. W. Le Quesne, *Tetrahedron Lett.*, 1976, 3249.
301. Z. Votický, E. Grossmann, J. Tomko, G. Massiot, A. Ahond and P. Potier, *Tetrahedron Lett.*, 1974, 3923.
302. L. Merlini, R. Mondelli, G. Nasini, F. W. Wehrli, E. W. Hagaman and E. Wenkert, *Helv. Chim. Acta*, 1976, **59**, 2254.
303. C. Cistaro, R. Mondelli and M. Anteunis, *Helv. Chim. Acta*, 1976, **59**, 2249.
304. C. Cistaro, L. Merlini, R. Mondelli and G. Nasini, *Gazz. chim. Ital.*, 1973, **103**, 153.
305. C. Cistaro, L. Merlini, R. Mondelli and G. Nasini, *Chem. Commun.*, 1972, 785.
306. G. Benz and E. Winterfeldt, *Chem. Ber.*, 1975, **108**, 1803.
307. E. Wenkert, E. W. Hagaman, B. Lal, G. E. Gutowski, A. S. Katner, J. C. Miller and N. Neuss, *Helv. Chim. Acta*, 1975, **58**, 1560.
308. D. E. Dorman and J. W. Paschal, *Org. Magn. Resonance*, 1976, **8**, 413.
309. S. S. Tafur, J. L. Occolowitz, T. K. Elzey, J. W. Paschal and D. E. Dorman, *J. Org. Chem.*, 1976, **41**, 1001.
310. P. Potier, N. Langlois, Y. Langlois and F. Guéritte, *J. Chem. Soc., Chem. Commun.*, 1975, 670.
311. R. Z. Andriamialisoa, N. Langlois and P. Potier, *Tetrahedron Lett.*, 1976, 2849.
312. N. Neuss, G. E. Mallet, D. R. Brannon, J. A. Mabe, H. R. Horton and L. L. Huckstep, *Helv. Chim. Acta*, 1974, **57**, 1886.
313. J. B. Bloxside, J. A. Elvidge, J. R. Jones, R. B. Mane, V. M. A. Chambers, E. A. Evans and D. Greenslade, *J. Chem. Research (S)*, 1977, 42.
314. Y. Rolland, N. Kunesch, J. Poisson, E. W. Hagaman, F. M. Schell and E. Wenkert, *J. Org. Chem.*, 1976, **41**, 3270.
315. E. Bombardelli, A. Lonati, B. Danieli, B. Gambetta, E. M. Martinelli and G. Mustich, *Experientia*, 1975, 139.

316. A. Cavé and J. Bruneton, *Tetrahedron Lett.*, 1973, 5081.
317. M. Daudon, M. H. Mehri, M. M. Plat, E. W. Hagaman and E. Wenkert, *J. Org. Chem.*, 1976, **41**, 3276.
318. B. C. Das, J. P. Cosson, G. Lukacs and P. Potier, *Tetrahedron Lett.*, 1974, 4299.
319. P. Rosoanaivo and G. Lukacs, *J. Org. Chem.*, 1976, **41**, 376.
320. E. Bombardelli, A. Bonati, B. Gabetta, E. M. Martinelli, G. Mustich and B. Danieli, *J. Chem. Soc., Perkin I*, 1976, 1432.
321. D. G. I. Kingston, B. B. Gerhart and F. Ionescu, *Tetrahedron Lett.*, 1976, 649.
322. H. Achenbach and E. Schaller, *Chem. Ber.*, 1976, **109**, 3527.
323. M. Damak, A. Ahond, H. Doucerain and C. Riche, *J. Chem. Soc., Chem. Commun.*, 1976, 510.
324. S. Sakai, N. Aimi, K. Yamaguchi, E. Yamanaka and J. Haginiwa, *Tetrahedron Lett.*, 1975, 719.
325. S. W. Pelletier, Z. Djarmati, S. Lajšić and W. H. De Camp, *J. Amer. Chem. Soc.*, 1976, **98**, 2617.
326. S. W. Pelletier and Z. Djarmati, *J. Amer. Chem. Soc.*, 1976, **98**, 2626.
327. A. J. Jones and M. H. Benn, *Canad. J. Chem.*, 1973, **51**, 486.
328. S. W. Pelletier, N. V. Mody, A. J. Jones and M. H. Benn, *Tetrahedron Lett.*, 1976, 3025.
329. R. Aneja, D. M. Locke and S. W. Pelletier, *Tetrahedron*, 1973, **29**, 3297.
330. S. W. Pelletier and J. Bhattacharyya, *Tetrahedron Lett.*, 1976, 4679.
331. S. W. Pelletier, N. V. Mody and H. S. Puri, *J. Chem. Commun.*, 1977, 12.
332. S. W. Pelletier and N. V. Mody, *J. Amer. Chem. Soc.*, 1977, **99**, 284.
333. S. W. Pelletier, N. V. Mody, Z. Djarmati, I. V. Mićović and J. K. Thakkar, *Tetrahedron Lett.*, 1976, 1055.
334. S. W. Pelletier, N. V. Mody, Z. Djarmati and S. D. Lajšić, *J. Org. Chem.*, 1976, **41**, 3042.
335. S. W. Pelletier, Z. Djarmati and N. V. Mody, *Tetrahedron Lett.*, 1976, 1749.
336. N. K. Hart, S. R. Johns, J. A. Lamberton, H. Soares and R. I. Willing, *Austral. J. Chem.*, 1976, **29**, 1295.
337. Y. Ichinohe, M. Yamaguchi and K. Matsushita, *Chem. Lett. (Japan)*, 1974, 1349.
338. K. Wiesner, P.-T. Ho, D. Chang, Y. K. Lam, C. S. J. Pan and W. Y. Ren, *Canad. J. Chem.*, 1973, **51**, 3978.
339. T. T. Nakashima, P. P. Singer, L. M. Browne and W. A. Ayer, *Canad. J. Chem.*, 1975, **53**, 1936.
340. E. Wenkert, B. Chauncy, K. G. Dave, A. R. Jeffcoat, F. M. Schell and H. P. Schenk, *J. Amer. Chem. Soc.*, 1973, **95**, 8427.
341. M. Castillo, L. A. Loyola, G. Morales, I. Singh, C. Calvo, H. L. Holland and D. B. MacLean, *Canad. J. Chem.*, 1976, **54**, 2893.
342. M. Castillo, L. A. Loyola, G. Morales, I. Singh, C. Calvo, H. L. Holland and D. B. MacLean, *Canad. J. Chem.*, 1976, **54**, 2900.

Carbon-13 NMR Spectroscopy of Steroids

W. B. SMITH

*Department of Chemistry, Texas Christian University,
Fort Worth, Texas, USA*

I. Introduction	199
II. Applications of chemical shift reagents	200
III. Applications of relaxation studies	203
IV. Substituent effects	211
V. Steroid stereochemistry	221
Acknowledgement	223
References	223

I. INTRODUCTION

Although most current papers on steroid chemistry and biochemistry do not include data on ^{13}C NMR spectra, the increasing availability of suitable instrumentation and assigned spectra ensures that the technique will find favour in steroid research just as proton NMR did in the past. The original intent of this review was a general coverage of steroid ^{13}C NMR. However, during the initial stages of preparation the author was made aware of an impending review by Blunt and Stothers (1) who graciously provided a preprint of their work. Their manuscript is subdivided into four parts: experimental conditions; spectral assignments; shielding data; substituent effects. Without repeating in detail the contents of each of these sections, it is worth stating briefly that the assignments for some 413 steroids are tabulated; 50 of these were previously unpublished. The authors have altered the assignments of a number of carbon atoms in previously published work. These re-assignments are not made without cause, and their tabulation will prove of great value in the future.

The present review is designed to bring the literature up to date well

into mid-1977. Certain aspects of the subject not covered in detail in the Blunt-Stothers review are discussed here. In addition, the assignments for a number of steroids available from studies in this laboratory are given.

The bibliography has been composed on the basis of a computer search of the literature. (11, 15-21, 36, 37, 46, 47, 51-101) The descriptors nuclear magnetic resonance, NMR, carbon, carbon-13, steroid, and steroids are used. The search has encompassed the Chemical Abstracts Condensates maintained by Lockheed Information Systems and the Medline file of the National Medical Library. Citations from the two sources do not completely overlap; the latter provides items of more medical interest. Furthermore, neither source is entirely complete. A number of citations from the author's own search are also included.

An early report (2) on steroid ^{13}C NMR includes discussion of the carbon chemical shifts of model compounds, single-frequency off-resonance decoupling, induced shifts upon acetylation, and deuterium exchange. These techniques are all amply reviewed by Blunt and Stothers (1) and are not specifically treated here. A particularly readable account of the off-resonance decoupling experiment is given in the text by Wehrli and Wirthlin. (3)

It is convenient to divide the subject into four sections. The first two, on chemical shift reagents and on relaxation studies, deal with techniques of line assignments and other facets of steroid behavior. The third, on substituent effects, lays the background for predicting steroid ^{13}C chemical shifts and interactions of substituents with the steroid framework. In the fourth section the use of ^{13}C NMR to solve problems in steroid stereochemistry is discussed. All chemical shift data are reported on the delta scale.

II. APPLICATIONS OF CHEMICAL SHIFT REAGENTS

As a matter of historical introduction it is noted that the first application (4) of a paramagnetic lanthanide chemical shift reagent involved the simplification of the proton NMR spectrum of cholesterol by means of $\text{Eu}(\text{dpm})_3\cdot 2\text{py}$. The applications and development of these valuable reagents are the subject of a book (5) and a recent review. (6)

The first applications of lanthanide induced shifts (LIS) in ^{13}C NMR appeared in 1971. (7-10) Shortly thereafter it was shown (11) that $\text{Eu}(\text{dpm})_3$ induced chemical shift changes in cholesterol which extended from the coordination site at C-3 clear across the ring system, the assignments used being those of Roberts' group. (2) Although the LIS

clearly reflected the necessity of reversing the initial assignments of carbons 12 and 16, this was not then discussed.

The basis for applying the LIS quantitatively to problems in stereochemistry depends upon expressions including the term $(3 \cos^2 \theta - 1)r^{-3}$, where r is the distance from the carbon to the lanthanide ion and the angle θ is defined by the symmetry axis of the complex and the vector from the lanthanide ion to the carbon in question. This application depends on a LIS imposed entirely by the "pseudocontact" mechanism. It has been shown that the "contact" mechanism is important for europium and praseodymium complexes in ^{13}C NMR for distances up to four bonds from the site of complexation, and that ytterbium complexes interact with ^{13}C nuclei largely, if not entirely, by the "pseudocontact" process. (12, 13)

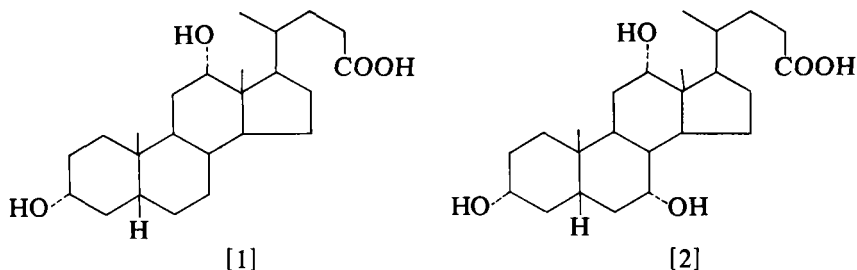
A systematic approach to the application of expressions involving $(3 \cos^2 \theta - 1)r^{-3}$ may be made by means of a computer program to find the optimum location of the lanthanide ion using the geometry of the molecule and seeking a best fit to the spectral data by an iterative process. (14) This approach to making line assignments in steroids was tested first on cholesterol (15) where it was found that the error in locating the Eu site in the $\text{Eu}(\text{dpm})_3$ complex is excessive if the LIS for carbons 2, 3, and 4 are included. The same is not true for the $\text{Yb}(\text{dpm})_3$ complex where the "contact" contribution is nil. The $\text{Yb}(\text{dpm})_3$ data for i-cholesterol and epi-i-cholesterol have been used to make line assignments. Essentially the same approach has been applied to the assignment of a series of hydroxy- and keto-androstanes using Eu and Pr LIS and excluding carbons close to the coordination site. (16) Comparison of the predicted and experimental values of the LIS at these excluded carbons gives an estimate of what turns out to be an appreciable "contact" contribution.

Subsequently, Chadwick and Williams (17) have pointed out that the above approaches are rather naive since no one fixed location for the lanthanide ion should be assumed. The LIS values derived from $\text{Yb}(\text{dpm})_3$ and 5α -cholestan- 3β -ol have been corrected at carbons close to the coordination site for a complex formation shift by using the LIS produced by the diamagnetic $\text{La}(\text{dpm})_3$ compound. Given this correction, the Yb ion is computer positioned by assuming an equal population of sites symmetrically disposed about the $-\text{O}-\text{C}(3)-\text{H}(3)$ plane.

Given some feeling for the diminution of the LIS with distance from the coordination site, it is unlikely that such detailed studies as those above are required for most assignment tasks. We have found it convenient to determine decoupled spectra after one or two increments of $\text{Yb}(\text{tfn})_3$ have been made to the steroid solution. This derivative of

tetradecafluorononanedione is a liquid and quite soluble in chloroform. It is, in addition, one of the strongest Lewis acids among the available chemical shift reagents.

The effectiveness of a chemical shift reagent is influenced by the steric environment of the coordination site. It has been reported (18) that the 3-hydroxyl group in methyl 3,12-dihydroxycholanate [1] complexes



about twenty times as strongly as the 12-hydroxyl group. In methyl 3,7,12-trihydroxycholanate [2] we have found the LIS of $\text{Yb}(\text{tfn})_3$ to be in the order $3 > 7 \gg 12$, the same as that found for ease of hydroxyl acetylation.

In some cases steric hindrance is so great that no complexation with hydroxyl occurs. In Fig. 1 are given the relative LIS for $\text{Yb}(\text{tfn})_3$ and a number of steroids of past or present interest in our laboratory.

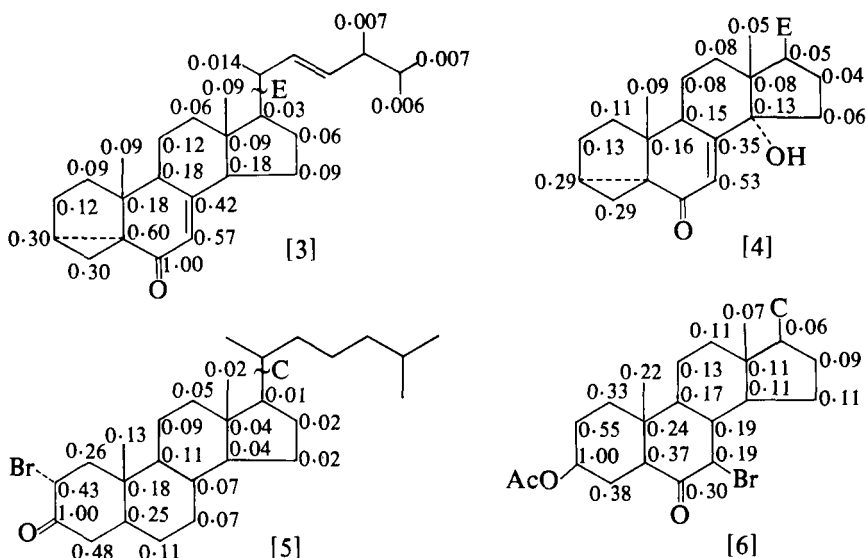


FIG. 1. Relative LIS effects of $\text{Yb}(\text{tfn})_3$ on the ^{13}C spectra of some steroids.

Comparing [3] and [4], it is seen that the 14α -hydroxyl group is not complexed within experimental error. In 2-bromo-3-cholestanone [5] a rather normal pattern is observed, and the same is found for the 2,4-dibromo-3-one (not shown). However, 2,2-dibromocholestan-3-one fails to show any LIS with even a large amount of the reagent. Whether this reflects an unusual steric or electronic effect is not clear.

Reagents other than paramagnetic shift reagents have been employed in steroid systems. Bose and Srinivasan (19) have studied the effects of titanium tetrachloride in chloroform on steroid α,β -unsaturated ketones. The carbonyl and β -carbons are markedly deshielded, while the α -carbon shows little effect. The magnitude of this deshielding is larger than that given by an equal amount of Eu(fod)_3 . The effect is due to complex formation and the alteration of charge distribution within the conjugated system. Rather similar observations have been made (20) on a series of steroid ketones by means of boron trifluoride in methylene chloride at -15°C . At sufficiently low temperatures two sets of signals are observed corresponding to free and complexed steroid.

It is probably stretching the point to consider the proton as a chemical shift reagent. However, it is convenient here to mention that the treatment of androst-4-ene-3,17-dione with 15 M H_2SO_4 also leads to a marked deshielding of both the carbonyl and β -carbon atoms with a very small effect on the α -carbon. (21) The 17-keto group also is protonated.

III. APPLICATIONS OF RELAXATION STUDIES

For many years the province of the physicist, FT NMR has been applied to many analytical problems. (22) Now one can readily obtain high resolution ^{13}C relaxation times together with much molecular structure information. Partially relaxed Fourier transform (PRFT) spectra are of particular importance in making line assignments.

Carbon-13 relaxation measurements have been covered in a number of texts (3, 23–25) and reviews. (26–30) For steroids it is clearly established that ^{13}C relaxation is almost entirely due to interactions (dipole–dipole) with attached or nearby protons. (31–33) The relaxation process is kinetically first-order, characterized by a rate constant T_1^{-1} . For steroids, at useful concentrations, ^{13}C T_1 values range from 0.02 to 5 s. Since T_1 is markedly affected by molecular tumbling, it is necessary carefully to control and state solvents, concentrations, and temperatures in acquiring and reporting T_1 values. Given all of these variables, T_1 reproducibilities are usually found to be around $\pm 10\%$, while reports from different laboratories not infrequently differ by 20%.

The first measurement of steroid ^{13}C T_1 values was reported (31) for cholesteryl chloride in 1 M carbon tetrachloride at 42°C using the conventional $180^\circ-\tau-90^\circ$ inversion-recovery technique. The values obtained are given in Fig. 2.

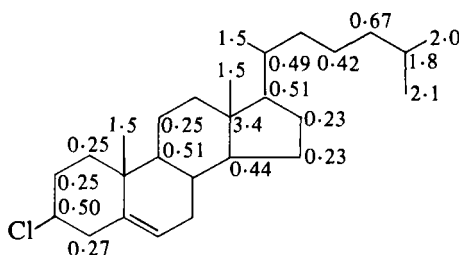


FIG. 2. Carbon relaxation times (s) for 1 M cholesteryl chloride in carbon tetrachloride. (31)

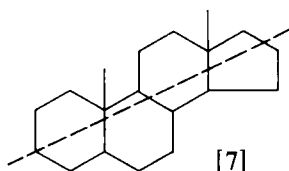
By studying the signal enhancement afforded by the NOE, on completely proton decoupled spectra, the authors concluded that the relaxation occurs entirely by the dipole-dipole mechanism. For this type of relaxation, assuming isotropic molecular tumbling, one can write:

$$\frac{1}{T_1} = \frac{1}{T_2} = \frac{N \gamma_C^2 \gamma_H^2}{\sum (r_{CH})^6} \tau_c \quad (1)$$

where γ_C and γ_H are the appropriate gyromagnetic ratios, r_{CH} is the distance between the carbon nucleus and an attached or nearby proton, τ_c is the molecular rotational correlation time which may be conceptualized as the time taken for the molecule to rotate through 1 radian, and N is the number of directly attached protons. Since the ring methylene and methine carbons are found to have T_1 values in the ratio 1:2, it is concluded that the molecule undergoes isotropic tumbling. The angular methyl carbons and those of the side chain enjoy additional degrees of freedom and require considerations beyond those of equation (1). In the extremes, if the angular methyl groups are not rotating their T_1 values will be 0.33 of those of the methine carbons; if freely rotating they will have $T_1 = 3T_1^{\text{CH}}$. As can be seen in Fig. 2, it is this latter value that is found. The enhanced T_1 values for C-23 and C-24, as well as for the terminal methyls at C-25 and C-26, are due to the segmental motions of the side chain.

ApSimon, Beierbeck, and Saunders (32) have extended this work to include a series of androstanes and cholestanes. They too find for the ring methylenes and methines that the T_1 values of the former are one-half those of the latter, thus signifying mainly isotropic tumbling.

However, a steroid has one long axis running close to C-3 as shown in [7]. For 5α -androstan- 3β -ol and 5α -androstan- 3α -ol the average NT_1



values for the ring methylenes and methines (1 M solutions in CDCl_3 , 35°C) are 2.1 s. The C-3 value for the former is 2.0 s, but for the latter the value is 1.5 s. We have seen the same sort of effect in 5α -cholestan- 3β -ol and its 3α -epimer. The rationalization is the same as that given (33, 34) for the *para* carbon compared with the *ortho* and *meta* carbons of the monosubstituted benzenes, i.e. in the 3α -steroid the C(3)-H bond is equatorial, and its correlation time is somewhat larger if there is a preference for rotation about the long axis of the molecule. The net result is a lowering of T_1 for a carbon atom with its attached proton along this axis. It appears, therefore, that steroid tumbling is not completely isotropic.

It has been postulated that methyl group relaxation times reflect energy differences between preferred conformations and the transition state for rotation. (32) Decreasing the number of diaxial 1,3-steric interactions lowers the energy of the preferred conformation but increases the energy of activation for the rotational process. Rotation rates are decreased but the efficiency of the relaxation process is enhanced, i.e. T_1 is decreased. In Fig. 3 are shown the T_1 data for a related series of steroids of interest to us. As can be seen, loss of 1,3-diaxial interactions does markedly reduce methyl T_1 values. This is particularly evident for the change to an Δ /B-*cis* ring fusion as in compound [11].

Noting the similarity between NMR relaxation and dielectric relaxation effects, Bloembergen, Purcell, and Pound (35) adapted the Debye theory for the latter to the problems of the former to obtain equation (2).

$$\tau_c = \frac{4\pi a^3}{3kT} \eta = \frac{V_m}{RT} \eta \quad (2)$$

In this approach the molecule is treated as a sphere of radius a in a uniform cavity characterized by a microviscosity η and an apparent molar volume V_m . Over the years many studies correlating T_1 with solution viscosity have been carried out. The record of linear correlations is patchy, partly because the microviscosity is not an experimentally available number. However, in large, relatively flat

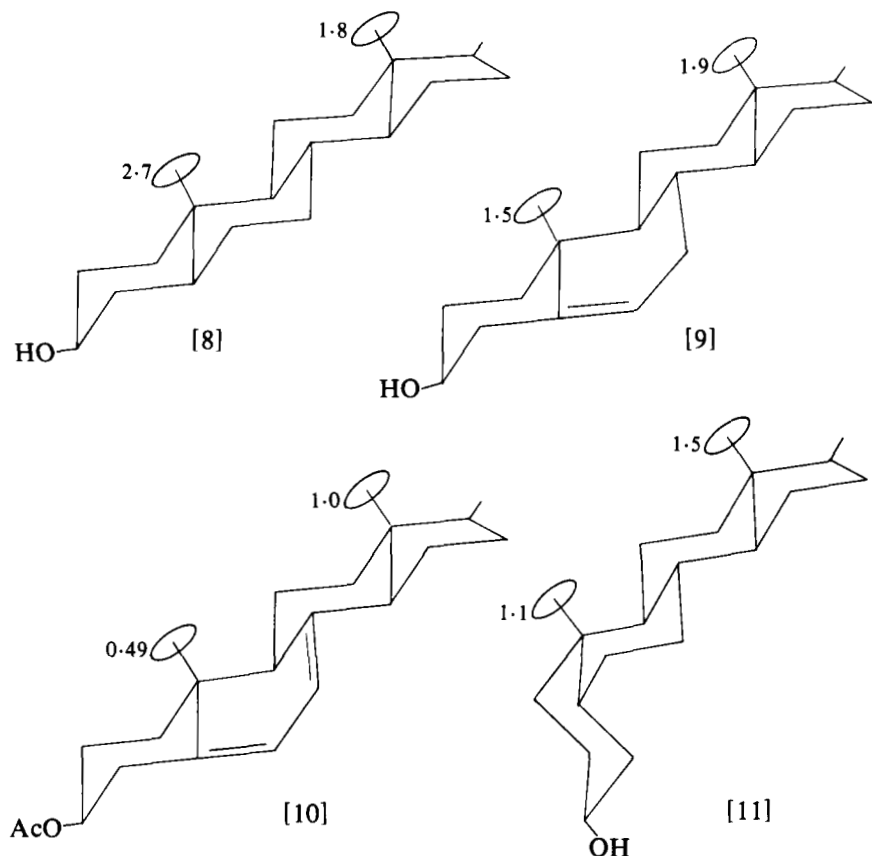


FIG. 3. Methyl relaxation times (s) for various steroids (200 mg/ml) in chloroform at 35°C.

molecules like steroids, tumbling of the molecule must move a large number of solvent molecules out of the way. Under such conditions microviscosity and translational viscosity should be equal or at least proportional. This hypothesis has been tested for solutions of cholesteryl chloride and cholesteryl acetate in deuteriochloroform. (36) Good linear behaviour between T_1^{-1} and η is obtained. Furthermore, an excellent linear fit of T_1 vs. $[M]$ is found (Fig. 4). This relationship has no basis in theory but seems to result from the viscosity-concentration relationships for these compounds over the range of concentrations utilized. From the experimental apparent molar volume of 1 M cholesteryl acetate in chloroform one calculates a τ_c of 4.1×10^{-10} s. The NMR determined value is 1.2×10^{-10} s, which can be considered as

providing good agreement since the steroid is hardly a spherical molecule in a spherical cavity.

With steroids bearing hydroxyl groups the linear behaviour between T_1 and molar concentration no longer holds. Cholesterol and a series of bile acid methyl esters have been studied. (36) The curves are concave

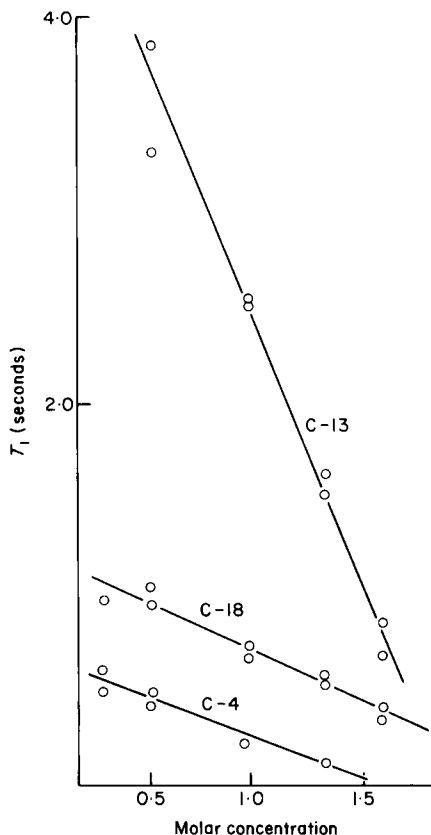


FIG. 4. The relationship between T_1 for several carbons in cholesteryl acetate and molar concentration, in deuteriochloroform at 35°C.

upwards and the nonlinearity increases with increasing number of available hydroxyl groups. This behaviour reflects the hydrogen bonding association of these molecules in chloroform. The same trend is reflected in the T_1 values at some standard concentration. Thus for the average values of the ring methylenes at 0.5 M in chloroform at 35°C, one finds cholesterol 0.55 s, methyl 3-hydroxychohanate 0.39 s, methyl 3,12-dihydroxychohanate 0.16 s, methyl 3,7-dihydroxychohanate 0.13 s,

and methyl 3,7,12-trihydroxycholesterol 0.04 sec. Even the greater steric hindrance at the 12-hydroxyl as opposed to the 7-hydroxyl position is reflected in these data.

Concentration effects on the quality of steroid spectra have been described by Wehrli (27, 28) who noted a resolution degradation in solutions of increasing concentration of cholesterol-3-one. The effect is one of line broadening and peak height loss. The methylene carbons are first affected, followed by those of the methine groups.

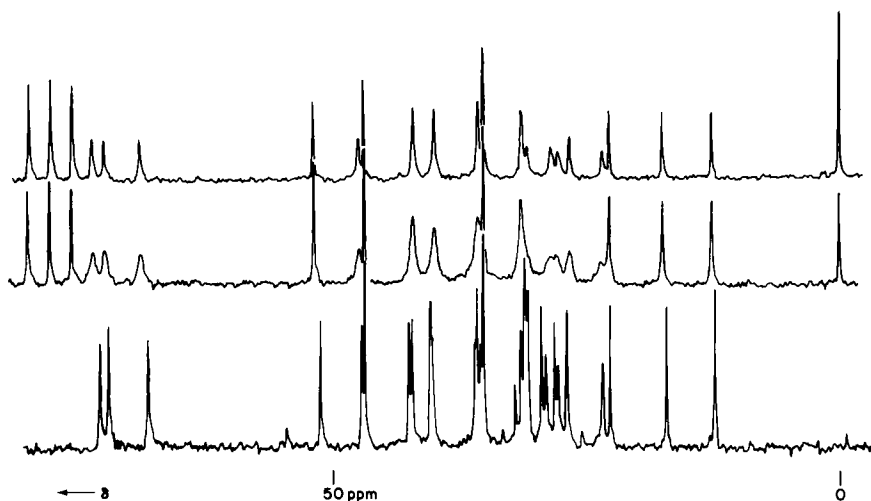


FIG. 5. ^{13}C spectra of methyl 3,7,12-trihydroxycholesterol taken at 15 MHz, for 1 M in acetone (bottom), 1 M in CDCl_3 (middle), and 0.5 M in CDCl_3 (top).

For steroids, at most accessible NMR frequencies, $T_1 = T_2$ and T_2^{-1} controls the line width. As the concentration increases both T_1 and T_2 decrease. Eventually a point is reached where T_2 is so small that line broadening in excess of that due to field inhomogeneity occurs. The effect can be seen in solutions of methyl 3,7,12-trihydroxycholesterol (Fig. 5). The improvement in resolution in going from 1 M to 0.5 M is apparent but even more striking is the improvement of the 1 M solution in acetone. Since acetone should serve as a good hydrogen bond acceptor, it is apparent that the aggregations of the steroid are broken up in this solvent. One caveat for the practitioner now becomes obvious: speeding acquisition times, by going to more concentrated solutions, can result in a loss of spectral quality.

The utility of PRFT spectra in making steroid spectral assignments has been reported. (27, 28, 31) In this technique the sample is given a spin inverting 180° pulse followed, after a brief waiting time, by an observing 90° pulse. Those carbons which relax slowly are inverted, while the fast relaxing methylenes appear as normal. The effect is shown in Fig. 6 for 2,2-dibromocholestan-3-one. Qualitatively one may separate the carbons into three categories; slow, medium, and fast

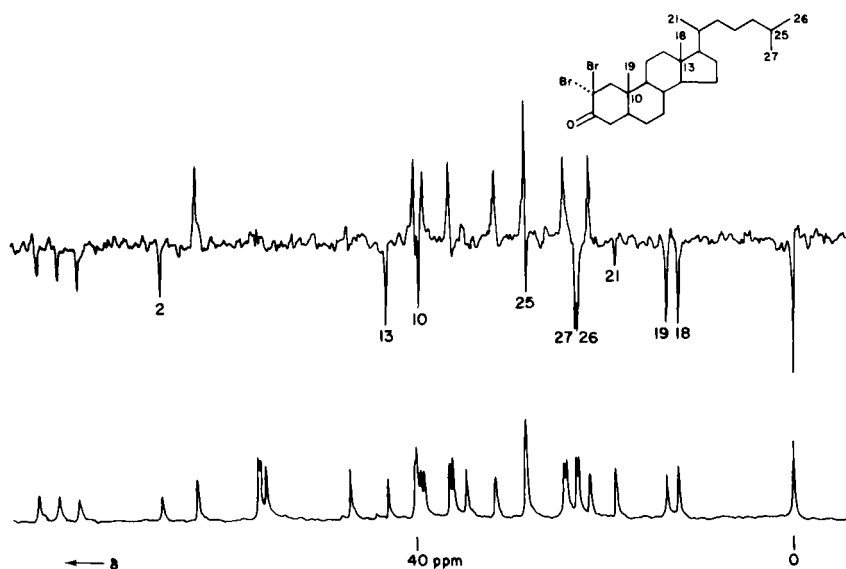


FIG. 6. Partially relaxed (top) and normal ^{13}C spectra of 2,2-dibromocholestan-3-one.

relaxers. Quaternary carbons 10, 13, and 2 and terminal methyl groups 26 and 27 fall in the slow division. Because of segmental motion the 21-methyl and 25-methine carbon are medium-slow. The eight ring methylene carbons are fast relaxers as is C-22. Because of segmental motion C-23 and C-24 fall in the medium-fast category and may be in the baseline. By proper adjustment of the pulse interval the methine carbon signals (medium) are nulled. This sort of spectrum is particularly helpful when coupled with incremental additions of a chemical shift reagent, since it makes tracking the line movements much easier.

An application combining information from relaxation and shift reagent studies is shown in Fig. 7. In the spectrum of 5α -cholestan-3-one there is a cluster of four lines, as shown, around 36 ppm. These have

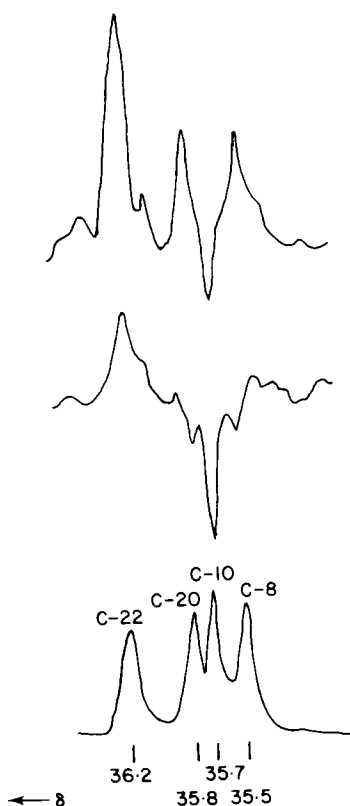


FIG. 7. The normal (lower) and partially relaxed spectra of 5 α -cholestan-3-one in the region around 36 ppm.

been assigned in several different perturbations by various laboratories but all agree that carbons 8, 10, 20, and 22 are involved. As seen here, the signal at 35.7 ppm is that of a slow relaxer and belongs to carbon 10. The methylene carbon-22 is a fast relaxer and is at 36.2 ppm. The methylenes C-8 and C-20 cannot be differentiated on the basis of T_1 values but in 5 α -cholestan-3 β -ol the line at 35.5 ppm is significantly more affected by Yb(tfn)₃ than that at 35.9 ppm. Since the change from a carbonyl to a hydroxyl will not influence these distant carbons the correct assignments are as shown in Fig. 7.

At present the number of steroid ¹³C NMR studies on molecules of biological interest is very small. The spectra of cholesteryl linoleate alone and in aqueous codispersions of egg phosphatidylcholine have been reported. (37) Line width considerations are used to draw conclusions of steroid organization and molecular motion. These results have been compared with the changes in the spectra of human serum

low density lipoprotein, and it is concluded that, at temperatures below the order-disorder transition, the cholesteryl esters are organized into a liquid crystal structure. (37) Above this temperature the structure is partially melted but it is still restricted compared with that of the ester in solution.

IV. SUBSTITUENT EFFECTS

The carbon chemical shifts for steroids are the most readily available data from a routine ^{13}C NMR determination. Since they reflect the electronic and steric environments of the various carbon nuclei, they provide sensitive insights to the configurational and conformational features of such molecules. While much interesting work on *ab initio* molecular orbital calculations of carbon chemical shifts is now appearing, it is probably true that the difficulties of carrying out such calculations on large molecules will prevent their applications to steroids for some time. We are limited, therefore, to a more empirical approach to steroid carbon chemical shifts. (3, 38)

The chemical shifts of carbons attached directly to various substituents generally reflect the electronegativity of the given substituent (the α -effect). In the vast majority of cases the α -effect produces deshielding. However, primary carbons attached to iodine may show the opposite effect (the heavy atom effect) owing to an increase in the nuclear shielding arising from the large number of non-bonded electrons.

Carbons β to the point of substituent attachment are, with few exceptions, also deshielded. The β -effect is not overly sensitive to the nature of the substituent. There appears to be no good explanation of the β -effect beyond the rationalization that it is the sum of two conflicting effects.

For substituents three bonds away from the carbon of interest, a more complex pattern of behaviour appears. If the substituent is a carbon bearing hydrogen, and if a *gauche* orientation is possible, then the γ -*gauche* effect is observed. This may be exemplified by comparing the C-19 chemical shifts of 5α -cholestan- 3β -ol [12] and cholest-5-en- 3β -ol (cholesterol) [13]. In [13] there is one less γ -*gauche* interaction owing to

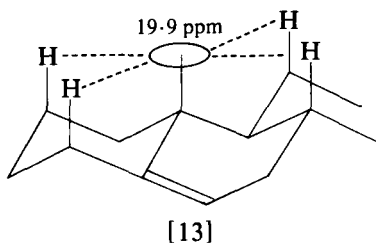
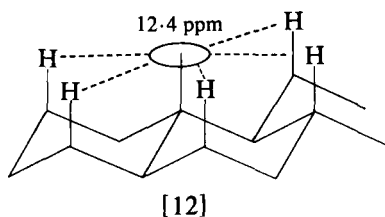


TABLE I

Some steroid ^{13}C chemical shift data from these laboratories (CDCl_3)

No. (1)	Steroid	C-1	C-2	C-3	C-4	C-5	C-6	C-7	C-8	C-9	C-10	C-11
211.	Cholest-5-en-3 β -ol (Cholesterol)	37.2	31.6	71.8	42.3 ^a	140.6	121.4	31.9 ^a	31.9 ^a	50.2	36.5	21.1
212.	Cholest-5-en-3 β -yl acetate	37.1	27.8	73.8	38.2	140.2	122.9	31.9 ^a	31.9 ^a	50.1	36.6	21.1
414.	Cholest-5-ene-3 β ,7 α -diol	37.5	31.4	71.3	42.2	146.4	123.9	65.4	37.2	42.4	37.6	20.8
415.	Cholest-5-ene-3 β ,7 α -diol 3-acetate	36.7	27.5	73.4	37.9	148.7	124.8	65.2	37.5 ^a	42.1 ^a	37.5 ^a	20.7
416.	Cholest-5-en-3 β -ol 7 α -hydro- peroxide	36.9	31.4	76.5	42.3	147.5	120.1	78.5	37.2	43.7	37.5	21.0
417.	Cholest-5-en-3 β -ol 7 α -hydro- peroxide 3-acetate	36.3	27.6	73.6	38.3	74.0	121.2	78.1	37.2	43.7	37.5	21.0
418.	Cholest-6-ene-3 β ,5 α -diol	28.6	30.6	67.1	41.0	74.0	133.1	133.4	38.5	45.1	38.1	21.1
419.	Cholest-6-ene-3 β ,5 α -diol 3-acetate	28.3	26.4	70.6	37.2	73.4	132.7 ^b	133.3 ^b	38.4	44.7	38.0	21.0
420.	Cholest-6-en-3 β -ol 5-hydro- peroxide	29.4	31.7	66.2	37.1	82.9	132.2	133.2	39.1	44.3	38.7	21.3
143.	5 α -Cholestan-3-one	38.6	38.0	210.4	44.6	46.7	29.0	31.8	35.6	53.9	35.4	21.5
421.	2 β -Bromo-5 α -cholestan-3-one	51.7	54.5	201.0	43.9	47.4	28.4	31.5	34.9	53.6	39.0	21.5
422.	2,2-Dibromo-5 α -cholestan-3- one	62.5	66.2	194.9	38.8	46.5	28.1 ^a	31.3	34.3	55.3	39.1	21.4
423.	2 β ,4 β -Dibromo-5 α -cholestan- 3-one	51.2	51.7	192.8	60.0	55.5	28.0 ^a	31.4	34.9	54.0	41.1	21.6
176.	5 α -Cholestan-6-on-3-yl acetate	36.4	26.9	72.8	26.2	56.4	209.8	46.6	37.9	53.9	40.9	21.5
424.	5 α -Bromocholestan-6-on-3-yl acetate	30.3	26.0	70.8	34.8	79.7	203.5	40.3	36.1 ^a	47.2	42.6	21.6
425.	7 β -Bromo-5 α -cholestan-6-on- 3-yl acetate	36.1	26.7	72.3	25.8	49.8	203.5	58.5	45.8	40.1	41.2	20.8

^a Overlapping lines.^b Assignment may be reversed.

the loss of the axial hydrogen at C-6 and a resulting decrease in the screening of the 19-carbon.

Indications that the simple steric polarization model for the γ -gauche interaction (39, 40) may be insufficient now come from a variety of sources. There are a number of examples in the literature where the three bond interaction involves a heteroatom which may have unshared pairs of electrons but no bond to hydrogen by which the steric polarization model could be evoked. An illustration of this may be seen from some steroid ^{13}C data recently acquired in our laboratory. These are shown in Table I where the numbering system initiated in the Blunt and Stothers review (1) is continued.

The introduction of the 5 α -bromine (compound 424) into 5 α -cholestan-6-on-3-yl acetate (compound 176) introduces a γ -gauche interaction at carbons 1, 3, 7, and 9 of -6.1 , -2.8 , -6.3 , and -6.7 ppm respectively. Presumably the effect at C-3 is partially compensated

C-12	C-13	C-14	C-15	C-16	C-17	C-18	C-19	C-20	C-21	C-22	C-23	C-24	C-25	C-26	C-27	Other carbons
39.8	42.3 ^a	56.8	24.3	28.3	56.1	11.9	19.4	35.8	18.7	36.2	23.8	39.5	28.0	22.6	22.8	
39.8	42.3	56.7	24.3	28.2	56.3	11.9	19.3	35.9	18.8	36.3	23.9	39.6	28.0	22.6	22.8	21.3 (Me)
39.3	42.3	49.5	24.4	28.3	56.0	11.7	18.3	35.9	18.8	36.3	23.8	39.6	28.1	22.6	22.8	
39.2	42.1 ^a	49.4	24.2	28.3	55.8	11.6	18.2	35.8	18.7	36.2	23.7	39.5	28.0	22.6	22.8	21.4 (Me)
39.2	42.4	49.1	24.5	28.2	55.9	11.4	18.2	35.8	18.8	36.3	23.8	39.6	28.1	22.6	22.8	
39.2	42.4	49.1	24.4	28.3	55.9	11.4	18.2	35.9	18.8	36.6	23.8	39.6	28.1	22.6	22.8	21.3 (Me)
40.1	43.7	54.0	23.9 ^a	28.3	56.2	12.1	14.7	35.8	18.7	36.2	32.9 ^a	39.5	28.0	22.5	22.9	
40.0	43.6	53.8	23.8 ^a	28.3	56.0	12.1	14.5	35.8	18.6	36.1	23.8 ^a	39.5	28.0	22.6	22.8	21.4 (Me)
40.4	43.7	53.8	24.0 ^a	28.2 ^a	56.3	12.2	15.5	36.1	18.8	36.5	24.0 ^a	39.8	28.2 ^a	22.7	22.8	
40.0	42.6	56.3	24.3	28.3	56.3	12.1	11.4	35.8	18.7	36.2	23.9	39.6	28.0	22.6	22.8	
39.7	42.6	56.1 ^a	24.2	28.2	56.1 ^a	12.1	12.1	35.7	18.7	36.1	23.8	39.5	28.0	22.6	22.8	
39.6	42.6	55.9	24.1	28.1 ^a	56.1	12.1	13.3	35.7	18.7	36.1	23.8	39.5	28.1 ^a	22.6	22.8	
39.7	42.6	56.0	24.1	28.2	56.3	12.1	13.2	35.8	18.7	36.1	23.9	39.5	28.0 ^a	22.6	22.8	
39.5	43.0	56.7	24.0	28.0 ^a	56.2	12.0	13.0	35.7	18.7	36.1	23.8	39.5	28.0 ^a	22.6	22.8	21.2 (Me)
39.2	43.0	55.9	23.7	27.9 ^a	56.1	12.0	14.4	35.6	18.6	36.1	23.7	39.4	27.9 ^a	22.6	22.8	21.2 (Me)
																170.0 (CO ₂)
38.7	42.6	52.2	22.8	27.8	55.7	12.3	12.6	35.6	18.7	36.1	23.8	39.4	27.9	22.6	22.8	21.2 (Me)
																170.2 (CO ₂)

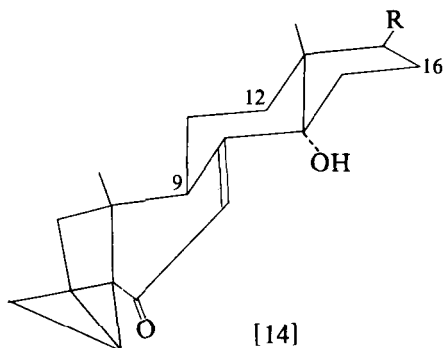
for by the acetoxy group. While substituent effects are often smaller at more highly substituted carbons, the C-9 methine shows the same γ -*gauche* effect as the C-1 and C-7 methylenes, which suggests that the effect at C-3 results from something other than just the fact of a methine hydrogen being there.

Similar, shielding, γ -*gauche* effects are evidenced at carbons 9 and 14 when a 7 α -hydroxy (compound 414) or a 7 α -hydroperoxy (compound 416) group is substituted into cholesterol (compound 211). The effects of bromine, hydroxyl, and hydroperoxy are -6 to -7 ppm for groups without hydrogen or with hydrogen and certainly of differing physical size.

The γ -*gauche* effect involving only C-H bonds has been recently investigated by means of a modified version of the INDO finite perturbation theory of ^{13}C chemical shifts, using butane as a model. (41) While the expected geometrical dependence on the methyl chemical

shifts is observed, i.e. as the *gauche* interaction of the methyl increases its ^{13}C chemical shift moves to lower frequencies, there is no such correlation with the computed electron densities. It has been suggested (42) that the γ -*gauche* effect arises from a coupling of bond angle distortions with changes in torsion angles. If so, steroid substituent effects may prove of value in that the X-ray structures for something in excess of 234 steroids now exist. (43) It has been contended that β , γ , and δ effects are better understood as a consequence of the removal of a hydrogen on the β -carbon. (81)

While the steric polarization model may be called into question by the considerations presented above, it would be hard to reject the obvious parallels of steric interaction and the γ -*gauche* shielding effect. A case in point is the highly strained molecule [14] (compound 480). The effects



of the 14α -hydroxyl at carbons 12 and 17 are -7.2 and -6.0 ppm respectively. That at C-9 is only -4.4 ppm while the effect at C-16 is an even smaller -1.1 ppm. The X-ray determination of a related molecule has been carried out and shows a highly strained structure which is also reflected in the Dreiding model of [14]. The latter shows the C-9 hydrogen slanting somewhat away from the 14α -hydroxyl, while the envelope conformation of the D-ring twists the C-16 protons to a perceptibly greater distance than the methine proton at C-17. Thus, the γ -*gauche* effect at these positions clearly reflects a change in the steric interactions with the 14α -hydroxyl group.

When the γ -substituent is antiperiplanar to the carbon, either low- or high-frequency shifts may be experienced, and the deciding factor appears to be the state of substitution of the intervening carbons. The situation has been discussed at length (44) and amply illustrated by recent research. (45)

Both extremes of the anti γ -effect have been found to operate in

steroids. Thus, C-1 in 5 α -cholestan-3 β -ol is 1.6 ppm more shielded than its hydrocarbon precursor, while in [14] the C-18 methyl appears at 3.6 ppm to high frequency of that without the 14 α -hydroxyl (compound 479). Similarly, C-10 in 2 α -bromo-5 β -cholestan-3-one (compound 421) is 3.6 ppm less shielded than it is in the 3-ketone (compound 143).

In general δ -substituent effects are small, but a marked exception exists when the substituent and the carbon in question have a *syn*-diaxial relation. While the steric interactions suggest a shielding of the carbon, in fact an appreciable deshielding is found. Thus, the C-19 methyls in the 2 β - and 4 β -hydroxy-5 α -cholestanes are 2.5 and 2.4 ppm to high frequency of the value in 5 α -cholestane itself. This type of evidence has also been advanced against the operation of the steric polarization mechanism.

As part of their review, Blunt and Stothers developed from their data a table of substituent chemical shifts for a variety of substituents at a wide range of positions. When applied to the appropriate steroid framework it becomes possible to make reasonably good predictions of steroid ^{13}C chemical shifts. The appropriate warnings about multiple substituent interactions are given. Considerable data on the interactions of multiple hydroxyl groups have been generated, (46, 47) and these provide useful guides for other substituents as well.

It seems of interest to attempt to provide a simple set of guidelines for predicting steroid ^{13}C chemical shifts. These should be self-contained in order to relieve one of the necessity of having a complex set of tables. The point of departure is a simple set of predictive rules given by Dr. B. A. Shoulders to his students at the University of Texas. His parameters have been modified slightly for steroids, and additions have been made to handle the various effects introduced by ring geometry as set forth above. No pretence is made that the following are in their best or final form. But they may serve as a starting point for others, and may be enlarged or altered as the need presents itself.

Steroid ^{13}C prediction rules

1. For a given carbon, count the number of α - and β -carbons and multiply the sum by 7.3 ppm.
2. If the carbon is in a six-membered ring subtract 2.4 ppm, or 3.8 ppm if in a five-membered ring. Carbons at ring fusion points are corrected for the larger ring only.
3. If the carbon is trisubstituted or tetrasubstituted, count the number of β -carbons. Subtract this number times 1.5 ppm if trisubstituted, or this number times 4.4 ppm if tetrasubstituted.

TABLE II

Some recently reported steroid ^{13}C chemical shifts (CDCl_3)

No. (1)	Steroid	C-1	C-2	C-3	C-4	C-5	C-6	C-7	C-8	C-9	C-10	C-11	C-12
426.	4-Oestrene	29.0	22.3	25.5	119.8	140.7	35.8	32.7	41.6	42.3	50.7	25.6	39.0
427.	4-Oestren-17-one	28.8	22.1	25.3 ^a	120.5	139.8	35.4	31.7	40.6	42.0	50.6 ^a	25.5 ^a	31.0
428.	17 α -Ethyl-4-oestren-17 β -ol	29.0	22.3	25.3	120.0	140.5	35.6	31.6 ^a	42.1 ^a	42.0 ^a	50.4	25.1	33.5
429.	4-Oestren-17 α -ol	29.0	22.7	25.5	120.0	140.4	35.7	32.6	41.5	42.2	50.2	25.2	31.5
430.	17 α -Fluoro-4-oestrene	28.9	22.2	25.7	120.1	140.2	35.6	32.5	41.3	42.1	50.1	25.4	31.3
431.	17 α -Chloro-4-oestrene	28.8	22.2	25.5	120.1	140.1	35.6	32.4	41.6	42.1	49.8	25.0	33.8
432.	4-Oestren-17 β -ol	28.9	22.2	25.5	120.0	140.4	35.6	31.7	41.2	42.1	50.5	25.2	36.8
433.	5 α -Cholestane-1 α ,2 β -diol	74.3	72.3	29.0	23.7	39.6	28.5	31.7	34.7	48.1	39.6	20.5	39.9
434.	5 α -Cholestane-1 α ,3 α -diol	72.7	36.2	67.8	33.6 ^a	32.2 ^a	28.4	31.7	35.4	46.8	40.3	20.2	39.7
435.	5 α -Cholestane-1 α ,3 β -diol	73.2	38.3 ^a	66.7	38.1 ^a	37.4	28.6	31.7	35.5	46.9	39.8	20.7	39.8
436.	(25R)-5 α -Spirostane-2 α ,3 β -diol	40.9	69.0 ^a	69.1 ^a	34.3	38.1	27.6	32.0	34.4	54.2	37.0	20.7	40.0
437.	5 α -Cholestane-2 β ,3 α -diol 3-acetate	40.0	68.5	73.0	28.7	40.5	28.2	31.9	34.9	55.1	35.4	20.9	40.0
438.	(25R)-5 α -Spirostane-2 α ,3 β -diol	45.1 ^a	73.0	76.4	35.6	44.9 ^a	27.9	32.1	39.5	54.3	37.6	21.2	40.0
439.	(25R)-5 α -Spirostane-2 β ,3 α -diol	40.1	71.7	70.6	31.8	39.0	28.2	32.1	34.6	55.2	35.9	20.8	40.1
440.	5 α -Cholestane-3 α ,4 α -diol	31.5 ^a	27.1	69.5	72.0	45.8	22.8	31.7 ^a	35.3	54.4	37.1	21.0	40.1
441.	5 α -Cholestane-3 α ,4 β -diol	31.7	24.6	70.3	76.1	44.0	25.2	32.4	35.6	55.2	35.9	20.3	40.0
442.	5 α -Cholestane-3 α ,4 β -diol 4 β -acetate	31.5	24.8	67.0	77.0	42.7	25.0	32.2	35.5	55.1	35.9	20.5	40.0
443.	5 α -Cholestane-3 α ,4 β -diol diacetate	32.0	22.3	69.6	73.3	44.1	24.7	32.0	35.4	55.0	35.6	20.4	40.0
444.	(25R)-5 α -Spirostane-3 α ,4 β -diol	31.7	24.6	70.2	76.0	43.8	25.0	32.5	35.1	55.1	35.9	20.0	39.9
445.	(25R)-5 α -Spirostane 3 α ,4 β - diacetate	32.0	22.2	69.4	73.2	44.0	24.6	32.0	34.9	54.9	35.6	20.2	39.8
446.	5 α -Cholestane-3 β ,4 α -diol	36.2	28.3	76.4	75.6	50.8	22.7	31.5	35.0	54.4	37.3	21.0	40.0
447.	5 α -Cholestane-3 β ,4 α -diacetate	35.8	26.0	75.4 ^a	74.0 ^a	49.3	22.9	31.3	35.0	54.2	37.3	21.0	40.0
448.	5 α -Cholestane-3 β ,4 β -diol	37.0	26.0	72.2	74.8	48.9	26.0	32.4	35.6 ^a	55.3	35.4 ^a	20.6	40.0
449.	5 α -Cholestane-3 α ,5 α -diol	25.5 ^a	29.0	67.5	39.4	75.0	34.0	26.5 ^a	34.8	45.7		21.0	40.0
450.	5 α -Cholestane-3 α ,5 α -diol 3 α -acetate	25.6 ^a	25.6 ^a	70.8	37.5	73.0	33.6	26.8 ^a	34.9	45.2		20.9	40.1
451.	5 α -Androstane-3 β ,5 α -diol	31.0	31.0	67.2	44.0	75.2	34.5	26.3	35.1	46.2	38.9	21.4	38.9
452.	5 α -Cholestane-3 β ,6 β -diol 6 β -acetate	38.3	31.3	71.3	35.0	46.4	73.6	36.5	31.1	54.0	35.5	21.1	39.9
453.	5 α -Cholestane-3 β ,6 β -diacetate	38.0	27.3	73.3	31.0	46.2	73.3	36.4	31.0	53.8	35.5	21.0	39.8
454.	5 α -Cholestane-3 β ,7 α -diol 3 β -acetate	36.9	27.4	73.5	33.6	36.1	36.5	67.7	39.5	45.7	35.5	21.0	39.5
455.	5 α -Cholestane-4 α ,5 α -diol	30.5	19.5	30.0	71.3	75.1	28.4	26.0	34.5	45.9	40.2	20.9	40.0
456.	5 α -Cholestane-4 α ,5 α -diol 4 α -acetate	30.4	19.4	26.3	75.2	74.2	29.2	25.9	34.5	45.4	40.7	20.9	40.0
457.	5 α -Cholestane-5 α ,6 α -diol	31.8	20.7	20.4	28.5	75.0	70.9	35.8	33.6	45.0	39.6	20.7	39.9
458.	5 α -Cholestane-6 α ,7 α -diol	38.6	21.8	26.2	22.8	45.3	12.2	71.3	38.4	45.4	36.7	20.6	39.5
459.	5 α -Cholestane-6 β ,7 α -diol	40.3	22.0	27.0	25.5	43.3	76.5	71.9	34.6	45.7	36.2	20.4	39.6
460.	5 α -Cholestane-12 β ,15 α -diol	38.8	22.1	26.7	28.9	46.8	28.9	32.0	34.5	53.5	36.4	29.8	79.1

[illegible]

TABLE II—*cont.*

No. (1)	Steroid	C-1	C-2	C-3	C-4	C-5	C-6	C-7	C-8	C-9	C-10	C-11	C-12
461.	5 α -Androstane-15 β ,17 β -diol	38.8	22.2	26.9	29.1	47.4	28.9	31.5	31.5	55.5	36.6	20.4	38.5
462.	5 α -Androstane-16 β ,17 β -diol	38.7	22.2	26.8	29.0	47.1	28.9	31.9	35.0	55.1	36.4	20.2	37.5
463.	1 α ,2 α -Epoxy-5 α -cholestane	59.4	52.8	23.5	28.1	37.2	28.1	31.7	35.5	48.9	36.5	21.2	
464.	1 α ,2 α -Epoxy-3 α -methyl-5 α -cholestane	60.0	56.9	25.6	34.3	31.5	28.1	31.8	35.5	49.3	36.3	21.3	
465.	1 α ,2 α -Epoxy-4 β -methyl-5 α -cholestane	59.3	52.6	33.1	26.5	43.4	23.2	31.7	34.8	48.9	36.8	21.3	
466.	1 β ,2 β -Epoxy-5 α -cholestane	59.3	54.3	26.6	22.7	45.6	27.7	32.0	35.7	51.1	35.9	21.6	
467.	1 β ,2 β -Epoxy-3 α -methyl-5 α -cholestane	59.8	58.9	28.4	30.0	39.6	27.7	32.0	35.8	51.2	36.0	21.6	
468.	1 β ,2 β -Epoxy-4 β -methyl-5 α -cholestane	59.4	54.1	35.8	24.9	51.2	22.6	32.0	35.8	51.2	36.7	21.8	
469.	2 α ,3 α -Epoxy-5 α -cholestane	38.2	50.4	51.7	29.0	36.2	28.2	31.1	35.4	53.5	33.6	20.9	
470.	2 α ,3 α -Epoxy-1 α -methyl-5 α -cholestane	35.5	56.0	53.2	30.0	30.8	28.8	31.5	35.4	46.6	35.7	21.3	
471.	2 α ,3 α -Epoxy-4 β -methyl-5 α -cholestane	38.2	51.9	57.4	31.8	43.2	24.8	31.8	35.2	53.6	34.5	20.9	
472.	2 β ,3 β -Epoxy-5 α -cholestane	38.1	52.6	51.5	28.2	41.2	28.4	31.3	34.7	55.3	34.3	20.8	
473.	2 β ,3 β -Epoxy-1 α -methyl-5 α -cholestane	35.7	58.8	50.6	28.7	34.0	28.7	31.5	34.8	49.1	36.1	20.5	
474.	2 β ,3 β -Epoxy-4 β -methyl-5 α -cholestane	38.1	53.2	57.7	31.0	48.9	25.7	31.9	34.6	55.6	34.6	20.9	
475.	3 α ,4 α -Epoxy-5 α -cholestane	30.4	21.3	51.9	55.6	46.7	26.7	31.4	35.3	52.6	34.0	21.3	
476.	3 α ,4 α -Epoxy-1 α -methyl-5 α -cholestane	32.8	28.5	52.5	56.3	38.5	27.0	31.8	35.3	47.9	36.7	20.3	
477.	3 β ,4 β -Epoxy-5 α -cholestane	33.6	21.2	50.3	57.6	46.2	25.3	31.8	35.4	54.7	35.7	20.7	
478.	3 β ,4 β -Epoxy-1 α -methyl-5 α -cholestane	33.0	29.1	49.7	57.3	38.7	25.0	32.2	35.4	49.3	37.1	19.8	
276.	Ergosta-5,7,22-trien-3 β -ol (Ergosterol)	38.4	32.1	70.5	40.9	139.8	119.7	116.4	141.4	46.3	37.1	21.2	39.2
479.	3 α ,5 α -Cyclocholestan-6-one	33.6	25.9	34.9	11.5	46.3	209.1	44.8	35.0	46.3	46.8	22.9	39.8
480.	3 α ,5 α -Cycloergosta-7,22-dien-6-one	33.9	26.8	34.8	13.1	43.7	196.0	123.6	163.9	42.1	45.1	22.7	39.1
481.	3 α ,5 α -Cycloergosta-7,22-dien-14 α -ol-6-one	33.7	26.8	35.4	13.7	43.9	198.2	123.3	164.6	37.8	45.2	21.8	31.9
482.	3 β -Acetoxy-5 α -ergosta-7,22-dien-6-one	29.3	25.5	67.7	29.6	51.5	202.1	121.3	165.9	38.3	36.2	22.2	39.0
483.	3 β -Acetoxy-5 β -ergosta-7,22-diene-6-one	36.3	26.8	72.9	26.4	53.1	198.9	123.0	164.0	50.0	38.2	21.8	38.7
484.	Soladulcidine	37.0	31.5	71.1	38.2	44.9	28.6	32.3	35.2	54.4	35.6	21.1	40.1
485.	Solasodine	37.3	31.5	71.7	42.3	140.9	121.3	32.1	31.5	50.2	36.7	20.9	40.0
486.	Tomatidine	37.0	31.5	71.0	38.2	44.9	28.6	32.3	35.0	54.4	35.5	21.1	40.2
487.	Demissidine	37.1	31.6	71.3	38.3	45.0	28.8	32.3	35.4	54.6	35.6	21.1	40.2
488.	Δ^5 -Solaniidine	37.3	31.6	71.7	42.3	140.8	121.6	32.1	31.6	50.2	36.7	21.0	40.0
489.	Jurubidine	37.7	30.9	50.9	37.6	45.5	28.6	32.3	35.2	54.5	35.6	21.0	40.1
490.	Solanocapsine	37.6	30.1	51.2	39.3	45.8	28.7	32.5	35.1	55.1	35.7	20.5	39.3

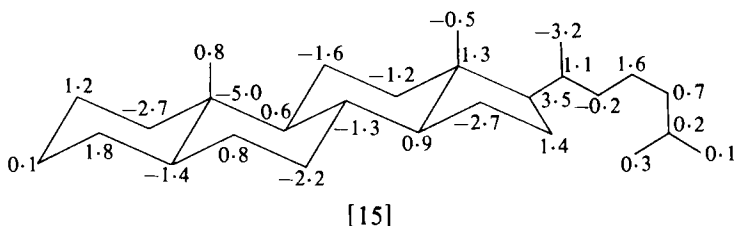
^a Line assignments may be reversed.

- For a methylene or methine carbon with an axial γ -methyl interaction subtract 5.8 ppm; for a methyl with n -axial γ -methylene proton interactions subtract $n \times 3.6$ ppm.
- For alkyl side chains the following addenda are required: (a) If

C-13	C-14	C-15	C-16	C-17	C-18	C-19	C-20	C-21	C-22	C-23	C-24	C-25	C-26	C-27	C-28	Other carbons	Ref.
42.4	56.1	69.4	43.1	81.4	13.9	12.3											47
42.5	47.6	35.0	70.1	80.9	12.0	12.3										Me	47
						11.4											56
						11.4										18.2	56
						12.1										19.4	56
						10.6											56
						10.8										17.5	56
						11.6										19.2	56
						12.9											56
						14.6										10.6	56
						13.8										16.2	56
						14.0											56
						15.7										12.1	56
						15.2										18.7	56
						13.4											56
						15.5										16.3	56
						14.0											56
						16.8										14.7	56
42.9	54.6	23.0	28.3	55.8	12.1	16.3	40.4	21.2	135.6	132.1	42.9	33.1	19.7	20.0	17.6		102
42.8	57.2	23.9	28.2	56.2	12.0	19.7	35.8	18.8	36.2	24.1	39.6	28.1	22.6	22.8	17.6		102
44.4	56.2	23.3	27.9	56.2	12.7	19.4	40.3	21.2	135.0	132.4	42.9	33.1	19.7	20.0	17.5		102
46.3	85.1	30.6	26.8	50.3	16.3	19.2	40.0	21.3	135.5	132.4	42.8	33.1	19.7	20.0	17.6		102
45.2	56.2	22.3	27.9	56.2	12.6	24.2	40.2	21.1	134.8	132.3	42.8	33.0	19.6	19.9	17.6	21.3 (Me)	102
44.4	55.7	22.6	27.8	56.1	12.6	13.2	40.2	21.1	135.0	132.5	42.8	33.1	19.7	19.9	17.6	21.3 (Me)	102
41.0	56.3	32.1	80.0	62.6	16.5	12.4	41.6	15.0	98.3	33.3	29.6	30.3	46.9	19.1			100
40.5	56.6	32.1	79.0	62.9	16.4	19.3	41.3	15.2	98.4	34.1	30.3	31.5	47.7	19.3			100
40.9	55.8	32.6	78.5	62.0	16.9	12.3	43.0	15.8	99.3	26.6	28.6	31.0	50.2	19.3			100
40.6	57.4	33.5	69.0	63.3	17.1	12.4	36.7	18.3	74.7	29.3	31.1 ^a	31.3 ^a	60.2	19.5			100
40.3	57.6	33.3	69.1	62.9	16.8	19.4	36.7	18.1	74.7	29.1	30.9 ^a	31.1 ^a	60.2	19.4			100
40.6	56.4	31.7	80.9	62.1	16.5	12.3	42.2	14.3	109.7	27.1	25.8 ^a	26.0 ^a	65.1	16.1			100
41.9	55.1	33.1	74.5	60.6	13.7	12.3	46.3	15.1	68.9	96.1	39.3 ^a	31.9 ^a	55.1	18.7			100

there is a methyl γ to a carbon of interest ($C-C-C-CH_3$) subtract 2.3 ppm if the penultimate carbon is *not* a methylene, or 0.4 ppm if it is. (b) If the carbon atom is third from a chain end and is also a methylene, add 2.3 ppm.

Applying the above rules to 5 α -cholestane [15] and comparing with the experimental values leads to the differences shown in [15], i.e.



experimental — predicted. The average deviation for all carbons is ± 1.4 ppm, though clearly the numbers at carbons 10, 17, and 21 account for a substantial amount of this.

Certain value judgments not built into the rules need to be applied. Thus, the envelope conformation accepted for the D-ring (43) suggests that a γ -interaction should be allowed for the calculation of C-15 and C-18 but not for C-16 since the hydrogens on the latter are tilted away from C-18. Similarly, there is a *gauche* interaction between C-18 and C-20 in the side chain which influences the chemical shift of both carbons. It is likely that the difficulties at C-17 and C-21 arise from steric interactions which are difficult to account for without assigning a specific conformation to the side chain. The result at C-10 is more difficult to rationalize.

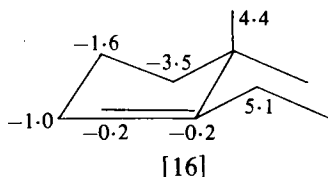
To account for carbon-carbon double bonds a sixth rule is added.

6. (a) The base value for an olefinic carbon is 121.5 ppm. Count the number of carbons α and β to the carbon in question and subtract the number of α' carbons. Multiply the total by 5.2 and add to the base value. Rule 2 applies. (b) Saturated carbon adjacent to a double bond are counted as usual, but if they are part of an acyclic chain 3.8 ppm is added to the value as an α -effect of the double bond, and 5.0 ppm is subtracted if the double bond is *cis*-substituted.

Applying the above to cholest-4-ene [16] yields for instance:

$$\text{C-3} = 4 \times 7.3 - 2.4 = 26.8 \quad (25.8 \text{ ppm exp})$$

$$\text{C-5} = 121.5 + (6 - 1)5.2 - 2.4 = 145.1 \quad (144.9 \text{ ppm exp})$$



The structure [16] illustrates the fact that introduction of the Δ^4 double bond alters the conformation of the A-ring to that of a half-chair. Examination of the Dreiding model shows that the 1,3-interactions of the C-19 methyl with the C-2 and C-6 axial protons are substantially reduced. Similarly, the *gauche* interaction of the C-4 and C-6 equatorial protons is greatly reduced.

From the available data on γ -*gauche* and *syn*-diaxial interactions of hydroxyl groups it appears that one might treat this group as a methyl with the appropriate correction at the α -carbon.

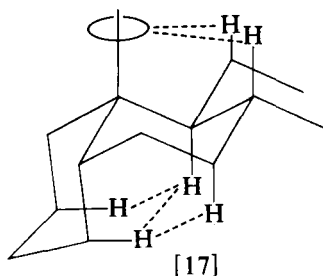
The frustrations of attempting rational explanations of substituent effects are exemplified by the various bromo-ketones in Table I. It has been known for many years that ketone carbonyl stretching frequencies are increased by about 23 cm^{-1} upon α -substitution with a coplanar equatorial bromine. (48) Axial bromines have no effect on the adjacent carbonyl stretching frequency. The suggested reason for these observations is that a field type interaction of the C-Br dipole with the carbonyl group suppresses the contribution of the $\text{C}^{\oplus}\text{-O}^{\ominus}$ structure to the carbonyl hybrid. While there is a small amount of data on the point from an unrelated system, (49) it seems worthwhile to probe whether or not a coplanar bromine will have a substantially different substituent effect from one essentially perpendicular to the carbonyl. The substituent chemical shifts of an equatorial bromine (compound 421), a second, but axial, bromine (compound 422), a second, but equatorial, bromine (compound 423), a single axial bromine (compound 424), and its comparable equatorial counterpart (compound 425) are -9.3 , -6.6 , -8.2 , -6.3 , and -6.3 ppm respectively. Thus, there is only a very slight effect upon altering the relative orientation of the two dipoles. Normally the β -effect of bromine produces a high frequency shift as evidenced at the adjacent methylenes in the compounds mentioned above. The low frequency shifts of the carbonyl carbon have been ascribed to the suppression of the $\text{C}^{\oplus}\text{-O}^{\ominus}$ contribution, (50) but it is clear that this is not the result of a geometry dependent field effect.

V. STEROID STEREOCHEMISTRY

Regardless of the mechanistic details, it is the obvious correlation of the γ -*gauche* effect with steric crowding which provides the bulk of the information on steroid stereochemistry. Early evidence of this was reported (51) for a series of A/B-*cis* steroids (i.e. 5β). It is found that the C-19 methyl signal moves to high frequency by 11–12 ppm, compared with that of their 5α counterparts. Very shortly thereafter the same

observation was made in rationalizing the chemical shifts of a series of bile acids and esters. (18)

As shown in the case of [12] previously, and in that of [17], in the 5α -steroid C-19 has five γ -*gauche* interactions, while the 5β -steroid reduces



these to three. At the same time, the C-7 and C-9 carbons acquire new steric interactions between their axial hydrogens and their counterparts at C-2 and C-4. In going from A/B-*trans* to A/B-*cis* the signals from carbons 2, 4, 7, 9, and 19 are altered by -0.8 , -2.0 , -5.3 , -14.5 , and $+12.0$ ppm respectively. The values for C-2 and C-4 reflect the loss of the methyl interaction compensated by the new interactions with C-7 and C-9. The latter clearly reflect these new interactions, while the C-19 methyl moves to higher frequency owing to the loss of the C-2 and C-4 interactions.

Just as the C-19 methyl values may be used to assign the stereochemistry of the A/B ring junction, similar observations have been made on the C-18 resonances of a series of C/D-*cis* polypregnanes. (52, 53)

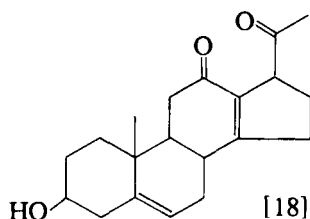
The stereochemical effects of one or more hydroxyl groups have been thoroughly investigated. (46, 47, 54) Mention of the expected effects has been made in the preceding section. There is not yet an example of an unknown steroid where the configuration of a hydroxyl group has been determined by ^{13}C NMR. However, one may expect that such an obvious application will be made soon.

The γ -effect is also evidenced by steroid epoxides. (55) Thus, the α -epoxide of 17β -acetoxy- 5α -androst-2-ene shows a 5.3 ppm shielding at C-5 compared with the β -epoxide. A variety of other epoxides have also been studied. When a methyl group is adjacent to the epoxy function rather unusual effects are noted due to deformations of the half chair conformations of the steroid ring bearing the epoxide. (56)

Letourneux *et al.* (57) have determined the ^{13}C chemical shifts for a series of (22*R*)- and (22*S*)-substituted cholesterol derivatives. The magnitudes of the β -effect are significantly different (2.7 ppm) for the

two series. Smaller differences are found at the γ -carbons. Configurational decisions at this position are important in studies of the biodegradation of the cholesterol side chain.

One final example of the utility of ^{13}C NMR data in the field of steroid chemistry is cited. Fukujusonorone [18] is the first 18-nor-steroid to be



isolated from a natural source. (58) The usual chromatographic techniques have led to the conclusion of a pure sample being present. The ^{13}C NMR spectrum shows a surprising doubling of the lines assignable to carbons about the 17-position. Subsequent deuterium exchange experiments have confirmed that the material isolated is a mixture of 17-epimers, thus demonstrating the superiority of ^{13}C NMR studies.

Acknowledgement

The data reported herein, as acquired in these laboratories, resulted from the generous support of the Robert A. Welch Foundation to whom thanks are expressed.

REFERENCES

1. J. W. Blunt and J. B. Stothers, *Org. Magn. Resonance*, 1977, **9**, 439.
2. H. J. Reich, M. Jautelat, M. T. Messe, F. J. Weigert and J. D. Roberts, *J. Amer. Chem. Soc.*, 1969, **91**, 7445.
3. F. W. Wehrli and T. Wirthlin, "Interpretation of Carbon-13 NMR Spectra", Heyden, London, 1976.
4. C. C. Hinkley, *J. Amer. Chem. Soc.*, 1969, **91**, 5160.
5. R. A. Sievers (ed.), "NMR Shift Reagents", Academic Press, New York, 1973.
6. O. Hofer, in "Topics in Stereochemistry", N. L. Allinger and E. L. Eliel (eds.), Wiley, New York, 1976.
7. J. Briggs, F. A. Hart, G. P. Moss and E. W. Randall, *J.C.S., Chem. Comm.*, 1971, 364.
8. M. Christl, H. J. Reich and J. D. Roberts, *J. Amer. Chem. Soc.*, 1971, **93**, 3463.
9. O. A. Gansow, M. R. Willcott and R. E. Lenkinski, *J. Amer. Chem. Soc.*, 1971, **93**, 4297.
10. E. Wenkert, D. W. Cochran, E. W. Hagaman, R. B. Lewis and F. M. Schell, *J. Amer. Chem. Soc.*, 1971, **93**, 6271.
11. W. B. Smith and D. L. Deavenport, *J. Magn. Resonance*, 1972, **6**, 256.
12. B. F. G. Johnson, J. Lewis, P. McArdle and J. R. Norton, *J.C.S., Chem. Comm.*, 1972, 535.

13. O. A. Gansow, P. A. Loeffler, M. R. Willcott and E. Lenkinski, *J. Amer. Chem. Soc.*, 1973, **95**, 3389.
14. M. R. Willcott, R. E. Lenkinski and R. E. Davis, *J. Amer. Chem. Soc.*, 1972, **94**, 1742.
15. W. B. Smith, D. L. Deavenport, J. A. Swanzy and G. A. Pate, *J. Magn. Resonance*, 1973, **12**, 15.
16. J. W. ApSimon, H. Beierbeck and J. K. Saunders, *Can. J. Chem.*, 1973, **51**, 3874.
17. D. J. Chadwick and D. H. Williams, *J.C.S., Perkin II*, 1974, 1903.
18. D. Leibfritz and J. D. Roberts, *J. Amer. Chem. Soc.*, 1973, **95**, 4996.
19. A. K. Bose and P. R. Srinivasan, *Tetrahedron Lett.*, 1975, 1571.
20. A. Fratiello and C. S. Stover, *J. Org. Chem.*, 1975, **40**, 1244.
21. A. R. Butler, *J.C.S., Perkin II*, 1976, 959.
22. W. B. Smith and T. W. Proulx, *J. Chem. Ed.*, 1976, **53**, 700.
23. G. C. Levy and G. L. Nelson, "13C NMR for Organic Chemists", Wiley, New York, 1972.
24. D. Shaw, "Fourier Transform NMR Spectroscopy", Elsevier, Amsterdam, 1976.
25. T. C. Farrar and E. D. Becker, "Pulse and Fourier Transform NMR", Academic Press, New York, 1971.
26. J. R. Lyerla and G. C. Levy, in "Topics in 13C NMR Spectroscopy", G. C. Levy (ed.), 1974, **1**, 79.
27. F. W. Wehrli, in "Topics in 13C NMR Spectroscopy", G. C. Levy (ed.), 1972, **2**.
28. F. W. Wehrli, *Advances in Mol. Relax. Processes*, 1974, **6**, 139.
29. G. C. Levy and I. R. Peat, *J. Magn. Resonance*, 1975, **18**, 500.
30. E. Breitmaier, K. H. Spohn and S. Berger, *Angew. Chem. Internat. Edition*, 1975, **14**, 144.
31. A. Allerhand, D. Doddrell and R. A. Komaraski, *J. Chem. Phys.*, 1971, **55**, 189.
32. J. W. ApSimon, H. Beierbeck and J. K. Saunders, *Can. J. Chem.*, 1975, **53**, 338.
33. G. C. Levy and U. Edlund, *J. Amer. Chem. Soc.*, 1975, **97**, 5031.
34. G. C. Levy, J. D. Cargioli and F. A. L. Anet, *J. Amer. Chem. Soc.*, 1973, **95**, 1528.
35. N. Bloembergen, E. M. Purcell and R. V. Pound, *Phys. Rev.*, 1948, **73**, 679.
36. W. B. Smith, *J. Phys. Chem.*, in the press.
37. B. Sears, R. J. Deckelbaum, M. J. Janiak, G. C. Shiple and D. M. Small, *Biochemistry*, 1976, **15**, 415.
38. G. E. Maciel, in "Topics in 13C NMR Spectroscopy", G. C. Levy (ed.), 1974, **1**, 53.
39. D. M. Grant and B. V. Cheney, *J. Amer. Chem. Soc.*, 1967, **89**, 5315.
40. D. K. Dalling and D. M. Grant, *J. Amer. Chem. Soc.*, 1967, **89**, 6612.
41. K. Seidman and G. E. Maciel, *J. Amer. Chem. Soc.*, 1977, **99**, 659.
42. D. G. Gorenstein, *J. Amer. Chem. Soc.*, 1977, **99**, 2254.
43. W. L. Daux, C. M. Weeks, and D. C. Rohrer, in "Topics in Stereochemistry", N. L. Allinger and E. L. Eliel (eds.), 1976, **9**, 271.
44. E. L. Eliel, W. F. Bailey, L. D. Kopp, R. L. Willer, D. M. Grant, R. Bertrand, K. A. Christensen, D. K. Dalling, M. W. Duch, E. Wenkert, F. M. Schell and D. W. Cochran, *J. Amer. Chem. Soc.*, 1975, **97**, 322.
45. W. A. Ayer, L. M. Browne, S. Fung and J. B. Stothers, *Org. Magn. Resonance*, in the press.
46. J. W. Blunt, *Aust. J. Chem.*, 1975, **28**, 1017.
47. C. L. Van Antwerp, H. Eggert, G. D. Meakins, J. O. Miners and C. Djerassi, *J. Org. Chem.*, 1977, **42**, 789.
48. R. N. Jones, D. A. Ramsey, F. Herling and K. Dobriner, *J. Amer. Chem. Soc.*, 1952, **74**, 2828.
49. E. Wenkert, A. O. Clouse, D. W. Cochran and D. Doddrell, *J.C.S., Chem. Comm.*, 1969, 1433.
50. J. B. Stothers, "13C NMR Spectroscopy", Academic Press, New York, 1972, p. 288.

51. J. L. Gough, J. P. Guthrie and J. B. Stothers, *J.C.S., Chem. Comm.*, 1972, 979.
52. T. Yamagishi, K. Hayashi, H. Mitsuhashi, M. Imanari and K. Matsushita, *Tetrahedron Lett.*, 1973, 3527.
53. T. Yamagishi, K. Hayashi, H. Mitsuhashi, M. Imanari and K. Matsushita, *Tetrahedron Lett.*, 1973, 3531.
54. H. Eggert, C. L. Van Antwerp, N. S. Bhacca and C. Djerassi, *J. Org. Chem.*, 1976, **41**, 71.
55. K. Tori, T. Komeno, M. Sangare, B. Septe, B. Delpach, A. Ahand and G. Lukacs, *Tetrahedron Lett.*, 1974, 1157.
56. M. Sangare, B. Septe, G. Belanger, G. Lukacs, K. Tori and T. Komeno, *Tetrahedron Lett.*, 1977, 699.
57. Y. Letourneux, H. Q. Khuong, M. Gut and G. Lukacs, *J. Org. Chem.*, 1975, **40**, 1674.
58. P. H. Solomon, K. Nakanishi, W. E. Fallon and Y. Shimizey, *Chem. Pharm. Bull.* (Tokyo), 1974, **22**, 1971.
59. C. Konno and H. Hikino, *Tetrahedron*, 1976, **32**, 325.
60. H. J. Schneider, W. Gschwendtner and U. Buchheit, *J. Magn. Resonance*, 1977, **26**, 175.
61. K. Tori, S. Seo, Y. Yoshimura, H. Arita and Y. Tomita, *Tetrahedron Lett.*, 1977, 179.
62. G. Lukacs, A. Picot, X. Lusinch, H. J. Kock and A. S. Perlin, *C.R. Acad. Sci. Ser. C*, 1971, **272**, 2171.
63. B. Balogh, D. M. Wilson and A. L. Burlingame, *Nature*, 1971, **233**, 261.
64. G. Lukacs, X. Lusinch, E. W. Hagman, B. L. Buckwalter, F. M. Schell and E. Wenkert, *C.R. Acad. Sci. Ser. C*, 1972, **274**, 1458.
65. J. B. Grutzner, *Lloydia*, 1972, **35**, 375.
66. H. Q. Khuong, G. Lukacs, A. Pancrazi and R. Goutarel, *Tetrahedron Lett.*, 1972, 3579.
67. O. Suzuki, *Yukagaku*, 1972, **21**, 199.
68. N. S. Bhacca, D. D. Giannini, W. S. Jankowski and M. E. Wolff, *J. Amer. Chem. Soc.*, 1973, **95**, 8421.
69. T. A. Wittstruck and I. H. K. Williams, *J. Org. Chem.*, 1973, **38**, 1542.
70. H. Eggert and C. Djerassi, *J. Org. Chem.*, 1973, **38**, 3788.
71. S. A. Knight, *Tetrahedron Lett.*, 1973, 83.
72. K. Toni, H. Ishii, Z. W. Wolkowski and C. Chachaty, *Tetrahedron Lett.*, 1973, 1077.
73. S. H. Grover and J. B. Stothers, *Can. J. Chem.*, 1974, **52**, 870.
74. D. L. Deavenport, *Diss. Abst. Int. B*, 1974, **35**, 2096.
75. A. K. Bose and J. J. Savarese, *Experientia*, 1974, **30**, 1489.
76. W. Stoffel, B. D. Tunggal, O. Zierenbers, E. Schreibers and E. Binczek, *Z. Physiol. Chem.*, 1974, **355**, 1367.
77. D. D. Giannini, P. A. Kollman, N. S. Bhacca and M. E. Wolff, *J. Amer. Chem. Soc.*, 1974, **96**, 5462.
78. G. Engelhardt, G. Schneider, I. Weisz-Vincze and A. Vass, *J. Prakt. Chem.*, 1974, **316**, 391.
79. H. Repmann, *Z. Naturforschung*, 1974, **29a**, 1172.
80. W. Stoffel and K. Bister, *Biochemistry*, 1975, **14**, 2841.
81. H. Beierbeck and J. K. Saunders, *Can. J. Chem.*, 1976, **54**, 2985.
82. H. Hikino, T. Okuyama, C. Koro and T. Takemoto, *Chem. Pharm. Bull.* (Tokyo), 1975, **23**, 125.
83. J. R. Hanson and M. Sivers, *J.C.S., Perkin I*, 1975, 1110.
84. J. R. Hanson and M. Sivers, *J.C.S., Perkin I*, 1975, 1956.
85. S. Lang, D. N. Lincoln and V. Wray, *J.C.S., Perkin II*, 1975, 344.
86. R. J. Abraham and J. R. Monasterios, *J.C.S., Perkin II*, 1975, 662.
87. P. Genard, M. Palem-Vliers, J. Dendel, H. Van Cauwenberge and W. Eechuate, *J. Steroid Biochem.*, 1975, **6**, 201.

88. V. Wray and S. Lang, *Tetrahedron*, 1975, **31**, 2815.
89. K. Tori, T. Komeno, J. M. Takam and G. Lukacs, *Tetrahedron Lett.*, 1975, 135.
90. H. Eggert and C. Djerassi, *Tetrahedron Lett.*, 1975, 3635.
91. G. Engelhardt, D. Zeigan, B. Schoenecker and K. Parsold, *Z. Chem.*, 1975, **15**, 60.
92. S. Tanaka, S. Toda, C. Nagata, K. Kanohta, S. Hashimoto, I. Nagoya, K. Musha and K. Yamaguchi, *Bunseki Kagaku*, 1976, **25**, 206.
93. W. A. Ayer, L. M. Browne, S. Fung and J. B. Stothers, *Can. J. Chem.*, 1976, **54**, 3272.
94. D. J. Kim, L. D. Colebrook and T. J. Adley, *Can. J. Chem.*, 1976, **54**, 3766.
95. D. Satoh and T. Hashimoto, *Chem. Pharm. Bull.* (Tokyo), 1976, **24**, 1950.
96. A. R. Butler and H. A. Jones, *J.C.S., Perkin II*, 1976, 963.
97. M. J. Gasic, Z. Djarmati and S. W. Pelletier, *J. Org. Chem.*, 1976, **41**, 1219.
98. R. J. Cushley and J. D. Filipenko, *Org. Magn. Resonance*, 1976, **8**, 308.
99. G. Engelhardt, H. Jancke and D. Zeigan, *Org. Magn. Resonance*, 1976, **8**, 655.
100. R. Radeaglia, G. Adam and H. Ripperger, *Tetrahedron Lett.*, 1977, 903.
101. H. Ishii, S. Seo, K. Tori, T. Tozyo and Y. Yoshimura, *Tetrahedron Lett.*, 1977, 1227.
102. W. B. Smith, *Org. Magn. Resonance*, 1977, **9**, 644.

Problems in Theory and Analysis of Dynamic Nuclear Magnetic Resonance Spectra

S. SZYMAŃSKI AND M. WITANOWSKI

Institute of Organic Chemistry, Polish Academy of Sciences, Warsaw, Poland

AND

A. GRYFF-KELLER

*Institute of Organic Chemistry and Technology, Polytechnical University, Warsaw,
Poland*

1. Introduction	228
II. Some fundamental concepts in lineshape theory	229
A. Density matrices and observables	230
B. Density matrix of a subsystem	231
C. Spin density matrix of a spin system at thermal equilibrium with a lattice	231
D. Superoperator formalism in the theory of NMR spectra	232
E. Equation of motion for a spin density matrix	235
1. Equation of motion in the laboratory frame	235
2. Factorization of the equation of motion	236
F. Lineshape of an unsaturated steady-state spectrum	237
III. Theory of NMR lineshapes for exchanging spin systems	238
A. Kinetics of a system at equilibrium	239
B. Equation of motion for a spin system in dynamic equilibrium	241
C. Evaluation of a spin density matrix after exchange	244
1. Reaction mechanisms	244
2. Basis function sets for reactions	247
3. Permutation operator	247
4. Density matrix of molecular fragments	249
5. Exchange superoperator	249
D. Equation of motion in the linear approximation	251
E. Exchange superoperators in the linear approximation	252
F. Properties of the exchange superoperator in composite Liouville space	254
G. Renormalization of the composite Liouville space	257
H. Lineshape equation for an exchanging system	258

IV. Computation and analysis of dynamic NMR spectra	259
A. Simulation of dynamic NMR spectra	259
1. Introductory remarks	259
2. Point by point methods	260
3. Diagonalization method	262
4. Conclusions	263
B. Analysis of dynamic NMR spectra	263
1. Unsophisticated methods	263
2. The least-squares method	264
V. Some practical problems	267
A. Selecting a model for exchange	268
1. Neglecting some spin-spin couplings	268
2. Multiplet components treated as signals from different nuclei	269
3. Weak coupling approximation	270
4. Single-nucleus representation of a group	271
B. Initial estimates of rates of exchange	272
C. Natural line-width	273
D. Chemical shifts and spin-spin couplings in dynamic NMR spectra	276
E. Parameters for a dynamic equilibrium	278
F. Intensity coefficient and base-line position	280
G. Significance of the results of a dynamic lineshape analysis	281
Appendix A. Composite indices. Some properties of direct (Kronecker) products	284
Appendix B. Differential form of the equation of motion	286
References	287

I. INTRODUCTION

In this article we consider problems concerning the interpretation of unsaturated, steady-state NMR spectra of spin systems which are in a state of dynamic equilibrium. Spin exchange processes may occur with frequencies between a few sec^{-1} and several thousand sec^{-1} and thus modify the spectral lineshapes. In this case we use the terms dynamic NMR and dynamic spectra. The analysis of dynamic NMR lineshapes constitutes an important, and often unique, source of information about intra- and inter-molecular reaction rates. This is especially true for degenerate reactions where the products are chemically identical with the substrates. For this and similar reasons, dynamic NMR analysis has attracted considerable attention for about twenty years.

In the first stage of its development, up to about 1965, reaction rate determinations by means of dynamic NMR were rather semi-quantitative. Increased precision in the results became possible only after the elimination of numerous systematic errors by improved experimental techniques. Equally important is a development in the theory of the lineshapes of dynamic NMR spectra and its presentation in a form suitable for practical applications in spectral analysis. Advances

in computer techniques, and their widespread applications, have enabled investigators to avoid the fallacies of crude approximations in the analysis of dynamic spectra, thus allowing them to shift towards engaging the entire available theory for extracting spectral information about the kinetic and thermodynamic parameters of reactions from the total lineshapes of dynamic spectra.

The history of the developments in dynamic NMR has been presented in an interesting article by Gutowsky in a monograph devoted to the subject. (1, 2) The latter contains articles concerning various other problems in the theory and practice of dynamic NMR, and presents a review of results obtained by dynamic NMR methods. It is certainly a valuable reference book for all potential users of these methods. Recently, a few reviews on dynamic NMR have also been published. (3–5) In the present article we refrain from presenting another review of the pertinent literature; instead we use a more synthetic and general approach together with the inclusion of some of our own ideas in the field.

After a discussion of the fundamental concepts in Section II, we present, in Section III, an approach to the lineshape theory of dynamic NMR spectra which comprises the most general case, namely that of a multi-component system where various intra- and inter-molecular exchange processes take place. We believe that a fully correct NMR theory of such an equilibrium has not been put forward yet. Section IV is concerned with the methods of simulation and analysis of complicated dynamic spectra. In Section V, we present our views on solving the numerous practical problems which usually appear upon the application of the theory to the analysis of dynamic spectra.

II. SOME FUNDAMENTAL CONCEPTS IN LINESHAPE THEORY

We shall shortly consider such fundamental concepts as density matrices and the superoperator formalism which are convenient to use in a formulation of the lineshape theory of NMR spectra. The general equation of motion for the density matrix of a non-exchanging spin system is formulated in the laboratory (non-rotating) reference frame. The lineshape of a steady-state, unsaturated spectrum is given as the Fourier transform of the free induction decay after a strong radio-frequency pulse. The equations provide a starting point for the formulation of the theory of dynamic NMR spectra presented in Section III. The reader who may be interested in a more detailed consideration of the problems is referred to the fundamental works of Abragam and

Slichter as well as to the articles by Lynden-Bell, Hoffman, and Nageswara Rao. (6–10)

A. Density matrices and observables

An isolated microscopic system is fully determined, in the quantum mechanical sense, when its state function ψ is known. In the Dirac formalism of quantum mechanics, the state function can be identified with a vector of state, $|\psi\rangle$. (11) The system in the $|\psi\rangle$ state may equivalently be described by a Hermitian operator, the so-called density matrix $\hat{\rho}$ of a pure state,

$$\hat{\rho} = |\psi\rangle \langle\psi| \quad (1)$$

where the vector $\langle\psi|$ (the “bra”) is the Hermitian adjoint of the vector $|\psi\rangle$ (the “ket”). If the vectors $|\phi_i\rangle$, $i = 1, 2, \dots$, constitute a basis set for the space of the states, the $|\psi\rangle$ state is a superposition of the states of the basis set:

$$|\psi\rangle = \sum c_i |\phi_i\rangle \quad (2)$$

The corresponding bra is given by the expression:

$$\langle\psi| = \sum c_i^* \langle\phi_i| \quad (3)$$

where the asterisk denotes the complex conjugate of c_i . The density matrix has the following representation within the basis set:

$$\hat{\rho}_{ij} = c_i c_j^* \quad (4)$$

Every macroscopic sample on which measurements are made is an aggregate of microscopic systems whose states are, in principle, unknown. A theoretical model can only provide the density of probabilities of individual states in the sample. In order to describe such a macroscopic sample, we use the density matrix which is defined as the weighted average over an ensemble of possible pure states:

$$\bar{\rho} = \overline{|\psi\rangle \langle\psi|} \quad (5)$$

where the horizontal line denotes the corresponding statistical averaging. The matrix thus defined describes a mixed state. The density matrix of a mixed state is also a Hermitian operator, like that for a pure state. The two types of matrices have unit traces in the orthonormal basis. Pure and mixed states are differentiated by the corresponding squares of the density matrices:

$$\hat{\rho}^2 = \hat{\rho} \quad (6)$$

$$\text{Tr}(\bar{\rho}^2) < 1 \quad (7)$$

The horizontal line is deleted in our further considerations; this should not lead to any confusion.

The expectation value of an observable \hat{A} is given by the expression,

$$\langle \hat{A} \rangle = \text{Tr}(\hat{A}\hat{\rho}) \quad (8)$$

where Tr denotes the trace of the matrix involved. For a pure state, equation (8) is equivalent to the well-known formula for the expectation value:

$$\langle \hat{A} \rangle = \langle \psi | \hat{A} | \psi \rangle \quad (9)$$

B. Density matrix of a subsystem

The density matrix of a mixed state can be constructed even for a system which has no quantum mechanical states since it is not isolated and constitutes only a subsystem of a larger system. For example, the spin system of a molecule in a liquid is not isolated owing to the presence of interactions between the degrees of freedom of the spins and other, mostly rotational, degrees of freedom which are usually called the lattice. The state of the entire system may be represented by the basis set which is formed from the direct product of the basis sets of its subsystems:

$$|\theta_{i\alpha}\rangle = |\Phi_i\rangle \otimes |\chi_\alpha\rangle \quad (10)$$

where Φ_i , $i = 1, 2, \dots, N$, is the basis function set of the spin space, and χ_α , $\alpha = 1, 2, \dots$, is that for the space of angular momentum. The density matrix $\hat{\rho}$ of a spin system can be obtained by the contraction of the matrix of the entire system:

$$\hat{\rho} = \text{Tr}_{\text{lattice}}(\hat{\rho}_{\text{spin} + \text{lattice}}) \quad (11)$$

Within the basis set defined by equation (10), the operation of matrix contraction takes the form:

$$\hat{\rho}_{ij} = \sum_{\alpha} (\hat{\rho}_{\text{spin} + \text{lattice}})_{i\alpha, j\alpha} \quad (12)$$

C. Spin density matrix of a spin system at thermal equilibrium with a lattice

A spin system placed in a constant homogeneous magnetic field B_0 finally attains thermal equilibrium with the lattice. This relaxation is induced by fluctuations of local magnetic fields which result from molecular motions. At equilibrium, the spin system is described by the equilibrium density matrix $\hat{\rho}_0$:

$$\hat{\rho}_0 = \exp(-\hbar\hat{H}_s/kT) / \text{Tr}[\exp(-\hbar\hat{H}_s/kT)] \quad (13)$$

where \hat{H}_s is the Hamiltonian of the spin system characterized by chemical shifts $\delta_i \times 10^6$ (ppm) and spin-spin coupling constants J_{ij} (Hz):

$$\hat{H}_s = - \sum \omega_{0_i}(1 - \delta_i)\hat{I}_{z_i} + 2\pi \sum_{i>j} J_{ij} \hat{I}_i \hat{I}_j \quad (14)$$

In equation (14), $\omega_{0_i} = \gamma_i B_0$, where γ_i is the magnetogyric ratio of nucleus i , and \hat{I}_i denotes the vector operator of the spin of nucleus i ; the z -axis is taken to be parallel to B_0 . We shall express Hamiltonian operators in frequencies.

At temperatures which are not too low, i.e. when $\hbar\omega_0 \ll kT$, the exponential function in equation (13) may be approximated as:

$$\hat{\rho}_0 = (\hat{E} - \hbar\hat{H}_s/kT)/\text{Tr}(\hat{E} - \hbar\hat{H}_s/kT) \quad (15)$$

where \hat{E} is the unit operator. For homonuclear systems at commonly used magnetic fields B_0 , corresponding to $\omega_0/2\pi \geq 40$ MHz for protons, the $\hat{\rho}_0$ matrix may be simplified further. This is due to the fact that chemical shifts are usually of the order of 10^{-5} , and coupling constants are not larger than a few hundred Hz:

$$\hat{\rho}_0 = [\hat{E} + (\hbar\omega_0/kT)\hat{F}_z]/\text{Tr}(\hat{E}) \quad (16)$$

where \hat{F}_z is the z component of the total spin of the system, $\hat{F} = \sum \hat{I}_i$.

D. Superoperator formalism in the theory of NMR spectra

Before writing an equation for the motion of a spin system, we introduce a convenient notation system, the so-called superoperator formalism. It was used for the first time in a description of NMR phenomena by Banwell and Primas, and later developed by Binsch. (12–15)

In a set of all linear operators which operate on the space of states (Hilbert space), we define the following scalar product:

$$(\hat{A}, \hat{B}) = \text{Tr}(\hat{A}\hat{B}^\dagger) \quad (17)$$

where the dagger (\dagger) denotes the Hermitian adjoint of the operator. Let us consider the set of all the N^2 projection operators $|\Phi_i\rangle\langle\Phi_j|$, constructed from the vectors of the orthonormal basis of product spin functions $|\Phi_i\rangle$, $i = 1, 2, \dots, N$. Such operators form the basis of a new space, called the Liouville space, where the operators from the Hilbert space may be considered as vectors. The basis is orthonormal as far as the scalar product in equation (17) is concerned:

$$\begin{aligned} (\mathbf{v}_{ij}, \mathbf{v}_{mn}) &= (|\Phi_i\rangle\langle\Phi_j|, |\Phi_m\rangle\langle\Phi_n|) \\ &= \text{Tr}(|\Phi_i\rangle\langle\Phi_j| |\Phi_m\rangle\langle\Phi_n|) \\ &= \delta_{jn} \delta_{im} \end{aligned} \quad (18)$$

where the vector \mathbf{v}_{ij} in Liouville space corresponds to the operator $|\Phi_i\rangle\langle\Phi_j|$. Vectors in Liouville space are denoted by small Latin or Greek letters in boldface. An operator \hat{A} , with the representation \hat{A}_{ij} in the basis set of the $|\Phi_i\rangle$ vectors, corresponds to the vector \mathbf{a} in the Liouville space with doubly-subscripted coordinates \hat{A}_{ij} within the basis set of \mathbf{v}_{ij} :

$$\mathbf{a} = \sum_{i,j} \hat{A}_{ij} \mathbf{v}_{ij} \quad (19)$$

It follows that:

$$\begin{aligned} (\mathbf{a}, \mathbf{v}_{ij}) &= \text{Tr}(\hat{A} |\Phi_j\rangle\langle\Phi_i|) \\ &= \sum_k \langle\Phi_k| \hat{A} |\Phi_j\rangle \langle\Phi_i|\Phi_k\rangle \\ &= \hat{A}_{ij} \end{aligned} \quad (20)$$

The scalar product of two vectors, $\mathbf{a} = \sum \hat{A}_{ij} \mathbf{v}_{ij}$ and $\mathbf{b} = \sum \hat{B}_{ij} \mathbf{v}_{ij}$, is calculated in this basis set as:

$$(\mathbf{a}, \mathbf{b}) = \sum_{i,j} \hat{A}_{ij} \hat{B}_{ij}^* \quad (21)$$

The product is also denoted by the symbol:

$$(\mathbf{a}, \mathbf{b}) \equiv \mathbf{b}^\dagger \mathbf{a} \quad (22)$$

by considering \mathbf{a} , \mathbf{b} as column vectors, and \mathbf{a}^\dagger , \mathbf{b}^\dagger as row vectors. The double dagger (\dagger) denotes, with respect to the Liouville space, the Hermitian adjoint of the vector concerned. In this notation, equation (8) for the expectation value of an observable \hat{A} takes the form:

$$\langle \hat{A} \rangle = (\mathbf{a}^\dagger)^\dagger \mathbf{p} \quad (23)$$

where \mathbf{a}^\dagger is the column vector which corresponds to the operator \hat{A}^\dagger . Notice that the density matrix becomes a vector in the Liouville space and as such is denoted by \mathbf{p} rather than $\hat{\rho}$.

The differentiation between Hilbert space and Liouville space, used throughout the literature and in the present article, has only a physical sense. Mathematically, both of them are Hilbert spaces.

Every linear transformation of a set of linear operators onto the same set (e.g. premultiplication or postmultiplication of the operators by a given operator) may be represented in Liouville space as a matrix (a superoperator). We shall calculate, for example, the representation of the commutator $[\hat{A}, \]$, the so-called derivation superoperator, and its components, the superoperators of pre- and post-multiplication, $\hat{A} \cdot$ and $\cdot \hat{A}$, respectively. The latter are known as the left-translation, \mathbf{A}^L , and right-translation, \mathbf{A}^R , superoperators.

Superoperators in Liouville space are denoted by capital Latin or Greek letters, in boldface. The representation of the derivation superoperator \mathbf{A}^D within the basis set of \mathbf{v}_{ij} vectors is given by:

$$\begin{aligned}
 \mathbf{A}_{ij,mn}^D &= \mathbf{v}_{ij}^\dagger \mathbf{A}^D \mathbf{v}_{mn} \\
 &= (\hat{A} |\Phi_m\rangle \langle \Phi_n| - |\Phi_m\rangle \langle \Phi_n| \hat{A}, |\Phi_i\rangle \langle \Phi_j|) \\
 &= \mathbf{A}_{ij,mn}^L - \mathbf{A}_{ij,mn}^R \\
 &= \text{Tr}(\hat{A} |\Phi_m\rangle \langle \Phi_n| \Phi_j) \langle \Phi_i| - \text{Tr}(|\Phi_m\rangle \langle \Phi_n| \hat{A} |\Phi_j) \langle \Phi_i|) \\
 &= \delta_{nj} \hat{A}_{im} - \delta_{mi} \hat{A}_{nj}
 \end{aligned} \tag{24}$$

It is evident that if the operator \hat{A} is Hermitian, then the superoperators \mathbf{A}^D , \mathbf{A}^L , and \mathbf{A}^R are also Hermitian.

Let $\{|\Phi_i\rangle\}$ be an orthonormal basis in Hilbert space such that:

$$|\psi_i\rangle = \sum_k \hat{U}_{ik} |\Phi_k\rangle \tag{25}$$

The transformation \hat{U} is unitary:

$$\hat{U}^\dagger = \hat{U}^{-1} \tag{26}$$

The corresponding unitary supertransformation \mathbf{U} transforms the basis set $\{\mathbf{v}_{ij}\}$ into $\{\mathbf{w}_{ij}\}$, where \mathbf{w}_{ij} corresponds to $|\psi_i\rangle \langle \psi_j|$:

$$\mathbf{w}_{ij} = \sum_{k,n} \mathbf{U}_{ij,kn} \mathbf{v}_{kn} \tag{27}$$

$$\mathbf{U}_{ij,kn} = \hat{U}_{ik} \hat{U}_{jn}^* \tag{28}$$

The representation of the superoperators considered may be expressed in terms of the direct products of the representations of the appropriate operators:

$$\mathbf{A}^D = \hat{A} \otimes \hat{E} - \hat{E} \otimes \hat{A} \tag{29}$$

$$\mathbf{A}^L = \hat{A} \otimes \hat{E} \tag{30}$$

$$\mathbf{A}^R = \hat{E} \otimes \hat{A}^* \tag{31}$$

$$\mathbf{U} = \hat{U} \otimes \hat{U}^* \tag{32}$$

where \hat{A} is a Hermitian operator, the asterisk denotes the corresponding complex conjugate. The direct product of the matrices \mathbf{M} and \mathbf{N} is defined as:

$$(\mathbf{M} \otimes \mathbf{N})_{ij,mn} = M_{im} N_{jn} \tag{33}$$

Some properties of direct multiplication (called also Kronecker or tensor multiplication) are given in Appendix A.

E. Equation of motion for a spin density matrix

1. Equation of motion in the laboratory frame

In an NMR experiment, the energy of the lattice is practically constant (the lattice has a large heat capacity). It is therefore assumed that the lattice is always in a state of thermodynamic equilibrium. Thus, it is possible to use a semi-classical description of its interactions with the spin system. Within this approach, the Liouville–von Neumann equation of motion for a spin system is given by:

$$d\hat{\rho}/dt = -i[\hat{H}_s + \hat{H}_I(t) + \hat{H}_{sl}(t), \hat{\rho}] \quad (34)$$

where $\hat{H}_I(t)$ denotes the Hamiltonian describing interactions of the spin system with external radio-frequency fields, and $\hat{H}_{sl}(t)$ is the Hamiltonian describing interactions between the spin system and the lattice (it is randomly varying with time). Equation (34) provides a starting point for the production of a formulation of the equation of motion for the ensemble-averaged density matrix of a spin system. (9, 16–20) It is known as the Wangness–Bloch–Redfield (WBR) master equation. It contains a relaxation term which may be represented in the superoperator formalism by a Hermitian matrix \mathbf{R} , called the relaxation matrix. The latter acts on the vector which represents a measure of the deviation of the spin system from thermal equilibrium with the lattice. The WBR equation is usually formulated in the rotating frame. Its conversion to the laboratory frame assumes the form:

$$d\mathbf{\rho}/dt = -i\mathbf{H}^D\mathbf{\rho} + \mathbf{R}(\mathbf{\rho} - \mathbf{\rho}_0) \quad (35)$$

In pulse-type NMR experiments, the super-Hamiltonian \mathbf{H}^D constitutes a superoperator representation of the commutator with the spin Hamiltonian \hat{H}_s which is defined by equation (14):

$$\mathbf{H}_s^D\mathbf{\rho} \equiv [\hat{H}_s, \hat{\rho}] \quad (36)$$

In continuous-wave experiments (single resonance), the super-Hamiltonian \mathbf{H}^D includes an additional component which represents interactions with the radio-frequency magnetic field B_1 rotating in the same direction as the Larmor precession: (21)

$$\mathbf{H}^D = \mathbf{H}_s^D - \gamma B_1(\mathbf{F}_x^D \cos \omega t - \mathbf{F}_y^D \sin \omega t) \quad (37)$$

where \mathbf{F}_u^D ($u = x, y$) is the representation of the commutator:

$$\mathbf{F}_u^D\mathbf{\rho} \equiv [\hat{F}_u, \rho] \quad (38)$$

The components of the relaxation matrix in the basis set adopted are real numbers. They may be computed from the correlation functions of the molecular rotations or, more precisely, from their Fourier transforms.

In our further considerations we assume that the components of the relaxation matrix are known in advance. This is a realistic assumption provided that unsaturated NMR spectra are being dealt with. One should note that equation (35) can be used for the description of motion of the system during time spans which are much longer than the typical correlation times for molecular rotation in liquids (about 10^{-11} – 10^{-12} sec). The processes of intra- and inter-molecular exchange which are considered here are characterized by half-life times longer than 10^{-5} sec. It seems justified to consider these processes independently of molecular rotations, in spite of the fact that they all participate in the relaxation.

2. Factorization of the equation of motion

The matrices in equation (35) for a system of n spins of $1/2$ have dimensions of 2^{2n} . This means that, for example, a four-spin system must be considered within a space of 256 dimensions. If we deal with the motion of a spin system in a static magnetic field (as in pulse-type experiments), significant simplifications are possible owing to the rules of commutation. Namely, if the Hermitian operators \hat{A} and \hat{B} commute in Hilbert space, then all the corresponding superoperators \mathbf{A}^L , \mathbf{A}^R , \mathbf{A}^D , \mathbf{B}^L , \mathbf{B}^R , and \mathbf{B}^D in Liouville space also commute. The proof of this is given in reference (12). In Hilbert space, the following commutation takes place:

$$[\hat{H}_s, \hat{F}_z] = 0 \quad (39)$$

Hence, in Liouville space, the energy superoperator \mathbf{H}_s^D commutes with all the mutually commuting superoperators \mathbf{F}_z^L , \mathbf{F}_z^R , and \mathbf{F}_z^D :

$$[\mathbf{H}_s^D, \mathbf{F}_z^Q] = 0 \quad (40)$$

where $Q = L, R, D$, and the \mathbf{F}_z^Q superoperators are defined by equation (24). The relaxation superoperator \mathbf{R} commutes also with \mathbf{F}_z^D : (22)

$$[\mathbf{R}, \mathbf{F}_z^D] = 0 \quad (41)$$

The \mathbf{v}_{ij} vectors are the eigenvectors of the superoperators \mathbf{F}_z^D , \mathbf{F}_z^R , and \mathbf{F}_z^L . We demonstrate this for the \mathbf{F}_z^D superoperator:

$$\begin{aligned} \mathbf{F}_z^D \mathbf{v}_{ij} &\equiv [\hat{F}_z, |\Phi_i\rangle \langle \Phi_j|] = F_{z_i} |\Phi_i\rangle \langle \Phi_j| - F_{z_j} |\Phi_i\rangle \langle \Phi_j| \\ &\equiv (F_{z_i} - F_{z_j}) \mathbf{v}_{ij} = F_{z_0}^D \mathbf{v}_{ij} \end{aligned} \quad (42)$$

where F_{z_i} is an eigenvalue of the \hat{F}_z operator, namely that associated with the eigenfunction Φ_i , and $F_{z_0}^D$ is an analogous eigenvalue of \mathbf{F}_z^D associated with the vector \mathbf{v}_{ij} . Arranging the \mathbf{v}_{ij} vectors according to the eigenvalues $F_{z_0}^D$ results in a factorization of the matrices \mathbf{H}_s^D and \mathbf{R} into blocks of dimensions equal to the degeneracies of the eigenvalues.

In the absence of a radio-frequency magnetic field B_1 , the density matrix components concerned with an eigenvalue $F_{z_0}^D (=k)$ change with time according to:

$$d\rho_{(k)}/dt = -iH_{s(k)}^D \rho_{(k)} + \mathbf{R}_{(k)}(\rho_{(k)} - \rho_{0(k)}) \quad (43)$$

where, for n spins of $1/2$, $k = -n, -n + 1, \dots, n - 1, n$; the index (k) denotes blocks. The matrix $\mathbf{R}_{(0)}$ is analogous to the relaxation rate, $1/T_1$, in the classical approach, whilst the $\mathbf{R}_{(+1)}$ and $\mathbf{R}_{(-1)}$ matrices correspond to $1/T_2$. It has been shown that, in an eigenbasis $\{\mathbf{v}_{ij}\}$ of the superoperators F_z^L , F_z^R , and F_z^D , the relaxation matrix has the properties: (9)

$$\mathbf{R}_{jk, lm} = \mathbf{R}_{kj, ml}^* = \mathbf{R}_{lm, jk}^* = \mathbf{R}_{ml, kj} \quad (44)$$

Any derivation superoperator \mathbf{A}^D which is constructed of a Hermitian operator $\hat{\mathbf{A}}$ obeys the relation:

$$\mathbf{A}_{jk, lm}^D = (\mathbf{A}_{lm, jk}^D)^* = -(\mathbf{A}_{kj, ml}^D)^* = -\mathbf{A}_{ml, jk}^D \quad (45)$$

which follows from equation (24). Within the basis set of the \mathbf{v}_{ij} vectors, the asterisks may be deleted. The relations from equations (44) and (45) express the conservation of Hermitian character by the operator ρ in equation (35). Thus, the expectation value of any Hermitian operator $\hat{\mathbf{B}}$ is given by the expression [see also equation (23)]:

$$\begin{aligned} \langle \hat{\mathbf{B}} \rangle &= \mathbf{b}^\dagger \rho \\ &= \mathbf{b}_{(0)}^\dagger \rho_{(0)} + \sum_{k=-n}^{-1} (\mathbf{b}_{(k)}^\dagger \rho_{(k)} + q_k) \end{aligned} \quad (46)$$

where $q_k = (\mathbf{b}_{(k)}^\dagger \rho_{(k)})^*$.

F. Lineshape of an unsaturated steady-state spectrum

If a spin system in thermal equilibrium with the lattice (i.e. that described by the vector ρ_0) is subjected, immediately prior to the moment $t = 0$, to a strong radio-frequency pulse, then, after the pulse ceases, the vector corresponding to the density matrix of the system becomes: (23, 99)

$$\rho_{(0)} = (\mathbf{e}^\dagger \mathbf{e})^{-1} [\mathbf{e} + (\hbar\omega_0/kT)(\mathbf{f}_x \sin \alpha + \mathbf{f}_z \cos \alpha)] \quad (47)$$

where \mathbf{e} , \mathbf{f}_x , and \mathbf{f}_z are vectors which correspond to the $\hat{\mathbf{E}}$, $\hat{\mathbf{F}}_x$, and $\hat{\mathbf{F}}_z$ operators, respectively; α is a measure of the pulse intensity (the "flip angle"), and the scalar product $\mathbf{e}^\dagger \mathbf{e}$ equals $\text{Tr } \hat{\mathbf{E}}$. The recovery of the system towards equilibrium in a static magnetic field is revealed as a train of decaying oscillations of the magnetic field in the x direction,

provided that $\alpha \neq n\pi$. According to equation (23), for the expectation value of an observable, the free induction decay signal M_x^{FID} is given by:

$$M_x^{\text{FID}}(t) = \langle \hat{F}_x \rangle = \mathbf{f}_x^\dagger \boldsymbol{\rho}(t) \quad (48)$$

The vector $\boldsymbol{\rho}(t)$ is obtained upon solving equation (35) with the super-Hamiltonian \mathbf{H}_s^D and the initial condition according to equation (47). Considering the fact that the only non-zero elements of the \mathbf{f}_x vector are $\mathbf{f}_{x(1)}$ and $\mathbf{f}_{x(-1)}$, and that for all $k \neq 0$ the following holds:

$$\mathbf{e}_{(k)} = \mathbf{f}_{z(k)} = \boldsymbol{\rho}_{0(k)} = 0 \quad (49)$$

the $M_x^{\text{FID}}(t)$ function may simply be written in the form:

$$M_x^{\text{FID}}(t) = K \{ \mathbf{f}_{x(-1)}^\dagger \exp[(-i\mathbf{H}_{s(-1)}^D + \mathbf{R}_{(-1)})t] \mathbf{f}_{x(-1)} + q_{-1}(t) \} \quad (50)$$

In equation (50), $K = (\hbar\omega_0/kT)(\mathbf{e}^\dagger \mathbf{e})^{-1} \sin(\alpha)$, and $q_{-1}(t)$ is the complex conjugate of the first component within the braces.

The lineshape function which describes the absorption and dispersion modes of an unsaturated, steady-state NMR spectrum is proportional to the Fourier transform of the function $M_x^{\text{FID}}(t)$: (24, 25, 99)

$$f(\omega) \sim \int_0^\infty \exp(+i\omega t) M_x^{\text{FID}}(t) dt \quad (51)$$

In the integral in expression (51), the only significant contribution comes from the first of the two components of the sum within braces in equation (50). The contribution from $q_{-1}(t)$ is about $2\omega_0$ times smaller, and it may safely be neglected. (23) Therefore, the final form of the lineshape function is:

$$f(\omega) = -C \mathbf{f}_- [-i(\mathbf{H}_{s(-1)}^D - \omega \mathbf{E}_{(-1)}) + \mathbf{R}_{(-1)}]^{-1} \mathbf{f}_- \quad (52)$$

where $\mathbf{f}_- = \mathbf{f}_x - i\mathbf{f}_y$ is the vector which corresponds to the so-called lowering operator, and C is a real, positive proportionality coefficient. The corresponding absorption and dispersion mode spectra are given by the real (Re) and imaginary (Im) parts of $f(\omega)$ respectively:

$$f_{\text{abs.}}(\omega) = \text{Re}[f(\omega)] \quad (53)$$

$$f_{\text{disp.}}(\omega) = \text{Im}[f(\omega)] \quad (54)$$

III. THEORY OF NMR LINESHAPES FOR EXCHANGING SPIN SYSTEMS

The first theoretical treatment of dynamic NMR was formulated in 1953 by Gutowsky, McCall, and Slichter. (26) It was subsequently developed in the works of Gutowsky *et al.*, McConnell, and Sack. (27–

30) Their theory, based on the classical Bloch equations, (31) describes the exchange of non-coupled spin systems in terms of their magnetizations. An equivalent description of the phenomena of dynamic NMR has been given by Anderson and by Kubo in terms of a stochastic model of exchange. (32, 33) In the latter approach, the spectrum of a spin system is identified with the Fourier transform of the so-called relaxation function.

A quantum mechanical treatment combined with the density matrix formalism extends the description to include the dynamic spectra of spin-coupled systems. (34–38) Further developments in the theory and presentation thereof, in a form suitable for computer calculations, are due to Binsch *et al.*, and to Kaplan *et al.* (14, 15, 39) However, even the recent theories are not rigorous in certain aspects and contain some errors. This is particularly true in the case of the intermolecular exchange of spins.

In this section, we discuss the assumptions which constitute the foundation of the theory, and derive final equations as rigorously as possible. We also give a theoretical description of the most general case of spin exchange, that in a multi-component system where both intra- and inter-molecular processes take place. The theory presented in this section involves only homonuclear systems of spins. An extension over individual heteronuclear systems should be quite straightforward.

A. Kinetics of a system at equilibrium

Let us consider a system of substances A_i , $i = 1, 2, \dots, S$, which undergo Ω different reactions. A reaction will be understood here as a one-way process for the formation of certain products and the disappearance of certain substrates. We take into account also degenerate reactions, e.g. intramolecular rearrangements which preserve the chemical identity of the reagents involved. The reactions are numbered by subscripts α , belonging to the set $\{1, 2, \dots, \Omega\}$. For any reaction α , there is exactly one opposite reaction, that denoted by the subscript $\omega(\alpha)$, where the ω function has the property:

$$\omega(\omega(\alpha)) = \alpha \quad (55)$$

We assume that in the state of equilibrium, for any molecule of the type A_i , there is a determined probability $p_i(t, t')$ that the molecule should appear at time t' , and that it should not react further within the period $[t', t]$, where $t' < t$:

$$p_i(t, t') = (1/\tau_i) \exp[-(t - t')/\tau_i] dt' \quad (56)$$

There are also definite probabilities $\pi_{i,\alpha}$ that a molecule of the A_i type, if formed, is a product of the reaction α . The following condition exists:

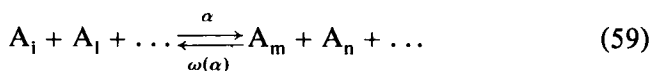
$$\sum_{\alpha=1}^{\Omega} \pi_{i,\alpha} = 1 \quad (57)$$

Obviously, some of the probabilities may be zero. The two equations (56) and (57) may be considered as postulates or else they can be derived by assuming Markovian character for the mass transfer in the equilibrium in a way analogous to that given in reference (33). We now present an interpretation of such an approach from the point of view of chemical kinetics.

It is known from the theory of chemical kinetics that a system of S chemical substances in dynamic equilibrium can be described by rate constants of the pseudo-first order, $K_{i,\alpha}$ ($i = 1, 2, \dots, S$; $\alpha = 1, 2, \dots, \Omega$). Some of the rates may assume zero values. The rate of depletion of substance A_i in the reaction $\omega(\alpha)$, $V_{i,\omega(\alpha)}^-$, and that of its formation in the reverse reaction α , $V_{i,\alpha}^+$, must equal each other at equilibrium:

$$V_{i,\alpha}^+ = V_{i,\omega(\alpha)}^- = K_{i,\alpha} c_i \quad (58)$$

where c_i is the equilibrium concentration of A_i expressed in, for example, units of molar concentration. Notice that for reactions with unit stoichiometric coefficients:



the following equalities hold:

$$V_{r,\alpha}^+ = V_{q,\omega(\alpha)}^- \quad (60)$$

where $r = m, n, \dots$, and $q = i, 1, \dots$. Equations (58) and (60) represent the consequences of the detailed balancing condition for processes α and $\omega(\alpha)$ in equation (59). The probabilities $\pi_{i,\alpha}$ have the following interpretation in terms of chemical kinetics:

$$\pi_{i,\alpha} = V_{i,\alpha}^+ / \sum_{\beta=1}^{\Omega} V_{i,\beta}^+ = K_{i,\alpha} / \sum_{\beta=1}^{\Omega} K_{i,\beta} \quad (61)$$

Let the symbol $c_i'(\tau)$, $\tau \geq 0$, denote the concentration of the A_i molecules which do not undergo any reaction within the period $[t', t' + \tau]$. Obviously, $c_i'(0) = c_i$. The change in the concentration with increasing time τ is given by:

$$dc_i'(\tau)/d\tau = - \left(\sum_{\alpha=1}^{\Omega} K_{i,\alpha} \right) c_i'(\tau) \quad (62)$$

Upon integration we obtain:

$$c'_i(\tau) = c_i \exp \left[\left(- \sum_{\alpha=1}^{\Omega} K_{i,\alpha} \right) \tau \right] \quad (63)$$

From the point of view of a single molecule, the quotient $c'_i(\tau)/c_i$ may be regarded as the probability that a molecule of the A_i type does not undergo any reaction within the time τ . The probability can also be calculated from equation (56) as the sum of the probabilities that a molecule of the A_i type is formed at any time within the period $[-\infty, t']$ and that it persists in the A_i form until $t' + \tau$. The following equality holds:

$$\begin{aligned} c'_i(\tau)/c_i &= \exp \left[\left(- \sum_{\alpha=1}^{\Omega} K_{i,\alpha} \right) \tau \right] \\ &= (1/\tau_i) \int_{-\infty}^{t'} \exp[-(t' + \tau - \theta)/\tau_i] d\theta \end{aligned} \quad (64)$$

Upon integration, we obtain the interpretation of the time τ_i as:

$$(1/\tau_i) = \sum_{\alpha=1}^{\Omega} K_{i,\alpha} \quad (65)$$

in terms of kinetic rate constants of the pseudo-first order.

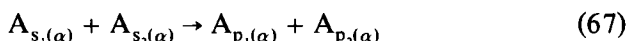
B. Equation of motion for a spin system in dynamic equilibrium

As far as an NMR experiment is concerned the state of the products of reaction α is unambiguously determined, within the so-called sudden approximation, (40) by the state of the substrates involved just prior to the reaction as well as by the reaction mechanism. This problem is considered in detail in Section III.C. Needless to say, the states involved are understood as the corresponding spin density matrices. In a description of the dynamic equilibrium considered, we may take into account all the stereochemically feasible reactions or we may divide the entire set of the latter into subsets of NMR-nondifferentiable reactions and then consider only one reaction from each of the subsets. (41, 42) In the latter method, the probability $\pi'_{i,\alpha}$, which refers to subset α , is the sum of probability given by:

$$\pi'_{i,\alpha} = \pi_{i,\alpha} + \sum_{\beta} \pi_{i,\beta} \quad (66)$$

where the summation over β includes all the reactions that cannot be distinguished from the reaction α from the point of view of NMR. The prime sign on the symbol π is deleted in our further considerations. For some systems it may be difficult to take into account all possible reactions, and the partition into subsets may pose a serious problem.

In our description of an equilibrium situation, we introduce the concept of an empty set of nuclei, A_0 , which enables us to write a general scheme for the reactions involved:



where s_k and p_k belong to the set $\{0, 1, 2, \dots, S\}$. In other words, we consider only unimolecular and bimolecular processes. More complicated processes appear to be of negligible importance.

Both intra- and inter-molecular processes, which occur in liquids, affect the relaxation rates of the spin systems involved. Our considerations are concerned with reactions and rearrangements which are characterized by life-times that are appreciably longer than typical correlation times for molecular rotations. The latter are included in the derivation of the equation (35) of motion. It seems, therefore, that the equation should be valid for the description of a spin system during the period between reactions.

The spin density matrix $\bar{\rho}_i(t)$ which describes the properties of any spin system of a molecule A_i is defined as follows. We assume that the density matrices $\bar{\rho}_j(0)$, $j = 1, 2, \dots, S$, which describe the individual components of the dynamic equilibrium at any arbitrary time zero, are known explicitly, and that at any time t' such that $t > t' > 0$ the $\bar{\rho}_j(t')$ matrices are already defined. Our reasoning is applied to a pulse-type NMR experiment, and we therefore construct the equation of motion in a static magnetic field. The $\bar{\rho}_i(t)$ matrix is the weighted average over the states involved, according to equation (5). The state of a molecule A_i , formed at the moment t' and persisting as such until t , is given by the solution of equation (35) with the super-Hamiltonian H_s^D :

$$\rho_i(t, t') = \exp[(-iH_s^D + R_i)(t - t')][\bar{\rho}_i^f(t') - \rho_{0i}] + \rho_{0i} \quad (68)$$

The density matrix $\bar{\rho}_i^f(t')$ describes the state of a molecule A_i which is formed at the moment t' . It is a shorthand description of the fact that, within the model assumed, the state of a molecule is unambiguously determined by the mean density matrices $\bar{\rho}_j(t')$ of all the components of the equilibrium considered and by the probabilities $\pi_{i,\alpha}$:

$$\bar{\rho}_i^f(t') = \sum_{\alpha=1}^{\Omega} \pi_{i,\alpha} G_{r_i,\alpha} [\bar{\rho}_{s_1(\alpha)}(t') \otimes \bar{\rho}_{s_2(\alpha)}(t')] \quad (69)$$

where the density matrices $\bar{\rho}_{s(\alpha)}(t')$ describe the state of the substrates of reaction α at the moment t' . The superoperators $G_{r_i,\alpha}$ describe contractions similar to those in equation (11): $r_i = 1$ for $i = p_1(\alpha)$ or $r_i = 2$ for $i = p_2(\alpha)$ [equation (67)]. The superoperators $G_{r_i,\alpha}$ are discussed in the following section. We now state only that they are time-independent.

This property is related directly to the assumption that a molecule stays for an infinitely short time in an active complex.

In our model the $\bar{\rho}_i(t)$ matrix represents the sum of contributions of two groups of states, those of molecules which are formed before the moment zero at which the pulse is applied, and the states $\rho_i(t, t')$ of molecules which are created later, at the moment t' within the period $[0, t]$:

$$\bar{\rho}_i(t) = \left\{ \int_{-\infty}^0 (1/\tau_i) \exp[-(t-t')/\tau_i] dt' \right\} \rho_i(t) + \int_0^t (1/\tau_i) \exp[-(t-t')/\tau_i] \rho_i(t, t') dt' \quad (70)$$

The integral within the braces in equation (70) represents the probability that a molecule of the A_i type is formed within the period $[-\infty, 0]$. All such molecules are in the same state ρ_i which is independent of the states preceding the moment zero. This state can be obtained by solving equation (35) with the initial condition $\rho_i(0) = \bar{\rho}_i(0)$:

$$\rho_i(t) = \exp[-i\mathbf{H}_{s_i}^D + \mathbf{R}_i]t [\bar{\rho}_i(0) - \rho_{0_i}] + \rho_{0_i} \quad (71)$$

By differentiating both sides of equation (70), with respect to t , we obtain the equation of motion in the commonly known differential form (computational details are given in Appendix B):

$$d\bar{\rho}_i(t)/dt = -i\mathbf{H}_{s_i}^D \bar{\rho}_i(t) + \mathbf{R}_i[\bar{\rho}_i(t) - \rho_{0_i}] + (1/\tau_i)[\bar{\rho}_i^f(t) - \bar{\rho}_i(t)] \quad (72)$$

where $i = 1, 2, \dots, S$. This equation can also be derived for a continuous-wave NMR experiment to yield a more general solution which includes, for example, saturated NMR spectra. In this case, a rotating system of coordinates has been employed together with rotating-frame super-Hamiltonians. (103) However, in such considerations of continuous-wave NMR, the justification for the assumption of the knowledge of $\bar{\rho}_i(0)$ is obscure.

For a pulse-type NMR experiment, the assumption has a straightforward interpretation, since the pulse applied at the moment zero breaks down the dynamic history of the spin system involved. The reasoning presented here, which leads to the equation of motion in the form of equation (72), bears some resemblance to Kaplan and Fraenkel's approach to the quantum-mechanical description of continuous-wave NMR. (39) The crucial point in our treatment is the introduction of the probabilities $\pi_{i,\alpha}$ which are expressed in terms of pseudo-first-order rate constants. This makes possible a definition of the mean density matrix $\bar{\rho}^f$ of a molecule at the moment of its creation, even for complicated multi-reaction systems. The definition of the $\bar{\rho}^f$ matrix makes unnecessary the distinction between intra- and inter-molecular spin exchange which has so far been employed in the literature.

Attention is drawn to the fact that the equation of motion in its integral form is erroneous if constructed by neglecting the states described by equation (71). It is somewhat mysterious how the correct differential form of the equation is derived from an erroneous integral form, as has been done in the literature. (39) In a number of fundamental works in the field, the differential form of the equation of motion, that corresponding to equation (72), has been formulated on a purely phenomenological basis. It seems that the integral approach has more heuristic value, giving a better insight into the phenomena of dynamic NMR.

Another approach, that based on the theory of Markovian processes, has been employed in the classical description of magnetization by Anderson and by Kubo. (32, 33) The idea behind this method is that the solutions of the differential equation, which describes the motion of magnetization vectors, are averaged over the trajectories of the Markovian process which is assumed to constitute the (scalar) operator in the equation of motion. A generalization of these results over the density matrices and superoperators for intra-molecular processes has been given by Johnson. (43, 44) Owing to recent advances in the theory of stochastic differential equations, the generalization acquires a rigorous mathematical foundation. (45).

C. Evaluation of a spin density matrix after exchange

Let us consider a reaction of the type:



where A, B, C, and D denote groups of nuclei which are exchanged among molecules. Some of the symbols may represent empty sets of nuclei so that the scheme describes all possible kinds of unimolecular and bimolecular exchange processes. A convenient procedure for the determination of the density matrices of the products, from those of the substrates, has been given by Kaplan and Fraenkel for a Hilbert space. (39) The method consists of a judicious selection of the appropriate basis function sets in the spaces of the reagents in order to provide an easy route to contractions such as those in equations (11) and (12). The method presented in this section is a generalization of Kaplan and Fraenkel's approach.

1. Reaction mechanisms

We shall arbitrarily number the positions occupied by nuclei in molecular frameworks (nuclear coordinates or stereochemical positions)

of individual reagents, using subscripted natural numbers. Let the symbol Z_{KL} denote a set of such numbers for the species KL:

$$Z_{KL} = \{1_{KL}, 2_{KL}, \dots, n_{KL}\}$$

where n_{KL} is the number of nuclei in the molecule KL. Reagents which are chemically identical (such as those in mutual reactions) have the same numbering of their nuclear coordinates. Magnetic nuclei in the substrates and in the products are numbered with subscripted natural numbers i_K , and we denote by the symbol Z_K a set of numbers assigned to nuclei which migrate, say, from KL to KM:

$$Z_K = \{1_K, 2_K, \dots, n_K\} \quad (74)$$

From the point of view of an NMR experiment, the reaction mechanism is defined by a one-to-one correspondence between the stereochemical positions of the nuclei in the products and those in the substrates. Such a mechanism may be written in terms of four functions, M_{AB}^s , M_{CD}^s , M_{AC}^p , and M_{BD}^p , where "s" stands for substrates and "p" for products, which assign the corresponding elements of the Z_K and Z_L sets to each of the elements of the Z_{KL} sets involved. Needless to say, the number of elements in the Z_{KL} set is equal to the sum of numbers of elements in Z_K and Z_L , $n_{KL} = n_K + n_L$. Mathematically speaking, the M_{KL} functions map the sets Z_{KL} ($KL = AB, CD, AC, BD$) onto the sums of the corresponding sets Z_K and Z_L :

$$M_{AB}^s : Z_{AB} \rightarrow Z_A \cup Z_B \quad (75a)$$

$$M_{AC}^p : Z_{AC} \rightarrow Z_A \cup Z_C \quad (75b)$$

The notation of reaction mechanisms is illustrated by the three following examples, where the symbols without parentheses denote the stereochemical positions (elements of Z_{KL} sets) whilst those within parentheses represent the numbering of individual nuclei which belong to the corresponding Z_K and Z_L sets.

(i) The inversion of configuration of the bonds at the nitrogen atom of aziridine (Fig. 1). This is an intramolecular process; therefore the B, C, and D sets are empty and the AB and AC molecules are chemically equivalent.

(ii) An intermolecular proton exchange between the NH group of aziridine and its environment with the retention of configuration of the bonds at the nitrogen atom (Fig. 2). In this case the sets B and C contain only one proton each; therefore AB is equivalent to AC, and CD is equivalent to BD.

(iii) The same as in the preceding example but with a change in the configuration at the nitrogen atom (Fig. 3). With this example we wish

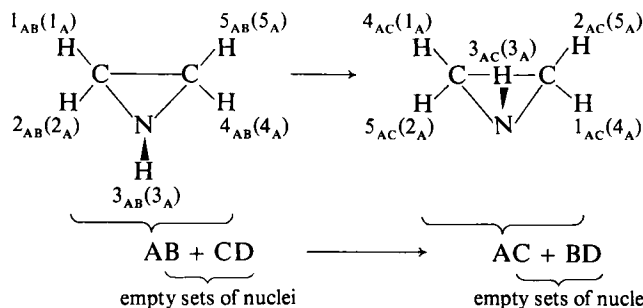


FIG. 1. Inversion of configuration of the bonds at the nitrogen atom of aziridine.

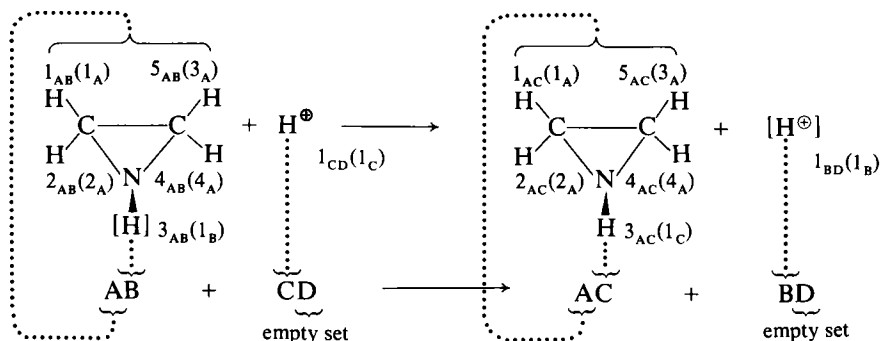


FIG. 2. Proton exchange between the NH group of aziridine and its environment, with the retention of configuration at the nitrogen atom.

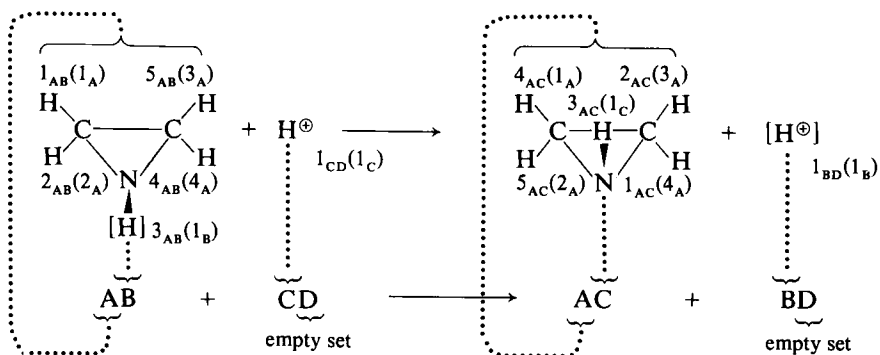


FIG. 3. Proton exchange between the NH group of aziridine and its environment, with a change in the configuration at the nitrogen atom.

to illustrate the meaning of the M_{KL} functions: $M_{AB}^s(1_{AB}) = 1_A$, $M_{AB}^s(2_{AB}) = 2_A$, $M_{AB}^s(3_{AB}) = 1_B$, $M_{AB}^s(4_{AB}) = 4_A$, $M_{AB}^s(5_{AB}) = 3_A$, and $M_{AC}^p(1_{AC}) = 4_A$, $M_{AC}^p(2_{AC}) = 3_A$, $M_{AC}^p(3_{AC}) = 1_C$, $M_{AC}^p(4_{AC}) = 1_A$, $M_{AC}^p(5_{AC}) = 2_A$.

2. Basis function sets for reactions

Let us denote by the symbol B_K a complete set of product spin functions $|\Phi_i^K\rangle$:

$$\Phi_i^K = \varphi_i(1_K) \varphi_i(2_K) \dots \varphi_i(n_K) \quad (76)$$

where φ is an eigenfunction (α or β) of the I_z operator for a single nucleus. Each of the B_K sets spans the spin space H_K , which may be termed the spin space of the molecular fragment K .

The set $B_{(KL)}$, composed of the products of the vectors from the sets B_K and B_L and lexicographically ordered according to the sequence of the indices K and L , spans the spin space $H_K \otimes H_L$ which may be called the space of fragment pairs:

$$\begin{aligned} B_{(KL)} &= \{|\Phi_1^K\rangle \otimes |\Phi_1^L\rangle, |\Phi_1^K\rangle \otimes |\Phi_2^L\rangle, \dots, |\Phi_{n_K}^K\rangle \otimes |\Phi_{n_L}^L\rangle\} \\ &= \{|\Theta_1^{(KL)}\rangle, |\Theta_2^{(KL)}\rangle, \dots, |\Theta_{n_{KL}}^{(KL)}\rangle\} \end{aligned} \quad (77)$$

The spaces $H_K \otimes H_L$ are related to the spin spaces H_{KL} of the reagents by the permutation transformation \hat{Q}_{KL} which is defined by the reaction mechanism in terms of the M_{KL} functions from equations (75a) and (75b):

$$\begin{aligned} \hat{Q}_{KL}^u [|\varphi(1_K)\varphi(2_K) \dots \varphi(n_K)\rangle \otimes |\varphi(1_L)\varphi(2_L) \dots \varphi(n_L)\rangle] \\ = |\varphi[M_{KL}^u(1_{KL})]\varphi[M_{KL}^u(2_{KL})] \dots \varphi[M_{KL}^u(n_{KL})]\rangle \end{aligned} \quad (78)$$

where $u = s$ if KL is a substrate or $u = p$ if KL is a product. We denote by the symbol B_{KL} an ordered set of vectors $|\chi_i^{KL}\rangle$ from the H_{KL} space:

$$|\chi_i^{KL}\rangle = \hat{Q}_{KL}^u |\Theta_i^{(KL)}\rangle \quad (79)$$

where $|\Theta_i^{(KL)}\rangle$ belongs to the set $B_{(KL)}$.

Lexicographically ordered sets of projection operators (Section II.D) which are composed of the vectors of the corresponding sets B_K , B_L , $B_{(KL)}$, and B_{KL} which span the Liouville spaces L_K , L_L , $L_K \otimes L_L$ and L_{KL} are called the basic function sets of a reaction.

3. Permutation operator

Within the basis sets of a reaction, the operator \hat{Q}_{KL}^u (or the superoperator \mathbf{Q}_{KL}^u) is represented by a unit matrix. In an arbitrary orthonormal basis $\{|\epsilon_i^{KL}\rangle\}$ in the space H_{KL} , the operator is represented by the inverse of the unitary matrix \hat{U} of the basis set transformation:

$$(\hat{Q}_{KL}^u)_{ji} = (\hat{U}^{-1})_{ij} = \hat{U}_{ji}^* \quad (80)$$

where the matrix \hat{U} transforms the basis set of vectors $|\chi_j^{KL}\rangle$ into that of the vectors $|\varepsilon_m^{KL}\rangle$ according to the relation:

$$|\varepsilon_m^{KL}\rangle = \sum_j \hat{U}_{mj} |\chi_j^{KL}\rangle \quad (81)$$

Transformation properties of the superoperator \mathbf{Q}_{KL}^u , which are connected with the change in the basis set in the H_{KL} space, can be derived from the corresponding properties of the operator \hat{Q}_{KL}^u . Let the set of vectors $\{\eta_{ij}^{KL}\}$, where η_{ij}^{KL} corresponds to $|\varepsilon_i^{KL}\rangle \langle \varepsilon_j^{KL}|$, constitute a basis set in the L_{KL} space. We define the basis set $\{\eta_{ijmn}^{(KL)}\}$ in the $L_K \otimes L_L$ space as:

$$\eta_{ijmn}^{(KL)} = \eta_{ij}^K \otimes \eta_{mn}^L \quad (82)$$

where the vectors η_{ij}^O constitute the basis set of a reaction in the L_O space:

$$\eta_{ij}^O \equiv |\Phi_i^O\rangle \langle \Phi_j^O| \quad (83)$$

The representation of the superoperator \mathbf{Q}_{KL}^u in the basis sets $\{\eta_{ijmn}^{(KL)}\}$ and $\{\eta_{pq}^{KL}\}$ becomes:

$$(\mathbf{Q}_{KL}^u)_{pq, ijmn} = (\mathbf{U}\mathbf{P})_{pq, ijmn} \quad (84)$$

where $\mathbf{U} = \hat{U}^* \otimes \hat{U}$. The permutation matrix \mathbf{P} transforms the basis set $\{\eta_{pqrs}^{(KL)}\}$ into the basis set of a reaction in the space $L_K \otimes L_L$:

$$\mathbf{P}\eta_{pqrs}^{(KL)} = \mathbf{w}_{a(p,r)a(q,s)}^{(KL)} \quad (85)$$

where the vectors \mathbf{w}_{ij} correspond to the operators $|\Theta_i^{KL}\rangle \langle \Theta_j^{KL}|$. The function "a" from equation (85) is defined implicitly by equation (77). The function assigns pairs of subscripts i,j , which are attached to Φ_i^K and Φ_j^L , to single subscripts $a(i,j)$ which characterize $\Theta_{a(i,j)}^{(KL)}$:

$$|\Theta_{a(i,j)}^{(KL)}\rangle = |\Phi_i^K\rangle \otimes |\Phi_j^L\rangle \quad (86)$$

In further considerations of spaces of the $L_K \otimes L_L$ type we always assume the basis set of vectors $\eta_{ijmn}^{(KL)}$.

All the operations which are carried out here on multi-subscripted matrices and vectors follow the general rules for doubly-subscripted matrices and singly-subscripted vectors. In all such operations, composite subscripts are replaced with single subscripts whose values result from lexicographical ordering (Appendix A).

The operators \hat{Q} commute with all those which are independent of nuclear coordinates:

$$\hat{Q}_{KL}^{-1} \hat{F}_{u_{KL}} \hat{Q}_{KL} = \hat{F}_{u_K} \otimes \hat{E}_L + \hat{E}_K \otimes \hat{F}_{u_L} \quad (87)$$

where $u = x, y, z$. In equation (87), the operator $\hat{F}_{u_{KL}}$ acts on the space

H_{KL} , and the operator $\hat{F}_{u_K} \otimes \hat{E}_L + \hat{E}_K \otimes \hat{F}_{u_L}$ acts on the space $H_K \otimes H_L$. The same is true for the corresponding superoperators Q_{KL} :

$$Q_{KL}^{-1} F_{u_{KL}}^S Q_{KL} = F_{u_K}^S \otimes E_L + E_K \otimes F_{u_L}^S \quad (88)$$

where $S = L, R, D$. Moreover, the following relations hold for the vectors $f_{u_{KL}}$ and e_{KL} which correspond to the operators $\hat{F}_{u_{KL}}$ and \hat{E}_{KL} , respectively:

$$Q_{KL}^{-1} f_{u_{KL}} = f_{u_K} \otimes e_L + e_K \otimes f_{u_L} \quad (89)$$

$$Q_{KL}^{-1} e_{KL} = e_K \otimes e_L \quad (90)$$

4. Density matrix of molecular fragments

Within appropriate basis function sets, the representations of the contraction superoperators of the type given by equation (11) take the form:

$$Tr_L^{KL} = E_K \otimes e_L^\dagger \quad (91a)$$

$$Tr_K^{KL} = e_K^\dagger \otimes E_L \quad (91b)$$

where E_Q is the unit superoperator of the spin space L_Q , and e_Q is the vector which corresponds to the unit operator in the corresponding space H_Q . If $\bar{\rho}_{KL}$ is the density matrix of the entire system in the basis set $\{\eta_{pqrs}^{(KL)}\}$, then the superoperators in equation (91a) and (91b) define the density matrices of the subsystems in the basis sets $\{\eta_{pq}^K\}$ and $\{\eta_{rs}^L\}$ respectively:

$$(E_K \otimes e_L^\dagger) \bar{\rho}_{KL} = \bar{\rho}_K \quad (92a)$$

$$(e_K^\dagger \otimes E_L) \bar{\rho}_{KL} = \bar{\rho}_L \quad (92b)$$

If the fragments K and L do not interact with each other, then:

$$\bar{\rho}_K \otimes \bar{\rho}_L = \bar{\rho}_{KL} \quad (93)$$

Otherwise, the equality does not hold. The contractions presented in equations (91a) and (91b) result in a loss of information relating to the whole system.

5. Exchange superoperator

Using the concepts derived above the density matrices of the products, at the moment of their formation, can be presented as the direct products of the density matrices of the molecular fragments involved (independently of the choice of basis function sets in the spaces of the reagents), e.g.:

$$\bar{\rho}_{AC}^f = \{Q_{AC}^p [(E_A \otimes e_B^\dagger) \otimes (E_C \otimes e_D^\dagger)] [(Q_{AB}^s)^{-1} \otimes (Q_{CD}^s)^{-1}]\} (\bar{\rho}_{AB} \otimes \bar{\rho}_{CD}) \quad (94)$$

Thus, the term within braces in equation (94) defines the superoperator \mathbf{G} given in equation (69) for the reaction represented by equation (73). In the notation of equation (94) we make use of certain properties of direct products (see Appendix A).

In order to formulate the superoperators for complicated equilibria, it is only necessary to modify the notation system. The superoperators \mathbf{G}_r^α , from equation (69), may be expressed as:

$$\mathbf{G}_1^\alpha = \mathbf{Q}_{p_1(\alpha)}[(\mathbf{E}_{11}^\alpha \otimes \mathbf{e}_{21}^{\alpha\dagger}) \otimes (\mathbf{E}_{12}^\alpha \otimes \mathbf{e}_{22}^{\alpha\dagger})](\mathbf{Q}_{s_1(\alpha)}^{-1} \otimes \mathbf{Q}_{s_2(\alpha)}^{-1}) \quad (95a)$$

$$\mathbf{G}_2^\alpha = \mathbf{Q}_{p_2(\alpha)}[(\mathbf{e}_{11}^{\alpha\dagger} \otimes \mathbf{E}_{21}^\alpha) \otimes (\mathbf{e}_{12}^{\alpha\dagger} \otimes \mathbf{E}_{22}^\alpha)](\mathbf{Q}_{s_1(\alpha)}^{-1} \otimes \mathbf{Q}_{s_2(\alpha)}^{-1}) \quad (95b)$$

In equations (95a) and (95b) the symbol \mathbf{E}_{kr}^α (or \mathbf{e}_{kr}^α) denotes the unit superoperator (or operator) in the space $L_{(A_{kr}^\alpha)}$, where A_{kr}^α is a group of nuclei which is transferred from a molecule with the substrate s_r to the product p_k ($k, r = 1, 2$) in the reaction represented by equation (67); $\mathbf{Q}_{p_k(\alpha)}$ and $\mathbf{Q}_{s_k(\alpha)}$ denote the permutation superoperators defined by the mechanisms $M_{p_k(\alpha)}$ and $M_{s_k(\alpha)}$, respectively (Sections III.C.1 and III.C.3).

It is convenient to express the exchange superoperator for the reaction $\omega(\alpha)$, i.e. that which is opposite to a reaction α , in the same terms as that for the reaction α :

$$\mathbf{G}_1^{\omega(\alpha)} = \mathbf{Q}_{s_1(\alpha)}(\mathbf{E}_{11}^\alpha \otimes \mathbf{e}_{12}^{\alpha\dagger} \otimes \mathbf{E}_{21}^\alpha \otimes \mathbf{e}_{22}^{\alpha\dagger})(\mathbf{Q}_{p_1(\alpha)}^{-1} \otimes \mathbf{Q}_{p_2(\alpha)}^{-1}) \quad (96a)$$

$$\mathbf{G}_2^{\omega(\alpha)} = \mathbf{Q}_{s_2(\alpha)}(\mathbf{e}_{11}^{\alpha\dagger} \otimes \mathbf{E}_{12}^\alpha \otimes \mathbf{e}_{21}^{\alpha\dagger} \otimes \mathbf{E}_{22}^\alpha)(\mathbf{Q}_{p_1(\alpha)}^{-1} \otimes \mathbf{Q}_{p_2(\alpha)}^{-1}) \quad (96b)$$

Equations (96a) and (96b) are valid providing that the reaction $\omega(\alpha)$ is represented by the same scheme as the reaction α , the only difference being the reversed direction of the arrows such as those given in Figs. 1–3 and the assumption:

$$s_i[\omega(\alpha)] = p_i(\alpha) \quad (97a)$$

$$p_i[\omega(\alpha)] = s_i(\alpha) \quad (97b)$$

Hence:

$$\mathbf{A}_{ij}^\alpha = \mathbf{A}_{ji}^{\omega(\alpha)} \quad (98)$$

which means that a group of nuclei transferred from the first substrate to the second product in the reaction α is identical with that transferred from the second substrate to the first product in the opposite reaction $\omega(\alpha)$ etc.

In order to make the notation self-consistent, we assume that all quantities which refer to empty sets of nuclei are set to (scalar) unity.

D. Equation of motion in the linear approximation

In a pulse-type NMR experiment the density matrix $\rho(t)$ of a non-exchanging system approaches the thermal equilibrium ρ_0 which is described satisfactorily by equation (16). The same matrices ρ_0 approximate, with good accuracy, the time-independent solution of the system of differential equations (72). This can be inferred from equation (99) which is derived from equations (95a) and (95b):

$$\mathbf{G}_k(\rho_{0_{s_1}} \otimes \rho_{0_{s_2}}) = \rho_{0_{p_k}} + \mathbf{O}(\hbar\omega_0/kT) \quad (99)$$

where $\mathbf{O}(\hbar\omega_0/kT)$ represents terms of an order higher than $(\hbar\omega_0/kT)$. The latter are negligibly small throughout the common range of temperatures at which NMR measurements are carried out. Thus, the matrices ρ_0 , which are defined in equation (16) for non-exchanging systems, describe the state of thermal equilibrium with the lattice also in a system of exchanging spins:

$$\bar{\rho}_{0_i} = \rho_{0_i} \quad (100)$$

It follows that, in a pulse-type experiment on an exchanging spin system, the initial conditions from equation (47) can be rewritten as:

$$\bar{\rho}_i(0) = 2^{-(n_i)} [\mathbf{e}_i + (\hbar\omega_0/kT)(\mathbf{f}_{x_i} \sin \alpha + \mathbf{f}_{z_i} \cos \alpha)] \quad (101)$$

In equation (101), α denotes the flip angle from equation (47).

One may assume, as in the case of no exchange, that in a pulse-type experiment, the matrix $\bar{\sigma}$ defined by equation (102) has the elements of the order of $(\hbar\omega_0/kT)$: (98, 99)

$$\bar{\sigma}_i(t) = 2^{(n_i)} \bar{\rho}_i - \mathbf{e}_i \quad (102)$$

In the direct product of the density matrices in equation (72), one may therefore neglect the term $\bar{\sigma}_i \otimes \bar{\sigma}_j$, which is of the order of $(\hbar\omega_0/kT)^2$ without any appreciable loss in accuracy:

$$\bar{\rho}_i \otimes \bar{\rho}_j \simeq 2^{-(n_i+n_j)} (\bar{\sigma}_i \otimes \mathbf{e}_j + \mathbf{e}_i \otimes \bar{\sigma}_j + \mathbf{e}_i \otimes \mathbf{e}_j) \quad (103)$$

This approximation is equivalent to those employed in references 36 and 39 for continuous-wave experiments. It is valid when both the high-temperature and high-field conditions are fulfilled. (98, 99) Kaplan's claims to the contrary (references 100 and 101) seem to be unjustified. (98, 99, 102)

As far as the $\bar{\sigma}_i$ matrices are concerned, the linear approximation of equation (72) takes the form:

$$\begin{aligned} d\bar{\sigma}_i/dt \simeq & -i\mathbf{H}_{s_i}^D\bar{\sigma}_i + \mathbf{R}_i(\bar{\sigma}_i - \bar{\sigma}_{0_i}) \\ & + (1/\tau_i) \left\{ \sum_{\alpha} [\pi_{i,\alpha} \mathbf{G}_{k_i}(\bar{\sigma}_{s_1(\alpha)} \otimes \mathbf{e}_{s_2(\alpha)} \right. \\ & \left. + \mathbf{e}_{s_1(\alpha)} \otimes \bar{\sigma}_{s_2(\alpha)}) 2^{(n_1 - n_{s_1(\alpha)} - n_{s_2(\alpha)})} - \bar{\sigma}_i \right\} \end{aligned} \quad (104)$$

where $i = 1, 2, \dots S$. Which follows from the fact that:

$$\mathbf{G}_{k_i}[2^{(n_1 - n_j - n_m)} \mathbf{e}_j \otimes \mathbf{e}_m] = \mathbf{e}_i \quad (105)$$

For purely intramolecular equilibria the system of differential equations (72) is already linear and the procedure described above transforms the system into the form of equation (104) exactly without any approximations. For such equilibria further simplification of equations (72) and (104) is possible by deleting all those quantities which refer to empty sets of nuclei.

E. Exchange superoperators in the linear approximation

The superoperators in the summation given in equation (104) can be presented in a form which is more convenient for further consideration. We therefore define:

$$\mathbf{Y}_{k1}^{\alpha}(\bar{\sigma}_{s_1(\alpha)}) = \mathbf{G}_k^{\alpha}[\bar{\sigma}_{s_1(\alpha)} \otimes \mathbf{e}_{s_2(\alpha)}] 2^{(q_{k,\alpha})} \quad (106a)$$

$$\mathbf{Y}_{k2}^{\alpha}(\bar{\sigma}_{s_2(\alpha)}) = \mathbf{G}_k^{\alpha}[\mathbf{e}_{s_1(\alpha)} \otimes \bar{\sigma}_{s_2(\alpha)}] 2^{(q_{k,\alpha})} \quad (106b)$$

where $k = 1, 2$ and $q_{k,\alpha} = n_{p_k(\alpha)} - n_{s_1(\alpha)} - n_{s_2(\alpha)}$. From the properties of direct products (Appendix A) it follows that the superoperators \mathbf{Y} can be written in the form:

$$\mathbf{Y}_{11}^{\alpha} = \mathbf{Q}_{p_1(\alpha)}(\mathbf{E}_{11}^{\alpha} \otimes \mathbf{e}_{21}^{\alpha\dagger} \otimes \mathbf{e}_{12}^{\alpha})(\mathbf{Q}_{s_1(\alpha)})^{-1} d_{11}^{\alpha} \quad (107a)$$

$$\mathbf{Y}_{12}^{\alpha} = \mathbf{Q}_{p_1(\alpha)}(\mathbf{e}_{11}^{\alpha} \otimes \mathbf{E}_{12}^{\alpha} \otimes \mathbf{e}_{22}^{\alpha\dagger})(\mathbf{Q}_{s_2(\alpha)})^{-1} d_{12}^{\alpha} \quad (107b)$$

$$\mathbf{Y}_{21}^{\alpha} = \mathbf{Q}_{p_2(\alpha)}(\mathbf{e}_{11}^{\alpha\dagger} \otimes \mathbf{E}_{21}^{\alpha} \otimes \mathbf{e}_{22}^{\alpha})(\mathbf{Q}_{s_1(\alpha)})^{-1} d_{21}^{\alpha} \quad (107c)$$

$$\mathbf{Y}_{22}^{\alpha} = \mathbf{Q}_{p_2(\alpha)}(\mathbf{e}_{21}^{\alpha} \otimes \mathbf{e}_{12}^{\alpha\dagger} \otimes \mathbf{E}_{22}^{\alpha})(\mathbf{Q}_{s_2(\alpha)})^{-1} d_{22}^{\alpha} \quad (107d)$$

The coefficients d_{uv}^{α} , where $u, v = 1, 2$ assume values:

$$d_{uv}^{\alpha} = 2^{(n_{uv}^{\alpha} - n_{s_v(\alpha)})} \quad (108)$$

where n_{uv}^{α} is the number of nuclei in the group which is transferred from the substrate s_v to the product p_u in the reaction α .

It follows from equation (84) that the superoperators \mathbf{Q} in equations (107a) to (107d) are represented by unitary matrices. Thus, their inverses can be replaced by their Hermitian adjoints:

$$\mathbf{Q}^{-1} = \mathbf{Q}^\dagger \quad (109)$$

It is seen from equations (96) and (109), as well as from the properties of direct products, that the following relations exist between the exchange superoperators of reactions α and $\omega(\alpha)$:

$$(\mathbf{d}_{ij}^\alpha)^{-1} \mathbf{Y}_{ij}^\alpha = (\mathbf{d}_{ji}^{\omega(\alpha)})^{-1} (\mathbf{Y}_{ji}^{\omega(\alpha)})^\dagger \quad (110)$$

where $i, j = 1, 2$.

Let the symbol \mathbf{X}_{uv}'' (where $u, v = 1, 2, \dots, S$) denote the properly weighted sum of the superoperators \mathbf{Y}^α which transform the vectors $\bar{\sigma}_v$ into $\bar{\sigma}_u$. The summation is taken over the set of reactions Λ_{uv} , which is composed of all of the reactions where A_u is formed from A_v :

$$\mathbf{X}_{uv}'' = (1/\tau_u) \left(\sum_{\alpha} \pi_{u,\alpha} \mathbf{Y}_{q_u, q_v}^\alpha \right) \quad (111)$$

where α belongs to the set Λ_{uv} , and $q_u, q_v = 1, 2$ depending upon the equation of the reaction α . The superoperators of the types \mathbf{X}_{0v}'' and \mathbf{X}_{u0}'' can obviously be neglected.

The superoperator \mathbf{X}_{vu}'' , which transforms the vectors of the space of a compound A_u into those of the space of A_v , can be calculated by the summation over the same set Λ_{uv} as in equation (111):

$$\mathbf{X}_{vu}'' = (1/\tau_v) \left(\sum_{\alpha} \pi_{v,\omega(\alpha)} \mathbf{Y}_{q_v, q_u}^{\omega(\alpha)} \right) \quad (112)$$

where α belongs to the set Λ_{uv} . Using the superoperators \mathbf{X}_{uv}'' , we may write the system of differential equations (104) for a space which is the direct sum of the Liouville spaces of individual components A_i . We call this, after Binsch, a composite Liouville space. (14) If we introduce the following notation:

$$\bar{\sigma}' = \bigoplus_{i=1}^S \bar{\sigma}_i \quad (113)$$

$$\mathbf{H}_s^D = \bigoplus_{i=1}^S \mathbf{H}_{s_i}^D \quad (114)$$

$$\mathbf{R} = \bigoplus_{i=1}^S \mathbf{R}_i \quad (115)$$

then the system of equations (104) takes the form:

$$d\tilde{\sigma}'/dt = -iH_S^D\tilde{\sigma}' + R(\tilde{\sigma}' - \tilde{\sigma}'_0) + X'\tilde{\sigma}' \quad (116)$$

The superoperator X' can be expressed as the sum of two matrices:

$$X' = X'' + \bar{K} \quad (117)$$

where the matrix X'' is composed of the superoperators X''_{ij} :

$$X'' = \begin{pmatrix} X''_{11} & X''_{12} & \dots & X''_{1S} \\ \dots & \dots & \dots & \dots \\ X''_{S1} & X''_{S2} & \dots & X''_{SS} \end{pmatrix} \quad (118)$$

and \bar{K} is the direct sum:

$$\bar{K} = \bigoplus_{i=1}^S (-1/\tau_i) E_i \quad (119)$$

Equation (116) has a form which is similar to that of the equation (35) of motion for non-exchanging spin systems. The analogy is even closer, as is shown later, since a judicious renormalization of the vectors in the composite Liouville space can convert equation (116) into one in which all the superoperators become Hermitian. Firstly we wish to draw attention to some of the properties of the exchange superoperator X' .

F. Properties of the exchange superoperator in composite Liouville space

The exchange superoperator X' commutes with the superoperator F_z^D in composite Liouville space:

$$X'F_z^D = F_z^DX' \quad (120)$$

where

$$F_z^D = \bigoplus_{i=1}^S F_{z_i}^D \quad (121)$$

In order to prove this it is sufficient to show that:

$$F_{z_i}^DX''_{ij} = X''_{ij}F_{z_j}^D \quad (122)$$

or [as follows from equation (111)] that:

$$F_{z_i}^DY_{q_i, q_j}^\alpha = Y_{q_i, q_j}^\alpha F_{z_j}^D \quad (123)$$

where q_i, q_j assume values from the set $\{1, 2\}$ depending on the equation

for the reaction α . We will demonstrate this in an example using the superoperator \mathbf{Y}_{11} . In other cases, the proof is analogous.

It is evident from equations (88) and (107a) that in order to prove equation (123) it is sufficient to show that:

$$(\mathbf{F}_{z_{11}}^D \otimes \mathbf{E}_{12} + \mathbf{E}_{11} \otimes \mathbf{F}_{z_{12}}^D)(\mathbf{E}_{11} \otimes \mathbf{e}_{21}^\dagger \otimes \mathbf{e}_{12}) \\ = (\mathbf{E}_{11} \otimes \mathbf{e}_{21}^\dagger \otimes \mathbf{e}_{12})(\mathbf{F}_{z_{11}}^D \otimes \mathbf{E}_{21} + \mathbf{E}_{11} \otimes \mathbf{F}_{z_{21}}^D) \quad (124)$$

where the subscripts ij refer to the space $L_{(A_{ij}^0)}$. Since the vectors $\mathbf{F}_{z_{12}}^D \mathbf{e}_{12}$ and $\mathbf{e}_{21}^\dagger \mathbf{F}_{z_{21}}^D$ are zero the products on both sides of equation (124) are equal to $\mathbf{F}_{z_{11}}^D \otimes \mathbf{e}_{21}^\dagger \otimes \mathbf{e}_{12}$. This proves that the commutation expressed by equation (120) is valid. One should note that for \mathbf{F}_z^L and \mathbf{F}_z^R equation (124) is valid only in those cases where all of the sets A_{ij} , with $i \neq j$, are empty, namely those referring to the intramolecular exchange of spins.

The superoperator \mathbf{X}' may always be reduced to diagonal form by a proper similarity transformation, because there is always one which can convert \mathbf{X}' into a Hermitian form \mathbf{X} :

$$\mathbf{X} = \mathbf{B}\mathbf{X}'\mathbf{B}^{-1} \quad (125)$$

where \mathbf{B} is the direct sum of the corresponding unit matrices which have been multiplied by proper coefficients:

$$\mathbf{B} = \bigoplus_{i=1}^S (c_i/2^{(n_i)})^{1/2} \mathbf{E}_i \quad (126)$$

In order to prove the Hermitian character of the superoperator \mathbf{X} it is sufficient to show that:

$$(b_i/b_j)\mathbf{X}_{ij}'' = (b_j/b_i)\mathbf{X}_{ji}''^\dagger \quad (127)$$

where $b_i = (c_i/2^{(n_i)})^{1/2}$. Upon consideration of equations (110), (111), and (112), it is sufficient to show that for any reaction in which A_j is formed from A_i the following holds:

$$b_i^2 d_{q_i, q_j}^\alpha \pi_{i, \alpha} / \tau_i = b_j^2 d_{q_j, q_i}^{\omega(\alpha)} \pi_{j, \omega(\alpha)} / \tau_j \quad (128)$$

where $q_i, q_j = 1, 2$. Using the definition of d_{uv}^α given by equation (108) we notice that:

$$2^{(-n_i)} d_{q_i, q_j}^\alpha = 2^{(-n_j)} d_{q_j, q_i}^{\omega(\alpha)} = 2^{(n_{q_i, q_j} - n_i - n_j)} \quad (129)$$

Moreover, it is evident from equations (60), (61) and (65) that:

$$c_i \pi_{i, \alpha} / \tau_i = c_i K_{i, \alpha} = c_j K_{j, \omega(\alpha)} = c_j \pi_{j, \omega(\alpha)} / \tau_j \quad (130)$$

Equations (129) and (130) prove that equation (128) and, hence equation (127), are valid. This shows the Hermitian character of the

superoperator \mathbf{X} . This property of the superoperator \mathbf{X} has been reported in the literature only for some special cases of equilibria. (47, 48)

For any equilibrium, either intra- or inter-molecular, the block of the superoperator \mathbf{X} , which is concerned with the eigenvalue -1 of the superoperator \mathbf{F}_z^D , is nonpositive. One may rigorously prove this point by using Levy-Hadamard's theorem (e.g. reference 49). It is also necessary to consider that the sum of the moduli of the elements in each of the rows of the matrix \mathbf{X}'' , from equation (118), is not larger than the modulus of the corresponding diagonal element of the $\bar{\mathbf{K}}$ matrix [equation (119)]. The inequality results from the fact that in the basis set of product spin functions the sum of the moduli of the elements in each of the rows of the \mathbf{Y}_{ij}^α matrix equals either 0 or 1. In addition, if any of the rows of the \mathbf{Y}_{ij}^α matrix has non-zero elements, then the same row in the $\mathbf{Y}_{i,q_j}^\alpha$ matrix, where $q_j = 1$ if $j = 2$ or else $q_j = 2$ if $j = 1$, contains only zeros.

Frequently, the form of the exchange superoperator is simplified. For intramolecular processes the equations (72) are already linear and the superoperators \mathbf{G} and \mathbf{Y} are equal to certain permutation matrices (in the basis sets of product spin functions):

$$\mathbf{G}^\alpha = \mathbf{Y}^\alpha = \mathbf{Q}_{p(\alpha)} \mathbf{Q}_{s(\alpha)}^\dagger \equiv \bar{\mathbf{Q}}^\alpha \quad (131)$$

In particular, for the simplest case of mutual exchange, the superoperator $\bar{\mathbf{Q}}^\alpha$ is equal to the direct product of the exchange operators $\hat{\mathbf{P}}$ introduced by Alexander: (36)

$$\bar{\mathbf{Q}}^\alpha = \hat{\mathbf{P}} \otimes \hat{\mathbf{P}} \quad (132)$$

For non-mutual intramolecular equilibria, if compounds A_i and A_j are converted into one another in only one way, the basis sets can be chosen such that the superoperators $\bar{\mathbf{Q}}$ become unit matrices. Thus, the superoperators \mathbf{X}'_{ij} take the form:

$$\mathbf{X}'_{ij} = \mathbf{E} \mathbf{K}_{ij} \quad (133a)$$

$$\mathbf{X}'_{ii} = \left(- \sum_{j \neq i} \mathbf{K}_{ij} \right) \mathbf{E} = (-1/\tau_i) \mathbf{E} \quad (133b)$$

where $i = 1, 2, \dots, S$, and \mathbf{K}_{ij} is the first-order rate constant for the formation of A_i from A_j ($\mathbf{K}_{ij} \equiv \mathbf{K}_{i,\alpha}$). For this particular case, (47) the superoperator \mathbf{X} assumes the form:

$$\mathbf{X}_{ij} = (\mathbf{K}_{ij} \mathbf{K}_{ji})^{1/2} \mathbf{E} \quad (134a)$$

$$\mathbf{X}_{ii} = \mathbf{X}'_{ii} \quad (134b)$$

G. Renormalization of the composite Liouville space

It has already been mentioned that the equation (116) of motion can be presented in a symmetric form provided that the basis sets of the individual subspaces of the composite space are properly normalized. Namely, if we substitute:

$$\mathbf{a} = \mathbf{B} \left(\bigoplus_{i=1}^s \mathbf{a}_i \right) \quad (135)$$

for each of the vectors \mathbf{a} of the composite Liouville space, and:

$$\mathbf{D} = \mathbf{B} \mathbf{D}' \mathbf{B}^{-1} \quad (136)$$

for each of the superoperators \mathbf{D}' , then the equation (116) of motion becomes:

$$d\bar{\sigma}/dt = -i\mathbf{H}_s^D \bar{\sigma} + \mathbf{R}(\bar{\sigma} - \bar{\sigma}_0) + \mathbf{X}\bar{\sigma} \quad (137)$$

This is due to the fact that the superoperators \mathbf{H}_s^D and \mathbf{R} , which have the structure of a direct sum according to equations (114) and (115), are invariant under such a renormalization.

In composite Liouville space, the expectation values of renormalized observables, calculated by using the renormalized $\bar{\sigma}$ matrix, are expressed by:

$$\langle \mathbf{v} \rangle = C' [\mathbf{v}^\dagger (\bar{\sigma} + \mathbf{e}^r)] \quad (138)$$

where C' is the corresponding proportionality coefficient:

$$C' = \left(\sum_{i=1}^s c_i \right)^{-1} \quad (139)$$

and

$$\mathbf{e}^r = \mathbf{B} \left(\bigoplus_{i=1}^s \mathbf{e}_i \right) \quad (140)$$

It may easily be checked that the expectation value of the observable \mathbf{v} is proportional to the sum of the expectation values of the individual components which have been weighted by the corresponding concentrations:

$$\langle \mathbf{v} \rangle = C' \sum_{i=1}^s c_i \mathbf{v}_i^\dagger \bar{\rho}_i \quad (141)$$

H. Lineshape equation for an exchanging system

In the renormalized composite Liouville space the superoperator F_z^D , defined by equation (121), commutes with all the (Hermitian) superoperators H_s^D , R , and X . Therefore, upon the proper rearrangement of the basis set in this space, one can obtain a factorization of the equation (137) of motion into blocks which are connected with individual eigenvalues of the superoperator F_z^D . This resembles the analogous procedure in the case of static NMR spectra, i.e. those for non-exchanging spin systems (Section II.E.2). The equations for the free induction decay M_x^{FID} and for the lineshape of an unsaturated steady-state spectrum, in terms of quantities from composite Liouville space, are therefore obtained for exchanging spin systems in a way which is analogous to that for non-exchanging systems (Section II.F).

Upon solving the equation (137) of motion with the renormalized initial condition:

$$\hat{\sigma}(0) = B \left\{ \bigoplus_{i=1}^S (\hbar\omega_0/kT)(f_{x_i} \sin \alpha + f_{z_i} \cos \alpha) \right\} \quad (142)$$

we obtain the free induction decay function in a form which is strictly analogous to that given in equation (50):

$$M_x^{FID}(t) = 2C f_{x(-1)} \exp[(-iH_{s(-1)}^D + R_{(-1)} + X_{(-1)})t] f_{x(-1)} + q_{-1}(t) \quad (143)$$

In equation (143), the subscript (-1) denotes the subspace of the composite Liouville space which is concerned with the eigenvalue -1 of the superoperator F_z^D (the subspace of single-quantum transitions). The vector f_x is normalized according to equation (135) and the $q_{-1}(t)$ function has the same meaning as in equation (50). The coefficient C is given by [equation (139)]:

$$C = C'(\hbar\omega_0/kT)(e^{\dagger} e^{\dagger})^{-1} \sin \alpha \quad (144)$$

The lineshape function, which is equal to the Fourier transform of M_x^{FID} , (98, 99) is given by:

$$f(\omega) = -C f_-^{\dagger} [-i(H_{s(-1)}^D - \omega E_{(-1)}) + R_{(-1)} + X_{(-1)}]^{-1} f_- \quad (145)$$

where the lowering operator f_- is normalized according to equation (135). We delete the subscripts (-1) in our further considerations.

For a system of S substances the dimension D of the subspace of the single-quantum transitions is equal to the sum of the dimensions of the subspaces for the individual substances D_i . The latter is given by:

$$D_i = \sum_{k=0}^{n_i-1} \binom{n_i}{k} \binom{n_i}{k+1} \quad (146)$$

Needless to say, the so-called combination transitions are also considered in this subspace. Lineshape equations for special forms of the relaxation matrix can also be written in terms of the Hilbert space. However, the notation becomes quite involved. This is probably the source of some erroneous simplifications which consist of neglecting combination transitions in the equations of lineshape. (50)

One should note that in reports on intermolecular spin exchange there are often errors in the renormalization of the vectors in composite Liouville space. (14, 51, 78) Such errors lead to erroneous lineshape equations in cases where the numbers of nuclei in the components of an equilibrium are not equal.

IV. COMPUTATION AND ANALYSIS OF DYNAMIC NMR SPECTRA

A. Simulation of dynamic NMR spectra

1. Introductory remarks

In a typical situation we are interested in the absorption mode of a dynamic spectrum, $f_{\text{abs.}}(\omega)$, which equals the real part of the complex function $f(\omega)$ given by equation (145). In most cases of unsaturated spectra the relaxation matrix which describes single-quantum transitions can be replaced by a constant $-\mathbf{E}/T_{2(\text{effective})}$ which is characteristic of the experimental conditions involved and reflects the inhomogeneity of the external magnetic field B_0 . The absorption mode spectrum is given by:

$$f_{\text{abs.}}(\omega) = C \operatorname{Re} \{ \mathbf{f}_-^\dagger [i(\mathbf{H}_s^D - \omega \mathbf{E}) + \mathbf{T}]^{-1} \mathbf{f}_- \} \quad (147)$$

where $\mathbf{T} = \mathbf{E}/T_{2(\text{effective})} - \mathbf{X}$. The computation of $f_{\text{abs.}}(\omega)$ often poses technical problems concerned with the size of the matrices appearing in equation (147). For intramolecular exchange the size can be reduced because of the mutually commuting superoperators \mathbf{F}_z^L and \mathbf{F}_z^R which also commute with the superoperators \mathbf{H}_s^D and \mathbf{T} in the single-quantum transition subspace. (15) This leads to a factorization into blocks in a properly ordered basis function set.

By analogy with non-exchanging spin systems the superoperators which commute with both the super-Hamiltonian and the superoperator \mathbf{T} in composite Liouville space may be called the constants of the motion. In some instances there may be additional constants of the motion which result from the conservation of some molecular symmetry in the exchange, from the magnetic equivalence of some nuclei, and from weak spin-spin coupling. (15, 52) For example,

in an exchange of the $ABCD \rightleftharpoons EFGH$ type the matrix of single-quantum transitions in equation (147) has a total size of 112×112 . However, it can be factorized owing to the commutation of F_z^L and F_z^R with H_s^D and T into blocks none of which is larger than 48×48 . For the four-spin system $A_3B \rightleftharpoons C_3D$ the largest block has a size of 4×4 due to magnetic equivalence factorization. Unfortunately for intermolecular exchange processes, and combinations thereof with intramolecular spin exchange, the superoperators F_z^L and F_z^R are not constants of the motion and the corresponding simplifications are not possible.

If the matrices which appear in the calculations do not exceed the size of 2×2 one can analytically derive the lineshape function, and this tends to make the computation rather trivial. Such cases are represented by all $A \rightleftharpoons B$ exchange processes and some other two-site exchange systems which give first-order spectra, as well as by the mutual $AB \rightleftharpoons BA$ exchange. The same is possible in calculations on spectral fragments of certain more complicated systems as reported in a previous review in this series by Sutherland. (53)

The general methods of computing dynamic NMR spectra which have so far been reported may be divided into two groups. One involves the point by point approach while the other is based on the diagonalization method.

2. Point by point methods

These consist of calculating values for the lineshape function (e.g. its absorption mode) at discrete points on the frequency axis of a dynamic spectrum. Their characteristic feature is that they require the repetition of all the calculations involved in the generation of the function at each of the selected spectral points. Thus the computational effort is proportional to the number of the points. The point by point calculation of the function $f_{\text{abs}}(\omega)$ can be directly performed by means of equation (147). Specialized procedures have been reported which are capable of computing the inverses of the complex matrices which appear in such problems. (54) However, methods based on calculating inverses of complex matrices are not very effective. Consequently the significant computational effort involved often leads to obtaining the rather useless information relating to the dispersion mode. A more effective point by point method has been employed by Newmark and Sederholm, in a program for simulating the dynamic NMR spectra of two- and three-spin systems. These are considered to exchange among, at most, three configurations within the same molecule. (55) They have reported an equation for the absorption mode of a dynamic spectrum which does not include any complex numbers. The calculation involves solving a system

of real linear equations for each of the selected points on the frequency axis of a spectrum. Use of the matrix identity has been made:

$$(\mathbf{W} + i\mathbf{V})^{-1} = (\mathbf{V}\mathbf{W}^{-1}\mathbf{V} + \mathbf{W})^{-1} - i\mathbf{W}^{-1}\mathbf{V}(\mathbf{V}\mathbf{W}^{-1}\mathbf{V} + \mathbf{W})^{-1} \quad (148)$$

The absorption spectrum can be expressed by:

$$f_{\text{abs.}}(\omega) = \mathbf{C}\mathbf{f}_-^\dagger[\mathbf{H}_s^D - E\omega]\mathbf{T}^{-1}(\mathbf{H}_s^D - E\omega) + \mathbf{T}]^{-1}\mathbf{f}_- \quad (149)$$

Equation (149) is valid provided that the matrix \mathbf{T} and that within the brackets are non-singular. It has been shown that this is always true in the case considered. (47) Since Newmark and Sederholm have used the exchange superoperator in its non-Hermitian form, such as that given in equation (117), their method is rather time-consuming. Probably, this is the reason why the method has been largely forgotten.

Recently an effective method of calculating the absorption mode of a dynamic NMR spectrum by the point by point approach has been suggested. (47) It is based on the symmetric form of the lineshape equation (147). One can always choose a real unitary matrix \mathbf{U} such that only the last element of the vector $\mathbf{f}'_- = \mathbf{U}\mathbf{f}_-$ is non-zero. The matrix ought to have its last column equal to the vector $(\mathbf{f}_-^\dagger\mathbf{f}_-)^{-1/2}\mathbf{f}_-$. Upon a transformation of equation (149), with the matrix \mathbf{U} , one obtains the $f_{\text{abs.}}(\omega)$ function in the form:

$$f_{\text{abs.}}(\omega) = \mathbf{C}_1[(\mathbf{H}_s^{D'} - E\omega)\mathbf{T}'^{-1}(\mathbf{H}_s^{D'} - E\omega) + \mathbf{T}']_{nn}^{-1} \quad (150)$$

where n is the size of the matrix, $\mathbf{C}_1 = \mathbf{C}(\mathbf{f}_-^\dagger\mathbf{f}_-)$, and the primed matrices are obtained by the unitary transformation, $\mathbf{T}' = \mathbf{U}^\dagger\mathbf{T}\mathbf{U}$, $\mathbf{H}_s^{D'} = \mathbf{U}^\dagger\mathbf{H}_s^D\mathbf{U}$. The method discussed consists of determining, at each of the spectral points considered, a lower triangular matrix \mathbf{N} such that the following matrix equation is obeyed:

$$\mathbf{N}\mathbf{N}^T = (\mathbf{H}_s^{D'} - E\omega)\mathbf{T}'^{-1}(\mathbf{H}_s^{D'} - E\omega) + \mathbf{T}' \quad (151)$$

where the superscript T denotes the transpose of a matrix. The decomposition into triangular matrices is always feasible since the matrix on the right-hand side of equation (151) is positive definite for all values of ω . (56) Thus, the equation for the absorption mode of a dynamic spectrum can finally be expressed in terms of the last diagonal element of the \mathbf{N} matrix:

$$f_{\text{abs.}}(\omega) = \mathbf{C}_1(\mathbf{N}_{nn})^{-2} \quad (152)$$

For computational purposes the right-hand side of equation (150) can conveniently be presented in the form:

$$f_{\text{abs.}}(\omega) = \mathbf{C}_1\{[\mathbf{Z} - \omega\mathbf{A} + \omega^2\mathbf{T}'^{-1}]^{-1}\}_{nn} \quad (153)$$

where $\mathbf{Z} = \mathbf{H}_s^{D'}\mathbf{T}'^{-1}\mathbf{H}_s^{D'} + \mathbf{T}'$, and $\mathbf{A} = \mathbf{H}_s^{D'}\mathbf{T}'^{-1} + \mathbf{T}'^{-1}\mathbf{H}_s^{D'}$. Obviously,

the ω -independent matrices \mathbf{Z} , \mathbf{A} , and \mathbf{T}'^{-1} have to be computed only once for the entire spectrum. The algorithm described above is employed in the ASES (Absorption Spectrum of Exchanging Systems) program which has been written in the Algol 1204 language. (47) The program can be used for simulating the dynamic NMR spectra of the spin-spin coupled systems which participate in intramolecular exchange among any number of conformations or configurations. The present version of the program allows one to take advantage of the simplifications which may result from one symmetry element of the spin system, from magnetic equivalence of the nuclei, and from weak spin-spin couplings.

The program considers mutual exchange as an exchange between different species. It appears that the method of simulation of dynamic NMR spectra employed in the ASES program is the most effective among point by point methods.

3. Diagonalization method

Contrary to the point by point approach the diagonalization method consists of the generation of an entire lineshape function in one step. (13, 14, 57–60) Time-consuming calculations are carried out only once. The resulting set of complex numbers can be used for a simple calculation of the lineshape (absorption and dispersion modes) at any desired point on the frequency axis. Thus, the complex matrix from equation (147) can be diagonalized by a similarity transformation using an ω -independent complex matrix \mathbf{W} :

$$\mathbf{\Lambda} - i\omega\mathbf{E} = \mathbf{W}^{-1}[\mathbf{i}(\mathbf{H}_s^D - \omega\mathbf{E}) - \mathbf{T}]\mathbf{W} \quad (154)$$

where $\mathbf{\Lambda} = \mathbf{i}\mathbf{\Omega} + \mathbf{\Gamma}$ and the real diagonal matrices $\mathbf{\Omega}$ and $\mathbf{\Gamma}$ are ω -independent. If we denote the number $(\mathbf{f}_-^+\mathbf{W})_k(\mathbf{W}^{-1}\mathbf{f}_-)_k$ by the symbol u_k , then the lineshape function can be expressed as the sum:

$$f(\omega) = C \sum_{k=1}^n u_k [i(\Omega_{kk} - \omega) + \Gamma_{kk}]^{-1} \quad (155)$$

where n is the matrix dimension. The absorption mode is given by:

$$f_{\text{abs.}}(\omega) = C \sum_{k=1}^n [\Gamma_{kk} \text{Re}(u_k) + (\Omega_{kk} - \omega) \text{Im}(u_k)] [(\Omega_{kk} - \omega)^2 + \Gamma_{kk}^2]^{-1} \quad (156)$$

where Re and Im denote the corresponding real and imaginary parts, respectively. Thus, any dynamic absorption spectrum is a sum of absorption-dispersion Lorentzian curves.

The method discussed above has been used in the algorithm of the DNMR-3 program for calculating the dynamic NMR spectra of

systems which participate in multi-site intramolecular spin exchange. (61) The program includes possible simplifications due to one symmetry element of the spin systems as well as to magnetic equivalence. The mutual exchange case can be treated in this program within the spin space of a single nuclear configuration (by the so-called mutual factorization). However, the DNMR-3 program is based on the non-symmetric form of the lineshape equation which is derived from the non-symmetric form of the equation (116) of motion. For the symmetric form of the lineshape equation, the diagonalization method can be simplified to a certain extent by selecting the diagonalizing matrix \mathbf{W} in such a way that $\mathbf{W}^{-1} = \mathbf{W}^T$.

4. Conclusions

It appears that programs which are based on the diagonalization method are the most efficient as regards computer time. However, in practical problems it is seldom necessary to calculate a dynamic NMR spectrum within a broad range of frequencies. Usually those parts of the spectral curve where only the baseline makes a significant contribution provide relatively little information about the dynamic spectrum considered. Often the point by point approach can favourably compete with the diagonalization approach since methods which operate on real matrices require less memory space in a computer than those which diagonalize complex matrices. Moreover, the diagonalization of complex matrices is impossible for certain combinations of spectral parameters. (23, 48)

Currently available computer programs can in theory deal with any intramolecular exchange type as far as spectrum simulation is concerned. Limitations result only from computer speed and capacity. However, no general algorithm has so far been suggested for intermolecular spin exchange.

B. Analysis of dynamic NMR spectra

1. Unsophisticated methods

Practical applications of the theory of NMR lineshapes of dynamic spectra can be divided into two general groups. One concerns investigations of intra- and inter-molecular reaction mechanisms. The other deals with the determination of kinetic and thermodynamic parameters for equilibria. In the former case the verification of reaction mechanisms usually consists of qualitative comparisons between experimental spectra and those simulated for various values of the rate constants using either visual inspection or visual fitting.

The other case may be properly termed spectral analysis since it involves procedures for extracting quantitative information about rate constants and equilibrium concentrations. For simple spin systems, such as that of a single nucleus A which is exchanging between two sites or that of a simple $AB \rightleftharpoons BA$ mutual exchange, a number of unsophisticated methods have been devised. They consider, for example, only one of the lineshape parameters concerned or only the coalescence point of the corresponding resonance signals. So far the most common practice is to use the method of visual fitting even in attempts to obtain quantitative information. If the visual comparison of entire spectral curves is involved the method is frequently called a total lineshape analysis. This term may be too optimistic in such cases. Such simple methods have been discussed in detail in the literature. (62–66) However, it seems that, from a methodological point of view, methods based on the least-squares fitting of theoretical lineshapes to experimental spectra are more justified. We therefore consider some fundamental problems of the least-squares approach.

2. The least-squares method

In this method the comparability criterion, for theoretical and experimental curves is the sum of the squares of deviations: (67)

$$\varepsilon = \sum_{i=1}^{D_y} [f_{\text{abs.}}(\omega_i) - y(\omega_i)]^2 \quad (157)$$

where $y(\omega_i)$ is the experimental value of the absorption measured with some random error at a frequency $\omega_i/2\pi$ ($i = 1, 2, \dots, D_y$). For a given experiment the set of frequencies (channels) $\omega_i/2\pi$ is fixed. Thus the ε function depends only on the parameters which define the superoperators in the lineshape equation. These lineshape parameters may be treated as the components of a D_g -dimensional vector \mathbf{g} . The g_i parameters may include those of the corresponding static spectra of the components of the equilibrium considered, e.g. chemical shifts and coupling constants (the magnetic parameters), as well as kinetic parameters (rate constants or combinations thereof), thermodynamic parameters (equilibrium concentrations of components), and some experimental quantities such as the intensity coefficient, the field inhomogeneity and the baseline equation which are characteristic of the experimental conditions employed. Equation (157) can be concisely written using vector notation in order to point out explicitly the functional dependence, on the lineshape parameters, of the vector \mathbf{f} :

$$\varepsilon(\mathbf{g}) = [\mathbf{f}(\mathbf{g}) - \mathbf{y}]^T [\mathbf{f}(\mathbf{g}) - \mathbf{y}] \quad (158)$$

where $\mathbf{f}^T = [f_{\text{abs.}}(\omega_1, \mathbf{g}), \dots, f_{\text{abs.}}(\omega_{D_y}, \mathbf{g})]$ and $\mathbf{y}^T = [y(\omega_1), \dots, y(\omega_{D_y})]$.

The solution of a least-squares problem consists of finding a set of parameters \mathbf{g}_{\min} such that the function $\varepsilon(\mathbf{g})$ attains a minimum value at the point \mathbf{g}_{\min} . The gradient of the function becomes zero at this point:

$$[d\varepsilon(\mathbf{g})/d\mathbf{g}]_{\mathbf{g}=\mathbf{g}_{\min}} = 2[d\mathbf{f}(\mathbf{g})/d\mathbf{g}]_{\mathbf{g}=\mathbf{g}_{\min}} [\mathbf{f}(\mathbf{g}_{\min}) - \mathbf{y}] = 0 \quad (159)$$

In equation (159) the column vector $d\varepsilon/d\mathbf{g}$ consists of the derivatives:

$$[d\varepsilon(\mathbf{g})/d\mathbf{g}]_i = \partial\varepsilon(\mathbf{g})/\partial g_i \quad (i = 1, 2, \dots, D_g) \quad (160)$$

The $d\mathbf{f}/d\mathbf{g}$ matrix has the elements:

$$[d\mathbf{f}(\mathbf{g})/d\mathbf{g}]_{ij} = \partial f_{\text{abs.}}(\omega_j, \mathbf{g})/\partial g_i \quad (161)$$

where $i = 1, 2, \dots, D_g$, and $j = 1, 2, \dots, D_y$.

In problems concerning dynamic NMR spectra the relationship between \mathbf{f} and the parameters \mathbf{g} is non-linear and therefore the determination of the minimum must be carried out by an iterative procedure. This is often a complicated computational problem and the procedure need not converge.

The least-squares methods may generally be applied using one of two possible approaches. One of them requires a computation of the function gradients whilst the other does not. Gradient methods use iterative computation of corrections to consecutive approximate solutions $\mathbf{g}^{(i)}$ according to the equation:

$$\mathbf{g}^{(i+1)} = \mathbf{g}^{(i)} - \alpha_i (\mathbf{A}^{(i)} + \mathbf{E}\beta_i)^{-1} [d\varepsilon(\mathbf{g})/d\mathbf{g}]_{\mathbf{g}=\mathbf{g}^{(i)}} \quad (162)$$

where α_i and β_i denote properly adjusted coefficients. $\mathbf{A}^{(i)}$ is a positive definite matrix which usually changes after each iteration step. If we assume that:

$$\mathbf{A}_{(\mathbf{g})}^{(i)} = \{[d\mathbf{f}(\mathbf{g})/d\mathbf{g}]_{\mathbf{g}=\mathbf{g}^{(i)}}\} \{[d\mathbf{f}(\mathbf{g})/d\mathbf{g}]_{\mathbf{g}=\mathbf{g}^{(i)}}\}^T \quad (163)$$

we obtain the Gauss-Newton method. The matrices $d\mathbf{f}/d\mathbf{g}$, and hence the gradients $d\varepsilon(\mathbf{g})/d\mathbf{g}$, can either be calculated from exact equations or approximated by the corresponding quotients of small finite increments.

Methods which do not employ gradients are diversified, between the most primitive ones, which use a trial-and-error approach to the best solution among a finite set $\mathbf{g}^{(1)} \dots \mathbf{g}^{(n)}$, and sophisticated procedures such as the Powell method. (69)

The matrix \mathbf{A} given by equation (163) is used for the evaluation of errors in the estimated values of individual parameters. It is usually assumed that the standard deviation of a parameter g_i is given by the expression:

$$dg_i = \sqrt{\{\varepsilon(\mathbf{g}_{\min})/(D_y - D_g)\} \mathbf{A}^{-1}(\mathbf{g}_{\min})_{ii}} \quad (164)$$

where the $\varepsilon \mathbf{A}^{-1}/(D_y - D_g)$ matrix plays the role of the covariance matrix

of the vector \mathbf{g} whose elements are random variables. Strictly speaking equation (164) gives the standard deviation of a parameter g_i only in those cases where the function fitted is linearly dependent on the vector \mathbf{g} and the errors in the experimental function have normal distributions. (67) Otherwise the interpretation of the results as standard deviations is only approximate.

A number of algorithms and computer programs for iterative analysis of dynamic NMR spectra have been reported. (51, 70–79) Most of them are only suited to those cases where the lineshape function can be expressed without invoking matrices. Only a few procedures are known which have a more general character. The GPLONK and CLSFIT programs have been prepared in order to analyse dynamic NMR spectra within the classical approximation of multi-site exchange. The spectra examined can be approximated in terms of those of non-coupled nuclei which exchange among sites characterized by different chemical shifts. (70–73) The diagonalization method is employed in the programs for computing the lineshape function. No details are given on the procedure for searching for a minimum of the function ϵ . It is reported that the algorithm is efficient, from the point of view of computer time, owing to a considerable reduction in the most time consuming step—the diagonalization of a complex matrix. This is achieved for each step by using the diagonalizing matrices obtained in the preceding step. The programs have been successfully employed in the dynamic NMR analysis of spectra of weakly spin–spin coupled systems. Often the fitting procedure includes simultaneously the rate constants and the line positions involved.

Recently the ASESIT program has been reported which is based on the quantum mechanical theory of dynamic NMR spectra. (77) It can deal with any spin system, strongly or weakly coupled, which is exchanging between two molecular configurations. The program includes simplifications resulting from one symmetry element, magnetic equivalence, and weak coupling. The computation of the lineshape function is carried out by the point by point method which is described in Section IV.A.2 for the ASES procedure. The gradient of the function ϵ is calculated by using exact equations. The latter are obtained by differentiating the $f_{\text{abs.}}(\omega)$ function from equation (150) with respect to the parameters \mathbf{g} and using equations (151) and (152). They have the following form which is convenient for computation:

$$\begin{aligned} \partial f_{\text{abs.}}(\omega_i, \mathbf{g}) / \partial g_j = & -C_1(N_{nn})^{-2}(\mathbf{N}^{-1})_n \\ & \times \{ \partial[(\mathbf{H}_s^{\text{D}'} - \mathbf{E}\omega_i)\mathbf{T}'^{-1}(\mathbf{H}_s^{\text{D}'} - \mathbf{E}\omega_i) + \mathbf{T}'] / \partial g_j \} (\mathbf{N}^{-1})_n^{\text{T}} \end{aligned} \quad (165)$$

where $(\mathbf{N}^{-1})_n$ denotes the last row of the inverse of the lower triangular matrix \mathbf{N} from equation (151). In the calculation of a dynamic NMR spectrum by a method such as that employed in the ASES procedure (Section IV.A.2) the $(\mathbf{N}^{-1})_n$ vector, which is common to all derivatives at a given value of ω_i , can be obtained with only a slight increase in computational effort. The evaluation of the derivatives of the matrix with respect to the parameters g_j is rather straightforward. It results from the fact that the matrix \mathbf{U} , which transforms the unprimed matrices into the primed ones, may be chosen such that its elements are simple functions of the equilibrium concentrations of exchanging species. For a two-site exchange such a matrix \mathbf{U} transforms the matrix \mathbf{T} into its diagonal form and this yields a further simplification in the calculation. The ASESIT program has been successfully tested on simulated spectra which are perturbed with artificial random noise as well as on practical examples of spin-coupled and non-coupled systems. (80, 81) In the case of an $\text{AB}_n \rightleftharpoons \text{CD}_n$ exchange it is possible simultaneously to optimize nine parameters: the rate parameter and the population for either of the components, the four chemical shifts, the two coupling constants, and the intensity coefficient.

It is difficult to judge from the available literature data which of the iterative methods of dynamic NMR analysis will prove to be the most efficient. One should note, however, that the evaluation of the D_g -dimensional gradient of the $\varepsilon(\mathbf{g})$ function in the ASESIT program takes less time than computing D_g times the value of the function. This suggests that gradient methods are more efficient than those which do not use gradients as far as the point by point approach is concerned. In our opinion the opposite is true for the diagonalization method. In this case the methods which employ gradients require time-consuming numerical differentiation of the lineshape function. This may offset the efficiency of the diagonalization approach.

V. SOME PRACTICAL PROBLEMS

In the preceding sections the theory of the lineshape of dynamic NMR spectra as well as methods of analysis are considered in detail. However, in practical applications some additional problems must be solved.

It is quite important for the spectra measured to represent the pure absorption mode with neither saturation nor transient effects. They should be measured in a homogenous external magnetic field B_0 in order to obtain purely Lorentzian lineshapes for individual spectral transitions. The signal-to-noise ratio should be as high as possible and experimental

conditions ought to be clearly determined. In theory it is possible to consider various deviations from such ideal conditions but this requires the introduction of some additional parameters. The latter may make the somewhat involved process of dynamic NMR analysis even more complicated.

Methods for obtaining good dynamic spectra have been discussed in the literature. (64, 82) We are not going to pursue that problem in this article. There are other questions to be considered such as the choice of a model for spin exchange, selection of the parameters which are to be fitted, assignment of the tentative values which are required at the beginning of an iterative process, and the estimation of errors. We recommend some ways of dealing with such problems which are based on methods available in the literature as well as on those obtained from our own experience. Whilst we do not pretend that these represent the only solution they do reflect our views on the correctness and generality of such methods.

A. Selecting a model for exchange

If all possible long-range couplings are considered most of the molecules, which constitute interesting objects for investigation by dynamic NMR methods, represent quite complicated spin systems. We are usually compelled to make some simplifications in the model of exchange by considering lineshape functions for simpler spin systems. Otherwise the computational effort involved may go beyond reasonable limits. In this section we discuss such approximations in detail.

1. Neglecting some spin-spin couplings

It is intuitively clear that the neglect of very weak couplings, those which do not result in observable signal splitting or broadening in a static NMR spectrum, should not lead to any significant error in the total lineshape analysis of the corresponding dynamic spectra. However, it is not easy to formulate a general method of validation for such assumptions. The history of the investigation of internal rotations in *N,N*-dimethylformamide and *N,N*-dimethylacetamide as well as the recent testing of calculations by Drakenberg *et al.* provide a warning. (83, 84) One should note, however, that an analysis of Drakenberg's calculations suggests that a change of only 0.1 Hz in the natural linewidth, assumed in the consideration of the theoretical spectra, practically compensates for the entire effect of neglecting long-range couplings. In some cases, especially those where the relative chemical shifts between different magnetic environments are small, weak

couplings may certainly determine the accuracy of the method employed.

An extreme example of this type of approximation is provided by the work of Bushweller *et al.* which is concerned with the ring inversion of 1,1-dimethyl-1-silacyclohexane. (85) The authors have assumed that the averaging of the signals of the axial and equatorial protons in positions 2 and 6 can be described by a simple $A \rightleftharpoons B$ model of two spectral lines which are characterized by unequal widths. However, the precision of the results obtained by such approximations seems to be rather undetermined.

2. Multiplet components treated as signals from different nuclei

When the lineshape equation (147) is applied to intramolecular exchange, i.e. when the exchange superoperators are given by equation (134), it can be expressed by using a proper unitary supertransformation U_i in terms of the eigenbases of the super-Hamiltonians $H_{s_i}^P$ of the individual molecular configurations. In the eigenbasis the diagonal elements of each H_s^P represent the positions of spectral lines on the energy (frequency) scale for the corresponding static spectrum. The squares of the elements of the vectors f_{-i} are then proportional to the intensities of the corresponding spectral lines. The off-diagonal blocks derived from the exchange superoperator have the form:

$$\tilde{X}_{ij} = (K_{ij}K_{ji})^{1/2}U_i^\dagger U_j \quad (166)$$

However, if all the spin Hamiltonians of the molecules involved commute with each other, then $U_i^\dagger U_j = E$ and $\tilde{X} = X$. Equation (147) then becomes identical with a special case of the classical equation given by Sack for multi-site exchange. (30) This happens when the latter equation is transformed into its symmetric form. In the case considered each of the spectral lines may be assumed to arise from the resonance absorption of a group of non-coupled nuclei. The entire equation is partitioned into as many sub-equations as there are lines in the spectra of any of the conformations involved because each line has its counterparts in the spectra of the remaining conformations. Thus, the entire exchange process may be expressed in terms of independent exchange processes within each of the groups of mutually corresponding spectral lines.

We indicate two cases where the super-Hamiltonians which describe a spin system in various conformations commute. This occurs either when only first-order splittings are observed in a static spectrum (corresponding to Hamiltonians which are diagonal in the basis sets of product spin functions) or when the spectra of individual conformations are identical

but shifted from each other on the frequency scale, i.e. when $J_{ij}^{(1)} = J_{ij}^{(2)} = \dots$ and $\delta_i^{(1)} = \delta_i^{(2)} + \Delta\delta^{(1,2)} = \dots$. Such conditions are seldom fulfilled entirely. More often both of them simultaneously exist to a certain extent, and they mutually enhance each other's effects. A practical example may be found in the spectra of *N,N*-diethyl-amides where dynamic effects are observed due to rotation around the N-CO bond. (86) A general program for the iterative analysis of dynamic NMR spectra within this approach has been reported by Reeves and Shaw (Section IV.B.2). (70-73)

A similar simplification is commonly used in the description of the dynamic effects observed for protons which are attached to carbon atoms which in turn are bonded to an ammonium group where the ammonium protons are exchanging with the environment. (87)

3. Weak coupling approximation

If a spin system, in all its conformations, is composed of two (or more) weakly-coupled groups G_A and G_X such that the exchange does not alter the assignments of the nuclei to the groups G_A and G_X , and if the A and X sub-spectra are significantly shifted from each other on the frequency scale, we can then delete the AX off-diagonal terms in the Hamiltonians. This means that interactions between the groups are treated as first-order perturbations, and that the calculation of the corresponding dynamic spectra is much simplified. (52) Weak coupling is defined here in the same way as for static spectra, i.e. all chemical shifts $\Delta\delta_{AX}$ should be much larger than the largest coupling constant J_{AX} . Such a simplification has been applied to the description of the spectral lineshape for *N*-acetylpyrrole where dynamic effects arise from the rotation of the acetyl group. (89) The ring protons are assumed to represent an ABXY \rightleftharpoons BAYX system, and a good fit is obtained between the experimental and theoretical spectra.

The ASesIT program (Section IV.B.2) can readily be used with the inclusion of weak-coupling simplifications. It appears that the weak-coupling approximation does not adversely affect the accuracy of the results if employed for heteronuclear systems and homonuclear spin-spin couplings of the long-range type. Unfortunately, in most cases where homonuclear couplings give rise to what is apparently considered as first-order splitting in the spectra, the intensities of the components of the spectral multiplets show measurable deviations from those predicted from the corresponding first-order splitting patterns. Usually within a pair of multiplets the innermost components show enhanced intensity whilst the outer components are weaker. Such effects can be allowed for by introducing empirical coefficients which modify the corresponding

intensities. (52) However, it is difficult to estimate the errors involved in such methods.

4. *Single-nucleus representation of a group*

If the spin system $A_nXYZ\dots$ contains a group A_n of n equivalent nuclei, and if the signals of the A_n group are clearly distinguished in all molecular configurations which exchange, the lineshape of A_n is almost independent of the number n apart from the total intensity. If we are interested in the computation of the spectrum of the A_n group only, it is convenient to assume the much simpler $AXYZ\dots$ model. The rationale for the approximation lies in the fact that a dynamic spectrum of the $A_nXYZ\dots$ system, which exchanges between different configurations, can be exactly divided into $E(n/2) + 1$ subspectra of so-called spin isomers of the $A^IXYZ\dots$ type. (15) Here $E(x)$ means the integer part of x , and A^I represents a nucleus with spin $I = n/2, n/2 - 1, \dots, n/2 - E(n/2)$. Differences among the subspectra in the A part of the spectrum tend to vanish with a decrease in the coupling between the A group and the remaining spins. This approximation has been employed in an investigation of the rotation of the diethylamino group in N,N -diethylbenzamide. (81)

All the approximations discussed introduce significant simplifications into the calculations and reduce the amount of computer time required to solve dynamic NMR problems. It has been mentioned before that such approximations constitute a compromise between the complexity of the objects investigated and the efficiency of the scientific tools available. This compromise need not introduce serious systematic errors. Nor should it reduce the accuracy of the results obtained, particularly if both very slow and very fast exchange rates are excluded from consideration. Sometimes it is possible to test this by theoretical calculations of dynamic spectra, possibly without any approximations, followed by an analysis of the calculated lineshapes by one of the approximate methods. The degree of self-consistency of the procedure, from the point of view of kinetic parameters, can serve as a measure of the validity of the approximation employed. If we have to use drastic approximations in the model of exchange, such as those in the case of 1,1-dimethyl-1-silacyclohexane, (85) the results may contain considerable systematic errors. These can occur in spite of using even the most refined and time-consuming methods of analysis. In such cases the accuracy is rather indefinite as far as the enthalpy and entropy of activation are concerned. The only thermodynamic parameter that can be interpreted in a reasonable way is the free energy of activation, ΔG^\ddagger .

B. Initial estimates of rates of exchange

The evaluation of kinetic parameters (rate constants) is usually the principal aim of dynamic NMR measurements. The parameters are optimized by spectrum fitting procedures. Since these are non-linear there is a necessity for making some initial assumptions about the parameters. Therefore, the question arises as to how accurate should the initial guess be. The acceptable range of such an initial error depends on the algorithm employed. If it is too small the convergence of the fitting process may often be slow or the procedure may even diverge. In the case of the ASESIT program, which is applicable to two-site exchange, the initial guess may be within a factor of 2 with respect to the true value of the rate constant considered. For multi-site exchange processes, where several kinetic parameters affect the lineshape, the problem may be quite difficult. For initial estimates of rates of exchange, one can profitably employ any of the approximate methods described in the literature. A good method is to compare visually an experimental spectrum with that simulated for a set of assumed parameters. However, in most cases simple methods which employ only one lineshape parameter should be satisfactory. Especially useful is the following equation, where w_e is the dynamic broadening of any spectral line of conformer i:

$$1/\tau_i = \pi \Delta w_e \quad (167)$$

This is valid, as shown by Alexander, for any spin system in the slow-exchange range provided that the broadened lines do not overlap appreciably with each other. (36) The following three equations can also be useful:

$$K = 2^{-1/2} \pi |\delta_A - \delta_B| \quad (168)$$

This gives the rate of a symmetric $A \rightleftharpoons B$ exchange at the coalescence point, i.e. when the minimum between the two peaks involved disappears; (64)

$$K = 2^{-1/2} \pi [(\delta_A - \delta_B)^2 + 6J_{AB}^2]^{1/2} \quad (169)$$

which gives the rate of mutual $AB \rightleftharpoons BA$ exchange at the coalescence point of the spectrum; (62) and

$$(K_{12} + K_{21})/2 = 2\pi p_1 p_2 (\delta_A - \delta_B)^2 / \Delta w_e \quad (170)$$

which applies to any $A \rightleftharpoons B$ exchange process in the fast-exchange limit. (90) In equation (170) p_1 and p_2 are the corresponding populations, Δw_e is the exchange broadening of the observed singlet, and the left-hand side represents the means of the forward and reverse conversion rates. These three equations describe only specific cases of exchange. However, if

they are used judiciously, initial estimates of exchange rates may be obtained for less simple models of exchange.

The approximate evaluation of kinetic parameters can also be carried out using other simple equations: for example, those derived for symmetric $A \rightleftharpoons B$ systems, (64, 66) diagrams constructed for unsymmetric $A \rightleftharpoons B$ systems, (65) or those for the case of averaged pairs of doublets of the type $A_nX \rightleftharpoons B_nY$ where $J_{AX} = J_{BY}$ etc. (52)

As soon as results are obtained from a dynamic spectrum at any temperature, initial approximations of the rate of exchange at other temperatures can be calculated from the Eyring equation under the assumption that the entropy of activation, ΔS^\ddagger , is zero.

C. Natural line-width

It has already been mentioned in Section IV.A.1 that relaxation effects in dynamic NMR spectra are usually dealt with by replacing the relaxation matrix with an experimentally adjusted quantity $(T_{2(\text{effective})})^{-1}E$ where $(T_{2(\text{effective})})^{-1}$ is the so-called natural line-width. It is a common assumption that the natural line-width in a dynamic NMR spectrum is the width at the half-height of a hypothetical Lorentzian lineshape function which represents the resonance signals of the spectrum under the conditions of measurement but either without exchange or with a very fast exchange rate. In order to determine this quantity we may measure the actual signal width at the half-height for a standard substance. This is generally justified since, under the usual experimental conditions for recording dynamic NMR spectra, the relaxation of spins of 1/2 is slow. Hence the widths of those signals which are not affected by exchange are determined mainly by field inhomogeneity which is the same for all of the nuclei involved. However, in spite of this experimental advantage, accurate measurement of the natural line-width may be difficult for several reasons. For example, difficulties may arise due to minor differences between the widths of the signal from the standard employed and those of the exchanging spin systems; some residual dynamic effects may be present in the spectra which are considered to represent very slow or very fast exchange. Overlapping of spectral lines may also occur.

The significance of the natural line-width for estimating dynamic NMR parameters, particularly the enthalpy and entropy of activation, has been pointed out in the literature. (91–93) It follows from our experience that an error of 0.2 Hz in the natural line-width for a symmetric $A \rightleftharpoons B$ system, characterized by $\Delta G^\ddagger = 60 \text{ kJ mol}^{-1}$ and $\Delta\delta_{AB} = 20 \text{ Hz}$, can result in an error of 3 kJ mol^{-1} in ΔH^\ddagger and 10 $\text{J mol}^{-1} \text{ K}$ in ΔS^\ddagger . An overestimation of the natural line-width results in a

decrease in the apparent rate of exchange estimated from a spectrum in the slow-exchange limit, and in a corresponding increase in the fast-exchange range. In such a case the straight line in the Eyring plot is apparently pivoted around the coalescence point, and the deviation increases with the increasing range of exchange rates. Thus, an unjustified extension of the range of temperature over which dynamic NMR measurements are carried out may result in a serious error in the values obtained for the activation parameters.

A recommended method for the estimation of natural line-widths in the dynamic range of an NMR spectrum is based on the line-width of a standard signal, w_0 , which is not affected by the exchange:

$$w = w_0 + \Delta w_0 \quad (171)$$

The correction, Δw_0 , which represents a difference in line-width resulting from different relaxation times and weak spin-spin couplings that are not considered in an explicit form in the model of exchange, should be as small as possible. It is estimated by a comparison of the line-width of the standard with that of the system being investigated outside the range of dynamic effects in the spectrum. Allowance is made for Δw_c which represents broadening due to unresolved splittings resulting explicitly from the assumed model of the exchanging spin system. If this is not possible then the comparison should be made at the limits of the dynamic range, making allowance for Δw_c and Δw_e , where the latter correction is the dynamic (residual) broadening at the limits of the range. If the value of Δw_0 thus obtained is large it implies either that the spectra are saturated or that some factors are operating which promote relaxation, e.g. the presence of quadrupolar nuclei, paramagnetic contaminations, or a high viscosity of the sample. The compensation of such effects, by introducing corrections to the natural width, is hardly justified. It should be considered as the last resort when no better solution is available.

Next we deal with the nature of the correction Δw_c . The resonance signals in a spectrum may be composed of overlapping, closely spaced components. Usually this is caused by either weak spin-spin couplings (we consider here only those which *are included* explicitly in the assumed model of an exchanging spin system) or by almost degenerate transitions in the spin multiplets. (81) Such effects should be compensated for by the correction Δw_c which can be determined from measurement of an apparent line-width, w_a , in a theoretical spectrum calculated for a reasonably assumed value of the natural line-width, w_{theor} . The correction ($w_a - w_{\text{theor}}$) is virtually independent of the value of w_{theor} .

It is well known that, under conditions of very fast or very slow exchange, dynamic NMR spectra consist of almost purely Lorentzian lines which are only slightly broadened with respect to the corresponding static spectra. The observed line-width can therefore be partitioned into the following approximate contributions:

$$w_{\text{obs}} = w + \Delta w_c + \Delta w_e = w_0 + \Delta w_0 + \Delta w_c + \Delta w_e \quad (172)$$

where Δw_e is the exchange broadening. This decreases with an increase in difference between the rate of exchange involved and that corresponding to the coalescence point of individual spectra. However, it is not always possible to extend measurements over sufficiently low and high rates of exchange in order to make the exchange broadening Δw_e insignificant. In the case of a symmetric $A \rightleftharpoons B$ interconversion where $\Delta\delta_{AB} = 20$ Hz, $\Delta G^\ddagger = 60$ kJ mol⁻¹, and $\Delta S^\ddagger = 0$, if we assume the temperature at which the signals collapse $T_{\text{coalescence}} = 10^\circ\text{C}$, the residual exchange broadening at -40°C and at $+80^\circ\text{C}$ amounts to about 0.05 Hz. In order to determine accurately the natural line-width involved, one must therefore estimate the value of Δw_e for the spectra at the lowest and the highest temperatures employed.

The following extrapolation procedure may be used which is based on the fact that the exchange rate determined from signal coalescence is that which is the least dependent on the natural width of the signals. Additionally in most cases the entropy of activation ΔS^\ddagger is small. One may therefore employ the total lineshape analysis in order to determine the rate of exchange and ΔG^\ddagger from one or more spectra within the range of coalescence by means of the assumption that $w = w_0$. From the Eyring equation and the values obtained for ΔG^\ddagger , assuming that $\Delta S^\ddagger = 0$, one can estimate the rates of exchange from equations (167) and (170) or from a plot of $\Delta w_e = f(K)$ drawn for simulated spectra. The approximate value of Δw_0 obtained from equation (172) may then be applied to the total lineshape analysis of the spectra over the entire range of temperatures used. If the value of ΔS^\ddagger obtained in this way is markedly different from zero one should continue the iteration until convergence, with respect to the entropy, is reached. After the first step in such an iteration it is unnecessary to use the full lineshape analysis since the previously found rate parameters can properly be corrected using relations of the type $\Delta w_e = f(K)$.

It sometimes happens that different values of Δw_0 are obtained for the low- and high-rate limits of exchange. In such cases interpolated values of Δw_0 should be used for the spectra within the intermediate range of exchange rates.

It is obvious from the discussion that the procedure of natural line-

width determination is quite complicated. One might express some doubt as to whether introducing corrections of the order of 0.1 Hz is reasonable, since even in carefully controlled experiments the accuracy in the line-width determination is usually not better than 0.1 Hz. We should remember, however, that the error introduced due to neglect of Δw_0 is systematic whilst that in w_0 is random.

The natural line-width parameter, w , can in principle be determined together with the other parameters of an exchanging spin system by using the lineshape fitting procedure. However, this method is not effective as far as the line-width is concerned. The natural line-width, w , constitutes an excessive parameter in most cases. (75) It is correlated with the kinetic parameter (rate of exchange) in dynamic spectra which are characterized by small values of Δw_e . It is virtually impossible to determine w using the lineshape analysis if approximations such as a neglect of weak spin-spin couplings etc. are used. All this, as well as the fact that the procedure discussed for obtaining the natural line-width by using a standard seems to be reliable, indicate that attempts to include the line-width into a set of parameters which are estimated from spectrum fitting procedures are not justified.

D. Chemical shifts and spin-spin couplings in dynamic NMR spectra

In this section problems concerning the extraction of chemical shifts and spin-spin coupling constants from dynamic NMR spectra are discussed by means of the example of a two-configuration exchange. It is the most commonly investigated case and an extension of these considerations to that of multi-configuration exchange is not difficult. We additionally assume that the populations of the two exchanging species involved are known in advance. We shall consider the case of unknown populations in the following section.

A static NMR spectrum, that representing a non-exchanging spin system, contains full information about the chemical shifts and coupling constants of the system. This is also apparently true for dynamic spectra in the range of slow exchange where the fine structure of the spectrum is still visible. Static spectra are analysed by standard methods which usually consider spectral line positions. (94) Recently methods based on spectral lineshape fitting have been suggested. (95)

It seems to be necessary in the analysis of dynamic NMR spectra in the slow-exchange region to optimize simultaneously the kinetic parameters and those involving the chemical shifts and spin-couplings. This is true even if the latter are not of direct interest. This arises because the magnetic parameters significantly affect the lineshape in this range of exchange rates. One expects that errors involved in assuming constant

values for such parameters, combined with unavoidable errors in spectrum recording (e.g. those in calibration), can lead to a serious deterioration in the accuracy of the estimated kinetic parameters. On the other hand, upon simultaneously fitting the whole set of parameters that describe the spectral system, small deviations of the fitted values of the shifts and coupling constants from those expected have only a slight influence on the accuracy of the estimated rates of exchange. This is due to the fact that in the slow-exchange region the information relating to these rates is contained mostly in the line-widths rather than in the line positions.

Upon increasing the rate of exchange the magnetic environments of the nuclei involved gradually become averaged out. Finally, at high exchange rates, a static spectrum is obtained for the averaged system which is characterized by the corresponding mean chemical shifts and mean coupling constants:

$$\delta_i^{\text{av.}} = p_1 \delta_i^{(1)} + p_2 \delta_i^{(2)} \quad (173)$$

$$J_{ij}^{\text{av.}} = p_1 J_{ij}^{(1)} + p_2 J_{ij}^{(2)} \quad (174)$$

where p_k is the mole fraction of species K. Thus, an exchanging system of two spins $CD \rightleftharpoons EF$ is transformed into an AB system, $ABCD \rightleftharpoons ABDC$ into ABE_2 , $ABCD \rightleftharpoons BADC$ into $EE'FF'$, etc.

In the range of intermediate rates of exchange, where the fine structure of a spectrum begins to disappear, the set of parameters to be fitted must be selected using common sense. The choice is difficult since the parameters that unequivocally determine the spectrum need not include the magnetic parameters as such but they may comprise any linear combination thereof. One should note, however, that at fast rates of exchange the most reasonable selection seems to include the mean parameters $\delta_i^{\text{av.}}$ and $J_{ij}^{\text{av.}}$ whilst $(\delta_i^{(1)} - \delta_i^{(2)})$ and $(J_{ij}^{(1)} - J_{ij}^{(2)})$ should be assumed using extrapolation from the slow-exchange region. A reversed procedure will probably lead to a divergence of the iterative fitting of the lineshape because of the correlation of the kinetic parameter with the differences in the chemical shifts. The choice of parameters to be fitted has therefore a significant influence on the accuracy of the results.

Sometimes the usefulness of such a choice can be estimated from the corresponding covariance matrix. This problem has been partially solved by Dimitrov for the $A \rightleftharpoons B$ case. The solution has been employed in a computational algorithm for lineshape fitting. (75) However, the author has admitted that the problem of strong correlations between the parameters is not yet overcome. Some limitation on the choice of parameters to be fitted results from difficulties in the extrapolation of

some magnetic parameters. Since there is a correlation between the kinetic parameter and the shifts in the fast-exchange region, it seems that it is more dangerous to try and fit too many parameters rather than too few. However, if a spectrum is recorded correctly, the parameters that can be evaluated using a fitting procedure should include the kinetic parameter K and at least those which are needed to describe completely the corresponding static spectrum at the fast-exchange extreme.

It seems clear from the discussion that, without some knowledge of the accurate values of at least some of the magnetic parameters concerned, it is generally impossible to analyse a dynamic NMR spectrum. The necessary information is usually obtained from the corresponding slow-exchange spectra and from equations (173) and (174) for the fast-exchange range. Spin-spin coupling constants are rather invariant with temperature, and thus their values in the range of dynamic effects in an NMR spectrum are usually known with good accuracy. On the contrary, chemical shifts are often temperature-dependent, and the temperature relationship may be quite involved. For this reason no particular extrapolation system is preferred, e.g. that employing a linear or logarithmic correlation between δ and either T or $1/T$. The choice should be made on the basis of a possible smooth fit to the experimental data within a sufficiently broad range of temperatures. Because of the lack of a good physical model of the temperature dependence of chemical shifts, the most reliable values are those which show the least variation with temperature in the accessible range of observation. The significance of errors in an extrapolation of chemical shifts increases with the decreasing differences in chemical shifts (and coupling constants) between the magnetic environments involved in the spin exchange.

E. Parameters for a dynamic equilibrium

It is obvious that independently of the rate of exchange the NMR spectrum of a system subject to a dynamic equilibrium depends on the relative concentrations of the components present. These may be expressed as mole fractions or, in the case of intramolecular exchange, as conformer populations. Sometimes the populations are governed by symmetry effects alone and are independent of the experimental conditions. This is always the case for mutual exchange when the process does not alter the chemical identity of a molecule. Examples of such exchange may be drawn from rotations of the *t*-butyl group in $(\text{CH}_3)_3\text{C}-\text{C}(\text{R}^1)(\text{R}^2)(\text{R}^3)$, and those about the $\text{CO}-\text{N}$ bond in *N,N*-dimethyl-substituted amides $(\text{CH}_3)_2\text{N}-\text{C}(=\text{O})\text{R}$. Other examples include ring inversions such as those in 1,2-*cis*-dimethylcyclohexane, 1,3-*trans*-

dimethylcyclohexane, 1,4-*cis*-dimethylcyclohexane, or the inversion of configuration at the nitrogen atom in 1,2,3-*trans*-trimethylaziridine.

The equilibrium concentrations are also known accurately in most of the intermolecular exchange processes. This is the case in the exchange process of ammonium protons in acidified aqueous solutions of ammonium salts. In such circumstances, the mole fractions of the species involved in the equilibrium are unambiguously determined by the composition of the sample under investigation. In other cases equilibrium parameters (concentrations) have to be determined experimentally. They are usually as interesting as are the corresponding kinetic parameters.

If an exchange of spins is slow enough, standard methods can be used (e.g. signal integration in proton spectra which are characterized by uniform T_2 relaxation times) for the determination of populations. However, when dynamic effects occur the problem becomes more complicated. In general one may say that, at low rates of exchange, the information concerning populations is contained mostly in the corresponding line intensities whilst, when signal coalescence occurs, these data appear mainly in the positions of the spectral lines. On the other hand, information about the corresponding kinetic parameters is contained, in either case, in the line-widths. One may therefore expect that total lineshape analysis in the region of slow-exchange will yield not only the corresponding kinetic and magnetic parameters but also the populations involved. However, within the range of intermediate and fast rates of exchange one is compelled to make assumptions about either the magnetic parameters or the equilibrium constants. Thus the investigator has to make a choice as to which parameters should be evaluated by the spectrum fitting procedure and which must be assumed in advance.

Contrary to the situation with magnetic parameters, the temperature dependence of an equilibrium constant is known to obey the simple equation:

$$\ln (p_1/p_2) = -\Delta G_0/RT \quad (175)$$

Besides this, in a typical range of temperatures where dynamic effects are observed in an NMR spectrum, i.e. about 50°C, the mole fractions of the species involved change only slightly. These two facts make possible a reasonably accurate estimation of the populations by extrapolation from the slow-exchange region.

It seems that the only case where the populations can be determined with satisfactory precision throughout the entire range of temperatures used in dynamic NMR measurements is that for a two-configuration exchange when the coupling constants are markedly different for the

exchanging species. In such a case, however, the equilibrium constant can also be determined from the averaged coupling observed for fast exchange rates and, by interpolation, for intermediate rates. Of course this is true only when the fast-exchange limit is experimentally accessible.

One should remember that, for multi-site exchange among n centres, there are only $(n - 1)$ independent populations. Owing to the condition of detailed balancing, any of the four parameters p_i , p_j , K_{ij} , and K_{ji} can be expressed as a function of the remaining three. Thus the number of independent parameters which describe the equilibrium and the kinetics of a given system does not exceed $n(n + 1)/2 - 1$.

F. Intensity coefficient and base-line position

In order to compare theoretical and experimental spectra, the theoretical lineshape function $f_{\text{abs.}}(\omega, \mathbf{g})$ used in Section IV.B.2 must be replaced:

$$\tilde{f}_{\text{abs.}}(\omega, \mathbf{g}) = M f_{\text{abs.}}(\omega, \mathbf{g}) + A \quad (176)$$

where the coefficient M and the term A are determined by spectrometer settings. They define the calibration of the energy absorption axis (intensity coefficient M) and the position of the base-line (term A).

The degree of fit expressed in terms of the sum of squares of deviations between experimental and theoretical spectra is critically dependent on these parameters. Their values must be fitted, together with those of the other parameters, in spite of the fact that the former are rather uninteresting by-products of the procedure of spectrum fitting.

It seems that the method of circumventing the problem by a straightforward assumption of the base-line position by inspection and by normalizing the spectrum to a certain integral (74, 96, 97) may lead to significant errors. It has little justification, since optimizing M and A by the least-squares method while the other parameters remain constant is performed in one step (the lineshape function is linear with respect to M and A). This provides a reasonable initial guess for M and A . However, in order to be certain that a minimum is attained for the ϵ function (Section IV.B.2) in the lineshape fitting one must simultaneously optimize the entire set of parameters which determine the spectrum considered. This is also the fastest route to such a minimum.

One should remember that apparently distant signals can significantly disturb the base-line in the vicinity of the signal considered. Sometimes it is necessary to introduce corrections of the form $B(\omega - \omega_0)^{-2}$ or to carry out a fitting procedure for a slanting background line. A Lorentzian signal characterized by a half-height width of w (Hz) and a

height h (in arbitrary units) has still an intensity of more than one unit of height within the range $\pm 0.5w(h - 1)^{1/2}$.

G. Significance of the results of a dynamic lineshape analysis

If the analysis of a dynamic NMR spectrum is carried out by an iterative least-squares fitting method, the results are accompanied by estimates of the errors. These are proportional to the square root of the sum of the squares of the deviations of the theoretical spectrum from the experimental one, as well as to the sensitivity of the sum to changes in the value of the parameter considered within the region where the sum attains a minimum. These estimates constitute a measure of the effects, on the resulting parameter values, of random errors. They do not include any effects due to systematic errors such as those involved in the assumed values of certain parameters. Moreover, because of the non-linearity of the least-squares fitting procedure employed, estimates of the errors have only an approximate statistical significance (Section IV.B.2 and reference 67).

The data of critical importance, as far as the accuracy of the kinetic parameter is concerned, are the natural line-width (in the slow- and fast-exchange regions) and the difference in chemical shifts (for fast exchange). Even small changes in such parameters can significantly affect the results without appreciably altering the corresponding sum of the squares of the deviations.

Probably the most accurate and least practical method for estimating the effects of systematic errors in line-widths and chemical shifts on the results of a dynamic NMR analysis involves an estimation of their maximum errors. This is then followed by a multiple iterative analysis with various combinations of their extreme values. Frequently one may try and estimate the contributions of such errors by a method based upon that for a symmetric $A \rightleftharpoons B$ exchange. (81) For this type of exchange a number of approximate equations have been suggested. These relate the rate of exchange to the difference in chemical shifts, $\delta_A - \delta_B = \Delta\delta_{AB}$, and to the exchange broadening of the signals, Δw_e . If Δw_e refers to very slow exchange or to that above the coalescence point, the approximate equation:

$$K = C(\Delta w_e)^n(\Delta\delta_{AB})^{1-n} \quad (177)$$

which yields a rather poor approximation of the rate K , can be used effectively in the estimation of errors. Upon comparing the latter equation with equations (169), (170), and (172), the following simple substitutions result:

$$\begin{aligned} C &= \pi, n = 1 \text{ for very slow exchange;} \\ C &= \pi/\sqrt{2}, n = 0 \text{ for signal coalescence;} \\ C &= \pi/2, n = -1 \text{ for very fast exchange.} \end{aligned}$$

For intermediate rates the values of C and n should be interpolated. The following relation can be derived from equation (177):

$$\frac{(dK)_s}{K} = |n| \frac{d\Delta w_e}{\Delta w_e} + (1 - n) \frac{d\Delta\delta_{AB}}{\Delta\delta_{AB}} \quad (178)$$

for the value of a systematic error $(dK)_s$. The error $d\Delta w_e$ is equal to a systematic error in Δw_0 whilst the systematic error $d\Delta\delta_{AB}$ results from extrapolation of the chemical shifts.

In order to estimate the uncertainty in the value obtained for the rate parameter K , one should also consider random errors. There are two sources of random error in this case: the least-squares fitting which gives an error $(dK)_{ls}$ due to random noise in the experimental spectrum [equation (164)] and the measurement of w_0 the line-width of the standard employed. The total random error in K is approximated by:

$$\frac{(dK)_r}{K} = \left\{ \left[n \frac{dw_0}{\Delta w_e} \right]^2 + \left[\frac{(dK)_{ls}}{K} \right]^2 \right\}^{1/2} \quad (179)$$

The exchange broadening Δw_e may be either measured directly from the spectrum or calculated from equation (177) upon substituting for K the value obtained from the iterative analysis. The procedure, after due modifications, can be employed for the estimation of errors for more complicated exchanging systems.

Most frequently dynamic NMR measurements are carried out in order to obtain activation parameters which are calculated from the temperature dependence of the exchange rates estimated from the spectra. The Eyring equation is usually employed to draw a straight line according to the least-squares fit:

$$\ln (K/T) = \ln (\kappa k/h) + \Delta S^\ddagger/R - \Delta H^\ddagger/(RT) \quad (180)$$

One can also calculate ΔG^\ddagger at individual temperatures using another form of the Eyring equation:

$$\Delta G^\ddagger = -RT \ln \left(\frac{\kappa kT}{hK} \right) \quad (181)$$

and then draw a straight line plot:

$$\Delta G^\ddagger = \Delta H^\ddagger - T\Delta S^\ddagger \quad (182)$$

in order to obtain the values of the enthalpy and entropy of activation. The uncertainty involved in the values of ΔH^\ddagger and ΔS^\ddagger is usually measured by their standard deviations from the least-squares fit. Due statistical weights should be assigned to individual values of ΔG^\ddagger at various temperatures if ΔH^\ddagger and ΔS^\ddagger are to be determined from the least-squares fit according to equation (182). From equation (181) the variance of ΔG^\ddagger is given by the first-order expansion in a Taylor series:

$$(\Delta \Delta G^\ddagger)^2 = (RT)^2 \left\{ \left[1 + \ln \left(\frac{\kappa kT}{hK} \right) \right]^2 \left(\frac{dT}{T} \right)^2 + \left(\frac{dK}{K} \right)^2 \right\} \quad (183)$$

and the corresponding statistical weights are proportional to $(1/\Delta \Delta G^\ddagger)^2$. The relative standard error dT/T is governed by experimental conditions. The relative error in the rate K , dK/K , can be estimated from equation (179). Since the latter is derived for a symmetric $A \rightleftharpoons B$ case, the exchange broadening Δw_e for more complicated systems should be assumed to equal the largest observed line-broadening in the spectrum considered. Since equation (179) represents a rather crude approximation it is sufficient to assume $n = 0$ for the maximum value of Δw_e in the entire set of dynamic spectra at the various temperatures employed. Similarly $n = \pm 1$ is taken for $\Delta w_e = 0$ according to equation (177), and interpolated values of n are used for intermediate broadenings Δw_e . An analogous procedure can be employed in the case of equation (180); the statistical weights for the corresponding $\ln(K/T)$ values then become:

$$[1/d \ln(K/T)]^2 = \left[\left(\frac{dK}{K} \right)^2 + \left(\frac{dT}{T} \right)^2 \right]^{-1} \quad (184)$$

In order to obtain estimates of the effects of systematic errors in K and T on the values of ΔH^\ddagger and ΔS^\ddagger , one can use a graphic method. For each of the temperatures employed one should recalculate K from the value of ΔG^\ddagger or $\ln(K/T)$ which results from the least-squares fit, then add to and subtract from this value the assumed maximum systematic error in K from equation (178). Two limiting values of ΔG^\ddagger , or $\ln(K/T)$, should then be computed for $K \pm (dK)_s$. These should be combined with two limiting values of T , or $1/T$, resulting from an assumed systematic error in T , to give four pairs of coordinates which describe a rectangle. Two straight lines with a maximum difference in their slopes should be drawn through the set of such rectangles obtained for all experimental points to yield limiting values of ΔH^\ddagger and ΔS^\ddagger .

The activation barrier is often described also in terms of the Arrhenius equation which was originally formulated in the differential form:

$$d \ln K/dT = E_a/(RT^2) \quad (185)$$

By differentiating the Eyring equation (180) with respect to T the following relationship is obtained, assuming that ΔH^\ddagger and ΔS^\ddagger are independent of temperature:

$$\Delta H^\ddagger = E_a - RT \quad (186)$$

However, by assuming that E_a is temperature-independent, the integrated form of equation (185) results:

$$\ln K = \ln A - E_a/(RT) \quad (187)$$

It has not yet been proven whether equation (187) or (180) provides the better description of the experimental results. Problems concerning the analysis of errors in E_a and A are virtually the same as those appearing in the case of the Eyring equation.

APPENDIX A. COMPOSITE INDICES. SOME PROPERTIES OF DIRECT (KRONECKER) PRODUCTS

In the linear spaces which have been employed in this article a convenient system of subscripts for basis set vectors is used which involves composite indices. Thus the elements of all the matrices and vectors in the spaces are subscripted with composite indices. All operations on such matrices and vectors are performed in the same manner as in the case of singly-subscripted vectors and doubly-subscripted matrices. For example the product of the matrices in equation (86) is expressed as:

$$(\mathbf{UP})_{pq,ijmn} = \sum_k \sum_l U_{pq,kl} P_{kl,ijmn} \quad (\text{A1})$$

Composite subscripts can always be replaced with single subscripts using, for example, equation (A2) which gives the so-called lexicographical order of composite indices:

$$a^{n_1, \dots, n_k}(j_1, \dots, j_k) = 1 + \sum_{i=1}^k \left[(j_i - 1) \prod_{r=k+1}^k n_r \right] \quad (\text{A2})$$

where $j_i = 1, 2, \dots, n_i$. The single subscript "a" defined by equation (A2) assumes values from the set $\{1, 2, \dots, \prod_{i=1}^k n_i\}$. If $n_u = 1$ for any u , then the index j_u can be deleted from the corresponding composite index:

$$\begin{aligned} a^{n_1, \dots, n_{u-1}, 1, n_{u+1}, \dots, n_k}(j_1, \dots, j_{u-1}, j_u, j_{u+1}, \dots, j_k) \\ = a^{n_1, \dots, n_{u-1}, n_{u+1}, \dots, n_k}(j_1, \dots, j_{u-1}, j_{u+1}, \dots, j_k) \end{aligned} \quad (\text{A3})$$

Let us denote by the symbol $\mathbf{A}^{m,n}$ a matrix with m rows and n columns. The symbols $\mathbf{A}^{1,1}$, $\mathbf{A}^{n,1}$, and $\mathbf{A}^{1,n}$ then denote a scalar, a column vector, and a row vector, respectively. The direct product of two matrices is defined by equation (A4) (see, for example, reference 46):

$$\mathbf{C}_{ij,kl}^{u,v} \equiv (\mathbf{A}^{m,n} \otimes \mathbf{B}^{p,q})_{ij,kl} \equiv \mathbf{A}_{i,k}^{m,n} \mathbf{B}_{j,l}^{p,q} \quad (\text{A4})$$

where $u = mp$ and $v = nq$. The resulting matrix \mathbf{C} has composite subscripts which can be replaced with single subscripts using equation (A2).

Properties of direct products result directly from equations (A4) and (A3):

(i) The operation of direct multiplication is linear with respect to both factors involved:

$$\mathbf{A}^{m,n} \otimes (\mathbf{bB}^{p,q} + \mathbf{cC}^{p,q}) = \mathbf{bA}^{m,n} \otimes \mathbf{B}^{p,q} + \mathbf{cA}^{m,n} \otimes \mathbf{C}^{p,q} \quad (\text{A5})$$

$$(\mathbf{aA}^{m,n} + \mathbf{dD}^{m,n}) \otimes \mathbf{C}^{p,q} = \mathbf{aA}^{m,n} \otimes \mathbf{C}^{p,q} + \mathbf{dD}^{m,n} \otimes \mathbf{C}^{p,q} \quad (\text{A6})$$

where a , b , c , and d are scalars.

(ii) Direct multiplication is associative:

$$\mathbf{A}^{m,n} \otimes (\mathbf{B}^{p,q} \otimes \mathbf{C}^{r,s}) = (\mathbf{A}^{m,n} \otimes \mathbf{B}^{p,q}) \otimes \mathbf{C}^{r,s} = \mathbf{A}^{m,n} \otimes \mathbf{B}^{p,q} \otimes \mathbf{C}^{r,s} \quad (\text{A7})$$

(iii) The Hermitian adjoint of a direct product equals the direct product of the corresponding Hermitian adjoints:

$$(\mathbf{A}^{m,n} \otimes \mathbf{B}^{p,q})^\dagger = (\mathbf{A}^{m,n})^\dagger \otimes (\mathbf{B}^{p,q})^\dagger \quad (\text{A8})$$

(iv) Direct multiplication is distributive with respect to ordinary multiplication:

$$(\mathbf{A}^{m,n} \otimes \mathbf{B}^{p,q})(\mathbf{C}^{n,r} \otimes \mathbf{D}^{q,s}) = (\mathbf{AC})^{m,r} \otimes (\mathbf{BD})^{p,s} \quad (\text{A9})$$

(v) If a row vector and a column vector are involved, the direct multiplication is commutative:

$$\mathbf{A}^{1,m} \otimes \mathbf{B}^{n,1} = \mathbf{B}^{n,1} \otimes \mathbf{A}^{1,m} \quad (\text{A10})$$

It follows from property (iv) that:

$$(\mathbf{A}^{m,n} \mathbf{B}^{n,p})^{m,p} \otimes \mathbf{C}^{q,1} = (\mathbf{A}^{m,n} \otimes \mathbf{C}^{q,1}) \mathbf{B}^{n,p} \quad (\text{A11})$$

since $\mathbf{C}^{q,1} = \mathbf{C}^{q,1} \mathbf{1}^{1,1}$, where $\mathbf{1}^{1,1}$ is a 1×1 matrix, equal to (scalar) unity.

Direct multiplication of matrices, which are subscripted with composite indices, is carried out in the same manner as that of doubly-subscripted matrices; e.g. the direct product in equation (93a) can be expressed as:

$$[\mathbf{E}^{n,n} \otimes (\mathbf{e}^\dagger)^{1,m}]_{ij,rs} = \mathbf{E}_{ij,rs}^{n,n} \mathbf{e}_{1,pq}^{\dagger,1,n} \quad (\text{A12})$$

APPENDIX B. DIFFERENTIAL FORM OF THE EQUATION OF MOTION

We define the following terms,

$$\mathbf{A}_k = -i\mathbf{H}_{s_k}^D + \mathbf{R}_k - \mathbf{E}_k/\tau_k \quad (\text{B1})$$

$$\lambda_k^f(t) = \bar{\rho}_k^f(t) - \rho_{0_k} \quad (\text{B2})$$

$$\lambda_k(t) = \bar{\rho}_k(t) - \rho_{0_k} \quad (\text{B3})$$

and consider that:

$$\int_{-\infty}^t (1/\tau_k) \exp[(t' - t)/\tau_k] dt' = 1 \quad (\text{B4})$$

$$\int_{-\infty}^0 (1/\tau_k) \exp[(t' - t)/\tau_k] dt' = \exp(-t/\tau_k) \quad (\text{B5})$$

in order to express equation (70) in the form:

$$\lambda_k(t) = \exp(\mathbf{A}_k t) \lambda_k(0) + \int_0^t \boldsymbol{\eta}_k(t, t') dt' \quad (\text{B6})$$

where the vector $\boldsymbol{\eta}_k(t, t')$ is given by:

$$\boldsymbol{\eta}_k(t, t') = (1/\tau_k) \exp[\mathbf{A}_k(t - t')] \lambda_k^f(t') \quad (\text{B7})$$

Differentiation of both sides of equation (B6) with respect to t yields:

$$\begin{aligned} d\lambda_k(t)/dt &= \mathbf{A}_k \exp(\mathbf{A}_k t) \lambda_k(0) \\ &+ \lim_{\Delta t \rightarrow 0} \frac{\int_0^{t+\Delta t} \boldsymbol{\eta}_k(t + \Delta t, t') dt' - \int_0^t \boldsymbol{\eta}_k(t, t') dt'}{\Delta t} \end{aligned} \quad (\text{B8})$$

It follows from equation (B7) that:

$$\boldsymbol{\eta}_k(t + \Delta t, t') = \boldsymbol{\eta}_k(t, t') + \frac{\partial \boldsymbol{\eta}_k(t, t')}{\partial t} \Delta t + \mathbf{o}(\Delta t) \quad (\text{B9})$$

where the vector $\mathbf{o}(\Delta t)$ has the property:

$$\lim_{\Delta t \rightarrow 0} \left[\frac{\mathbf{o}(\Delta t)}{\Delta t} \right] = 0 \quad (\text{B10})$$

The limit in equation (B8) can therefore be expressed as:

$$\frac{d}{dt} \int_0^t \boldsymbol{\eta}_k(t, t') dt' = \int_0^t \frac{\partial \boldsymbol{\eta}_k(t, t')}{\partial t} dt' + \boldsymbol{\eta}_k(t, t) \quad (\text{B11})$$

In order to calculate the integral on the right-hand side of equation (B11) we notice that:

$$\int_0^t \frac{\partial \boldsymbol{\eta}_k(t, t')}{\partial t} dt' = \mathbf{A}_k \int_0^t \boldsymbol{\eta}_k(t, t') dt' \quad (\text{B12})$$

The integral on the right-hand side of equation (B12) can be calculated using equation (B6):

$$\int_0^t \eta_k(t, t') dt' = \lambda_k(t) - \exp(A_k t) \lambda_k(0) \quad (\text{B13})$$

Therefore, equation (B8) assumes the form:

$$\frac{d\lambda_k(t)}{dt} = A_k \lambda_k(t) + (1/\tau_k) \lambda_k^f(t) \quad (\text{B14})$$

Upon substituting A_k , λ_k^f , and λ_k according to equations (B1), (B2), and (B3), respectively, we obtain equation (72).

REFERENCES

1. H. S. Gutowsky, reference 2, p. 1.
2. "Dynamic Nuclear Magnetic Resonance Spectroscopy", L. M. Jackman and F. A. Cotton (eds), Academic Press, New York, 1975.
3. T. Drakenberg and H. Wennerström, in "Specialist Periodical Report on NMR", R. K. Harris (ed.), 1975, **4**, 141.
4. T. Drakenberg and H. Wennerström, in "Specialist Periodical Report on NMR", R. K. Harris (ed.), 1976, **5**, 163.
5. P. D. Buckley, K. W. Jolly and D. N. Pinder, in "Progress in NMR Spectroscopy", J. Emsley, J. Feeney and L. H. Sutcliffe (eds.), 1975, **10**, 1.
6. A. Abragam, "The Principles of Nuclear Magnetism", Oxford University Press, 1961.
7. C. P. Slichter, "Principles of Magnetic Resonance", Harper, New York, 1963.
8. R. M. Lynden-Bell, in "Progress in NMR Spectroscopy", J. Emsley, J. Feeney and L. H. Sutcliffe (eds.), 1967, **2**, 163.
9. R. A. Hoffman, in "Advances in Magnetic Resonance", J. S. Waugh (ed.), 1970, **4**, 87.
10. B. D. Nageswara Rao, in "Advances in Magnetic Resonance", J. S. Waugh (ed.), 1970, **4**, 271.
11. P. A. M. Dirac, "Principles of Quantum Mechanics", Clarendon Press, Oxford, 1958.
12. C. N. Banwell and H. Primas, *Mol. Phys.*, 1962, **6**, 225, and references therein.
13. G. Binsch, *Mol. Phys.*, 1968, **15**, 469.
14. G. Binsch, *J. Amer. Chem. Soc.*, 1969, **91**, 1304.
15. D. A. Kleier and G. Binsch, *J. Magn. Resonance*, 1970, **3**, 146.
16. R. K. Wangness and F. Bloch, *Phys. Rev.*, 1953, **89**, 728.
17. F. Bloch, *Phys. Rev.*, 1956, **102**, 104.
18. F. Bloch, *Phys. Rev.*, 1957, **105**, 1206.
19. A. G. Redfield, *IBM J. Res. Develop.*, 1957, **1**, 19.
20. A. G. Redfield, in "Advances in Magnetic Resonance", J. S. Waugh (ed.), 1965, **1**, 1.
21. F. Bloch and A. Siegert, *Phys. Rev.*, 1940, **57**, 522.
22. See reference 9, pp. 108, 115.
23. R. Kaiser, *J. Magn. Resonance*, 1971, **5**, 220.
24. See reference 6, pp. 98–113.
25. I. J. Lowe and R. E. Norberg, *Phys. Rev.*, 1957, **107**, 46.
26. H. S. Gutowsky, D. W. McCall and C. P. Slichter, *J. Chem. Phys.*, 1953, **21**, 279.
27. H. S. Gutowsky and A. Saika, *J. Chem. Phys.*, 1953, **21**, 1688.
28. H. S. Gutowsky and C. H. Holm, *J. Chem. Phys.*, 1956, **25**, 1228.

29. H. M. McConnell, *J. Chem. Phys.*, 1958, **28**, 430.
30. R. A. Sack, *Mol. Phys.*, 1958, **1**, 163.
31. F. Bloch, *Phys. Rev.*, 1946, **70**, 460.
32. P. W. Anderson, *J. Phys. Soc. Japan*, 1954, **9**, 316.
33. R. Kubo, *J. Phys. Soc. Japan*, 1954, **9**, 935.
34. J. I. Kaplan, *J. Chem. Phys.*, 1958, **28**, 278.
35. J. I. Kaplan, *J. Chem. Phys.*, 1958, **28**, 462.
36. S. Alexander, *J. Chem. Phys.*, 1962, **37**, 967, 974.
37. S. Alexander, *J. Chem. Phys.*, 1963, **38**, 1787.
38. S. Alexander, *J. Chem. Phys.*, 1964, **40**, 2741.
39. J. I. Kaplan and G. Fraenkel, *J. Amer. Chem. Soc.*, 1972, **94**, 2907.
40. L. I. Schiff, "Quantum Mechanics", McGraw-Hill, New York, 1949, p. 211; see also reference 39.
41. W. G. Klemperer, in reference 2, p. 23, and references therein.
42. R. Willem, J. Brocas and D. Fastenakel, *Theor. Chim. Acta*, 1975, **40**, 25.
43. C. S. Johnson, *J. Chem. Phys.*, 1964, **41**, 3277.
44. C. S. Johnson, in "Advances in Magnetic Resonance", J. S. Waugh (ed.), 1965, **1**, 33.
45. J. A. Morrison, *J. Math. Phys.*, 1972, **13**, 299.
46. P. L. Corio, "Structure of High Resolution NMR Spectra", Academic Press, New York, 1966, p. 98.
47. S. Szymański and A. Gryff-Keller, *J. Magn. Resonance*, 1974, **16**, 182.
48. E. B. Feldman, *Theoret. Eksperiment. Khim.*, 1974, **10**, 787.
49. E. Bodewig, "Matrix Calculus", North-Holland, Amsterdam, 1959, p. 67.
50. J. I. Kaplan, *J. Magn. Resonance*, 1976, **21**, 153.
51. S. I. Alber, G. V. Lagodzinskaya, G. B. Manelis and E. B. Feldman, *Izv. Akad. Nauk. SSSR, Ser. Khim.*, 1974, 1719.
52. A. Gryff-Keller and S. Szymański, *Rocz. Chem.*, 1973, **47**, 1889.
53. I. O. Sutherland, in "Annual Reports on NMR Spectroscopy", E. F. Mooney (ed.), 1971, **4**, 71.
54. J. R. Yandle and J. P. Maher, *J. Chem. Soc. (A)*, 1969, 1549.
55. R. A. Newmark and C. H. Sederholm, *J. Chem. Phys.*, 1965, **43**, 602.
56. See reference 49, p. 125.
57. R. G. Gordon and R. P. McGinnis, *J. Chem. Phys.*, 1968, **49**, 2455.
58. R. E. Schirmer, J. H. Noggle and D. F. Gaines, *J. Amer. Chem. Soc.*, 1969, **91**, 6240.
59. L. W. Reeves and K. N. Shaw, *Can. J. Chem.*, 1970, **48**, 3641.
60. P. Meakin, E. L. Muttarties, F. N. Tebbe and J. P. Jesson, *J. Amer. Chem. Soc.*, 1971, **93**, 4701.
61. D. A. Kleier and G. Binsch, "DNMR 3: A Computer Program for the Calculation of Complex Exchange-broadened NMR Spectra. Modified Version for Spin Systems Exhibiting Magnetic Equivalence or Symmetry", 1970, Program 165, Quantum Chemistry Program Exchange, Indiana University, Bloomington, USA.
62. R. J. Kurland, M. B. Rubin and W. B. Wise, *J. Chem. Phys.*, 1964, **40**, 2426.
63. See reference 44, p. 66.
64. A. Allerhand, H. S. Gutowsky, J. Jonas and R. A. Meinzer, *J. Amer. Chem. Soc.*, 1966, **88**, 3185.
65. S. I. Alber, G. V. Lagodzinskaya, G. B. Manelis and E. B. Feldman, *Izv. Akad. Nauk SSSR, Ser. Khim.*, 1974, 1632.
66. V. S. Dimitrov, *Org. Magn. Resonance*, 1974, **6**, 16.
67. S. Brandt, "Statistical and Computational Methods in Data Analysis", North-Holland, Amsterdam, 1970.

68. J. M. Ortega and W. C. Rheinboldt, "Iterative Solutions of Nonlinear Equations in Several Variables", Academic Press, New York, 1970, pp. 267–268.
69. M. J. D. Powell, *Computer Journal*, 1964, **7**, 155.
70. L. W. Reeves and K. N. Shaw, *Can. J. Chem.*, 1971, **49**, 3671.
71. L. W. Reeves, R. C. Shaddick and K. N. Shaw, *Can. J. Chem.*, 1971, **49**, 3683.
72. E. A. Allan, M. G. Hogben, L. W. Reeves and K. N. Shaw, *Pure Appl. Chem.*, 1972, **32**, 9.
73. S. O. Chan and L. W. Reeves, *J. Amer. Chem. Soc.*, 1973, **95**, 673.
74. J. Gelan, *J. Magn. Resonance*, 1973, **10**, 37.
75. V. S. Dimitrov, *J. Magn. Resonance*, 1976, **22**, 71.
76. P. Moore, *J.C.S., Faraday Trans. I*, 1976, 826.
77. S. Szymański and A. Gryff-Keller, *J. Magn. Resonance*, 1976, **22**, 1.
78. G. Binsch, in reference 2, p. 45, and references therein.
79. J. D. Swalen, T. R. Lusebrink and D. Ziesow, *Magnetic Resonance Review*, 1973, **2**, 165.
80. S. Szymański, L. Stefaniak, M. Witanowski and A. Ejchart, *Org. Magn. Resonance*, 1977, **9**, 699.
81. A. Gryff-Keller and P. Szczeciński, *Org. Magn. Resonance*, 1978, **11**, 258.
82. N. F. Chamberlain, "The Practice of NMR Spectroscopy", Plenum Press, London and New York, 1974, p. 15.
83. P. T. Inglefield, E. Krakower, L. W. Reeves and R. Stewart, *Mol. Phys.*, 1968, **15**, 65.
84. T. Drakenberg and R. E. Carter, *Org. Magn. Resonance*, 1975, **7**, 307.
85. C. H. Bushweller, J. W. O'Neil and H. S. Bilofsky, *Tetrahedron*, 1971, **27**, 3605.
86. T. H. Siddal III, W. E. Stewart and F. C. Knight, *J. Phys. Chem.*, 1970, **74**, 3580.
87. E. Grunwald and E. K. Ralph, in reference 2, p. 621, and references therein.
88. See reference 46, p. 283.
89. K. I. Dahlqvist and S. Forsén, *J. Phys. Chem.*, 1969, **73**, 4124.
90. L. H. Piette and W. A. Anderson, *J. Chem. Phys.*, 1959, **30**, 899.
91. R. Mukherjee and R. M. Moriarty, *J. Magn. Resonance*, 1971, **3**, 201.
92. T. Drakenberg, K. I. Dahlqvist and S. Forsén, *Acta Chem. Scand.*, 1970, **24**, 694.
93. R. E. Carter and T. Drakenberg, *J.C.S., Perkin II*, 1975, 1690.
94. P. Diehl, H. Kellerhals and E. Lustig, in "NMR. Basic Principles and Progress", P. Diehl, E. Fluck and R. Kosfeld (eds.), Springer-Verlag, Berlin, 1972, Vol. VI, p. 30.
95. P. Diehl, S. Sykora and J. Vogt, *J. Magn. Resonance*, 1975, **19**, 67.
96. S. I. Alber, G. V. Lagodzinskaya, G. B. Manelis and E. B. Feldman, *Theoret. Eksperiment. Khim.*, 1974, **10**, 223.
97. S. S. Zumdahl and R. S. Drago, *J. Amer. Chem. Soc.*, 1967, **89**, 4319.
98. R. R. Ernst, *J. Chem. Phys.*, 1973, **59**, 989.
99. R. R. Ernst, W. P. Aue, E. Bartholdi, A. Höhener and S. Schaublin, *Pure Appl. Chem.*, 1974, **37**, 47.
100. J. I. Kaplan, *J. Chem. Phys.*, 1972, **57**, 5615.
101. J. I. Kaplan, *J. Chem. Phys.*, 1973, **59**, 990.
102. J. I. Kaplan, P. P. Yang and G. Fraenkel, *J. Chem. Phys.*, 1974, **60**, 4840.
103. S. Szymański, *Bull. Acad. Polon. Sci., Ser. Chim.*, 1978, in press.

Chemical Shifts of ^{119}Sn Nuclei in Organotin Compounds

PETER J. SMITH

International Tin Research Institute, Greenford, Middlesex, UB6 7AQ, England

AND

ALGIRDAS P. TUPČIAUSKAS

*Institute of Biochemistry, Academy of Sciences of the Lithuanian SSR,
Lenino av. 3, 232600 Vilnius MTP-1, USSR*

I. Introduction	292
II. Measurement of ^{119}Sn chemical shifts	293
A. Continuous wave methods	293
B. $^1\text{H}-\{^{119}\text{Sn}\}$ double magnetic resonance	293
C. Fourier transform NMR	298
III. Factors influencing ^{119}Sn chemical shifts	299
A. Coordination number	299
1. Chemical interactions with solvents	299
2. Auto-association	303
3. Discrete five- and six-coordinate organotin complexes	310
B. Substituent effects in $\text{R}_n\text{SnX}_{4-n}$ compounds	311
1. Effect of changing the organic group, R	311
2. Effect of changing the inorganic radical, X	311
3. Dependence of chemical shifts on multiple substitution	313
4. Variation in bond angles at tin	316
C. Isotope effects	317
1. Primary effects	317
2. Secondary effects	318
D. Temperature dependence	318
IV. Survey of ^{119}Sn chemical shift data	320
A. Presentation of tables	320
B. Tables of data	320
Acknowledgements	367
References	367

I. INTRODUCTION

The first NMR measurements on ^{119}Sn nuclei were made in 1960 by Burke and Lauterbur, (1) although the magnetic moments of the tin nuclei were determined as early as 1949 by Proctor. (2) Burke and Lauterbur's measurements were made by direct observation of the resonance of the ^{119}Sn nuclei at a frequency of 8.5 MHz. They found that the range of ^{119}Sn chemical shifts exceeds 1800 ppm. (1)

Elemental tin contains ten naturally occurring isotopes, and only three of these have non-zero nuclear magnetic moments: ^{115}Sn , ^{117}Sn , and ^{119}Sn (Table I). Each of the three magnetic tin isotopes has a nuclear

TABLE I

Nuclear magnetic moments and natural abundance of tin isotopes (3)

Isotope	Nuclear magnetic moment, μ (nuclear magnetons)	Natural abundance (%)	Relative NMR sensitivity ^a
^{112}Sn	—	1.01	—
^{114}Sn	—	0.68	—
^{115}Sn	-0.9132	0.35	3.5×10^{-2}
^{116}Sn	—	14.28	—
^{117}Sn	-0.9949	7.67	4.5×10^{-2}
^{118}Sn	—	23.84	—
^{119}Sn	-1.0409	8.68	5.2×10^{-2}
^{120}Sn	—	32.75	—
^{122}Sn	—	4.74	—
^{124}Sn	—	6.01	—

^a At constant field ($^1\text{H} = 1.00$).

spin of $\frac{1}{2}$ and therefore zero quadrupole moment. All three isotopes have approximately equal nuclear magnetic moments. However, in NMR investigations of tin compounds the chemical shifts are usually measured for ^{119}Sn nuclei because of the greater intensity of their NMR signals and because of their higher natural abundance (see Table I).

In this review, the measurement of, and factors influencing, ^{119}Sn chemical shifts of organotin compounds are discussed, and ^{119}Sn chemical shift data are tabulated for the period from 1960 to mid-1977. With the exception of Table XV, all chemical shifts are presented in ppm, with respect to Me_4Sn , high-frequency shifts being taken as positive.

II. MEASUREMENT OF ^{119}Sn CHEMICAL SHIFTS

A. Continuous wave methods

There are great difficulties in determining the chemical shifts of ^{119}Sn nuclei by direct observation, owing to their low natural abundance. In the early experiments, large samples, rapid sweep-rates (to minimize saturation effects), high RF power levels, and isotopic enrichment were all used (1, 4–6) but the resulting ^{119}Sn NMR spectra were often badly resolved and with a low signal-to-noise ratio, so application of this technique to structural investigations of organotin compounds is very limited.

B. ^1H - $\{^{119}\text{Sn}\}$ double magnetic resonance

In 1969, the possibility of determining ^{119}Sn chemical shifts of organotin compounds was increased when McFarlane and coworkers (7) suggested the ^1H - $\{^{119}\text{Sn}\}$ heteronuclear double magnetic resonance (HDMR) method, based on the use of ^1H NMR spectra.

It is known that, in many cases, the ^1H NMR spectra of organotin compounds show satellites caused by spin-spin coupling of the ^{119}Sn and ^{117}Sn nuclei with protons in the molecule. If the sample is simultaneously irradiated with a second radiofrequency (RF) at the ^{119}Sn (or ^{117}Sn) resonance frequency, the ^{119}Sn (or ^{117}Sn) satellites are decoupled, i.e. collapsed into the central peak. Depending on the amplitude of the second RF field and the accuracy of the RF setting, such irradiation can cause perturbation of the energy levels in the spin system. The perturbation patterns indicate the positions of individual lines in the ^{119}Sn spectrum and determine ^{119}Sn chemical shifts in the organotin molecule under investigation. In favourable conditions, the position of a particular line in the ^{119}Sn spectrum can be determined with an accuracy of 0.5 Hz, (7) but, more often, the ^{119}Sn spectra are very complicated and therefore such accuracy cannot be achieved.

The ^1H - $\{^{119}\text{Sn}\}$ HDMR method has certain advantages over the direct observation of ^{119}Sn NMR spectra. For example, ^{119}Sn chemical shifts may be measured with greater accuracy and for much weaker concentrations of a substance, since the proton magnetic resonance yields stronger signals than those of ^{119}Sn nuclei in direct observation (see Table I). The restriction of the HDMR method is also clear: the chemical shifts of ^{119}Sn nuclei can be determined only if spin-spin coupling constants $J(^{119}\text{Sn}-\text{H})$ are significant in the proton spectrum. For most organotin compounds this presents no great problems.

The ^1H - $\{^{119}\text{Sn}\}$ HDMR experimental set-up does not require any great modifications to commercial high-resolution NMR spectrometers,

(8–10) the second RF being received from a commercial frequency synthesizer such as the Rhode and Schwarz Model XUA, General Radio 1164-A7C, Hewlett-Packard 5105, Shomandl ND-30MB, or Schlumberger FS 30.

The second RF field may be introduced into the high-resolution NMR spectrometer probe either by winding an extra transmitter coil (11) or by double-tuning the existing transmitter coil. (12, 13)

The stabilization of the field–frequency ratio, which is required for HDMR experiments in the INDOR mode, can be obtained by locking the NMR spectrometer field–frequency ratio to the resonance condition of a strong and sharp signal in the sample under investigation. (14) Additional stabilization can be achieved by locking together the main frequency of the spectrometer and master oscillator of the synthesizer. (15, 16) In this case, the drift in the frequency of the synthesizer is balanced by the change in the main frequency of the spectrometer.

The first results of experiments with a wide range of organotin compounds (1, 4, 7) showed that the ^{119}Sn chemical shifts exceed a range of 1000 ppm. If the $^1\text{H}-\{^{119}\text{Sn}\}$ HDMR experiment is carried out using a spectrometer with a resonance frequency for protons equal to 100 MHz, the second irradiating field, B_2 , must be changed in the range of approximately 40 kHz to cover this range of chemical shifts. The location of the centre of the ^{119}Sn spectrum can therefore sometimes causes difficulties. However, using a strong irradiating field B_2 , i.e. $\gamma(^{119}\text{Sn})B_2/2\pi > 1000$ Hz, it is possible to determine the range of ^{119}Sn resonance frequencies for the compound under investigation. (9) Scanning the range of changes of ^{119}Sn chemical shifts by intervals of a few kHz determines the values where the ^{119}Sn satellite lines begin to collapse. Figure 1 shows the $^1\text{H}-\{^{119}\text{Sn}\}$ HDMR spectra for the compound Me_4Sn at different deviations, η , of the second frequency, ν_2 . $\eta = [\nu_2 - \nu_0(^{119}\text{Sn})]$, where $\nu_0(^{119}\text{Sn})$ is the exact resonance frequency for the ^{119}Sn nuclei in the compound under investigation.

On the basis of a theory proposed by Anderson and Freeman, (17, 18) the following expression is given (19) for evaluating the second field, B_2 , from the $^1\text{H}-\{^{119}\text{Sn}\}$ HDMR spectra:

$$[\gamma(^{119}\text{Sn})B_2/2\pi]^2 = \frac{1}{4}\{[J(^{119}\text{Sn}-\text{H})/2\nu_1]^2 - 1\} \\ \times \{[2\eta - (2m_1 - 1)J(^{119}\text{Sn}-\text{H})]^2 - (2\nu_1)^2\} \quad (1)$$

where $\gamma(^{119}\text{Sn})$ is the gyromagnetic ratio for ^{119}Sn nuclei, ν_1 is the position of the perturbed ^{119}Sn satellite line relative to the centre of the multiplet in the proton spectrum (in Hz), and m_1 is the projection of the total magnetic moment for protons.

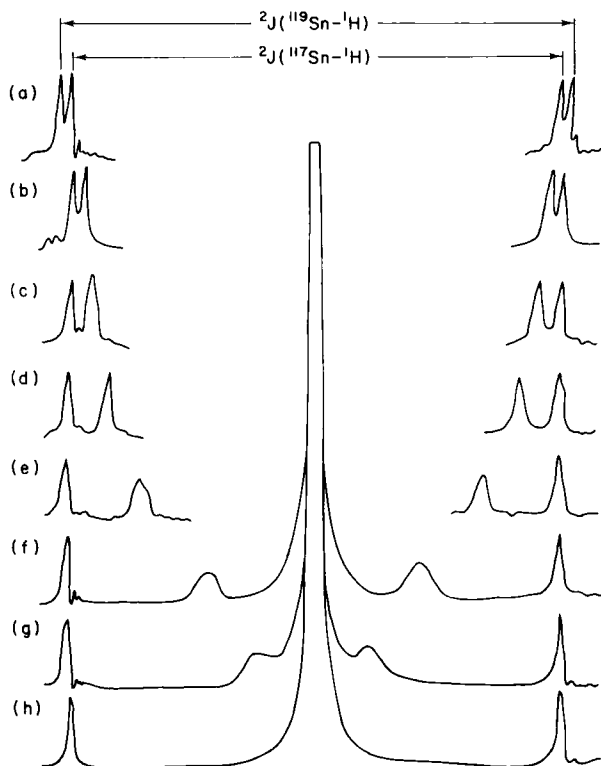


FIG. 1. Experimental $^1\text{H}-\{^{119}\text{Sn}\}$ spectrum for Me_4Sn with different frequency deviations η of the strong RF field. The ^{117}Sn satellite lines are unchanged. (9) (a) No irradiation; (b) $\eta = 5000$ Hz; (c) 4000 Hz; (d) 3000 Hz; (e) 2000 Hz; (f) 1000 Hz; (g) 500 Hz; (h) 0 Hz.

If the second field is absent, i.e. $\chi(^{119}\text{Sn})B_2/2\pi = 0$, the position of the ^{119}Sn satellite line, ν_1 , is equal to $\pm J(^{119}\text{Sn}-\text{H})/2$.

The B_2 value calculated from expression (1) depends upon the value of the projection of the magnetic moment, m_1 . Table II demonstrates this dependence for hydrogen nuclei in the compound Me_4Sn , when $\eta = 5000$ Hz, and the positions of the perturbed ^{119}Sn satellite lines are defined by the frequency $\nu_1 = \pm 24.1$ Hz [Fig. 1(b)].

When the frequency deviation, η , is smaller than the value $\chi(^{119}\text{Sn})B_2/2\pi$, the ^{119}Sn satellite lines are broadened a little [see Fig. 1(e-g)].

Using the strong irradiating field, B_2 , it is possible to determine the centre of the ^{119}Sn multiplet with an accuracy of 200–300 Hz. A convenient method for a more accurate determination of the line positions in the ^{119}Sn spectrum is the use of the HDMR experiment in

TABLE II

The various values of the total magnetic moment projection m_1 and the B_2 values determined from $^1\text{H}-\{^{119}\text{Sn}\}$ HDMR spectra when $\eta = 5000$ Hz

m_1	$\gamma(^{119}\text{Sn})B_2/2\pi$ (Hz)	B_2 (μT)
6	2398	151.1
5	2425	152.8
4	2453	154.6
3	2480	156.3
2	2508	158.0
1	2536	159.8
0	2564	161.6
-1	2590	163.2
-2	2617	164.9
-3	2646	166.7
-4	2674	168.5
-5	2701	170.2
-6	2728	171.9

the INDOR mode. (20) The power of the second irradiating field B_2 in the INDOR mode must be chosen so that the condition $\gamma(^{119}\text{Sn})B_2/2\pi \geq \Delta\nu$ is satisfied, where $\Delta\nu$ is the breadth of the perturbed line in Hz. (18)

Following the usual terminology, the $^1\text{H}-\{^{119}\text{Sn}\}$ HDMR experiment in the INDOR mode can be defined as the double magnetic resonance experiment in which the detecting frequency is set exactly on the resonance of some ^{119}Sn satellite line in the proton spectrum, while the

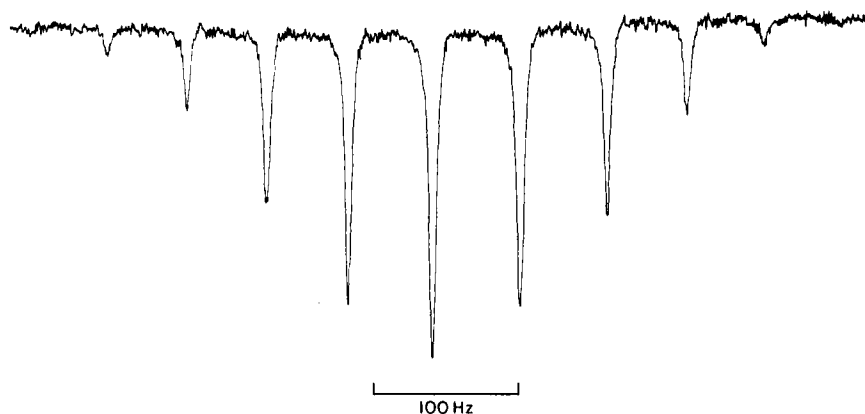


FIG. 2. ^{119}Sn INDOR spectrum of Me_4Sn . (21)

perturbing frequency ν_2 is swept over the resonance of the ^{119}Sn nuclei present in the sample. For example, the $^1\text{H}-\{^{119}\text{Sn}\}$ HDMR spectrum in the INDOR mode for Me_4Sn (21) is illustrated in Fig. 2. Other ^{119}Sn INDOR spectra have also been reported. (7, 8, 22–24)

The $^1\text{H}-\{^{119}\text{Sn}\}$ HDMR experiments may often be applied to the analysis of type A_nX spin systems* with degenerate transitions and only two groups of magnetically equivalent nuclei. For example, the energy level diagram for an A_3X system is shown in Fig. 3.

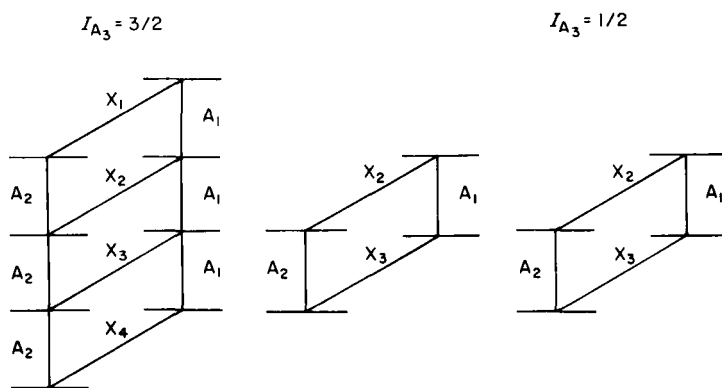


FIG. 3. Energy level diagram for an A_3X system.

It is evident that if the monitoring frequency ν_1 is set on one of the ^{119}Sn satellite lines, say A_1 , composed of five coincident transitions, then the ^{119}Sn , say X , spectrum will always reveal at least one transition with the same energy level as the transitions being observed. When the perturbing frequency ν_2 sweeps over the ^{119}Sn spectrum the intensity of the ^{119}Sn satellite, observed in the proton spectrum, changes according to the population redistribution amongst the energy levels due to the general Overhauser effect. (26)

The centre of the ^{119}Sn multiplet can be determined from the changes in intensity of the ^{119}Sn satellite line. The perturbing frequency corresponding to the centre of the ^{119}Sn multiplet must be reduced to conditions in which the resonance frequency for the protons of Me_4Si (TMS) is exactly equal to the main resonance frequency of the spectrometer. The reduction can be made by means of the following expression: (9, 27)

$$\nu_{\text{TMS}} = \nu_{\text{obs}}[1 \pm (\nu_m \pm C\delta)/\nu_0] \quad (2)$$

* The nuclei under the influence of the second perturbing field are denoted by the last Latin alphabet letters, and the observed nuclei by the initial ones. (25)

where ν_{TMS} is the resonance frequency for ^{119}Sn nuclei of the organotin compound in the magnetic field at which protons of the TMS reference display their signal exactly at the main resonance frequency of the spectrometer (in Hz), ν_{obs} is the observed resonance frequency of the ^{119}Sn nuclei corresponding to the centre of the spectrum of the ^{119}Sn multiplet (in Hz), ν_m is the modulation frequency of the internal stabilization system (in Hz), ν_0 is the main resonance frequency of the spectrometer for protons (in Hz), C is the main resonance frequency of the spectrometer for protons (in MHz), and δ is the proton chemical shift of the internal stabilization signal from TMS.

The signs of the second term in square brackets in equation (2) depend upon whether the upper (−) or lower (+) sideband is used to record the spectrum.

If the main resonance frequency of the spectrometer for protons, ν_0 , differs by $\pm E$ from the nominal one, then equation (2) is transformed to:

$$\nu_{\text{TMS}} = \nu_{\text{obs}} [1 \pm (\nu_m \pm C\delta \pm E)/\nu_0] \quad (3)$$

Equation (3) is a generalized one for the reduction of the observed ^{119}Sn resonance frequency. It considers all possible features for the determination of this frequency: the sign and value of the sideband frequency used for recording; the proton chemical shift of the standard signal used for the stabilization of the magnetic field; the main resonance frequency of the spectrometer and its drift. This expression can be used to determine ^{119}Sn chemical shifts by the HDMR experiment in either the INDOR or the frequency sweep mode. The ^{119}Sn resonance frequency is usually quoted in terms of a polarizing field strength in which TMS gives a proton resonance at exactly 100 MHz. For Me_4Sn this is $37\,290\,665 \pm 2$ Hz. (7)

It should be noted here that there are a number of surveys devoted to the theory and application of HDMR. (27–33) and, additionally, a review on all aspects of NMR of organotins, (34) and on ^{119}Sn NMR. (23)

C. Fourier transform NMR

Fourier transform NMR spectroscopy, although used extensively to study ^{13}C and ^{15}N nuclei, has only very recently been applied to ^{119}Sn . (27, 35–40, 42–44)

Lauterbur (41) has tried to increase the comparatively low intensity of the ^{119}Sn nuclei in the CW mode by using a strong decoupling interaction $^{119}\text{Sn}-\{^1\text{H}\}$, but the effect is negligible. However, in the pulsed FT mode, proton decoupling significantly increases the signal-to-noise ratio in the ^{119}Sn spectrum. A ^{119}Sn FT spectrum recently obtained (21) for a mixture of $\text{Me}_2\text{SnH}_n\text{D}_{2-n}$ compounds is shown in Fig. 4.

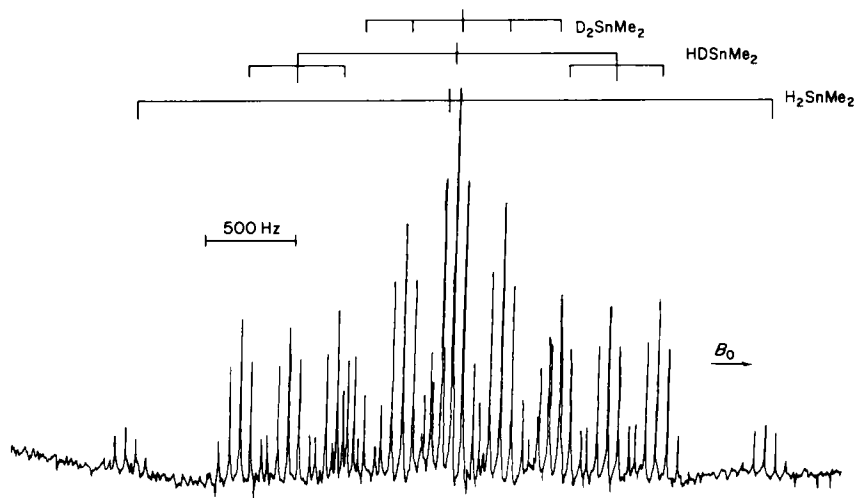


FIG. 4. ^{119}Sn FT spectrum of $\text{Me}_2\text{SnH}_2 + \text{Me}_2\text{SnDH} + \text{Me}_2\text{SnD}_2$, recorded using 21 000 pulses. (21)

For ^{119}Sn , the nuclear Overhauser effect does not give an overall intensity gain (23) owing to the negative sign of its magnetic moment (see Table I). Under appropriate conditions, the decrease in intensity due to the NOE can be avoided by the use of gated decoupling. (129)

Pulse FT NMR has been used to study the spin-lattice relaxation times, T_1 , of ^{119}Sn in a number of organic (37, 38, 40, 42, 43) and inorganic (44) tin compounds. The most important relaxation mechanism for this nucleus in a series of tetraorganotins appears to be spin-rotation (SR) (38, 43) although for larger molecules, such as hexabutyltin, dipole-dipole (DD) relaxation is important, even at room temperature. (37)

III. FACTORS INFLUENCING ^{119}Sn CHEMICAL SHIFTS

A. Coordination number

1. Chemical interactions with solvents

Various workers have observed (1, 4, 7) that five- and six-coordinate organotin compounds show ^{119}Sn signals which occur at much lower frequencies than those of the four-coordinate derivatives. For this reason, the choice of solvent in preparing samples for NMR measurements may affect the value of the observed ^{119}Sn chemical shift.

Hunter and Reeves have noted (4) that dilution of trimethyltin chloride and bromide in non-coordinating solvents such as benzene and

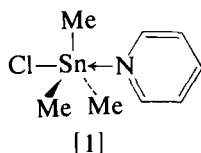
carbon tetrachloride has only a very slight effect on ^{119}Sn chemical shifts. The lack of large changes in chemical shift with dilution in these solvents indicates that (a) no complexing occurs between the organotin compound and the solvent, and (b) self-association is absent in these trimethyltin halides (see Section III.A.2). Some results for the dilution of trimethyltin chloride in carbon tetrachloride (19) are shown in Table III, and the ^{119}Sn chemical shifts are seen to be essentially independent of both concentration and temperature.

TABLE III
 ^{119}Sn chemical shifts (ppm) for Me_3SnCl dissolved in carbon tetrachloride (19)

Concentration (mol %)	Temperature ($^{\circ}\text{C}$)		
	-5	+20	+35
40	+159.5	+159.5	+159.6
20	+160.7	+160.6	+159.9
10	+159.9	+159.7	+159.8
5	+159.8	+159.6	+159.2
3	+159.8	+159.5	+159.7

Polar coordinating solvents, such as acetone, dimethyl sulfoxide (DMSO), or pyridine, can produce large variations in the ^{119}Sn chemical shift, dependent on the concentration. For example, the addition of pyridine to a solution of trimethyltin chloride in carbon tetrachloride (45) produces a change in chemical shift from +159 to -9 ppm as the mole ratio of Me_3SnCl to pyridine is altered from 1:0 to 1:12. The greatest change in shift occurs over the range of mole ratios from 1:0 to 1:1, and further increases take place slowly as more pyridine is added.

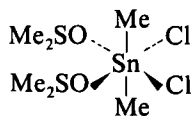
This is consistent with the formation of a five-coordinate trigonal bipyramidal 1:1 adduct, [1], which is known from X-ray studies (46) to



exist in the solid state. This complex dissociates when dissolved in non-polar solvents, (47) and the change in chemical shift is a reflection of the increase in coordination number of the tin as a complex is formed.

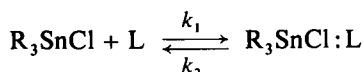
Similarly, the ^{119}Sn chemical shift of a saturated solution of dimethyltin dichloride in DMSO (-246 ppm) is almost 400 ppm to low

frequency of that in CH_2Cl_2 or CCl_4 (48) and probably corresponds to the six-coordinate octahedral complex $\text{Me}_2\text{SnCl}_2 \cdot 2\text{DMSO}$, [2], the crystal structure of which has been determined. (49)



[2]

A more detailed study (50) of the ^{119}Sn chemical shifts of trimethyl- and triethyl-tin chloride as a function of concentration and temperature in various polar solvents has revealed the effect of complexing on chemical shift. The formation of a 1 : 1 complex of trialkyltin chloride in a polar donor solvent, L, may be written as:



In this case, the equilibrium constant, K , can be calculated (4) from the concentration dependences found for the ^{119}Sn chemical shifts:

$$K = \frac{k_1}{k_2} = \frac{\delta_0(\delta_c - c\delta_0)}{\delta_0^2(1 - c) + c\delta_0^2 - \delta_0\delta_c} \quad (4)$$

where δ_0 is the ^{119}Sn chemical shift for the uncomplexed trialkyltin chloride, δ_c is the ^{119}Sn chemical shift for the complexed trialkyltin chloride, and c is the initial molar fraction of R_3SnCl .

Using equation (4), Torocheshnikov *et al.* (50) have calculated the values of δ_c and K for Me_3SnCl and Et_3SnCl in acetone, acetonitrile, and dioxan. The molar enthalpy of complex formation, ΔH , can be obtained from a $\ln K$ vs. $1/T$ plot (Fig. 5) using the Van't Hoff relationship:

$$d(\ln K)/dT = \Delta H/RT^2 \quad (5)$$

The values of ΔH obtained are listed in Table IV and are found to be close to those calculated by thermochemical methods. (51)

Reported changes in chemical shift (50) with temperature and concentration of trimethyltin chloride in methanol or ethanol indicate a more complicated process than a simple monomer = complex equilibrium. It has been suggested that ionization of the organotin compound occurs in these solvents, probably forming a solvated five-coordinate $(\text{R}_3\text{SnL}_2)^{\oplus}$ cationic species.

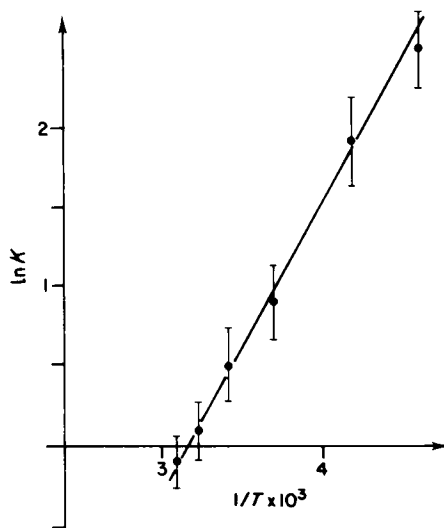
FIG. 5. Dependence of $\ln K$ on $1/T$ for trimethyltin chloride in acetone.

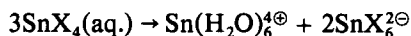
TABLE IV

Molar enthalpy ΔH values for complexes of Me_3SnCl and Et_3SnCl with acetone, acetonitrile, and dioxan. (50)

Complex	ΔH (kcal mol ⁻¹)	
$\text{Me}_3\text{SnCl}/\text{acetone}$	4.2 (± 1.3)	5.7 ^a
$\text{Me}_3\text{SnCl}/\text{acetonitrile}$	4.1 (± 1.15)	4.8 ^a
$\text{Me}_3\text{SnCl}/\text{dioxan}$	5.1 (± 1.5)	—
$\text{Et}_3\text{SnCl}/\text{acetone}$	3.3 (± 1.4)	—
$\text{Et}_3\text{SnCl}/\text{acetonitrile}$	2.8 (± 1.25)	—

^a From Bolles and Drago. (51)

Fratiello (52) has investigated ionization processes for SnCl_4 and SnBr_4 in water–acetone mixtures. The ^{119}Sn chemical shifts demonstrate the presence of ionization of the stannic tetrahalides as:



This process is confirmed by dielectric constant changes of the solute.

Tetraorganotin compounds, R_4Sn , show weak acceptor properties and do not form solid adducts, with the possible exception of Me_3SnCF_3 , which is reported (53) to form a 1:1 complex with hexamethylphosphortriamide. Tetramethyltin, for example, has little or no tendency to form complexes with a wide range of solvents, (9) since the chemical shift changes are very small (Table V).

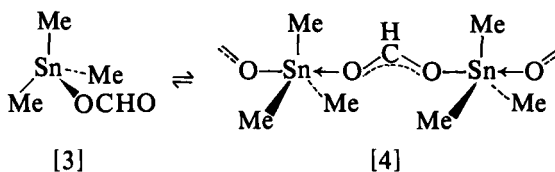
TABLE V
 ^{119}Sn chemical shifts (ppm) for Me_4Sn in various
 solvents (9)

Solvent	δ	Solvent	δ
Neat	0	Me_2CO	+0.5
C_6H_{12}	+0.8	$(\text{Me}_2\text{N})_3\text{PO}$	-1.7
$\text{C}_4\text{H}_8\text{O}$	-1.4	MeOH	+0.4
CCl_4	0	MeCN	-0.2
PhH	-2.0	DMSO	-1.6
CS_2	-6.7	$(\text{Me}_2\text{N})_2\text{CO}$	-3.3
CH_2Cl_2	+0.5	Et_3N	+0.4

It is, however, interesting to note that tetrakis(*m*-trifluoromethylphenyl)tin in DMSO shows (54) a ^{119}Sn chemical shift which is *ca.* 10 ppm to low frequency of that of the same compound in CDCl_3 , whereas a low frequency shift of only 1.6 ppm is found (9) for tetramethyltin in similar solvents (Table V).

2. Auto-association

The ^{119}Sn chemical shift of dimethyltin dichloride in carbon tetrachloride and other non-polar solvents remains practically invariant to large changes in concentration. It has a value of *ca.* +140 ppm. This indicates the ease with which the molecules are able to dissociate into discrete tetrahedral species in solution as a result of the very weak intermolecular $\text{Sn} \dots \text{Cl}$ bonds which exist in crystalline dimethyltin dichloride. (55) On the other hand, a chemical shift-concentration study of trimethyltin formate in deuteriochloroform solution (56) has revealed a dramatic change in chemical shift from +2.5 ppm for a 3 M solution to +152 ppm on dilution to 0.05 M in the same solvent. This has been attributed to self-association of monomeric tetrahedral trimethyltin formate molecules, [3]. As the concentration is increased, five-coordinate oligomeric or polymeric species, [4], could be formed. These are known to exist in the solid state. (57)

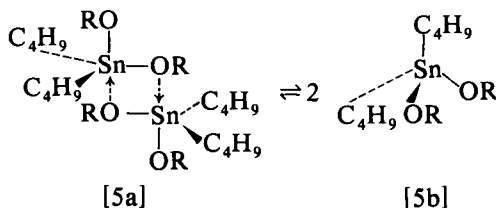


Trimethyltin hydroxide and isothiocyanate, which are also self-associated polymers in the solid state, (58, 59) show rather smaller

changes in chemical shift on dilution in non-coordinating solvents (data given in Table XVI). Trimethyltin acetate, another polymeric trialkyltin carboxylate in the solid state, (60) is found to have a chemical shift of +129 ppm, when studied as a saturated solution in CDCl_3 . (45) This value does not change on dilution. However, trimethyltin acetate is so sparingly soluble in CDCl_3 (*ca.* 0.04 g cm^{-3}) that even a saturated solution is extremely dilute and monomeric species might therefore be expected in this case.

The ^{119}Sn chemical shifts have been used extensively to study intermolecular association in various organotin alkoxides, $\text{R}_n\text{Sn}(\text{OR}')_{4-n}$, where $n = 1-3$.

On the basis of molecular weight measurements and infrared spectroscopy it has been suggested (61, 62) that dibutyltin dimethoxide, di-*n*-propoxide, and di-*n*-butoxide are associated into dimers in the pure liquid state, [5a], whilst the di-*t*-butoxide is monomeric, [5b].



The ^{119}Sn chemical shifts for a series of di- and tri-*n*-butyltin alkoxides, (63) as the neat liquids at room temperature, are presented in Table VI.

TABLE VI

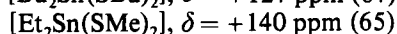
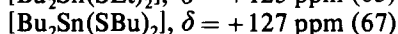
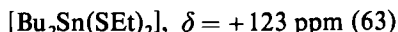
^{119}Sn chemical shifts (ppm) of di- and tri-
butyltin alkoxides (63)

R	$\text{Bu}_2\text{Sn}(\text{OR})_2$	Bu_3SnOR
Me	-165 (2)	+83 (7)
Et	-161 (2)	+86 (5)
^nPr	-159 (5)	+87 (2)
^iPr	-90 (5)	+76 (2)
^nBu	-161 (5)	+91 (5)
^iBu	-150 (2)	+82 (5)
^sBu	-34 (2)	+80 (2)
^tBu	-34 (5)	+60 (2)

The chemical shifts clearly enable one to differentiate between the two species [5a] and [5b]; dibutyltin dimethoxide, diethoxide, di-*n*-propoxide, and di-*n*-butoxide all show low-frequency shifts (-159 to -165 ppm), whereas the di-*t*-butoxide and di-*s*-butoxide, in which the

bulky R groups prevent dimerization, display shifts to much higher frequency (-34 ppm). Similar chemical shift trends are observed in the dimethyl- and diethyl-tin dialkoxides. (64, 65)

Replacement of the two oxygen atoms in these dialkoxides by sulphur, a poorer bridging atom, decreases the tendency to intermolecular association and prevents the formation of dimers. (66) The high-frequency ^{119}Sn chemical shifts found for $\text{R}_2\text{Sn}(\text{SR}')_2$ compounds reflect this behaviour:



The tributyltin alkoxides (Table VI) also show high-frequency chemical shifts, independent of the nature of the alkoxy substituent, and are thus monomeric tetrahedral species in the neat liquid at room temperature. At 80 K, however, both tributyltin methoxide and phenoxide are self-associated. (63)

The changes in chemical shift as a function of concentration and temperature for the dibutyltin dialkoxides (63) are shown in Fig. 6.

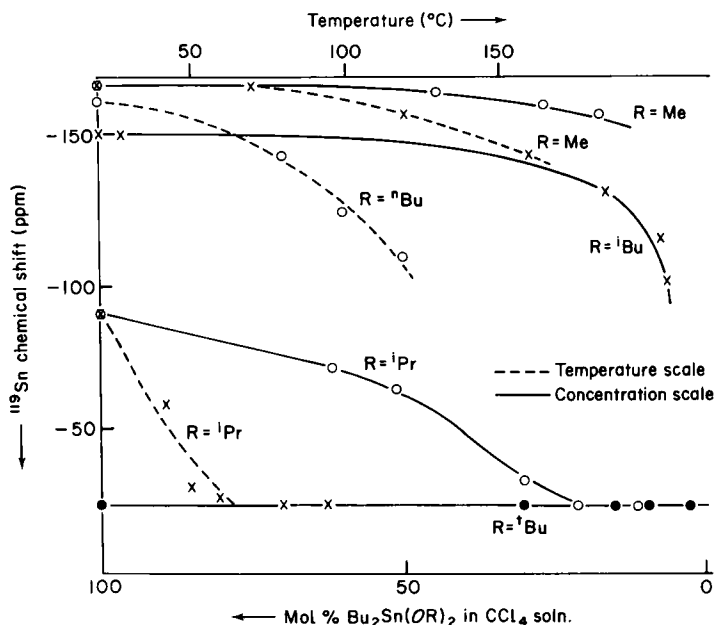


FIG. 6. Effect of dilution and temperature on ^{119}Sn chemical shifts of $\text{Bu}_2\text{Sn}(\text{OR})_2$ compounds. (63)

The molar enthalpy ΔH values for the reaction $\text{dimer} \rightleftharpoons 2(\text{monomer})$ for dibutyltin di-*i*-propoxide and di-*n*-butoxide have been estimated. The degree of dissociation, α , is written in terms of the observed ^{119}Sn chemical shift, δ_{obs}^* , and that of the dimer, δ_{D}^* ,

$$\alpha = 1 - \delta_{\text{obs}}^* / \delta_{\text{D}}^* \quad (6)$$

where $\delta_{\text{obs}}^* = \delta_{\text{obs}} - \delta_{\text{M}}$ and $\delta_{\text{D}}^* = \delta_{\text{D}} - \delta_{\text{M}}$ are chemical shift values expressed relative to the chemical shift of the monomer, δ_{M} . The equilibrium constant, K , for the $\text{dimer} \rightleftharpoons 2(\text{monomer})$ reaction is given by:

$$K = 4\alpha^2 n / (1 - \alpha) v \text{ mol l}^{-1} \quad (7)$$

where n is the number of moles of dimer before dissociation and v is the volume.

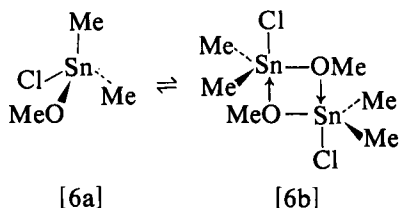
Using the Van't Hoff equation, (5) molar enthalpy ΔH values have been obtained (63, 68) from the equilibrium constants determined at various temperatures (Table VII).

TABLE VII

**Thermochemical data for the dissociation of dialkyltin
dialkoxide dimers (neat liquids)**

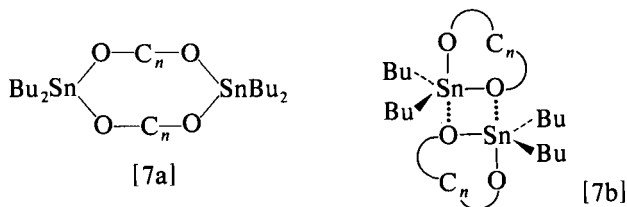
Compound	ΔH (kcal mol $^{-1}$)	Ref.
$\text{Bu}_2\text{Sn}(\text{OPh})_2$	19 ± 0.5	68
$\text{Bu}_2\text{Sn}(\text{O}^i\text{Pr})_2$	24 ± 4	63
	19 ± 1.5	68
$\text{Bu}_2\text{Sn}(\text{O}^n\text{Bu})_2$	14 ± 3	63
$\text{Bu}_2\text{Sn}(\text{O}^i\text{Bu})_2$	18 ± 0.5	68
$\text{Me}_2\text{Sn}(\text{O}^i\text{Pr})_2$	17 ± 1	68
$\text{Me}_2\text{Sn}(\text{O}^n\text{Bu})_2$	18 ± 0.5	68

A dilute solution of dimethyltin methoxide chloride, $\text{Me}_2\text{Sn}(\text{OMe})\text{Cl}$, in dichloromethane shows (69) two ^{119}Sn signals at +126 and -90 ppm. This is compatible with the presence of an equilibrium between the simple tetrahedral monomer [6a] and the symmetrical dimer [6b]



containing five-coordinate tin. In line with this, the proportion of dimer [6b] is found to increase with increasing concentration.

The ^{119}Sn chemical shifts have been used (63) as a criterion of dimerization in the investigation of cyclic dialkyltin alkoxides, $\text{R}_2\text{SnOC}_n\text{O}$. Two structures have been suggested (61) for the dimer in solution: the large ring, [7a], in which the tin atoms are four-coordinate and tetrahedral, and the oxygen-bridged dimer, [7b], in which the two tin atoms are occupying a trigonal bipyramidal *cis*- R_2SnX_3 geometry.



The ^{119}Sn chemical shifts for a series of cyclic dibutyltin alkoxides (63) are shown in Table VIII.

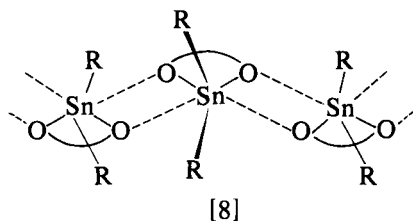
Structure [7b], which is very similar to that suggested for the acyclic dimeric dialkoxides in the pure liquids, [5a], is identified by a low-

TABLE VIII

 ^{119}Sn chemical shifts (ppm) of cyclic dibutyltin alkoxides (63)

Tin alkoxide	Solution conditions	δ
	satd. CDCl_3	-189 (5)
	satd. CDCl_3	-164 (5)
	satd. CDCl_3	-155 (5)
	satd. CDCl_3	-228 (10)
	neat liquid (120°C)	-213 (5)
	satd. CCl_4	-235 (5)

frequency ^{119}Sn signal. The lowest frequency ^{119}Sn chemical shifts (-213 to -233 ppm) are ascribed (63) to oligomeric species, [8], containing six-coordinate tin atoms. This structure has subsequently been confirmed by X-ray crystallography (70) for $\text{Bu}_2\text{SnO}(\overline{\text{CH}_2})_3\text{O}$.



The cyclic dialkyltin thioalkoxides, $\text{R}_2\text{Sn}(\overline{\text{SC}}_n)_2$, are, like their acyclic counterparts, unassociated monomeric species in solution and, accordingly, show high-frequency ^{119}Sn signals. (63, 65, 71)

Their ^{119}Sn NMR spectroscopy has been used to study auto-association in methyl- and butyl-tin trialkoxides (64, 68, 72). Figure 7 illustrates the variation of chemical shift with temperature for the neat liquid butyltin trialkoxides, $\text{BuSn}(\text{OR})_3$. (72)

The butyltin trialkoxides exhibit a substantial range of chemical shifts, from *ca.* -205 ppm for the tri-*t*-butoxide to *ca.* -425 ppm for the linear chain trialkoxides. It has therefore been suggested (72) that the chemical shifts appearing at around -425 ppm are indicative of six-coordination in these butyltin trialkoxides. In line with this, the higher viscosity of these butyltin trialkoxides suggests that six-coordination may involve an oligomeric or polymeric degree of interaction. The value of -205 ppm observed for the tri-*t*-butoxide butyltin chemical shift may be ascribed to essentially monomeric, tetrahedral species in the neat liquid. This is confirmed by the failure of the ^{119}Sn NMR signal to change significantly on heating (Fig. 7) or dilution. It parallels the behaviour of the, similarly monomeric, dibutyltin di-*t*-butoxide. In the case of *n*-butyltin tri-*i*-butoxide, the extra 2-methyl substituent increases the steric hindrance to association over that observed in the straight-chain trialkoxides. This compound, although essentially six-coordinate at room temperature, shows an increased tendency towards dissociation as the temperature is decreased. Finally, the effect of a third 2-alkyl substituent, as in the tri-neopentoxide, or of a second 1-alkyl substituent, as in the tri-*s*-butoxide, is even more pronounced and for steric reasons six-coordination is completely inhibited. (72)

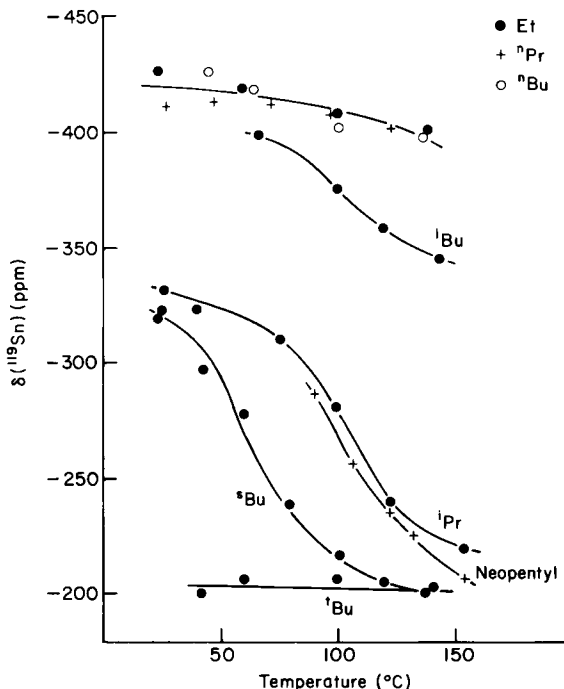


FIG. 7. Variation of $\delta(^{119}\text{Sn})$ with temperature for the neat liquid butyltin trialkoxides, $\text{BuSn}(\text{OR})_3$, (72)

As an extension of the auto-association in organotin compounds, the ^{119}Sn chemical shifts of a series of functionally disubstituted symmetrical distannoxanes, $\text{X} \cdot \text{R}_2\text{SnOSnR}_2 \cdot \text{X}$, containing a range of X substituents have been measured (5, 6, 37, 73) and some results are shown in Table IX.

The ^{119}Sn chemical shifts for the distannoxanes provide evidence for the existence of a dimeric ladder structure [9] in solution. (73) The tetrabutyl-dichloro- and -dibromo-distannoxanes and tetramethyl-bis-(trimethylsiloxy)distannoxane show two well-resolved ^{119}Sn signals

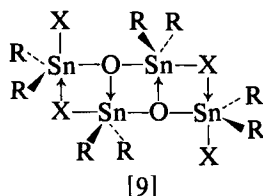


TABLE IX

¹¹⁹Sn chemical shifts (ppm) for X·R₂SnOSnR₂·X compounds

R	X	Solution conditions	δ	Ref.
Bu	F	satd. CCl ₄	−168 (14)	73
Bu	Cl	satd. CCl ₄	−145 (5); −94 (5)	73
Bu	Cl	satd. CCl ₄	−142.7 (0.1); −89.6 (0.1)	37
Bu	Br	satd. PhH	−141 (5); −87 (5)	73
Bu	NCS	satd. PhH	−159 (9)	73
Bu	OSiMe ₃	satd. PhH	−163 (5)	73
Bu	OCOMe	satd. PhH	−221 (5)	73
Me	OSiMe ₃	satd. CCl ₄	−130 (2); −156 (2)	6
Me	OSiMe ₃	satd. CCl ₄	−137 (2); −153 (2)	73

separated by about 1000 Hz; the other distannoxanes give a single, very broad ¹¹⁹Sn resonance. The low-frequency signals observed for all the distannoxanes are consistent with both tin atoms occupying very similar five-coordinate trigonal bipyramidal environments in solution. Subsequent X-ray work has demonstrated the presence of this ladder structure, [9], in the solid state for R = Bu, X = O.CO.CCl₃; (74) R = Me, X = NCS; (75) and R = Me, X = OSiMe₃. (57) The Δ*H* value for the dimer=2(monomer) dissociation reaction of tetramethyl-bis(trimethylsiloxy)distannoxane is 9 ± 1 kcal mol^{−1}. (6)

3. Discrete five- and six-coordinate organotin complexes

The ¹¹⁹Sn chemical shifts of some discrete five- and six-coordinate organotin complexes are collected in Table X.

An increase in the amount of s-character in the Sn–C bonds (78, 79) is usually accompanied by a signal shift to low frequency. (80) No ¹¹⁹Sn NMR data have been reported for seven-coordinate organotin com-

TABLE X

¹¹⁹Sn chemical shifts (ppm) of some discrete organotin complexes

Complex	Probable geometry	δ	Ref.
Me ₂ Sn(SCSNiEt ₂)Cl ^a	Trig. bipy. <i>cis</i> -R ₂ SnX ₃	−204	7
Et ₂ Sn(ox) ₂	Octahedral <i>cis</i> -R ₂ SnX ₄	−264	65
Me ₂ Sn(SCSNiEt ₂) ₂	Octahedral <i>trans</i> -R ₂ SnX ₄	−336	7
Me ₂ Sn(acac) ₂ ^b	Octahedral <i>trans</i> -R ₂ SnX ₄	−366	23
BuSn(ox) ₂ Cl	Octahedral RSnX ₅	−395	71

^a X-ray structure of Me₂Sn(SCSNMe₂)Cl available. (76)

^b X-ray structure available. (77)

plexes, although these are becoming increasingly more common, e.g. $\text{MeSn}(\text{SCSNet}_2)_3$. (78)

B. Substituent effects in $\text{R}_n\text{SnX}_{4-n}$ compounds

1. Effect of changing the organic group, R

As the electron releasing power of the alkyl group increases, the tin atom becomes progressively more shielded and the ^{119}Sn chemical shift should thus move to lower frequencies. This effect is illustrated in Table XI for each of the three series of alkyltin chlorides, RSnCl_3 , R_2SnCl_2 , and R_3SnCl . The Taft σ^* constants for the organic groups, (81) which are a better guide to polar effects than electronegativity, correlate roughly with δ (Table XI). A rough correlation between σ^* and δ has been found (82) for a number of tetra-alkyltin compounds.

TABLE XI

^{119}Sn chemical shifts (ppm) of alkyl- and phenyl-tin chlorides

R	RSnCl_3	R_2SnCl_2	R_3SnCl	Taft $\sigma^*(\text{R})$
Me	+20	+141	+164	0.000
Et	+6.5	+126	+155	-0.100
^nBu	+6.0	+122	+141	-0.130
^tBu	—	+52	—	-0.225
Ph	-63	-32	-48	+0.600

See Section IV.B for references.

If the alkyl groups in any $\text{R}_n\text{SnX}_{4-n}$ series are replaced by phenyl, the ^{119}Sn signal moves to lower frequencies (Table XI), which is inconsistent with the greater electron withdrawing capability of a phenyl substituent on tin. Similar effects are found with benzyl, vinyl, and allyl groups (Tables XXX and XXXI) and may be due to the increased polarizability of these unsaturated substituents. (23) This topic is discussed further in Section III.B.3.

2. Effect of changing the inorganic radical, X

In a series of compounds, R_3SnX , the ^{119}Sn chemical shift should move to higher frequency with increased inductive withdrawing power of X. (4) This is clearly illustrated in Fig. 8 for a number of unassociated trimethyltin compounds, Me_3SnX , where a plot of δ against the Pauling electronegativity of X results in a good linear correlation. (80)

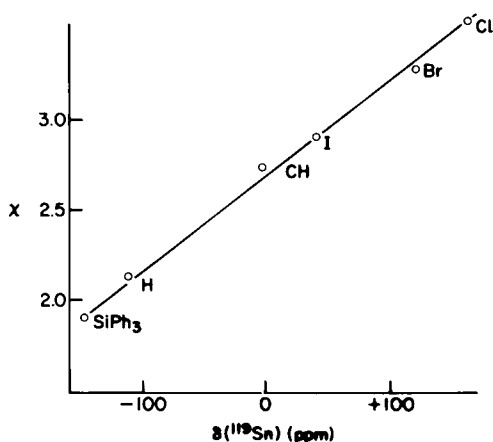


FIG. 8. Dependence of ^{119}Sn chemical shifts (ppm) upon Pauling electronegativity χ of substituent for some Me_3SnX compounds. (80)

McFarlane and Wood (56) have determined the ^{119}Sn chemical shifts of a number of trineophyl- and triphenyl-tin carboxylates, $(\text{Me}_2\text{PhCCH}_2)_3\text{SnOCOR}$ and Ph_3SnOCOR , in which the electron withdrawing ability of the carboxylate group can be assessed from the $\text{p}K_a$ value of the parent acid. It is found that increased inductive electron withdrawal from tin gives progressively larger δ values. Similarly, in a series of trimethyl- and triphenyl-tin thiophenoxides (19, 83) and trimethyltin phenoxides (19) with various *para*-substituents, X, in the aromatic ring, it is found that electron withdrawing substituents decrease the tin shielding (Table XII).

TABLE XII

^{119}Sn chemical shifts (ppm) of trimethyltin phenoxides and triphenyltin thiophenoxides (19, 83)

X	$\text{Me}_3\text{SnOC}_6\text{H}_4\text{X-4}$	$\text{Ph}_3\text{SnSC}_6\text{H}_4\text{X-4}$
H	+131.8	-65.2
OMe	+131.4	-65.2
NO_2	+147.5	-61.8
Cl	+138.8	-64.4
Me	—	-67.4

A plot of chemical shift against the Taft σ^* value of R for Me_3SnSR , where R = Me, Et, ^iPr , and ^tBu , is linear indicating that inductive effects

are dominant. (48) The trimethyltin alkoxides, Me_3SnOR , show similar behaviour as R is varied. (68)

3. Dependence of chemical shifts on multiple substitution

The theory of ^{119}Sn magnetic shielding is in its infancy. (23) Following the approach of Saika and Slichter, (84) the shielding, $\sigma(^{119}\text{Sn})$, may be divided into three contributions:

$$\sigma(^{119}\text{Sn}) = \sigma_d + \sigma_p + \sigma_n \quad (8)$$

where σ_d is the diamagnetic contribution to the ^{119}Sn shielding, σ_n defines the magnetic effects due to electronic circulation associated with other atoms in the molecule and should give contributions of comparable magnitude for all nuclei. Although the shifts arising from diamagnetic anisotropy and ring current are important for protons, they can be ignored in connection with tin nuclei because the overall chemical shift range is so large. For ^{119}Sn , the main factor determining the chemical shift differences is the paramagnetic contribution, σ_p , which may be written as: (85)

$$\sigma_p = - \frac{\mu_0 e^2 \hbar^2}{6\pi m^2 \Delta E} (\langle r^{-3} \rangle_p P_i + \langle r^{-3} \rangle_d D_i) \quad (9)$$

where e , \hbar , and m are the usual constants, ΔE is a mean electronic excitation energy, P_i and D_i are the amounts of electron imbalance associated with the tin atom's valence p and d orbitals, and $\langle r^{-3} \rangle_p$ and $\langle r^{-3} \rangle_d$ are the average values of r^{-3} , where r refers to the separation between the ^{119}Sn nucleus and the valence p and d electrons respectively. ΔE may be treated as being approximately constant for a related series of tin compounds. (4, 7) The values of P_i and D_i depend on coordination number, hybridization of atomic orbitals in bonding, and ionicity of the bonds. In the case of spherically symmetrical electron shells, the values of P_i and D_i are zero, whereas large values of P_i and D_i correspond to highly imbalanced p and d electron distributions.

Hence, in a series of tetrahedral compounds, R_3SnX , an increase in the electronegativity of X should increase P_i and, therefore, σ_p [equation (9)], i.e. the ^{119}Sn magnetic shielding is decreased. This is found to be the case in the two series $\text{Me}_3\text{SnCH}_2\text{Cl} \rightarrow \text{Me}_3\text{SnCCl}_3$ and $\text{Me}_3\text{SnCH}_2\text{Br} \rightarrow \text{Me}_3\text{SnCBr}_3$. (7)

Consequently, increasing substitution of R by X in four-coordinate organotin compounds, $\text{R}_n\text{SnX}_{4-n}$, produces an initial decrease in shielding followed by a progressive increase, to give a characteristic U-

shaped dependence of δ on n (Fig. 9). Similar curves have been reported for a wide range of R and X groups, including the series:

$\text{Me}_n\text{SnCl}_{4-n}$ (7, 9, 22)	$\text{Me}_n\text{SnBr}_{4-n}$ (22)	$\text{Me}_n\text{SnI}_{4-n}$ (22)
$\text{Me}_n\text{Sn}(\text{NMe}_2)_{4-n}$ (86)	$\text{Me}_n\text{Sn}(\text{SR})_{4-n}$ (22, 48)	
$\text{Me}_n\text{Sn}(\text{OR})_{4-n}$ (68, 86)	$\text{Me}_n\text{Sn}(\text{SeR})_{4-n}$ (87)	
$\text{Me}_n\text{Sn}(\text{C}_5\text{H}_5)_{4-n}$ (88)	$\text{Et}_n\text{SnCl}_{4-n}$ (9, 65)	
$\text{Et}_n\text{SnBr}_{4-n}$ (65)	$\text{Bu}_n\text{SnCl}_{4-n}$ (4, 9, 80)	
$\text{Bu}_n\text{Sn}(\text{NEt}_2)_{4-n}$ (80)	$\text{Bu}_n\text{Sn}(\text{O}^t\text{Bu})_{4-n}$ (68, 72)	
$\text{Ph}_n\text{SnCl}_{4-n}$ (7)	$(\text{PhCH}_2)_n\text{SnCl}_{4-n}$ (82)	

However, the origins of this effect are still not completely understood.

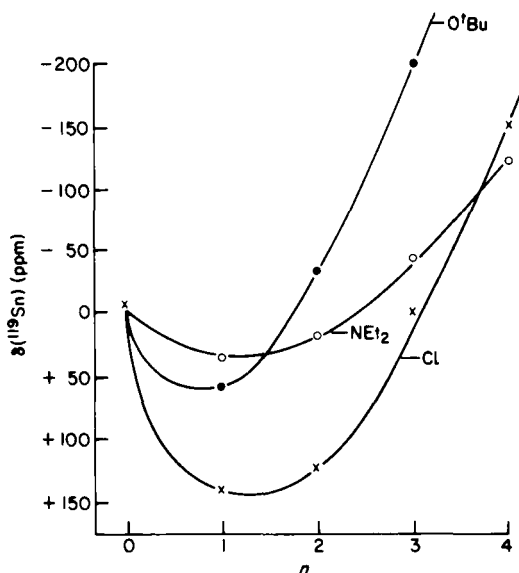


FIG. 9. ^{119}Sn chemical shifts (ppm) for unassociated butyltin compounds, $\text{Bu}_{4-n}\text{SnX}_n$ (80) as a function of n .

Normally, an increase in effective electronegativity of a particular group attached to the tin atom is expected to increase the imbalance in the population of the p orbitals and so give a shift to higher frequencies but any use of the tin d orbitals to form π bonds would tend to offset this effect. If the overall number of electronegative substituents is increased, the effective electronegativity of the tin atom itself will also increase and so the p electron imbalance in each bond may decrease and the tin nucleus may experience increased shielding.

The population of the tin d orbitals may result from both $(d \rightarrow p)-\pi$ and $(d \rightarrow d)-\pi$ bonding. These two effects should increase over the series of substitutions of $\text{Cl} \rightarrow \text{Br} \rightarrow \text{I}$, since the more distant p and d electrons of the halogen have higher probabilities of delocalization into the tin d orbitals and are characterized by an increase in the energy of the d orbitals.

In contrast to the foregoing, organotin compounds of the following $\text{R}_n\text{SnR}'_{4-n}$ types show a linear increase in shielding with progressive substitution of R' groups:

$\text{Me}_n\text{Sn}(\text{vinyl})_{4-n}$ (4, 32)	$\text{Me}_n\text{SnPh}_{4-n}$ (32)
$\text{Me}_n\text{Sn}(\text{allyl})_{4-n}$ (88)	$\text{Et}_n\text{SnPh}_{4-n}$ (65)
$\text{Et}_n\text{Sn}(\text{vinyl})_{4-n}$ (65)	$\text{Et}_n\text{Sn}(\text{CH}_2\text{Ph})_{4-n}$ (65)
$\text{Et}_n\text{Sn}(\text{ethynyl})_{4-n}$ (65)	$\text{Bu}_n\text{SnPh}_{4-n}$ (54)
$\text{Bu}_n\text{Sn}(\text{C}_6\text{H}_4\text{CF}_3-3)_{4-n}$ (54)	$\text{Me}_n\text{SnH}_{4-n}$ (Fig. 10).

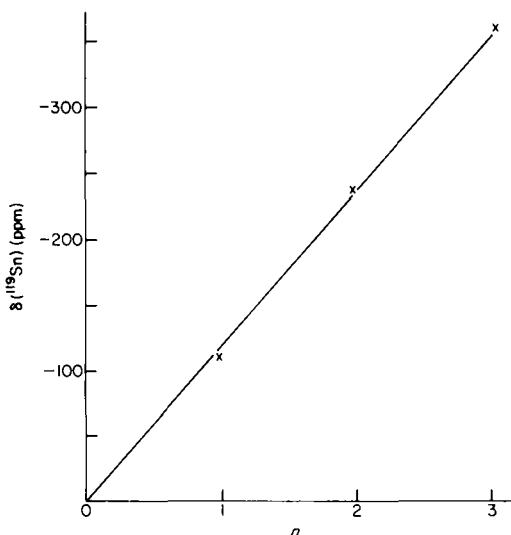


FIG. 10. ^{119}Sn chemical shifts (ppm) for methyltin hydrides, $\text{Me}_{4-n}\text{SnH}_n$, as a function of n (data from Table XXXIV).

This effect cannot be explained in terms of electronegativity, since the most strongly electron withdrawing groups give the lowest frequency shifts. McFarlane has suggested (23) that substituent polarizability may be important here.

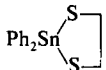
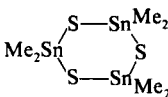
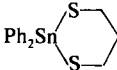
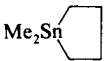
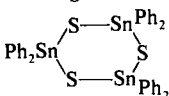
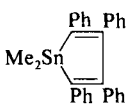
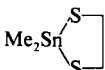
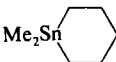
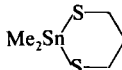
A theoretical interpretation of substituent effects in unassociated alkyltin compounds has recently been given. (89)

4. Variation in bond angles at tin

It has been reported that, when the tin atom is incorporated into a five- or six-membered ring system, the ^{119}Sn nuclear shielding is markedly dependent upon the ring size (Table XIII). (90)

TABLE XIII

^{119}Sn chemical shifts (ppm) for some diorganostanna-cycloalkanes and -thiocycloalkanes (4, 10, 90)

Compound	δ	Compound	δ
	+ 78		+ 129
	+ 28.5		+ 53.5
	+ 19.5		+ 52.0
	+ 190		-42.5
	+ 149		

Incorporation of tin into a five-membered ring has the effect of shifting the ^{119}Sn resonance to high frequency of its position in the six-membered ring analogue. The higher frequency shifts for the five-membered ring compounds are ascribed (90) to a deformation of the X-Sn-X bond angle ($\text{X} = \text{S}$ or $-\text{CH}_2-$) from the tetrahedral value, i.e. a "ring strain" effect.

In line with this, the geometry of the tin atom in 1-dimethylstanna-2,5-dithiacyclopentane is known by X-ray crystallography to be considerably distorted from tetrahedral, (91) whereas the tin atoms in the cyclic dimethyl- and diphenyl-tin sulphide trimers are in an almost regular tetrahedral environment, the S-Sn-S bond angles being 107.7° (92) and 111.9° (93) respectively. Changes of C-Sn-C bond angles have also been invoked to account for the observed changes of ^{119}Sn shielding in a series of norbornenyltrimethyltins, (94) and it is probable that some of the apparently random variations in the chemical shifts of tetra-alkyltins can be accounted for by variations in interbond angles arising from bulky groups or constraints due to closed rings. (23)

C. Isotope effects

1. Primary effects

The results of research on the NMR spectra of elements with different isotopic composition have been reported. (95) The particular interest of these investigations lies in the possibility of applying perturbation theory to account for the contribution of vibrational states to the shielding of nuclei. (96, 97) In addition, the measurement of nuclear g factors of isotopic pairs, with great accuracy, is required for evaluating small hyperfine structure anomalies. (39, 98)

The evaluation of the primary isotopic effect for ^{117}Sn and ^{119}Sn nuclei, having the resonance frequencies $\nu_{\text{TMS}}(^{117}\text{Sn})$ and $\nu_{\text{TMS}}(^{119}\text{Sn})$, can be made from equation (10).

$$\begin{aligned} \frac{\nu_{\text{TMS}}(^{117}\text{Sn})}{\nu_{\text{TMS}}(^{119}\text{Sn})} &= \frac{\gamma(^{117}\text{Sn})[1 - \sigma(^{117}\text{Sn})]}{\gamma(^{119}\text{Sn})[1 - \sigma(^{119}\text{Sn})]} \\ &\simeq \frac{\gamma(^{117}\text{Sn})}{\gamma(^{119}\text{Sn})} \{1 - [\sigma(^{117}\text{Sn}) - \sigma(^{119}\text{Sn})]\} \end{aligned} \quad (10)$$

For the ^{117}Sn and ^{119}Sn isotopes the resulting expressions for the chemical shifts are:

$$\delta(^{117}\text{Sn}) = \sigma(^{117}\text{Sn}) - \sigma_0(^{117}\text{Sn}) \quad (11)$$

$$\delta(^{119}\text{Sn}) = \sigma(^{119}\text{Sn}) - \sigma_0(^{119}\text{Sn}) \quad (12)$$

where $\sigma_0(^{117}\text{Sn})$ and $\sigma_0(^{119}\text{Sn})$ are the shielding constants for the ^{117}Sn and ^{119}Sn nuclei in a standard compound, Me_4Sn . The primary isotopic effect for the pair of ^{117}Sn and ^{119}Sn isotopes may then be expressed as:

$$\begin{aligned} \Delta &= \sigma(^{117}\text{Sn}) - \sigma(^{119}\text{Sn}) \\ &= [\delta(^{117}\text{Sn}) - \delta(^{119}\text{Sn})] + [\sigma_0(^{117}\text{Sn}) - \sigma_0(^{119}\text{Sn})] \end{aligned} \quad (13)$$

The chemical shift difference, $[\delta(^{117}\text{Sn}) - \delta(^{119}\text{Sn})]$, has been measured for a number of organotin compounds in non-coordinating solvents with the result that the primary isotopic effect, whilst negligibly low in most cases, appears to be significant for tetraethyltin, triethyltin chloride, and tetra(cyclopentadienyl)tin. (99) However, McFarlane (65) has pointed out that these differences are greatest for molecules in which the tin spectrum is very complex and, in these cases, it may therefore be difficult to measure the tin chemical shift accurately. The absence of any significant primary isotope effect on the tin shielding has also been observed for tetramethyltin, (99, 100) dimethyltin dichloride, (99, 100) and bis(trimethyltin) sulphide. (100)

If the primary isotopic effect is neglected, very accurate values may be obtained for the gyromagnetic constant ratio $\gamma(^{117}\text{Sn})/\gamma(^{119}\text{Sn})$ [equation (10)] from the ratio of the tin resonance frequencies, $\nu_{\text{TMS}}(^{117}\text{Sn})/\nu_{\text{TMS}}(^{119}\text{Sn})$. The ratios of resonance frequencies measured for pairs of tin isotopes with different accuracies by various authors are compared in Table XIV.

TABLE XIV

Ratios of resonance frequencies for pairs of tin isotopes

$\nu(^{115}\text{Sn})/\nu(^{117}\text{Sn})$	$\nu(^{119}\text{Sn})/\nu(^{117}\text{Sn})$	Ref.
0.91794 ($\pm 1 \times 10^{-4}$)	1.0465 ($\pm 1 \times 10^{-4}$)	2
0.9182341 ($\pm 6 \times 10^{-7}$)	1.0465410 ($\pm 6 \times 10^{-7}$)	39
—	1.04654122 ($\pm 2 \times 10^{-8}$)	100
—	1.046541 ($\pm 5 \times 10^{-7}$)	99
—	1.046541275 ($\pm 3 \times 10^{-9}$)	21

2. Secondary effects

Very little information is available relating to secondary isotopic effects on ^{119}Sn chemical shifts.

Gillies has measured the ^{119}Sn chemical shifts for Me_2SnH_2 , Me_2SnHD , and Me_2SnD_2 , and found (101) a shift of approximately 1 ppm to lower frequencies per substitution of H by D (see also Fig. 4). Similarly, in the series $\text{SnMe}_4 \rightarrow \text{Sn}(\text{CD}_3)_4$, Lassigne and Wells have observed a total 3 ppm ^{119}Sn shift to low frequency. (43) This result, together with the already derived value of the paramagnetic term σ_p , for the ^{119}Sn nucleus in Me_4Sn , of -3200 ppm (43) indicates that full deuteration of the molecule causes only a 0.1% change in the paramagnetic contribution to the total shielding constant.

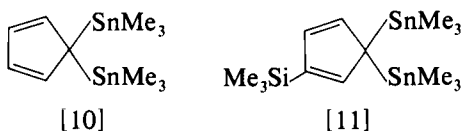
D. Temperature dependence

As described in Sections III.A.1 and III.A.2, organotin compounds which are complexed with polar solvents or are auto-associated usually show a change in chemical shift to high frequency as the temperature is increased, and this allows the calculation of ΔH values. On the other hand, Mitchell has observed (37) a low-frequency chemical shift change as the temperature is increased in di- and tri-isopropyltin bromides. These molecules are unlikely to be self-associated under the conditions used.

The following values are obtained for $^i\text{Pr}_2\text{SnBr}_2$: -10°C , $\delta + 100.1$

ppm, linewidth (LW) 17 Hz; 50°C , $\delta + 93.2$ ppm, LW 62 Hz; 100°C , $\delta + 88.3$ ppm, LW 73 Hz. Over the same temperature range, the shift of $^1\text{Pr}_3\text{SnBr}$ varies between $+125.7$ and $+108.9$ ppm, while the LW is practically invariant at 33 ± 2 Hz. The changes in linewidth are ascribed to variations in the relaxation time of the ^{119}Sn nucleus.

Torocheshnikov (88) has studied the temperature variation of ^{119}Sn chemical shifts in two trimethylstannyl derivatives of cyclopentadiene, [10] and [11]. In these two compounds, a non-degenerate metallotropic



rearrangement takes place and the ^{119}Sn chemical shifts exhibit a strong dependence upon temperature (Table XV), reflecting a displacement of the fast metallotropic equilibrium.

TABLE XV

Temperature dependence of ^{119}Sn chemical shifts^a for neat $\text{C}_5\text{H}_4(\text{SnMe}_3)_2$ and $\text{Me}_3\text{SiC}_5\text{H}_3(\text{SnMe}_3)_2$ (88)

$\text{C}_5\text{H}_4(\text{SnMe}_3)_2$		$\text{Me}_3\text{SiC}_5\text{H}_3(\text{SnMe}_3)_2$	
T ($^\circ\text{C}$)	Shift	T ($^\circ\text{C}$)	Shift
26	336.4	26	227.4
42	321.9	42	209.4
58	305.8	52	194.5
68	297.4	63	182.5
79	287.0	85	162.4
90	274.7	95	155.4
127	244.4	105	144.4
141	232.2	115	138.2
151	222.4	120	130.0
		136	111.5
		145	103.9

^a Quoted in Hz relative to Me_4Sn .

It has been reported (72) that three unassociated methyltin compounds with highly shielded tin nuclei show linear increases in chemical shift with temperature: $\text{Me}_2\text{Sn}(\text{O}^i\text{Bu})_2 + 0.06$ ppm K^{-1} ; $\text{MeSn}(\text{O}^i\text{Bu})_3 + 0.11$ ppm K^{-1} ; $\text{MeSnI}_3 + 0.26$ ppm K^{-1} .

IV. SURVEY OF ^{119}Sn CHEMICAL SHIFT DATA

A. Presentation of tables

XVI	Methyltin compounds, MeSnX_3 .
XVII	Dimethyltin compounds, Me_2SnX_2 and $\text{Me}_2\text{SnXX}'$.
XVIII	Trimethyltin compounds, Me_3SnX .
XIX	Ethyltin compounds, EtSnX_3 .
XX	Diethyltin compounds, Et_2SnX_2 .
XXI	Triethyltin compounds, Et_3SnX .
XXII	n-Butyltin compounds, BuSnX_3 .
XXIII	Di-n-butyltin compounds, Bu_2SnX_2 .
XXIV	Tri-n-butyltin compounds, Bu_3SnX .
XXV	n-Octyltin compounds, $\text{Oct}_n\text{SnX}_{4-n}$.
XXVI	Phenyltin compounds, PhSnX_3 .
XXVII	Diphenyltin compounds, Ph_2SnX_2 .
XXVIII	Triphenyltin compounds, Ph_3SnX .
XXIX	Other compounds, RSnX_3 .
XXX	Other compounds, R_2SnX_2 and $\text{RR}'\text{SnX}_2$.
XXXI	Other compounds, R_3SnX , $\text{RR}'_2\text{SnX}$, and $\text{RR}'\text{R}''\text{SnX}$.
XXXII	Symmetrical tetraorganotin compounds, R_4Sn .
XXXIII	Unsymmetrical tetraorganotin compounds, $\text{R}_n\text{SnR}'_{4-n}$.
XXXIV	Organotin hydrides, $\text{R}_n\text{SnH}_{4-n}$.
XXXV	Compounds containing tin-metal bonds: (a) Sn-Sn, Sn-Si, and Sn-Li bonds; (b) Tin-transition metal bonds.
XXXVI	Organotin oxides (containing an Sn-O-Sn bond): (a) Unsubstituted organotin oxides, $\text{R}_3\text{SnOSnR}_3$; (b) 1,3-Disubstituted distannoxanes, $\text{X} \cdot \text{R}_2\text{SnOSnR}_2 \cdot \text{X}$.
XXXVII	Stannasiloxanes (containing an Sn-O-Si bond).
XXXVIII	Organotin sulphides, selenides, and tellurides (containing an Sn-X-Sn bond).
XXXIX	Organotin derivatives of carboranes.
XL	Covalent organotin halide complexes.
XLI	Ionic organotin halide complexes.

B. Tables of data

The formula of each compound is followed by:

- (a) The solution conditions. The measurement refers to that at room temperature (r.t.) (*ca.* 25°C) unless otherwise indicated. If the same compound has been run at different dilutions, the relevant values of the ^{119}Sn chemical shifts are normally included.

- (b) The value of the ^{119}Sn chemical shift in ppm relative to tetramethyltin, together with the error (shown in brackets) if quoted.
- (c) The literature reference. If a compound has been examined by more than one group of workers, all the appropriate shift values are listed. The literature is completely covered up to mid-1977.

Note added in proof (July, 1978).

Since this review was submitted, further reports of ^{119}Sn chemical shift data have appeared for compounds of the type $\text{Bu}_2\text{Sn}(\text{OCH}_2\text{CH}_2)_2\text{NR}$, (131) $\text{Me}_n\text{Sn}(2\text{-furyl})_{4-n}$, (132) R_2SnXY , (133) $\text{R}_3\text{Sn}^i\text{Bu}$, (134) $\text{R}_n\text{Sn}(\text{C}\equiv\text{CR}')_{4-n}$, (135, 136) $\text{Ph}_3\text{SnCH}_2\text{X}$, (137) $\text{R}_3\text{SnSnR}'_3$, (124) and 1-stannacyclopentadienes, (138) which are not included in the tables.

Compound	Solution	Shift	Ref.
XVI. Compounds of the type MeSnX₃			
MeSnCl ₃	3–20% in PhH or CHCl ₃	+21	22
	+10% PhH	+19 (0.3)	7
	3 mol % in PhH	+20.03 (0.47)	105
	8 mol % in PhH	+16.23 (0.09)	105
	satd. PhH	+18.73 (0.04)	105
	satd. PhH (60°C)	+8.67 (2.0)	45
	neat liquid (74°C)	+6.03 (1.2)	105
	various solns. in Me ₂ CO	–103.6 to –151.2	4
	various solns. in H ₂ O	–474 to –481	4
	5 M in CCl ₄	–15.2 (0.1)	40
	23 mol % in Me ₂ S	–167	48
	CH ₂ Cl ₂	+4.4	121
	3–20% in PhH or CHCl ₃	–165	22
MeSnBr ₃	CH ₂ Cl ₂	–170 (0.05)	7
MeSnI ₃	3–20% in PhH or CHCl ₃	–600 (extrap.)	22
	satd. CCl ₄	–699.5 (1)	83
MeSnI ₂ Cl	20% MeSnI ₃ /MeSnCl ₃ in PhH	–436 (3)	83
MeSnICl ₂	20% MeSnI ₃ /MeSnCl ₃ in PhH	–202 (5)	83
MeSn(OEt) ₃	50% v/v in mesitylene	–434 (10)	68
	50% v/v in mesitylene (72°C)	–407 (5)	68
	PhH	–130.59	86
	neat liquid	–302 (2)	23, 64, 68
MeSn(O ⁱ Bu) ₃	neat liquid	–177 (1)	64
	neat liquid	–177.2 (0.2)	68
	neat liquid	–167	23
	50% v/v in mesitylene	–452 (5)	68
MeSn(O ^t Bu) ₃	50% v/v in mesitylene (65°C)	–406 (10)	68

Compound	Solution	Shift	Ref.
$\text{MeSn}(\text{SMe})_3$	3–20% in PhH or CHCl_3	+167	22
	30% v/v in DMSO	+103	48
	30% v/v in Me_2S	+160	48
	CH_2Cl_2	+155	121
$\text{MeSn}(\overline{\text{OCH}_2\text{CH}_2})_3\text{N}$?	–352 to –540	127
$\text{MeSn}(\text{SEt})_3$	neat liquid	+144	48
$\text{MeSn}(\text{SEt})_2\text{I}$	10% $\text{MeSnI}_3/\text{MeSn}(\text{SEt})_3$ in CH_2Cl_2	–2 (5)	83
$\text{MeSn}(\text{SEt})\text{I}_2$	10% $\text{MeSnI}_3/\text{MeSn}(\text{SEt})_3$ in CH_2Cl_2	–274 (2)	83
$\text{MeSn}(\text{S}^i\text{Pr})_3$	neat liquid	+119.5	48
$\text{MeSn}(\text{S}^i\text{Bu})_3$	neat liquid	+65	48
$\text{MeSn}(\text{S}^i\text{Bu})_2\text{I}$	10% $\text{MeSnI}_3/\text{MeSn}(\text{S}^i\text{Bu})_3$ in CH_2Cl_2	–84 (4)	83
$\text{MeSn}(\text{S}^i\text{Bu})\text{I}_2$	10% $\text{MeSnI}_3/\text{MeSn}(\text{S}^i\text{Bu})_3$ in CH_2Cl_2	–321 (2)	83
$\text{MeSn}(\text{S}^o\text{Oct})_3$	neat liquid	+123.6	23
$\text{MeSn}(\text{SPh})_3$	neat liquid	+101.5	48
$\text{MeSn}(\text{SPh})_2\text{I}$	10% $\text{MeSnI}_3/\text{MeSn}(\text{SPh})_3$ in CH_2Cl_2	+45 (2)	83
$\text{MeSn}(\text{SPh})\text{I}_2$	10% $\text{MeSnI}_3/\text{MeSn}(\text{SPh})_3$ in CH_2Cl_2	–294 (1)	83
$\text{MeSn}(\overline{\text{SCH}_2\text{CH}_2\text{S}})\text{S}(\text{CH}_2)_2\text{S}-\overline{\text{Sn}(\text{Me})\text{SCH}_2\text{CH}_2\text{S}}$	dil. CH_2Cl_2	+173	90
$\text{MeSn}(\overline{\text{DMSO}})(\overline{\text{SCH}_2\text{CH}_2\text{S}})\text{S}(\text{CH}_2)_2\text{S}-\overline{\text{Sn}(\text{Me})(\text{DMSO})\text{SCH}_2\text{CH}_2\text{S}}$	dil. DMSO	+24 (2.5)	90
$\text{MeSn}(\overline{\text{DMSO}})(\overline{\text{SCH}_2\text{CH}_2\text{S}})\text{S}(\text{CH}_2)_2\text{S}-\overline{\text{Sn}(\text{Me})(\text{DMSO})\text{SCH}_2\text{CH}_2\text{S}}$	satd. DMSO	+23.8 (2.5)	23
$\text{MeSn}(\text{SeMe})_3$	neat liquid	+14.8	87
$\text{MeSn}(\text{SePh})_3$	neat liquid	–16.5	87
$\text{MeSn}(\text{NMe}_2)_3$	25% v/v in PhH	–15.1	114
$\text{MeSn}(\text{NEt}_2)_3$	25% v/v in PhH	–24	114
	neat liquid	–28 (2)	23
$(\text{MeSnCl}.\text{NEt}_2)_3$	PhH	–156 (1.5)	7

Compound	Solution	Shift	Ref.
XVII. Compounds of the type Me_2SnX_2 and $\text{Me}_2\text{SnXX}'$			
Me_2SnCl_2	1.5 mol % in PhH	+140.1 (0.04)	45
	3.5 mol % in PhH	+136.7 (0.04)	45
	6 mol % in PhH	+136.8 (0.04)	45
	3–20% in PhH or CHCl_3	+140	22
	satd. PhH	+134.2 (2.0)	80
	satd. CCl_4	+141.2	40
	CH_2Cl_2	+126.6	121
	5 mol % in CH_2Cl_2	+137.5 (0.5)	9, 99
	20% in CH_2Cl_2	+137 (0.3)	7
	Me_2CO	+36 (2.0)	1
	Me_2CO	+19.6 (0.1)	40
	6 mol % in Me_2S	+50	48
	neat liquid at m.p.	+132.5 (0.8)	80
Me_2SnBr_2	CHCl_3	+74.3	4
	3–20% in PhH or CHCl_3	+70	22
	3–20% in PhH or CHCl_3	–159	22
Me_2SnI_2	20% in CH_2Cl_2	–157 (0.5)	10
Me_2SnICl	20% $\text{Me}_2\text{SnI}_2/\text{Me}_2\text{SnCl}_2$ in PhH	+15 (5)	83
$\text{Me}_2\text{Sn(OMe)}_2$	PhH	–126.32	86
$\text{Me}_2\text{Sn(OMe)Cl}$	dil. CH_2Cl_2	+126 and –90	69
$\text{Me}_2\text{Sn(OEt)}_2$	25% v/v in mesitylene	–126 (2)	64, 68
	PhH	–125.90	86
	neat liquid	–129 (1)	23, 68
$\text{Me}_2\text{Sn(O}^i\text{Pr)}_2$	neat liquid	–73.0 (2)	68
	neat liquid (74°C)	–72.5	23
	14 mol % in mesitylene	–92.5	23
	neat liquid	–133 (1)	68
$\text{Me}_2\text{Sn(O}^n\text{Bu)}_2$	neat liquid		

Compound	Solution	Shift	Ref.
$\text{Me}_2\text{Sn}(\text{O}^i\text{Bu})_2$	neat liquid	-121 (1)	68
$\text{Me}_2\text{Sn}(\text{O}^s\text{Bu})_2$	neat liquid	-93 (1)	68
$\text{Me}_2\text{Sn}(\text{O}^i\text{Bu})_2$	neat liquid	-2 (1)	64
	neat liquid	-1.8 (0.1)	68
$\text{Me}_2\text{Sn}(\text{O}^{\text{neo}}\text{Pent})_2$	neat liquid (110°C)	+12 (1)	68
	neat liquid (131°C)	+15	23
$\text{Me}_2\text{Sn}(\text{acac})_2$	10% in CDCl_3	-366	23
$\text{Me}_2\text{Sn}(\text{SMe})_2$	3-20% in PhH or CHCl_3	+144	22
	CH_2Cl_2	+136.7	121
$\text{Me}_2\text{Sn}(\text{SEt})_2$	neat liquid	+127	48
$\text{Me}_2\text{Sn}(\text{S}^i\text{Pr})_2$	neat liquid	+110	48
$\text{Me}_2\text{Sn}(\text{S}^i\text{Pr})\text{I}$	50% $\text{Me}_2\text{SnI}_2/\text{Me}_2\text{Sn}(\text{S}^i\text{Pr})_2$ in PhH	+26 (2)	83
$\text{Me}_2\text{Sn}(\text{S}^i\text{Bu})_2$	neat liquid	+75	48
$\text{Me}_2\text{Sn}(\text{SPh})_2$	neat supercooled liquid	+122.5	48
	10% in CH_2Cl_2	+125.6 (0.1)	83
$\text{Me}_2\text{Sn}(\text{SPh})\text{I}$	20% $\text{Me}_2\text{Sn}(\text{SPh})_2/\text{Me}_2\text{SnI}_2$ in PhH	+28 (2)	83
$\text{Me}_2\text{Sn}(\text{SC}_6\text{H}_4\text{Cl-4})_2$	15% in CH_2Cl_2	+128.3 (0.2)	83
$\text{Me}_2\text{Sn}(\text{SC}_6\text{H}_4\text{Br-4})_2$	10% in CH_2Cl_2	+127.6 (0.2)	83
$\text{Me}_2\text{Sn}(\text{SC}_6\text{H}_4\text{NO}_2\text{-4})_2$	10% in CH_2Cl_2	+130.8 (0.1)	83
$\text{Me}_2\text{Sn}(\text{SC}_6\text{H}_4\text{NH}_2\text{-4})_2$	5% in CH_2Cl_2	+121.6 (0.1)	83
$\text{Me}_2\text{Sn}(\text{SC}_6\text{H}_4\text{Me-4})_2$	15% in CH_2Cl_2	+123.5 (0.1)	83
$\text{Me}_2\text{Sn}(\text{SC}_6\text{H}_4^i\text{Bu-4})_2$	10% in CH_2Cl_2	+124.7 (0.1)	83
$\text{Me}_2\text{SnSCH}_2\text{CH}_2\text{S}$	10% in CDCl_3	+194 (0.9)	65, 71
	dil. CH_2Cl_2	+190	90
	20% in CH_2Cl_2	+194 (0.05)	10
	dil. DMSO	-72.6	90
$\text{Me}_2\text{Sn}[\overline{\text{SCH}_2\text{CH}_2\text{S}}]_2\text{DMSO}$	DMSO	-72.6	23
$\text{Me}_2\text{SnS}(\text{CH}_2)_3\text{S}$	dil. CH_2Cl_2	+149	90
	dil. DMSO	-56.1 (2)	90

Compound	Solution	Shift	Ref.
$[\text{Me}_2\text{SnS}(\text{CH}_2)_3\text{S}]_n$	dil. CH_2Cl_2	+132 (3)	90
$[\text{Me}_2\text{SnS}(\text{CH}_2)_3\text{CH}_2]_n$	dil. CH_2Cl_2	+88 (2)	90
$[\text{Me}_2\text{SnS}(\text{CH}_2)_4\text{S}]_n$	dil. CH_2Cl_2	+134 (3)	90
$\text{Me}_2\text{Sn}(\text{SeMe})_2$	neat liquid	+57.1	87
$\text{Me}_2\text{Sn}(\text{SePh})_2$	neat supercooled liquid	+54.1	87
$\text{Me}_2\text{Sn}(\text{SCSNEt}_2)_2$	CH_2Cl_2	-336 (0.05)	7
$\text{Me}_2\text{Sn}(\text{SCSNEt}_2)\text{Cl}$	CH_2Cl_2	-204 (0.05)	7
$\text{Me}_2\text{Sn}(\text{SCSNEt}_2)\text{Br}$	CH_2Cl_2	-233 (0.05)	7
$\text{Me}_2\text{Sn}(\text{SCSNEt}_2)\text{I}$	CH_2Cl_2	-292 (0.05)	7
$\text{Me}_2\text{Sn}[\text{SCSN}(\text{CH}_2)_4]_2$	CH_2Cl_2	-310	23
$\text{Me}_2\text{Sn}(\text{NMe}_2)_2$	25% v/v in PhH	+58.8	114
$\text{Me}_2\text{Sn}(\text{NEt}_2)_2$	+50% PhH	+41 (0.05)	7
	25% v/v in PhH	+45	114
$(\text{Me}_2\text{SnNEt})_3$	+10% PhH	+76 (0.1)	7
XVIII. Compounds of the type Me_3SnX			
Me_3SnCl	5 mol % in CS_2	+152.7	9
	5 mol % in DMSO	+179.3	9
	14 mol % in Me_2S	+126	48
	5 mol % in cyclo- C_6H_{12}	+153.5	9
	various solns. in cyclo- C_6H_{12}	+155.7 to +158.6	4
	14.6 mol % in CDCl_3	+171.2 (0.23)	45
	33.7 mol % in CDCl_3	+165.7 (0.12)	45
	67.3 mol % in CDCl_3	+159.5 (0.09)	45
	+5% CH_2Cl_2	+166 (0.3)	7
	5 mol % in CH_2Cl_2	+168.9	9
	12.1 mol % in CH_2Cl_2	+165.6 (0.23)	45
	32.2 mol % in CH_2Cl_2	+161.8 (0.23)	45

Compound	Solution	Shift	Ref.
Me ₃ SnCl	73 mol % in CH ₂ Cl ₂	+155.1 (0.09)	45
	CH ₂ Cl ₂	+152	121
	3–20% in PhH or CHCl ₃	+164.2	22
	2.4 mol % in PhH	+159.0 (2.2)	45
	5.0 mol % in PhH	+161.6	9
	6.5 mol % in PhH	+159.3 (0.47)	45
	16.4 mol % in PhH	+159.7 (0.23)	45
	35.9 mol % in PhH	+159.5 (0.09)	45
	76.5 mol % in PhH	+156.4 (0.04)	45
	5 M in CCl ₄	+160.0	40
	5.0 mol % in CCl ₄	+158.0	9
	10.0 mol % in CCl ₄	+165.8 (0.47)	45
	30.6 mol % in CCl ₄	+164.0 (0.23)	45
	74.5 mol % in CCl ₄	+161.9 (0.04)	45
	1:0.64 M Me ₃ SnCl/Pyrid. + CCl ₄	+55.07 (0.04)	45
	1:1.3 M	+36.52 (0.09)	45
	1:2.5 M	+13.05 (0.23)	45
	1:4.5 M	−0.45 (0.09)	45
	1:12.7 M	−9.52 (0.12)	45
	3 mol % in MeCN (−20°C)	+92.7	50
	(−5°C)	+101.6	50
	(r.t.)	+110.8	50
	(40°C)	+119.5	50
	(60°C)	+126.4	50
	(70°C)	+129.0	50
	5 mol % in MeCN (−20°C)	+95.2	50
	(−5°C)	+103.4	50
	(r.t.)	+111.5	50
	(40°C)	+120.4	50

Compound	Solution	Shift	Ref.
Me ₃ SnCl	5 mol % in MeCN	(60°C)	+127.1
		(70°C)	+129.6
	10 mol % in MeCN	(-20°C)	+98.2
		(-5°C)	+105.0
		(r.t.)	+113.2
		(40°C)	+123.6
		(60°C)	+128.7
		(70°C)	+131.1
	20 mol % in MeCN	(-20°C)	+101.7
		(-5°C)	+108.7
		(r.t.)	+116.2
		(40°C)	+126.1
		(60°C)	+130.9
		(70°C)	+133.5
	40 mol % in MeCN	(-20°C)	+107.3
		(-5°C)	+114.7
		(r.t.)	+118.9
		(40°C)	+129.3
		(60°C)	+135.6
		(70°C)	+137.5
	2 mol % in dioxan	(r.t.)	+120.4
		(37°C)	+125.5
		(50°C)	+131.6
		(68°C)	+136.4
		(82°C)	+140.1
	5 mol % in dioxan	(r.t.)	+121.5
		(37°C)	+126.3
		(50°C)	+132.5
		(68°C)	+136.9
		(82°C)	+140.7

Compound	Solution	Shift	Ref.
Me_3SnCl	10 mol % in dioxan (r.t.)	+123.8	50
	(37°C)	+127.6	50
	(50°C)	+133.7	50
	(68°C)	+137.9	50
	(82°C)	+141.4	50
	15 mol % in dioxan (r.t.)	+124.3	50
	(37°C)	+128.0	50
	(50°C)	+134.1	50
	(68°C)	+138.3	50
	(82°C)	+141.9	50
	20 mol % in dioxan (r.t.)	+125.3	50
	(37°C)	+129.1	50
	(50°C)	+135.2	50
	(68°C)	+139.6	50
	84.5 mol % in dioxan	+137.1 (0.23)	45
	2 mol % in Me_2CO (−55°C)	+77.8	50
	(−34°C)	+87.5	50
	(−2°C)	+98.4	50
	(r.t.)	+108.5	50
	(37°C)	+116.4	50
	(50°C)	+121.0	50
	5 mol % in Me_2CO (−55°C)	+79.0	50
	(−34°C)	+89.0	50
	(−2°C)	+100.4	50
	(r.t.)	+109.3	50
	(37°C)	+117.4	50
	(50°C)	+121.7	50
	10 mol % in Me_2CO (−55°C)	+80.8	50
	(−34°C)	+90.4	50

Compound	Solution	Shift	Ref.
Me_3SnCl	10 mol % in Me_2CO (-2°C)	+101.5	50
	(r.t.)	+110.3	50
	(37°C)	+118.5	50
	(50°C)	+122.9	50
	15 mol % in Me_2CO (-55°C)	+82.5	50
	(-34°C)	+91.3	50
	(-2°C)	+102.7	50
	(r.t.)	+111.8	50
	(37°C)	+119.8	50
	(50°C)	+124.1	50
	20 mol % in Me_2CO (-55°C)	+84.8	50
	(-34°C)	+92.7	50
	(-2°C)	+104.3	50
	(r.t.)	+113.2	50
	(37°C)	+121.3	50
	(50°C)	+125.5	50
	30.5 mol % in Me_2CO	+119.8 (0.04)	45
	71.9 mol % in Me_2CO	+136.6 (0.12)	45
	10–22 mol % in $\text{Me}_2\text{CO}/\text{H}_2\text{O}$	range of <i>ca.</i> 25	4
	2–14 mol % in H_2O	range of <i>ca.</i> 23	4
	10–22 mol % in MeOH	range of <i>ca.</i> 10	4
	2 mol % in MeOH (-13°C)	+28.6	50
	(1°C)	+34.0	50
	(r.t.)	+40.9	50
	(33°C)	+43.9	50
	(56°C)	+51.9	50
	4 mol % in MeOH (-13°C)	+29.3	50
	(1°C)	+34.6	50
	(r.t.)	+41.7	50

Compound	Solution	Shift	Ref.
Me_3SnCl	4 mol % in MeOH (33°C)	+44.4	50
	(56°C)	+52.8	50
	7 mol % in MeOH (−13°C)	+30.3	50
	(1°C)	+35.9	50
	(r.t.)	+43.0	50
	(33°C)	+45.5	50
	(56°C)	+54.1	50
	12 mol % in MeOH (−13°C)	+34.1	50
	(1°C)	+39.9	50
	(r.t.)	+48.2	50
	(33°C)	+52.1	50
	(56°C)	+61.2	50
	20 mol % in MeOH (−13°C)	+36.6	50
	(1°C)	+42.3	50
	(r.t.)	+51.1	50
	(33°C)	+54.4	50
	(56°C)	+64.4	50
	2 mol % in EtOH (−35°C)	+21.4	50
	(0°C)	+35.7	50
	(r.t.)	+43.7	50
	(30°C)	+51.7	50
	(50°C)	+62.3	50
	5 mol % in EtOH (−35°C)	+22.7	50
	(0°C)	+35.8	50
	(r.t.)	+44.6	50
	(30°C)	+52.6	50
	(50°C)	+63.5	50
	10 mol % in EtOH (−35°C)	+24.9	50
	(0°C)	+37.1	50

Compound	Solution	Shift	Ref.
Me_3SnCl	10 mol % in EtOH (r.t.)	+47.9	50
	(30°C)	+54.0	50
	(50°C)	+65.2	50
	15 mol % in EtOH (−35°C)	+26.7	50
	(0°C)	+40.1	50
	(r.t.)	+50.7	50
	(30°C)	+57.5	50
	(50°C)	+68.5	50
	20 mol % in EtOH (−35°C)	+27.7	50
	(0°C)	+42.2	50
	(r.t.)	+51.8	50
	(30°C)	+60.2	50
	(50°C)	+69.4	50
Me_3SnBr	PhH	+128 (0.3)	7
	3–20% in PhH or CHCl_3	+128	22
	3–5 mol % in H_2O	range of <i>ca.</i> 6	4
	9–34 mol % in $\text{H}_2\text{O}/\text{Me}_2\text{CO}$	range of <i>ca.</i> 30	4
	neat liquid	+130.7	4
Me_3SnI	3–20% in PhH or CHCl_3	+38.6	22
Me_3SnOH	satd. CDCl_3	+76.7 (0.04)	45
	MeOH	+51.8	4
	satd. CH_2Cl_2	+118 (1)	100
	2% in CHCl_3	+128.09	86
	8% in CHCl_3	+122.24	86
Me_3SnOMe	PhH	+120.87	86
	satd. PhH	+129 (2)	68
Me_3SnOEt	PhH	+110.49	86
	50% v/v in PhH	+119 (2)	68
	neat liquid	+114.3 (0.1)	64

Compound	Solution	Shift	Ref.
Me ₃ SnO ^t Pr	50% v/v in PhH	+109 (2)	68
Me ₃ SnO ^t Bu	neat liquid	+89.5 (0.1)	64
	50% v/v in PhH	+91 (2)	68
Me ₃ SnOPh	10% m C ₆ H ₁₂	+134.3 (0.1)	130
	10% m PhH	+131.8 (0.2)	130
Me ₃ SnOC ₆ H ₄ OMe-4	10% m PhH	+131.4 (0.2)	130
Me ₃ SnOC ₆ H ₄ NO ₂ -4	10% m PhH	+147.5 (0.4)	130
Me ₃ SnOC ₆ H ₄ Cl-4	10% m C ₆ H ₁₂	+138.8 (0.1)	130
	40% m C ₆ H ₁₂	+144.9 (0.1)	130
Me ₃ SnOC ₆ H ₄ Cl-3	10% m C ₆ H ₁₂	+148.5 (0.1)	130
Me ₃ SnON=C(cyclo-C ₆ H ₁₁) ₂	50% in PhH	+20 (0.1)	10
Me ₃ SnON=C ₆ H ₁₀	20% in CH ₂ Cl ₂	+132 (0.9)	10
(Me ₃ SnO) ₃ P=O	neat liquid	+24.9	4
Me ₃ SnOPH. Ph	10% in PhH	+13 (0.3)	10
Me ₃ SnOCHO	3 m CDCl ₃	+2.5	56
	0.05 m CDCl ₃	+150	56
Me ₃ SnOCOMe	satd. CDCl ₃	+129	45
Me ₃ SnSMe	3–20% in PhH or CHCl ₃	+90	22
	CH ₂ Cl ₂	+85.1	121
Me ₃ SnSEt	neat liquid	+78	48
Me ₃ SnS ^t Pr	neat liquid	+69.5	48
Me ₃ SnS ^t Pr, W(CO) ₃	satd. PhH	+132 (1)	23
Me ₃ SnS ^t Bu	neat liquid	+55.5	48
Me ₃ SnSCPh ₃	50% in CH ₂ Cl ₂	+67.4 (2)	83
Me ₃ SnSPH	neat liquid	+90.5	48
	25% in CH ₂ Cl ₂	+91.3 (0.2)	83
	10% m PhH	+90.1 (0.2)	130
	40% m PhH	+90.1 (0.2)	130
Me ₃ SnSC ₆ H ₄ Me-4	25% in CH ₂ Cl ₂	+92.9 (0.2)	83
	10% m PhH	+89.9 (0.2)	130

Compound	Solution	Shift	Ref.
$\text{Me}_3\text{SnSC}_6\text{H}_4^t\text{Bu}-4$	25% in CH_2Cl_2	+89.7 (0.2)	83
$\text{Me}_3\text{SnSC}_6\text{H}_4\text{OMe}-4$	10% m PhH	+90.2 (0.2)	130
$\text{Me}_3\text{SnSC}_6\text{H}_4\text{NH}_2-4$	25% in CH_2Cl_2	+90.7 (0.2)	83
$\text{Me}_3\text{SnSC}_6\text{H}_4\text{NMe}_2-4$	10% m PhH	+87.4 (0.2)	130
$\text{Me}_3\text{SnSC}_6\text{H}_4\text{Cl}-4$	25% in CH_2Cl_2	+95.1 (0.2)	83
$\text{Me}_3\text{SnSC}_6\text{H}_4\text{Cl}-3$	10% m PhH	+101.5 (0.2)	130
$\text{Me}_3\text{SnSC}_6\text{H}_4\text{Br}-4$	CH_2Cl_2	+98.7 (0.2)	83
$\text{Me}_3\text{SnSC}_6\text{H}_4\text{NO}_2-4$	CH_2Cl_2	+103.7 (0.2)	83
	10% m PhH	+99.5 (0.2)	130
$\text{Me}_3\text{SnS}(\text{CH}_2)_2\text{SSnMe}_3$	neat liquid	+82.3	90
$\text{Me}_3\text{SnS}(\text{CH}_2)_3\text{SSnMe}_3$	neat liquid	+81.5	90
$\text{Me}_3\text{SnS}(\text{CH}_2)_4\text{SSnMe}_3$	neat liquid	+80.5	90
Me_3SnSeMe	neat liquid	+45.6	87
Me_3SnSePh	neat liquid	+55.0	87
$\text{Me}_3\text{SnNMe}_2$	10% v/v in PhH	+75.5	114
	25% v/v in PhH	+75.0	114
	40% v/v in PhH	+75.0	114
	80% v/v in PhH	+74.7	114
$\text{Me}_3\text{SnNEt}_2$	neat liquid + 50% PhH	+58 (0.1)	7
	25% v/v in PhH	+60	114
	cyclo- C_6H_{12}	+50.1	67
$\text{Me}_3\text{SnNH} \cdot \text{CH}_2\text{Ph}$	neat liquid	+56 (2)	23
$(\text{Me}_3\text{Sn})_2\text{NCH}_2\text{Ph}$	neat liquid	+80	23
Me_3SnNHPh	neat liquid	+47 (2)	23
$\text{Me}_3\text{Sn}^{15}\text{NHPh}$	neat liquid + 10% PhH	+46.4 (2)	83
$(\text{Me}_3\text{Sn})_2\text{NPh}$	neat liquid	+61 (2)	23
$\text{Me}_3\text{SnNPh} \cdot \text{SiMe}_3$	50% in PhH	+64 (0.05)	10
$\text{Me}_3\text{SnN}=\text{C}(\text{CF}_3)_2$?	+73	23
Me_3SnNCS	satd. CCl_4	+59.4 (0.04)	45

Compound	Solution	Shift	Ref.
Me_3SnNCS	20% in PhH	+58.71	123
	1.25% in PhH	+67.95	123
Me_3SnNCO	20% in PhH	+82.74	123
	1.25% in PhH	+86.55	123
Me_3SnPPh	10% in PhH	+18 (0.4)	10, 104
$\text{Me}_3\text{SnPPh}_2$	neat liquid + 25 mol % dioxan	-4	102
	50% in PhH	-3 (0.1)	10, 104
	neat liquid + <i>ca.</i> 35% PhH	-2.3 (0.1)	116
$\text{Me}_3\text{SnPPh}_2\text{W}(\text{CO})_5$	PhH	+33.7 (0.2)	116
$(\text{Me}_3\text{Sn})_2\text{PPh}$	neat liquid + <i>ca.</i> 10% CH_2Cl_2	+14.2 (0.1)	116
$(\text{Me}_3\text{Sn})_2\text{PPhCr}(\text{CO})_5$	PhH	+39.7 (0.1)	116
$(\text{Me}_3\text{Sn})_2\text{PPhW}(\text{CO})_5$	PhH	+41.6 (1.0)	116
$(\text{Me}_3\text{Sn})_3\text{P}$	neat liquid + <i>ca.</i> 35% PhH	+36.3 (0.1)	116
$(\text{Me}_3\text{Sn})_3\text{PCr}(\text{CO})_5$	PhH	+64.2 (0.1)	116
$(\text{Me}_3\text{Sn})_3\text{PW}(\text{CO})_5$	PhH	+63.4 (0.1)	116
$\text{Me}_3\text{SnB}(\text{NMe}_2)_2$	neat liquid	-150 (1)	117
$\text{Me}_3\text{SnB}(\text{NMe}_2)\text{Cl}$	neat liquid	-139 (1)	117
XIX. Compounds of the type EtSnX_3			
EtSnCl_3	CCl_4	+6.5 (1.2)	99
	CCl_4	+4.2	9
	30% in CCl_4	+6.0 (0.5)	65
	neat liquid + 3 drops CH_2Cl_2 (-5°C)	+2.0 (1.5)	105
	(<i>r.t.</i>)	+3.0 (2.0)	105
EtSnBr_3	(50°C)	+2.0 (2.0)	105
	50% in CCl_4	-141 (0.3)	65

Compound	Solution	Shift	Ref.
XX. Compounds of the type Et_2SnX_2			
Et_2SnCl_2	CH_2Cl_2	+125 (0.8)	7
	30% in $\text{CCl}_4 + \text{CH}_2\text{Cl}_2$	+121 (1.3)	65
	CCl_4	+126.3	9
	CCl_4	+122.5 (2.0)	69
	Me_2CO	+62 (1.0)	1
Et_2SnBr_2	CH_2Cl_2	+99 (3.0)	7
	20% in CCl_4	+96 (0.5)	65
	CCl_4	+92.5 (4.0)	69
	15% in CCl_4	+53 (1.1)	65
Et_2SnI_2	10% in PhH	-165 (1.1)	65, 71
$\text{Et}_2\text{Sn(OMe)}_2$	neat liquid	-181 (1.1)	65, 71
	10% in PhH	-165 (1.1)	65, 71
$\text{Et}_2\text{Sn(O}^t\text{Bu)}_2$	neat liquid	-31 (1.3)	65
$\text{Et}_2\text{Sn}(\overline{\text{OCH}_2\text{CH}_2\text{O}})$	25% in CDCl_3	-177 (1.3)	65, 71
$\text{Et}_2\text{Sn(ox)}_2$	25% in CH_2Cl_2	-264 (3.0)	65
$\text{Et}_2\text{Sn(SMe)}_2$	20% in CCl_4	+140 (0.8)	65, 71
$\text{Et}_2\text{Sn}(\overline{\text{SCH}_2\text{CH}_2\text{S}})$	20% in $\text{CH}_2\text{Cl}_2 + \text{CDCl}_3$	+199 (0.1)	65, 71
$\text{Et}_2\text{Sn(NMe}_2)_2$	20% in CCl_4	-67 (1.3)	65
$\text{Et}_2\text{Sn(NEt}_2)_2$	neat liquid	+21 (1.1)	65
	dil. $\times 8$ with PhH	+21 (1.1)	65
XXI. Compounds of the type Et_3SnX			
Et_3SnCl	CH_2Cl_2	+153.4	9
	30% in CCl_4	+155 (0.5)	65
	CCl_4	+150.5 (1.2)	99
	10 mol % in MeCN (-9°C)	+111.6	50

Compound	Solution	Shift	Ref.
Et ₃ SnCl	10 mol % in MeCN (r.t.)	+120.2	50
	(35°C)	+124.8	50
	(48°C)	+127.4	50
	(63°C)	+130.1	50
	25 mol % in MeCN (−9°C)	+115.5	50
	(r.t.)	+124.0	50
	(35°C)	+127.6	50
	(48°C)	+130.7	50
	(63°C)	+133.2	50
	50 mol % in MeCN (−9°C)	+127.2	50
	(r.t.)	+134.8	50
	(35°C)	+137.2	50
	(48°C)	+139.7	50
	(63°C)	+141.9	50
	75 mol % in MeCN (−9°C)	+139.7	50
	(r.t.)	+141.8	50
	(35°C)	+145.4	50
	(48°C)	+147.9	50
	(63°C)	+149.0	50
	90 mol % in MeCN (−9°C)	+146.8	50
	(r.t.)	+148.6	50
	(35°C)	+151.8	50
	(48°C)	+153.1	50
	(63°C)	+154.7	50
	10 mol % in Me ₂ CO (−20°C)	+108.0	50
	(−10°C)	+111.7	50
	(r.t.)	+121.3	50
	(35°C)	+127.7	50
	(48°C)	+129.2	50

Compound	Solution	Shift	Ref.
Et ₃ SnCl	25 mol % in Me ₂ CO (−20°C)	+112.2	50
	(−10°C)	+115.9	50
	(r.t.)	+125.5	50
	(35°C)	+131.6	50
	(48°C)	+133.7	50
	50 mol % in Me ₂ CO (−20°C)	+125.0	50
	(−10°C)	+128.3	50
	(r.t.)	+134.8	50
	(35°C)	+140.0	50
	(48°C)	+142.3	50
	75 mol % in Me ₂ CO (−20°C)	+136.8	50
	(−10°C)	+139.7	50
	(r.t.)	+147.5	50
	(35°C)	+147.8	50
	(48°C)	+149.4	50
	90 mol % in Me ₂ CO (−20°C)	+146.2	50
	(−10°C)	+147.5	50
	(r.t.)	+149.0	50
	(35°C)	+150.9	50
	(48°C)	+152.7	50
	neat liquid	+151 (2)	1
	neat liquid	+155.9	4
Et ₃ SnBr	neat liquid	+148 (0.5)	65
Et ₃ SnOMe	CH ₂ Cl ₂	+100.3	67
Et ₃ SnOCOMe	CH ₂ Cl ₂	+102.4	67

Compound	Solution	Shift	Ref.
XXII. Compounds of the type BuSnX₃			
BuSnCl ₃	CCl ₄	+6.0	9, 67
	neat liquid	-1.4 (0.2)	105
	neat liquid	-3.0 (1)	1
	neat liquid	+4.6 (0.1)	82
BuSn(ox) ₂ Cl	satd. CH ₂ Cl ₂	-395 (5)	72
BuSn(OEt) ₃	16 mol % in PhH	-432 (9)	72
	33 mol % in PhH	-432 (9)	72
	48 mol % in PhH	-432 (9)	72
	neat liquid (r.t.)	-428 (14)	72
	(60°C)	-423 (5)	72
	(100°C)	-412 (5)	72
	(138°C)	-405 (5)	72
BuSn(O ⁿ Pr) ₃	18 mol % in PhH	-387 (9)	72
	23 mol % in PhH	-387 (5)	72
	32 mol % in PhH	-396 (9)	72
	neat liquid (r.t.)	-414 (10)	72
	(47°C)	-415 (9)	72
	(71°C)	-417 (5)	72
	(99°C)	-412 (5)	72
BuSn(O ⁱ Pr) ₃	(122°C)	-405 (5)	72
	10 mol % in PhH	-307 (10)	72
	20 mol % in PhH	-323 (5)	72
	46 mol % in PhH	-327 (5)	72
	76 mol % in PhH	-330 (5)	72
	neat liquid (40°C)	-327 (2)	72
	(76°C)	-311 (5)	72
	(97°C)	-284 (2)	72
	(122°C)	-240 (5)	72
	(154°C)	-222 (9)	72

Compound	Solution	Shift	Ref.
BuSn(O ⁿ Bu) ₃	12 mol % in PhH	-387 (9)	72
	22 mol % in PhH	-405 (9)	72
	38 mol % in PhH	-418 (9)	72
	neat liquid (38°C)	-428 (14)	72
	(65°C)	-423 (9)	72
	(100°C)	-406 (9)	72
	(138°C)	-405 (5)	72
BuSn(O ⁱ Bu) ₃	16 mol % in PhH	-392 (14)	72
	27 mol % in PhH	-397 (10)	72
	44 mol % in PhH	-397 (10)	72
	neat liquid (66°C)	-401 (5)	72
	(100°C)	-378 (5)	72
	(120°C)	-360 (5)	72
	(143°C)	-347 (5)	72
BuSn(O ^s Bu) ₃	19 mol % in PhH	-275 (5)	72
	25 mol % in PhH	-284 (5)	72
	32 mol % in PhH	-298 (5)	72
	41 mol % in PhH	-312 (5)	72
	neat liquid (r.t.)	-325 (5)	72
	(45°C)	-298 (5)	72
	(62°C)	-280 (2)	72
	(80°C)	-240 (14)	72
	(100°C)	-217 (2)	72
	(120°C)	-209 (5)	72
BuSn(O ^t Bu) ₃	(140°C)	-206 (5)	72
	12 mol % in PhH	-199 (5)	72
	18 mol % in PhH	-199 (5)	72
	33 mol % in PhH	-199 (5)	72

Compound	Solution	Shift	Ref.
BuSn(O ^t Bu) ₃	neat liquid (r.t.)	-200 (5)	72
	(60°C)	-208 (5)	72
	(98°C)	-208 (5)	72
	(136°C)	-204 (5)	72
BuSn(^{neo} Pent) ₃	neat liquid (92°C)	-289 (2)	72
	(108°C)	-259 (2)	72
	(122°C)	-236 (5)	72
	(131°C)	-227 (2)	72
	(153°C)	-212 (2)	72
BuSn(NEt ₂) ₃	neat liquid	-44 (2)	103
	50% v/v in PhH	-44 (2)	103
	25% v/v in PhH	-44 (2)	103
XXIII. Compounds of the type Bu₂SnX₂			
Bu ₂ SnCl ₂	CCl ₄	+123·1	9
	CH ₂ Cl ₂	+123·4	67
	+10% PhH	+122 (0·3)	7
	CS ₂	+114 (2·0)	1
	Me ₂ CO	+71 (2·0)	1
	Me ₂ CO	+56	4
Bu ₂ Sn(OMe) ₂	18·9 mol % in CCl ₄	-159 (2)	45
	27·3 mol % in CCl ₄	-161 (2)	45
	45·2 mol % in CCl ₄	-163 (2)	45
	neat liquid (r.t.)	-165 (2)	63
	(70°C)	-165 (2)	45
	(120°C)	-159 (2)	45
	(160°C)	-147 (2)	45

Compound	Solution	Shift	Ref.
Bu ₂ Sn(OEt) ₂	50% in CCl ₄	-154 (4)	80
	neat liquid	-161 (2)	63
Bu ₂ Sn(O ⁿ Pr) ₂	neat liquid	-159 (5)	63
Bu ₂ Sn(O ⁱ Pr) ₂	10.2 mol % in CCl ₄	-31 (5)	45
	12.2 mol % in CCl ₄	-29 (5)	45
	15.4 mol % in CCl ₄	-31 (5)	45
	21 mol % in CCl ₄	-29 (5)	80
	30 mol % in CCl ₄	-40 (5)	80
	52 mol % in CCl ₄	-71 (5)	80
	62 mol % in CCl ₄	-76 (5)	80
	neat liquid (r.t.)	-90 (5)	63
	(r.t.)	-100 (2)	68
	(41°C)	-65 (5)	80
	(50°C)	-38 (5)	80
	(59°C)	-33 (5)	80
	(80°C)	-27 (5)	80
	(93°C)	-27 (5)	80
Bu ₂ Sn(O ⁿ Bu) ₂	neat liquid (r.t.)	-161 (5)	63
	(80°C)	-146 (5)	80
	(99°C)	-126 (5)	80
	(118°C)	-115 (5)	80
Bu ₂ Sn(O ⁱ Bu) ₂	7 mol % in CCl ₄	-105 (2)	80
	9 mol % in CCl ₄	-114 (2)	80
	17 mol % in CCl ₄	-132 (2)	80
	neat liquid	-150 (2)	63
	neat liquid	-154 (4)	68
Bu ₂ Sn(O ^s Bu) ₂	neat liquid	-34 (2)	63
Bu ₂ Sn(O ^t Bu) ₂	4-100 mol % in CCl ₄	-34 (5)	45, 63
	neat liquid	-34 (5)	63

Compound	Solution	Shift	Ref.
$\text{Bu}_2\text{Sn}(\text{OPh})_2$	satd. CCl_4 or PhH	-138 (2)	63
	neat liquid (49°C)	-120 (2)	63
	supercooled liquid	-142 (4)	68
$\text{Bu}_2\text{Sn}(\overline{\text{OCH}_2\text{CH}_2\text{O}})$	satd. CDCl_3	-189 (5)	63
$\text{Bu}_2\text{Sn}(\overline{\text{OCHMeCH}_2\text{O}})$	satd. CDCl_3	-164 (5)	63
$\text{Bu}_2\text{Sn}(\overline{\text{OCHMeCHMeO}})$	satd. CDCl_3	-155 (5)	63
$\text{Bu}_2\text{Sn}(\overline{\text{OCH}_2\text{CH}_2\text{CH}_2\text{O}})$	satd. CDCl_3	-228 (10)	63
$\text{Bu}_2\text{Sn}(\overline{\text{OCH}_2\text{CH}_2\text{CH}_2\text{O}})$	neat liquid (96°C)	-228 (2)	63
$\text{Bu}_2\text{Sn}(\overline{\text{OCH}_2\text{CMe}_2\text{CH}_2\text{O}})$	neat liquid (120°C)	-213 (5)	63
$\text{Bu}_2\text{Sn}(\overline{\text{OCH}_2\text{CMe}^n\text{PrCH}_2\text{O}})$	satd. CCl_4	-233 (5)	63
$\text{Bu}_2\text{Sn}(\overline{\text{O}(\text{CH}_2)_4\text{O}})$	50% in CCl_4	-154 (5)	80
	satd. CCl_4	-154 (5)	63
	neat liquid	-161 (2)	63
$\text{Bu}_2\text{Sn}(\overline{\text{OCH}_2\text{CH}_2\text{S}})$	50% in CDCl_3	-30 (5)	80
	satd. CDCl_3	-32 (2)	63
	satd. PhH	-28 (5)	80
	neat liquid (100°C)	-24 (5)	80
	(128°C)	-24 (5)	63
$\text{Bu}_2\text{Sn}(\text{SEt})_2$	25% in PhH	+123 (2)	80
	25% in PhH (60°C)	+123 (2)	80
	neat liquid (r.t.)	+123 (2)	63
	(60°C)	+123 (2)	80
	(100°C)	+123 (2)	80
$\text{Bu}_2\text{Sn}(\text{SBu})_2$	CCl_4	+127 (2)	67
$\text{Bu}_2\text{Sn}(\overline{\text{SCH}_2\text{CH}_2\text{S}})$	25% in CDCl_3	+193 (0.8)	65, 71
$\text{Bu}_2\text{Sn}[\overline{\text{SCSN}(\text{CH}_2\text{Ph})_2}]_2$	CH_2Cl_2	-340	23
$\text{Bu}_2\text{Sn}[\overline{\text{SCSN}(\text{CH}_2)_4}]_2$	CH_2Cl_2	-313	23

Compound	Solution	Shift	Ref.
$\text{Bu}_2\text{Sn}(\text{NET}_2)_2$	neat liquid	-18 (2)	103
$\text{Bu}_2\text{Sn}(\text{OCOMe})_2$	neat liquid	-195 (1)	1
XXIV. Compounds of the type Bu_3SnX			
Bu_3SnCl	CH_2Cl_2 or CCl_4	+141.2	9, 67
	neat liquid	+143 (2)	1
	neat liquid	+139	4
Bu_3SnBr	+10% PhH	+134 (0.8)	7
Bu_3SnOMe	neat liquid	+83 (7)	63
Bu_3SnOEt	neat liquid	+86 (5)	63
$\text{Bu}_3\text{SnOCH}_2\text{CF}_3$	+20% PhH	+122 (0.5)	7
$\text{Bu}_3\text{SnOCH}_2\text{Ph}$	+20% PhH	+100 (0.5)	7
$\text{Bu}_3\text{SnO}^n\text{Pr}$	neat liquid	+87 (2)	63
$\text{Bu}_3\text{SnOCH}_2\text{CF}_2\text{CF}_2\text{H}$	neat liquid	+119 (7)	80
$\text{Bu}_3\text{SnO}^i\text{Pr}$	neat liquid	+76 (2)	63
$\text{Bu}_3\text{SnO}^n\text{Bu}$	neat liquid	+91 (5)	63
$\text{Bu}_3\text{SnO}^i\text{Bu}$	neat liquid	+82 (5)	63
$\text{Bu}_3\text{SnO}^s\text{Bu}$	neat liquid	+80 (2)	63
$\text{Bu}_3\text{SnO}^t\text{Bu}$	neat liquid	+60 (2)	63
Bu_3SnOPh	neat liquid (r.t.)	+105 (7)	63
	(50°C)	+107 (2)	80
	(85°C)	+105 (2)	80
$\text{Bu}_3\text{SnOO}^i\text{Bu}$	CH_2Cl_2	+105 (1.1)	7
$\text{Bu}_3\text{SnNET}_2$	neat liquid	+36 (2.0)	103
Bu_3SnCN	CH_2Cl_2	-48 (1.3)	7
	satd. CH_2Cl_2	-38 (5.0)	45
	dil. $\times 2$ in PhH	-74 (5.0)	45
	satd. PhH	-83 (2.0)	45

Compound	Solution	Shift	Ref.
Bu_3SnCN	satd. CHCl_3	-42 (2.0)	45
	dil. $\times 3$ in Pyr.	-85 (2.0)	45
	satd. Pyr.	-91 (2.0)	45
$\text{Bu}_3\text{SnOCOMe}$	CH_2Cl_2	+96 (0.8)	7
$\text{Bu}_3\text{SnOCOC}_6\text{H}_4\text{OCOMe-2}$	CH_2Cl_2	+115 (1.3)	7
Bu_3SnOx	neat liquid	+29 (4)	103
$\text{Bu}_3\text{SnOCH}_2\text{CH}_2\text{NEt}_2$	neat liquid	+99.4	120
XXV. Compounds of the type $\text{Oct}_n\text{SnX}_{4-n}$			
$\text{Oct}_3\text{SnCl}_3$	neat liquid	+5.3 (0.1)	37
	neat liquid	+0.5 (2)	105
$\text{Oct}_2\text{SnCl}_2$	CCl_4	+114	80
$\text{Oct}_2\text{SnOCH}_2\text{CH}_2\text{S}$	satd. CDCl_3	-30 (5)	63
XXVI. Compounds of the type PhSnX_3			
PhSnCl_3	CH_2Cl_2	-63	7
	CDCl_3	-64 (2)	80
	neat liquid	-60.5	105
PhSn(SMe)_3	30% in CH_2Cl_2	+107 (2)	83
PhSn(SEt)_3	30% in CH_2Cl_2	+90 (2)	83
$\text{PhSn(S}^i\text{Pr)}_3$	30% in CH_2Cl_2	+69.5 (2)	83
$\text{PhSn(S}^t\text{Bu)}_3$	30% in CH_2Cl_2	+11 (2)	83
$\text{PhSn(SCH}_2\text{Ph)}_3$	30% in CH_2Cl_2	+87.5 (2)	83
PhSn(SeMe)_3	30% in CH_2Cl_2	-21 (1)	83

Compound	Solution	Shift	Ref.
XXVII. Compounds of the type Ph_2SnX_2			
Ph_2SnCl_2	CH_2Cl_2	-32 (0.8)	7
$\text{Ph}_2\text{Sn}(\text{SeMe})_2$	30% in CH_2Cl_2	-20 (1)	83
$\text{Ph}_2\text{Sn}(\text{SMe})_2$	30% in CH_2Cl_2	+38.5 (1)	83
$\text{Ph}_2\text{Sn}(\text{SEt})_2$	30% in CH_2Cl_2	+33 (2)	83
$\text{Ph}_2\text{Sn}(\text{S}^i\text{Pr})_2$	30% in CH_2Cl_2	+9.5 (2)	83
$\text{Ph}_2\text{Sn}(\text{S}^i\text{Bu})_2$	30% in CH_2Cl_2	+30.4 (2)	83
$\text{Ph}_2\text{Sn}(\text{SCH}_2\text{Ph})_2$	30% in CH_2Cl_2	+26 (2)	83
$\text{Ph}_2\text{Sn}[\overline{\text{SCH}_2\text{CH}_2\text{S}}]$	dil. CH_2Cl_2	+78 (2)	90
	dil. DMSO	-67.7 (2)	90
$\text{Ph}_2\text{Sn}[\overline{\text{SCH}_2\text{CH}_2\text{S}}]_2\text{DMSO}$	DMSO	-67.5 (2)	23
$\text{Ph}_2\text{SnS}(\text{CH}_2)_3\text{S}$	dil. CH_2Cl_2	+28.5 (2)	90
	dil. DMSO	-85.4 (5)	90
$\text{Ph}_2\text{Sn}(\text{S} \cdot \text{CO} \cdot \text{Ph})_2$	CHCl_3	-101.2	4
$\text{Ph}_2\text{Sn}[\text{SCSN}(\text{CH}_2)_4]_2$	CH_2Cl_2	-481	23
$\text{Ph}_2\text{Sn}[\text{SCSN}(\text{CH}_2\text{Ph})_2]_2$	CH_2Cl_2	-490	23
XXVIII. Compounds of the type Ph_3SnX			
Ph_3SnCl	CH_2Cl_2	-48 (0.8)	7
	neat liquid	-46	4
Ph_3SnI	CCl_4	-114.5	67
Ph_3SnOH	<0.5 M CDCl_3	-86	56
$\text{Ph}_3\text{SnOO}^i\text{Bu}$	CH_2Cl_2	-95 (1.3)	7
$\text{Ph}_3\text{SnOOCMe}_2\text{Ph}$	CH_2Cl_2	-91 (1.3)	7
$\text{Ph}_3\text{SnOCOMe}$	<0.5 M CDCl_3	-121	56
$\text{Ph}_3\text{SnOCOCH}_2\text{F}$	<0.5 M CDCl_3	-90	56

Compound	Solution	Shift	Ref.
$\text{Ph}_3\text{SnOCOCH}_2\text{Cl}$	$<0.5 \text{ M CDCl}_3$	-95	56
$\text{Ph}_3\text{SnOCOCHCl}_2$	$<0.5 \text{ M CDCl}_3$	-79	56
$\text{Ph}_3\text{SnOCOCCl}_3$	$<0.5 \text{ M CDCl}_3$	-80	56
$\text{Ph}_3\text{SnOCOEt}$	$<0.5 \text{ M CDCl}_3$	-121	56
$\text{Ph}_3\text{SnOCOCHEt}(\text{CH}_2)_3\text{Me}$	CHCl_3	-115.3	4
Ph_3SnSMe	30% in CH_2Cl_2	-47 (1)	83
Ph_3SnSEt	30% in CH_2Cl_2	-54.4 (2)	83
$\text{Ph}_3\text{SnS}^i\text{Pr}$	30% in CH_2Cl_2	-62 (1)	83
$\text{Ph}_3\text{SnS}^i\text{Bu}$	30% in CH_2Cl_2	-84.2 (1)	83
$\text{Ph}_3\text{SnSCH}_2\text{Ph}$	30% in CH_2Cl_2	-54.5 (2)	83
Ph_3SnSPh	CH_2Cl_2	-65.2 (1)	83
$\text{Ph}_3\text{SnSC}_6\text{H}_4\text{Me-4}$	CH_2Cl_2	-67.4 (1)	83
$\text{Ph}_3\text{SnSC}_6\text{H}_4^i\text{Bu-4}$	CH_2Cl_2	-66.3 (1)	83
$\text{Ph}_3\text{SnSC}_6\text{H}_4\text{NH}_2\text{-4}$	CH_2Cl_2	-69.2 (1)	83
$\text{Ph}_3\text{SnSC}_6\text{H}_4\text{Cl-4}$	CH_2Cl_2	-64.4 (1)	83
$\text{Ph}_3\text{SnSC}_6\text{H}_4\text{NO}_2\text{-4}$	CH_2Cl_2	-61.8 (1)	83
$\text{Ph}_3\text{SnSC}_6\text{H}_4\text{Br-4}$	CH_2Cl_2	-63.6 (1)	83
$\text{Ph}_3\text{SnSC}_6\text{H}_4\text{OMe-4}$	CH_2Cl_2	-65.8 (1)	83
$\text{Ph}_3\text{SnS}(\text{CH}_2)_2\text{SSnPh}_3$	dil. CH_2Cl_2	-54	90
$\text{Ph}_3\text{SnS}(\text{CH}_2)_3\text{SSnPh}_3$	dil. CH_2Cl_2	-55	90
Ph_3SnSeMe	satd. CH_2Cl_2	-69 (1)	83, 87
$\text{Ph}_3\text{SnSCSNMe}_2$	CHCl_3	-94.5	4
$\text{Ph}_3\text{SnSCSNET}_2$	CH_2Cl_2	-194.5	23
XXIX. Other compounds, RSnX_3			
$(\text{C}_6\text{H}_4\text{CF}_3\text{-3})\text{SnCl}_3$	neat liquid	-69 (2)	54
$(\text{C}_6\text{H}_4\text{CF}_3\text{-2})\text{SnCl}_3$	+ 35 mol % Bu_2SnCl_2	-85 (2)	54
$\text{C}_3\text{H}_{11}\text{SnCl}_3$	neat liquid	+5.3 (0.1)	37

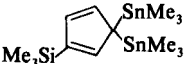
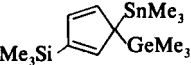
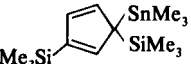
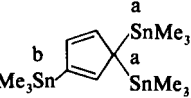
Compound	Solution	Shift	Ref.
$C_6H_{13}SnCl_3$	neat liquid	+2.0 (0.1)	37
	5% in n-hexane	+5.9 (0.1)	37
$C_7H_{15}SnCl_3$	neat liquid	+1.0 (0.1)	37
XXX. Other compounds, R_2SnX_2 and $RR'SnX_2$			
iBu_2SnCl_2	neat liquid (50°C)	+52 (5)	23
$^iBu_2Sh(OCH_2CH_2)_2NMe$	CH_2Cl_2	-205	127, 131
$(PhCH_2)_2SnCl_2$	satd. CH_2Cl_2	+35	82
iPr_2SnBr_2	neat liquid (-10°C)	+100.1 (0.1)	37
	(50°C)	+93.2 (0.1)	37
	(100°C)	+88.3 (0.1)	37
$(CH_2=CH)_2SnCl_2$	neat liquid	-40.9	4
$(CH_2=CHCH_2)_2SnBr_2$	neat liquid	-16.8	67
$(\alpha\text{-thienyl})_2SnCl_2$	CCl_4	-38.4	67
$BuPhSnCl_2$	CCl_4	+22.2	67
$BuMeSnCl_2$	neat liquid	+128.5 (0.1)	37
$(C_5H_{11})MeSnCl_2$	neat liquid	+128.4 (0.1)	37
$(C_6H_{13})MeSnCl_2$	neat liquid	+124.4 (0.1)	37
$(C_7H_{15})MeSnCl_2$	neat liquid	+124.8 (0.1)	37
$OctMeSnCl_2$	neat liquid	+126.3 (0.1)	37
XXXI. Other compounds, R_3SnX, RR'_2SnX, and $RR'R''SnX$			
$(PhCH_2)_3SnCl$	satd. CH_2Cl_2	+53	82
	CCl_4	+43	67
	$CDCl_3$	+52 (2)	80
$(4\text{-}FC_6H_4CH_2)_3SnCl$	satd. CH_2Cl_2	+53	82

Compound	Solution	Shift	Ref.
$(4\text{-ClC}_6\text{H}_4\text{CH}_2)_3\text{SnCl}$	satd. CH_2Cl_2	+50	82
$(\text{PhMe}_2\text{CCH}_2)_3\text{SnF}$	conc. CDCl_3	+138 (0.5)	107
	<0.5 M CDCl_3	+139	56
$(\text{PhMe}_2\text{CCH}_2)_3\text{SnCl}$	<0.5 M CDCl_3	+118	56
$(\text{PhMe}_2\text{CCH}_2)_3\text{SnOH}$	<0.5 M CDCl_3	+161	56
$(\text{PhMe}_2\text{CCH}_2)_3\text{SnOCHO}$	<0.5 M CDCl_3	+98	56
$(\text{PhMe}_2\text{CCH}_2)_3\text{SnOCOMe}$	<0.5 M CDCl_3	+79	56
$(\text{PhMe}_2\text{CCH}_2)_3\text{OCOCHCl}_2$	<0.5 M CDCl_3	+131	56
$(\text{PhMe}_2\text{CCH}_2)_3\text{SnOCOCF}_3$	<0.5 M CDCl_3	+146	56
$^i\text{Pr}_3\text{SnBr}$	neat liquid (-10°C)	+125.7 (0.1)	37
	(100°C)	+108.9 (0.1)	37
$\text{Me}_2\text{Sn}(\text{CH}_2\text{Cl})\text{Cl}$	CCl_4	+113.5 (0.15)	67, 99
Me_2BuSnCl	neat liquid	+157.1 (0.1)	37
$\text{Me}_2(\text{C}_5\text{H}_5)_3\text{SnCl}$	CCl_4	+101.6	88
$\text{Me}_2(\text{C}_5\text{H}_{11})_3\text{SnCl}$	neat liquid	+157.1 (0.1)	37
$\text{Me}_2(\text{C}_6\text{H}_{13})_3\text{SnCl}$	neat liquid	+156.9 (0.1)	37
$\text{Me}_2(\text{C}_7\text{H}_{15})_3\text{SnCl}$	neat liquid	+156.7 (0.1)	37
$\text{Me}_2\text{OctSnCl}$	neat liquid	+156.9 (0.1)	37
$\text{Et}_2(\text{C}_2\text{F}_5)_3\text{SnI}$	10% in CH_2Cl_2	-17 (0.3)	10
$\text{Me}^i\text{Pr}(\text{cyclo-C}_6\text{H}_{11})_3\text{SnBr}$	CH_2Cl_2	+122 (0.5)	7
XXXII. Symmetrical tetraorganotin compounds, R_4Sn			
Et_4Sn	20% in CCl_4	-1.4 (0.5)	65
	CCl_4	-5.97 (0.3)	67, 99
	50% in PhH	+1.0 (0.3)	10
	neat liquid	-6.7	4
Pr_4Sn	neat liquid	-16.8	4

Compound	Solution	Shift	Ref.
$^1\text{Pr}_4\text{Sn}$	neat liquid	-43.9	4
Bu_4Sn	neat liquid	-12.0 (1)	1
	CCl_4	-6.6	9, 67
$(\text{PhCH}_2)_4\text{Sn}$	satd. CH_2Cl_2	-36	82
Ph_4Sn	estimated value	-120 (20)	7, 65
	estimated value	-140 (10)	54
	CHCl_2 , CH_2Cl (110°C)	-137 (2)	23
$(\text{C}_6\text{H}_4\text{CF}_3)_4\text{Sn}$	satd. CDCl_3	-128 (2)	54
	satd. DMSO	-139 (2)	54
$(\text{CH}_2=\text{CH})_4\text{Sn}$	CCl_4	-157.4	67
	neat liquid + 30% TMS	-119	109
	neat liquid	-165.1	4
	neat liquid	-161.5	106
$(\text{CH}_2=\text{CH} \cdot \text{CH}_2)_4\text{Sn}$	neat liquid	-147.9	67
	CCl_4	-147.5	67
$(\text{CH}\equiv\text{C})_4\text{Sn}$	20% in Et_2O	-279 (0.8)	65
$(\text{C}_3\text{H}_5)_4\text{Sn}$	CCl_4 (50°C)	-25.89 (0.15)	99
	CCl_4 (20°C)	-24.4	88
XXXIII. Unsymmetrical tetraorganotin compounds, $\text{R}_n\text{SnR}'_{4-n}$			
$\text{MeSn}(\text{CH}=\text{CH}_2)_3$	neat liquid	-124	106
$\text{MeSn}(\text{C}_3\text{H}_5)_3$	CCl_4	-7.0	88
MeSnPh_3	+20% CH_2Cl_2	-93 (0.5)	7
Me_2SnEt_2	20% in CCl_4	+7 (1.0)	65
$\text{Me}_2\text{Sn}^n\text{PrEt}$	+20% PhH	-2 (0.5)	7
$\text{Me}_2\text{Sn}^n\text{Pr}_2$	neat liquid	-4.5	90
Me_2SnBu_2	neat liquid	+0.4	4
$\text{Me}_2\text{Sn}(\overline{\text{CH}_2})_3\text{CH}_2$	neat liquid	+53.5 (2)	90

Compound	Solution	Shift	Ref.
$\text{Me}_2\text{Sn}(\overline{\text{CH}_2})_4\text{CH}_2$	neat liquid	-42.5 (2)	90
	30% in CH_2Cl_2	-42 (2)	23
$\text{Me}_2\text{SnCPh}=\text{CPh} \cdot \text{CPh}=\text{CPh}$	satd. CH_2Cl_2	+52 (0.3)	10
$\text{Me}_2\text{Sn}(\text{C}_3\text{H}_5)_2$	CCl_4	+23.2	88
$\text{Me}_2\text{Sn}(\text{CH}=\text{CH}_2)_2$	neat liquid	-79.4	4
	neat liquid	-84	106
Me_2SnPh_2	neat liquid	-59.8	4
$\text{Me}_2\text{SnPh}[\text{PhCr}(\text{CO})_3]$	10% in CH_2Cl_2	-31 (0.8)	10
$\text{Me}_2\text{Sn}[\text{PhCr}(\text{CO})_3]_2$	5% in CH_2Cl_2	-4 (0.8)	10
$\text{Me}_2\text{SnPh}(\text{C}_6\text{H}_4\text{F}-4)$	C_6H_{12}	-56.3	67
$\text{Me}_2\text{Sn}(\text{C}_6\text{H}_4\text{F}-4)_2$	C_6H_{12}	-53.2	67
$\text{Me}_2\text{Sn}(\text{C}_6\text{H}_4\text{F}-4)(\text{C}_6\text{H}_4\text{Cl}-4)$	C_6H_{12}	-53.2	67
$\text{Me}_2\text{Sn}(\text{C}_6\text{H}_4\text{F}-4)(\text{C}_6\text{H}_4\text{Cl}-3)$	10% m C_6H_{12}	-53.2 (0.5)	130
$\text{Me}_2\text{Sn}(\text{C}_6\text{H}_4\text{F}-4)(\text{C}_6\text{H}_4\text{OMe}-4)$	C_6H_{12}	-54.5	67
$\text{Me}_2\text{Sn}(\text{C}_6\text{H}_4\text{F}-4)(\text{C}_6\text{H}_4\text{OMe}-3)$	10% m C_6H_{12}	-54.2 (0.5)	130
$\text{Me}_2\text{Sn}(\text{C}_6\text{H}_4\text{F}-4)(\text{C}_6\text{H}_2\text{Cl}_3-3,4,5)$	10% m C_6H_{12}	-46.9 (0.4)	130
$\text{Me}_3\text{SnCH}=\text{CH}_2$	neat liquid	-35.4	4
	neat liquid	-40	106
	10% in CCl_4	-39	23
$\text{Me}_3\text{SnC}\equiv\text{CBu}$	25% v/v in CH_2Cl_2	-72.0 (0.2)	122
$\text{Me}_3\text{SnC}\equiv\text{CPh}$	50% in PhH	-69 (0.08)	10
$\text{Me}_3\text{SnCCl}_3$	+10% PhH	+85 (0.05)	7
$\text{Me}_3\text{SnCHCl}_2$	PhH	+33 (0.03)	7
$\text{Me}_3\text{SnCH}_2\text{Cl}$	PhH	+4.0 (0.3)	7
	CCl_4	+4.95 (0.15)	99
	CCl_4	+4.8	67
$\text{Me}_3\text{SnCBr}_3$	+10% PhH	+101 (0.05)	7
$\text{Me}_3\text{SnCHBr}_2$	PhH	+42 (0.1)	7
$\text{Me}_3\text{SnCH}_2\text{Br}$	PhH	+6 (0.1)	7

Compound	Solution	Shift	Ref.
$\text{Me}_3\text{SnCH}_2\text{CH}=\text{CH}_2$?	-5.4 (0.4)	108
$\text{Me}_3\text{SnCH}_2^t\text{Bu}$	25% v/v in CH_2Cl_2	-14.2 (0.2)	122
$\text{Me}_3\text{SnCH}_2\text{Ph}$	10% M C_6H_{12}	+4.1 (0.4)	130
	50% in CH_2Cl_2	+4 (0.8)	10
$\text{Me}_3\text{SnCH}_2\text{Ph.Cr(CO)}_3$	10% in CH_2Cl_2	+8 (0.1)	10
$\text{Me}_3\text{SnCH}_2\text{C}_6\text{H}_4\text{Cl-4}$	10% M C_6H_{12}	+10.4 (0.2)	130
$\text{Me}_3\text{SnCH}_2\text{TiCl}(\pi\text{-C}_5\text{H}_5)_2$	satd. PhH	+14 (1)	111
$\text{Me}_3\text{SnCH}_2\text{TiCH}_2\text{SiMe}_3(\pi\text{-C}_5\text{H}_5)_2$	satd. PhH	+4 (2)	111
$\text{Me}_3\text{SnCH}_2\text{ZrCl}(\pi\text{-C}_5\text{H}_5)_2$	satd. PhH	+15 (1)	111
$\text{Me}_3\text{SnCH}_2\text{HfCl}(\pi\text{-C}_5\text{H}_5)_2$	satd. PhH	+16.5 (2)	111
Me_3SnEt	neat liquid	+5.9	4
	neat liquid	-2.7 (0.1)	37
	CCl_4	+3.0 (0.1)	7
	30% in PhH	+3.0 (0.5)	65
	25% v/v in CH_2Cl_2	+4.2 (0.2)	122
$\text{Me}_3\text{Sn}^n\text{Pr}$	25% v/v in CH_2Cl_2	-2.3 (0.1)	122
	neat liquid	-2.9	4
	neat liquid	-1.96 (0.1)	37
$\text{Me}_3\text{Sn(cyclo-C}_3\text{H}_7)$	25% v/v in CH_2Cl_2	+14.0 (0.2)	122
$\text{Me}_3\text{Sn}^i\text{Pr}$	25% v/v in CH_2Cl_2	+8.6 (0.2)	122
	neat liquid	+9.9	4
$\text{Me}_3\text{Sn(CH}_2)_2\text{CH}=\text{CH}_2$?	+1.6 (0.2)	108
$\text{Me}_3\text{Sn(CH}_2)_3\text{CH}=\text{CH}_2$?	-0.5 (0.2)	108
$\text{Me}_3\text{Sn}^n\text{Bu}$	+10% PhH	-2 (0.3)	7
	neat liquid	-0.55 (0.1)	37
	25% v/v in CH_2Cl_2	-1.0 (0.2)	122
$\text{Me}_3\text{Sn}^t\text{Bu}$	neat liquid	+17.5	4
	neat liquid	+19.5	128
$\text{Me}_3\text{SnCHMe.CH}=\text{CHMe}$	25% v/v in CH_2Cl_2	-13.8 (0.2)	122

Compound	Solution	Shift	Ref.
$\text{Me}_3\text{SnC}_5\text{H}_5$	CCl_4	+23.3	67
	CCl_4	+26.0	88
	50% in CCl_4 /dioxan	+28	86
$\text{Me}_3\text{SnC}_5\text{H}_5\text{SiMe}_3$	CCl_4	+11.5	88
$\text{Me}_3\text{SnC}_5\text{H}_5\text{GeMe}_3$	CCl_4	+11.5	88
$(\text{Me}_3\text{Sn})_2\text{C}_5\text{H}_4$	CCl_4	+10.6	88
	variable temp. study	see ref.	88
	CCl_4	+7.0	88
	variable temp. study	see ref.	88
	CCl_4	+8.8	88
	CCl_4	+9.0	88
	CCl_4 (20°C)	-11.7	88
	toluene (-80°C) Tin a	+11.1	88
	Tin b	-49.8	88
$(\text{Me}_3\text{Sn})_4\text{C}_5\text{H}_2$	toluene	-20.2	88
$\text{Me}_3\text{SnC}_5\text{H}_{11}$	neat liquid	-0.55 (0.1)	37
$\text{Me}_3\text{Sn}(\text{cyclo-C}_6\text{H}_{11})$	neat liquid	-1.7	4
	25% v/v in CH_2Cl_2	-4.7 (0.2)	122
	+10% CH_2Cl_2	-5.0 (0.5)	7
$\text{Me}_3\text{SnC}_6\text{H}_{13}$	neat liquid	-0.55 (0.1)	37
$\text{Me}_3\text{SnC}_7\text{H}_{15}$	neat liquid	-0.55 (0.1)	37

Compound	Solution	Shift	Ref.
Me ₃ Sn ⁿ Oct	neat liquid	-0.55 (0.1)	37
2-(Me ₃ Sn)py	dilute n-C ₆ H ₁₄	-50.7	119
3-(Me ₃ Sn)py	dilute n-C ₆ H ₁₄	-27.4	119
4-(Me ₃ Sn)py	dilute n-C ₆ H ₁₄	-27.8	119
Me ₃ SnPh	20% in CH ₂ Cl ₂	-28.6 (0.2)	83
	10% m PhH	-24.1 (0.2)	130
	50% v/v in CCl ₄	-30.3 (0.2)	122
	neat liquid	-30.3	4
	10% m C ₆ H ₁₂	-23.3 (0.2)	130
Me ₃ SnPh. Cr(CO) ₃	5% in CH ₂ Cl ₂	+3 (1.0)	10
Me ₃ SnC ₆ H ₄ CF ₃ -2	50% v/v in CCl ₄	-16.6 (0.2)	122
Me ₃ SnC ₆ H ₄ CF ₃ -3	50% v/v in CCl ₄	-23.9 (0.2)	122
Me ₃ SnC ₆ H ₄ F-2	50% v/v in CCl ₄	-28.5 (0.2)	122
Me ₃ SnC ₆ H ₄ F-3	50% v/v in CCl ₄	-25.0 (0.2)	122
Me ₃ SnC ₆ H ₄ F-4	50% v/v in CCl ₄	-25.9 (0.2)	122
	C ₆ H ₁₂	-25.9 (0.5)	67
Me ₃ SnC ₆ H ₄ Cl-2	50% v/v in CCl ₄	-24.2 (0.2)	122
Me ₃ SnC ₆ H ₄ Cl-3	50% v/v in CCl ₄	-24.5 (0.2)	122
	10% m C ₆ H ₁₂	-23.8 (0.2)	130
Me ₃ SnC ₆ H ₄ Cl-4	50% v/v in CCl ₄	-25.6 (0.2)	122
Me ₃ SnC ₆ H ₄ Br-4	50% v/v in CCl ₄	-25.0 (0.2)	122
Me ₃ SnC ₆ H ₄ Me-2	50% v/v in CCl ₄	-34.0 (0.2)	122
	20% in CH ₂ Cl ₂	-33.0 (0.8)	10, 122
Me ₃ SnC ₆ H ₄ Me-3	50% v/v in CCl ₄	-29.9 (0.2)	122
Me ₃ SnC ₆ H ₄ Me-4	50% v/v in CCl ₄	-29.9 (0.2)	122
	20% in CH ₂ Cl ₂	-28.3 (0.2)	83
	10% m C ₆ H ₁₂	-29.1 (0.2)	130
Me ₃ SnC ₆ H ₄ Et-2	50% v/v in CCl ₄	-35.1 (0.2)	122
Me ₃ SnC ₆ H ₄ ^t Bu-4	50% v/v in CCl ₄	-30.6 (0.2)	122

Compound	Solution	Shift	Ref.
$\text{Me}_3\text{SnC}_6\text{H}_4\text{OMe-2}$	50% v/v in CCl_4	-34.6 (0.2)	122
$\text{Me}_3\text{SnC}_6\text{H}_4\text{OMe-3}$	50% v/v in CCl_4	-28.0 (0.2)	122
$\text{Me}_3\text{SnC}_6\text{H}_4\text{OMe-4}$	50% v/v in CCl_4	-28.8 (0.2)	122
	20% in CH_2Cl_2	-27.4 (0.2)	83
$\text{Me}_3\text{SnC}_6\text{H}_4\text{OEt-2}$	50% v/v in CCl_4	-35.4 (0.2)	122
$\text{Me}_3\text{SnC}_6\text{H}_4\text{OEt-4}$	50% v/v in CCl_4	-28.6 (0.2)	122
$\text{Me}_3\text{SnC}_6\text{H}_4\text{NMe}_2\text{-2}$	50% v/v in CCl_4	-46.3 (0.2)	122
$\text{Me}_3\text{SnC}_6\text{H}_4\text{NMe}_2\text{-4}$	50% v/v in CCl_4	-30.2 (0.2)	122
	C_6H_{12}	-30.0	67
$1,4\text{-(Me}_3\text{Sn)}_2\text{C}_6\text{H}_4$	50% v/v in CCl_4	-30.5 (0.2)	122
	20% in CH_2Cl_2	-29.0 (0.8)	10
$1,4\text{-(Me}_3\text{Sn)}_2\text{C}_6\text{H}_4\cdot\text{Cr(CO)}_3$	5% in CH_2Cl_2	+4 (1.3)	10
$1,2\text{-(Me}_3\text{Sn)}_2\text{C}_6\text{H}_4$	50% v/v in CCl_4	-33.8 (0.2)	122
$\text{Me}_3\text{SnC}_6\text{H}_3(\text{CF}_3)_2\text{-2,6}$	50% v/v in CCl_4	-8.9 (0.2)	122
$\text{Me}_3\text{SnC}_6\text{H}_3\text{F}_2\text{-2,6}$	50% v/v in CCl_4	-28.4 (0.2)	122
$\text{Me}_3\text{SnC}_6\text{H}_3\text{Cl}_2\text{-2,6}$	50% v/v in CCl_4	-11.6 (0.2)	122
$\text{Me}_3\text{SnC}_6\text{H}_3\text{Me}_2\text{-2,6}$	50% v/v in CCl_4	-51.4 (0.2)	122
$\text{Me}_3\text{SnC}_6\text{H}_3(\text{OMe})_2\text{-2,6}$	50% v/v in CCl_4	-43.7 (0.2)	122
$\text{Me}_3\text{SnC}_6\text{H}_3(\text{OEt})_2\text{-2,6}$	50% v/v in CCl_4	-46.0 (0.2)	122
$\text{Me}_3\text{SnC}_6\text{H}_3(\text{CF}_3)_2\text{-3,5}$	50% v/v in CCl_4	-17.0 (0.2)	122
$\text{Me}_3\text{SnC}_6\text{H}_3\text{Cl}_2\text{-3,5}$	10% m C_6H_{12}	-16.9 (0.2)	130
$\text{Me}_3\text{SnC}_6\text{H}_3\text{Me}_2\text{-2,3}$	50% in CH_2Cl_2	-34 (0.8)	10
$\text{Me}_3\text{SnC}_6\text{H}_3(\text{CF}_3)_2\text{-2,4}$	50% v/v in CCl_4	-6.6 (0.2)	122
$\text{Me}_3\text{SnC}_6\text{H}_3\text{Me}_2\text{-2,4}$	50% v/v in CCl_4	-34.0 (0.2)	122
$\text{Me}_3\text{SnC}_6\text{H}_3\text{Me}_2\text{-3,4}$	50% v/v in CCl_4	-30.9 (0.2)	122
$\text{Me}_3\text{SnC}_6\text{H}_2(\text{OMe})_3\text{-2,4,6}$	50% v/v in CCl_4	-43.8 (0.2)	122
$\text{Me}_3\text{SnC}_6\text{H}_2\text{Me}_3\text{-2,4,6}$	50% in CH_2Cl_2	-50.0 (0.8)	10
$\text{Me}_3\text{SnC}_6\text{H}_2\text{Cl}_3\text{-3,4,5}$	10% m C_6H_{12}	-9.5 (0.3)	130
$\text{Me}_3\text{SnC}_6\text{Cl}_5$	satd. CH_2Cl_2	+123 (0.3)	10

Compound	Solution	Shift	Ref.
Me ₃ Sn(adamantane-1)	25% v/v in CH ₂ Cl ₂	-6.9 (0.2)	122
Me ₃ Sn(adamantane-2)	25% v/v in CH ₂ Cl ₂	-13.7 (0.2)	122
Me ₃ Sn(norbornane-1)	25% v/v in CH ₂ Cl ₂	+4.4 (0.2)	122
Me ₃ Sn(norbornane-7)	25% v/v in CH ₂ Cl ₂	-9.2 (0.2)	122
Me ₃ Sn(<i>syn</i> -norbornene-7)	25% v/v in CH ₂ Cl ₂	-11.3 (0.2)	122
	PhH	-13.2	94
Me ₃ Sn(<i>anti</i> -norbornene-7)	25% v/v in CH ₂ Cl ₂	-25.6 (0.2)	122
Me ₃ Sn(naphthalene-1)	25% v/v in CH ₂ Cl ₂	-31.8 (0.2)	122
<i>endo</i> -5-Me ₃ Sn(norborn-2-ene)	PhH	-1.2	94
<i>exo</i> -5-Me ₃ Sn(norborn-2-ene)	PhH	+7.8	94
3-Me ₃ Sn(nortricyclene)	PhH	-11.4	94
1-Me ₃ Sn(indene)	neat liquid	+31.3	67, 88
EtSn(CH ₂ Ph) ₃	40% in CH ₂ Cl ₂	-23 (0.5)	65
EtSnPh ₃	30% in CCl ₄	-98 (0.5)	65
	C ₆ H ₁₂	-111.1	67
EtSn(CH=CH ₂) ₃	50% in CCl ₄	-124 (1.3)	65
Et ₂ Sn(C ₂ F ₅) ₂	10% in CH ₂ Cl ₂	-65 (0.3)	10
Et ₂ Sn(CH ₂ Ph) ₂	40% in PhH	-13 (0.8)	65
Et ₂ Sn ^t Bu ₂	30% in CCl ₄	-19 (0.5)	65
Et ₂ Sn(C ₅ H ₅) ₂	C ₆ H ₁₂	+14.6	88
Et ₂ SnPh ₂	50% in CH ₂ Cl ₂	-66 (1.0)	65
Et ₂ Sn(C ₆ H ₄ Me-2) ₂	30% in CCl ₄	-63 (0.5)	65
Et ₂ Sn(C ₆ H ₄ Me-3) ₂	30% in CCl ₄	-63 (0.5)	65
Et ₂ Sn(C ₆ H ₄ Me-4) ₂	30% in CCl ₄	-63 (0.5)	65
Et ₂ Sn(CH=CH ₂) ₂	20% in CCl ₄	-81 (1.0)	65
Et ₂ Sn(C≡CH) ₂	30% in CCl ₄	-141 (0.8)	65
Et ₃ SnMe	20% in CCl ₄	+9 (0.5)	65
Et ₃ SnCH ₂ CONMe ₂	CH ₂ Cl ₂	+90	67
Et ₃ SnCH ₂ CH ₂ SiMe ₂ CH=CHMe	PhH	-2.8	67

Compound	Solution	Shift	Ref.
$\text{Et}_3\text{SnCH}_2\text{Ph}$	satd. CCl_4	-6 (1.3)	65
$\text{Et}_3\text{Sn}^t\text{Bu}$	neat liquid	-0.5	128
Et_3SnPh	25% in CCl_4	-34 (0.5)	65
$\text{Et}_3\text{SnCH}=\text{CH}_2$	50% in CCl_4	-42 (1.0)	65
	CCl_4	-37.6	67
$\text{Et}_3\text{SnC}\equiv\text{CH}$	30% in CCl_4	-52 (0.8)	65
$\text{Pr}_3\text{Sn}^t\text{Bu}$	neat liquid	-11.8	128
$\text{Pr}_3\text{SnCH}=\text{CHOBu}$	CCl_4	-50.6	67
$^i\text{Pr}_3\text{Sn}^t\text{Bu}$	neat liquid	-48.7	128
BuSnPh_3	C_6H_{12}	-110.5	67
$\text{BuSn}(\text{C}_6\text{H}_4\text{CF}_3-3)_3$	neat liquid	-95 (2)	54
$\text{BuSn}(\text{CH}_2\text{CH}=\text{CH}_2)_3$	neat liquid	-34.3	67
Bu_2SnPh_2	neat liquid	-65.9	4
$\text{Bu}_2\text{Sn}(\text{C}_6\text{H}_4\text{CF}_3-3)_2$	neat liquid	-68 (2)	54
$\text{Bu}_2\text{Sn}(\text{CH}=\text{CH}_2)_2$	neat liquid	-86.4	4
$\text{Bu}_3\text{SnCH}_2\text{CH}_2\text{OEt}$	CCl_4	-14.6	67
$\text{Bu}_3\text{Sn}^t\text{Bu}$	neat liquid	-7.9	128
Bu_3SnPh	neat liquid	-45 (2)	54
	neat liquid	-41.7	4
$\text{Bu}_3\text{SnC}_6\text{H}_4\text{CF}_3-2$	neat liquid	-25 (2)	54
$\text{Bu}_3\text{SnC}_6\text{H}_4\text{CF}_3-3$	neat liquid	-38 (2)	54
$\text{PhSn}(\text{cyclo-C}_6\text{H}_{11})_3$	CHCl_3	-102.5	4
$\text{Ph}_2\text{Sn}(\text{cyclo-C}_6\text{H}_{11})_2$	CHCl_3	-106.5	4
$\text{Ph}_3\text{Sn}(\text{cyclo-C}_6\text{H}_{11})$	CHCl_3	-113.7	4
$\text{Ph}_3\text{Sn}(\text{CH}_2)_6\text{Me}$	CH_2Cl_2	-96 (2)	54
$\text{Ph}_3\text{SnCH}_2\text{SPh}$	30% in CH_2Cl_2	+118.0 (0.5)	83
$\text{Ph}_3\text{SnCH}_2\text{SC}_6\text{H}_4\text{NO}_2-4$	20% in CH_2Cl_2	+118.2 (0.5)	83
$\text{Ph}_3\text{SnCH}_2\text{SC}_6\text{H}_4\text{Cl-4}$	15% in CH_2Cl_2	+118.5 (0.5)	83
$\text{Ph}_3\text{SnCH}_2\text{SC}_6\text{H}_4\text{Br-4}$	20% in CH_2Cl_2	+118.5 (1)	83

Compound	Solution	Shift	Ref.
$\text{Ph}_3\text{SnCH}_2\text{SC}_6\text{H}_4^t\text{Bu-4}$	20% in CH_2Cl_2	+119.0 (0.5)	83
$\text{Ph}_3\text{SnCH}_2\text{SC}_6\text{H}_4\text{OMe-4}$	15% in CH_2Cl_2	+119.5 (1.5)	83
$\text{Ph}_3\text{SnCH}_2\text{SC}_6\text{H}_4\text{NH}_2\text{-4}$	15% in CH_2Cl_2	+120.7 (0.5)	83
XXXIV. Organotin hydrides, $\text{R}_n\text{SnH}_{4-n}$			
MeSnH_3	60% in toluene (-35°C)	-346 (2)	23
	30% in Et_2O /toluene (-35°C)	-347 (4)	23
Me_2SnH_2	10% in C_6H_{12} (-20°C)	-225	110
	neat liquid (27°C)	-229 (2)	101
Me_3SnH	PhH	-104.5	67
EtSnH_3	50% in Bu_2O	-282 (1.3)	10
Et_2SnH_2	80% in PhH	-231 (0.3)	10
Et_3SnH	50% in PhH	-40 (0.4)	10
$^n\text{Pr}_3\text{SnH}$	neat liquid	-89	101
Bu_3SnH	CCl_4	-91.4	67
	neat liquid	-95 (2)	101
	neat liquid	-89 (4)	23
PhSnH_3	neat liquid (-15°C)	-320 (2)	101
Ph_2SnH_2	20% in TMS (30°C)	-234	110
	neat liquid (27°C)	-243 (2)	101
Ph_3SnH	neat liquid (27°C)	-148 (2)	101
XXXV. Compounds containing a tin-metal bond			
(a) Sn-Sn, Sn-Si, and Sn-Li bonds			
$\text{Me}_3\text{SnSnMe}_3$	+ 10% PhH	-113 (0.03)	7
	neat liquid	-109	4
	neat liquid	-108.7	118

Compound	Solution	Shift	Ref.
$\text{Me}_3\text{SnSiMe}_3$	90% in PhH	-126.7	117
$\text{Me}_3\text{SnPbMe}_3$?	-57	112
$\text{Et}_3\text{SnSnEt}_3$	neat liquid	-59.9	118
$^1\text{Pr}_3\text{SnSn}^1\text{Pr}_3$	neat liquid	-29.1	118
$\text{Bu}_3\text{SnSnBu}_3$	neat liquid	-83.2	118
	neat liquid	-79.5	4
$^1\text{Pr}_2^1\text{BuSnSn}^1\text{Pr}_2^1\text{Bu}$	neat liquid	-21.5	118
$\text{Me}_3\text{Sn}^a\text{Sn}^b\text{Et}_3$	neat liquid Tin a	-108.1	118
	Tin b	-61.8	118
$\text{Me}_3\text{Sn}^a\text{Sn}^b\text{Bu}_3$	neat liquid Tin a	-105.3	118
	Tin b	-45.3	118
$\text{Me}_3\text{Sn}^a\text{Sn}^b(\text{C}_6\text{H}_{11})_3$	neat liquid Tin a	-103.8	118
	Tin b	-78.3	118
$\text{Me}_3\text{Sn}^a\text{Sn}^b\text{Ph}_3$	satd. CDCl_3 Tin a	-91.5	118
	satd. CH_2Cl_2 Tin a	-91.5	117
	satd. CDCl_3 Tin b	-150.6	118
	satd. CH_2Cl_2 Tin b	-153 (2)	117
$\text{Me}_3\text{SnSiPh}_3$	40% in CDCl_3 + 20 mol % dioxan	-149	102
$\text{Et}_3\text{Sn}^a\text{Sn}^b\text{Bu}_3$	neat liquid Tin a	-65.7	118
	Tin b	-79.7	118
$\text{Et}_3\text{Sn}^a\text{Sn}^b\text{Ph}_3$	neat liquid Tin a	-48.7	118
	Tin b	-140.4	118
$^1\text{Bu}_3\text{Sn}^a\text{Sn}^b(\text{C}_6\text{H}_{11})_3$	satd. CDCl_3 Tin a	-93.2	118
	Tin b	-85.2	118
$^1\text{Bu}_3\text{Sn}^a\text{Sn}^b\text{Ph}_3$	satd. CDCl_3 Tin a	-86.8	118
	Tin b	-146.9	118
$\text{Me}_2\text{Sn}^a(\text{Sn}^b\text{Me}_3)_2$	conc. PhH Tin a	-263 (1.5)	113
	neat liquid Tin a	-261.7	124
	conc. PhH Tin b	-100.8 (2)	113
	neat liquid Tin b	-99.5	124

Compound	Solution		Shift	Ref.
$\text{Me}_2\text{Sn}^a(\text{Sn}^b\text{Et}_3)_2$	neat liquid	Tin a	-199.1	124
		Tin b	-99.1	124
$\text{Me}_2\text{Sn}^a(\text{Sn}^b\text{}^1\text{Pr}_3)_2$	neat liquid	Tin a	-139.5	124
		Tin b	-97.0	124
$\text{Et}_2\text{Sn}^a(\text{Sn}^b\text{Me}_3)_2$	neat liquid	Tin a	-272.8	124
		Tin b	-56.0	124
$\text{Et}_2\text{Sn}^a(\text{Sn}^b\text{Et}_3)_2$	neat liquid	Tin a	-205.9	124
		Tin b	-54.8	124
$\text{Et}_2\text{Sn}^a(\text{Sn}^b\text{}^1\text{Pr}_3)_2$	neat liquid	Tin a	-139.3	124
		Tin b	-57.3	124
$\text{Et}_2\text{Sn}^a(\text{Sn}^b\text{}^1\text{Bu}_3)_2$	neat liquid	Tin a	-214.4	124
		Tin b	-63.9	124
$\text{}^1\text{Pr}_2\text{Sn}^a(\text{Sn}^b\text{Me}_3)_2$	neat liquid	Tin a	-272.1	124
		Tin b	-34.3	124
$\text{}^1\text{Pr}_2\text{Sn}^a(\text{Sn}^b\text{Et}_3)_2$	neat liquid	Tin a	-206.7	124
		Tin b	-31.0	124
$\text{}^1\text{Pr}_2\text{Sn}^a(\text{Sn}^b\text{}^1\text{Pr}_3)_2$	neat liquid	Tin a	-132.9	124
		Tin b	-35.0	124
$\text{}^1\text{Bu}_2\text{Sn}^a(\text{Sn}^b\text{}^1\text{Bu}_3)_2$	neat liquid	Tin a	-236.2	124
		Tin b	-92.8	124
$(\text{cyclo-C}_6\text{H}_{11})_2\text{Sn}^a(\text{Sn}^b\text{}^1\text{Bu}_3)_2$	conc. PhH	Tin a	-224.8	124
		Tin b	-84.3	124
$\text{Ph}_2\text{Sn}^a(\text{Sn}^b\text{}^1\text{Bu}_3)_2$	conc. PhH	Tin a	-221.0	124
		Tin b	-138.2	124
Me_3SnLi	20% in THF		-183 (0.1)	10
			-180.7 (0.5)	115
$(\text{Me}_3\text{Sn}^b)_3\text{Sn}^a\text{Li}\cdot 3\text{THF}$	THF	Tin a	-1031 to 1042	113
		Tin b	-104.6 to 107.1	113
$(\text{Me}_3\text{Sn}^b)_3\text{Sn}^a\text{Fe}(\eta\text{-C}_5\text{H}_5)\text{P}(\text{OPh})_3$	conc. PhH	Tin a	-401.1 (0.5)	113
		Tin b	-103 (0.5)	113

Compound	Solution		Shift	Ref.
$(\text{Me}_3\text{Sn}^a)_3\text{Sn}^b\text{Me}$	neat liquid	Tin a	-89.5	126
		Tin b	-489.7	126
$(\text{Me}_3\text{Sn}^a)_3\text{Sn}^b\text{Et}$	neat liquid	Tin a	-89.3	126
		Tin b	-440.9	126
$(\text{Me}_3\text{Sn}^a)_4\text{Sn}^b$	PhH	Tin a	-80	120
		Tin b	-806	120
$(\text{Me}_3\text{Sn}^a)_3\text{Sn}^b\text{Bu}$	neat liquid	Tin a	-90.3	126
		Tin b	-459.9	126
$(\text{Me}_3\text{Sn}^a)_3\text{Sn}^b\text{}^i\text{Bu}$	neat liquid	Tin a	-90.8	126
		Tin b	-480.4	126
$(\text{Me}_3\text{Sn}^a)_3\text{Sn}^b\text{}^n\text{C}_5\text{H}_{11}$	neat liquid	Tin a	-90.1	126
		Tin b	-460.5	126
$(\text{Me}_3\text{Sn}^a)_3\text{Sn}^b\text{Ph}$	neat liquid	Tin a	-83.2	126
		Tin b	-434.2	126
$\text{Me}_2\text{Sn}^a\text{Sn}^a\text{Me}_2\text{SSn}^b\text{Me}_2\text{S}$	conc. PhH	Tin a	+43.8	125
		Tin b	+176.4	125
$\text{Me}_2\text{Sn}^a\text{Sn}^a\text{Me}_2\text{SeSn}^b\text{Me}_2\text{Se}$	conc. PhH	Tin a	+21.3	125
		Tin b	+82.2	125
$\text{Me}_2\text{Sn}^a\text{Sn}^a\text{Me}_2\text{TeSn}^b\text{Me}_2\text{Te}$	conc. PhH	Tin a	-38.0	125
		Tin b	-163.8	125
(b) Tin-transition metal bonds				
$\text{Me}_3\text{SnTaH}_2(\pi\text{-C}_5\text{H}_5)_2$	satd. PhH		+53 (2)	111
$\text{Me}_3\text{SnCr}(\text{CO})_3(\pi\text{-C}_5\text{H}_5)$	PhH		+161 (0.5)	111
$\text{Me}_3\text{SnMoH}(\pi\text{-C}_5\text{H}_5)_2$	satd. PhH		+123 (2)	111
$\text{Me}_3\text{SnMoCl}(\pi\text{-C}_5\text{H}_5)_2$	satd. PhH		+90 (2)	111
$\text{Me}_3\text{SnMoBr}(\pi\text{-C}_5\text{H}_5)_2$	satd. PhH		+90 (2)	111
$\text{Me}_3\text{SnMoI}(\pi\text{-C}_5\text{H}_5)_2$	satd. PhH		+96 (2)	111
$\text{Me}_3\text{SnMo}[\text{C}(\text{CO}_2\text{Me})=\text{C}(\text{CO}_2\text{Me})\text{H}](\pi\text{-C}_5\text{H}_5)_2$	satd. PhH		+119 (1)	111

Compound	Solution	Shift	Ref.
$\text{Me}_3\text{SnMo}(\text{CO})_3(\pi\text{-C}_5\text{H}_5)$	PhH	+121 (0.5)	111
$\text{Me}_3\text{SnWH}(\pi\text{-C}_5\text{H}_5)_2$	satd. PhH	-41 (2)	111
$\text{Me}_3\text{SnWCl}(\pi\text{-C}_5\text{H}_5)_2$	satd. PhH	-70 (5)	111
$\text{Me}_3\text{SnWBr}(\pi\text{-C}_5\text{H}_5)_2$	satd. PhH	-74 (2)	111
$\text{Me}_3\text{SnWI}(\pi\text{-C}_5\text{H}_5)_2$	satd. PhH	-74 (2)	111
$\text{Me}_3\text{SnW}(\text{CO})_3(\pi\text{-C}_5\text{H}_5)$	PhH	+43.1 (0.3)	111
$\text{Me}_3\text{SnW}[\text{C}(\text{CO}_2\text{Me})=\text{C}(\text{CO}_2\text{Me})\text{H}](\pi\text{-C}_5\text{H}_5)_2$	satd. PhH	-40 (2)	111
$\text{Me}_3\text{SnMn}(\text{CO})_5$	PhH	+63 (1)	111
	C_6H_{12}	+66.3	4
$\text{Me}_2\text{Sn}[\text{Mn}(\text{CO})_5]_2$	satd. PhH	+150 (1)	111
$\text{MeSn}[\text{Mn}(\text{CO})_5]_3$	satd. CDCl_3	+284 (2)	111
$\text{Me}_3\text{SnRe}(\text{CO})_5$	satd. PhH	-89 (1)	111
$\text{Me}_2\text{Sn}[\text{Re}(\text{CO})_5]_2$	satd. CDCl_3	-223 (2)	111
$(\text{Me}_3\text{Sn})_2\text{Fe}(\text{CO})_4$	PhH	+79 (1)	111
$[\text{Me}_2\text{SnFe}(\text{CO})_4]_2$	CDCl_3	+257 (2)	111
$\text{Me}_3\text{SnFe}(\text{CO})_2(\pi\text{-C}_5\text{H}_5)_2$	PhH	+147 (0.5)	111
$(\text{Me}_3\text{Sn}^b)_3\text{Sn}^a\text{Fe}(\eta\text{-C}_5\text{H}_5)[\text{P}(\text{OPh})_3]_2$	conc. PhH Tin a	-401.1 (0.5)	113
	Tin b	-103 (0.5)	113
$\text{Me}_3\text{SnCo}(\text{CO})_4$	PhH	+151 (0.2)	111
$\text{Me}_2\text{Sn}[\text{Co}(\text{CO})_4]_2$	satd. PhH	+293 (1)	111
$\text{MeSn}[\text{Co}(\text{CO})_4]_3$	satd. PhH	+483 (1)	111
$\text{Me}_3\text{SnRh}(\text{PPh}_3)_2(\text{C}\equiv\text{CPh})_2$	satd. CH_2Cl_2	+172 (1)	111
$\text{Me}_3\text{SnIr}(\text{PPh}_3)_2(\text{C}\equiv\text{CPh})_2$	satd. CH_2Cl_2	-106 (2)	111
$\text{Me}_3\text{SnIr}(\text{CO})(\text{PPh}_3)_2(\text{C}\equiv\text{CPh})_2$	satd. CH_2Cl_2	-123 (2)	111
<i>cis</i> - $[(\text{Ph}_3\text{P})_2\text{Pt}(\text{C}\equiv\text{CPh})\text{SnMe}_3]$	satd. CH_2Cl_2	-46 (2)	111
<i>cis</i> - $[(\text{MePh}_2\text{P})_2\text{Pt}(\text{C}\equiv\text{CPh})\text{SnMe}_3]$	satd. $[\text{}^2\text{H}_8]\text{toluene}$	-48 (1)	111
<i>cis</i> - $[(\text{Ph}_3\text{P})_2\text{Pt}(\text{CF}=\text{CF}_2)\text{SnMe}_3]$	satd. CDCl_3	0 (2)	111

Compound	Solution	Shift	Ref.
XXXVI. Organotin oxides (containing an Sn—O—Sn bond)			
(a) Unsubstituted organotin oxides			
Me ₃ SnOSnMe	neat liquid	+ 109.5	100
	neat liquid containing		
	20% v/v CH ₂ Cl ₂	+ 113.1 (1)	100
	50% v/v in CH ₂ Cl ₂	+ 117.1	100
Et ₃ SnOSnEt ₃	CCl ₄	+ 86.15 (0.4)	67, 99
	90% in CH ₂ Cl ₂	+ 87.0 (1.3)	10
ⁿ Pr ₃ SnOSn ⁿ Pr ₃	neat liquid	+ 77.8 (4.7)	45
ⁿ Bu ₃ SnOSn ⁿ Bu ₃	+ 10% PhH	+ 82 (0.8)	7
	CCl ₄	+ 84.5	67
	neat liquid	+ 77.8 (2.3)	45
(Me, ¹ Pr, cyclo-C ₆ H ₁₁ , Sn) ₂ O	CH ₂ Cl ₂	+ 64 (0.5)	7
Ph ₃ SnOSnPh ₃	CHCl ₃	- 80.6	4
Ph ₂ Sn(OSnPh ₃) ₂	CH ₂ Cl ₂	- 109 (1.3)	7
(b) 1,3-Disubstituted distannoxanes, (R ₂ SnX) ₂ O			
(Me ₂ SnOSiMe ₃) ₂ O	satd. CCl ₄	- 130 and - 156 (2)	6
	satd. CCl ₄	- 137 and - 153 (2)	73
(Bu ₂ SnF) ₂ O	satd. CCl ₄	- 168 (broad) (14)	73
(Bu ₂ SnCl) ₂ O	satd. CCl ₄	- 145 and - 94 (5)	73
	?	- 142.7 and - 89.6 (0.1)	37
(Bu ₂ SnBr) ₂ O	satd. CCl ₄	- 141 and - 92 (5)	80
	satd. PhH	- 141 and - 87 (5)	73
(Bu ₂ SnNCS) ₂ O	satd. PhH	- 159 (broad) (9)	73
(Bu ₂ SnOSiMe ₃) ₂ O	satd. PhH	- 163 (5)	73
(Bu ₂ SnOCOMe) ₂ O	satd. PhH	- 221 (broad) (5)	73
(Bu ₂ SnOCOC ₇ H ₁₅) ₂ O	neat liquid	one broad peak	5

Compound	Solution	Shift	Ref.
(Bu ₂ SnOPh) ₂ O	satd. PhH	-181 (broad) (5)	73
(Bu ₂ SnOC ₆ H ₄ Me-4) ₂ O	satd. PhH	-181 (2)	73
(Bu ₂ SnOC ₆ H ₄ OMe-4) ₂ O	satd. PhH	-188 (2)	73
(Bu ₂ SnOC ₆ H ₄ Cl-4) ₂ O	satd. PhH	-177 (broad) (5)	73
XXXVII. Stannasiloxanes (containing an Sn—O—Si bond)			
Me ₃ SnOSiPh ₃	satd. CCl ₄	+121 (1)	80
Me ₂ Sn(OSiPh ₃) ₂	CH ₂ Cl ₂	+2 (0·1)	7
Bu ₃ SnOSiPh ₃	neat liquid	+89 (2)	63
Bu ₃ SnOSiMe ₃	neat liquid	+71 (2)	63
Bu ₂ Sn(OSiPh ₃) ₂	satd. CCl ₄ or PhH	-36 (2)	63
Ph ₃ SnOSiPh ₃	neat liquid (82°C)	-45 (2)	63
Ph ₂ Sn(OSiPh ₃) ₂	CH ₂ Cl ₂	-103 (0·8)	7
	satd. CDCl ₃	-188 (5)	80
XXXVIII. Organotin sulphides, selenides, and tellurides (containing an Sn—X—Sn bond)			
(Me ₂ SnS) ₃	CS ₂	+125·6	4
	PhH	+128 (0·1)	7
	satd. CH ₂ Cl ₂	+129 (2)	90
	20% in CH ₂ Cl ₂	+131 (0·05)	10
	conc. PhH	+130·6	125
Me ₂ Sn ^a SSn ^a Me ₂ NEtSn ^b Me ₂ NEt	PhH	+88 (0·1)	7
	Tin a	+100 (0·1)	7
	Tin b	+114 (0·1)	7
Me ₂ Sn ^a SSn ^b Me ₂ NEtSn ^b Me ₂ S	PhH	+109 (0·1)	7
	Tin a	+43·8	125
	Tin b	+176·4	125
Me ₂ Sn ^a SSn ^b Me ₂ SSn ^a Me ₂	conc. PhH		

Compound	Solution	Shift	Ref.
$(\text{Me}_2\text{SnSe})_3$	satd. PhH	+42.3	125
$\text{Me}_2\text{Sn}^a\text{SeSn}^b\text{Me}_2\text{SeSn}^a\text{Me}_2$	conc. PhH Tin a	+21.3	125
	Tin b	+82.2	125
$(\text{Me}_2\text{SnTe})_3$	satd. PhH	-196.0	125
$\text{Me}_2\text{Sn}^a\text{TeSn}^b\text{Me}_2\text{TeSn}^a\text{Me}_2$	conc. PhH Tin a	-38.0	125
	Tin b	-163.8	125
$\text{Me}_3\text{SnSSnMe}_3$	neat liquid	+84.9	100
	neat liquid + 20% v/v CH_2Cl_2	+86.5 (0.3)	100
$(\text{Me}_3\text{Sn})_2\text{S}[\text{P}(\text{OMe})_3]\text{W}(\text{CO})_4$	PhH	+136.2	23
$(\text{Me}_2\text{SnCl})_2\text{S}$	20% in CH_2Cl_2	+144 (0.08)	10
$(\text{Me}_2\text{SnBr})_2\text{S}$	20% in CH_2Cl_2	+123 (0.5)	10
$(\text{Me}_2\text{SnI})_2\text{S}$	30% $\text{Me}_2\text{SnI}_2/(\text{Me}_2\text{SnS})_3$ in $\text{CH}_2\text{Cl}_2/\text{CCl}_4$	+13.5 (5)	83
$\text{Me}_3\text{SnSeSnMe}_3$	50% in CH_2Cl_2	+44.5	117
	neat liquid + 20% v/v CH_2Cl_2	+44.5	100
$\text{Me}_3\text{SnTeSnMe}_3$	70% in CH_2Cl_2	-66.8	117
	neat liquid + 20% v/v CH_2Cl_2	-66.8 (1)	100
$(\text{Bu}_2\text{SnS})_3$	CCl_4	+126.9	67
	neat liquid	+124 (2)	1
$\text{Bu}_3\text{SnSSnBu}_3$	CCl_4	+81.9	67
$\text{BrBu}_2\text{Sn}^a\text{SSn}^b\text{BuBr}_2$	CH_2Cl_2 Tin a	+109 (1.3)	7
	Tin b	+92 (1.3)	7
$(\text{Ph}_2\text{SnS})_3$	CHCl_3	+19.5	4
$\text{Ph}_3\text{SnSSnPh}_3$	neat liquid	-48.7	4
XXXIX. Organotin derivatives of carboranes			
$(\text{Me}_3\text{Sn})_2\text{C}_2\text{B}_{10}\text{H}_{10}$	CCl_4	+40.3	67
$\text{Et}_3\text{Sn}(p\text{-C}_2\text{B}_{10}\text{H}_{10})$	CS_2	+15.1	67

Compound	Solution	Shift	Ref.
XL. Covalent organotin halide complexes			
MeSnCl ₃ , 2DMSO	satd. DMSO	-457	48
MeSnI ₃ , 2DMSO	satd. DMSO	-795 (4)	23
Me ₂ SnCl ₂ , 2DMSO	satd. CH ₂ Cl ₂	-84 (0.08)	10
	satd. DMSO	-246	48
Me ₂ SnCl ₂ , 2Ph ₃ PO	satd. CH ₂ Cl ₂	-83 (0.3)	10
Me ₂ SnBr ₂ , bipy	satd. CH ₂ Cl ₂	-245 (3)	10
Me ₂ SnI ₂ , bipy	satd. CH ₂ Cl ₂	-237 (3)	10
Me ₂ SnI ₂ , 2DMSO	dil. DMSO	-315.5 (2)	23
Me ₃ SnCl, DMSO	satd. CH ₂ Cl ₂	-86 (1.3)	10
	8.5 mol % DMSO	-3	48
Me ₃ SnCl, Py	CHCl ₃	+25.4	4
	MeOH	+20.2	4
	1 : 12.7 M Me ₃ SnCl/Py + CCl ₄	-9.52 (0.12)	45
Me ₃ SnBr, PhNH ₂	CHCl ₃	+149.9	4
XLI. Ionic organotin halide complexes			
(MeSnCl ₃) ²⁻	H ₂ O	-464 (0.5)	7
(MeSnBr ₃) ²⁻	H ₂ O	-662 (0.5)	7
(MeSnBr ₃ Cl ₂) ²⁻	H ₂ O	-546 (0.5)	7
(Et ₄ N) ⁺ (Me ₃ SnCl ₂) ⁻	satd. Me ₂ CO	-53 (0.05)	10
(Me ₃ Sn, bipy) ⁺ (BPh ₄) ⁻	satd. CH ₂ Cl ₂	-18 (0.1)	10

Acknowledgements

The authors thank Dr. D. G. Gillies, Royal Holloway College, University of London, Dr. T. N. Mitchell, University of Dortmund, and Dr. D. S. Rycroft, University of Glasgow, for helpful comments and for providing ^{119}Sn NMR data in advance of publication. The International Tin Research Council, London, is gratefully acknowledged for permission to publish this article.

REFERENCES

1. J. J. Burke and P. C. Lauterbur, *J. Amer. Chem. Soc.*, 1961, **83**, 326.
2. W. G. Proctor, *Phys. Rev.*, 1950, **79**, 35.
3. R. C. West (ed.), "Handbook of Chemistry and Physics", 56th edn., The Chemical Rubber Co., Cleveland, Ohio, 1975.
4. B. K. Hunter and L. W. Reeves, *Can. J. Chem.*, 1968, **46**, 1399.
5. D. L. Alleston, A. G. Davies, M. Hancock and R. F. M. White, *J. Chem. Soc.*, 1963, 5469.
6. W. J. Considine, G. A. Baum and R. C. Jones, *J. Organometal. Chem.*, 1965, **3**, 308.
7. A. G. Davies, P. G. Harrison, J. D. Kennedy, T. N. Mitchell, R. J. Puddephatt and W. McFarlane, *J. Chem. Soc. (C)*, 1969, 1136.
8. W. McFarlane, *J. Chem. Soc. (A)*, 1968, 1630.
9. A. P. Tupčiauskas, N. M. Sergejev and Yu. A. Ustynyuk, *Liet. Fiz. Rink.*, 1971, **11**, 93.
10. P. G. Harrison, S. E. Ulrich and J. J. Zuckerman, *J. Amer. Chem. Soc.*, 1971, **93**, 5398.
11. D. G. Gillies and E. W. Randall, *J. Sci. Instr.*, 1966, **43**, 466.
12. R. C. Hopkins, *Rev. Sci. Instr.*, 1964, **35**, 1495.
13. A. Charles and W. McFarlane, *Mol. Phys.*, 1968, **14**, 299.
14. H. Primas and R. Ernst, *Discuss. Faraday Soc.*, 1962, **34**, 43.
15. R. Freeman, *J. Chem. Phys.*, 1964, **40**, 3571.
16. A. Charles, *J. Phys., E*, 1968, **1**, 64.
17. W. A. Anderson and R. Freeman, *J. Chem. Phys.*, 1962, **37**, 85.
18. R. Freeman and W. A. Anderson, *J. Chem. Phys.*, 1962, **37**, 2053.
19. A. P. Tupčiauskas, Cand. Diss., Moscow State University, 1972.
20. E. B. Baker, *J. Chem. Phys.*, 1962, **37**, 911.
21. D. G. Gillies, personal communication.
22. E. V. van den Berghe and G. P. van der Kelen, *J. Organometal. Chem.*, 1971, **26**, 207.
23. J. D. Kennedy and W. McFarlane, *Revs. Silicon, Germanium, Tin, Lead Compds.*, 1974, **1**, 235.
24. P. R. Wells, P. J. Banney and D. C. McWilliam, *J. Magn. Resonance*, 1970, **2**, 235.
25. E. W. Randall, *Discuss. Faraday Soc.*, 1962, **34**, 156.
26. F. Bloch, *Phys. Rev.*, 1956, **102**, 104.
27. W. McFarlane, in "Annual Reports on NMR Spectroscopy", E. F. Mooney (ed.), 1968, **1**, 135.
28. J. D. Baldeschwieler and E. W. Randall, *Chem. Rev.*, 1963, **63**, 81.
29. R. A. Hoffman and S. Forsen, in "Progress in NMR Spectroscopy", J. W. Emsley, J. Feeney and L. H. Sutcliffe (eds.), 1966, **1**, 15.
30. E. Lippmaa, *Zh. Strukt. Khim.*, 1967, **8**, 717.
31. V. J. Kowalewski, in "Progress in NMR Spectroscopy", J. W. Emsley, J. Feeney and L. H. Sutcliffe (eds.), 1969, **5**, 1.
32. P. R. Wells, in "Determination of Organic Structures by Physical Methods", F. C. Nachod and J. J. Zuckerman (eds.), 1971, **4**, 233.

33. W. McFarlane, in "Determination of Organic Structures by Physical Methods", F. C. Nachod and J. J. Zuckerman (eds.), 1971, **4**, 139.
34. V. S. Petrosyan, in "Progress in NMR Spectroscopy", J. W. Emsley, J. Feeney and L. H. Sutcliffe (eds.), 1977, **11**, 115.
35. D. D. Traficante and J. A. Simms, *Rev. Sci. Instr.*, 1972, **43**, 1122.
36. G. E. Maciel, in "NMR of Nuclei other than Protons", T. Axenrod and G. A. Webb (eds.), Wiley, New York, 1974, p. 347.
37. T. N. Mitchell, *Org. Magn. Resonance*, 1976, **8**, 34.
38. Yu. Kh. Puskar, T. A. Saluvere, E. Lippmaa, A. B. Permin and V. S. Petrosyan, *Dokl. Akad. Nauk. SSSR*, 1975, **220**, 112.
39. H. Krüger, O. Lutz, A. Nolle and A. Uhl, *Z. Naturforschung*, 1972, **27a**, 173.
40. C. R. Lassigne and E. J. Wells, *Can. J. Chem.*, 1977, **55**, 927.
41. P. C. Lauterbur, private communication, quoted in Ref. 28.
42. T. Hasebe, G. Soda and H. Chihara, *Bull. Chem. Soc. Japan*, 1976, **49**, 3684.
43. C. R. Lassigne and E. J. Wells, *J. Magn. Resonance*, 1977, **26**, 55.
44. R. R. Sharp, *J. Chem. Phys.*, 1972, **57**, 5321.
45. L. Smith, Ph.D. Thesis, University of London, 1972.
46. R. Hulme, *J. Chem. Soc.*, 1963, 1524.
47. E. V. van den Berghe and G. P. van der Kelen, *J. Organometal. Chem.*, 1968, **11**, 479.
48. J. D. Kennedy and W. McFarlane, *J.C.S., Perkin II*, 1974, 146.
49. N. W. Isaacs and C. H. L. Kennard, *J. Chem. Soc. (A)*, 1970, 1257.
50. V. N. Torocheshnikov, A. P. Tupčiauskas, N. M. Sergeyev and Yu. A. Ustynyuk, *J. Organometal. Chem.*, 1972, **35**, C25.
51. T. F. Bolles and R. S. Drago, *J. Amer. Chem. Soc.*, 1966, **88**, 1392.
52. A. Fratiello, S. Peak, R. E. Schuster and D. Davis, *J. Phys. Chem.*, 1970, **74**, 3730.
53. V. S. Petrosyan and O. A. Reutov, *Pure Appl. Chem.*, 1974, **37**, 147.
54. M. Barnard, P. J. Smith and R. F. M. White, *J. Organometal. Chem.*, 1974, **77**, 189.
55. A. G. Davies, H. J. Milledge, D. C. Puxley and P. J. Smith, *J. Chem. Soc. (A)*, 1970, 2862.
56. W. McFarlane and R. J. Wood, *J. Organometal. Chem.*, 1972, **40**, C17.
57. R. Okawara and M. Wada, in "Advances in Organometallic Chemistry", F. G. A. Stone and R. West (eds.), 1967, **5**, 137.
58. N. Kasai, K. Yasuda and R. Okawara, *J. Organometal. Chem.*, 1965, **3**, 172.
59. R. A. Forder and G. M. Sheldrick, *J. Organometal. Chem.*, 1970, **21**, 115.
60. H. Chih and B. R. Penfold, *J. Cryst. Mol. Struct.*, 1973, **3**, 285.
61. J. C. Pommier and J. Valade, *J. Organometal. Chem.*, 1968, **12**, 433.
62. J. Mendelsohn, J. C. Pommier and J. Valade, *Compt. Rend., Ser. C*, 1966, **263**, 921.
63. P. J. Smith, R. F. M. White and L. Smith, *J. Organometal. Chem.*, 1972, **40**, 341.
64. J. D. Kennedy, *J. Mol. Struct.*, 1976, **31**, 207.
65. W. McFarlane, J. C. Maire and M. Delmas, *J.C.S., Dalton*, 1972, 1862.
66. D. Sukhani, V. D. Gupta and R. C. Mehrotra, *J. Organometal. Chem.*, 1967, **7**, 85.
67. A. P. Tupčiauskas, N. M. Sergeyev and Yu. A. Ustynyuk, *Org. Magn. Resonance*, 1971, **3**, 655.
68. J. D. Kennedy, *J.C.S., Perkin II*, 1977, 242.
69. A. C. Chapman, A. G. Davies, P. G. Harrison and W. McFarlane, *J. Chem. Soc. (C)*, 1970, 821.
70. J. C. Pommier, F. Mendes and J. Valade, *J. Organometal. Chem.*, 1973, **55**, C19.
71. M. A. Delmas, J. C. Maire, W. McFarlane and Y. Richard, *J. Organometal. Chem.*, 1975, **87**, 285.
72. J. D. Kennedy, W. McFarlane, P. J. Smith, R. F. M. White and L. Smith, *J.C.S., Perkin II*, 1973, 1785.

73. A. G. Davies, L. Smith, P. J. Smith and W. McFarlane, *J. Organometal. Chem.*, 1971, **29**, 245.
74. R. Graziani, G. Bombieri, E. Forsellini, P. Furlan, V. Peruzzo and G. Tagliavini, *J. Organometal. Chem.*, 1977, **125**, 43.
75. Y. M. Chow, *Inorg. Chem.*, 1971, **10**, 673.
76. K. Furue, T. Kimura, N. Yasuoka, N. Kasai and M. Kakudo, *Bull. Chem. Soc. Japan*, 1970, **43**, 1661.
77. G. A. Miller and E. O. Schlemper, *Inorg. Chem.*, 1973, **12**, 677.
78. J. C. May, D. Petridis and C. Curran, *Inorg. Chim. Acta*, 1971, **5**, 511.
79. R. V. Parish and R. H. Platt, *Inorg. Chim. Acta*, 1970, **4**, 589.
80. P. J. Smith and L. Smith, in "Inorg. Chim. Acta Reviews", U. Croatto (ed.), 1973, **7**, 11.
81. R. W. Taft, Jr., in "Steric Effects in Organic Chemistry", M. S. Newman (ed.), ch. 13, Wiley, New York, 1956, p. 591.
82. L. Verdonck and G. P. van der Kelen, *J. Organometal. Chem.*, 1972, **40**, 139.
83. J. D. Kennedy, W. McFarlane, G. S. Pyne, P. L. Clarke and J. L. Wardell, *J.C.S., Perkin II*, 1975, 1234.
84. A. Saika and C. P. Slichter, *J. Chem. Phys.*, 1954, **22**, 26.
85. C. J. Jameson and H. S. Gutowsky, *J. Chem. Phys.*, 1964, **40**, 1714.
86. E. V. van den Berghe and G. P. van der Kelen, *J. Mol. Struct.*, 1974, **20**, 147.
87. J. D. Kennedy and W. McFarlane, *J.C.S., Dalton*, 1973, 2134.
88. V. N. Torocheshnikov, A. P. Tupčiauskas and Yu. A. Ustynyuk, *J. Organometal. Chem.*, 1974, **81**, 351.
89. R. Radeglia and G. Engelhardt, *Z. Chem.*, 1974, **14**, 319.
90. J. D. Kennedy, W. McFarlane and G. S. Pyne, *Bull. Soc. Chim. Belge.*, 1975, **84**, 289.
91. C. A. MacKay, Ph.D. Thesis, University of London, 1973.
92. B. Menzebach and P. Bleckmann, *J. Organometal. Chem.*, 1975, **91**, 291.
93. H. Schumann, *Z. Anorg. Allg. Chem.*, 1967, **354**, 192.
94. J. D. Kennedy, *J. Organometal. Chem.*, 1976, **104**, 311.
95. H. Batiz-Hernandez and R. A. Bernheim, in "Progress in NMR Spectroscopy", J. W. Emsley, J. Feeney and L. H. Sutcliffe (eds.), 1968, **3**, 63.
96. T. W. Marshall, *Mol. Phys.*, 1961, **4**, 61.
97. D. K. Hindermann and C. D. Cornwell, *J. Chem. Phys.*, 1968, **48**, 4148.
98. O. Lutz, *Phys. Lett.*, 1970, **31A**, 528.
99. A. P. Tupčiauskas, N. M. Sergeev and Yu. A. Ustynyuk, *Mol. Phys.*, 1971, **21**, 179.
100. J. D. Kennedy and W. McFarlane, *J. Organometal. Chem.*, 1975, **94**, 7.
101. M. J. Ahamed and D. G. Gillies, unpublished results.
102. H. Elser and H. Dreeskamp, *Ber. Bunsenges. Phys. Chem.*, 1969, **73**, 619.
103. J. D. Kennedy, personal communication.
104. P. G. Harrison, S. E. Ulrich and J. J. Zuckerman, *Inorg. Nucl. Chem. Lett.*, 1971, **7**, 865.
105. A. G. Davies, L. Smith and P. J. Smith, *J. Organometal. Chem.*, 1972, **39**, 279.
106. D. C. McWilliam, M.Sc. Thesis, University of Queensland, 1970.
107. W. McFarlane and R. J. Wood, *J.C.S., Chem. Comm.*, 1969, 262.
108. W. McFarlane, private communication, quoted in: R. G. Jones, P. Partington, W. J. Rennie and R. M. G. Roberts, *J. Organometal. Chem.*, 1972, **35**, 291.
109. K. Hildenbrand and H. Dreeskamp, *Z. Phys. Chem. (Frankfurt)*, 1970, **69**, 171.
110. C. Schumann and H. Dreeskamp, *J. Magn. Resonance*, 1970, **3**, 204.
111. D. H. Harris, M. F. Lappert, J. S. Poland and W. McFarlane, *J.C.S., Dalton*, 1975, 311.
112. J. D. Kennedy, W. McFarlane, R. J. Puddephatt and P. J. Thompson, *J.C.S., Dalton*, 1976, 874.
113. J. D. Kennedy and W. McFarlane, *J.C.S., Dalton*, 1976, 1219.

114. E. V. van den Berghe and G. P. van der Kelen, *J. Organometal. Chem.*, 1973, **61**, 197.
115. J. D. Kennedy and W. McFarlane, *J.C.S., Chem. Commun.*, 1974, 983.
116. W. McFarlane and D. S. Rycroft, *J.C.S., Dalton*, 1974, 1977.
117. J. D. Kennedy, W. McFarlane, G. S. Pyne and B. Wrackmeyer, *J.C.S., Dalton*, 1975, 386.
118. T. N. Mitchell, *J. Organometal. Chem.*, 1974, **70**, C1.
119. T. N. Mitchell, *Org. Magn. Resonance*, 1975, **7**, 610.
120. T. N. Mitchell, personal communication.
121. E. V. van den Berghe and G. P. van der Kelen, *J. Organometal. Chem.*, 1974, **72**, 65.
122. H. J. Kroth, H. Schumann, H. G. Kuivila, C. D. Schaeffer, Jr. and J. J. Zuckerman, *J. Amer. Chem. Soc.*, 1975, **97**, 1754.
123. E. V. van den Berghe and G. P. van der Kelen, *J. Organometal. Chem.*, 1974, **82**, 345.
124. T. N. Mitchell and G. Walter, *J.C.S., Perkin II*, 1977, 1842.
125. T. N. Mitchell and B. Mathiasch, unpublished results.
126. T. N. Mitchell and M. el-Behairy, *J. Organometal. Chem.*, 1977, **141**, 43.
127. A. Tzschach, A. Zschunke and K. Jurkschat, 2nd International Conference on Organometallic and Coordination Chemistry of Ge, Sn, and Pb, Nottingham, 1977, Abstract No. B.11.
128. T. N. Mitchell and G. Walter, *J. Organometal. Chem.*, 1976, **121**, 177.
129. A. Frangou and D. G. Gillies, unpublished results.
130. A. P. Tupčiauskas, *Liet. Fig. Rink.*, 1977, **17**, 233.
131. K. Jurkschat, C. Mügge, A. Zschunke, M. F. Larin, V. A. Pestunovich and M. G. Voronkov, *J. Organometal. Chem.*, 1977, **139**, 279.
132. M. Mägi, E. Lippmaa, E. Lukevics and N. P. Erčak, *Org. Magn. Resonance*, 1977, **9**, 297.
133. D. A. Armitage and A. Tarassdi, *Inorg. Chem.*, 1945, **14**, 1210.
134. A. Rahm, M. Pereyre, M. Petraud and B. Barbe, *J. Organometal. Chem.*, 1977, **139**, 49.
135. B. Wrackmeyer, *J. Organometal. Chem.*, 1978, **145**, 183.
136. T. N. Mitchell, *J. Organometal. Chem.*, 1977, **141**, 289.
137. P. G. Harrison and K. Molloy, *J. Organometal. Chem.*, 1978, **152**, 53.
138. L. Killian and B. Wrackmeyer, *J. Organometal. Chem.*, 1978, **148**, 137.

SUBJECT INDEX

*The numbers in **bold** indicate the pages on which the topic is discussed in detail*

A

- Accedine, ¹H NMR data on, 136
 Accedinisine, ¹H NMR data on, 174
N-Acetylmerrillicine, ¹H NMR data on, 9
 6-Acetylheteratisine, ¹³C NMR data on, 180
N-Acetyl methyl ester of clavicipitic acid, ¹H NMR data on, 116
N-Acetylnortiliacoronine A, ¹H NMR data on, 24
N-Acetyltiliamosine, ¹H NMR data on, 24
 Acridone alkaloids, **98**
 Adiantifoline, ¹H NMR data on, 26
 Adina bases, **152**
 Adlumine, ¹H NMR data on, 45
 Affinisine, ¹H NMR data on, 175
 Ajmalicine alkaloids, **117**
 Ajmalicine, ¹³C NMR data on, 120
 3-iso-19-epi-Ajmalicine, ¹³C NMR data on, 120
¹H NMR data on, 124
 Akagerine, ¹H NMR data on, 157
 Akuammigine, ¹³C NMR data on, 120
¹H NMR data on, 124
 Alatamine, ¹H NMR data on, 95
 Alchorneine, ¹H NMR data on, 106
 Alkaloid A from *Atalantia Ceylanica*, ¹H NMR data on, 102
 Alkaloid-L23, ¹³C NMR data on, 187
 Alkaloids, ¹³C NMR spectra of **3**
 Alkanes, effects of α -, β - and γ -methyl substituents on ¹³C shifts, 4
N-Alkylnoratropine derivatives, ¹³C NMR data on, 86
 Alkyltin Chloride, ¹¹⁹Sn chemical shifts of, 311
 Alllosecurinine, ¹H NMR data on, 71
 Amaryllidaceae alkaloids, **52**
 Ambresoline, ¹H NMR data on, 83
 4a-Aminomethylhexahydrophenanthrenes, ¹H NMR data on, 64
 Amphibin, ¹H and NMR data on, 6
 Anantine, ¹H NMR data on, 104
 Anagyrin, ¹³C NMR data on, 73
 Andrangine, ¹³C NMR data, 168
 Andranginine, **152**
¹³C NMR data on, 154
 Andrangininol, ¹H NMR data on, 154
 5 α -Androstan-3 α -ol, ¹³C *T*₁ data on, 205
 5 α -Androstan-3 β -ol, ¹³C *T*₁ data on, 205
 Androstanes, ¹³C *T*₁ data on, 204
 Angustoline, ¹H NMR data on, 126
 Anopterine, ¹³C NMR data on, 184
¹H NMR data on, 184
 Antirrhine- β -methochloride, ¹H NMR data on, 126
 Apomorphine, ¹H NMR data on, 10
 Aporphine alkaloids, **8**
 Aristolactams, **15**
 Aristoteline, ¹H NMR data on, 156
 ASES program, use of in simulating dynamic NMR spectra, 262
 ASESIT program, use of in dynamic NMR, 266
Aspergillus amstelodami, ¹³C NMR data on a substance isolated from, 111
Aspergillus fumigatus, ¹H NMR data on a metabolite of, 111
 Aspidophytine, ¹³C NMR data on, 145
¹H NMR data on, 147
 Aspidospermine alkaloids, **139**
 Atalanine, ¹H NMR data on, 102
 Atisine, ¹³C NMR data on, 181
¹H NMR data on, 181
 Austamide, ¹H NMR data on, 110
 Azafluoranthenes, **49**
 Aziridine, proton exchange reactions and configuration inversion of, **246**

B

Base-line position for dynamic NMR spectra, **280**

Benzoates of evonine, ^1H NMR data on, 95

Benzophenanthridines, **43**

Benzylisoquinoline alkaloids, **7**

Benzylisoquinoline-aporphine dimers, **24**

2-Benzyltropine type alkaloids, ^{13}C NMR data on, 89

Berberastine iodide, ^1H NMR data on, 38

Bicuculline, ^1H NMR data on, 47

Bicyclomahanimbine, revised structure of, 107

Bisbenzylisoquinolines, **17**

Bisindole alkaloids, **158**

Bonafousine, ^{13}C NMR data on, 175

Boron trifluoride, use of as a shift reagent on steroid ketones, 203

Brevianamide C, ^1H NMR data on, 109

2-Bromo-3-cholestanone, ^{13}C shifts of due to $\text{Yb}(\text{tfn})_3$, 203

Brucine, ^{13}C NMR data on, 133

n-Butyltin compounds, ^{119}Sn chemical shifts of, 339

Butyltin trialkoxides, variation of ^{119}Sn of with temperature, 309

C

^{13}C NMR spectra of alkaloids, **3**

^{13}C Substituent effects in substituted benzenes, **3**

Cabucine oxindole A, ^1H NMR data on, 127

Cabucine oxindole B, ^1H NMR data on, 127

Cadamine acetate, ^1H NMR data on, 156

Cadia purpurea alkaloid, ^{13}C NMR data on, 74

Camptothecin, ^{13}C NMR data on, 100

α -Canadine methochloride, ^{13}C NMR data on, 33

β -Canadine methochloride, ^{13}C NMR data on, 33

Canconine derivatives, ^1H NMR data on, 61

Cannabicyclol, ^1H NMR data on, 107

Cannivonine, ^{13}C shifts induced by Nickel acetylacetonate, 92

Carbazoles, **106**

Carbolines, **106**

16 α -Carbomethoxyquebrachamine, ^{13}C NMR data on, 142

16 β -Carbomethoxyquebrachamine, ^{13}C NMR data on, 142

5 α -Carbomethoxytetrahydroalstonine, ^1H NMR data on, 125

Cassamedine, ^1H NMR data on, 13

Catharanthine, ^{13}C NMR data on, 150

Catharanthine *N*-oxide rearrangement product, ^1H NMR data on, 153

Cathedulin-6, ^{13}C NMR data on, 97

Cathedulin-4, ^1H NMR data on, 96

Cephalotaxine alkaloids, **55**

Cepharadione B, ^1H NMR data on, 15

Cepharanone A, ^1H NMR data on, 16

Cepharanone B, ^1H NMR data on, 16

Chavicine, ^1H NMR data on, 93

Chemical shifts in dynamic NMR spectra, **276**

Chiral lanthanide shift reagent, effect of on the ^1H spectrum of (\pm)-glaucine, 9

Chitosenine, ^1H NMR data on, 136

Chloro-16-dehydro-1-tabersonine, ^{13}C NMR data on, 146

5 α -Cholestan-3 α -ol, ^{13}C T_1 data on, 205

5 α -Cholestan-3 β -ol, ^{13}C chemical shifts of, 211

^{13}C T_1 data on, 205, 210

5 α -Cholestan-3-one, PRFT data on, 210

Cholestanes, ^{13}C T_1 data on, 204

Cholest-5-en-3 β -ol, ^{13}C Chemical shifts of, 211

i-Cholesterol, ^{13}C assignments using $\text{Yb}(\text{dpm})_3$, 201

Cholesterol, ^{13}C T_1 data on, 207

Cholesterol, effects of $\text{Eu}(\text{dpm})_3$ on the ^{13}C chemical shifts of, 200

Cholesteryl acetate, ^{13}C relaxation studies on, 206

Cholesteryl chloride, ^{13}C T_1 data on, 204

^{13}C relaxation studies on, 206

Cholesteryl linoleate, ^{13}C NMR data on, 210

Cimicine, ^{13}C NMR data on, 144

^1H NMR data on, 144

Cinchona bases, **152**

Cinchonidine, ^{13}C NMR data on, 98

Solvent effects on the ^{13}C chemical shifts of, 99

Cinocorine, ^{13}C NMR data on, 172

Cleavamine, ^{13}C NMR data on, 143

CLSFT program, use of in dynamic NMR, 266

Codeine, ^{13}C NMR data on, 58

Colchicine, ^{13}C NMR data on, 50
 Composite indices, **284**
 Composite Liouville space, renormalization of, **257**
 Compounds with tin-metal bonds, ^{119}Sn chemical shifts of, 358
 Computation and analysis of dynamic NMR spectra, **259**
 Condoxine, ^1H NMR data on, 130
 Conopharynginol tosylate spiran, ^1H NMR data on, 153
 Coordination number, influence on ^{119}Sn chemical shifts, **299**
 Coralydine, ^{13}C NMR data on, 32
 Cordrastine I, ^1H NMR data on, 48
 Cordrastine II, ^1H NMR data on, 48
 Coronaridine, ^{13}C NMR data on, 151
 Corydalic acid methyl ester, ^1H NMR data on, 45
 Corydalinidzine, ^1H NMR data on, 35
 (\pm)-Corydaline, ^1H NMR data on, 36
 Corydalispirone, ^1H NMR data on, 42
 Corydamine hydrochloride, ^1H NMR data on, 44
 Corynantheidine, ^{13}C NMR data on, 117
 Corynantheidine derivatives, ^1H NMR data on, 125
 Corynantheine alkaloids, **117**
 Corynantheine, ^{13}C NMR data on, 117
 Corynoline, ^1H NMR data on, 43
 Couroupitine A, ^1H NMR data on, 156
 Covalent organotin halide complexes, ^{119}Sn chemical shifts of, 366
 Criophylline, ^{13}C NMR data on, 167
 Croalbinecine, ^1H NMR data on, 67
 Cryptaustoline, ^1H NMR data on, 51
 Cryptophorine, ^1H NMR data on, 90
 Cryptophorinine, ^1H NMR data on, 90
 Cryptopleurine, ^1H NMR data on, 75
 Cuanzine, ^1H NMR data on, 138
 (\pm)-Cularidine, ^1H NMR data on, 29
 Cularine, ^1H NMR data on, 30
 Cularines, **29**
 Curryanin, ^1H NMR data on, 107
 Cyclecurine, ^1H NMR data on, 21
 Cycleadrine, ^1H NMR data on, 20
 Cycleanorine, ^1H NMR data on, 20
 Cycleapeltine, ^1H NMR data on, 20
 Cyclic dialkyltin alkoxides, ^{119}Sn chemical shifts of, 307

Cyclohexanes, effects of α -, β -, and γ -methyl substituents on ^{13}C shifts, 4
 Cyclohexanoindole, ^{13}C NMR data on, 115
 Cynometrine, ^1H NMR data on, 105

D

Deacetylgeissovellin, ^1H NMR data on, 132
 ^{13}C NMR data on, 134
 Dehydroisolongistrobone, ^1H NMR data on, 105
 Dehydrodicentrine, ^1H NMR data on, 17
 Delphinine, ^{13}C NMR data on, 179
 Delphinium bicolor Nutt. ^{13}C NMR data on alkaloid A of, 179
 Delphirine, ^{13}C NMR data on, 181 ^1H NMR data on, 181
 Delphisine 1-acetate, ^{13}C NMR data on, 177
 Delphisine, ^{13}C NMR data on, 177 ^1H NMR data on, 177
 Dendrobium alkaloid intermediates, ^1H NMR data on, 69
 Density matrices, **230**
 Deoxyharringtonine, ^1H NMR data on, 57
 Deoxynupharidine, ^1H NMR data on, 79
 ^{13}C NMR data on, 80
 (\pm)-1,4 α -Diacetoxyaporphine, ^1H NMR data on, 12
 (\pm)-1,4 β -Diacetoxyaporphine, ^1H NMR data on, 11
O,O'-Diacetylbrunsvigine, ^1H NMR data on, 53
 3,11-*O,O'*-Diacetylhydroxycephalotaxine, ^1H NMR data on, 56
O,N-Diacetylmichelanugine, ^1H NMR data on, 11
 4,*O*-Diacetylthaliporphines, ^1H NMR data on, 11
 Dialkyltin dialkoxide dimers, thermochemical data on, 306
 Dilbenz[*d,f*]azonine alkaloids, **55**
 2,2-Dibromocholestan-3-one, PRFT data on, 209
 Dibutyltin alkoxides, ^{119}Sn chemical shifts of, 307
 Di-*n*-butyltin alkoxides, ^{119}Sn chemical shifts of, 304
 Di-*n*-butyltin compounds, ^{119}Sn chemical shifts of, 341
 1,3-Diethylpiperidinal, ^{13}C NMR data on, 161

- Diethyltin compounds, ^{119}Sn chemical shifts of, 336
- Dihydroalstonerine, ^1H NMR data on, 157
- 3 α -Dihydrocadambine, ^1H NMR data on, 155
- Dihydrocatharanthine, ^{13}C NMR data on, 150
- Dihydrochelirubine, ^1H NMR data on, 43
- Dihydrocorynantheine, ^{13}C NMR data on, 117
- (\pm)-8,9-Dihydroglaziovine, ^1H NMR data on, 14
- (\pm)-11,12-Dihydroglaziovine, ^1H NMR data on, 14
- Dihydrolycopodine, ^{13}C NMR data on, 186
- 14',15'-Dihydropycnanthine, ^{13}C NMR data on, 173
- ^1H NMR data on, 173
- Dihydrosanguinarine, ^1H NMR data on, 43
- Dihydrovindoline, ^{13}C NMR data on, 140
- Di-isopropyltin bromides, ^{119}Sn chemical shift of, 318
- Diketopiperazines, ^1H NMR data on, 110
- 10,11-Dimethoxyaporphine, ^1H NMR data on, 10
- O,O*-Dimethylkrukovine, ^1H NMR data on, 21
- 1,3-Dimethylpiperidine, ^{13}C NMR data on, 115
- Dimethyltin chloride, formation of DMSO adduct of, 301
- Dimethyltin compounds ^{119}Sn chemical shifts of, 324
- Dimethyltin dichloride, auto-association of, 303
- Diorganostannacycloalkanes, ^{119}Sn chemical shifts of, 316
- Diorganostannathiocycloalkanes, ^{119}Sn chemical shifts of, 316
- Dioscorine, ^{13}C NMR data on, 92
- Dioxoaporphines, 15
- Diphenyltin compounds, ^{119}Sn chemical shifts of, 346
- Direct products, some properties of, 284
- Distannoxanes, ^{119}Sn chemical shifts of, 309
- 1,3-Disubstituted distannoxanes, ^{119}Sn chemical shifts of, 363
- Diterpene alkaloids, 177
- DNMR-3 program, use of in simulating dynamic NMR spectra, 262
- Dregamine, ^{13}C NMR data on, 134
- Dynamic equilibrium parameters for, 278
- Dynamic lineshape analysis, significance of the results from, 281
- Dynamic NMR spectra, computation and analysis of, 259
- simulation of, 259
- analysis of, 263

E

- α,β and γ Effects on the ^{13}C chemical shifts of steroids, 211
- γ -Effect on ^{13}C chemical shifts of tetracycles, 121
- Emetine, 49
- ^{13}C NMR data on, 50
- Enamides, some ^1H NMR data on, 39
- Epialloyohimbane, ^{13}C NMR data on, 121
- 21-Epiandronginine, ^1H NMR data on, 154
- Epi-i-cholesterol, ^{13}C assignments using Yb(dpm)₃, 201
- 11-Epicorynoline, ^1H NMR data on, 44
- 7-Epideoxynupharidine, ^1H NMR data on, 79
- ^{13}C NMR data on, 80
- Epidihydrolycopodine, ^{13}C NMR data on, 186
- 16-Epidregamine, ^{13}C NMR data on, 135
- Epi-isopilosine, ^1H NMR data on, 104
- Epilupinin, ^{13}C NMR data on, 74
- Epimelosine, ^{13}C NMR data on, 103
- 7-Epinupharidine, ^{13}C NMR data on, 80
- Epi-guinidine, ^{13}C NMR data on, 99
- Epi-quinine, solvent effects on the ^{13}C chemical shifts of, 99
- Episcandomelonine, ^{13}C NMR data on, 169
- Δ^{14} -16-Epivincamine, ^1H NMR data on, 136
- 21-Epivincamine, ^{13}C NMR data on, 138
- 19'-Epivindoline (19S), ^{13}C NMR data on, 173
- ^1H NMR data on, 173
- 14,15 β -Epoxytabersonine, ^{13}C NMR data on, 168
- Equation of motion, differential form of, 286
- Equation of motion for a spin density matrix, 235
- in the linear approximation, 251
- Equation of motion for a spin system in dynamic equilibrium, 241
- Ergot alkaloids, 112
- Erythrina alkaloids, 55
- Erythrinanone, ^1H NMR data on, 55

Erythrinan-diones, ^1H NMR data on, 55
 Eseramine, ^{13}C NMR data on, 108
 6,14-*endo*-Ethenotetrahydrothebaines, ^{13}C NMR data on, 59
 Ethyltin compounds, ^{119}Sn chemical shifts of, 335
 Eu(fod)₃, effect of an ^1H spectrum of 10,11-dimethoxyaporphine, 10
 Evanimine, ^1H NMR data on, 94
 Exchange model, selection of, 268
 Exchange superoperators in the linear approximation, 252
 properties of in composite Liouville space, 254

F

Fagaronine methosulphate, ^1H NMR data on, 42
 Falaconitine, ^{13}C NMR data on, 181
 Febrifugine acetate di-hydrochloride, ^1H NMR data on, 91
 Festuclavine, ^{13}C NMR data on, 115
 structure of, 114
 Fetidine, ^1H NMR data on, 27
 Five-coordinate organotin complexes, ^{119}Sn chemical shifts of, 310
 Folicangine, ^{13}C NMR data on, 166
 Four-coordinate organotin compounds, effect of substitution on ^{119}Sn chemical shifts of, 313
 Fukujusonorone, ^{13}C NMR data on, 223
 Fumigaclavine B, ^{13}C NMR data on, 116

G

Gardmultine, ^1H NMR data on, 176
 Geissoschizine, ^{13}C NMR data on, 122
 ^1H NMR data on, 125
 Gelsemine, ^{13}C NMR data on, 129
 Gelseverine, ^{13}C NMR data on, 129
 Glaucine, ^1H NMR data on, 8
 GPLONK program, use of in dynamic NMR, 266

H

Halfordamine, ^1H NMR data on, 102
 Haplophytine, ^{13}C NMR data on, 145
 ^1H NMR data on, 147

HDMR method applied to the determination of ^{119}Sn chemical shifts, 293
 Heteratisine, ^{13}C NMR data on, 180
 Hexahydroechinulin, ^{13}C NMR data on, 109
 Heyneanine, ^{13}C NMR data on, 151
 Hilbert space, use of in the superoperator formalism, 232
 Histronicotoin, ^1H NMR data on, 94
 (\pm)-Homoargemonine, ^1H NMR data on, 51
 Homopavinane, ^1H NMR data on, 50
 Hydrastine, ^1H NMR data on, 45
 Hydrastine imide, ^1H NMR data on, 48
 Hydroxy-androstanes, ^{13}C assignments using shift reagents, 201
 6-Hydroxybuphanidrine, ^1H NMR data on, 52
 11-Hydroxycephalotaxine, ^1H NMR data on, 56
 12-Hydroxycorynoline, ^1H NMR data on, 44
 7-Hydroxy- α -isosparteine, ^{13}C NMR data on, 72
 19-Hydroxy-isovoacangin, ^1H NMR data on, 152
 1-Hydroxymethyl- β -carboline, ^1H NMR data on, 108
 13 β -Hydroxystylopine, ^1H NMR data on, 35
 6'-Hydroxythiobinupharidine, ^1H NMR data on, 77
 6-Hydroxythionuphlutine-B, ^1H NMR data on, 77
 Hyoscyamine, ^{13}C NMR data on, 87

I

Ibogaïne, ^{13}C NMR data on, 149
 Ibogamine alkaloids, 139
 Imeluteine, ^1H NMR data on, 51
 Imenine, ^1H NMR data on, 13
 Imerubrine, ^1H NMR data on, 52
 Imidazole alkaloids, 103
 Indole alkaloids, 106
 Indoles, methyl substituent effects on ^{13}C chemical shifts of, 107
 Indolizidine alkaloids, 70
 Indolizidine, ^{13}C NMR data on, 129
 Intensity coefficient for dynamic NMR spectra, 280
 Ionic organotinhalide complexes, ^{119}Sn chemical shifts of, 366
 Isoancistrocladine, ^1H NMR data on, 7

Isoatisine, ^{13}C NMR data on, 184
 Isochavicine, ^1H NMR data on, 93
 Isodesoxycamptothecin, ^{13}C NMR data on, 100
 Isodihydrocadambine acetate, ^1H NMR data on, 155
 19-Isokeyneanine, ^{13}C NMR data on, 151
 Isolongistrobine, ^1H NMR data on, 105
 D-Isolysergic acid dimethylamide, conformation of, 112
 (+)-Isomatrine, ^1H NMR data on, 75
 Isonarciclasine tetra-acetate, ^1H NMR data on, 53
 Isonauclefine, ^{13}C NMR data on, 124
 ^1H NMR data on, 126
 Isopilosine, ^1H NMR data on, 104
 Isopiperine, ^1H NMR data on, 93
 Isoquinoline alkaloids, 5
 Isorhyncophylline, ^{13}C NMR data on, 129
 α -Isosparteine, ^{13}C NMR data on, 72
 Isotope effects on ^{119}Sn chemical shifts, 317
 Isotryptoquivaline, ^1H NMR data on, 111
 Isovoafoline, ^{13}C NMR data on, 165

J

$^1\text{J}(\text{C}-\text{H})$ in episcandomelonine, 168
 $^1\text{J}(\text{C}-\text{H})$ in reserpine, 124
 $^1\text{J}(\text{C}-\text{H})$ in scandomelonine, 168
 $^1\text{J}(\text{C}-\text{H})$ in yohimbine, 124

K

Keto-androstanes, ^{13}C assignments using shift reagents, 201
 Kinetic parameters, initial estimates of from dynamic NMR, 272
 Kinetics of a system at equilibrium, 239
 Kreysigine derivatives, ^1H NMR data on, 49
 Krukovine, ^1H NMR data on, 21

L

Lanuginosine, ^1H NMR data on, 13
 Laurifinine, ^1H NMR data on, 56
 Lepistine, ^1H NMR data on, 93
 Leurosidine, ^{13}C NMR data on, 161
 Leurosine, ^{13}C NMR data on, 161
 Lineshape equation for an exchanging system, 258

Lineshape of an unsaturated steady-state spectrum, 237
 Lineshape theory, some fundamental concepts in, 229
 Liouville space, use of in the superoperator formalism, 233
 Longimammidine hydrochloride, ^1H NMR data on, 5
 Longimammosine hydrochloride, ^1H NMR data on, 5
 Lupanine and related alkaloids, 71
 Lupin alkaloids, ^{13}C NMR data on, 71
 Lupinin, ^{13}C NMR data on, 73
 Lycodoline, ^{13}C NMR data on, 186
 Lycopodine, ^{13}C NMR data on, 186
 Lycopodium alkaloids, 186
 Lycorenine, ^1H NMR data on, 52
 D-Lysergic acid dimethylamide, ^1H NMR data on, 112
 Lythraceae alkaloids, 82
 Lythrancine-IV, ^1H NMR data on, 83

M

Macralstonidine, ^{13}C NMR data on, 172
 Magellanine, ^1H NMR data on, 187
 Mamanine, ^{13}C NMR data on, 75
 Mappicine, ^1H NMR data on, 101
 Matrine derivatives, ^{13}C NMR data on, 74
 Maytine, ^1H NMR data on, 95
 Maytolidine, ^1H NMR data on, 95
 Maytoline, ^1H NMR data on, 95
 Melobaline, ^{13}C NMR data on, 144
 Meloscine, ^{13}C NMR data on, 103
 Mesembrenone, ^{13}C NMR data on, 54
 10-Methoxy-dihydrolysergic acids, ^1H NMR data on, 113
 ^{13}C NMR data on, 114
 12-Methoxy- Δ^{14} -vincamine, ^1H NMR data on, 137
 O-Methylancistrocladine, ^1H NMR data on, 7
 Methylbicycloalaphylline, ^1H NMR data on, 101
 O-Methylcapaurine, ^{13}C NMR data on, 31
 ^1H NMR data on, 34
 O-Methylcorytenchirine, ^{13}C NMR data on, 32
 Methyl 3,7-dihydroxycholanate, ^{13}C T_1 data on, 207

- Methyl 3,12-dihydroxycholanate, ^{13}C T_1 data on, 207
 coordination with shift reagents, 202
N-Methyl-4-dimethylallyltryptophan, ^1H NMR data on, 116
 2,3-Methylenedioxy-9,10-dimethoxy-13-methyloctotensane, ^1H NMR data on, 41
O-Methylgeissoschizine, ^{13}C NMR data on, 122
 Methyl-3-hydroxycholanate, ^{13}C T_1 data on, 207
N-Methylisoquinuclidine, ^{13}C NMR data on, 150
 Methyl-lagerine, ^1H NMR data on, 84
O-Methylnemuarine, ^1H NMR data on, 19
O-Methoxyacanthine, ^1H NMR data on, 18
 Methyl 1,4,5,6-tetrahydronicotinate, ^{13}C NMR data on, 139
N-methyltetrahydrostepinone, ^1H NMR data on, 29
 Methyltin compounds, ^{119}Sn chemical shifts of, 322
 Methyl 3,7,12-trihydroxycholanate, ^{13}C shifts of due to $\text{Yb}(\text{tfn})_3$, 202
 ^{13}C T_1 data on, 208
O-Methyltylophorinidine, ^1H NMR data on, 70
 Michelanugine hydrochloride, ^1H NMR data on, 11
 Miyaconine, ^{13}C NMR data on, 185
 Monomethyltetrandrinium chloride, ^1H NMR data on, 20
 Morphine alkaloids, 57
 Morphine alkaloids with the hasuban skeleton, 65
 Morphine alkaloids with the 4,5-oxide bridge, 57
 Morphine alkaloids without the 4,5-oxide bridge, 62
 Morphine, ^{13}C NMR data on, 59
 Morphine type alkaloids, 57
 Mould metabolites, 109
- N**
- 6 α -Naltrexol, ^{13}C NMR data on, 60
 6 β -Naltrexol, ^{13}C NMR data on, 60
 Narcotine, ^1H NMR data on, 45
 Natural line-widths in dynamic NMR, 273
 Nauclefine, ^{13}C NMR data on, 124
 ^1H NMR data on, 126
 Neoline, ^{13}C NMR data on, 180
 Neostychnine, ^1H NMR data on, 131
 Neothiobinupharidine, ^{13}C NMR data on, 82
 ^1H NMR data on, 79
 Nicotine, NOE studies on, 97
 NOE studies on nicotine, 97
 Nor-rufescine, ^1H NMR data on, 52
 Nuphar alkaloids, 76
 Nupharidine, ^{13}C NMR data on, 81
- O**
- Obaberine oxidation product, ^1H NMR data on, 24
 Ochrolifuanine A, ^{13}C NMR data on, 176
 Ochrolifuanine B, ^{13}C NMR data on, 176
 Ocobotrine, ^1H NMR data on, 64
 Octahydroquinolizin-4-one, ^1H NMR data on, 75
n-Octyltin compounds, ^{119}Sn chemical shifts of, 345
 Ohysovenine, ^{13}C NMR data on, 108
 Organotin alkoxides, ^{119}Sn chemical shifts of, 304
 Organotin derivatives of carboranes, ^{119}Sn chemical shifts of, 365
 Organotin dihalides, ^{119}Sn chemical shifts of, 348
 Organotin hydrides, ^{119}Sn chemical shifts of, 358
 Organotin monohalides, ^{119}Sn chemical shifts of, 348
 Organotin oxides, ^{119}Sn chemical shifts of, 363
 Organotin selenides, ^{119}Sn chemical shifts of, 365
 Organotin sulphides, ^{119}Sn chemical shifts of, 364
 Organotin tellurides, ^{119}Sn chemical shifts of, 365
 Organotin trihalides, ^{119}Sn chemical shifts of, 347
 Orientalidine, ^1H NMR data on, 37
 Oxa-aporphine alkaloids, 13
 6,7- β -Oxidodeoxynupharidine, ^1H NMR data on dimer of, 76
 Oxindole alkaloids, 127
 Oxindoles, ^1H NMR data on, 128
 ^{13}C NMR data on, 129

- 19-Oxodehydroheteratisine, ^1H NMR data on, 180
 4-Oxo- α -isosparteine, ^{13}C NMR data on, 73
 Oxolaureline, ^1H NMR data on, 13
 4-Oxosparteine, ^{13}C NMR data on, 73

P

- Pandine, ^{13}C NMR data on, 145
 Pandoline, ^{13}C NMR data on, 143
 Paniculatin, ^{13}C NMR data on, 188
 ^1H NMR data on, 188
 Palinine tetra-acetate, ^1H NMR data on, 156
 Panurensine, ^1H NMR data on, 19
 Paragracine, ^1H NMR data on, 106
 Paspoclavine, ^1H NMR data on, 116
 Pavines, **49**
 Pentadesacetylevonimine, ^1H NMR data on, 94
 Phlebicine, ^1H NMR data on, 22
 Phenanthrene alkaloids, **15**
 Phenethylisoquinolines, **49**
 Phenyltin chlorides, ^{119}Sn chemical shifts of, 311
 Phenyltin compounds, ^{119}Sn chemical shifts of, 345
cis(4-H,9a-H)-4-Phenylquinolizidine, ^1H NMR data on, 82
 Phthalideisoquinolines, **45**
 Phyllantidine, ^1H NMR data on, 71
 Physostigmine, ^{13}C NMR data on, 108
 Physostygmine type alkaloids, **106**
 Pilocarpine, ^1H NMR data on, 105
 Pilosinine, ^1H NMR data on, 103
 Piperidine alkaloids, **85**
 Piperine, ^1H NMR data on, 92
 Pleiocorine, ^{13}C NMR data on, 170
 ^1H NMR data on, 170
cis-Polyprenanes, ^{13}C NMR data on, 222
 Pontevedrine, ^{13}C NMR data on, 15
 PRFT applied to steroid ^{13}C spectra, 203, 209
 Proaporphine alkaloids, **14**
 Prostaphabyssine, ^1H NMR data on, 65
 Protoberberines, **31**
 Protoberberinium salts, ^1H NMR data on, 37
 Protopines, **31**
see Pseudostrychnine derivatives, ^1H NMR data on, 132
 Pseudoyohimbine, ^{13}C NMR data on, 118
 Pyridine alkaloids, **94**

- Pyrodelphinine, ^{13}C NMR data on, 178
 Pyrrole alkaloids, **66**
 Pyrrolizidine alkaloids, **66**

Q

- Quebrachamine alkaloids, **139**
 Quebrachamine, ^{13}C NMR data on, 141
 Quimbeline, ^1H NMR data on, 167
 Quinazoline alkaloids, **98**
 Quinidine, ^{13}C NMR data on, 98
 Quinine, ^{13}C NMR data on, 98
 Quinoline alkaloids, **98**
 Quinolizidine alkaloids, **71**
 Quinolizidine, ^{13}C NMR data on, 71
 Quinolizidin-4-one, ^{13}C NMR data on, 73
 Quinolizidone derivatives, ^{13}C NMR data on, 123
 [2,3-*a*]Quinolizine, ^{13}C NMR data on, 117

R

- iso-3-Rauniticine, ^{13}C NMR data on, 120
 Relaxation data for ^{119}Sn , 299
 Relaxation studies applied to the ^{13}C NMR spectra of steroids, **203**
 Repandine, ^1H NMR data on, 18
 Retroisosenine, ^1H NMR data on, 68
 Rhyncophylline, ^{13}C NMR data on, 129
 Ribalinidine, ^1H NMR data on, 101
 Roxburghine B, ^{13}C NMR data on, 158
 ^1H NMR data on, 159
 Roxburghine C, ^{13}C NMR data on, 158
 Roxburghine D, ^{13}C NMR data on, 158
 Roxburghine E, ^{13}C NMR data on, 159
 ^1H NMR data on, 160
 Roxburghines, **158**
 Rubenine, ^1H NMR data on, 155
 Rufescine, ^1H NMR data on, 51

S

- Sarpagine type alkaloids, **135**
 Scandomelonine, ^{13}C NMR data on, 169
 Sceletenone, ^{13}C NMR data on, 54
 Sceletium alkaloid A₄, ^1H NMR data on, 54
 Schöpfung's base-VI, ^1H NMR data on, 39
 Scopolamine, ^{13}C NMR data on, 88
 3,7-Secopandoline A, ^{13}C NMR data on, 143
 Self-association in tributyltin alkoxides, 305

- SFORD** measurements on deacetyl-geissovelline, 134
 spectra on alkaloids, 4
 data on meloscine, 103
 data on scandomelonine, 169
 data on steroids, 200
 data on tropine, 89
 data for vindoline, 140
 Shift reagents applied to ^{13}C NMR spectra of steroids, **200**
 Shihunine, ^{13}C NMR data on, 69
 Siamin, ^1H and ^{13}C NMR data on, 6
 Simple indoles, **106**
 Simple isoquinoline alkaloids, **5**
 Sinomenine, ^{13}C NMR data on, 63
 Six-coordinate organotin complexes, ^{119}Sn chemical shifts of, 310
 Smipine, ^1H NMR data on, 91
 ^{119}Sn chemical shifts, isotope effects on, **317**
 ^{119}Sn chemical shifts, measurement of, **293**
 factors influencing, **299**
 ^{119}Sn chemical shift range, 292
 Solvent effects on ^{119}Sn chemical shifts, **299**
 Spareteine, ^{13}C NMR data on, 72
 Spin density matrix after exchange, evaluation of, **244**
 Spin-spin couplings in dynamic NMR spectra, **276**
 Spin system at thermal equilibrium with a lattice, spin density matrix of, **231**
 Spirobenzylisoquinolines, **40**
 Stannasiloxanes, ^{119}Sn chemical shifts of, 364
 Staphidine, ^{13}C NMR data on, 183
 Staphigine, ^{13}C NMR data on, 183
 ^1H NMR data on, 183
 Staphinine, ^{13}C NMR data on, 183
 Staphisagnine, ^{13}C NMR data on, 184
 ^1H NMR data on, 184
 Staphisine, ^{13}C NMR data on, 183
 ^1H NMR data on, 181
 Stephamiersine, ^1H NMR data on, 65
 Stephasunoline, ^1H NMR data on, 65
 Stepinonine, ^1H NMR data on, 28
 Steric polarization model of ^{13}C chemical shifts in steroids, 214
 Steroid ^{13}C chemical shift prediction rules, 215
 Steroid epoxides, γ -effect on ^{13}C chemical shifts of, 222
 Steroids, ^{13}C chemical shifts of, **212, 216**
 Steroid stereochemistry, **221**
 Strychnine, ^1H NMR data on, 130
 ^{13}C NMR data on, 133
 Strychnine and related alkaloids, **130**
 Substituent effects on the ^{13}C NMR spectra of steroids, **211**
 Substituted benzenes, ^{13}C substituent effects in, 3
 Superoperators, **232**
 Swazine, ^1H NMR data on, 67
 Symmetrical tetraorganotin compounds, ^{119}Sn chemical shifts of, 349
 Syneilesine, ^1H NMR data on, 68
 Synthetic spirobenzylisoquinolines, ^1H NMR data on, 41
- T**
- Tabernaeanegantines, ^{13}C NMR data on, 171
 ^1H NMR data on, 170
 Tabernaemontanine, ^{13}C NMR data on, 135
 Tabersonine, ^{13}C NMR data on, 139
 Tetrahydrodibenzapyrrocines, **49**
 Tetramethyl tin, HDMR spectrum of, 295
 Tetramethyl tin, solvent effects on ^{119}Sn chemical shift of, 303
 2,3,9,10-Tetrasubstituted tetrahydroprotoberberines, ^1H NMR data on, 36
 Thalibrunimine, ^1H NMR data on, 22
 Thalibrunine, ^1H NMR data on, 19
 Thalicarpine, ^1H NMR data on, 25
 Thalictrine, ^1H NMR data on, 18
 Thalictrigamine, ^1H NMR data on, 26
 Thalictrone, ^1H NMR data on, 25
 Thalidoxine acetate, ^1H NMR data on, 28
 Thalidoxine, ^1H NMR data on, 26
 Thalistyline chloride, ^1H NMR data on, 23
 Thalmelatine, ^1H NMR data on, 25
 Thalsimine, ^1H NMR data on, 23
 Thebaine, ^{13}C NMR data on, 58
 Thebaine photoadduct, ^1H NMR data on, 61
 Theory of NMR lineshapes for exchanging spin systems, **238**
 Thiobinuphoridine, ^{13}C NMR data on, 81
 ^1H NMR data on, 78
 1-*epi*-1'-*epi*-Thiobinuphoridine, ^{13}C NMR data on, 81
 Thionupharoline, ^1H NMR data on, 78
 Tin isotopes, NMR data on, 292

Tin isotopes, ratios of resonance frequencies of, 318

Titanium tetrachloride, use of as a shift reagent on steroid α,β -unsaturated ketones, 203

Trialkyl tin chlorides, effect on ^{119}Sn chemical shifts due to complexing, 301

Tri-*n*-butyltin alkoxides, ^{119}Sn chemical shifts of, 304

Tri-*n*-butyltin compounds, ^{119}Sn chemical shifts of, 344

Triethyltin compounds, ^{119}Sn chemical shifts of, 336

Tri-isopropyltin bromides, ^{119}Sn chemical shift of, 318

2,5,7-Trimethylindole, ^{13}C NMR data on, 109

Trimethylstannyl derivatives of cyclopentadiene, ^{119}Sn chemical shifts of, 319

Trimethyl tin chloride, formation of a pyridine adduct of, 300

effect of concentration and temperature on the ^{119}Sn chemical shifts of, 300

Trimethyl tin complexes, molar enthalpy data for, 302

Trimethyltin compounds, ^{119}Sn chemical shifts of, 326

Trimethyltin phenoxides, ^{119}Sn chemical shifts of, 312

Trineophyltin carboxylates, ^{119}Sn chemical shifts of, 312

Triphenyltin carboxylates, ^{119}Sn chemical shifts of, 312

Triphenyltin compounds, ^{119}Sn chemical shifts of, 346

Triphenyltin thiophenoxides, ^{119}Sn chemical shifts of, 312

Tritium NMR data on vincalécoblastine sulphate, 163

Tropane alkaloids, 85

Tropine, ^{13}C NMR data on, 89

^1H NMR data on, 86

2,2,4,4- d_4 -Tropine *N*-oxides, ^1H NMR data on, 86

Tylophorinidine, ^1H NMR data on, 70

U

Unsymmetrical tetraorganotin compounds, ^{119}Sn chemical shifts of, 350

Uvariopsine, ^1H NMR data on, 16

V

Vandrikine, ^{13}C NMR data on, 164

Velbanamine, ^{13}C NMR data on, 144

Venalstonine, ^{13}C NMR data on, 141

Vertaline, ^1H NMR data on, 84

Villalstonine, ^{13}C NMR data on, 171

Vincadifformine, ^{13}C NMR data on, 139

Vincalécoblastine, ^{13}C NMR data on, 160

^1H NMR data on, 162

Vincalécoblastine and related alkaloids, 160

Vincalécoblastine ether, ^1H NMR data on, 163

Vincalécoblastine sulphate, ^3H NMR data on, 163

Vincamine, ^{13}C NMR data on, 137

Vincamine and related alkaloids, 136

Δ^{14} -Vincamine, ^1H NMR data on, 136

Vincarodine, ^1H NMR data on, 139

Vincathicine, ^{13}C NMR data on, 161

^1H NMR data on, 162

Vincovoline, ^1H NMR data on, 163

Vindoline, ^{13}C NMR data on, 140

Vindoline metabolite, ^1H NMR data on, 147

Vindolinine, ^{13}C NMR data on, 141

^1H NMR data on, 146

Vindolinine (19*R*), ^{13}C NMR data on, 173

^1H NMR data on, 173

Vinoxine, ^{13}C NMR data on, 157

Voacangine, ^{13}C NMR data on, 149

Voafolidine, ^{13}C NMR data on, 166

Voafoline, ^{13}C NMR data on, 165

Voaketone, ^1H NMR data on, 152

Vobasinol, ^1H NMR data on, 175

Vobtusine, ^{13}C NMR data on, 164

W

WBR master equation, 235

Y

Yb(tfn)₃, use of in ^{13}C assignments of steroids, 201

Yenhusomine, ^1H NMR data on, 41

Yohimbane, ^{13}C NMR data on, 118

Yohimbanes, ^1H NMR data on, 160

Yohimbine, ^{13}C NMR data on, 118

Yohimbine alkaloids, 117

α -Yohimbine, ^{13}C NMR data on, 119

3-*epi*- α -Yohimbine, ^{13}C NMR data on, 119